# Expanding the scope of nickel-catalyzed carbon-oxygen bond activation: Towards the employment of easily accessible chemicals in modern catalysis

By

**Adam Cook**

Thesis submitted to the University of Ottawa

in partial Fulfillment of the requirements for the degree of

**Doctor of Philosophy**

**in**

**Chemistry**

Department of Chemistry and Biomolecular Sciences

Faculty of Science

University of Ottawa

# ABSTRACT

**Expanding the scope of nickel-catalyzed carbon-oxygen bond activation: Towards the employment of easily accessible chemicals in modern catalysis**

**Adam Cook** **Advisor:**

**University of Ottawa, 2024** **Stephen G. Newman**

The field of transition metal catalysis has exploded, both in popularity and utility, over the course of the past half-century. Into modernity, chemists have sought to improve methods for the transition metal-catalyzed activation of increasingly strong bonds, leading to the emergence of the subfield of carbon-oxygen bond activation. Carbon–oxygen bonds are extraordinarily prevalent in the natural world, and unlocking methods to activate them will prove paramount in the push towards a greener, bio-based economy. Nickel has emerged as a privileged, sustainable transition metal catalyst for carbon-oxygen bond activation. This dissertation will focus on the development of methods to expand the boundaries of nickel-catalyzed carbon–oxygen bond activation.

After a detailed introduction, chapter two of this dissertation will explore the *defunctionalisation* of chemical compounds via a process which will be called deoxygenative reduction – installing carbon–hydrogen bonds where once there were carbon–oxygen. Utilizing a nickel catalyst alongside an abundant, inexpensive hydride source, the development of a method that enables the reduction of carbon–oxygen bonds found in esters, ketones, aldehydes, epoxides, ethers, and alcohols will be described. Primary, secondary, and tertiary carbon–oxygen bonds each prove reducible when present in π-activated *and* non-π-activated positions. Applications of this method are demonstrated towards catalytic deuteration and the reductive defunctionalization of complex molecules including NSAIDs, cholesterol, quinine, and biomass derivatives.

The ability of this method to activate carbon–oxygen bonds in tertiary, non-π-activated positions lays the foundation for chapter three, wherein attention will be turned towards the realm of *functionalization*. This chapter explores the discovery and development of a deoxygenative

Suzuki-Miyaura arylation that uses unprotected, non-π-activated alcohols as substrates. Once more, nickel catalysts prove uniquely capable of achieving this reaction, this time being employed alongside Lewis acid catalysts and organoboron coupling partners to forge synthetically valuable C($sp^3$)–C($sp^2$) bonds. Yet, this chapter concludes with unanswered questions regarding the nature of the active catalyst, the mechanism of transformation and the substrate scope restrictions.

Solutions to these questions form the basis for chapter four, wherein the $\beta$-silicon effect – a known phenomenon in physical organic chemistry – is exploited to overcome the limitations of the nickel-catalyzed deoxygenative Suzuki-Miyaura arylation presented in chapter three. A deeper understanding as to how this reaction works is obtained by systematically studying ligand effects and gathering evidence to support the existence of a key carbocation intermediate. This chapter also documents the isolation, characterization, and evaluation of a series of nickel complexes, shedding light on the role of a newly discovered ligand in achieving reactivity.

With the development of a method for the Suzuki-Miyaura arylation of non-π-activated alcohols in the rear-view mirror, chapter five describes efforts to employ non-π-activated alcohols in other transformations. A high-throughput approach is taken to explore the chemical space of this transformation, keeping the substrate and catalytic conditions constant while varying the nucleophilic coupling partner. Efforts in achieving the formation of C($sp^3$)–C($sp^3$), C($sp^3$)–C(sp) and C($sp^3$)–N bonds will be documented.

# Acknowledgements

Holy freaking smokes. What a ride the past five years have been! Grad school sure was a funky time, filled with a multitude of personal and professional changes with, of course, some really awesome science sprinkled in between. But this (semi)short section is for none of that. It's for giving thanks to those who have made an impact on my (semi)short years at the University of Ottawa. Who was it that said, "people are the cumulation of those they spend the most time around?" I'm not sure, and if writing this dissertation has taught me anything it has taught me that Google isn't going to help. However, as I write these acknowledgements in our lab's office, shrouded in memories of some of the best friends I've ever had, that quote certainly rings true.

Rule number one: you've got to take care of number one! This one's for you, boss. Hope that you know how much I mean it when I tell you that I couldn't have made it to the point I stand at now without you. And did it ever get rocky at times, huh?! But from the tough times through to the celebratory pizza lunches, the one constant is that you've been supportive of me and my goals. As someone with dreams of becoming a professor, I couldn't have picked someone better to learn from. You told me in my first year that your role is to facilitate my studies, rather than supervise them; this will echo eternally between my ears as I walk towards the future. Your willingness to chat about anything and everything was awesome, and your constant open door policy is unique, encouraging and… just awesome. In so many ways, you're the best boss that a student could ask for and I am grateful for my time spent on your team. Looking forward to the jump from "student" into "friend".

John Donne writes that "No man is an island, entire of itself. Every man is a piece of the continent, a part of the main." The work discussed within this dissertation is nothing if not a group effort. Of all the things I've done as a graduate student, I consider my greatest achievement to be the contributions I've made towards building the best research group out there. Together, we've met the highest of highs and the lowest of lows… and we've had a heck of a fun time along the way. To all those I've overlapped with, rest assured that you'll live forever in my thoughts, stories, and memories. Big shout out to "iteration one" of the Newman group, those who welcomed me kindly into the group and helped build me up in the first couple of years. That's Taoufik, Ryan (what an incredible person to look up to), Garrett (sorry about that one time, hahaha), Omid (remember that time you covered our bill at the bar? What a stand-up guy), Eric S., Prakash, Jacob,

Haydn, Rama (aka. my favourite undergrad of all time), Katie, Max, Yan-Long (and his work ethic that I will forever look up to), Amrah, Victoria, August, and Saeed (gone too early but forever in our hearts and minds).

One day I woke up, and the group I had been brought up within had changed entirely! Cheers to "iteration two" of the Newman group. In no particular order, that's Carlos, Hana, Kostya, Isuru, Fran, Kian and Zichuan (good luck at Cornell and beyond). Shajia & Aisha: I sure will miss the nighttime shifts, and the uncountable smiles that accompanied them. Promise that I'll call you both from California. Piyas: keep the dream alive… you are always welcome in Ajax, and I look forward to future Ramakrishna dates. Aref: man, you are one of a kind and I am lucky to have gotten to know you… keep the INTENSITY, keep the FOCUS and watch your dreams come together before your eyes. Piers: those conference memories will last forever! I will be wicked upset if we don't cross paths every now and then and am liable to show up in Orillia at random if ever you stop replying to my 5 am Facebook messages. Eric: The one person who's been by my side the entire way! I've nothing left to say that I haven't told you already. You're family, family. Shout out to everyone I met while working in the Lin lab at Cornell, as well: Andy, Pierre, Jonas, Bartosz, Yukun, Justin, Samson, and all… looking back on my time with you all feels like a dream.

Amongst everyone, three people deserve special recognition for their unwavering support at various points during this adventure. Z.K.: I probably wouldn't have embarked on this journey, and certainly wouldn't be where I am right now, if it weren't for the inspiration from you, your family… and of course the animals. It's crazy now to think that I almost dropped out to become a priest! Once upon a time, but what a time it was! T.S.: To you I owe a lot; you carried me through the toughest of times and your strength and general ability to tackle anything life throws at you will serve you well as you move through graduate school, and beyond. And Sofia: your work ethic is inspirational, and you've helped carried me through the busiest of times. These last couple of years would have been made immeasurably more difficult without you (and Twil). The future is ours, and I am excited.

I've been fortunate to have been taught and guided by a series of inspirational leaders over the years. Prof Organ: you've been a heck of a source of inspiration… talk about having someone unique to look up to! Prof Gagosz (oops, I mean Fabien): probably I didn't reach out as much as I should have over the years, but you've said some things to me that have really resonated. Most

recently: “pressure is good, but only if it comes from within.” Advice that applies far beyond the perils and pleasures of graduate school. Dr. Rashmi: Couldn’t have had half as fun as I did in graduate school without all of the opportunities you’ve granted me. Roxanne: As with Fabien, I probably didn’t reach out as much as I should have, but you’re the best in the game and I appreciate the tips and tricks you’ve offered over the years. Song: Thanks for welcoming me with open arms into your lab… without doubt those few months had a tremendous impact on who I will become.

I’ve been fortunate to go to a heck of a lot of conferences throughout graduate school; to anyone I’ve had the pleasure to meet, you probably had a bigger role in my development than you realize. Undergraduate school sure was a heck of a time, huh? Yuri: You’ll always be the man, thanks for opening my eyes to how much fun I can have as a chemist! JP: I miss playing catch in the commons! Kevin: I wouldn’t have even gotten a foot in the door without your unwavering support. Liliana: It’s always the highlight of my CSC week whenever we get to catch up… I’ll get those textbooks back to you soon! And to the ones at the beginning of the journey – Mrs. McCormack and Mrs. Ryan – the first steps of this adventure laid the groundwork for the rest.

Family! I’ve saved the most important thankyous for last. I arrived in graduate school without a penny in my pocket – I remember having to borrow $600 from my grandfather just to cover the first installment of rent and groceries. Sadly, gramps passed in October of 2021; I know that you’re looking upon us all now from above and can only hope that I’ve made you proud. Dad: this whole shebang is because of you! You couldn’t possibly begin to understand how big of a role you have played in the person I’ve become. I recall all those stupid stressed out nights as an undergraduate when you were the one to carry me through. All of this – and all I do in the future – is owed to you. Em: your support in the good times, and especially the bad times, has been invaluable. You are my best friend, and your resilience and toughness are inspirational. Make sure the car stops before you jump out, next time. Declan, Huddy: if only we had more time to spend with each other over the past five years! We will make up for it, one day when you’re less obsessed with beating the crap out of me. Mom: you’re the rock that I know will always be there when I need you. And Grandma: there’s nothing I look forward to each time I come home more than our chats. You and your willingness to dare have been inspirational to me over my whole life. Aunts, uncles, cousins and beyond: I’m dead convinced that no one comes from a family as supportive as ours, and I move through life in full knowledge that if ever I falter, you’ll all be there to pick me up.

Finally, I need not talk about my background here, but suffice to say that the achievement of a PhD is something that flies in the face of predetermination; this achievement for all of those who've been told that big things are out of their reach. To everyone I've crossed path with over the past five years – mentioned herein by name or not – the world is yours if you reach out for it. I like to think that I'll pop up in your memories as often as I am certain you will appear in mine. Remember that being in school is a privilege, not a right. And, in graduate school and beyond, you are the singular author of your own story. ***Produce more than you work, work more than you sleep (and beware the lab goblins)!*** Yet, never forget to enjoy the ride. If ever you find yourself climbing a mountain, take a moment to look behind you at the path you've already traversed. Oftentimes, you'll find that the beautiful parts are nestled within the toughest moments of the journey.

## Statement of Contributions

All work in this thesis is original and was performed by the author of this dissertation unless otherwise noted below. The work discussed in part A of chapter two was a result of collaboration with Dr. Prakash Sekar, who led the optimization of the ester reduction transformation and assisted in the scope expansion, and Dr. Yan-Long Zheng, who made the seminal discovery of the reduction reaction. Other colleagues, Haydn MacLean and Piers St. Onge, contributed to part B of this chapter, assisting in the optimization and reproduction of the reaction, respectively. The work discussed in chapter three was performed in collaboration with Piers St. Onge, wherein they assisted in the reproduction of the reaction. Dr. Yan-Long Zheng was also responsible for synthesizing the first batch of the ligand that proved to be optimal for reactivity. The work discussed in chapter four was performed in collaboration with colleagues Carlos Barbery, Aisha Kassymbek and Aref Vaezghaemi. Carlos, an undergraduate honours student, synthesized a range of ligands (including the ligand that ended up proving optimal), Aisha led efforts in the isolation and characterization of nickel-NHC complexes and Aref assisted in the synthesis of starting materials while also demonstrating the reproduction of this reaction. The work presented in chapter five was conducted by the author of this dissertation. Chapters two through four are derived from a series of submitted publications on which the author of this dissertation is lead author; in all cases, they were responsible for writing drafts of the manuscript and supporting information.

## Claims to Original Research

***List of Publications*:** Parts of this thesis have been submitted for publication in peer-reviewed journals. In all cases, works have been partially rewritten and expanded upon for this dissertation.

**8. Cook, A.**; Kassymbek, A.; Vaezghaemi, A.; Barbery, C.; Newman, S. G. An $S_N1$-Approach to Cross-coupling: Deoxygenative Arylation Facilitated by the *β*-Silicon Effect. *Submitted*, **2024**.

**7. Cook, A.**; Newman, S. G. Alcohols as Substrates in Transition Metal-Catalyzed Arylation, Alkylation and Related Methods. *Chem. Rev.* **2024**, *129*, 6078–6144. doi: 10.1021/acs.chemrev.4c00094

**6. Cook, A.**; St. Onge, P.; Newman, S. G. Deoxygenative Suzuki-Miyaura Arylation of Tertiary Alcohols Through Silyl Ethers. *Nature Synthesis* **2023**. 2, 663-669. doi: 10.1038/s44160-023-00275-w

**5. Cook, A.**; Bezaire, M.; Newman, S. G. Nickel-Catalyzed Desulfonylative Olefination of *β*-Hydroxysulfones. *Org. Chem. Front.*, **2023**, *10*, 1339-1404. doi: 10.1039/D2QO01999J

**4.** St. Onge, P.; Khan, S. I.; **Cook, A.**; Newman, S. G. Reductive Cleavage of $C(sp^2)$–$CF_3$ Bonds in Trifluoromethylpyridines. *Org. Lett.*, **2023**, *25*, 1030-1034. doi: 10.1021/acs.orglett.3c00258

**3. Cook, A.**; MacLean, H.; St. Onge, P.; Newman, S. G. Nickel-Catalyzed Reductive Deoxygenation of Diverse C–O Bond-Bearing Functional Groups. *ACS Catal.*, **2021**, *11*, 13337-13347. doi: 10.1021/acscatal.1c03980

**2. Cook, A.**; Clément, R.; Newman, S. G. Reaction Screening in Multiwell Plates: High-Throughput Optimization of a Buchwald-Hartwig Amination. *Nature Protocols* **2021**, *16*, 1152-1169. doi: 10.1038/s41596-020-00452-7

**1. Cook, A.**; Prakash, S.; Zheng, Y.-Z.; Newman, S. G. Exhaustive Reduction of Esters Enabled by Nickel Catalysis. *J. Am. Chem. Soc.* **2020**, *142*, 8109-8115. doi: 10.1021/jacs.0c02405

***List of Presentations:*** Parts of this thesis have been presented in conference proceedings and technical meetings:

**16.** Cook, A.; Newman, S. G. Nickel-catalyzed Suzuki-Miyaura arylation: From high-throughput to Hammett analysis. *33rd QOMSBOC held at Concordia University*, Nov. **2023**.

**15.** Cook, A.; Newman, S. G. Free alcohols: More than just a tool to attract people to your wedding. *Graduate Professional Seminar Series held at Cornell University*, October **2023**.

**14.** Cook, A.; Newman, S. G. Free alcohols: More than just a tool to attract people to your wedding. *Canadian Organic International Talks (virtual)*, Oct. **2023** [invited].

**13.** Cook, A.; Newman, S. G. Nickel-catalyzed Suzuki-Miyaura arylation: From high-throughput to Hammett analysis. *21st International Symposium on Organometallic Chemistry Directed Towards Organic Synthesis held in Vancouver*, July **2023**.

**12.** Cook, A.; Newman, S. G. Nickel-catalyzed Suzuki-Miyaura arylation: From high-throughput to Hammett analysis. *106th Canadian Chemistry Conference and Exhibition held in Vancouver*. June **2023**.

**11.** Cook, A.; Newman, S. G. Nickel-catalyzed Suzuki-Miyaura arylation: From high-throughput to Hammett analysis. *Ottawa-Carleton Chemistry Institute Day held at University of Ottawa*, May **2023**.

**10.** Cook, A.; Newman, S. G. Nickel-catalyzed deoxygenation: From high-throughput to Hammett analysis. *Quebec-Ontario Physical Organic Chemistry Mini-Symposium held at Royal Military College of Canada*, Nov. **2022**.

**9.** Cook, A.; Newman, S. G. Nickel-catalyzed Suzuki-Miyaura arylation: Quest for the ideal electrophilic coupling partner. *32nd QOMSBOC held at McMaster University,* Oct. **2022**.

**8.** Cook, A.; Newman, S. G. Nickel-catalyzed Suzuki-Miyaura arylation: Quest for the ideal electrophilic coupling partner. *105th Canadian Chemistry Conference and Exhibition held in Calgary.* June **2022**.

**7.** Cook, A.; Newman, S. G. Nickel-catalyzed Suzuki-Miyaura arylation: Quest for the ideal electrophilic coupling partner. *Ottawa-Carleton Chemistry Institute Day held at Carleton University,* May **2022**

**6.** Cook, A.; Newman, S. G. Nickel-catalyzed deoxygenation: The hunt for reactive intermediates. *24th Annual Chemistry and Biochemistry Graduate Research Conference (virtual),* Nov. **2021**.

**5.** Cook, A.; Newman, S. G. Nickel-catalyzed deoxygenation: The hunt for reactive intermediates. *31st QOMSBOC hosted by McMaster University (virtual),* Nov. **2021**.

**4.** Cook, A.; Newman, S. G. Nickel-catalyzed deoxygenation: In search of reactive intermediates. *51st IUPAC General Assembly and 104th Canadian Chemistry Conference and Exhibition (virtual)*. July **2021**.

**3.** Cook, A.; Newman, S. G. Nickel-catalyzed deoxygenation: In search of reactive intermediates. *Ottawa-Carleton Chemistry Institute Day (virtual).* May **2021**.

**2.** Cook, A.; Newman, S. G. Nickel-catalyzed deoxygenation: In search of reactive intermediates. *Quebec-Ontario Physical Organic Chemistry Mini-Symposium held at Royal Military College of Canada (virtual),* Nov. **2020**.

**1.** Cook, A.; Newman, S. G. Exhaustive reduction of esters enabled by nickel catalysis. *30th QOMSBOC held at University of Ottawa,* Nov. **2019**.

## Table of Contents

Abstract ……..……. II-III

Acknowledgements ……...… IV-VII

Statement of contributions ……..…….…….……..…… VII

Claims to original research …….……...…….…….. VIII-X

Table of Contents ……...……..……. XI-XVIII

List of Figures ……...……..……. XIX-XXI

List of Schemes ……..……. XXII-XXVII

List of Tables ……...……...…. XXVIII

List of Abbreviations ……...…… XXIX-XXXIII

**Chapter 1.** Transition metal cross-coupling towards the goal of employing oxo-chemicals as easily accessible substrates …… **1-122**

1.0. Setting the stage: Historical commentary and a prelude to the Sustainocene ……… 2-4

1.1. Reuse permissions ……...… 5

1.2. Basics of chemical catalysis ……..…….. 5-17

1.2.1. Selected theory and historical notes on catalysis ……...…. 5-13

1.2.2. Cross-coupling reactions: Passing the torch from palladium to nickel ……..…..... 13-15

1.2.3. Ligands in transition metal catalysis: *N*-heterocyclic carbenes …… 15-17

1.3. Cross-coupling reactions: Constructing complexity from C–O bonds ……... 17-24

1.4. Alcohols as substrates in transition metal catalyzed alkylation, arylation and related reactions …….. 24-75

1.4.1. Alcohols as alkylating agents by direct substitution through $S_N1$-type and related pathways ……..…… 26-43

1.4.1.1. Select developments prior to 2010 ……..…… 27-29

1.4.1.2. Developments after 2010 ……..…..……. 29-43

1.4.2. Deoxygenative functionalization via cross-coupling and related transformations ……..…….. 44-67

1.4.2.1. π-Activated alcohols with organoboron nucleophiles …….... 44-57

1.4.2.2. π-Activated alcohols with other organometallic nucleophiles ……..….. 58-60

1.4.2.3. π-Activated alcohols with other electrophiles ……... 60-67

1.4.3. Non-π-activated alcohol activation ……...…… 67-75

1.5. Beyond cross-coupling: Transition metal-catalyzed deoxygenative reduction of oxo-chemicals ……...……. 75-83

1.5.1. Reductive deoxygenation of ketones and aldehydes ……..…… 77-79

1.5.2. Reductive deoxygenation of ethers and alcohols ……..……. 79-83

1.6. Scope of this dissertation: Research goals and objectives ……..…….. 84-85

1.7. References ……..…….…… 86-122

**Chapter 2.** Deoxygenative reduction of diverse carbon-oxygen bond bearing functional groups ……...… **123-220**

2.1. Chapter outlook ……..……..... 124

2.2. Reuse permissions and contributions ……...…… 125-126

**2.3. Part A:** Exhaustive reduction of esters enabled by nickel catalysis ….....…. **127-161**

2.3.1. Introductory theory and background information ……..……... 127-128

2.3.2. Discovery and optimization ……..…… 129-136

2.3.2.1. Investigating alternative bases and hydride sources ……... 130-132

2.3.2.2. Investigating alternative catalyst systems ……..…….. 132-135

2.3.2.3. Control experiments ……..….. 135-136

2.3.3. Substrate scope …….. 136-143

2.3.3.1. Substrate scope overview ……..….. 136-139

2.3.3.2. Unsuccessful scope examples ……...….. 139-140

2.3.3.3. Controlling selectivity: Ester vs. ether reduction ……..….. 141-142

2.3.3.4. Extension to catalytic deuteration …….. 142-143

2.3.4. Preliminary mechanistic investigation ……...…. 144-157

2.3.4.1. Investigating potential reaction intermediates ……...…. 144-147

2.3.4.2. Variable time normalization analysis ……...…. 147-153

2.3.4.3. Kinetic isotope effect ……..…. 154-155

2.3.4.4. Speculative reaction mechanism and commentary …..…. 155-157
2.3.5. Failed directions ……... 157-160
2.3.6. Part A: Conclusions ……... 160-161
**2.4. Part B:** Reductive deoxygenation of diverse C–O bond bearing functional groups ……..... **161-190**
2.4.1. Introductory theory and background information …… 161-163
2.4.2. Development of reaction conditions ……. 163-166
2.4.2.1. Overview ……..…….. 163-165
2.4.2.2. Time-course study of ketone deoxygenation ……..…… 165-166
2.4.3. Substrate scope ……..…… 166-174
2.4.3.1. Substrate scope for alcohol deoxygenation ……...…..... 166-168
2.4.3.2. Substrate scope for ketone and aldehyde deoxygenation .. 169-170
2.4.3.3. Substrate scope for ether and epoxide deoxygenation ….. 171-172
2.4.3.4. Multi-site deoxygenation …….…….…….. 172-173
2.4.3.5. Unsuccessful scope examples ……...…. 173-174
2.4.4. Applications of this transformation ……..…… 174-177
2.4.4.1. Catalytic deuteration …….……. 174-175
2.4.4.2. Deprotection of benzyl-protected alcohols …… 175-176
2.4.4.3. Degradation of biomass-derived molecules …….. 176-177
2.4.5. Mechanistic evaluation ……..... 177-188
2.4.5.1. Kinetic isotope effect and plausible intermediates ……..... 177-178
2.4.5.2. Investigating potential olefin intermediate …...…….. 178-179
2.4.5.3. Investigating potential carbocation intermediate ……... 179-180
2.4.5.4. Investigating radical and organonickel intermediates ….... 180-183
2.4.5.5. Effect of chain length on reactivity ……..…. 183-185
2.4.5.6. Effect of drop-in additives ……...….. 185-186
2.4.5.7. Tentative mechanistic hypothesis …….…. 187-188
2.4.6. Additional commentary …… 189-190
2.4.7. Part B: Conclusions ……. 190
2.5. Conclusion, impact, future work and considerations …….. 191-197

2.5.1. Conclusion ..... 191
2.5.2. Impact and collaborations ..... 192-196
2.5.3. Future work and considerations ..... 196-197
2.6. Experimental ..... 198-203
2.6.1. General details ..... 198
2.6.2. Instrumentation ..... 198
2.6.3. Materials ..... 199
2.6.4. General procedures ..... 200-202
2.6.5. Characterization data of synthesized products ..... 203
2.7. References ..... 204-220

**Chapter 3.** Deoxygenative Suzuki-Miyaura arylation of tertiary alcohols through silyl ether intermediates ..... **221-284**
3.1. Chapter outlook ..... 222
3.2. Reuse permissions and contributions ..... 223
3.3. Introductory theory and background information ..... 224-225
3.4. Discovery, optimization, further investigations into the reaction conditions .. 226-239
3.4.1. Discovery and optimization synopsis ..... 226-227
3.4.2. Ligand investigation ..... 228-231
3.4.3. Investigations into the role of $Bi(OTf)_3$ .....231-233
3.4.4. Investigations into the role of chlorosilane additive ..... 234-237
3.4.5. Control reactions with drop-in additives ..... 238
3.4.6. Observed byproducts ..... 239
3.5. Substrate scope ..... 240-243
3.5.1. Substrate scope overview ..... 240-242
3.5.2. Unsuccessful scope examples ..... 242-243
3.6. Mechanistic investigations ..... 244-262
3.6.1. Investigating olefin and radical intermediates ..... 244-245
3.6.2. Hammett analysis ..... 245-246
3.6.3. Carbocation rearrangements ..... 246-247

3.6.4. Stereochemical erosion ……..…….. 248
3.6.5. Variable time normalization analysis ……...… 249-258
3.6.6. Eyring analysis ……. 259-260
3.6.7. Preliminary mechanistic hypothesis ……...…….. 261-262
3.7. Failed directions and additional commentary ……..……. 263-266
3.8. Conclusions, impact, future work and considerations ……..…… 267-271
3.8.1. Conclusions …….. 267
3.8.2. Impact ……..…. 267-269
3.8.3. Future work and considerations …… 270-271
3.9. Experimental …… 272-275
3.9.1. General details ……..... 272
3.9.2. Instrumentation …… 272
3.9.3. Materials …….. 273
3.9.4. General procedures ……..…. 273-275
3.9.6. Characterization data of synthesized products …….……. 275
3.10. References ……..…… 276-284

**Chapter 4.** An $S_N1$-approach to cross-coupling: Deoxygenative arylation facilitated by the *β*-silicon effect ……...…..... **285-374**
4.1. Chapter outlook ……..... 286
4.2. Reuse permissions and contributions ……... 287
4.3. Introductory theory and background information ……..…….. 288-291
4.4. Discovery and optimization of reaction conditions ……..... 291-299
4.4.1. Discovery and optimization synopsis ……..….. 291-294
4.4.2. Detailed ligand investigation ……..….. 294-299
4.4.3. Synthesis of β-hydroxysilanes ……..…… 299
4.5. Substrate scope …… 300-303
4.5.1. Substrate scope overview ……. 300-301
4.5.2. Derivatization of products ……..……. 302
4.5.3. Unsuccessful scope examples ……..…… 303

4.6. Mechanistic investigations …….. 304-323
4.6.1. Investigating nickel-**L2** complexes …….. 304-309
4.6.2. Kinetic evaluation of reaction mechanism ……...…… 310-319
4.6.2.1. Variable time normalization analysis …… 310-314
4.6.2.2. Eyring analysis ……..…… 315
4.6.2.3. Kinetic isotope effect ……..…….. 316
4.6.2.4. Time-course diagram comparison with different ligands .. 317-319
4.6.3. Miscellaneous mechanistic experiments ……..…. 319-322
4.6.4. Mechanistic hypothesis ……...….. 322-323
4.7. Additional commentary ……...…. 324-325
4.8. Conclusion, impact, future work and considerations ……..…. 326-330
4.8.1. Conclusion ……..……. 326
4.8.2. Impact, future work and considerations ……..……. 326-330
4.9. Experimental ……...…. 331-363
4.9.1. General details ……...….. 331
4.9.2. Instrumentation …… 331
4.9.3. Materials ……..…..… 332
4.9.4. General procedures ……..……..…. 332-334
4.9.5. Characterization details of starting materials ……..….. 334-339
4.9.6. Characterization details of products ……..… 340-350
4.9.7. Diversification of silane handle in reaction products ……..... 351-437
4.9.7.1. Procedure for oxidation of -$SiMe_3$ into -OH ……..…. 351-352
4.9.7.2. Procedure for protodesilylation of -$SiMe_3$ to -H ……...… 352-354
4.9.8. Other experimental details and procedures ……..….. 354-357
4.9.9. Synthesis of nickel-**L2** complexes …… 357-363
4.10. References ……. 364-374

**Chapter 5.** High-throughput evaluation of future directions for the deoxygenative functionalization of unprotected, non-π-activated alcohols ……..…..…….. **375-420**

5.1. Chapter outlook ……..…… 376
5.2. Reuse permissions ……..…. 377
5.3. Introductory theory and background information ……..……. 377-380
5.4. High-throughput exploration of nucleophilic coupling partners …..…… 380-382
5.5. Investigating C($sp^3$)–C($sp^3$) bond forming reactions ……...… 382-385
5.6. Investigating the allylation of tertiary alcohols ……..…. 385-386
5.7. Investigating the alkynylation of tertiary alcohols ……..… 386-388
5.8. Investigating the amination of tertiary alcohols ……..…….. 388-396
5.9. Conclusion, future outlook and considerations ……..…….. 397-400
5.9.1. Conclusions ……..……. 397
5.9.2. Future outlook and considerations …… 397-400
5.10. Experimental …….. 401-412
5.10.1. General details ……..…….. 401
5.10.2. Instrumentation ……..……. 401
5.10.3. Materials ……..……...……. 402
5.10.4. General procedures …….. 402-407
5.10.5. Characterization details ……..……. 407-412
5.11. References ……..…… 413-420

**Chapter 6.** Conclusions ……..…...… **421-**
6.0. Contents of this conclusion …….. 422
6.1. Summary of the work presented within this dissertation …….. 423-424
6.2. Critical analysis of the work presented within this dissertation ……..….. 424-432
6.2.1. Strengths ……..…….. 424-427
6.2.2. Weaknesses ……...…… 428-429
6.2.3. Overall contributions to the field of study: Summary …… 430-432
6.3. The future of C($sp^3$)–O bond activation, nickel catalysis: Enabling technologies in a modern era ……...…… 432-433
6.4. Epilogue: Diet for a new Chem-merica ……..…… 433-434
6.5. References …… 435-438

7. Appendix ……...…….. 439-509

## List of Figures

Figure 1.1. What does it take to get a chemical reaction to occur? ……..……. 6

Figure 1.2. Chemical catalysis: Basics …….……. 6

Figure 1.3. Transition metal-catalyzed transformations ……..…… 11

Figure 1.4. Comparing palladium and nickel ……...…… 15

Figure 1.5. Generic structures of *N*-heterocyclic carbenes (NHCs) and those that will be used within this dissertation …….…… 17

Figure 1.6. Bond dissociation energy (kcal/mol) of electrophilic coupling partners in cross-coupling reactions ……...……. 18

Figure 1.7. Early reports of the use of various alcohol derivatives in nickel-catalyzed Suzuki-Miyaura reactions ……...….. 20

Figure 1.8. Cleavage of aliphatic alcohols: Topics to be discussed herein …….. 25

Figure 1.9. Graphical outlook for this dissertation …….. 85

Figure 2.1. Nickel-catalyzed deoxygenative reduction of various oxo-functional groups ...…. 124

Figure 2.2. Contemporary methods to achieve the ester-to-methyl transformation ……..… 127

Figure 2.3. Alternative esters that could be reduced ……. 139

Figure 2.4. Unsuccessful substrates ……... 140

Figure 2.5. Variation in catalyst: vTNA plots suggest first order dependence ……..… 150

Figure 2.6. Variation in TMDSO: vTNA plots suggest first order dependence ……. 151

Figure 2.7. Variation in [**2.94**]: vTNA plots suggest first order dependence ……..… 152

Figure 2.8. Variation in KO$^t$Bu: vTNA plots suggest first order dependence ……... 153

Figure 2.9. Speculative reaction mechanism …….. 156

Figure 2.10. Methods for reductive deoxygenation ……... 162

Figure 2.11. Unsuccessful substrates in the deoxygenation of C–O bonds ……... 173

Figure 2.12. Systematic investigation into the effect of chain length on product yield …… 184

Figure 2.13. Tentative mechanistic hypothesis …….. 188

Figure 2.14. Attempted reduction of carbohydrate model compound **2.211** ……. 190

Figure 3.1. Lewis acid/transition metal dual catalyzed deoxygenative Suzuki-Miyaura arylation of tertiary alcohols ……,,,,.……. 222

Figure 3.2. Contemporary strategies for cross-coupling of unprotected alcohols ……. 225

Figure 3.3. Structures of ligands used in this optimization …… 230

Figure 3.4. Unsuccessful alcohol and boronate ester coupling partners …… 243

Figure 3.5. Variation in [Ni-**L1**] catalyst for the arylation of substrate **3.106**: Variable time normalization plots illustrate positive order dependency ……..…. 251

Figure 3.6. Variation in [PhBpin] for the arylation of substrate **3.106**: Variable time normalization plots illustrate positive order dependency …….. 252

Figure 3.7. Variation in [substrate] for the arylation of substrate **3.106**: Variable time normalization plots illustrate positive order dependency. …….. 253

Figure 3.8. Variation in [$Bi(OTf)_3$] for the arylation of substrate **3.106**: Variable time normalization plots illustrate positive order dependency. ……..… 254

Figure 3.9. Variation in [Ni-**L1**] for the arylation of substrate **3.98b**: Variable time normalization plots illustrate positive order dependency. ……..… 255

Figure 3.10. Variation in [PhBpin] for the arylation of substrate **3.98b**: Variable time normalization plots illustrate positive order dependency …….……. 256

Figure 3.11. Variation in [substrate] for the arylation of substrate **3.98b**: Variable time normalization plots illustrate positive order dependency ……..... 257

Figure 3.12. Variation in [$Bi(OTf)_3$] for the arylation of substrate **3.98b**: Variable time normalization plots illustrate positive order dependency …….. 258

Figure 3.13. Proposed reaction mechanism and related evidence ……..… 262

Figure 4.1. Graphical outlook for chapter four ……. 286

Figure 4.2. Exploiting the *β*-silicon effect in the arylation of *β*-hydroxysilanes ……... 291

Figure 4.3. Structures of ligands used in this optimization …… 296

Figure 4.4. Dissecting the structure of bis(NHC)s ……. 297

Figure 4.5. Unsuccessful substrates ……... 303

Figure 4.6. Investigating the rate dependence on [$Bi(OTf)_3$] …….. 311

Figure 4.7. Investigating the rate dependence on [substrate] ……..… 312

Figure 4.8. Investigating the rate dependence on [PhBpin] ……... 313

Figure 4.9. Investigating the rate dependence on [Ni-**L2**] catalyst …… 314

Figure 4.10. Time-course data for arylation in the presence of **L2**, **L7**, and dppp ……..... 318-319

Figure 4.11. Tentative reaction mechanism ……... 323

Figure 4.12. Exploring non-silicon based neighbouring groups …… 329

Figure 4.13. Extending this transformation towards stereocontrolled syntheses ……... 330

Figure 4.14. X-ray crystal structure of **L2** ……..…… 339

Figure 4.15. X-ray crystal structure of **4.59** …… 358

Figure 4.16. X-ray crystal structure of **4.60** …… 359

Figure 4.17. X-ray crystal structure of **4.61** …… 361

Figure 4.18. X-ray crystal structure of **4.62** …… 362

Figure 4.19. X-ray crystal structure of **4.63** …… 362

Figure 5.1. High-throughput expansion of nucleophilic coupling partners amenable to previously discussed alcohol activation ……... 376

Figure 5.2. High-throughput experimentation as a method for the rapid generation of data ….. 378

Figure 5.3. High-throughput reaction discovery: Alternative nucleophiles in the Lewis acid/transition metal catalyzed functionalization of tertiary alcohols ……. 381

Figure 5.4. Conventional methods for amination ……..…….. 389

Figure 5.5. Screening of amine nucleophilic coupling partners ……... 392

Figure 5.6. Speculating upon the 'optimal pKa window' for this reaction …….……... 393

Figure 5.7. bis(NHC) ligands that could be screened in these transformations ……...… 398

Figure 6.1. Summarizing the contents of this dissertation …….. 423

## List of Schemes

Scheme 1.1. Early efforts in transition metal catalysis ……..…… 8

Scheme 1.2. Early discoveries in Mizoroki-Heck reactions ……..……. 9

Scheme 1.3. Suzuki-Miyaura reaction ……. 13

Scheme 1.4. Efforts by the Newman group in the coupling of oxygenated chemical substrates ……. 19

Scheme 1.5. Transition metal cross-coupling of simple ethers ……...……. 22

Scheme 1.6. Silylation as a strategy towards the activation of alcohols …….…. 23

Scheme 1.7. $S_N1$-type deoxygenative functionalization: General details and representative examples ……..……..... 28

Scheme 1.8. Iridium/tin bimetallic catalysis for $S_N1$-type deoxygenative functionalization ……. 30

Scheme 1.9. Selected tin-catalyzed methods ……..…….. 31

Scheme 1.10. Selected copper-catalyzed methods ……..……. 32

Scheme 1.11. Selected silver- and gold-catalyzed methods ……..…….... 34

Scheme 1.12. Selected rhenium-catalyzed methods ……...…. 35

Scheme 1.13. Selected indium-catalyzed methods ….……. 36

Scheme 1.14. Selected iron-catalyzed methods ……...… 38

Scheme 1.15. Selected iron-catalyzed methods applied to heterocycle synthesis and functionalization …….…….. 39

Scheme 1.16. Selected scandium-catalyzed methods …….……. 40

Scheme 1.17. Selected titanium-catalyzed methods …… 41

Scheme 1.18. Selected zinc- and ytterbium-catalyzed methods …….. 42

Scheme 1.19. The Suzuki-Miyaura coupling of benzyl alcohols …… 45

Scheme 1.20. Copper-, nickel- and palladium-catalyzed cross-coupling methods ……. 47

Scheme 1.21. Molybdenum-catalyzed benzylation of benzyl alcohols ……..…. 48

Scheme 1.22. Early examples of the use of allyl alcohols as coupling partners with organoboron nucleophiles ……...….. 49

Scheme 1.23. Nickel-catalyzed cross-coupling methods ……..……..….. 50

Scheme 1.24. Engaging allyl alcohols with organoboron nucleophiles through a tandem isomerization/arylation mechanism ……. 51

Scheme 1.25. Enantioselective and enantiospecific cross-coupling of allyl alcohols with organoboron nucleophiles ……..… 52

Scheme 1.26. Asymmetric coupling of allylic alcohols with organoboron nucleophiles using phosphoramidite ligands ……... 53

Scheme 1.27. Palladium-catalyzed reactions of propargyl alcohols with organoboron nucleophiles ……..……..54

Scheme 1.28. Palladium/Brønsted acid and rhodium-catalyzed transformations of propargyl alcohols with organoboron nucleophiles …….……. 56

Scheme 1.29. Nickel-catalyzed coupling of benzyl and allyl alcohol with Grignard reagents …. 58

Scheme 1.30. Nickel-catalyzed coupling of allyl alcohols with organozinc reagents ……..… 59

Scheme 1.31. Iridium-catalyzed allyl alcohol cross-coupling with allylsilane reagents …...…... 60

Scheme 1.32. Cobalt-catalyzed cross-electrophile coupling of alcohols ……. 61

Scheme 1.33. Nickel- and titanium-catalyzed cross-electrophile coupling of unprotected alcohols via homolytic C–O cleavage …… 62

Scheme 1.34. Palladium-catalyzed cross-electrophile coupling of alcohols with α-bromo ketones ……... 63

Scheme 1.35. Nickel-catalyzed cross-electrophile coupling of alcohols with aryl (pseudo)halides ……... 64

Scheme 1.36. Diverse reactivity of allyl alcohols in cross-electrophile coupling ……... 65

Scheme 1.37. Nickel-catalyzed cross-electrophile coupling with alkyl tosylates, phosphonium salts and aryl chlorides …….……. 66

Scheme 1.38. Ruthenium-catalyzed methods for the coupling of alcohols with alkenes or phenols ……... 68

Scheme 1.39. In situ halogenation as a strategy towards the functionalization of non-π activated alcohols . ……..……. 70

Scheme 1.40. Deoxygenative radical generation as a strategy towards the activation of non-π activated alcohols …….…… 72

Scheme 1.41. Lewis acid catalysis as a technique towards the functionalization of non-π activated alcohols ……. 74

Scheme 1.42. Classical methods for the reductive deoxygenation of oxo-functional groups …. 76

Scheme 1.43. Merging traditional Wolff-Kishner chemistry with transition metal catalysis ….. 78

Scheme 1.44. Hydrosilanes as hydride sources in transition metal-catalyzed reductions of carbonyls …….. 79

Scheme 1.45. Early disclosures in the transition metal-catalyzed reduction of ethers …… 80

Scheme 1.46. Selected early developments in the transition metal-catalyzed deoxygenative reduction of alcohols using silanes as hydride sources …… 81

Scheme 1.47. Selected examples of recent methods used for the deoxygenations of alcohols ..... 83

Scheme 2.1. Nickel-catalyzed reductions mediated by organosilane reducing agents …… 128

Scheme 2.2. Scope of substrates tolerated in the methyl ester reduction …… 138

Scheme 2.3. Controlling selectivity between esters and ethers …… 142

Scheme 2.4. Applications of exhaustive reduction of esters …….. 143

Scheme 2.5. Time-course diagrams for the reduction of methyl-2-napthoate (**2.94**) and napthalene-2-methanol (**2.95**) ……..…. 147

Scheme 2.6. Apparent rate law determination by variable time normalization kinetic analysis …… 148

Scheme 2.7. Initial reaction progress in the presence of TMDSO or $d_2$-TMDSO ……. 154

Scheme 2.8. Competition experiments to determine deuterium incorporation ……..… 155

Scheme 2.9. Attempts to exploit esters as ‘masked’ methyl groups ……..…. 158

Scheme 2.10. Attempted extension to carboxylic acid reduction …….. 158

Scheme 2.11. Reduction of esters into aldehydes ……..…. 159

Scheme 2.12. Nickel-catalyzed reduction of esters into aldehydes ……...…… 160

Scheme 2.13. Time-course diagram for the deoxygenation of model substrate **2.109** …….. 166

Scheme 2.14. Substrate scope for alcohol deoxygenation ……..… 168

Scheme 2.15. Substrate scope for ketone & aldehyde deoxygenation ……..…… 170

Scheme 2.16. Substrate scope for ether and epoxide deoxygenation ……..…….…. 172

Scheme 2.17. Substrate scope for multi-site deoxygenation ……..…… 173

Scheme 2.18. Unsuccessful reduction of silyl ethers. ….……...…… 174

Scheme 2.19. Catalytic deuteration of ketones and alcohols ……...…. 175

Scheme 2.20. Deprotection of benzyl-protected alcohols ……...……. 176

Scheme 2.21. Biomass-derived molecule degradation ……..…….. 177

Scheme 2.22. Kinetic isotope effect study and plausible reactive intermediates ……..…….. 178

Scheme 2.23. Evidence against an olefin intermediate ……..……. 179

Scheme 2.24. Evidence against a carbocation intermediate ……..…….. 180

Scheme 2.25. Evidence against an exclusively free-radical pathway ……..…. 181

Scheme 2.26. Evidence against a non-radical nickel(0)/nickel(II) mechanistic pathway …..… 183

Scheme 2.27. Hammett study of *para*-substituted alcohols . ……..... 185

Scheme 2.28. Radical scavenging experiments ……..... 186

Scheme 2.29. Investigating the nature of the C–O bond reduction through Hg-poisoning experiments ……... 186

Scheme 2.30. Extensions of the exhaustive reduction of esters ……. 193

Scheme 2.31. Selected extensions of the reductive deoxygenation of alcohols ……..... 194

Scheme 2.32. TMDSO/KO$^t$Bu as a platform for the reductive cleavage of C($sp^2$)–$CF_3$ bonds in trifluoromethylpyridines …… 195

Scheme 2.33. Nickel-catalyzed desulfonylative olefination of *β*-hydroxysulfones …….. 196

Scheme 3.1. Synthesis of **L1** ……..…. 231

Scheme 3.2. Dependence of product yield on $Bi(OTf)_3$ catalyst loading …….. 233

Scheme 3.3. Comparing the rate of arylation for free alcohol **3.1** vs. TBS-protected alcohol **3.7** ……. 237

Scheme 3.4. Investigating the observed byproduct ……... 239

Scheme 3.5. Reaction scope of arylation reaction ……. 241

Scheme 3.6. Unsuccessful alcohol and boronate ester coupling partners ……. 243

Scheme 3.7. Bismuth-catalyzed chlorination of alcohols ……..…. 244

Scheme 3.8. Summarizing evidence against olefin and radical intermediates ……..… 245

Scheme 3.9. Investigating the effects of *p*-substitution on reactivity …… 246

Scheme 3.10. Evidence supporting a 1,2-alkyl shift ……..… 247

Scheme 3.11. Evidence supporting a 1,2-hydride shift …….. 247

Scheme 3.12. Erosion of stereochemical information in alcohol **3.105** occurs in both the standard reaction conditions and with Friedel–Crafts conditions. ……..……... 248

Scheme 3.13. Arylation of a benzylic (**3.98b**) and non-benzylic (**3.106**) silyl ether ……. 249

Scheme 3.14. No arylation in the absence of nickel catalyst ……..... 250

Scheme 3.15. Eyring plot for the arylation of compound **3.106** ……..... 260

Scheme 3.16. Eyring plot for the arylation of compound **3.98b** ……..... 260

Scheme 3.17. Attempts to isolate a nickel-**L1** complex ……...….. 264

Scheme 3.18. Other productive results from the high-throughput campaign ……..... 265

Scheme 3.19. Attempted arylation of chiral alcohols ..... 266

Scheme 3.20. Attempted trapping of carbocation intermediate ..... 266

Scheme 3.21. Extensions of this project within the Newman Lab ..... 268

Scheme 3.22. Key mechanistic steps of MacMillan's deoxygenative arylation ..... 269

Scheme 3.23. Further investigations into this deoxygenative arylation: Selected unanswered questions ..... 271

Scheme 4.1. Silicon as a synthetically and industrially useful heteroatom ..... 290

Scheme 4.2. Optimizing Lewis acid, precatalyst and silane in this arylation ..... 292

Scheme 4.3. Optimizing ligands in this arylation ..... 294

Scheme 4.4. Systematic investigation into the effect of NHC structures on reactivity ..... 298

Scheme 4.5. Synthesis of $\beta$-hydroxysilanes ..... 299

Scheme 4.6. Substrate scope ..... 301

Scheme 4.7. Derivatization of product compounds ..... 302

Scheme 4.8. Preparation and solid state structure of nickel(II)-peroxo complex ..... 305

Scheme 4.9. Preparation and solid state structure of nickel(I)-bromide complex ..... 306

Scheme 4.10. Preparation and solid state structure of nickel(0)-stilbene complex ..... 307

Scheme 4.11. Preparation and solid state structure of nickel(0)-cod complexes ..... 307

Scheme 4.12. Effect of bite angle on reactivity for a series of phosphine ligands ..... 308

Scheme 4.13. Reactivity of different nickel species ..... 309

Scheme 4.14. Kinetic data was obtained for the arylation of compound **4.64** ..... 310

Scheme 4.15. Eyring analysis for the arylation of compound **4.64** ..... 315

Scheme 4.16. Results of the kinetic isotope effect experiments ..... 316

Scheme 4.17. Comparing the mass balance of the reaction in the presence of three different ligands: **L2**, **L7** and dppp ..... 317

Scheme 4.18. Experiments refuting the existence of radical intermediates ..... 320

Scheme 4.19. Investigating the effects of substrate stereochemistry on reactivity ..... 321

Scheme 4.20. Comparing **L1** vs **L2** ..... 324

Scheme 4.21. Brook rearrangement ..... 325

Scheme 4.22. Attempts at stereoretentive arylation ..... 325

Scheme 4.23. Extending this transformation towards other cross-couplings ..... 328

Scheme 5.1. Initial hit: Coupling of 1-adamantanol and a benzylboronate ester ……...… 383
Scheme 5.2. Reproducing the hits from the high-throughput plate ……... 383
Scheme 5.3. Investigating the allylation of non-π-activated tertiary alcohols ……..…... 386
Scheme 5.4. Investigating the alkynylation of tertiary alcohols ……. 387
Scheme 5.5. Investigating the reaction of indole and carbazole with tertiary alcohols ……. 390
Scheme 5.6. Preliminary substrate scope …….. 394
Scheme 5.7. Evidence against a radical intermediate ……... 395
Scheme 5.8. Preliminary mechanistic investigation …… 396
Scheme 6.1. Procedures used to synthesize the optimal ligands in each chapter ……..… 425
Scheme 6.2. Illustrating select strengths of this dissertation …… 427
Scheme 6.3. Illustrating selected weaknesses within this dissertation ……..…… 429
Scheme 6.4. Installing –$CD_3$ groups ……..…. 431

# List of Tables

Table 2.1. Optimization of ester reduction reaction ……. 130

Table 2.2. Examining alternative bases in this reductive deoxygenation ……..…... 131

Table 2.3. Examining alternative organosilanes in this reductive deoxygenation ……..… 132

Table 2.4. Examining alternative metal sources in this reductive deoxygenation ……..… 133-134

Table 2.5. Examining alternative ligands in this reductive deoxygenation ……...…. 134-135

Table 2.6. Control experiments for this reductive deoxygenation ……..…. 135-136

Table 2.7. Reduction of proposed intermediates ……. 145

Table 2.8. Optimization of the ketone reduction reaction …… 164-165

Table 3.1. Reaction Optimization …….. 227

Table 3.2. Ligand Optimization ……..…..… 228-229

Table 3.3. Control experiments investigating the role of $Bi(OTf)_3$ in this arylation protocol ... 232

Table 3.4. Varying silane additive and pre-stirring conditions …… 234

Table 3.5. Investigating the reaction of free alcohol to form a chlorosilylether intermediate .... 235

Table 3.6. Control experiments pertaining to the arylation step …… 236

Table 3.7. Effect of drop-in additives on the arylation reaction …… 238

Table 4.1. Phosphine, pyridyl and other ligands tested in this arylation ……...…. 295-296

Table 4.2. Testing variables, including drop in additives, in this arylation ……..... 322

Table 5.1. Preliminary optimization for benzylation ……. 384

Table 5.2. Preliminary optimization of alkynylation reaction …… 387-388

Table 5.3. *N*-alkylation of carbazole with pyran-bearing alcohol ……..…… 391

# List of Abbreviations

| | |
|---|---|
| µm | micrometer |
| AcONa | sodium acetate |
| ACS | American Chemical Society |
| AIBN | azobisisobutyronitrile |
| Ar | aryl |
| $B_2pin_2$ | bis(pinacolato)diboron |
| BINAP | 2,2′-bis(diphenylphosphino)-1,1′-binaphthyl |
| Bn | benzyl |
| Bpy | 2,2’-bipyridine |
| $Bu_3SnH$ | tributyltin hydride |
| CCDC | Cambridge Crystallographic Data Centre |
| CCRI | Centre for Catalysis Research and Innovation |
| $CD_3$ | trideuteromethyl |
| $CDCl_3$ | deuterated chloroform |
| CEBO | 2-chloro-3-ethylbenzo[d]oxazol-3-ium salt |
| cod | 1,5-cyclooctadiene |
| Cp | cyclopentadienyl |
| Cp* | 1,2,3,4,5-pentamethylcyclopentadienyl |
| CPME | cyclopentyl methyl ether |
| Cy | cyclohexyl |
| $d_2$-TMDSO | deuterated 1,1,3,3-tetramethyldisiloxane |
| dba | dibenzylideneacetone |
| DBE | dibromoethane |
| DCE | 1,2-dichloroethane |
| DCM | dichloromethane |
| dct | dibenzocyclooctatetraene |
| dcype | 1,2-bis(dicyclohexylphosphino)ethane |

| | |
|---|---|
| DEPT | distortionless Enhancement by Polarization Transfer |
| DG | directing group |
| DIBAL-H | diisobutylaluminum hydride |
| DIC | diisopropylcarbodiimide |
| DIPEA | *N*,*N*-diisopropylethylamine (Hünig's base) |
| $D^{i}PP$ | diisopropylphenyl |
| DMA | *N*,*N*-dimethylacetamide |
| DMDC | dimethyldicarbonate |
| DMF | *N*,*N*-dimethylformamide |
| DMO | dimethyloxalate |
| dmpe | 1,2-bis(dimethylphosphino)ethane |
| DMSO | dimethylsulfoxide |
| DPEphos | bis[(2-diphenylphosphino)phenyl] ether |
| dppb | 1,3-bis(diphenylphosphino)butane |
| dppe | 1,2-bis(diphenylphosphino)ethane |
| Dppent | 1,5-bis(diphenylphosphino)pentane |
| dppf | 1,1'-bis(diphenylphosphino)ferrocene |
| dppp | 1,3-bis(diphenylphosphino)propane |
| dr | diastereomeric ratio |
| DTBMP | 2,6-di-tertbutyl-4-methylpyridine |
| dtbpy | 4,4'-ditertbutyl-2,2'-bipyridine |
| e.g. | for example |
| ee | enantiomeric excess |
| EPR | electron paramagnetic resonance spectroscopy |
| $Et_2O$ | diethyl ether |
| $Et_3SiD$ | deuterated triethylsilane |
| $Et_3SiH$ | triethylsilane |
| FTIR | Fourier-transform infrared spectroscopy |
| GC-FID | gas chromatography flame ionization detection |
| GC-MS | gas chromatography mass spectrometry |

| | |
|---|---|
| $H_2O$ | water |
| HATU | hexafluorophosphate azabenzotriazole tetramethyl uronium |
| HCl | hydrochloric acid |
| HFIP | 1,1,1,3,3,3-hexafluoroisopropanol |
| HMDS | hexamethyldisilazine |
| HSVM | high-speed vibration milling |
| HTE | high-throughput experimentation |
| Hz | Hertz |
| IAd·HCl | 1,3-bis(1-adamantyl)imidazolium chloride |
| ICy·$HBF_4$ | 1,3-dicyclohexylimidazolium tetrafluoroborate salt |
| IMes·HCl | 1,3-bis(2,4,6-trimethylphenyl)imidazolinium chloride |
| IPA | isopropyl alcohol |
| IPent·$HBF_4$ | 1,3-bis(2,6-di(3-pentyl)phenyl)imidazolium chloride |
| $^{i}$Pr | isopropyl group |
| IPr·HCl | 1,3-bis(2,6-diisopropylphenyl)imidazolium Chloride |
| ITT | iodine tris(trifluoroacetate) |
| KIE | kinetic isotope effect |
| KOAc | potassium acetate |
| LA | Lewis acid |
| LED | light-emitting diode |
| $LiAlD_4$ | lithium aluminum deuteride |
| $LiAlH_4$ | lithium aluminum hydride |
| $LiEt_3BD$ | lithium triethylborodeuteride |
| Me | methyl |
| MeCN | acetonitrile |
| MeOH | methanol |
| MTBE | methyl tert-butyl ether |
| MW | microwave |
| $NaBH_4$ | sodium aluminum hydride |
| NaO$^{t}$Bu | sodium tertbutoxide |

| | |
|---|---|
| *n*$Bu_2O$ | dibutylether |
| *n*$Bu_3N$ | tributylamine |
| NHC | *N*-heterocyclic carbene |
| NMP | *N*-methyl-2-pyrrolidone |
| NMR | nuclear magnetic resonance |
| NSAIDs | nonsteroidal anti-inflammatory drugs |
| NTf | nonafluorobutanesulfonates (nonaflate) |
| Nu | nucleophile |
| *o* | ortho substituent |
| OAc | acetate |
| OMs | mesylate |
| OPiv | pivalate |
| O$^t$Bu | *tert*-butoxide |
| OTf | triflate |
| OVAT | one-variable-at-a-time |
| *p* | para substituent |
| Pc | phthalocynine |
| $PCy_3$ | tricyclohexylphosphine |
| PEPPSI | pyridine-enhanced precatalyst preparation stabilization and initiation |
| PG | protecting group |
| Ph | phenyl group |
| PhBpin | phenylboronic acid pinacol ester |
| PhCl | chlorobenzene |
| phen | 1,10-phenanthroline |
| PhMe | toluene |
| PMHS | polymethylhydrosiloxane |
| $PPh_3$ | triphenylphosphine |
| rt | room temperature |
| *s*-BuOH | *sec*-butanol |
| SI | supporting information |

| | |
|---|---|
| SIPr·HCl | 1,3-bis-(2,6-diisopropylphenyl)imidazolinium chloride |
| stb | stilbene |
| $^{t}$AmOMe | *tert*-amyl methyl ether |
| TBAB | tetrabutylammonium bromide |
| TBAF | tetrabutyl ammonium fluoride |
| TBS | tert-butyldimethylsilyl |
| TEMPO | 2,2,6,6-tetramethylpiperidin-1-yl)oxyl |
| TESCl | triethylsilyl chloride |
| TFFH | tetramethylfluoroformamidinium hexafluorophosphate |
| TfOH | triflic acid |
| THF | tetrahydrofuran |
| TLC | thin-layer chromatography |
| TMDSO | 1,1,3,3-tetramethyldisiloxane |
| TMEDA | tetramethylethylenediamine |
| TMP | 2,2,6,6-tetramethylpiperidine |
| TMS | trimethylsilyl |
| TON | turnover number |
| Triphos | 1,1,1-tris(diphenylphosphinomethyl)ethane |
| UV | ultraviolet |
| VTNA | variable time normalization analysis |
| *β*-H | beta hydride |

# **Chapter 1**. Transition metal cross-coupling towards the goal of employing oxo-chemicals as easily accessible substrates

*"Nascentes morimur finisque ab origine pendet."*

- *Astronomica, Marcus Manilius, 30-40 AD*



*Chapter one references begin on page 86*

## 1.0. Setting the stage: Historical commentary and a prelude to the Sustainocene

A fundamental goal of synthetic chemistry is to develop methods for making (and breaking) chemical bonds. Philosophically, this goal mirrors that of humanity as we wander through the world looking to find new ways to make (*and break*) things. What do we start with? How do we make new things? How do we use what we are given to form new things? More importantly, how can we make things that we need out of the things that we have? Coming from a prohibitively low-income background, this is a question that I have learned to hold dear. And as I sit to write this dissertation, I hear it ringing between my ears louder than ever. This is the fundamental question that guides the study of organic chemistry.

*How can we make things that we need out of the things that we have?*

For centuries, humankind has been guided by this question. We *have* fire, we *have* meat… we *need* food; can we use the fire to cook the meat until it is edible? We *have* rocks, we *have* sand, we *have* gravel… can we mix these in specific proportions, alongside cement, to form concrete, from which we can build shelter? For millennia, the persistence, resilience and survival of humankind has been directed by the underlying question. *What do we have, and how can we use it to achieve our needs?*

In time, chemistry would be born out of this very question. In the earliest days of "chemistry", alchemists developed ways to access desired materials out of those that were preexisting. They found ways to purify materials, distilling desired chemicals out of abundant chemical substances. Aristotle wrote of the evaporation of seawater as a source for fresh water,[1a] work which was expanded upon using true distillation equipment by Alexander of Aphrodisias a few hundred years later.[1b] Early Greco-Egyptian alchemist Zosimos of Panapolis wrote of metallic



Chapter one references begin on page 86

transmutation, the desire to transform abundant metals (e.g. lead, copper) into those of value (e.g. gold, silver).[2] Moving further east, and a few hundred years into the future, Jābir ibn Hayyān described the derivation of inorganic salts (such as ammonium chloride) from abundant biological materials and valued elixirs from animal, vegetable and mineral substances.[3] Yet the goal remained the same; the age of alchemy centered around making desired substances out of abundant materials. One of my favourite instances of chemical lore is that of Henning Brand, who – in his seventeenth-century pursuit of the philosopher's stone – boiled his own urine, leading to the discovery of phosphorous (while simultaneously earning the chagrin of his neighbours, I'm sure).[6] As the age of alchemy bled into that of chemistry, goals became more specific – more *scientific* – in nature. Boyle studied the composition of matter, elements, and mixtures.[4] Lavoisier studied the process of combustion, becoming instrumental in the study of elements such as oxygen and hydrogen while also proving influential in the conversion of chemistry from qualitative to quantitative.[5]

Yet as the hands of time ticked on, this simple question – *how can we make things that we need out of the things that we have* – began to mold society. The pursuit of answers to this question led to innovation, which, in turn, led to modernization. Perkin's mauve was discovered serendipitously by eighteen-year old William H. Perkin over the easter holidays of 1856. He discovered this while searching for ways to synthesize medicinally important quinine, not knowing that his discovery would revolutionize the fashion industry and contribute to the development of some of the first chemical plants. Author Simon Garfield even suggested that Perkins' discovery of mauve "ultimately led to the development of explosives, perfume, photography and modern medicine".[7] Around the same time, Benjamin Silliman Jr., son of the very first professor of chemistry at Yale, developed a method for the fractional distillation of petroleum. In doing so, he



*Chapter one references begin on page 86*

demonstrated how one could take something that the earth has in abundance and transform it into fuels and plastics and all of the items that would give rise towards the petroleum industry. He even wrote that petroleum is "a raw material from which [one] can manufacture a very valuable product".[8] In time, these discoveries, and the millions of discoveries that would follow, came to shape the world as we know it. As a chemist, I know all too well that chemistry – driven by the search for making desirable compounds out of abundant ones – pumps the heart of modernity.

However, I also know that with each rising tide comes a plummeting wave. While modern society – built on the back of industrial, chemical, and technological revolution – reached new heights, the natural world suffered; as the heart of society beat, the heart of nature bled. Pollution, largely resulting from modern chemical plants and industrial waste, ran rampant and biodiversity faltered.[9] As a child, I can remember watching reports on human-driven climate change and hearing stories of islands the size of Texas in the Pacific Ocean composed solely of waste plastics.[10] Into modernity, global carbon emissions are rising, single-use plastics are all the rage, deforestation threatens natural ecosystems and the amount of plant and animal species approaching extinction continues to rise.[11] Some claim that we have entered the Anthropocene, an era in the history of the world that places humanity at its center.[12] Many even insist that we are in the midst of a human-driven mass extinction event.[13] I argue that we must rapidly pivot into the Sustainocene, an era in the history of the world where humankind focuses on living in harmony with the natural environment rather than utilizing its resources strictly to our benefit.

As we enter the Sustainocene, we observe as the angels on one shoulder of humanity attempt to bandage the wounds caused by the demons on its other. In this battle for sustainability, we observe as the angels wield perhaps their most powerful tool for healing… chemistry. Once more, we return to the question. *What do we have an abundance of, and what can we do with it?*



*Chapter one references begin on page 86*

## 1.1. Reuse permissions

Section 1.4 of this chapter has been derived with permission from the review article "Alcohols as Substrates in Transition Metal-Catalyzed Arylation, Alkylation and Related Methods" by Adam Cook and Stephen G. Newman. *Chem. Rev.* **2024**, *124*, 6078–6144. Copyright 2024 American Chemical Society. The dissertation author is the lead author of this manuscript. Aside from this section, the rest of chapter one is original and found exclusively within this dissertation.

## 1.2. Basics of chemical catalysis

### 1.2.1. Selected theory and historical notes on catalysis

Chemistry is defined as "the branch of science that deals with the identification of the substances of which matter is composed; the investigation of their properties and the ways in which they interact, combine, and change; and the use of these processes to form new substances."[14] Often referred to as "the central science," chemistry can also be broadly defined as the study of matter. This dissertation concerns organic chemistry; to many organic chemists, chemistry is the study of making and breaking chemical bonds such that some kind of desired compound is created; it is the art of molding what one has into something that they want.

To forge a chemical bond, two things must be true: (*i*) individual constituents (i.e. substrates) must combine with enough energy to overcome the activation energy barrier for a reaction, and (*ii*) they must do so with the proper orientation.[15] A great way to teach this concept is to remark that getting a chemical reaction to occur is like building a tower from plastic building



*Chapter one references begin on page 86*

blocks (Figure 1.1). To get individual building blocks to combine to build a tower, they must combine in the proper orientation and enough pressure (i.e. energy).

**Figure 1.1.** What does it take to get a chemical reaction to occur?

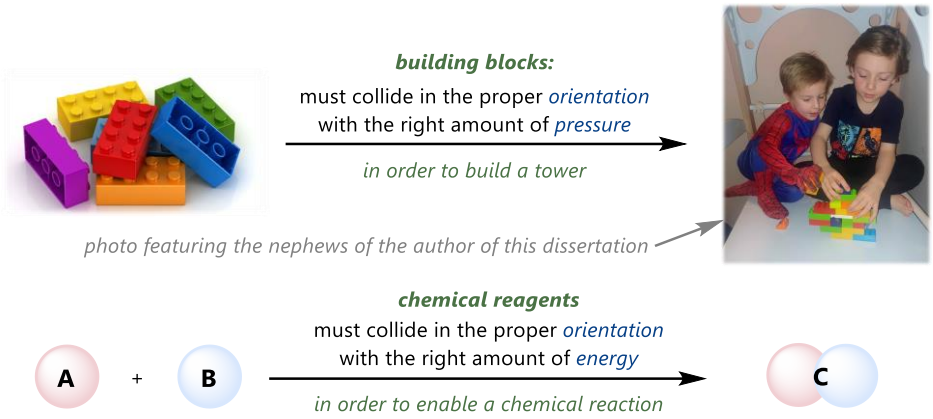


Catalysts lower the amount of energy required for a chemical transformation to take place (i.e. they reduce the activation energy barrier) (Figure 1.2). Often, they do this by providing an alternative, non-native pathway for reactivity. Catalysis itself is defined as the increase in rate of a chemical reaction due to the presence of a catalyst.[16] So then, what is a catalyst?

**Figure 1.2.** Chemical catalysis: Basics

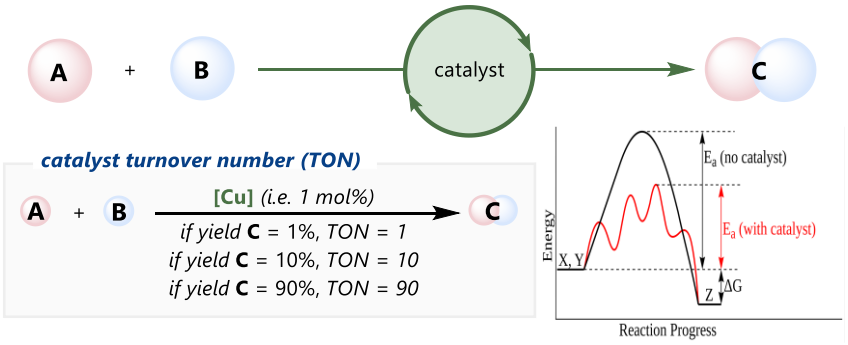


*(a) photo obtained from https://www.thoughtco.com/definition-of-catalyst-604402. Smokefoot, Wikipedia Commons.*



*Chapter one references begin on page 86*

A hallmark of catalysts is that they are often employed in substoichiometric amounts. For instance, a reaction that is 'catalytic in copper' is one that employs fewer molar equivalents of copper than there are molar equivalents of resulting product. Related is the idea of 'catalyst turnover', the number of times a catalyst can react in a given reaction. More specifically, catalyst turnover defines the number of moles of substrate that a mole of catalyst can convert into product before becoming inactivated.[17] Catalyst turnover numbers are a way to gauge the efficiency of a catalytic reaction. Catalysts can be homogeneous (entirely soluble and uniformly distributed in the reaction solution) or heterogeneous (chemical catalysts whose physical phase is different than the physical phase of the reactants and/or products that take part in a chemical reaction).[18] While many types of catalysts exist, this dissertation will primarily be concerned with homogeneous transition metal-catalyzed transformations, with a specific focus on cross-coupling chemistry.

The earliest breaths of homogeneous transition metal catalysis, with respect to cross-coupling reactions, were taken at the end of the 19$^{th}$ century. As chemists began exploring the use of sub-stoichiometric amounts of transition metals to stitch two molecular fragments together, names such as Ullmann (Scheme 1.1a),[19] Goldberg (Scheme 1.1b),[20] Job,[21] Meerwein (Scheme 1.1c),[22] and Kharasch (Scheme 1.1d)[23] began to make their marks on history.

While these efforts were substantial, they were generally plagued by limited functional group tolerance and uncontrollable selectivity, often leading to the observation of significant amounts of homocoupling product alongside cross-coupling product. In 1957, Chodkiewicz disclosed a selective copper catalyzed coupling of alkynyl halides with terminal alkynes (Scheme 1.1e).[24] Castro and Stephens extended this reactivity towards the selective coupling of cuprous acetylides, formed from terminal alkynes and copper salts, with aryl iodides in 1963.[25] With these



*Chapter one references begin on page 86*

discoveries, the idea that selective cross-coupling could be achieved between an electrophilic (i.e. organohalide) and nucleophilic (i.e. alkynyl cuprate) coupling partner was achieved.

**Scheme 1.1.** Early efforts in transition metal catalysis

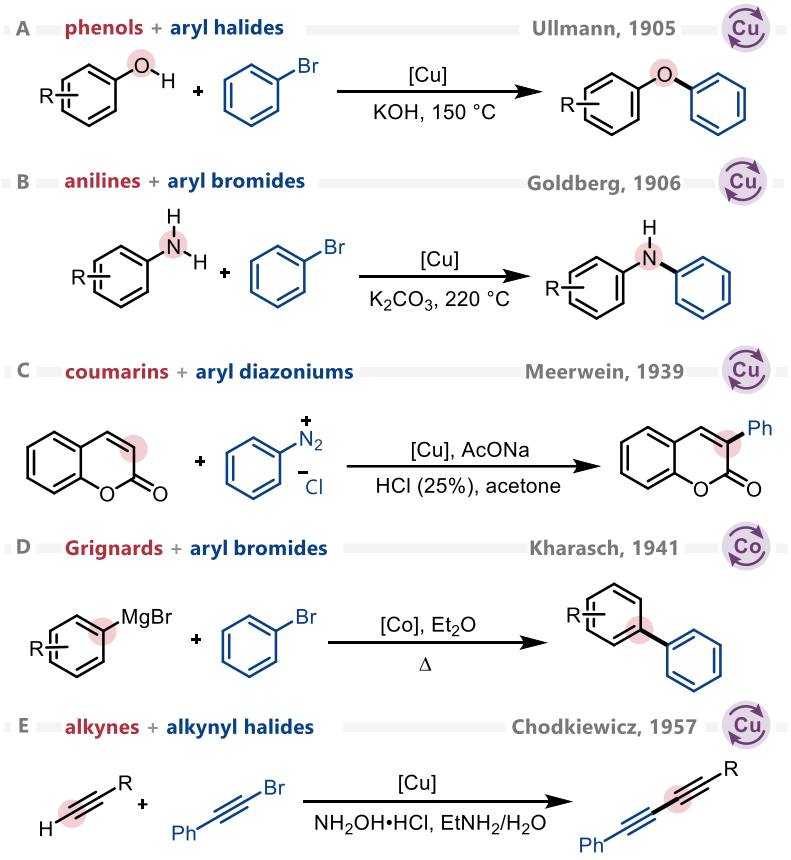


However, apart from the industrially relevant Wacker process,[26] transition metal catalyzed cross-coupling reactions remained predominantly in the shadows until pioneering discoveries by Heck in the late 1960s. Tasked with the duty of "doing something interesting with transition metals" at the Hercules Powder Company, Heck laid the foundations for a renaissance in transition metal catalysis with the publication of seven back-to-back lone-author publications in 1968… in J. Am. Chem. Soc., nonetheless![27] Within these pages, Heck documented the coupling of



Chapter one references begin on page 86

arylmercury compounds with olefins using palladium as a catalyst (Scheme 1.2a). In 1971 Mizoroki independently reported the use of less toxic aryl iodides in lieu of arylmercury compounds in a palladium-catalyzed carbon-carbon bond forming reaction (Scheme 1.2b).[28] On a personal note, the author of this dissertation thinks that this is phenomenal. Consider that Mizoroki worked on the complete opposite side of the globe from Heck at Japan's Tokyo Institute of Technology. As this was before the age of "click on this link that was sent to your email to access an online version of a scientific article published by a chemist working 6760 miles away", it is possible that Heck was not even the first person to run the reaction that now bears his name! Another very notable name in the early days of transition metal-catalyzed cross-coupling reactions is Kochi, who in the 1970s pioneered the first detailed investigations concerning the mechanism of some of the earliest processes in cross-coupling chemistry.[29a,b]

**Scheme 1.2**. Early discoveries in Mizoroki-Heck reactions

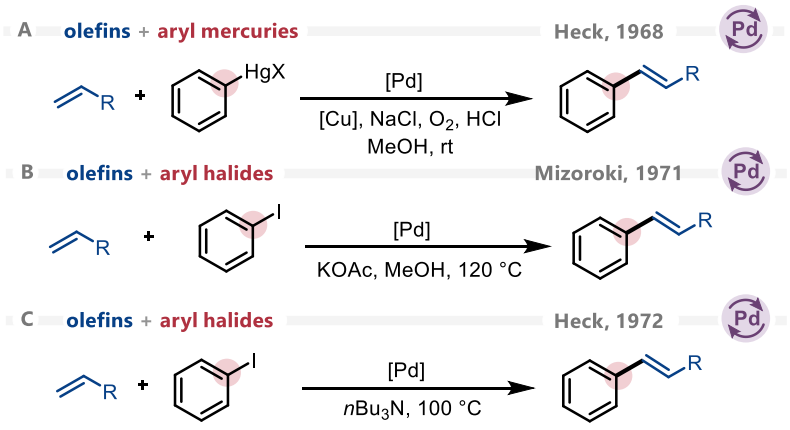


Unfortunately, Mizoroki would succumb to pancreatic cancer at a young age. Heck, however, became a professor at the University of Delaware shortly after his discoveries wherein he developed the practicality of this method (Scheme 1.2c). The discovery of the Mizoroki-Heck



Chapter one references begin on page 86

reaction paved the way for the development of other transition metal-catalyzed coupling reactions including those of aryl halides with organostannanes (Stille coupling)[30], Grignards (Kumada-Corriu coupling),[31] organozincs (Negishi coupling),[32] organosilicates (Hiyama-Denmark)[33] and alkynes (Sonogashira) (Figure 1.3a).[34] Each of these transformations played a key part in the modernization of the chemical industry, often featuring strong substrate scopes, benign conditions relative to alternative carbon-carbon bond forming processes at the time and the ability to reliably forge bonds to C($sp^2$)-hybridized coupling partners.

In time, chemists began to understand the mechanism of these transition metal-catalyzed cross-coupling reactions, which generally consist of a cycle of multiple catalytic steps. A generic catalytic cycle begins with the oxidative addition of a transition metal catalyst into the C–X bond of an organo(pseudo)halide (this species is colloquially termed the "electrophilic coupling partner"). Next, transmetallation occurs with an organometallic species (colloquially termed the "nucleophilic coupling partner") to exchange a charged X species with an organic group, thereby putting two organic groups onto a transition metal catalyst. Finally, reductive elimination from this transition metal complex forges the key bond while also regenerating active catalyst (Figure 1.3b).[35]



*Chapter one references begin on page 86*

**Figure 1.3.** Transition metal-catalyzed transformations

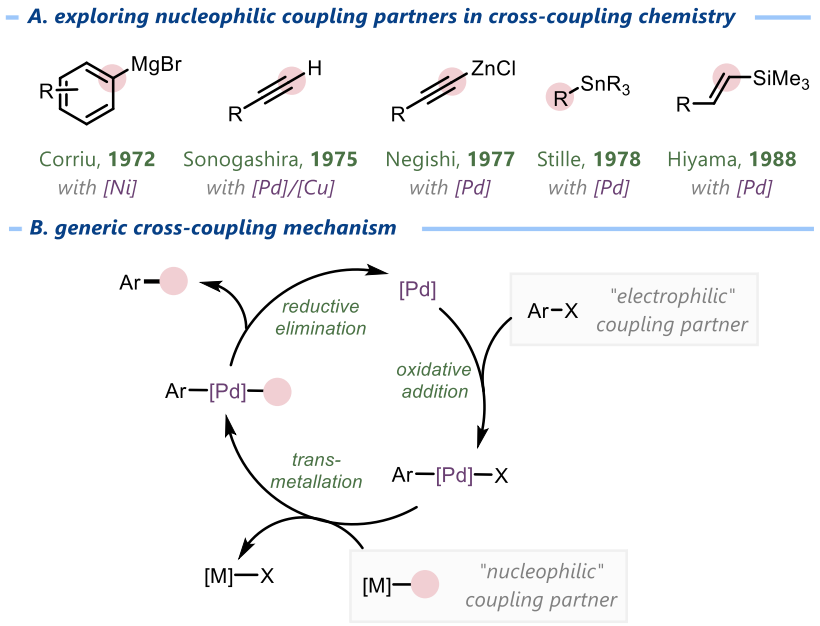


As the 1970s came to a close, however, these metal-catalyzed cross-coupling reactions still possessed limitations. The foremost of these was the requirement for such activated organometallic nucleophiles; the employment of Grignard reagents, organostannanes or organozincs as nucleophiles led to build up of oft-toxic inorganic waste products while also proving in many cases to be moisture sensitive and difficult to handle.

Shakedown, 1979. No, this is not referring to the hit single by the Smashing Pumpkins. In 1979, a new type of cross-coupling reaction was developed by Akira Suzuki and assistant professor Norio Miyaura (Scheme 1.3a).[36] Having returned to Japan after conducting a postdoc alongside boron expert H. C. Brown (winner of the 1979 Nobel Prize for… his work on organoboranes!), Suzuki was in the ideal position, alongside Miyaura, to revolutionize the study of cross-coupling



Chapter one references begin on page 86

reactions as they described the coupling of 1-alkenylboranes with 1-alkenyl and 1-alkynyl halides in the presence of a palladium catalyst. Suzuki and Miyaura expanded this reactivity to aryl halides later in the same year.[37]

Over the next 30+ years, the Suzuki-Miyaura reaction would rise to the forefront of cross-coupling reactions, being noted in a 2015 publication as the 5$^{th}$ most used transformation in industry.[38] The Suzuki-Miyaura reaction featured easy to prepare, easy to handle, stable, and lowly toxic organoboron nucleophiles. Further, Suzuki-Miyaura reactions could proceed under mild conditions with high functional group tolerance and tremendous versatility, often even under aqueous conditions.[39] Lastly, these reactions generally did not lead to the formation of toxic inorganic byproducts, as was observed with other cross-coupling reactions at the time. An important factor in the Suzuki-Miyaura reaction is the inclusion of base, as bases have been demonstrated to react in situ with the organoboron coupling partner to permit the formation of an activated "ate" complex, facilitating the transmetallation step. Apart from this difference, the general catalytic cycle of a Suzuki-Miyaura reaction resembles that of most cross-coupling reactions (Scheme 1.3b). Some notable uses of Suzuki-Miyaura reactions in modernity include its inclusion in the synthesis of losartan, ruxolitinib, and etoricoxib (Scheme 1.3c).[40] Chapters three and four of this dissertation will describe a modern approach that has been developed for the Suzuki-Miyaura reaction, wherein alcohols will be used in place of organohalides as the electrophilic coupling partner.



*Chapter one references begin on page 86*

**Scheme 1.3.** Suzuki-Miyaura reaction

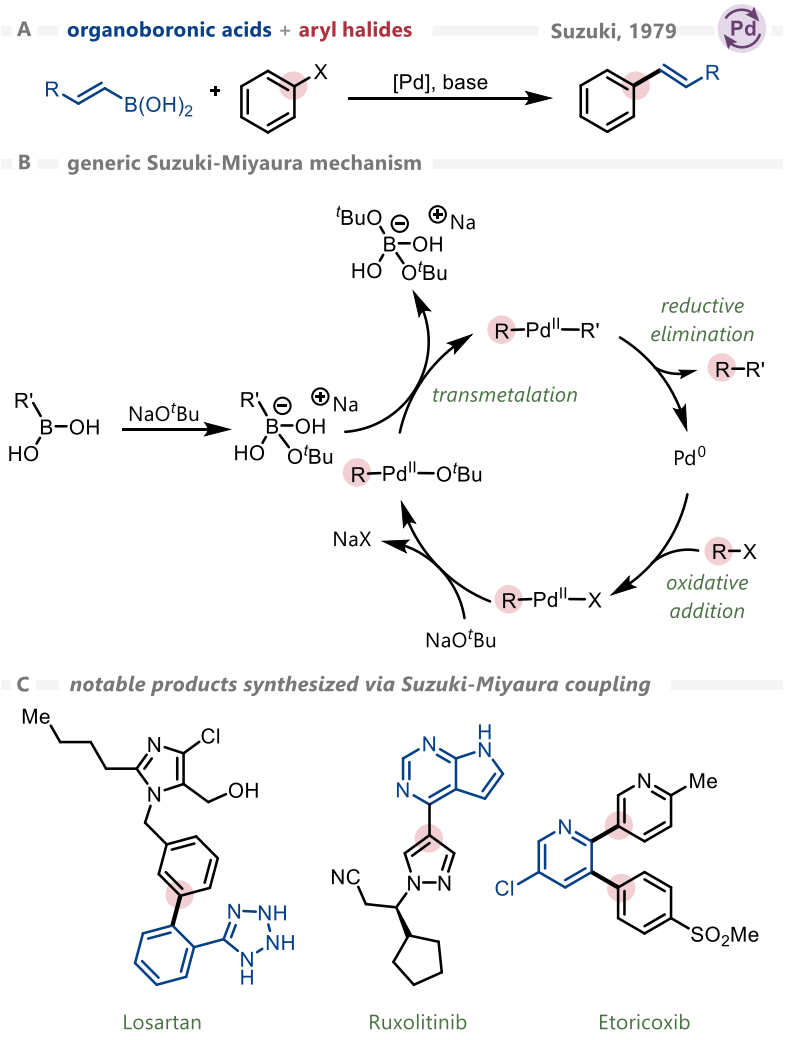


## 1.2.2. Cross-coupling reactions: Passing the torch from palladium to nickel

While exceptions exist, most early developments in cross-coupling chemistry used palladium as a catalyst. Palladium is a well understood transition metal catalyst whose electronic and steric environment can be manipulated through the inclusion of powerful ligands which lock on to it like a ball in a glove, leading towards the relatively facile isolation and characterization of



Chapter one references begin on page 86

palladium complexes.[41] Yet, a significant contemporary research focus in transition metal catalysis concerns the development of transition metal catalyzed transformations with metals *other* than palladium.

*Why?*

Firstly, palladium is expensive, costing approximately $3670 CAD/mol at the time of the submission of this dissertation.[42] Secondly, palladium is scarce. In 2023, the global supply of palladium was forecast to be around 6.2 million ounces, down from 6.4 million ounces in 2022.[43] Palladium is not just used for cross-coupling catalysis. The majority of palladium is used in the automotive industry and it also sees use in the dental, jewelry and electrical industries.[44] Eventually palladium will become a prohibitively scarce resource, posing an incredible problem of both chemical and societal importance. It is estimated that palladium catalysis is involved in the synthesis of 70% of pharmaceutical products on the contemporary market.[45] Imagine a future world where physicians have to tell patients that a medication that could save their life exists but is not available because chemists have lost the ability to synthesize it. This motivating factor prompts chemists to ask the question: what other metals can be used as cross-coupling catalysts?

One property of palladium that makes it ideal for use as a cross-coupling catalyst is its inherent ability to shift between various oxidation states.[35] Fortunately, this ability to shift between oxidation states is one which is shared amongst numerous transition metals. As the content to be presented in chapters two through five of this dissertation focuses almost exclusively on nickel catalysis, a comparison of palladium to nickel is warranted (Figure 1.4).

While ligand cost often drives the economics of a transition metal-catalyzed transformation, nickel is far more economically viable than palladium, being priced at approximately $1.21 CAD/mol at the time of the submission of this manuscript.[42] It is less



Chapter one references begin on page 86

electronegative and has a smaller atomic radius than palladium, making it more nucleophilic and easier to oxidize.[46] It can readily access the 0, +1, +2 and +3 oxidation states; the ability to access nickel(I) and nickel(III) oxidation states enables facile access to single electron chemistry. Nickel – particularly when present as a nickel(II)-alkyl intermediate – is less likely to undergo *β*-hydride elimination than palladium, which contributes to its efficiency in coupling alkyl-hybridized electrophiles in cross-coupling reactions.[47] Ultimately, nickel has been demonstrated to be better suited towards harnessing alcohols and their derivatives in cross-coupling chemistry relative to palladium.[48]

**Figure 1.4.** Comparing palladium and nickel

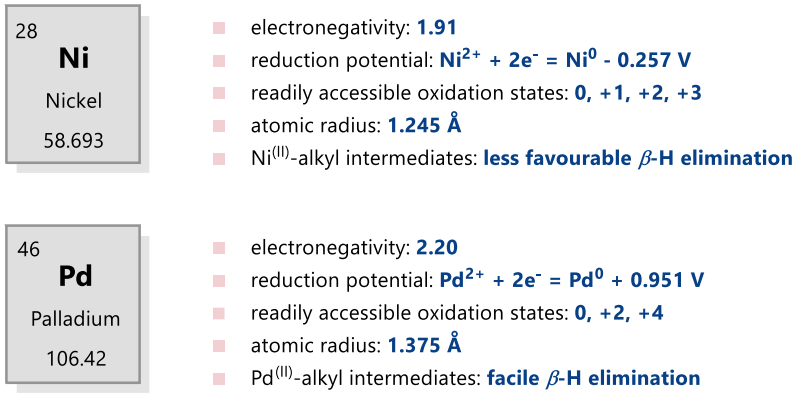


### 1.2.3. Ligands in transition metal catalysis: *N*-heterocyclic carbenes

Transition metals are often used in chemical reactions alongside large, often organic molecules called ligands. Ligands enshroud transition metals, increasing their solubility in organic solvents while allowing for precise modulation of their chemical reactivity. Most early developments in cross-coupling chemistry made use of phosphine ligands, which were ideal due to their accessibility, diversity, and inherent ability to bond tightly to transition metal centers. While the synergistic history of phosphines and transition metal catalysis is rich,[49] chapters two



Chapter one references begin on page 86

through five of this dissertation involve the use of a different type of ligand, *N*-heterocyclic carbenes.

*N*-heterocyclic carbenes (NHCs) are proficient at enabling cross-coupling reactions.[50] An early discovery in NHC synthesis was made by Arduengo in 1991, who discovered that NHCs could be complexed as a salt to enable them to be bench stable and "bottleable".[51] This breakthrough laid the foundations for the development of the wide variety of accessible NHCs that can be purchased or synthesized in modernity. In practice, NHCs are commonly employed in reactions as salts, of the form NHC·HX with the free carbene being generated in situ via deprotonation or upon heating. Most NHCs are 1,3-imidazolium salts (i.e. nitrogen-containing heterocycles with a lone pair of electrons present on the carbon in between two nitrogen atoms) (Figure 1.5). NHCs have tremendous structural versatility, as ring size, ring complexity and *N*-substitution can each be varied to the curious chemist's hearts content. NHCs have been used for a range of transition metal-catalyzed reactions, including C–C bond forming reactions, C–heteroatom bond forming reactions, olefin metathesis, cyclization reactions and addition reactions.[52] Relative to phosphines, NHCs are stronger σ-donors which aids in their facilitation of oxidative addition,[48] particularly in the nickel-catalyzed activation of strong bonds.[53] A comprehensive review of the structure and utility of NHC ligands was published by Glorius and colleagues in 2014.[54]



*Chapter one references begin on page 86*

**Figure 1.5.** Generic structures of *N*-heterocyclic carbenes (NHCs) and those that will be used within this dissertation

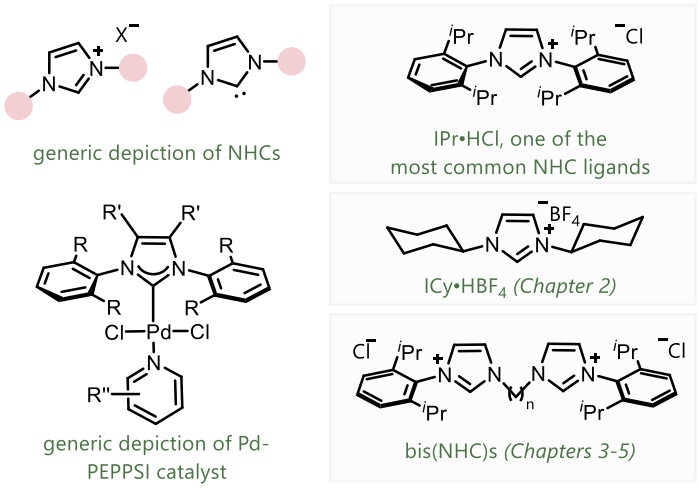


## 1.3. Cross-coupling reactions: Constructing complexity from C–O bonds

As described in Section 1.2, the mechanism of a transition metal cross-coupling reaction generally begins with the oxidative addition of a metal into a C–X bond on the electrophilic coupling partner. Conventional transition metal catalyzed cross-couplings make use of organohalides as electrophilic coupling partners. These species are frequently employed as substrates due to the relatively weak bond strength of carbon-halogen bonds (Figure 1.6).[55] While bond strengths represent the amount of energy required to cleave a bond homolytically, they are relatively representative of the ease-of-cleavage of each type of bond. As bond strengths increase, oxidative addition becomes more difficult. This is a significant factor as to why organobromides and organoiodides are often easier to implement than organochlorides and organofluorides in cross-coupling reactions.[56] Organo(pseudo)halides, such as triflates, mesylates, tosylates and



*Chapter one references begin on page 86*

related species, also possess relatively weak C–OR bonds, lending to their facile employment as electrophilic coupling partners in cross-coupling reactions.[57]

**Figure 1.6**. Bond dissociation energy (kcal/mol) of electrophilic coupling partners in cross-coupling reactions[55]

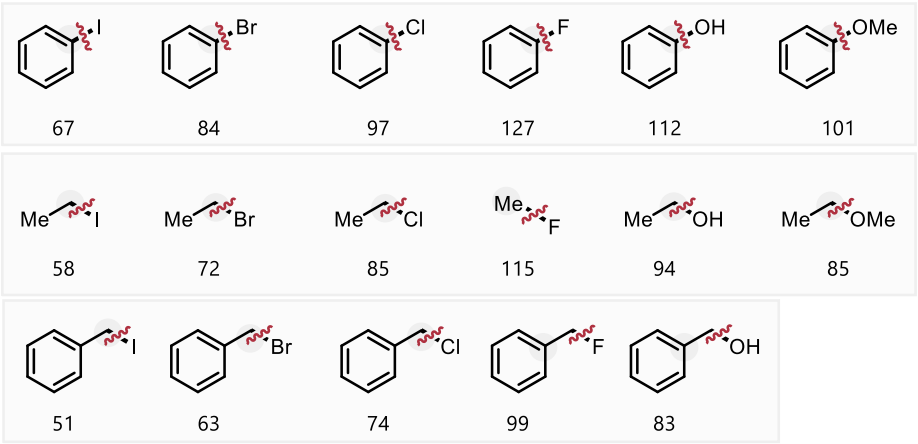


While reliable, the employment of organohalides in cross-coupling is associated with some notable limitations. Firstly, organohalides are not generally found in nature and must be synthesized inside of a laboratory. Common methods to synthesize alkyl halides include the radical halogenation of alkyl halides, allylic halogenation of alkenes or halogenation of an alcohol; methods to synthesize aryl halides include Sandmeyer reactions,[58a] Friedel-Crafts halogenations or Balz-Schiemann reactions.[58b] Secondly, the use of organohalides in cross-coupling chemistry leads to the generation of large amounts of heavy halogenated waste. As halogenated materials generally do not degrade readily in natural environments, they tend to accumulate. This problem is further exacerbated as their incineration can create large amounts of harmful byproducts, such as hydrohalogenated acids; notably, methods for microbial dehalogenation have been developed



*Chapter one references begin on page 86*

as a potential resolve to these environmental problems.[59] Finally, densely functionalized organohalides – particularly aryl iodides and aryl bromides – are of limited accessibility.[60]

As such, chemists have explored the use of alternative substrates as electrophiles in cross-coupling reactions. Previous research in the Newman group has focused on the development of methods to use esters in cross-coupling reactions, utilizing the C(acyl)–O bond as a surrogate for the C–X bond of an organohalide. Prior my arrival, researchers within the group had developed methods to employ esters in Suzuki-Miyaura-type couplings[61a,61b] (Scheme 1.4a), Heck-type reactions[61c] and amidations[61d-f] (Scheme 1.4b). Aldehydes[62a-d] (Scheme 1.4c) and alcohols (Scheme 1.4d)[63] were also explored as alternative oxygenated substrates in cross-coupling reactions.

**Scheme 1.4.** Efforts by the Newman group in the coupling of oxygenated substrates

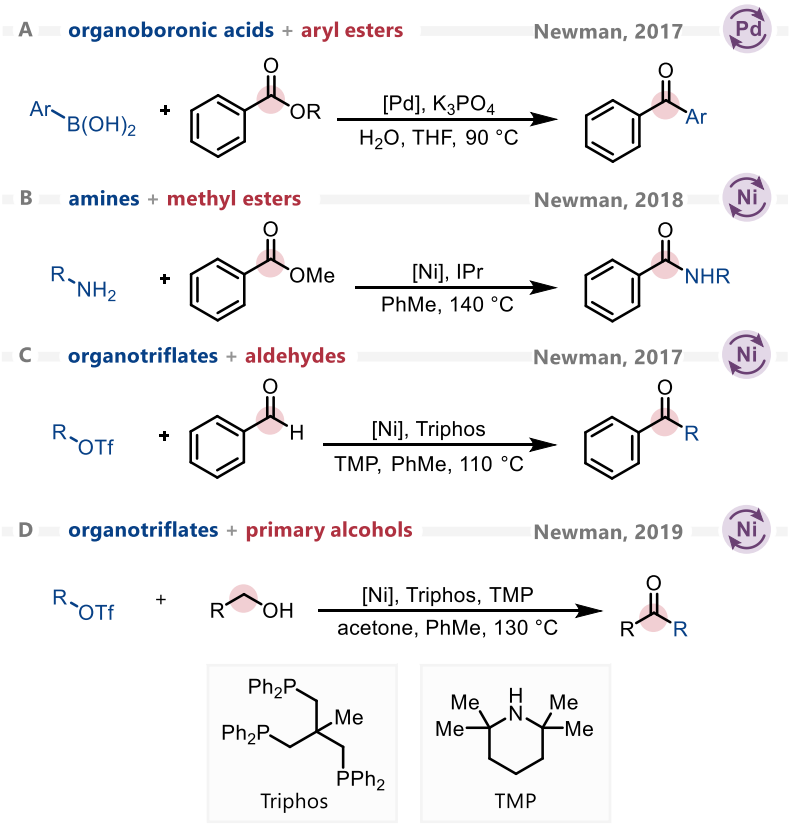




*Chapter one references begin on page 86*

Alcohols, phenols, and their derivatives exist as naturally abundant, easily accessible substrates.[64] They offer a separate substrate pool to synthetic chemists. In the case of phenols, this results in easier access to a variety of substitution patterns that are difficult to access for aryl halides. However, employing these species as electrophilic coupling partners in cross-coupling chemistry is comparatively difficult relative to organohalides. For this reason, most efforts in C–O bond activation revolve around the use of alcohol derivatives with significantly weakened C–O bonds such as those found in triflates,[65] mesylates,[66] phosphates,[67] pivalates,[68] carbamates,[69] carbonates[69] and sulfamates (Figure 1.7).[69] These species are colloquially referred to as organo(pseudo)halides.

**Figure 1.7.** Early reports of the use of various alcohol derivatives in nickel-catalyzed Suzuki-Miyaura reactions

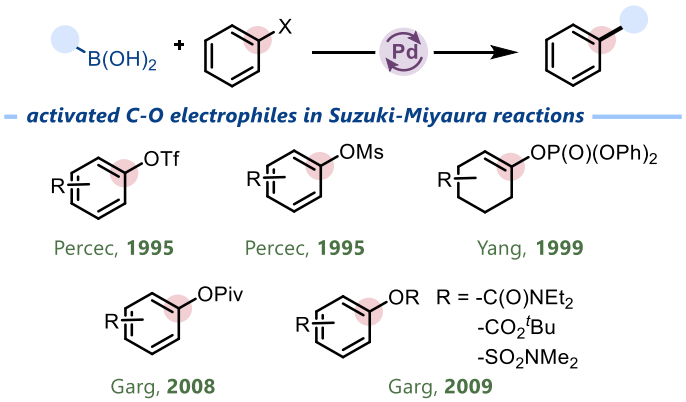


The simplest alcohol derivative is an ether and the activation of carbon–oxygen bonds in ethers serves as valuable precedent for the material that will be presented in chapters two through five of this dissertation. Ethereal carbon–oxygen bonds are abundant in biomass and natural products such as lignin, quinine, and many steroids. Finding ways to efficiently activate them would be advantageous to the chemical community.[60] An early example of catalytic C($sp^2$)–O



Chapter one references begin on page 86

bond activation was described by Wenkert who disclosed the coupling of aryl and vinyl ethers with a $Ni/PPh_3$ catalyst and Grignard reagents in 1979 (Scheme 1.5a).[70] Dankwardt expanded the scope and utility of this transformation in 2004 by using a $Ni/PCy_3$ catalyst (Scheme 1.5b).[71] Further advances, largely driven by ligand design, were disclosed independently by Shi,[72] Wang,[73] Nicasio[74] and Martin.[75] Shi extended the Kumada coupling of aryl alkyl ethers to benzyl alkyl ethers in 2008, permitting the coupling of primary and secondary benzyl alkyl ethers with Grignard reagents (Scheme 1.5c).[76] Soon after, Jarvo developed stereospecific nickel catalyzed reactions of enantioenriched benzyl alkyl ethers with various Grignard reagents.[77] In 2013, Shi and colleagues expanded these Kumada-Corriu-type reactions towards homobenzyl ethers using $FeF_2$ as a catalyst (Scheme 1.5d).[78] Beyond Kumada-Corriu reactions, Negishi,[79] Suzuki-Miyaura (Scheme 1.5e)[80] and Mizoroki-Heck[81] reactions are well known with ethers, proceeding through C–O activation.



*Chapter one references begin on page 86*

**Scheme 1.5.** Transition metal cross-coupling of simple ethers

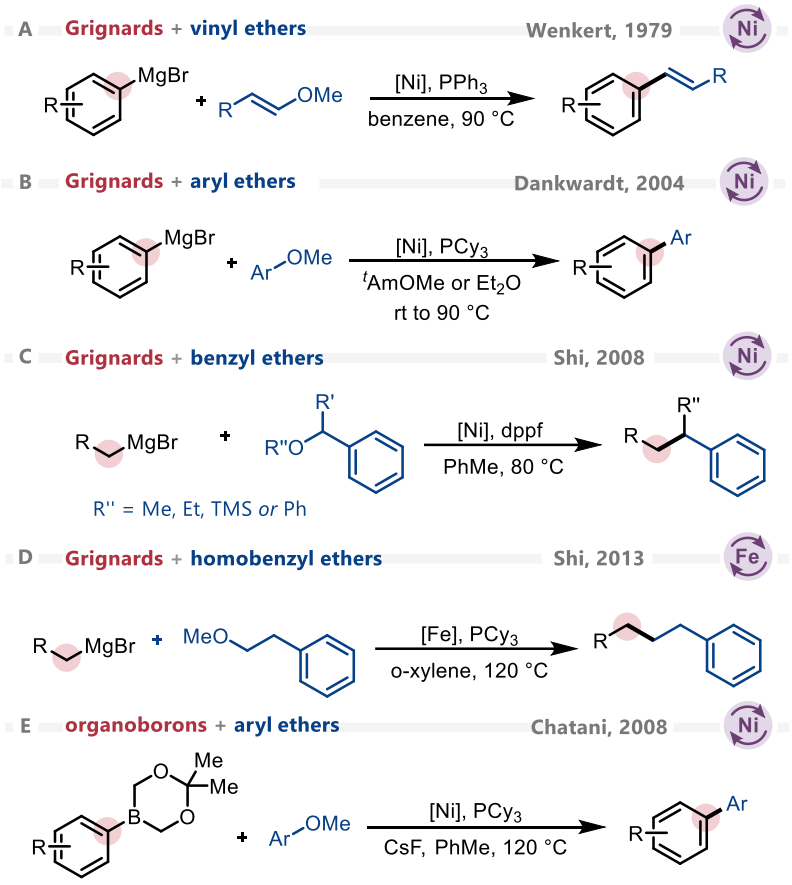


The use of silyl groups has also been explored towards the activation of carbon-oxygen bonds. Traditionally, silyl groups are considered a protecting group for hydroxyl functional groups. Montgomery and colleagues recognized that the strong nature of the silicon-oxygen bond in a silyl ether could activate the adjacent carbon-oxygen bond in a manner that enables deoxygenative functionalization, developing methods for the reduction,[82a] silylation,[82a] amination,[82b] and borylation[82c] of silyl-protected phenols (Scheme 1.6a, b). In related precedent, Kumada conducted a systematic study on the deoxygenative functionalization of silyl enol ethers with Grignard reagents in 1980 using nickel catalysts (Scheme 1.6c).[83] Other authors have also employed aryl



Chapter one references begin on page 86

and alkenyl silyl ethers in carbon-oxygen bond activating reactions.[68,84] Towards the activation of C($sp^3$)-O bonds, Grygorenko and colleagues used a desilylative approach towards the fluorination of a silyl ether in the synthesis of GABA analogues in 2020 (Scheme 1.6d).[85]

**Scheme 1.6.** Silylation as a strategy towards the activation of alcohols

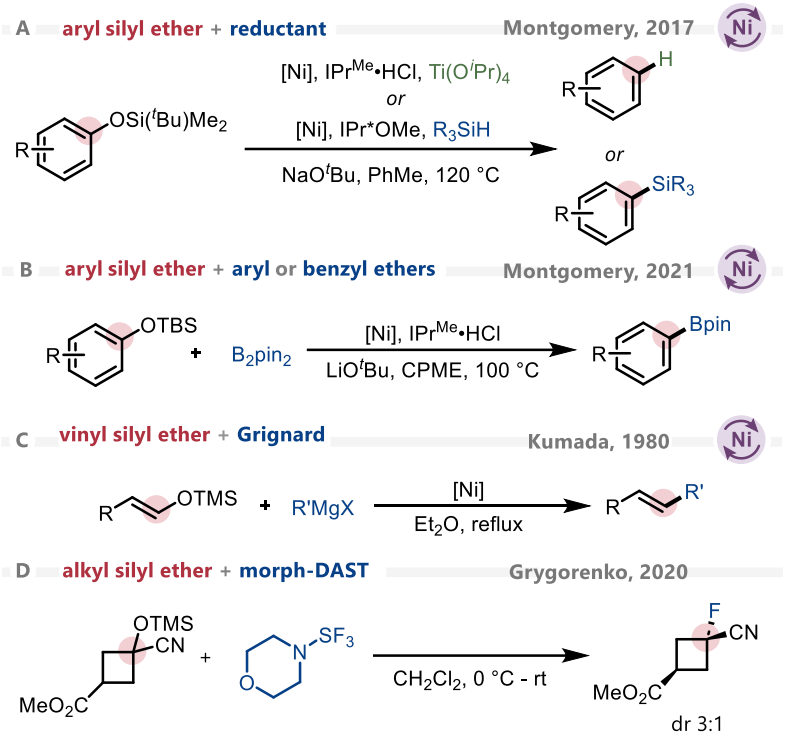


Many examples of C–O activation mentioned within this section have explored the activation of C($sp^2$)–O bonds of phenols and their derivatives. For a detailed account of the many transformations that proceed through C($sp^2$)–O bond activation of phenols and their derivatives, the reader is directed towards a 2020 review published by Li and colleagues.[86] Further, the examples presented thus far have only considered protected alcohols, ranging from highly activated sulfonates to less activated ethers. A detailed account of the coupling of C–O electrophiles was published by Percec and colleagues in 2011.[48] Less comprehensive, but more



Chapter one references begin on page 86

recent, accounts of new electrophiles in cross-coupling chemistry have been published by Campeau in 2019[87] and Garg in 2020.[53]

At this point, the readers are reminded that this is a dissertation that will detail methods that are used exclusively to activate C($sp^3$)–O bonds. Moreover, while chapter two will describe the catalytic activation of various oxo-functional groups (i.e. functional groups bearing an oxygen, such as ketones, aldehydes, esters, alcohols, etc.), the overwhelming majority of this dissertation will explore the transition metal-catalyzed activation of unprotected alcohols. Thus, the following section aims to give a comprehensive overview of transition metal-catalyzed methods to activate unprotected alcohols. It will focus primarily on methods that exploit the ability of transition metals to act as Lewis acid catalysts, or cross-coupling catalysts, to generate carbon-carbon bonds. The reader is further reminded that this section (Section 1.4) is derived with permission from the review article "Alcohols as Substrates in Transition Metal-Catalyzed Arylation, Alkylation and Related Methods" by Adam Cook and Stephen G. Newman. *Chem. Rev.* **2024**, 124, 6078–6144.

## 1.4. Alcohols as substrates in transition metal catalyzed alkylation, arylation and related reactions

In the push towards greener, more efficient chemical syntheses, alcohols present themselves as appealing and abundant building blocks. Alcohols are present in many renewable chemical sources (e.g., lignocellulosic biomass, carbohydrates) or they can be readily synthesized by a range of reliable methods.[88-91] However, alcohols are difficult to engage in cross-coupling reactions for a number of reasons. The foremost of these reasons is the high bond strength of the alcohol C–O bond, making the OH a poor leaving group. Secondly, alcohols are prone to ionization



Chapter one references begin on page 86

of their O–H bond, which commonly leads to the formation of either alkoxides which participate in catalyst inhibition of phenolic salts that enhance the energy of the C–O bond.[64] Lastly, aliphatic alcohols are prone to *β*-hydride elimination which can form undesired byproducts.

Section 1.4 is divided into two parts, differentiated by the mechanistic approach taken to cleave the C–O bond (Figure 1.8). Section 1.4.1 describes C–O bond functionalization through direct substitution, wherein the alcohol is used as a leaving group. This is primarily proposed to occur by a carbocation or carbocation-like intermediate. While $S_N1$-type functionalization of alcohols has been known for over a century, for example in Friedel–Crafts alkylation reactions, this section will primarily consider recent developments in mild, transition metal-catalyzed alternatives to render alcohols as good substrates for substitution chemistry.

**Figure 1.8.** Cleavage of aliphatic alcohols: Topics to be discussed herein

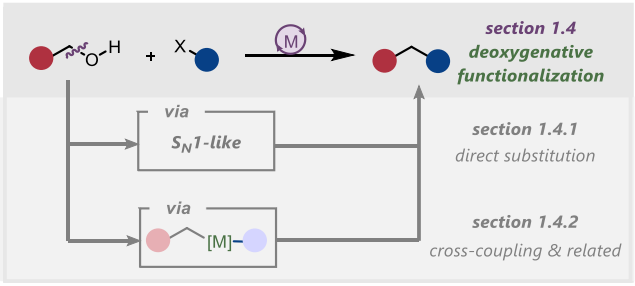


Section 1.4.2 describes C–O bond functionalization strategies that are proposed to proceed via the formation of a carbon–metal bond at some stage in the catalytic cycle. This is most frequently encountered in cross-coupling and related reactions, where the alcohol is used as a pseudohalide and cleaved via oxidative addition. Such reactions include advancements made in Suzuki-Miyaura coupling, cross-electrophile coupling, and couplings with C–H bonds.



Chapter one references begin on page 86

Within Section 1.4, several notable restrictions were made so as to not distract from the goals and theme of this dissertation. Firstly, only intermolecular, homogeneous, transition-metal catalyzed transformations of unprotected alcohols will be discussed. Secondly, only methods that forge carbon-carbon bonds will be discussed. Finally, transformations that result in fragmentation or extensive rearrangement of the alcohol scaffold will not be discussed, nor will specific reactions that are immense in scope (e.g. the Tsuji-Trost reaction).

### 1.4.1. Alcohols as alkylating agents by direct substitution through $S_N1$-type and related pathways

A suggestion from the 2005 ACS Green Chemistry Institute Pharmaceutical Roundtable identified such methods for the direct catalytic nucleophilic substitution of alcohols as a top priority.[92] The Friedel-Crafts reaction is a classic method for making C–C bonds via the reaction of arenes with carbon-based electrophiles such as alkyl or acyl halides.[93] Due to the modest nucleophilicity of arenes, a catalyst is often required to enhance the electrophilicity of the organohalide, for example by forming a carbocation in situ. Alcohols can also be utilized as electrophilic coupling partners in these reactions. While reliable, Friedel-Crafts reactions are often hampered by the necessity of harsh reaction conditions, prompting chemists to explore improved strategies for Friedel-Crafts and related chemistry, generally focusing on the development of mild, catalytic alternatives.

Section 1.4.1 catalogs developments in catalytic functionalization of unprotected alcohols wherein the alcohol is used as a leaving group to react with a carbon-based nucleophile such as an arene or ketone/enol. Carbocation intermediates are often invoked but mechanistic studies reveal many subtleties and edge-cases. Here, these reactions have been grouped together and described



*Chapter one references begin on page 86*

as reactions occurring via $S_N1$-type pathways, elaborating on key mechanistic details if known. In general, the activation of alcohols towards deoxygenative $S_N1$-type functionalization relies predominantly on the Lewis basicity of alcohols alongside carefully chosen Lewis acidic metal catalysts. As Cozzi and coworkers published a comprehensive review of these transformations in 2010,[94] a focus will be primarily placed on more recent developments, only briefly summarizing pioneering achievements.

#### 1.4.1.1. Select developments prior to 2010

Developments occurring before 2010 in the catalytic $S_N1$-type transformations of alcohols saw a range of metal catalysts used to permit them to act as alkylating reagents. A commonality between most of the methods detailed within this section include the use of (hetero)arenes, 1,3-dicarbonyl compounds, organosilanes, olefins and/or alkynes as nucleophilic reaction partners (Scheme 1.7a). Furthermore, most reactions feature π-activated (e.g. benzyl, allyl, propargyl) and/or tertiary alcohols as substrates. Generally, these transformations fit into variations of a unified mechanistic paradigm. Metals act as Lewis acid catalysts to activate C–O bonds towards cleavage, thereby resulting in the formation of a carbocation or carbocation-like intermediate. To form product, this intermediate is intercepted by the nucleophilic reaction partner. However, alternative pathways also exist. Dimerized ethereal intermediates, formed through self-reaction of a carbocation-like intermediate with alcohol substrate can be observed as a byproduct or intermediate. Other intermediates can involve the formation of alcohol or alkoxy-metal bonds rather than naked carbocations. Further, alternative transition metal-catalyzed methods of generating carbocations exist. Masked Brønsted acid catalyzed methods are known, for instance



Chapter one references begin on page 86

through the generation of triflic acid from $Bi(OTf)_3$. Highlighted reports by Ishii (Scheme 1.7b)[95,96] and Baba (Scheme 1.7c)[97,98] are both pioneering and representative.

**Scheme 1.7.** $S_N1$-type deoxygenative functionalization: General details and representative examples

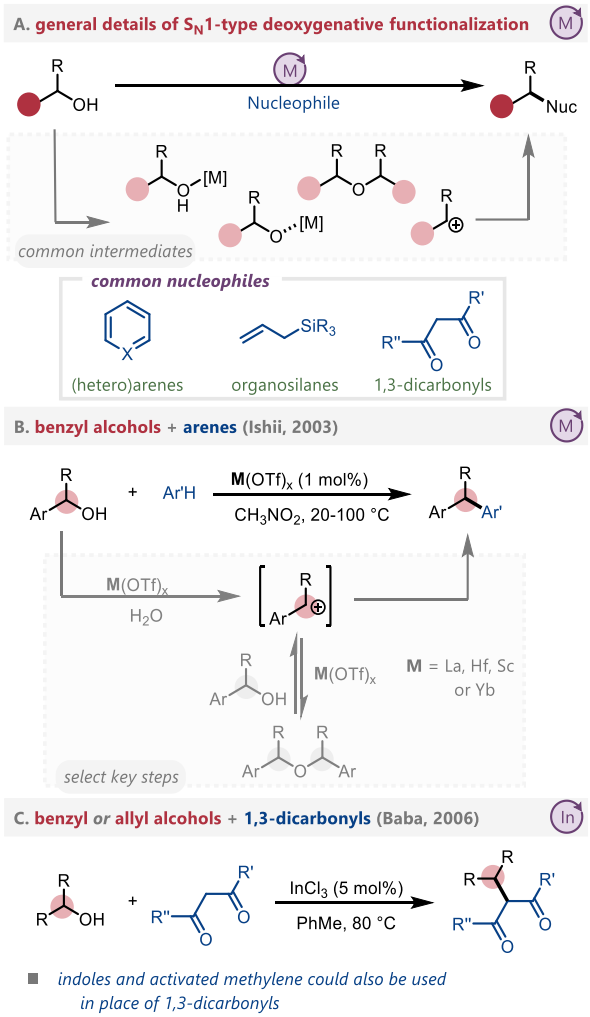


Metals featured in early reports in this field include bismuth,[99,100] cerium,[101,102] ruthenium,[103,104] niobium,[105] ytterbium,[106-108] molybdenum,[109-111] tungsten,[112] scandium,[113-115] aluminum,[116] and gold.[117] Indium catalysis has proven particularly common in these



Chapter one references begin on page 86

deoxygenative functionalization reactions,[118-123] as has iron catalysis, particularly utilizing $FeCl_3$ and its hydrated analogs.[124-133]

### 1.4.1.2. Developments after 2010

Recent advancements in this area have seen chemists further explore the range of metals that can be employed as catalysts, largely focusing on innovative uses and features of these transformations, including multicomponent reactions, stereochemical control, tandem reactions, and heterocycle synthesis. Works in the direct deoxygenative substitution of alcohols through carbocation intermediates published since 2010 are catalogued within this section, grouped according to the metal catalyst. Recent years have seen an increase in alternative strategies such as Brønsted-acid catalysis, ionic liquid catalysis, heterogeneous catalysis and organocatalysis. While these fall outside of the scope of this manuscript, a series of reviews have been published broadly detailing the developments in substitution reactions with alcohol electrophiles.[134-138]

#### Iridium/tin catalysis

Originating from earlier disclosures,[139-141] bimetallic iridium/tin catalysts were explored by Roy and coworkers in the deoxygenative functionalization of benzyl, allyl and propargyl alcohols with nucleophiles including 1,3-dicarbonyls, (hetero)arenes and organosilanes (Scheme 1.8).[142-144] The authors proposed a mechanism that involves Lewis acid/base interactions between tin and the alcohol oxygen atom alongside concurrent coordination between iridium and an adjacent π-electron system on the alcohol. Hammett analyses were performed that confirmed the build up of positive charge at the time of the transition state of this transformation. In 2012, Roy and



Chapter one references begin on page 86

colleagues disclosed a related palladium/tin bimetallic catalyst for similar deoxygenative functionalization of π-activated alcohols.[145]

**Scheme 1.8.** Iridium/tin bimetallic catalysis for $S_N1$-type deoxygenative functionalization

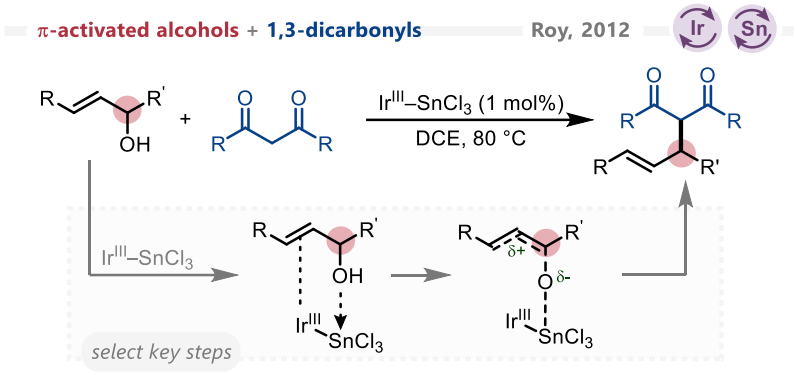


## Tin catalysis

Dunach and colleagues demonstrated the $S_N1$-type deoxygenative functionalization of hemiaminals with carbon nucleophiles including arenes, 1,3-dicarbonyls, simple carbonyls, and organosilanes in 2010 (Scheme 1.9a).[146] This transformation was proposed to proceed through tin-catalyzed generation of an *N*-acyliminium ion, allowing for the successful functionalization of an alcohol that does not contain an adjacent π-electron system. While hemiaminals are a form of activated alcohol, this work serves as precedent for later developments in $S_N1$-type alcohol activation.

The diastereoconvergent nucleophilic substitution of diastereomeric mixtures of diarylmethanols was achieved by Nakata in 2019 (Scheme 1.9b),[147] with the authors observing that a chiral auxiliary on the arene could enable highly stereoselective substitution. They proposed that the tin catalyst plays a dual role, activating both the alcohol and the 1,3-dicarbonyl. Ethers – likely resulting from the self reaction of activated alcohol substrates – were observed as



Chapter one references begin on page 86

byproducts. Tin catalysts were also exploited by Liu in the deoxygenative functionalization of xanthenols using a distannoxane catalyst,[148] Masuyama in the functionalization of propargyl alcohols[149] and Nakata in the functionalization of diarylmethanols (Scheme 1.9c).[150]

**Scheme 1.9.** Selected tin-catalyzed methods

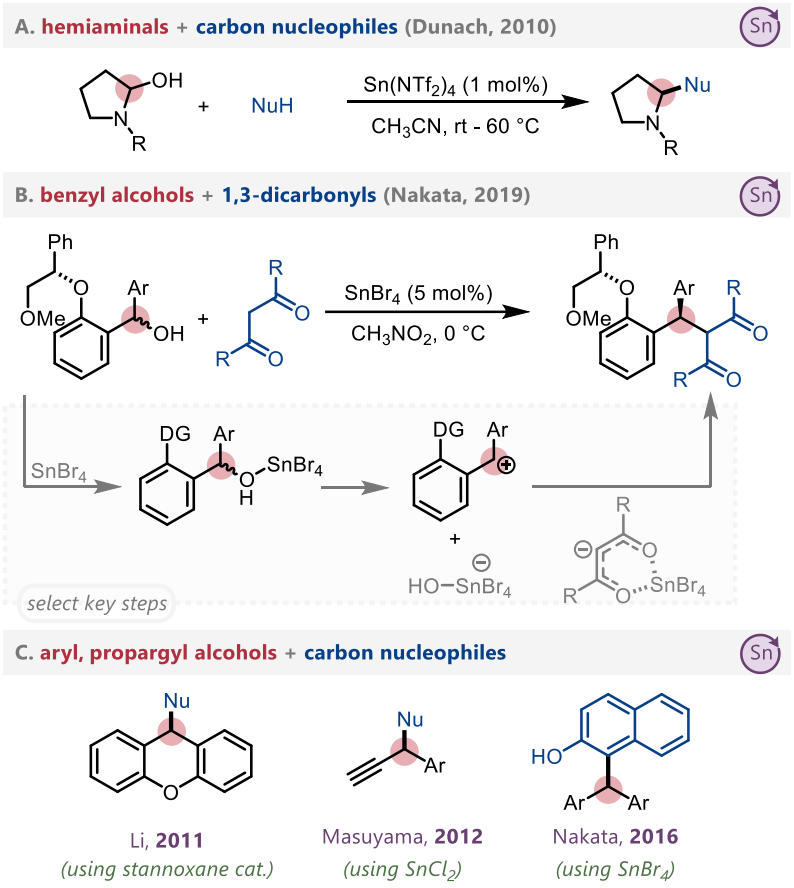


## Copper catalysis

Copper catalysis was employed in the direct substitution of benzyl alcohols with ketene dithioacetals towards the synthesis of polyfunctionalized O-heterocycles in 2010 by Liu (Scheme 1.10a).[151] The authors noted that *4H*-chromenes were formed when using dichloromethane as a solvent; however, dihydrocoumarins were obtained in acetonitrile. Mechanistic support was



Chapter one references begin on page 86

provided to suggest copper plays a dual-catalytic role, both activating the ketene dithioacetal as well as the benzyl alcohol. A notable example of enantioselective synthesis was demonstrated by Nishibayashi and colleagues as $Cu(OTf)_2$ was used alongside a chiral ligand in the alkylation of β-keto phosphonates with diarylmethanols (Scheme 1.10b).[152] Products were obtained in up to 92% ee, providing a rare example of asymmetric synthesis proceeding via a proposed carbocation intermediate. Other examples of copper catalysis in $S_N1$-type deoxygenative functionalization also exist, including the propargylation of indole scaffolds in 2012 by Wang,[153] the vinylation of propargyl alcohols to generate enynes by Zhang in 2013[154] and the addition of diketones on to allyl alcohols by Baeza in 2017,[155] among others (Scheme 1.10c).[156,157]

**Scheme 1.10.** Selected copper-catalyzed methods

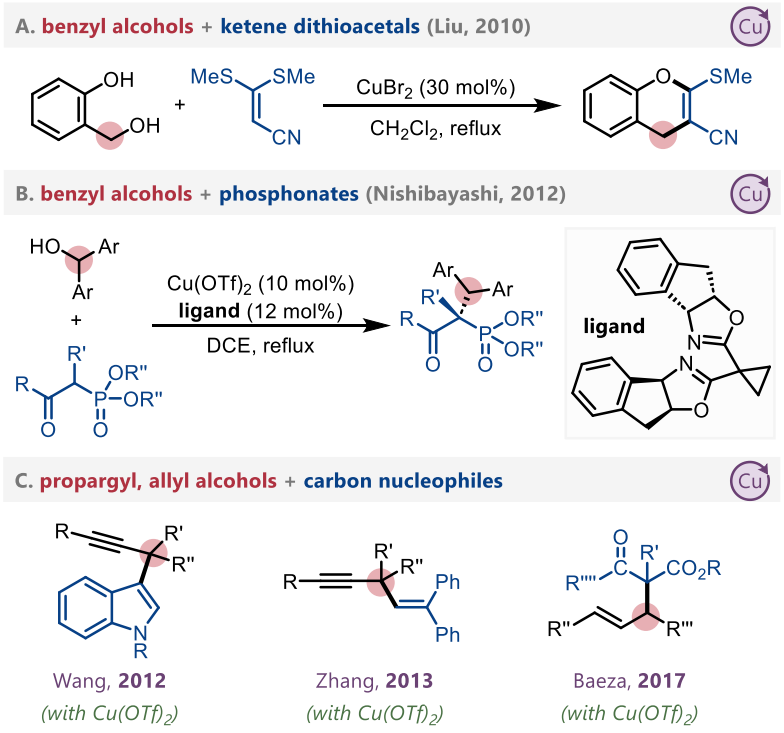




Chapter one references begin on page 86

## Silver and/or gold catalysis

Silver and gold have also been demonstrated to be effective catalysts for deoxygenative functionalization reactions. In 2012, Li and colleagues utilized gold/silver dual catalysis towards the synthesis of functionalized allenes through the substitution of propargyl alcohols with arenes (Scheme 1.11a).[158] Di-, tri- and tetrasubstituted allenes could be obtained, with the authors proposing the reaction proceeds through a carbocation intermediate due to observed loss of stereochemistry when performing the reaction with an enantiopure propargyl alcohol starting material. Another interesting demonstration of gold and silver catalyzed deoxygenative substitution reactions was disclosed by Bandini and colleagues in 2015, wherein the α-allyl enones were prepared from alcohols and allenamides (Scheme 1.11b).[159] In this work, allenamides were used as precursors to α-gold-substituted carbonyl compounds, with DFT results supporting the key role of this species as an active nucleophile. Silver and gold catalysts were further used in the deoxygenative functionalization of alcohols by Balamurugan,[160] Quillian,[161] Sheppard[162] and Azumaya;[163,164] Campagne has also explored gold-catalyzed substitutions of alcohols, providing an account of their research into the coupling of propargyl, allyl and benzyl alcohols with various nucleophiles in 2011 (Scheme 1.11c).[165]



Chapter one references begin on page 86

**Scheme 1.11.** Selected silver- and gold-catalyzed methods

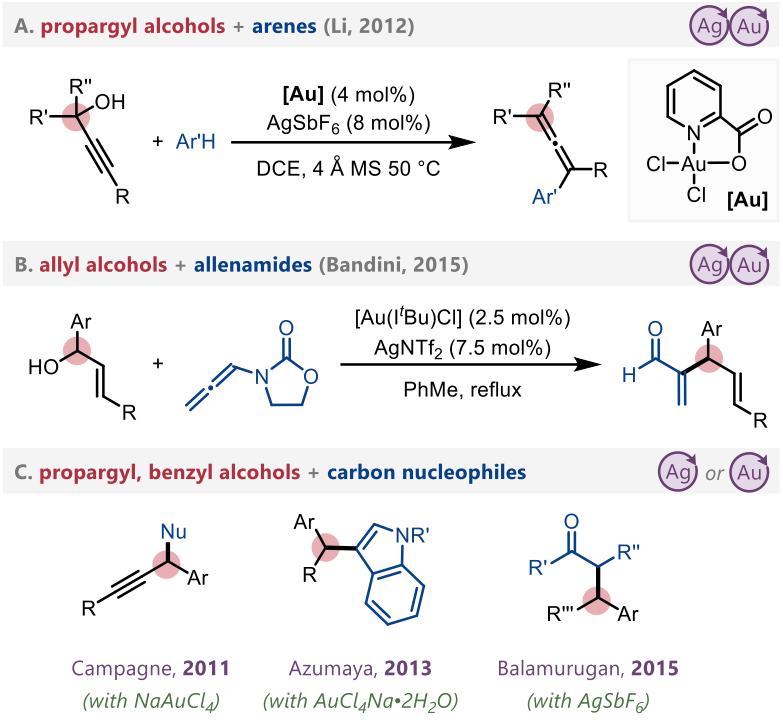


## Rhenium catalysis

Notable for its low catalyst loading and mechanistic discussion, Floreancig and coworkers disclosed in 2018 a rhenium-catalyzed Friedel-Crafts type reaction of benzyl alcohols with arenes to generate diarylmethanes (Scheme 1.12a).[166] The authors employed HFIP as a solvent and proposed the transient existence of perrhenate ester intermediates, from which C–O bond cleavage occurs to yield a benzyl carbocation. Other rhenium-catalyzed methods have been developed by Ghorai[167] and Nishiyama[168,169] for the activation of alcohols through $S_N1$-type pathways (Scheme 1.12b).



Chapter one references begin on page 86

**Scheme 1.12.** Selected rhenium-catalyzed methods

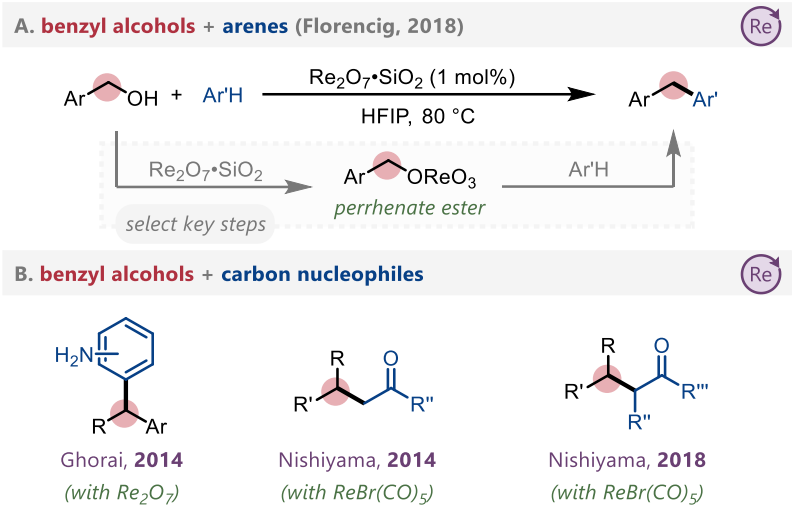


## Indium catalysis

Cozzi and colleagues demonstrated the stereoselective allylation of aldehydes with allyl alcohols using an $InBr_3$/imidazolidinone co-catalytic system in 2010 (Scheme 1.13a).[170] This merging of organocatalysis with Lewis acid catalysis allowed for the generation of products with up to 98% ee, providing an avenue for enantioselective synthesis proceeding through carbocation intermediates. This work was expanded to include the substitution of propargyl alcohols[171] and benzyl alcohols.[172] Another interesting application of indium in the deoxygenative functionalization of alcohols came from Xu and colleagues, who demonstrated in 2018 the iodoalkylation of alkynes via a multicomponent reaction of alkynes, benzyl alcohols and hydroiodic acid in the presence of an $InI_3$ catalyst (Scheme 1.13b).[173] The authors proposed the Lewis acid catalyzes generation of a carbocation intermediate that reacts with the alcohol starting material to form a key dimeric ether intermediate. Indium catalysis has also been employed by a



Chapter one references begin on page 86

number of other groups towards the deoxygenative functionalization of alcohols, including Xiao,[174] Ji,[175] and Singh (Scheme 1.13c).[176]

**Scheme 1.13.** Selected indium-catalyzed methods

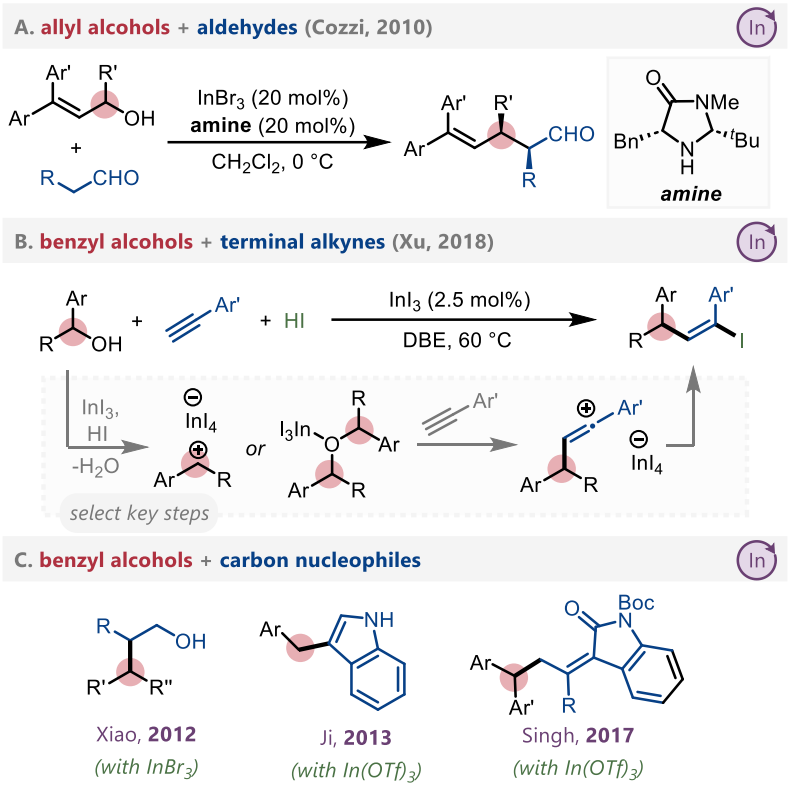


## Iron catalysis

The iron-catalyzed multicomponent synthesis of alkenyl iodides through the coupling of alcohols with alkynes in the presence of $I_2$ and NaI has been demonstrated by Ji and colleagues (Scheme 1.14a).[177] The authors used iron powder as a catalyst in 1,2-dibromoethane (DBE) as a solvent, gathering mechanistic evidence to support the existence of a dimeric ether intermediate. The iron-catalyzed decarboxylative alkylation of β-keto acids with alcohols was demonstrated by Tian and coworkers in 2012 (Scheme 1.14b).[178] Mechanistic evidence obtained through $^1$H-NMR



Chapter one references begin on page 86

experiments suggests that $S_N1$ alkylation occurs prior to decarboxylation, and benzyl, allyl and propargyl alcohols each proved capable of acting as alkylating reagents. While a range of Lewis acids could catalyze this transformation, iron catalysts consistently outperformed alternatives. Iron catalysis was also used by Gu in the substitution of benzyl alcohols with aryl methyl ketones in 2013, presenting a method for extending the scope of these transformations beyond 1,3-dicarbonyls (Scheme 1.14c).[179] Iron tribromide was used by Bi and colleagues to activate propargyl alcohols towards the synthesis of gem-bis(alkylthio)-substituted vinylallenes in 2013 (Scheme 1.14d).[180] The authors proposed that the reaction proceeds through a propargyl cation that is preferentially attacked by the electron-rich α-carbon of α-oxo ketene dithioacetal at the electrophilic alkyne carbon. Iron-catalyzed $S_N1$-type deoxygenative functionalization reactions of alcohols have been explored by others as well, being used towards the synthesis of indenes,[181] triarylmethanes,[182] stereospecific olefins,[183] cis-hexahydrobenzophenanthridines,[184] fluorenes,[185] and trifluoromethylated species,[186,187] as well as being used towards the functionalization of secondary benzylic alcohols,[188] and propargylation of diarylalkenes.[189] Functionalization of allylic alcohols using aqueous solvents was also demonstrated.[190]



*Chapter one references begin on page 86*

**Scheme 1.14.** Selected iron-catalyzed methods

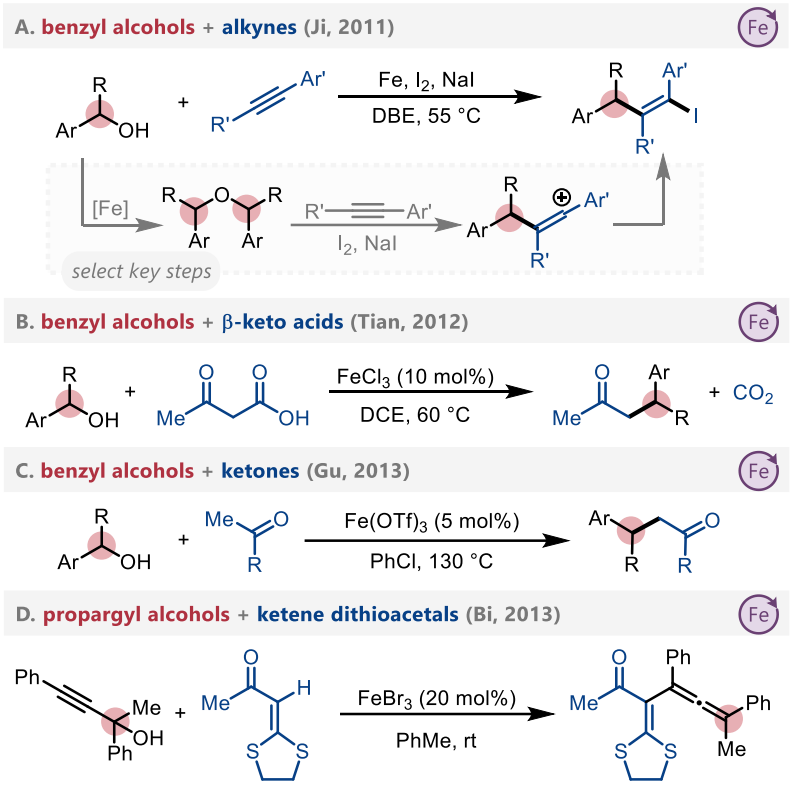


Iron catalysis was utilized by Itoh and colleagues in 2015 in the stereoretentive substitution of (hetero)benzyl alcohols with (hetero)arenes (Scheme 1.15a).[191] The authors invoke the conformational stability of *β*-silyl carbocations as a key feature that prevents loss of optical purity. Iron catalysis was also exploited in the stereoselective allylation of diarylmethanols with allylsilanes in 2018 by Nakata, wherein a chiral auxiliary on the arene was used to control diastereoselectivity in the reaction between a transient carbocation and allylsilane nucleophile.[192] The regio- and stereoselective synthesis of 1,2,3-trisubstituted indanes through the direct substitution of diarylmethanols with allylamides was demonstrated by Xu in 2016, who gathered evidence to suggest the reaction proceeds through a dimer intermediate that forms upon self-reaction of the activated diarylmethanol (Scheme 1.15b).[193] Various oxygenated and nitrogenated



Chapter one references begin on page 86

heterocycles, including dihydropyrans by Chang[194] (Scheme 1.15c) and dihydroquinolines by Jana[195] (Scheme 1.15d), have also been synthesized through tandem reactions of alcohols with unsaturated nucleophiles.[196,197]

**Scheme 1.15.** Selected iron-catalyzed methods applied to heterocycle synthesis and functionalization

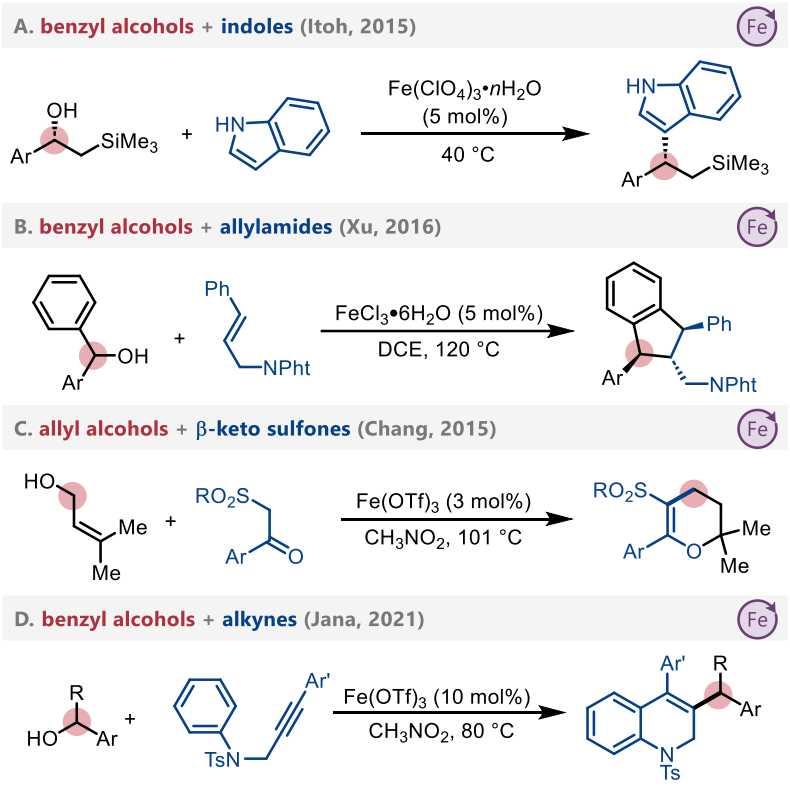


## Other metals

While the aforementioned metals are among the most common, a number of alternatives have also been demonstrated to act as catalysts for the direct $S_N1$-type deoxygenative functionalization of alcohols with carbon nucleophiles. A scandium-catalyzed strategy towards the synthesis of *N*-containing heterocycles was reported by Wang in 2013 (Scheme 1.16a).[198] The



Chapter one references begin on page 86

authors proposed that the scandium catalyst first coordinates to the aziridine ring, promoting the direct nucleophilic attack and subsequent ring opening by the benzyl alcohol substrate. The resulting intermediate undergoes rearrangement and subsequent deoxygenative Friedel-Crafts-type cyclization. Scandium catalysis was also employed by Bates in the allylation of benzyl alcohols with allyl silanes (Scheme 1.16b).[199] A hidden Brønsted acid-catalyzed transformation was proposed, wherein the $Sc(OTf)_3$ reacts with water in situ to generate triflic acid which facilitates the reaction. Scandium has been utilized by other authors towards these types of transformations as well.[200,201]

**Scheme 1.16.** Selected scandium–catalyzed methods

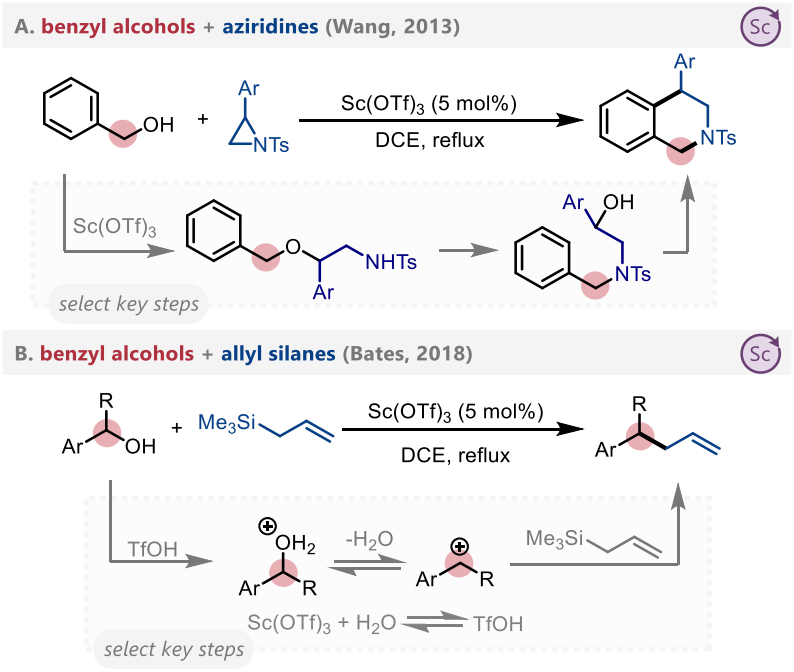


Donohoe and coworkers employed titanium catalysis in the presence of hexafluoroisopropanol (HFIP) towards the stereoselective synthesis of highly substituted oxygen heterocycles through the substitution of benzyl and allyl alcohols with homoallylic alcohols in



Chapter one references begin on page 86

2019 (Scheme 1.17a).[203] The authors proposed a key titanium-HFIP complex activates the C–O bond. Substitution via an $S_N1$-type pathway towards cyclization reactions was also developed by the Donohoe group in 2023, as they utilized the titanium-HFIP system to generate carbocations from benzyl or allyl alcohols in situ which proceed to initiate polyene cyclization cascades (Scheme 1.17b).[204] Using this method, the authors were able to generate three new carbon–carbon bonds in a single step. This technique has also been employed towards the stereoselective preparation of substituted pyrrolidines and piperidines from acyclic precursors.[205]

**Scheme 1.17.** Selected titanium-catalyzed methods

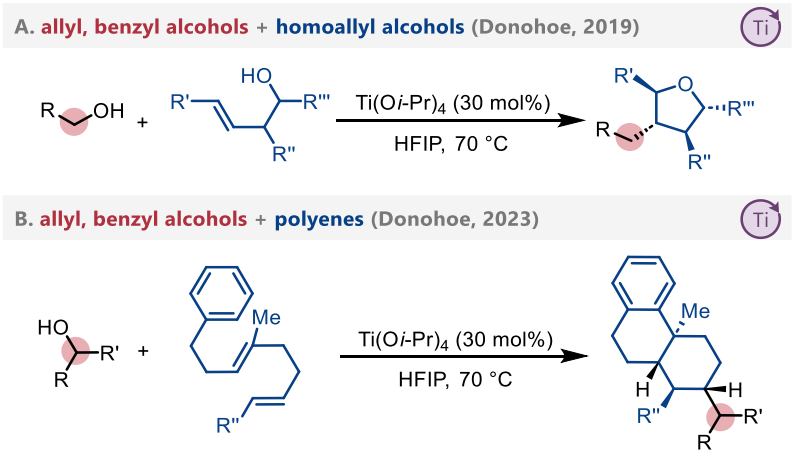


Zinc has been employed by Wang in the substitution of allyl alcohols with 1,3-dicarbonyl compounds and (hetero)arenes using mechanochemical high-speed vibration milling (HSVM) conditions (Scheme 1.18a),[206] and ytterbium has been employed in a cascade reaction towards the synthesis of carbazoles and naphthalenes from propargyl alcohols (Scheme 1.18b).[207] In the synthesis of carbazoles and naphthalenes, Wang and colleagues proposed that the reaction proceeds through the in situ generation of an allenium ion, cyclization with the benzyl alcohol, and a 1,2-aryl shift. Other metals that have been used in the deoxygenative functionalization of



*Chapter one references begin on page 86*

alcohols through $S_N1$-type pathways include bismuth,[208-211] cobalt,[212] gallium,[213] zirconium,[214] molybdenum,[215] mercury,[216] hafnium,[217,218] cerium,[219] aluminum,[220,221] lithium,[222] and platinum.[223] Lastly, Bisai and colleagues demonstrated the Friedel-Crafts alkylation of 3-hydroxy-2-oxindoles in the presence of various Lewis acids.[224-226]

**Scheme 1.18.** Selected zinc- and ytterbium-catalyzed methods

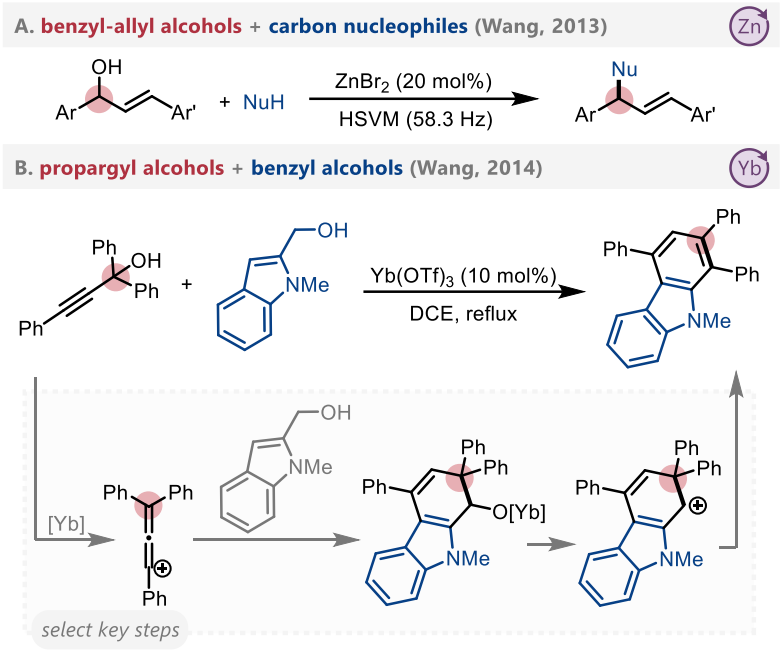


A multitude of methods for the deoxygenative functionalization of unprotected alcohols through $S_N1$-type and related pathways have been developed, including numerous pioneering discoveries in the late 1990s and early 2000s focused on metals such as iron and indium. Today, an assortment of reliable base metal-catalyzed methods are available for use to the contemporary chemist. Methods for coupling primary, secondary and tertiary alcohols have been described within this section, provided an adjacent π-system is present to aid in stabilization of intermediate carbocation or carbocation-like electrophile. Many applications towards stereocontrolled



Chapter one references begin on page 86

reactions, heterocycle synthesis and cascade reactions have been disclosed. As methods concerning the deoxygenative functionalization of unprotected alcohols continue to be developed, there remains a need for methods to employ non-π-activated alcohols, which are still rarely used. Further, there remains room for the development of diastereo- and enantioselective variations of these transformations, which requires new strategies to control facial attack of planar carbocations. Expansion of the type of reaction partners that can participate in this chemistry is also welcome, as most reports feature only nucleophilic arenes, 1,3-dicarbonyls, and related species.

Finally, while the scope of this discussion is restricted to homogeneous transition metal-catalyzed reactions of alcohols that form bonds to carbon, it is important to note that a range of heterogeneous catalysts, organocatalysts, acid catalysts, photo(redox)chemistry, electrochemistry, and stoichiometric methods that can facilitate this chemistry, and heteroatom nucleophiles can also be used. These topics, as well as much of the content discussed herein, are described in specialized reviews. A review on the catalytic alkylation of furans by π-activated alcohols was put forth by Butin in 2014.[227] Cozzi and colleagues reviewed the stereoselective alkylation of enols and enolates through $S_N1$-type mechanisms in 2017.[228] The use of 2-propargyl alcohols in organic synthesis was catalogued by Bi and colleagues in 2019,[229] highlighting their ability to act as excellent electrophiles. A comprehensive review concerning the nucleophilic allylic substitution of allyl alcohols with 1,3-dicarbonyl compounds was published in 2022 by Rezgui and coworkers.[230] A review on the generation of carbocations by organophotoredox catalysis was put forth by Ohmiya and Nagao in 2021.[231] For further general overviews of the field of $S_N1$-type transformations of alcohols, readers are referred to three reviews: a 2010[94] and 2021[232] review by Cozzi and a 2016 review by Moran.[233]



Chapter one references begin on page 86

### 1.4.2. Deoxygenative functionalization via cross-coupling and related transformations

Section 1.4.1 described the C–O functionalization reactions disclosed since 2010 that proceed by using Lewis acid catalysis to convert alcohols into good electrophiles for substitution chemistry. In most cases, the reactive intermediate was proposed to be a carbocation. This section will describe methods that proceed via the formation of an intermediate bearing a carbon–metal bond. In most cases, this is achieved by oxidative addition using low-valent metal catalysts with reaction mechanisms that proceed by a cross-coupling-type catalytic cycle.

This section will be sectioned based on the identity of the substrates used in each transformation. π-Activated alcohols, including benzyl and allyl alcohols, are particularly common. As such, Section 1.4.2.1. will discuss the reaction of π-activated alcohols with organoboron nucleophiles, Section 1.4.2.2. will discuss their use in reactions with other organometallic species and Section 1.4.2.3. will discuss their use in cross-electrophile like coupling. Section 1.4.3 will discuss various approaches towards using non-π-activated alcohols as reaction partners. As with other section, discussion will be primarily limited to reactions that feature homogeneous, transition metal-catalyzed arylation, alkylation and related transformations using unprotected alcohols with an emphasis on work published from 2010-2022.

#### 1.4.2.1. π-Activated alcohols with organoboron nucleophiles

Catalogued below are the methods that have been demonstrated to permit the coupling of unprotected π-activated alcohols with organoboron nucleophiles in Suzuki-Miyaura-type reactions[234] with an emphasis placed on the strategy used to facilitate C–O bond cleavage. As chapters three and four of this dissertation will explore the cross-coupling of non-π-activated



Chapter one references begin on page 86

alcohols with organoboron nucleophiles, the following examples (Scheme 1.19 to 1.28) serve as important precedent.

## Benzyl alcohols

The first report of the transition metal-catalyzed Suzuki-Miyaura coupling of unprotected benzyl alcohols was disclosed by the Shi group in 2015 (Scheme 1.19),[235] who discovered that $Pd(PPh_3)_4$ could be used to synthesize a range of diarylmethanes through coupling with triarylboroxines. The authors demonstrated that both π-extended (e.g. naphthalenes) and simple benzyl alcohols could be used. The C–O bond of the benzyl alcohol is proposed to be activated through Lewis acid/base coordination between its hydroxide group and the triarylboroxine, forming a boronate ester intermediate. This intermediate is then proposed to undergo oxidative addition with the active palladium catalyst. Notably, this Lewis acid/base coordination observed between the alcohol and organoboron reactant is a common proposal for the activation of alcohols in cross-coupling reactions that will be seen throughout this chapter.

**Scheme 1.19.** The Suzuki-Miyaura coupling of benzyl alcohols

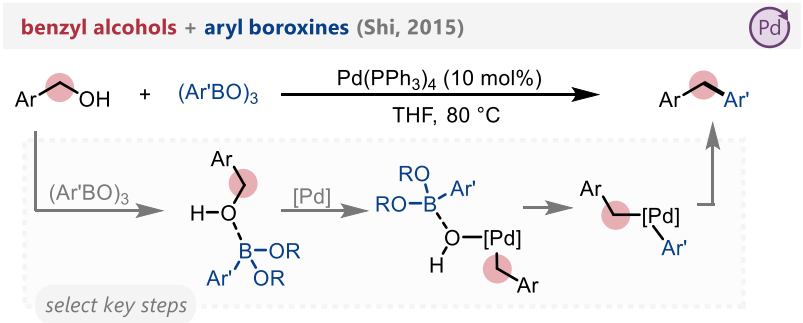




Chapter one references begin on page 86

In the following year, Rao and colleagues disclosed a method for the copper-catalyzed transformation of diarylmethanols into triarylmethanes upon reaction with arylboronic acids, demonstrating the synthetic utility of this method in the synthesis of large polyaromatic compounds as well as pharmaceutically relevant species (Scheme 1.20a).[236] The scope of benzyl alcohols that can be used was further expanded by Samec and colleagues who found that, in the presence of a nickel catalyst, both napthyl and quinolyl alcohols could be coupled (Scheme 1.20b).[237] A mechanism similar to that of Shi and coworkers was proposed, with NMR and ESI-HRMS studies suggesting coordination of the benzyl alcohol with the Lewis acidic boronic acid. The authors found two heating stages were necessary. Mixing at 80 °C enabled boronic ester formation, and subsequent heating to 100-125 °C allowed for the generation of final product. The Qin group explored a palladium-catalyzed Suzuki-Miyaura coupling of benzyl alcohols with arylboronic acids in 2019, utilizing various (hetero)benzylic alcohol derivatives and (hetero)arylboronic acids (Scheme 1.20c).[238] Sulfuryl fluoride ($SO_2F_2$), an inexpensive, abundant, and relatively inert gas was utilized to activate the alcohol *in situ*, generating fluorosulfonate esters that proceed to react with triethylamine to generate benzyltriethylammonium salts capable of undergoing oxidative addition with the palladium catalyst.

In 2022, the Morandi group disclosed a method to permit the palladium-catalyzed Suzuki-Miyaura coupling of benzyl alcohols employing diisopropylcarbodiimide (DIC) as an activating reagent (Scheme 1.20d).[239] This reagent combination permitted the generation of transient isoureas that were sufficiently activated to undergo oxidative addition with the palladium catalyst. Rapid (<5 minute) reactions were performed under these base-free reaction conditions with several base-sensitive boronic acids.



*Chapter one references begin on page 86*

**Scheme 1.20**. Copper-, nickel- and palladium-catalyzed cross-coupling methods

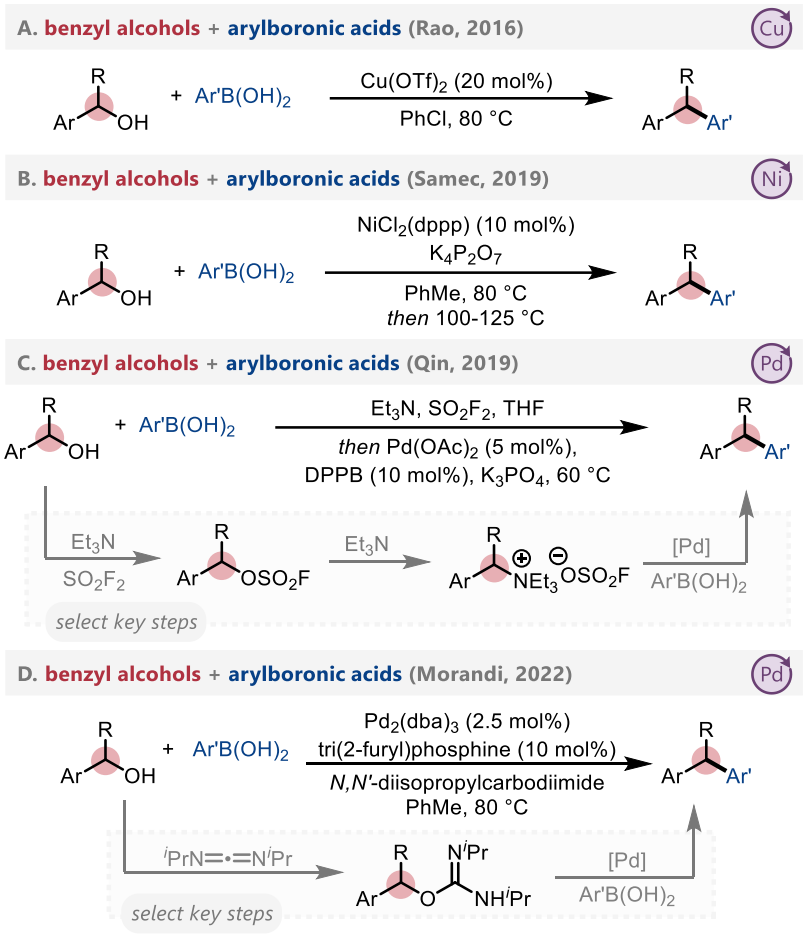


In 2022, the Xu group utilized a molybdenum-oxo catalyst that could permit the coupling of primary, secondary and tertiary benzyl alcohols with various benzyl trifluoroborate salts (Scheme 1.21).[240] Mechanistic studies suggested a distinct mechanism from conventional cross-coupling reactions. A Mo(VI) active catalyst is proposed to react with both the alcohol and organoboron coupling partners, and the key C–C bond formation is proposed to occur via 4-membered ring transition state.



Chapter one references begin on page 86

**Scheme 1.21.** Molybdenum-catalyzed benzylation of benzyl alcohols

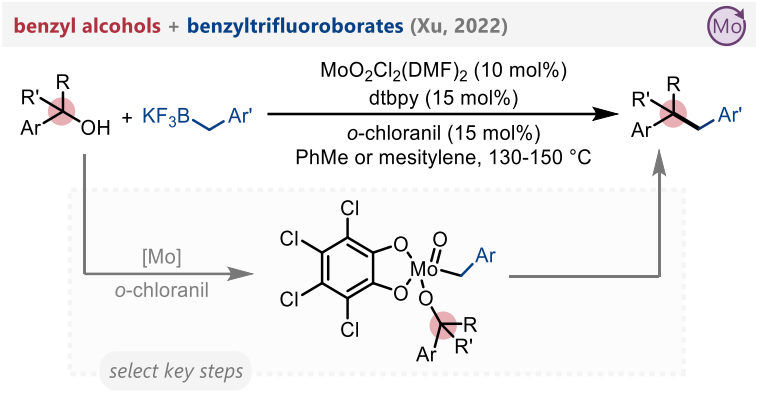


## Allyl alcohols

Selected reports of the coupling of allyl alcohols with organoboron nucleophiles disclosed prior to 2010 saw the use of rhodium catalysts by Kabalka[241] (Scheme 1.22a) and others,[242,243] and palladium catalysts by Tsukamoto[244] (Scheme 1.22b) and others.[245-247] A Lewis acid/base interaction between the organoboron and alcohol reaction partners is commonly proposed as a key step to facilitate the C–O bond activation. In the case of allyl alcohol functionalization, this bond cleavage is generally proposed to result in the formation of a π-allyl complex (Scheme 1.22c).



Chapter one references begin on page 86

**Scheme 1.22.** Early examples of the use of allyl alcohols as coupling partners with organoboron nucleophiles

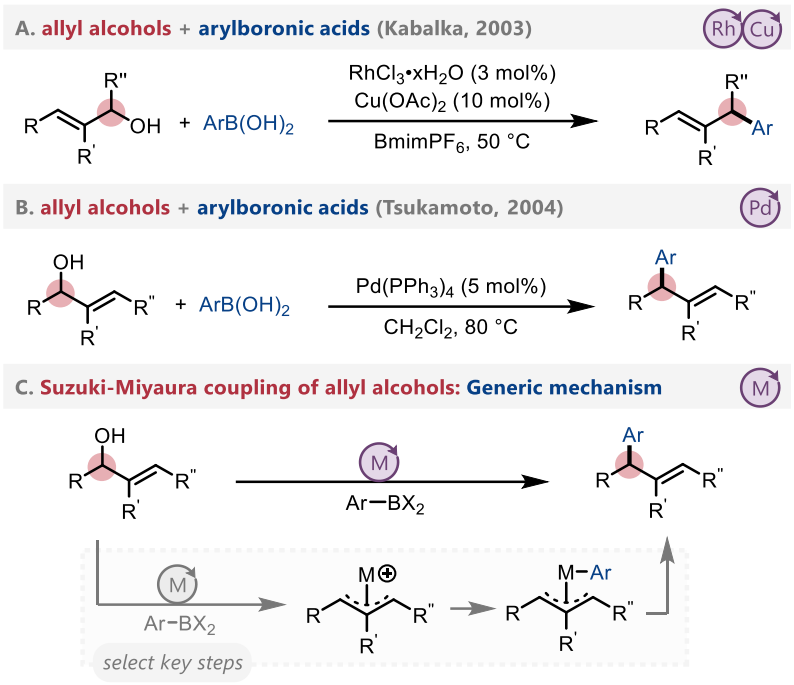


In 2011 the Kobayashi group reported the nickel-catalyzed coupling of allyl alcohols with allylboron nucleophiles (Scheme 1.23a).[248] The method was selective for the formation of 1,5-dienes with excellent linear- and γ-selectivity. Later, Michaelis and colleagues developed a nickel-catalyzed coupling of allyl alcohols with organoboron nucleophiles using a bidentate NHC/phosphine ligand (Scheme 1.23b).[249] A wide range of primary and secondary allylic alcohols were employed and X-ray crystallography was utilized to confirm the bidentate nature of this ligand, which the authors proposed extends the lifetime of the active catalyst. Applications of transition metal-catalyzed reactions of allyl alcohols with organoboron nucleophiles have been extended to permit this transformation to occur in neat water,[250] on sterically encumbered α-branched allyl alcohols[251,252] and under ligand-free conditions.[253,254]



Chapter one references begin on page 86

**Scheme 1.23**. Nickel-catalyzed cross-coupling methods

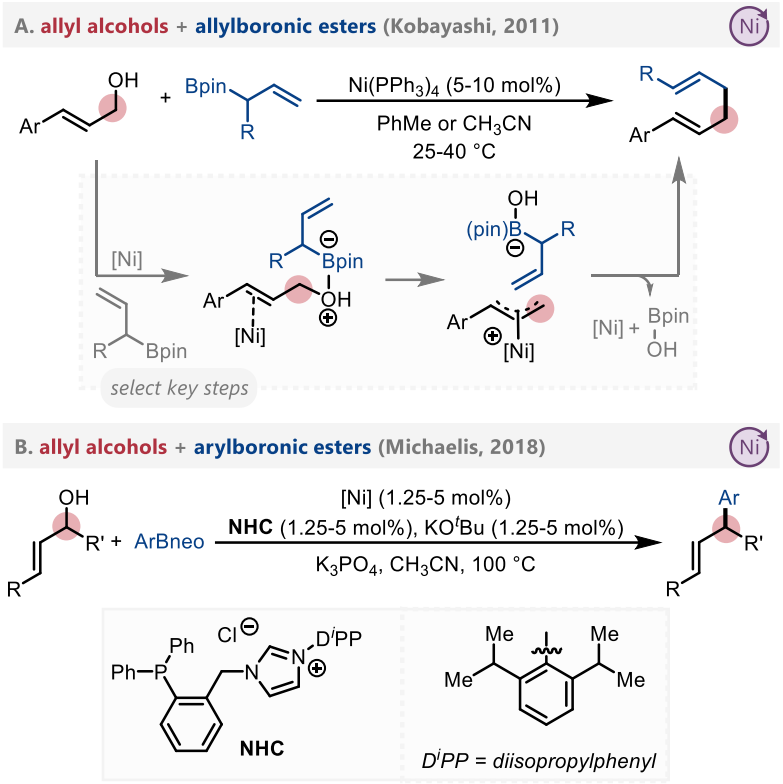


In 2022, Stanley and coworkers disclosed a nickel/Xantphos-catalyzed arylative substitution of homoallylic alcohols using arylboroxines (Scheme 1.24).[255] The authors found that the addition of *para*-methoxyphenylboronic acid was beneficial and proposed that it served to activate the alcohol substrate. Mechanistic experiments led the authors to proposed tandem catalytic cycles, wherein an olefin migration provides an allyl alcohol in situ, which then undergoes oxidative cleavage to form a π-allyl intermediate and subsequent transmetalation/reductive elimination with high regioselectivity towards formation of a conjugated alkene product.



*Chapter one references begin on page 86*

**Scheme 1.24**. Engaging allyl alcohols with organoboron nucleophiles through a tandem isomerization/arylation mechanism

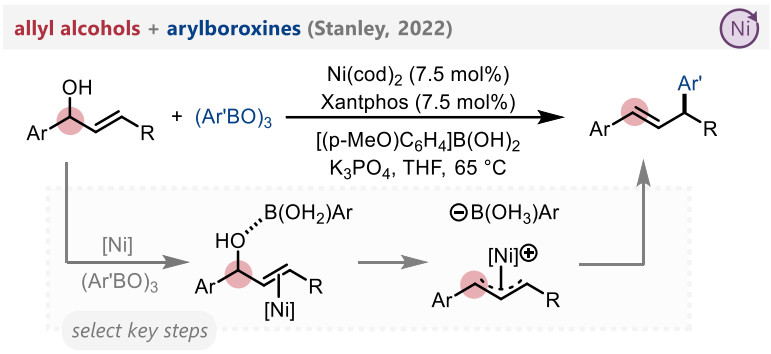


Further advances in the cross-coupling of allylic alcohols with organoboron nucleophiles have been demonstrated in the context of stereoselective transformations. In 2011, Shi and coworkers disclosed a method for the coupling of Morita-Baylis-Hilman allyl alcohols adducts with arylboronic acids in the presence of an axially chiral palladium catalyst bearing a bidentate ligand, allowing for the formation of 1,4-*(E)*-allylation products with 93-99% *ee* (Scheme 1.25a).[256] The palladium-catalyzed stereospecific coupling of enantioenriched allyl alcohols in the presence of arylboronic acids has also been demonstrated in the presence of *rac*-BINAP (Scheme 1.25b)[257] and TMEDA[258] as ligands. These reactions are proposed to occur by activation of the alcohol fragment with the boron electrophile, formation of a π-allyl complex with inversion of configuration, and stereoretentive transmetalation/reductive elimination.



*Chapter one references begin on page 86*

**Scheme 1.25**. Enantioselective and enantiospecific cross-coupling of allyl alcohols with organoboron nucleophiles

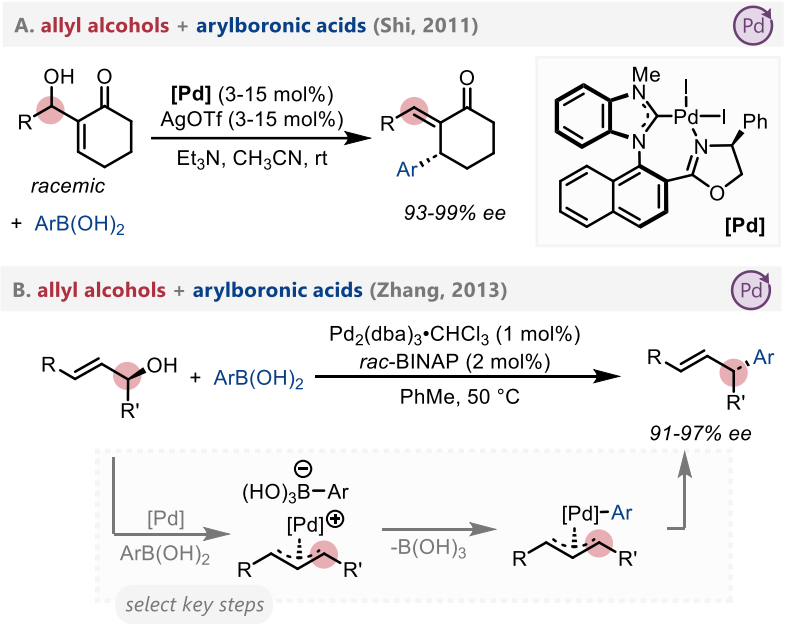


A powerful catalyst for asymmetric substitution of chiral racemic alcohols was developed by Carreira and coworkers.[259] In 2013, they disclosed the asymmetric substitution of allyl alcohols with vinyltrifluoroborate salts in the presence of this catalyst (Scheme 1.26a).[260] This reaction occurs at room temperature and allows for the synthesis of various chiral dienes and polyenes with >95% *ee*. The applicability of this work was demonstrated with respect to the synthesis of (-)-hinokiresinol, and later work demonstrated a related enantioselective alkynylation of allyl alcohols with alkynyl trifluoroborate salts (Scheme 1.26b).[261] This iridium-phosphoramidite catalyst system has been employed by Yang towards the asymmetric substitution of allyl alcohols (Scheme 1.26c).[262] In 2022, an alternative ligand was used in the alkynylation of allyl alcohols towards chiral enynes as disclosed by Wong and Cui.[263] Comprehensive reviews on enantioselective allylic



*Chapter one references begin on page 86*

substitution via iridium catalysis have been published, with You detailing advancements prior to 2018[264,265] and Takeuchi detailing advancements between 2018-2022.[266]

**Scheme 1.26**. Asymmetric coupling of allylic alcohols with organoboron nucleophiles using phosphoramidite ligands

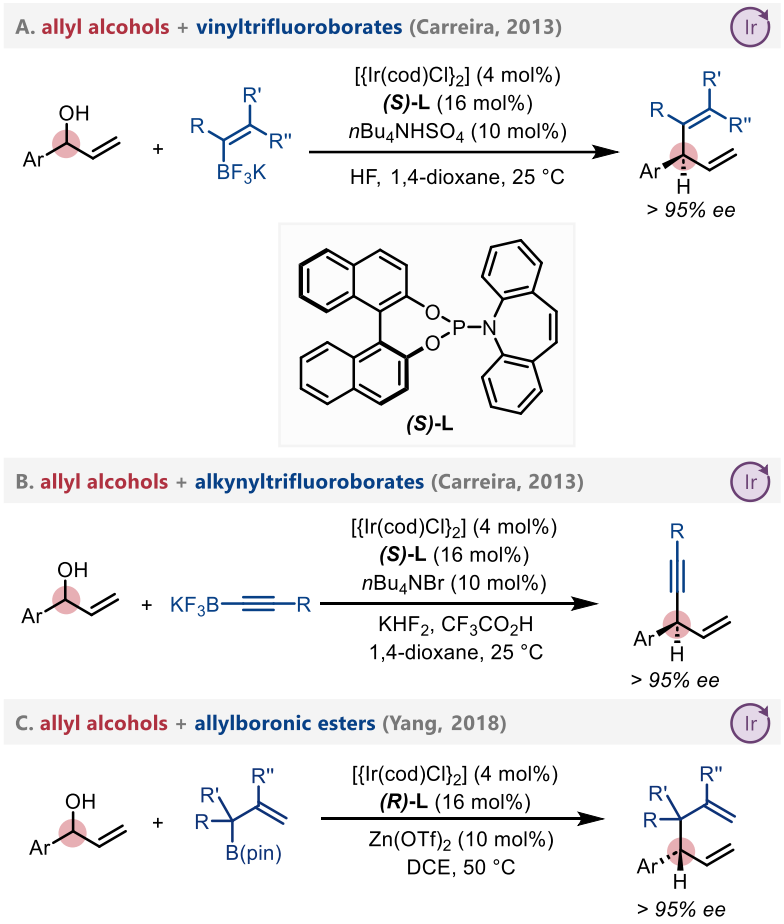


## Propargyl and allenyl alcohols

Propargyl and allenic alcohols are two further classes of π-activated alcohols that can be used in transition metal catalysis. Pioneering work into the coupling of diverse propargyl alcohols with arylboronic acids was disclosed by Yoshida and Ihara in 2004 (Scheme 1.27a).[267] Notably,



Chapter one references begin on page 86

arylated allenes were observed upon employing secondary or tertiary alcohols as substrates. In contrast, primary alcohols gave mixtures of arylated allenes and alkynes. The authors proposed that oxidative addition of palladium into the C–O bond of the alcohol reveals a propargyl organopalladium intermediate that exists in equilibrium with an allenic intermediate. The arylation of propargyl alcohols was expanded upon in 2016, with Kimber developing a base-free transformation to access dienes via isomerization of an intermediate aryl allene (Scheme 1.27b)[268] and Sherburn employing propargyl diols to gain access to highly substituted dienes via two-fold Suzuki-Miyaura coupling (Scheme 1.27c).[269]

**Scheme 1.27**. Palladium-catalyzed reactions of propargyl alcohols with organoboron nucleophiles

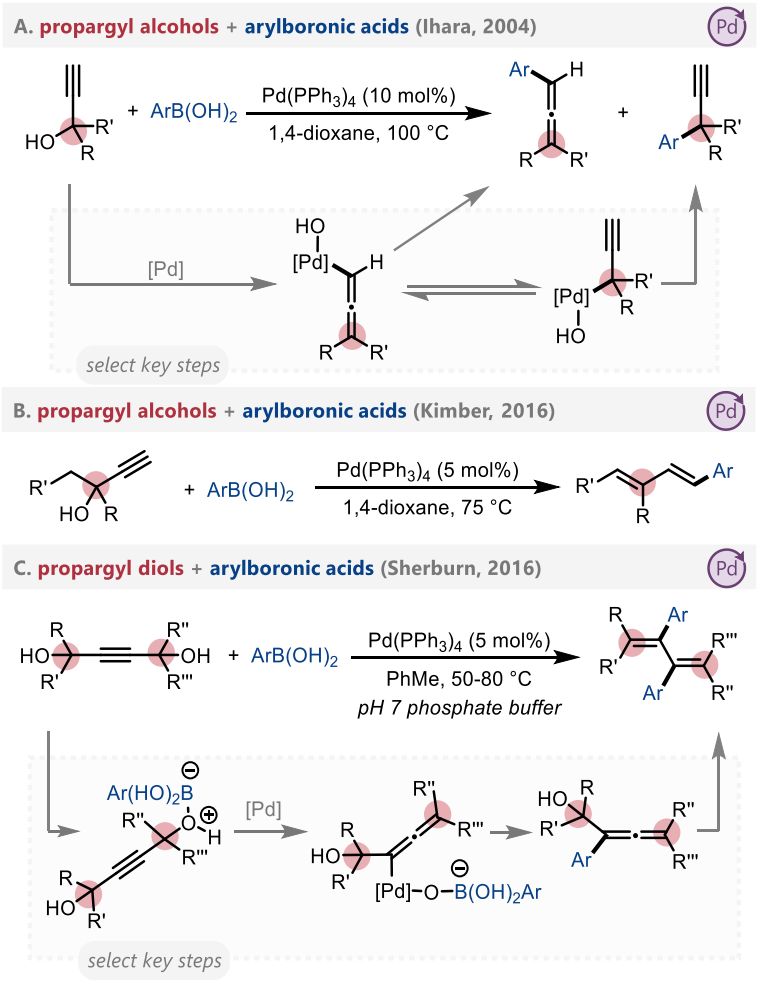




Chapter one references begin on page 86

Palladium/Brønsted acid dual catalysis was explored by Ma and coworkers in the reaction of propargyl alcohols with boronic acids to synthesize tri- and tetrasubtituted allenes in 2020 (Scheme 1.28a).[270] The authors proposed protonation of the alcohol renders the C–O bond susceptible towards oxidative addition by palladium. In 2022, Guo and coworkers utilized palladium catalysis in the Suzuki-Miyaura coupling of allyl-substituted propargyl alcohols, resulting in the generation of stereodefined polysubstituted conjugated enynes (Scheme 1.28b).[271] The coordination of an intermediate palladium π-allyl complex to the tethered alkyne is proposed to facilitate formation of the *Z*-alkene product.

In 2017, Duo and coworkers disclosed the rhodium-catalyzed arylation/dihydroxylation of tertiary propargyl alcohols towards the synthesis of tetrasubstituted allenes (Scheme 1.28c).[272] Unlike the palladium-catalyzed reactions described above that are proposed to proceed by oxidative addition of the allyl alcohol, the authors suggested this reaction proceeds by initial transmetalation to make a rhodium–aryl species that undergoes alkyne insertion and subsequent β-hydroxide elimination to form the allene. This work was expanded upon by the same group towards the arylation of propargyl diols[273] and benzylic propargyl alcohols.[274] In 2022, the Duo group developed a rhodium/Brønsted acid catalytic method for the tandem arylation-cyclization of propargyl alcohols with boronic acids towards the synthesis of benzo-*2H*-pyrans and benzofurans.[275] The authors proposed a similar insertion/elimination sequence as discussed above, with the acid co-catalyst facilitating intramolecular cyclization between the phenol and allene groups in the intermediate.



*Chapter one references begin on page 86*

**Scheme 1.28**. Palladium/Brønsted acid and rhodium-catalyzed transformations of propargyl alcohols with organoboron nucleophiles

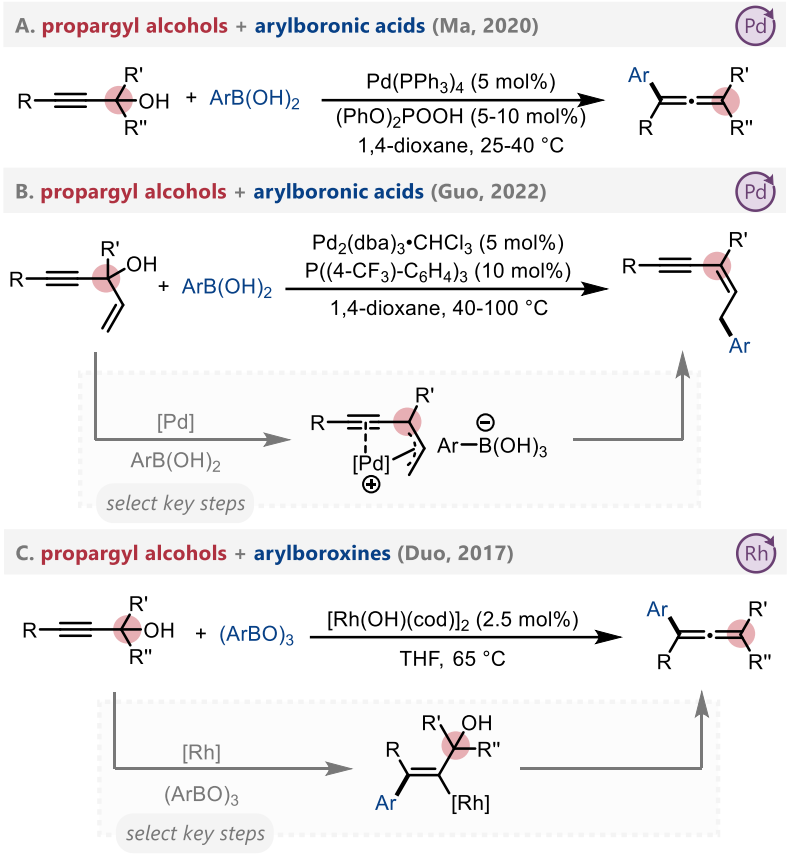


The palladium-catalyzed coupling of allenic alcohols with organoboron nucleophiles was demonstrated by Yoshida, Ihara, and colleagues in 2004,[276,277] using both aryl and alkenylboronic acids to generate poly-alkenylated products with high *E*-selectivity. Later, phosphinoyl-substituted allenic alcohols were successfully coupled with arylboronic acids by Wu and colleagues in the presence of a palladium catalyst.[278] Rhodium catalysis has also been explored by Murakami and colleagues for the coupling of allenic alcohols with organoboron nucleophiles.[279]



*Chapter one references begin on page 86*

Suzuki-Miyaura reactions and related couplings with organoboron nucleophiles represent powerful methods to generate molecular complexity. The deoxygenative cross-coupling of unprotected π-activated alcohols with organoboron reagents is no exception. Reactions with allyl alcohols are particularly common and have been done stereoselectively to prepare enantioenriched arylated products as well as stereodefined alkenes. Comparatively, there remains room for the development of methods to couple benzyl, propargyl and allenic alcohols with control of stereochemistry, as well as opportunities in asymmetric allene synthesis. Lastly, most examples feature C($sp^2$)-hybridized organoboron coupling partners. Use of alkylboron reactants would enable synthesis of useful C($sp^3$)–C($sp^3$) linkages and expand the 3-dimensional space accessible by C–O bond activation of π-activated alcohols.

### 1.4.2.2. π-Activated alcohols with other organometallic nucleophiles

In contrast to advancements in the coupling of unprotected alcohols with organoboron nucleophiles, methods to engage these species with alternative organometallic nucleophiles remain scarce. A likely reason for this disparity is that organoboron reagents have been commonly observed to serve a dual role as both the nucleophilic reaction partner and the alcohol activating agent. Conversely, more aggressive nucleophiles are sufficiently basic to deprotonate alcohols, leading to the generation of alkoxide salts and destruction of the organometallic reagent. Nonetheless, some reports exist of the cross-coupling of π-activated alcohols beyond Suzuki-Miyaura-type reactions.

Shi and colleagues report in 2012 the cross-coupling of unprotected benzyl alcohols with Grignard reagents in the presence of a nickel catalyst and stoichiometric methylmagnesium bromide (Scheme 1.29a).[280] The authors proposed that the benzyl alcohol is initially deprotonated



Chapter one references begin on page 86

to generate a magnesium alkoxide, which reacts with the nickel catalyst by oxidative addition. This reaction was extended towards the nickel-catalyzed coupling of allyl alcohols with primary alkyl Grignard reagents by Wang and coworkers in 2020 (Scheme 1.29b).[281] The authors found that only primary alkyl Grignard reagents could be utilized in this alkylation. The employment of secondary alkyl Grignard reagents, with the exception of cyclopropylmagnesium bromide, led towards production of the reduced product. The reduced product could also be formed upon employing a different nickel catalyst and a higher reaction temperature.

**Scheme 1.29**. Nickel-catalyzed coupling of benzyl and allyl alcohol with Grignard reagents

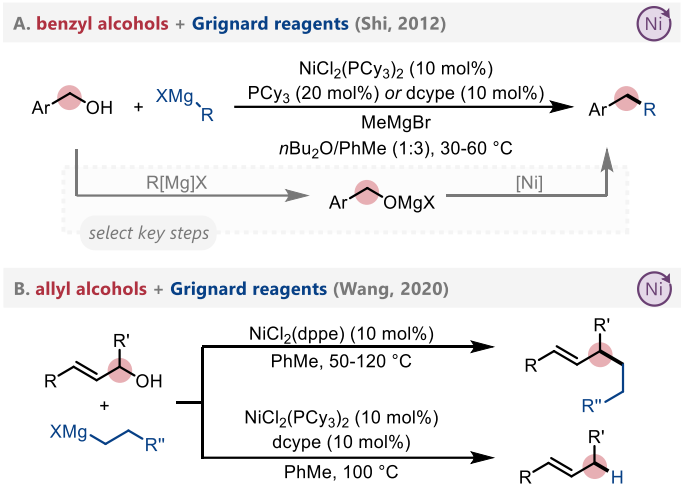


Wang and colleagues disclosed a Negishi-type coupling of allylic alcohols in 2017, demonstrating that both aryl and alkenylzinc chlorides could be coupled to primary or secondary alcohols in the presence of a $Ni(OTf)_2$ catalyst (Scheme 1.30a).[282] Similar to the work of Shi and coworkers above, stoichiometric amounts of MeZnCl were required. The authors found that adding two equivalents of lithium chloride could improve sluggish reactions. The reaction was not inhibited in the presence of radical traps, leading the authors to propose a nickel(0)/nickel(II) catalytic cycle rather than a radical pathway. This work was extended in 2021 by the same group



Chapter one references begin on page 86

towards the alkynylation of allyl alcohols using alkynyl zincs to form 1,4-enynes (Scheme 1.30b).[283] Stoichiometric amounts of MeZnCl were again required, forming zinc alkoxides in situ as reactive intermediates.

**Scheme 1.30**. Nickel-catalyzed coupling of allyl alcohols with organozinc reagents

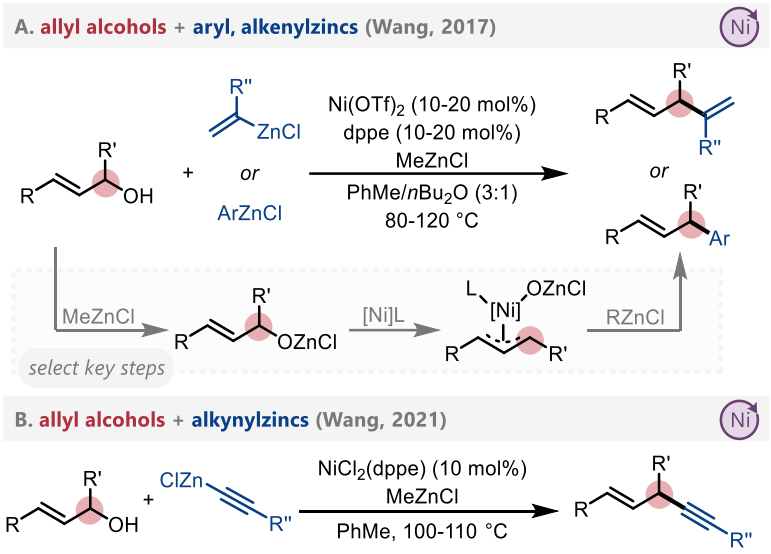


Carreira and coworkers demonstrated in 2014 the iridium-catalyzed enantioselective reaction between racemic allylic alcohols and allylsilanes, affording 1,5-dienes with >95% *ee* (Scheme 1.31).[284] Lewis acid co-catalysts were employed, and mono-, di-, tri- and tetrasubstituted allyl silanes could be used.



*Chapter one references begin on page 86*

**Scheme 1.31**. Iridium-catalyzed allyl alcohol cross-coupling with allylsilane reagents

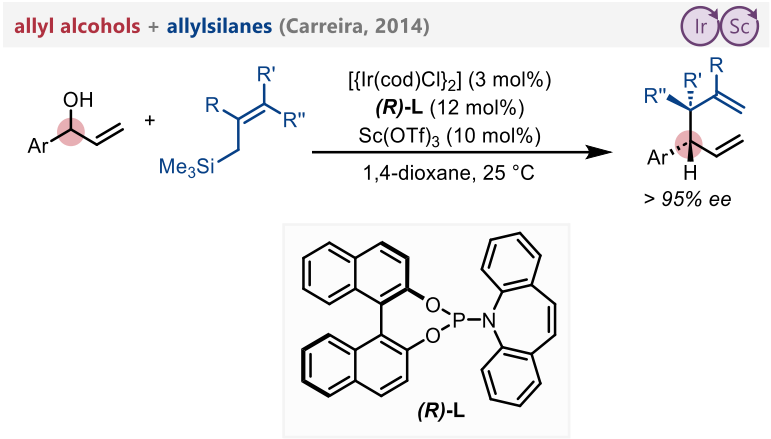


### 1.4.2.3. π -Activated alcohols with other electrophiles

Traditional cross-couplings – as covered in the previous sections – involve the reaction of a (pseudo)halide electrophile and an organometallic nucleophile. While many types of organometallic reagents exist, they are commonly derived from the corresponding organohalide starting material. Cross-electrophile couplings react two electrophiles with one another, obviating the requirement for nucleophile synthesis. A significant obstacle in cross-electrophile coupling reactions is selectivity, as it is difficult avoid deleterious side reactions such as homocoupling. Chemists have employed a range of innovative techniques to counteract this obstacle. In this section, methods that react unprotected π-activated alcohols with organo(pseudo)halides such as aryl bromides and triflates will be focused upon. As these represent cross-electrophile couplings, a common feature will be the employment of stoichiometric reductants to facilitate the reactions and turn over the catalyst.

An early example of transition metal-catalyzed cross-electrophile coupling of benzyl alcohols was disclosed by Weix in 2015 (Scheme 1.32a).[285] They used a cobalt/nickel dual catalyst



Chapter one references begin on page 86

system alongside stoichiometric $Ms_2O$ and zinc to enable deoxygenative coupling with aryl bromides. The authors proposed the nickel oxidatively adds into the aryl bromide bond while the cobalt activates the C–O bond to generate a benzyl radical. The aryl-nickel(II) intermediate combines with the benzyl radical and reductive elimination from nickel(III) produces product while zinc regenerates both metal catalysts.

Cobalt catalysis was once again employed in 2021 by the Shu group, this time towards the enantiospecific dynamic kinetic cross-electrophile coupling of allyl alcohols with vinyl triflates to give chiral 1,4-dienes (Scheme 1.32b).[286] Dimethyloxalate (DMO) was employed as an alcohol activating agent, which the authors proposed converts the alcohol into a good leaving group for anti-$S_N2$' oxidative addition with the cobalt catalyst. This results in the generation of a π-allyl complex that undergoes reduction and a second oxidative addition with the vinyl triflate. Reductive elimination affords product with inverted stereochemistry.

**Scheme 1.32**. Cobalt-catalyzed cross-electrophile coupling of alcohols

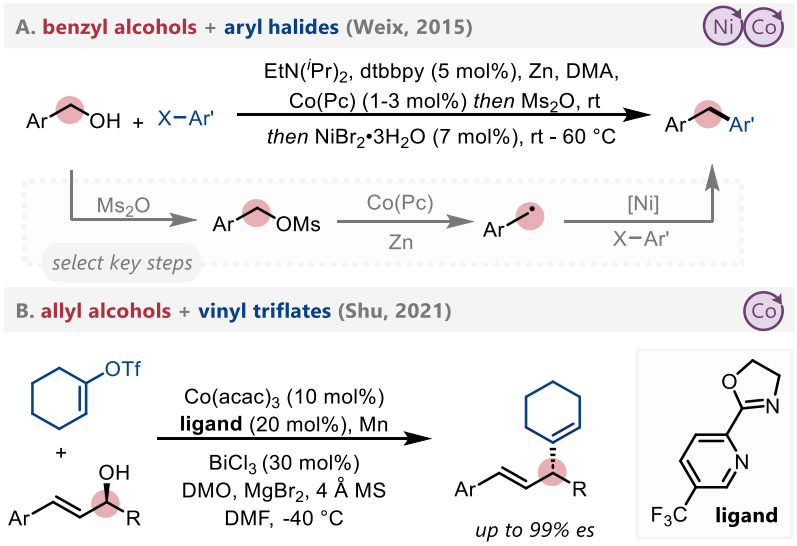




Chapter one references begin on page 86

Titanium has also been employed as an activating reagent in cross-electrophile coupling. Ukaji and colleagues demonstrated how low-valent titanium could be employed to enable deoxygenative nickel-catalyzed coupling with aryl (Scheme 1.33a)[287] or alkenyl[288] halides in the presence of manganese. Both benzyl and allyl alcohols could be used, which the authors proposed underwent homolytic cleavage upon coordination to in situ-formed low valent titanium, providing a radical that could be intercepted by a nickel oxidative addition complex. In 2021, Iwasawa disclosed a method for the dehydroxylative dimerization of benzyl alcohols – formally a cross-electrophile coupling, albeit without the formation of a carbon–metal bond-containing intermediate – with titanium as the only catalyst in the presence of light.[289] The reaction is proposed to occur via photomediated formation of titanium that reacts with benzyl alcohol substrates to generate benzyl radicals that undergo radical-radical. The isopropanol solvent is proposed to act as the reductant, resulting in the formation of acetone as a byproduct.

**Scheme 1.33.** Nickel--catalyzed cross-electrophile coupling of unprotected alcohols via homolytic C–O cleavage

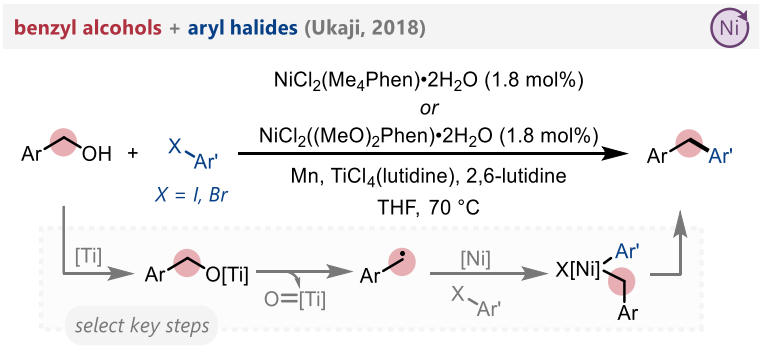


In 2019, Wu disclosed a palladium-catalyzed method for the cross-electrophile coupling of α-bromo ketones with primary and secondary allyl alcohols in the presence of stoichiometric



Chapter one references begin on page 86

$Mo(CO)_6$ (Scheme 1.34).[290] The authors proposed that a palladium-alkoxide intermediate forms that inserts CO from a $Mo(CO)_6$ additive and subsequently decarboxylates to form a π-allyl intermediate and carbon dioxide. Palladium catalysis was again explored in cross-electrophile coupling by Huang in 2021,[291] who coupled found allyl alcohols could be dimerized to generate 1,5-dienes using $H_2$ as the sole reductant.

**Scheme 1.34**. Palladium-catalyzed cross-electrophile coupling of alcohols with α-bromo ketones

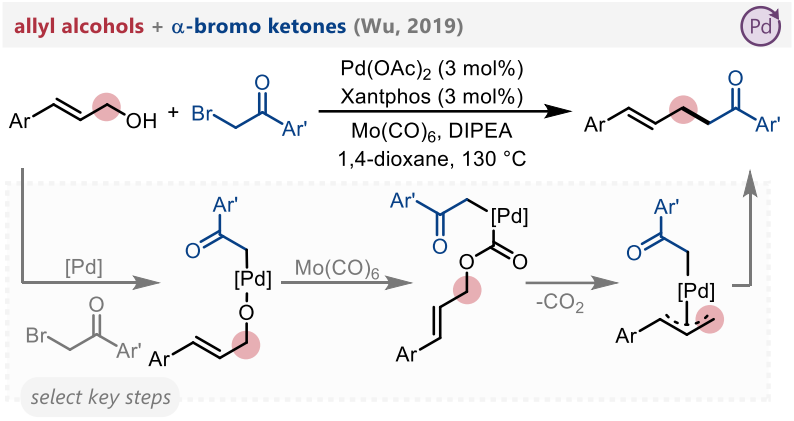


In 2018, Shu and coworkers utilized nickel- and Lewis acid-catalysis in the cross-electrophile coupling of allyl alcohols with (hetero)aryl halides (Scheme 1.35a).[292] The authors proposed the (hetero)aryl halide undergoes oxidative addition with the nickel catalyst while the allylic alcohol is activated by the Lewis acid. A subsequent disclosure by Shu demonstrated the dynamic kinetic cross-electrophile arylation of benzyl alcohols with (hetero)aryl halides and triflates in the presence of a nickel catalyst (Scheme 1.35b).[293] Dimethyl oxalate was employed as an activating agent, producing a more reactive benzyl alcohol derivative in situ by reversible transesterification., This intermediate was found to be sufficiently reactive for C–O bond cleavage with the nickel catalyst via a radical process. While primary and secondary benzyl alcohols were



Chapter one references begin on page 86

utilized in this transformation, attempted coupling with tertiary alcohols was not achieved. This work was extended towards the synthesis of dibenzyls through nickel-catalyzed homocoupling of benzyl alcohols in the same year.[294] Rahaim and colleagues investigated nickel-catalyzed cross-electrophile coupling towards the synthesis of diarylmethanes in 2020 (Scheme 1.35c).[295] They found that benzyl alcohols could be coupled with aryl bromides upon employing TMSCl as an alcohol activation reagent, with preliminary evidence supporting a radical mechanism.

**Scheme 1.35**. Nickel-catalyzed cross-electrophile coupling of alcohols with aryl (pseudo)halides

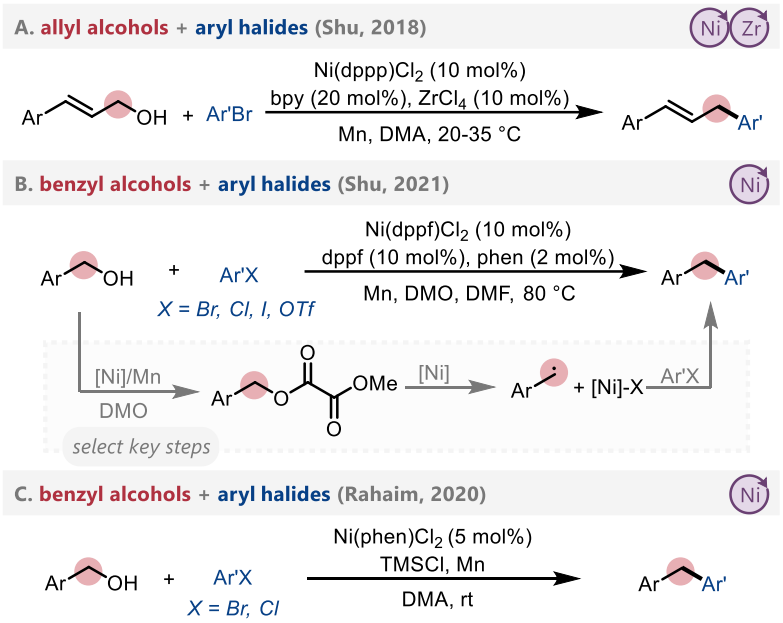


The nickel-catalyzed homocoupling of allyl alcohols was explored by Liu in 2020, who used $B_2pin_2$ en route towards the synthesis of 1,5-dienes (Scheme 1.36).[296] Non-dimeric products could also be obtained, for instance by including a second allyl alcohol or an aldehyde. The authors proposed that the reaction proceeds through in situ formation of an allyl boron intermediate, similar to a palladium-catalyzed transformation reported by Szabó and colleagues in 2008.[297]



Chapter one references begin on page 86

**Scheme 1.36**. Diverse reactivity of allyl alcohols in cross-electrophile coupling

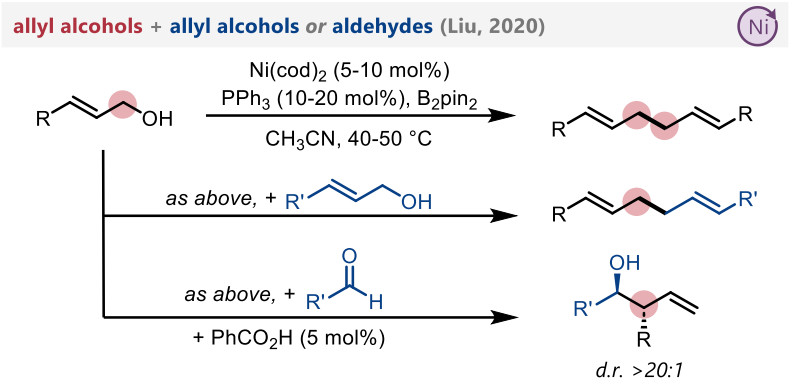


In 2021, Alexanian and coworkers disclosed a method for the stereospecific nickel-catalyzed cross-electrophile coupling of chiral alkyl tosylates with allyl alcohols (Scheme 1.37a).[298] Hexamethyldisilazane (HMDS) was used to activate the alcohol through in situ silylation, and vinyl magnesium chloride was employed as a reductant. An allyl magnesium nucleophile is proposed to be formed from the allyl alcohol, which undergoes an $S_N2$ addition to the alkyl tosylate electrophile with inversion of configuration. Also in 2021, Liang and coworkers disclosed the cross-electrophile coupling of allyl alcohols with (hetero)aryl phosphonium salts under dual nickel and Lewis acid co-catalysis (Scheme 1.37b).[299] The authors proposed the reaction proceeds by a series of oxidative additions and single electron reductions with manganese. Lastly, nickel-catalyzed cross-electrophile coupling of allyl alcohols has been explored by Wang and coworkers (Scheme 1.37c)[300] who demonstrated that branched allyl alcohols could be coupled with aryl chlorides in the presence of a $Ni(cod)_2$ catalyst and stoichiometric zinc and magnesium reductants. Linear allylation products were formed and good selectivity for the *E*-configuration was observed in cases where the product is a disubstituted alkene.



*Chapter one references begin on page 86*

**Scheme 1.37**. Nickel-catalyzed cross-electrophile coupling with alkyl tosylates, phosphonium salts and aryl chlorides

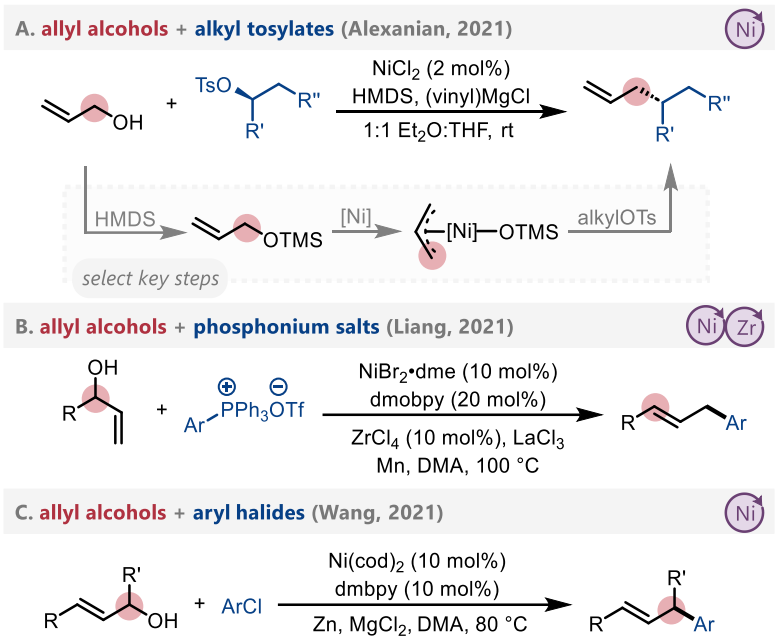


While many methods for cross-electrophile coupling of alcohols have been developed, most are very recent and the topic has much room for improvement. For example, coupling with sterically hindered reactants – regarding both the alcohol and the coupling partner – is still rare. Most reactions are limited to simple benzyl or allyl alcohols and activating more complex and/or non-π-activated alcohols would represent a substantial achievement, as would stereoselective and/or enantioselective variants. Furthermore, a major feature of using alcohols as cross-coupling electrophiles is their attractiveness relative to organohalides. Yet, most reports thus far feature the reaction of an alcohol with an organohalide coupling partner. The deoxygenative transition metal-catalyzed cross-coupling of two unprotected alcohols has scarcely been reported. For further discussion on related cross-electrophile coupling, this author recommends the account from Gong



Chapter one references begin on page 86

on the use of alcohol derivatives[301] and the review from Nicholas that describes diverse applications of alcohols and epoxides.[302]

### 1.4.3. Non-π-activated alcohol activation

As illustrated thus far in Section 1.4, enormous strides have been made in the catalytic functionalization of unprotected π-activated alcohols including benzyl, allyl, propargyl, and allenyl alcohols. Most of these examples rely on these neighbouring π-systems to weaken the C–O bond and facilitate the generation of conjugated carbocations, radicals, or organometallic species. Due to their ubiquity and ease-of-access, the development of methods for the activation of non-π-activated alcohols would greatly enhance the scope of alcohols amenable to deoxygenative functionalization reactions. In this section, strategies that have been taken to employ non-π-activated alcohols in deoxygenative functionalization methodologies will be explored.

In 2011, Yi and colleagues utilized a cationic ruthenium catalyst in the coupling of alcohols with alkenes to furnish alkylated olefins with high linear selectivity (Scheme 1.38a).[303] This method permitted the functionalization of both non-π-activated and π-activated primary alcohols. Secondary alcohols were found to react sluggishly. The authors proposed a vinyl ruthenium intermediate may form that activates the alcohol by oxidative addition/reductive elimination. The mechanism was studied in depth by Cavallo, Poater and coworkers,[304,305] who corroborated this hypothesis. The Yi group followed up this work with a succession of papers over the following decade, demonstrating the functionalization of phenols with diols or simple alcohols (Scheme 1.38b),[306] the etherification of two alcohols,[307] the reductive etherification of alcohols with



Chapter one references begin on page 86

aldehydes or ketones in the presence of $H_2$[308] and the synthesis of *N*-heterocycles from coupling with 1,2- and 1,3-diols.[309]

**Scheme 1.38**. Ruthenium-catalyzed methods for the coupling of alcohols with alkenes or phenols

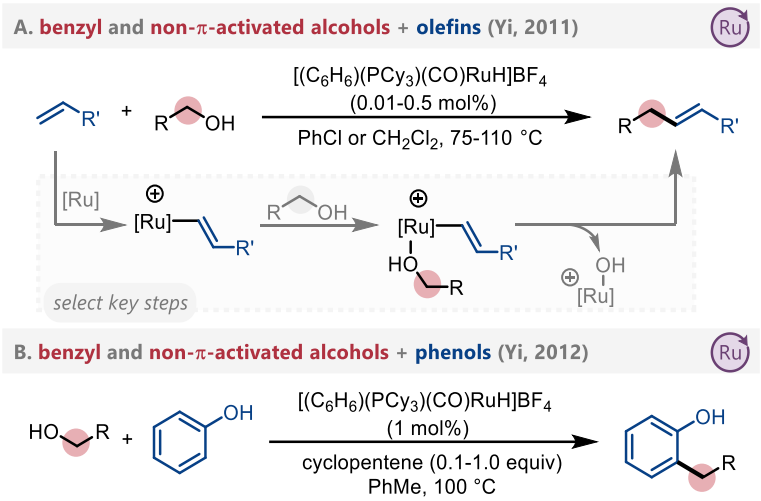


A common approach to functionalize simple alcohols is to first convert them into organohalides, which renders them good electrophiles for substitution chemistry and cross-coupling. Recent efforts have shown that organohalides can be formed from alcohols in situ and immediately captured in transition metal-catalyzed reactions. An early example of this approach came from the Huang group, who detailed in 2013 the titanium-catalyzed coupling of hemiaminals with alkenes (Scheme 1.39a),[310] inspiring future efforts towards reactions of unactivated alcohols. The authors use TMSCl as an additive to convert the hemiaminal into a chlorolactam in situ, and the ensuing carbon-chlorine bond undergoes homolysis in the presence of the titanocene catalyst. In 2021, Li employed a nickel/electrocatalytic system in the cross-electrophile coupling of non-π activated primary and secondary alcohols with aryl halides (Scheme 1.39b).[311] They proposed that the alcohol is activated in situ to form an alkyl halide through an anodic Appel reaction with



Chapter one references begin on page 86

$PPh_3Br_2$ (generated in situ) prior to entering the catalytic cycle. Gong and coworkers employed a related strategy using nickel catalysis (Scheme 1.39c).[312] Cross-electrophile coupling with aryl halides could be achieved using 2-chloro-3-ethylbenzo[d]oxazol-3-ium salt (CEBO) to enable bromination of alcohol substrates. While technically a two-step one-pot protocol, the halogenation step occurs within 1-5 minutes, making it a practical strategy to perform deoxygenative arylation of alcohols without requiring isolation of any reactive intermediates. Weix and coworkers also utilized nickel catalysis in the cross-electrophile coupling of non-π-activated primary and secondary alcohols via in situ halogenation with both aryl and vinyl halides as coupling partners (Scheme 1.39d).[313] Inclusion of a P(V) reagent proved essential to activate the alcohol prior to bromination.



*Chapter one references begin on page 86*

**Scheme 1.39**. In situ halogenation as a strategy towards the functionalization of non-π activated alcohols

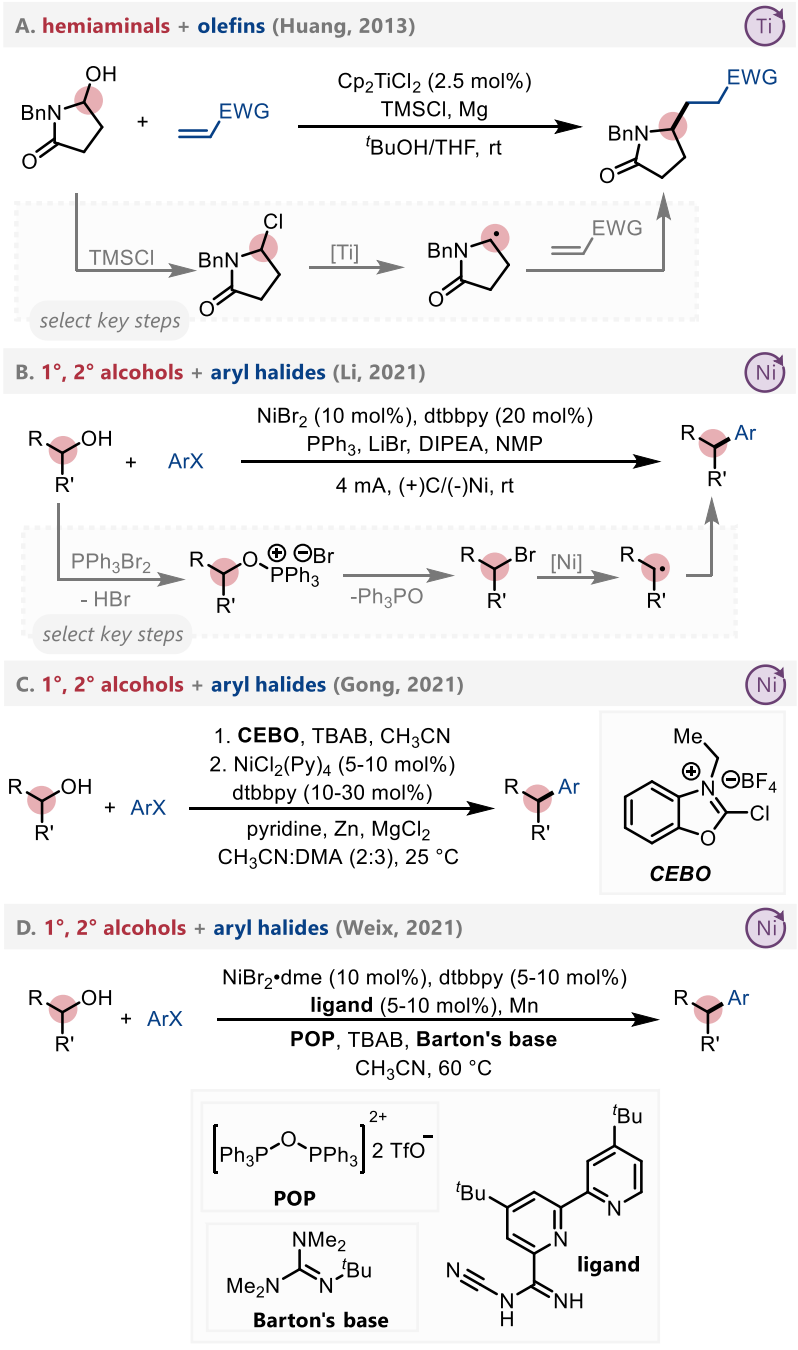


Deoxygenative formation of carbon-centered radicals is another strategy to engage non-π activated alcohols in catalysis. Shu and colleagues found in 2020 that catalytic titanium could be



Chapter one references begin on page 86

used to couple tertiary alcohols with olefins (Scheme 1.40a).[314] Mechanistic experiments corroborated titanium-catalyzed homolytic cleavage of the C–O bond, with catalytic regeneration of the active titanium catalyst being permitted through reaction with a silyl chloride and zinc. This approach was extended to include coupling with halostyrenes in 2022 (Scheme 1.40b),[315] which allowed retention of the π-bond by elimination of bromide.

Xanthate esters are well-established alcohol derivatives for a range of transformations, including Barton-McCombie deoxygenation.[316] In situ activation of alcohols via stoichiometric formation of xanthate esters or xanthate ions is also possible, enabling more direct deoxygenative functionalization.[317,318] A catalytic method to functionalize xanthate esters was reported in 2021 when Wu described a one-pot method for their in situ formation and photocatalytic activation with iridium. While photocatalytic methods are outside of the scope of this review, an exception is made for this method as it represents an innovative way to activate non-π-activated alcohols. The authors proposed a carbon-centered radical forms and reacts with an olefin via a Giese-type addition (Scheme 1.40c).[319] This strategy allowed for the coupling of non-π-activated primary, secondary and tertiary alcohols. Takemoto and coworkers adapted a similar approach the following year as they demonstrated the coupling of in situ generated xanthate salts with imines.[320] Finally, cobalt catalysis was employed by Liu and colleagues in the deoxygenative difluoromethylation of benzylic alcohols and α-hydroxy alcohols (Scheme 1.40d).[321] Xanthate esters were generated from alcohols in situ, which are proposed to be converted to carbon-centered radicals by the diazonium salt additive. The transformation was found to work with benzylic substrates as well as alcohols adjacent to esters, amides, and nitriles. While each of these methods using xanthate esters proceed through two-step procedures with isolation of the intermediate, they have been included within this section as methods to activate non-π-activated alcohols are rare.



Chapter one references begin on page 86

**Scheme 1.40**. Deoxygenative radical generation as a strategy towards the activation of non-π activated alcohols

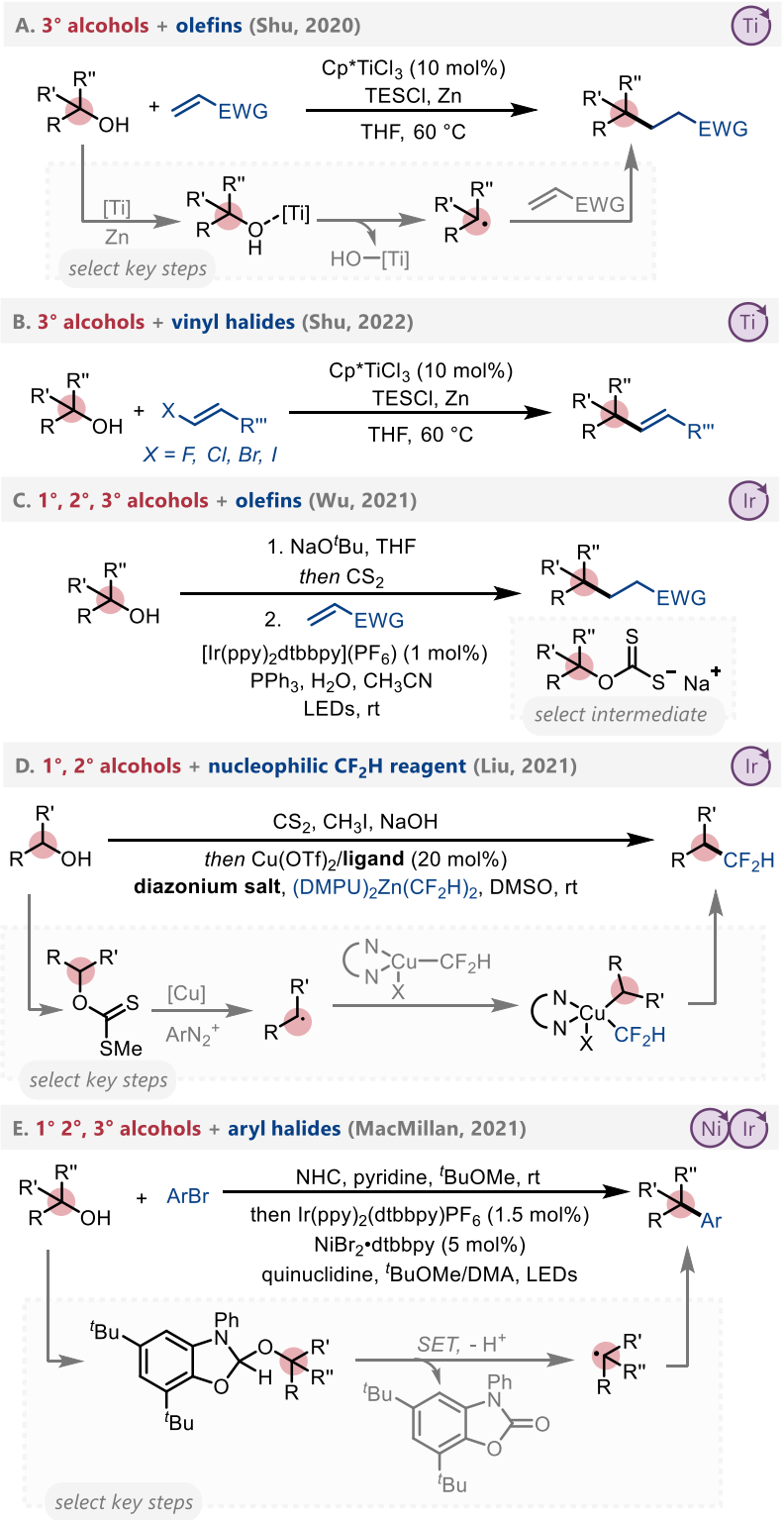




Chapter one references begin on page 86

A notable achievement in the coupling of non-π-activated alcohols was reported by the MacMillan group in 2021, who developed a NHC reagent for alcohol activation that could allow the coupling of primary, secondary and tertiary alcohols through metallaphotoredox-enabled deoxygenative arylation (Scheme 1.40e).[322] The authors proposed the reaction begins by stoichiometric generation of an NHC-alcohol adduct, which undergoes photomediated C–O bond homolysis to generate a carbon-centered radical that can react with a nickel-aryl oxidative addition complex. While still a recent development, this approach for activating alcohols has proven useful in a range of transformations.[323-325] A similar rationale was employed by Studer to enable the three-component radical coupling of aroyl fluorides, styrenes and alcohols[326] and Wang in the deoxygenative functionalization of alcohols with isocyanides.[327]

Another strategy to activate aliphatic alcohols involves the use of Lewis acids. Cook and coworkers utilized iron catalysis in the substitution of non-π-activated secondary alcohols with arenes in 2014 (Scheme 1.41a).[328] Intramolecular cyclizations were also demonstrated by this group, and an enantioenriched secondary alcohols was shown to cyclize with minimal loss of enantiomeric excess, suggesting this example may be an exception to the more commonly proposed $S_N1$-pathway in Lewis acid-mediated Friedel–Crafts-type alkylation. In a related transformation, non-π-activated tertiary alcohols were employed as substrates towards the formation of C–C bonds by Kou and coworkers, who explored synergistic Brønsted/Lewis acid catalysis in 2022 (Scheme 1.41b).[329] Quaternary carbon centers obtained, and the authors found the reaction to have a second order dependence in iron. DFT calculations supported the hypothesis that the combination of Lewis and Brønsted acid lowers the barrier towards carbocation formation in an $S_N1$-like reaction. While not strictly a metal catalyst, silylium ions have been shown to facilitate alcohol activation; for example, as demonstrated by Oestrich in 2023 in the use of



Chapter one references begin on page 86

methanol in Friedel-Crafts-type alkylation (Scheme 1.41c).[207] A methyl silyloxonium ion is proposed to be the key electrophilic methyl source, making this a rare example of deoxygenative arylation that is not thought to occur by an $S_N1$-type mechanism.

**Scheme 1.41.** Lewis acid catalysis as a technique towards the functionalization of non-π activated alcohols

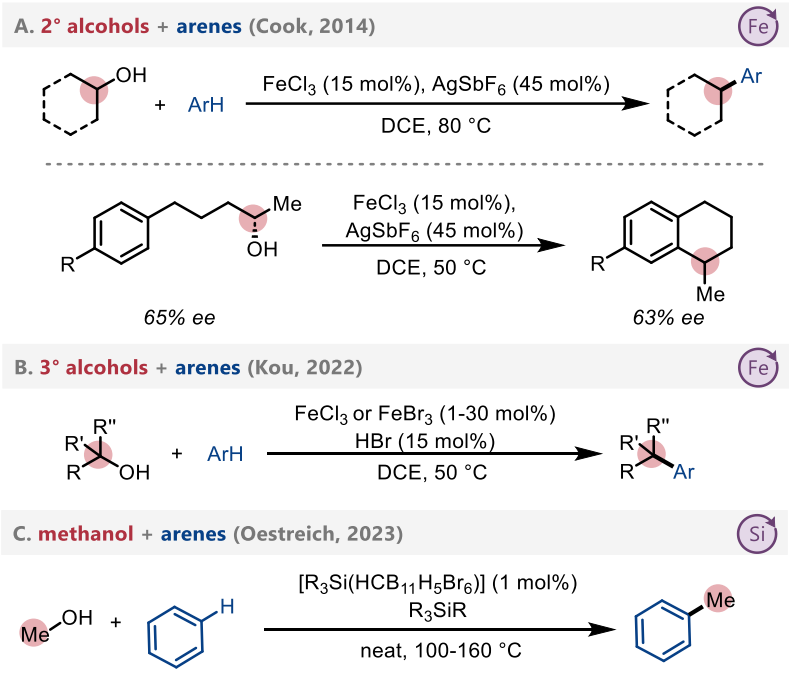


As it can be seen, relative to methods developed to functionalize π-activated alcohols, those developed to functionalize non-π activated alcohols are scarce and proceed through a limited number of mechanistic pathways. There remains significant room for the development of further methods, particularly as non-π activated alcohols represent a valuable source of alkyl fragments. Further, most of these contemporary efforts are restricted in substrate scope and require preactivation step and/or stoichiometric additives to proceed. Future developments may focus on dual-catalytic, biocatalytic and electro/photocatalytic methods to bypass these limitations,



Chapter one references begin on page 86

allowing access to transformations with a more diverse range of alcohols and coupling partners under less forcing conditions.

## 1.5. Beyond cross-coupling chemistry: Transition metal-catalyzed deoxygenative reduction of oxo-chemicals

In each of the preceding sections of this introduction, methods that lead to the *functionalization* of compounds, such as cross-coupling reactions, have been emphasized. While these reactions are paramount in the collective goal of synthesizing things that we need from things that we have, there is also significant value in the development of selective *defunctionalization* reactions, those that convert organic functional groups into hydrogen atoms.

Defunctionalization reactions are valuable whenever less functionalized products are more valuable than their corresponding raw materials. For instance, desulfurization and deamination can be used to prepare environmentally friendly fuels from crude liquid fuels,[330] environmental remediation makes use of the dechlorination of persistent polychlorinated biphenyls,[331] and high value compounds can be produced via the degradation of biomass.[332] Synthetically, defunctionalization reactions enable functional groups to act as transient, or "masked", moieties prior to removal.[333]

Chapter two of this dissertation will explore a subset of defunctionalization reactions, reductive deoxygenation reactions, or, reactions that transform carbon-oxygen bonds into carbon-hydrogen bonds. As with the functionalization methods discussed in Sections 1.3 and 1.4 of this introduction, the fundamental challenge of these types of reactions is selectively overcoming the strong bond-strengths in C–O bonds.



*Chapter one references begin on page 86*

Classical methods for reductive deoxygenation generally utilize stoichiometric amounts of metal hydrides (e.g. $LiAlH_4$, $NaBH_4$, DIBAL-H, $Bu_3SnH$) (Scheme 1.42).[334] While widely implemented, these strategies necessitate difficult purifications and the formation of inorganic salts as stoichiometric waste while often suffering from limited selectivity and functional group tolerance. An alternative is the use of pressurized gases over pyrophoric metals (e.g. $H_2$/Pd/C, $H_2$/Raney Ni).[335] Other reducing agents frequently encountered in classical transformations include hydrazines,[336] and metal amalgams.[337] Transition metal-catalyzed methods for reductive deoxygenation can provide convenient, selective, economically and environmentally friendlier alternatives to conventional stoichiometric approaches.

**Scheme 1.42.** Classical methods for the reductive deoxygenation of oxo-functional groups

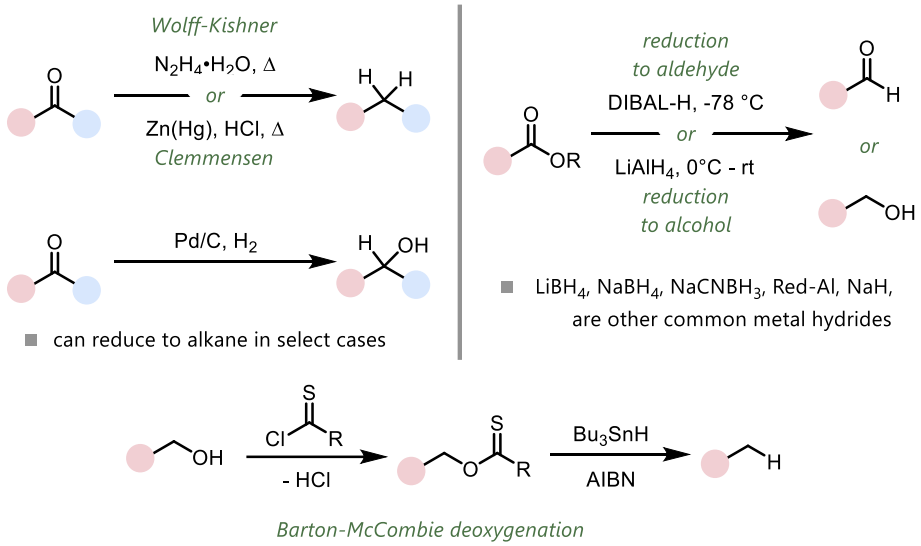


The use of boron Lewis acids (e.g. $B(C_6F_5)_3$), often alongside hydrosilanes, presents a well-established alternative to these methods. While these methods are effective, they will not be discussed within this dissertation as they have been thoroughly reviewed.[338] Other topics that will not be discussed to not distract from the objectives of this dissertation include heterogeneous-



Chapter one references begin on page 86

catalyzed reductions, electrocatalyzed reductions, photocatalyzed reductions, and transfer hydrogenations. The reduction of carbon dioxide and methanol will not be explored. Finally, this discussion will only consider *exhaustive* deoxygenative reductions, those that cleave carbon-oxygen bonds (e.g. reductions of ketones to the alcohol oxidation state, and similar transformations, will not be covered).

### 1.5.1. Reductive deoxygenation of ketones and aldehydes

Traditionally, the reductive deoxygenation of carbonyl groups is performed using Wolff-Kishner[336] or Clemmensen-type[337] chemistry, making use of hydrazines or metal amalgams. Transition metal-catalyzed alternatives can provide improved selectivity in these transformations while obviating the need for harsh reaction conditions, tough work ups or unfavourable reagents.

A subset of modern methods for the transition metal-catalyzed deoxygenation of ketones and aldehydes relies on modern variations of traditional Wolff-Kishner chemistry. For example, Cram and colleagues disclosed a method to perform the Wolff-Kishner reduction at room temperature using a pre-formed hydrazone alongside potassium *tert*-butoxide in 1962,[339] Caglioti developed a method to use tosylhydrazone alongside a hydride donor in 1963,[340] and Myers employed *N*-*tert*-butyldimethylsilyl hydrazones in 2004.[341] The Myers modification is notable as it combines classical Wolff-Kishner chemistry with modern transition metal catalysis, employing catalytic $Sc(OTf)_3$ to allow the transformation to proceed under mild conditions (Scheme 1.43a). Continuing the use of catalytic metals to enable the deoxygenation of ketones, Li and colleagues disclosed in 2022 that ruthenium can be used alongside $N_2H_4 \cdot H_2O$ to enable the deoxygenation of benzyl ketones (Scheme 1.43b).[342]



Chapter one references begin on page 86

**Scheme 1.43.** Merging traditional Wolff-Kishner chemistry with transition metal catalysis

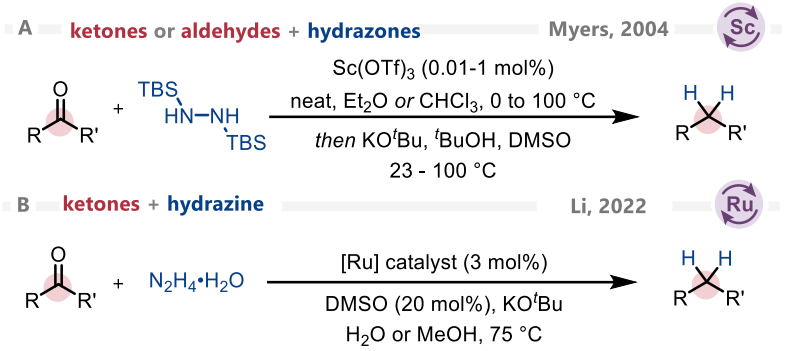


Another common approach towards the deoxygenation of carbonyls is to use a transition metal alongside a hydrosilane. Campagne and colleagues disclosed an iron-catalyzed method for the reduction of ketones in 2009 (Scheme 1.44a).[343] Polymethylhydrosiloxane (PMHS) was used as an inexpensive hydride source, and reactivity could be achieved on non-π-activated ketones and aldehydes. Inspired by this work, Wang and colleagues employed a heterogeneous Pd/$TiO_2$ plus homogeneous $FeCl_3$ catalyst, alongside PMHS, to achieve the deoxygenation of ketones.[344] PMHS was also used as a hydride source for the deoxygenation of benzylic ketones by Maleczka Jr. and colleagues in 2011.[345] $Pd(OAc)_2$ was employed as a catalyst in this transformation, with authors suggesting that the transformation proceeded through palladium nanoparticle-catalyzed hydrosilylation and subsequent C–O reduction facilitated by a chloroarene additive. Xu and colleagues used $PdCl_2$ and PMHS in methanol to catalyze the reduction of aromatic ketones (and benzyl alcohols) in 2013.[346] Adolfsson and colleagues achieved the mild deoxygenation of aromatic ketones and aldehydes using Pd/C and PMHS in 2015, demonstrating that the reaction could be performed on a 30 mmol scale in an open-to-air setup, at room temperature, using only 0.085% Pd/C (Scheme 1.44b).[347] Rhenium,[348] molybdenum,[349] and rhodium[350] have also been used as catalysts alongside hydrosilanes to achieve the deoxygenation of aromatic ketones.



Chapter one references begin on page 86

**Scheme 1.44.** Hydrosilanes as hydride sources in transition metal-catalyzed reductions of carbonyls

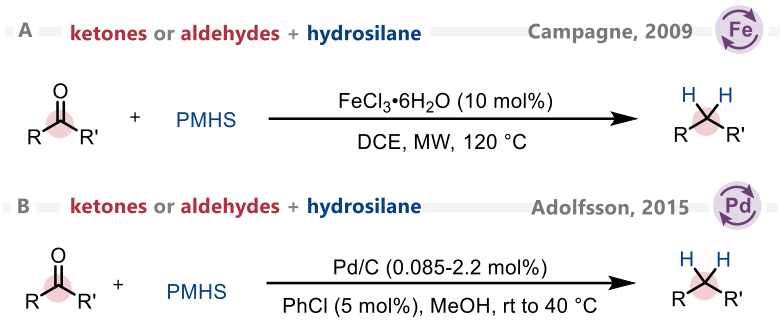


Beyond hydrosilanes the reduction of aromatic ketones has been achieved by Popowycz in 2014 using Pd/C alongside hypophosphites,[351] Yi in 2015 using $H_2$ alongside a ruthenium catalyst,[352] Zhou in 2020 using a range of hydride sources ($N_2H_4 \cdot H_2O$, $H_2$, $HCO_2NH_4$) alongside Pd/C[353] and Yang in 2020 using $HCO_2H$ alongside an iridium catalyst.[354]

### 1.5.2. Reductive deoxygenation of ethers and alcohols (including phenols)

As with the cross-coupling of alcohols, the high bond strengths of alcohols often means that they must be preconverted into an activated group, such as a sulfonate, to enable selective reduction.[48] As these species represent significantly activated alcohols, they will not be discussed in favour of less activated ethers, which are more representative of the species that will be reacted within this dissertation.

The reductive deoxygenation of ethers has been known in the presence of nickel since the early 20$^{th}$ century.[355] However, these methods proved to be nonselective, often hydrogenating the aromatic ring unpredictably alongside ethers. The selective, controllable reductive cleavage of



Chapter one references begin on page 86

C($sp^2$)–O bonds in aryl methyl ethers was accomplished in 2010 by Martin and colleagues using TMDSO, although it could generally only occur on π-extended systems (e.g. naphthalenes) (Scheme 1.45a).[356] Strong selectivity was demonstrated in this work, with the authors demonstrating that C($sp^2$)–OMe bonds could be activated in the presence of more reactive C($sp^3$)–OMe bonds. In 2011, Chatani reported a nickel-catalyzed reductive cleavage of C($sp^2$)–OMe bonds with Ni/$PCy_3$/$HSiMe(OMe)_2$ as a reductant (Scheme 1.45b).[357] Also in 2011, Hartwig developed a method for C($sp^2$)–O cleavage using hydrogen as a reductant and a nickel-NHC catalyst (Scheme 1.45c).[358] The authors applied this method to lignin defunctionalization and demonstrated how the reduction could be extended towards C($sp^3$)–O bonds in π-activated positions (i.e. benzyl ethers) upon including $AlMe_3$. Since, other approaches have been disclosed that enable the catalytic reduction of C($sp^2$)–O bonds in ethers.[359]

**Scheme 1.45.** Early disclosures in the transition metal-catalyzed reduction of ethers

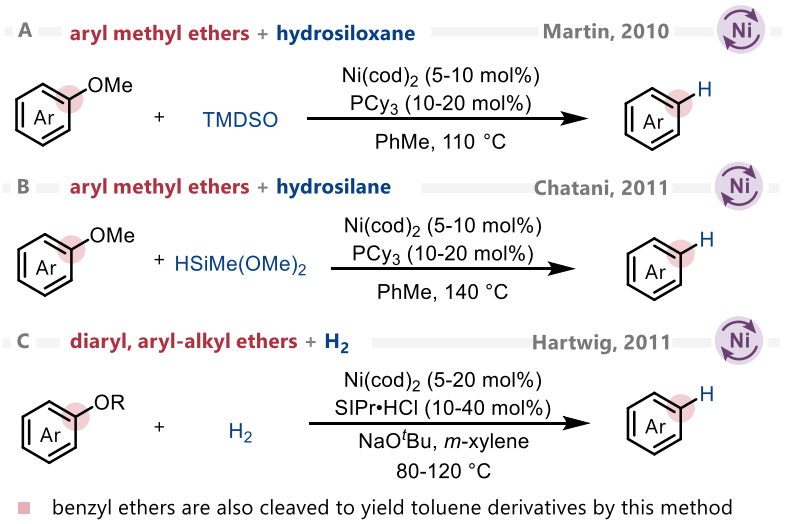


Transition metal-catalyzed methods for the reductive deoxygenation of alcohols have also been developed. The deoxygenation of alcohols in the presence of a transition metal catalyst was



Chapter one references begin on page 86

demonstrated by Baba and colleagues in 2001 (Scheme 1.46a).[360] The authors utilized catalytic amounts of indium trichloride to achieve this transformation on benzylic primary and secondary alcohols, as well as select aliphatic alcohols, using a chlorohydrosilane. They proposed that the mechanism involved formation of Lewis acid-activated silylated alcohols that underwent C–O bond cleavage to yield a carbocation. Beyond this work, Nishibayashi utilized ruthenium catalysts alongside a hydrosilane to reduce propargylic alcohols in 2006 (Scheme 1.46b),[361] Mirza-Aghayan extended this work towards the reduction of benzyl alcohols using a palladium catalyst alongside $Et_3SiH$ in 2009,[362] and Zhou employed iron catalysis in 2009 to achieve the deoxygenative reduction of allylic alcohols, ethers and acetates with benzyl alcohols.[363]

**Scheme 1.46.** Selected early developments in the transition metal-catalyzed deoxygenative reduction of alcohols using silanes as hydride sources

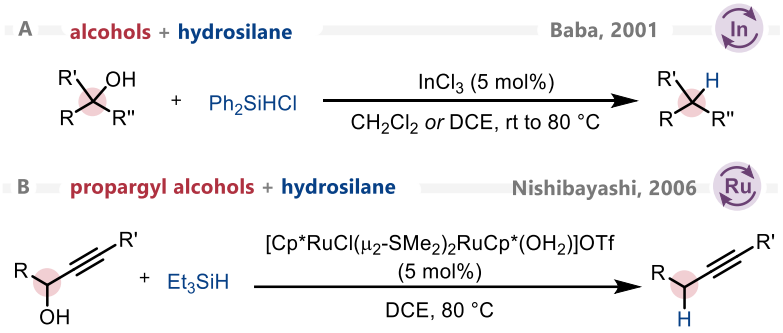


Advancements in the deoxygenation of alcohols continued after 2010, with Kim demonstrating the reductive deoxygenation of benzylic alcohols using PMHS and $FeCl_3$ in 2011 (Scheme 1.47a),[364] Laali demonstrating that propargylic, allylic and benzylic alcohols could be reduced using $Bi(OTf)_3$ and $Et_3SiH$ in ionic liquids in 2012,[365] and Niggemann exploring the calcium-catalyzed deoxygenation of propargylic alcohols – including tertiary propargylic alcohols – with triethylsilane in 2012.[366] Lalic demonstrated in 2013 the copper catalyzed reduction of



Chapter one references begin on page 86

primary and secondary alcohols through in situ triflation (Scheme 1.47b).[367] TMDSO was used as a hydride source in this reaction; notably, this is a rare examples of the deoxygenation of non-π-activated alcohols. In 2015, iron catalysis was explored by Bi and colleagues in the chemo- and regioselective reductive deoxygenation of 1-en-4-yn-ols into 1,4-enynes,[368] and in 2016 Nicholas and colleagues demonstrate the rhenium-catalyzed reduction and reductive dimerization of alcohols in 2016.[369] Li and colleagues demonstrated a method for the deoxygenation of non-π-activated primary alcohols in 2016 (Scheme 1.47c).[370] A ruthenium-catalyst was used alongside hydrazine, with the transformation proceeding through a Wolff-Kishner-type pathway. The same authors have explored the use of iridium and manganese in other deoxygenations of alcohols.[371] The iridium-catalyzed site-selective deoxygenation of primary, secondary and tertiary alcohols was realized by Xu and colleagues in 2018.[372] A 4-(*N*-substituted amino)aryl directing group was required, formic acid acted as a hydride donor and the authors gain evidence to suggest an $S_N1$-type pathway. Gallium was used alongside isopropanol as a hydride donor by Sai in 2018 in the reduction of benzylic alcohols.[373] Lastly, Carreira and colleagues demonstrated the asymmetric reductive deoxygenation of racemic tertiary alcohols using iridium/bismuth dual catalysis in 2019.[374]



*Chapter one references begin on page 86*

**Scheme 1.47.** Selected examples of recent methods used for the deoxygenations of alcohols

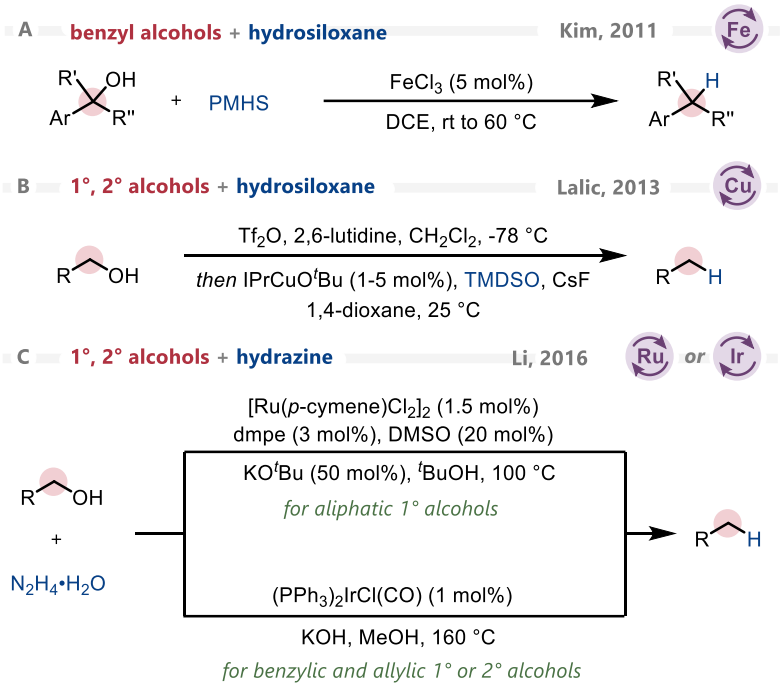


Classical methods for the deoxygenative reduction of oxo-functional groups often involve harsh reagents, forcing conditions or difficult purifications. As can be seen, a variety of transition metal-catalyzed methods have been developed as alternatives. Numerous transition metals including palladium, ruthenium, iridium, and nickel have been employed in these transformations, and hydrosilanes are frequently used as inexpensive and relatively benign hydride sources. A significant limitation in these transition metal-catalyzed transformations is that they often only permit the reduction of C–O bonds that are located adjacent to a π-electron system. With scarce exceptions, aliphatic, non-π-activated C($sp^3$)–O bonds prove difficult to reduce. Recall that this restriction was also frequently encountered in Section 1.4 of this dissertation. Consequently, the development of methods to achieve the activation of non-π-activated C($sp^3$)–O bonds in alcohols and other oxo-functional groups is highly desired.



Chapter one references begin on page 86

## 1.6. Scope of this dissertation: Research goals and objectives

The employment of oxo-functional groups and other naturally abundant compounds as substrates in synthetic chemistry is of paramount importance in the push towards a greener future. Previous research in the Newman group has explored the expansion of reaction partners in transition metal catalysis. Most notably, previous researchers have established numerous methods for the cross-coupling of esters. The motivation of this dissertation is to expand this goal further by utilizing a range of oxo-chemicals as substrates in nickel-catalyzed transformations (Figure 1.9). As alcohols exist as the simplest and most naturally abundant oxo-chemical, **the foremost goal of this dissertation is to develop nickel-catalyzed transformations that can utilize alcohols as substrates in valuable chemical reactions.**

Chapter two explores this goal towards deoxygenative reduction reactions. This chapter begins with a description of efforts made towards the development of a nickel-catalyzed method for the exhaustive reduction of esters. The second half of this chapter delves into efforts made in to extend this transformation, developing glovebox-free conditions that permit the deoxygenation of ketones, aldehydes, epoxides, ethers and alcohols.

Chapters three and four explore this goal towards deoxygenative functionalization reactions, culminating in the development of a dual nickel/bismuth-catalyzed method for the Suzuki-Miyaura arylation of primary, secondary, and tertiary alcohols. Notably, this work represents the first successful implementation of unprotected, non-π-activated alcohols in Suzuki-Miyaura coupling. Proceeding through an $S_N1$-type reaction mechanism, this work also represents a new way to envision mechanisms in cross-coupling chemistry.



*Chapter one references begin on page 86*

Chapter five builds upon the methods developed in Chapters Three and Four, exploring the use of alcohols in other deoxygenative coupling reactions. In this chapter, a high-throughput exploration of the chemical space surrounding the newly disclosed nickel/bismuth catalyst system is presented towards the coupling of tertiary alcohols. A strong focus is placed on expanding the scope of amenable coupling partners, particularly through the use of *N*-heterocycles as coupling partners. While unpublished at the time of the submission of this dissertation, Chapter five significantly lowers the barrier for future researchers in the Newman group *en route* towards a continued push towards implementing easily accessible in synthetic chemistry.

**Figure 1.9.** Graphical outlook for this dissertation

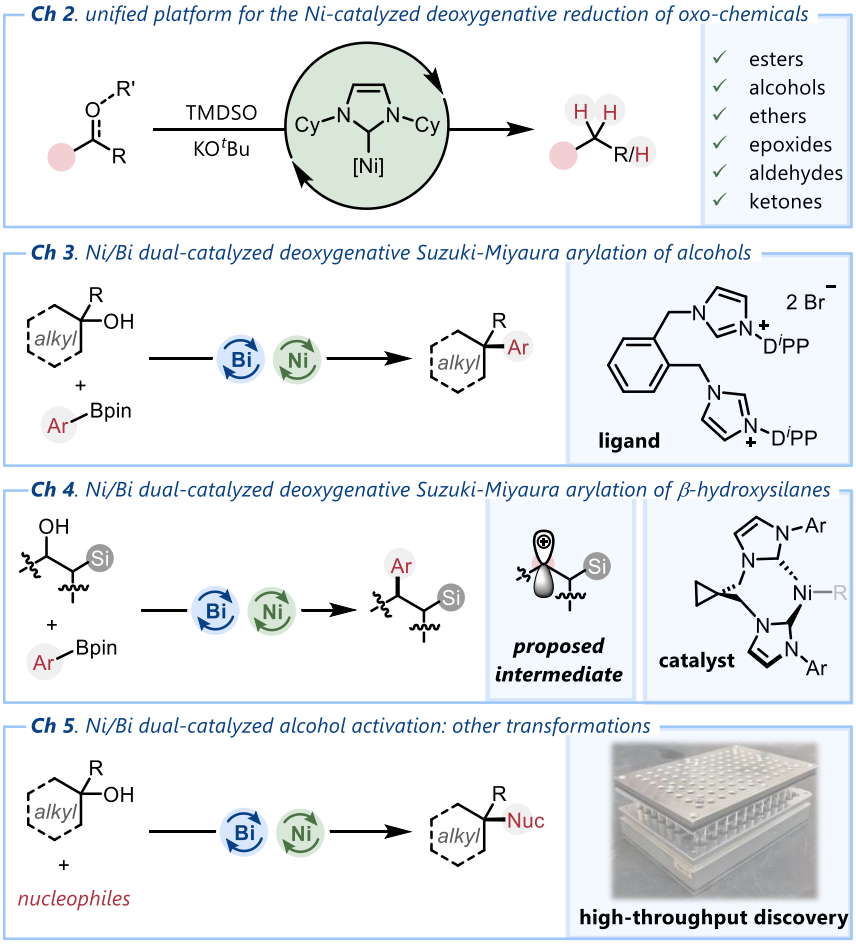




*Chapter one references begin on page 86*

## 1.9. References


(1) (a) Aristotle. (1952) [c. 340 BC]. *Meteorologica* (in Ancient Greek and English). Translated by Lee, H. D. P. Harvard University Press. pp. 2.3, 358b. (b) Forbes, R. J. (1970). *A Short History of the Art of Distillation: From the Beginnings Up to the Death of Cellier Blumenthal*. BRILL. p. 14.

(2) Sherwood Taylor, F. (1937). "The Visions Of Zosimos". *Ambix*. **1** (1): 88–92.

(3) Holmyard, E. J. Jābir Ibn Hayyān. *Proc. R. Soc. Med.* **1923**, *16* (Sect_Hist_Med), 46–57.

(4) "Phosphorus Starts With Pee In This Tale Of Scientific Serendipity". *NPR.org*. Retrieved 2023-01-24).

(5) Principe, Lawrence M.. "Robert Boyle". *Encyclopedia Britannica*, 21 Jan. 2024, https://www.britannica.com/biography/Robert-Boyle. Accessed 30 January 2024.

(6) Donovan, Arthur (1996). *Antoine Lavoisier: Science, Administration, and Revolution*. Cambridge: Cambridge University Press.

(7) Garfield, Simon (2001). *Mauve: How One Man Invented a Color that Changed the World*. W. W. Norton & Company

(8) Yergin, Daniel (1991). *The Prize, The Epic Quest for Oil, Money & Power*. New York: Simon & Schuster. pp. 19–29

(9) Ahmed, F.; Ali, I.; Kousar, S.; Ahmed, S. The Environmental Impact of Industrialization and Foreign Direct Investment: Empirical Evidence from Asia-Pacific Region. *Environ. Sci. Pollut. Res. Int.* **2022**, *29*, 29778–29792.

(10) National Geographic Society. “Great Pacific Garbage Patch”. https://education.nationalgeographic.org/resource/great-pacific-garbage-patch

(11) (a) Naidu, R.; Biswas, B.; Willett, I. R.; Cribb, J.; Kumar Singh, B.; Paul Nathanail, C.; Coulon, F.; Semple, K. T.; Jones, K. C.; Barclay, A.; Aitken, R. J. Chemical Pollution: A Growing Peril and Potential Catastrophic Risk to Humanity. *Environ. Int.* **2021**, *156*, 106616. (b) Johnston, J.; Cushing, L. Chemical Exposures, Health, and Environmental Justice in Communities Living on the Fenceline of Industry. *Curr. Environ. Health Rep.* **2020**, *7*, 48–57. (c) Woodruff, T. J. et al. A Science-Based Agenda for Health-Protective Chemical Assessments and Decisions: Overview and Consensus Statement. *Environ. Health* **2023**, *21* (S1). doi: 10.1186/s12940-022-00930-3.

(12) Steffen, W. Introducing the Anthropocene: The Human Epoch. Theme: Anthropocene. *Ambio* **2021**, *50*, 1784–1787. doi. 10.1007/s13280-020-01489-4.

(13) Ceballos, G.; Ehrlich, P. R.; Barnosky, A. D.; García, A.; Pringle, R. M.; Palmer, T. M. Accelerated Modern Human–Induced Species Losses: Entering the Sixth Mass Extinction. *Sci. Adv.* **2015**, *1*, 5.

(14) "Definition of CHEMISTRY". Merriam-Webster. Archived from the original on 7 August 2020. Retrieved 6 February 2024.

(15) Espenson, James (1995). *Chemical Kinetics and Reaction Mechanisms*. McGraw-Hill.

(16) (a) Steinfeld, Jeffrey I.; Francisco, Joseph S.; Hase, William L. (1999). *Chemical Kinetics and Dynamics* (2nd ed.). Prentice Hall. p. 147 (b) Atkins, Peter; de Paula, Julio (2006). *Atkins' Physical Chemistry* (8th ed.). W.H. Freeman. p. 839.

(17) Bligaard, T.; Bullock, R. M.; Campbell, C. T.; Chen, J. G.; Gates, B. C.; Gorte, R. J.; Jones, C. W.; Jones, W. D.; Kitchin, J. R.; Scott, S. L. Toward Benchmarking in Catalysis Science: Best Practices, Challenges, and Opportunities. *ACS Catal.* **2016**, *6*, 2590–2602.

(18) (a) an Leeuwen, P. W. N. M.; Chadwick, J. C. (2011). *Homogeneous Catalysts: Activity - Stability - Deactivation*. Wiley-VCH, Weinheim.

(19) Ullmann, F.; Sponagel, P. Ueber Die Phenylirung von Phenolen. *Ber. Dtsch. Chem. Ges.* **1905**, *38*, 2211–2212.

(20) Goldberg, I. Ueber Phenylirungen Bei Gegenwart von Kupfer Als Katalysator. *Ber. Dtsch. Chem. Ges.* **1906**, *39*, 1691–1692.

(21) A. Job, R. Reich,C. R. Hebd. *Seances Acad. Sci*.**1924**,*179*, 330 –332

(22) Meerwein, H.; Büchner, E.; van Emster, K. Über Die Einwirkung Aromatischer Diazoverbindungen Auf α,B-ungesättigte Carbonylverbindungen. *J. Prakt. Chem.* **1939**, *152*, 237–266.

(23) Kharasch, M. S.; Fields, E. K. Factors Determining the Course and Mechanisms of Grignard Reactions. IV. The Effect of Metallic Halides on the Reaction of Aryl Grignard Reagents and Organic Halides. *J. Am. Chem. Soc.* **1941**, *63*, 2316–2320.

(24) Chodkiewicz, W. *Ann. Chim. Paris* **1957**, *2*, 819–69.



*Chapter one references begin on page 86*

(25) Stephens, R. D.; Castro, C. E. The Substitution of Aryl Iodides with Cuprous Acetylides. A Synthesis of Tolanes and Heterocyclics. *J. Org. Chem.* **1963**, *28*, 3313–3315.

(26) (a) Jira, R. Acetaldehyde from Ethylene—A Retrospective on the Discovery of the Wacker Process. *Angew. Chem. Int. Ed.* **2009**, *48*, 9034–9037. (b) Fernandes, R. A.; Jha, A. K.; Kumar, P. Recent Advances in Wacker Oxidation: From Conventional to Modern Variants and Applications. *Catal. Sci. Technol.* **2020**, *10*, 7448–7470.

(27) Heck, R. F. Acylation, Methylation, and Carboxyalkylation of Olefins by Group VIII Metal Derivatives. *J. Am. Chem. Soc.* **1968**, *90*, 5518–5526.

(28) Mizoroki, T.; Mori, K.; Ozaki, A. Arylation of Olefin with Aryl Iodide Catalyzed by Palladium. *Bull. Chem. Soc. Jpn.* **1971**, *44*, 581–581.

(29) (a) Sheldon, Roger; Kochi, Jay (1981). *Metal-catalyzed oxidations of organic compounds: mechanistic principles and synthetic methodology including biochemical processes.* New York: Academic Press. (b) Chirik, P. J. Pioneers and Influencers in Organometallic Chemistry: A Profile of Professor Jay Kochi. *Organometallics* **2020**, *39*, 775–777.

(30) Milstein, D.; Stille, J. K. A General, Selective, and Facile Method for Ketone Synthesis from Acid Chlorides and Organotin Compounds Catalyzed by Palladium. *J. Am. Chem. Soc.* **1978**, *100*, 3636–3638.

(31) Corriu, R. J. P.; Masse, J. P. Activation of Grignard Reagents by Transition-Metal Complexes. A New and Simple Synthesis of Trans-Stilbenes and Polyphenyls. *J. Chem. Soc. Chem. Commun.* **1972**, No. 3, 144a.

(32) King, A. O.; Okukado, N.; Negishi, E.-I. Highly General Stereo-, Regio-, and Chemo-Selective Synthesis of Terminal and Internal Conjugated Enynes by the Pd-Catalysed Reaction of Alkynylzinc Reagents with Alkenyl Halides. *J. Chem. Soc. Chem. Commun.* **1977**, No. 19, 683.

(33) Hatanaka, Y.; Hiyama, T. Cross-Coupling of Organosilanes with Organic Halides Mediated by a Palladium Catalyst and Tris(Diethylamino)Sulfonium Difluorotrimethylsilicate. *J. Org. Chem.* **1988**, *53*, 918–920.



*Chapter one references begin on page 86*

(34) Sonogashira, K.; Tohda, Y.; Hagihara, N. A Convenient Synthesis of Acetylenes: Catalytic Substitutions of Acetylenic Hydrogen with Bromoalkenes, Iodoarenes and Bromopyridines. *Tetrahedron Lett.* **1975**, *16*, 4467–4470.

(35) Johansson Seechurn, C. C. C.; Kitching, M. O.; Colacot, T. J.; Snieckus, V. Palladium-catalyzed Cross-coupling: A Historical Contextual Perspective to the 2010 Nobel Prize. *Angew. Chem. Int. Ed.* **2012**, *51*, 5062–5085.

(36) Miyaura, N.; Yamada, K.; Suzuki, A. A New Stereospecific Cross-Coupling by the Palladium-Catalyzed Reaction of 1-Alkenylboranes with 1-Alkenyl or 1-Alkynyl Halides. *Tetrahedron Lett.* **1979**, *20*, 3437–3440.

(37) Miyaura, N.; Suzuki, A. Stereoselective Synthesis of Arylated (*E*)-Alkenes by the Reaction of Alk-1-Enylboranes with Aryl Halides in the Presence of Palladium Catalyst. *J. Chem. Soc. Chem. Commun.* **1979**, No. 19, 866.

(38) (a) Brown, D. G.; Boström, J. Analysis of Past and Present Synthetic Methodologies on Medicinal Chemistry: Where Have All the New Reactions Gone?: Miniperspective. *J. Med. Chem.* **2016**, *59*, 4443–4458. (b) Miyaura, N.; Suzuki, A. Palladium-Catalyzed Cross-Coupling Reactions of Organoboron Compounds. *Chem. Rev.* **1995**, *95*, 2457–2483.

(39) Li, Z.; Gelbaum, C.; Heaner, W. L., IV; Fisk, J.; Jaganathan, A.; Holden, B.; Pollet, P.; Liotta, C. L. Palladium-Catalyzed Suzuki Reactions in Water with No Added Ligand: Effects of Reaction Scale, Temperature, pH of Aqueous Phase, and Substrate Structure. *Org. Process Res. Dev.* **2016**, *20*, 1489–1499.

(40) Buskes, M. J.; Blanco, M.-J. Impact of Cross-Coupling Reactions in Drug Discovery and Development. *Molecules* **2020**, *25*, 3493.

(41) Biffis, A.; Centomo, P.; Del Zotto, A.; Zecca, M. Pd Metal Catalysts for Cross-Couplings and Related Reactions in the 21st Century: A Critical Review. *Chem. Rev.* **2018**, *118*, 2249–2295.

(42) Prices of nickel and palladium obtained from https://www.dailymetalprice.com/ on May 28th, 2024.

(43) Data obtained from statista.com, accessed on Feb 12, 2024. https://www.statista.com/statistics/418218/global-palladium-



*Chapter one references begin on page 86*

supply/#:~:text=In%202023%2C%20the%20global%20supply,than%206.4%20million%20ounces%20worldwide

(44) Kielhorn, J.; Melber, C.; Keller, D.; Mangelsdorf, I. Palladium – A Review of Exposure and Effects to Human Health. *Int. J. Hyg. Environ. Health* **2002**, *205*, 417–432.

(45) *Catalytic process improves speed and efficiency of medicines manufacture*. The Engineer. https://www.theengineer.co.uk/content/news/catalytic-process-improves-speed-and-efficiency-of-medicines-manufacture/ (accessed 2024-01-29)

(46) Ananikov, V. P. Nickel: The "Spirited Horse" of Transition Metal Catalysis. *ACS Catal.* **2015**, *5*, 1964–1971.

(47) Chernyshev, V. M.; Ananikov, V. P. Nickel and Palladium Catalysis: Stronger Demand than Ever. *ACS Catal.* **2022**, *12*, 1180–1200.

(48) Rosen, B. M.; Quasdorf, K. W.; Wilson, D. A.; Zhang, N.; Resmerita, A.-M.; Garg, N. K.; Percec, V. Nickel-Catalyzed Cross-Couplings Involving Carbon−Oxygen Bonds. *Chem. Rev.* **2011**, *111*, 1346–1416.

(49) (a) Martin, R.; Buchwald, S. L. Palladium-Catalyzed Suzuki−Miyaura Cross-Coupling Reactions Employing Dialkylbiaryl Phosphine Ligands. *Acc. Chem. Res.* **2008**, *41*, 1461–1473. (b) Paul C. J. Kamer, Piet W. N. M. van Leeuwen, ed. (2012). *Phosphorus(III)Ligands in Homogeneous Catalysis: Design and Synthesis.* New York: Wiley.

(50) Fortman, G. C.; Nolan, S. P. *N*-Heterocyclic Carbene (NHC) Ligands and Palladium in Homogeneous Cross-Coupling Catalysis: A Perfect Union. *Chem. Soc. Rev.* **2011**, *40*, 5151.

(51) Arduengo, A. J., III; Harlow, R. L.; Kline, M. A Stable Crystalline Carbene. *J. Am. Chem. Soc.* **1991**, *113*, 361–363.

(52) B. Gudimetla, V.; P. Joy, B.; Paul, S. Imidazolium-Based *N*-Heterocyclic Carbenes (NHCs) and Metal-Mediated Catalysis. In *Carbene*; IntechOpen, **2022**.

(53) Boit, T. B.; Bulger, A. S.; Dander, J. E.; Garg, N. K. Activation of C–O and C–N Bonds Using Non-Precious-Metal Catalysis. *ACS Catal.* **2020**, *10*, 12109–12126.

(54) Hopkinson, M. N.; Richter, C.; Schedler, M.; Glorius, F. An Overview of *N*-Heterocyclic Carbenes. *Nature* **2014**, *510*, 485–496.



*Chapter one references begin on page 86*

(55) Blanksby, S. J.; Ellison, G. B. Bond Dissociation Energies of Organic Molecules. *Acc. Chem. Res.* **2003**, *36*, 255–263.

(56) Iwasaki, T.; Kambe, N. Cross- and Multi-coupling Reactions Using Monofluoroalkanes. *Chem. Rec.* **2023**, *23*, 9.

(57) Luo, Y.-R. *Handbook of Bond Dissociation Energies in Organic Compounds*; CRC Press, 2002.

(58) (a) Sandmeyer, T. Ueber Die Ersetzung Der Amidgruppe Durch Chlor in Den Aromatischen Substanzen. *Ber. Dtsch. Chem. Ges.* **1884**, *17*, 1633–1635.

(59) Fetzner, S.; Lingens, F. Bacterial Dehalogenases: Biochemistry, Genetics, and Biotechnological Applications. *Microbiol. Rev.* **1994**, *58*, 641–685.

(60) Cornella, J.; Zarate, C.; Martin, R. Metal-Catalyzed Activation of Ethers via C–O Bond Cleavage: A New Strategy for Molecular Diversity. *Chem. Soc. Rev.* **2014**, *43*, 8081–8097.

(61) (a) Ben Halima, T.; Zhang, W.; Yalaoui, I.; Hong, X.; Yang, Y.-F.; Houk, K. N.; Newman, S. G. Palladium-Catalyzed Suzuki–Miyaura Coupling of Aryl Esters. *J. Am. Chem. Soc.* **2017**, *139*, 1311–1318. (b) Masson-Makdissi, J.; Vandavasi, J. K.; Newman, S. G. Switchable Selectivity in the Pd-Catalyzed Alkylative Cross-Coupling of Esters. *Org. Lett.* **2018**, *20*, 4094–4098. (c) Zheng, Y.-L.; Newman, S. G. Nickel-catalyzed Domino Heck-type Reactions Using Methyl Esters as Cross-coupling Electrophiles. *Angew. Chem. Int. Ed.* **2019**, *58*, 18159–18164. (d) Ben Halima, T.; Vandavasi, J. K.; Shkoor, M.; Newman, S. G. A Cross-Coupling Approach to Amide Bond Formation from Esters. *ACS Catal.* **2017**, *7*, 2176–2180. (e) Ben Halima, T.; Masson-Makdissi, J.; Newman, S. G. Nickel-catalyzed Amide Bond Formation from Methyl Esters. *Angew. Chem. Int. Ed.* **2018**, *57*, 12925–12929. (f) Zheng, Y.-L.; Newman, S. G. Methyl Esters as Cross-Coupling Electrophiles: Direct Synthesis of Amide Bonds. *ACS Catal.* **2019**, *9*, 4426–4433.

(62) (a) Isbrandt, E.; Vandavasi, J.; Zhang, W.; Jamshidi, M.; Newman, S. Catalytic Deuteration of Aldehydes with $D_2O$. *Synlett* **2017**, *28*, 2851–2854. (b) Vandavasi, J. K.; Hua, X.; Halima, H. B.; Newman, S. G. A Nickel-catalyzed carbonyl-Heck Reaction. *Angew. Chem. Int. Ed.* **2017**, *56*, 15441–15445. (c) Newman, S.; Vandavasi, J.



*Chapter one references begin on page 86*

A High-Throughput Approach to Discovery: Heck-Type Reactivity with Aldehydes. *Synlett* **2018**, *29*, 2081–2086.

(63) Verheyen, T.; van Turnhout, L.; Vandavasi, J. K.; Isbrandt, E. S.; De Borggraeve, W. M.; Newman, S. G. Ketone Synthesis by a Nickel-Catalyzed Dehydrogenative Cross-Coupling of Primary Alcohols. *J. Am. Chem. Soc.* **2019**, *141*, 6869–6874.

(64) Yu, D.-G.; Li, B.-J.; Shi, Z.-J. Exploration of New C−O Electrophiles in Cross-Coupling Reactions. *Acc. Chem. Res.* **2010**, *43*, 1486–1495.

(65) Oh-e, T.; Miyaura, N.; Suzuki, A. Palladium-Catalyzed Cross-Coupling Reaction of Aryl or Vinylic Triflates with Organoboron Compounds. *Synlett* **1990**, *1990*, 221–223.

(66) Percec, V.; Bae, J.-Y.; Hill, D. H. Aryl Mesylates in Metal Catalyzed Homocoupling and Cross-Coupling Reactions. 2. Suzuki-Type Nickel-Catalyzed Cross-Coupling of Aryl Arenesulfonates and Aryl Mesylates with Arylboronic Acids. *J. Org. Chem.* **1995**, *60*, 1060–1065.

(67) Nan, Y.; Yang, Z. Nickel-Catalyzed Cross-Couplings of Cyclohexenyl Phosphate and Arylboronic Acids. *Tetrahedron Lett.* **1999**, *40*, 3321–3324.

(68) Quasdorf, K. W.; Tian, X.; Garg, N. K. Cross-Coupling Reactions of Aryl Pivalates with Boronic Acids. *J. Am. Chem. Soc.* **2008**, *130*, 14422–14423.

(69) Quasdorf, K. W.; Riener, M.; Petrova, K. V.; Garg, N. K. Suzuki−Miyaura Coupling of Aryl Carbamates, Carbonates, and Sulfamates. *J. Am. Chem. Soc.* **2009**, *131*, 17748–17749.

(70) (a) Wenkert, E.; Michelotti, E. L.; Swindell, C. S. Nickel-Induced Conversion of Carbon-Oxygen into Carbon-Carbon Bonds. One-Step Transformations of Enol Ethers into Olefins and Aryl Ethers into Biaryls. *J. Am. Chem. Soc.* **1979**, *101*, 2246–2247. (b) Wenkert, E.; Michelotti, E. L.; Swindell, C. S.; Tingoli, M. Transformation of Carbon-Oxygen into Carbon-Carbon Bonds Mediated by Low-Valent Nickel Species. *J. Org. Chem.* **1984**, *49*, 4894–4899.

(71) Dankwardt, J. W. Nickel-catalyzed Cross-coupling of Aryl Grignard Reagents with Aromatic Alkyl Ethers: An Efficient Synthesis of Unsymmetrical Biaryls. *Angew. Chem. Int. Ed.* **2004**, *43*, 2428–2432.



*Chapter one references begin on page 86*

(72) Guan, B.-T.; Xiang, S.-K.; Wu, T.; Sun, Z.-P.; Wang, B.-Q.; Zhao, K.-Q.; Shi, Z.-J. Methylation of Arenes via Ni-Catalyzed Aryl C–O/F Activation. *Chem. Commun.* **2008**, *12*, 1437.

(73) (a) Xie, L.-G.; Wang, Z.-X. Cross-coupling of Aryl/Alkenyl Ethers with Aryl Grignard Reagents through Nickel-catalyzed C–O Activation. *Chemistry* **2011**, *17*, 4972–4975. (b) Xie, L.-G.; Wang, Z.-X. Nickel-catalyzed Cross-coupling of Non-activated or Functionalized Aryl Halides with Aryl Grignard Reagents. *Chemistry* **2010**, *16*, 10332–10336.

(74) Iglesias, M. J.; Prieto, A.; Nicasio, M. C. Kumada–Tamao–Corriu Coupling of Heteroaromatic Chlorides and Aryl Ethers Catalyzed by (IPr)Ni(Allyl)Cl. *Org. Lett.* **2012**, *14*, 4318–4321.

(75) Cornella, J.; Martin, R. Ni-Catalyzed Stereoselective Arylation of Inert C–O Bonds at Low Temperatures. *Org. Lett.* **2013**, *15*, 6298–6301.

(76) Guan, B.-T.; Xiang, S.-K.; Wang, B.-Q.; Sun, Z.-P.; Wang, Y.; Zhao, K.-Q.; Shi, Z.-J. Direct Benzylic Alkylation via Ni-Catalyzed Selective Benzylic $sp^3$ C−O Activation. *J. Am. Chem. Soc.* **2008**, *130*, 3268–3269.

(77) (a) Taylor, B. L. H.; Swift, E. C.; Waetzig, J. D.; Jarvo, E. R. Stereospecific Nickel-Catalyzed Cross-Coupling Reactions of Alkyl Ethers: Enantioselective Synthesis of Diarylethanes. *J. Am. Chem. Soc.* **2011**, *133*, 389–391. (b) Greene, M. A.; Yonova, I. M.; Williams, F. J.; Jarvo, E. R. Traceless Directing Group for Stereospecific Nickel-Catalyzed Alkyl−Alkyl Cross-Coupling Reactions. *Org. Lett.* **2012**, *14*, 4293–4296. (c) Taylor, B. L. H.; Harris, M. R.; Jarvo, E. R. Synthesis of Enantioenriched Triarylmethanes by Stereospecific Cross-coupling Reactions. *Angew. Chem. Int. Ed.* **2012**, *51*, 7790–7793. (d) Tollefson, E. J.; Hanna, L. E.; Jarvo, E. R. Stereospecific Nickel-Catalyzed Cross-Coupling Reactions of Benzylic Ethers and Esters. *Acc. Chem. Res.* **2015**, *48*, 2344–2353.

(78) Luo, S.; Yu, D.-G.; Zhu, R.-Y.; Wang, X.; Wang, L.; Shi, Z.-J. Fe-Promoted Cross Coupling of Homobenzylic Methyl Ethers with Grignard Reagents via sp3 C–O Bond Cleavage. *Chem. Commun.* **2013**, *49*, 7794.

(79) Wang, C.; Ozaki, T.; Takita, R.; Uchiyama, M. Aryl Ether as a Negishi Coupling Partner: An Approach for Constructing C–C Bonds under Mild Conditions. *Chemistry* **2012**, *18*, 3482–3485.



*Chapter one references begin on page 86*

(80) (a) Kakiuchi, F.; Usui, M.; Ueno, S.; Chatani, N.; Murai, S. Ruthenium-Catalyzed Functionalization of Aryl Carbon−Oxygen Bonds in Aromatic Ethers with Organoboron Compounds. *J. Am. Chem. Soc.* **2004**, *126*, 2706–2707. (b) Tobisu, M.; Shimasaki, T.; Chatani, N. Nickel-catalyzed Cross-coupling of Aryl Methyl Ethers with Aryl Boronic Esters. *Angew. Chem. Int. Ed.* **2008**, *47*, 4866–4869. (c) Shimasaki, T.; Konno, Y.; Tobisu, M.; Chatani, N. Nickel-Catalyzed Cross-Coupling Reaction of Alkenyl Methyl Ethers with Aryl Boronic Esters. *Org. Lett.* **2009**, *11*, 4890–4892.

(81) (a) Matsubara, R.; Jamison, T. F. Nickel-Catalyzed Allylic Substitution of Simple Alkenes. *J. Am. Chem. Soc.* **2010**, *132*, 6880–6881. (b) Harris, M. R.; Konev, M. O.; Jarvo, E. R. Enantiospecific Intramolecular Heck Reactions of Secondary Benzylic Ethers. *J. Am. Chem. Soc.* **2014**, *136*, 7825–7828.

(82) (a) Wiensch, E. M.; Todd, D. P.; Montgomery, J. Silyloxyarenes as Versatile Coupling Substrates Enabled by Nickel-Catalyzed C–O Bond Cleavage. *ACS Catal.* **2017**, *7*, 5568–5571. (b) Wiensch, E. M.; Montgomery, J. Nickel-catalyzed Amination of Silyloxyarenes through C–O Bond Activation. *Angew. Chem. Int. Ed.* **2018**, *57*, 11045–11049. (c) Pein, W. L.; Wiensch, E. M.; Montgomery, J. Nickel-Catalyzed Ipso-Borylation of Silyloxyarenes via C–O Bond Activation. *Org. Lett.* **2021**, *23*, 4588–4592.

(83) Hayashi, T.; Katsuro, Y.; Kumada, M. Nickel-Catalyzed Cross-Coupling of Silyl Enol Ethers with Grignard Reagents. Regio- and Stereocontrolled Synthesis of Olefins. *Tetrahedron Lett.* **1980**, *21*, 3915–3918.

(84) (a) Zhao, F.; Yu, D.-G.; Zhu, R.-Y.; Xi, Z.; Shi, Z.-J. Cross-Coupling of Aryl/Alkenyl Silyl Ethers with Grignard Reagents through Nickel-Catalyzed C–O Bond Activation. *Chem. Lett.* **2011**, *40*, 1001–1003. (b) Ohgi, A.; Nakao, Y. Selective Hydrogenolysis of Arenols with Hydrosilanes by Nickel Catalysis. *Chem. Lett*. **2016**, *45*, 45–47. (c) Yang, Z.-K.; Wang, D.-Y.; Minami, H.; Ogawa, H.; Ozaki, T.; Saito, T.; Miyamoto, K.; Wang, C.; Uchiyama, M. Cross-coupling of Organolithium with Ethers or Aryl Ammonium Salts by C−O or C−N Bond Cleavage. *Chem. Eur. J.*, **2016**, *22*, 15693–15699.

(85) Feskov, I. O.; Golub, B. O.; Vashchenko, B. V.; Levterov, V. V.; Kondratov, I. S.; Grygorenko, O. O.; Haufe, G. GABA Analogues and Related Mono-/Bifunctional Building



*Chapter one references begin on page 86*

Blocks Derived from the Fluorocyclobutane Scaffold. *European J. Org. Chem.* **2020**, *30*, 4755–4767.

(86) Qiu, Z.; Li, C.-J. Transformations of Less-Activated Phenols and Phenol Derivatives via C–O Cleavage. *Chem. Rev.* **2020**, *120*, 10454–10515.

(87) Campeau, L.-C.; Hazari, N. Cross-Coupling and Related Reactions: Connecting Past Success to the Development of New Reactions for the Future. *Organometallics* **2019**, *38*, 3–35.

(88) Ertl, P.; Schuhmann, T. A Systematic Cheminformatics Analysis of Functional Groups Occurring in Natural Products. *J. Nat. Prod.* **2019**, *82*, 1258–1263.

(89) Henkel, T.; Brunne, R. M.; Müller, H.; Reichel, F. Statistical Investigation into the Structural Complementarity of Natural Products and Synthetic Compounds. *Angew. Chem. Int. Ed.*, **1999**, *38*, 643–647.

(90) Rinaldi, R.; Jastrzebski, R.; Clough, M. T.; Ralph, J.; Kennema, M.; Bruijnincx, P. C. A.; Weckhuysen, B. M. Paving the Way for Lignin Valorisation: Recent Advances in Bioengineering, Biorefining and Catalysis. *Angew. Chem. Int. Ed.*, **2016**, *55*, 8164–8215.

(91) Bauer, E. B. Transition Metal Catalyzed Glycosylation Reactions – an Overview. *Org. Biomol. Chem.* **2020**, *18*, 9160–9180.

(92) Constable, D. J. C.; Dunn, P. J.; Hayler, J. D.; Humphrey, G. R.; Leazer, J. L., Jr; Linderman, R. J.; Lorenz, K.; Manley, J.; Pearlman, B. A.; Wells, A.; Zaks, A.; Zhang, T. Y. Key Green Chemistry Research Areas—a Perspective from Pharmaceutical Manufacturers. *Green Chem.* **2007**, *9*, 411–420.

(93) Price, C. C. The Alkylation of Aromatic Compounds by the Friedel-Crafts Method. *Organic Reactions*. Wiley March 15, 2011, pp 1–82.

(94) Emer, E.; Sinisi, R.; Capdevila, M. G.; Petruzziello, D.; De Vincentiis, F.; Cozzi, P. G. Direct Nucleophilic $S_N1$-type Reactions of Alcohols. *Eur. J. Org. Chem.*, **2011**, 647–666.

(95) Noji, M.; Ohno, T.; Fuji, K.; Futaba, N.; Tajima, H.; Ishii, K. Secondary Benzylation Using Benzyl Alcohols Catalyzed by Lanthanoid, Scandium, and Hafnium Triflate. *J. Org. Chem.* **2003**, *68*, 9340–9347.

(96) Noji, M.; Konno, Y.; Ishii, K. Metal Triflate-Catalyzed Cationic Benzylation and Allylation of 1,3-Dicarbonyl Compounds. *J. Org. Chem.* **2007**, *72*, 5161–5167.



*Chapter one references begin on page 86*

(97) Yasuda, M.; Somyo, T.; Baba, A. Direct Carbon–Carbon Bond Formation from Alcohols and Active Methylenes, Alkoxyketones, or Indoles Catalyzed by Indium Trichloride. *Angew. Chem. Int. Ed.*, **2006**, *45*, 793–796.

(98) Nishimoto, Y.; Onishi, Y.; Yasuda, M.; Baba, A. α-Alkylation of Carbonyl Compounds by Direct Addition of Alcohols to Enol Acetates. *Angew. Chem. Int. Ed.*, **2009**, *48*, 9131–9134.

(99) Rueping, M.; Nachtsheim, B. J.; Ieawsuwan, W. An Effective Bismuth-Catalyzed Benzylation of Arenes and Heteroarenes. *Adv. Synth. Catal.* **2006**, *348*, 1033–1037.

(100) Rueping, M.; Nachtsheim, B. J.; Kuenkel, A. Efficient Metal-Catalyzed Direct Benzylation and Allylic Alkylation of 2,4-Pentanediones. *Org. Lett.* **2007**, *9*, 825–828.

(101) Li, J.-H.; Liu, W.-J.; Yin, D.-L. An Efficient and Inexpensive Catalyst System for Friedel-Crafts Alkylation of Aromatic Compounds with Benzyl and Allyl Alcohols. *Synth. Commun.* **2004**, *34*, 3161–3165.

(102) Xu, X.; Jiang, R.; Zhou, X.; Liu, Y.; Ji, S.; Zhang, Y. Cerium Ammonium Nitrate: An Efficient Catalyst for Carbon–Carbon Bond Formation from Ferrocenyl Alcohol Substrate. *Tetrahedron* **2009**, *65*, 877–882.

(103) Liu, P. N.; Zhou, Z. Y.; Lau, C. P. The Lewis Acidic Ruthenium-complex-catalyzed Addition of *β*-diketones to Alcohols and Styrenes Is in Fact Brønsted Acid Catalyzed. *Chem. Eur. J.* **2007**, *13*, 8610–8619.

(104) Zaitsev, A. B.; Gruber, S.; Pregosin, P. S. Fast, Efficient Ru(IV)-Catalysed Regioselective Allylation of Indoles Using Allyl Alcohol (without Additives) under Mild Conditions. *Chem. Commun.* **2007**, 4692.

(105) Yadav, J. S.; Bhunia, D. C.; Vamshi Krishna, K.; Srihari, P. Niobium(V) Pentachloride: An Efficient Catalyst for C–, N–, O–, and S–Nucleophilic Substitution Reactions of Benzylic Alcohols. *Tetrahedron Lett.* **2007**, *48*, 8306–8310.

(106) Huang, W.; Wang, J.; Shen, Q.; Zhou, X. $Yb(OTf)_3$-Catalyzed Propargylation and Allenylation of 1,3-Dicarbonyl Derivatives with Propargylic Alcohols: One-Pot Synthesis of Multi-Substituted Furocoumarin. *Tetrahedron* **2007**, *63*, 11636–11643.

(107) Huang, W.; Shen, Q.-S.; Wang, J.-L.; Zhou, X.-G. Direct Substitution of the Hydroxy Group at the Allylic/Propargylic Position with Carbon- and Heteroatom-Centered Nucleophiles Catalyzed by $Yb(OTf)_3$. *Chin. J. Chem.* **2008**, *26*, 729–735.



*Chapter one references begin on page 86*

(108) Shen, M.-G.; Cai, C.; Yi, W.-B. Yb[N($SO_2C_8F_{17}$)$_2$]$_3$-Catalyzed Allylation of 1,3-Dicarbonyl Compounds with Allylic Alcohols in a Fluorous Biphase System. *J. Fluor. Chem.* **2009**, *130*, 595–599.

(109) Shimizu, I.; Khien, K. M.; Nagatomo, M.; Nakajima, T.; Yamamoto, A. Molybdenum-Catalyzed Aromatic Substitution with Olefins and Alcohols. *Chem. Lett.* **1997**, *26*, 851–852.

(110) Yamamoto, Y.; Itonaga, K. Versatile Friedel–Crafts-type Alkylation of Benzene Derivatives Using a Molybdenum Complex/*Ortho*-chloranil Catalytic System. *Chem. Eur. J.* **2008**, *14*, 10705–10715.

(111) Yang, H.; Fang, L.; Zhang, M.; Zhu, C. An Efficient Molybdenum(VI)-catalyzed Direct Substitution of Allylic Alcohols with Nitrogen, Oxygen, and Carbon Nucleophiles. *Eur. J. Org. Chem.*, **2009**, 666–672.

(112) Wang, G.-W.; Shen, Y.-B.; Wu, X.-L. Phosphotungstic Acid Catalyzed Direct Benzylation of *β*-dicarbonyl Compounds. *Eur. J. Org. Chem.*, **2008**, 4999–5004.

(113) El Gihani, M. T.; Heaney, H.; Shuhaibar, K. F. Scandium and Copper Triflate-Catalysed Acylaminoalkylation and Friedel-Crafts Alkylation Reactions. *Synlett* **1996**, 871–872.

(114) Tsuchimoto, T.; Tobita, K.; Hiyama, T.; Fukuzawa, S.-I. Scandium(III) Triflate Catalyzed Friedel-Crafts Alkylation with Benzyl and Allyl Alcohols. *Synlett* **1996**, 557–559.

(115) Tsuchimoto, T.; Tobita, K.; Hiyama, T.; Fukuzawa, S.-I. Scandium(III) Triflate-Catalyzed Friedel−Crafts Alkylation Reactions. *J. Org. Chem.* **1997**, *62*, 6997–7005.

(116) Piao, C.-R.; Zhao, Y.-L.; Han, X.-D.; Liu, Q. $AlCl_3$-Mediated Direct Carbon−Carbon Bond-Forming Reaction of *α*-Hydroxyketene-*S*,*S*-Acetals with Arenes and Synthesis of 3,4-Disubstituted Dihydrocoumarin Derivatives. *J. Org. Chem.* **2008**, *73*, 2264–2269.

(117) Rao, W.; Chan, P. W. H. Gold-Catalysed Allylic Alkylation of Aromatic and Heteroaromatic Compounds with Allylic Alcohols. *Org. Biomol. Chem.* **2008**, *6*, 2426.

(118) Sun, H.-B.; Li, B.; Chen, S.; Li, J.; Hua, R. An Efficient Synthesis of Unsymmetrical Diarylmethanes from the Dehydration of Arenes with Benzyl Alcohols Using $InCl_3 \cdot 4H_2O$/Acetylacetone Catalyst System. *Tetrahedron* **2007**, *63*, 10185–10188.



*Chapter one references begin on page 86*

(119) Radha Krishna, P.; Raja Sekhar, E.; Lakshmi Prapurna, Y. $InCl_3$ Catalyzed C–C Coupling of Aryl Alcohols and TosMIC. *Tetrahedron Lett.* **2007**, *48*, 9048–9050.

(120) Vicennati, P.; Cozzi, P. G. Facile Access to Optically Active Ferrocenyl Derivatives with Direct Substitution of the Hydroxy Group Catalyzed by Indium Tribromide. *Eur. J. Org. Chem.*, **2007**, 2248–2253.

(121) Cozzi, P. G.; Zoli, L. Nucleophilic Substitution of Ferrocenyl Alcohols "on Water." *Green Chem.* **2007**, *9*, 1292.

(122) Yadav, J. S.; Reddy, B. V. S.; Aravind, S.; Kumar, G. G. K. S. N.; Reddy, A. S. InBr3 as a Versatile and Highly Efficient Catalyst for the Synthesis of 3-Allyl- and 3-Benzylindoles. *Tetrahedron Lett.* **2007**, *48*, 6117–6120.

(123) Nishimoto, Y.; Kajioka, M.; Saito, T.; Yasuda, M.; Baba, A. Direct Coupling of Alcohols with Alkenylsilanes Catalyzed by Indium Trichloride or Bismuth Tribromide. *Chem. Commun.* **2008**, 6396.

(124) Iovel, I.; Mertins, K.; Kischel, J.; Zapf, A.; Beller, M. An Efficient and General Iron-catalyzed Arylation of Benzyl Alcohols and Benzyl Carboxylates. *Angew. Chem. Int. Ed.*, **2005**, *44*, 3913–3917.

(125) Yuan, Y.; Shi, Z.; Feng, X.; Liu, X. Solvent-free Reactions of Alcohols with *β*-dicarbonyl Compounds Catalyzed by Iron(III) Chloride. *Appl. Organomet. Chem.* **2007**, *21*, 958–964.

(126) Kischel, J.; Mertins, K.; Michalik, D.; Zapf, A.; Beller, M. A General and Efficient Iron-catalyzed Benzylation of 1,3-dicarbonyl Compounds. *Adv. Synth. Catal.* **2007**, *349*, 865–870.

(127) Jana, U.; Maiti, S.; Biswas, S. An $FeCl_3$-Catalyzed Highly C3-Selective Friedel–Crafts Alkylation of Indoles with Alcohols. *Tetrahedron Lett.* **2007**, *48*, 7160–7163.

(128) Jana, U.; Biswas, S.; Maiti, S. A Simple and Efficient $FeCl_3$-Catalyzed Direct Alkylation of Active Methylene Compounds with Benzylic and Allylic Alcohols under Mild Conditions. *Tetrahedron Lett.* **2007**, *48*, 4065–4069.

(129) Jana, U.; Biswas, S.; Maiti, S. Iron(III)-catalyzed Addition of Benzylic Alcohols to Aryl Alkynes – A New Synthesis of Substituted Aryl Ketones. *Eur. J. Org. Chem.*, **2008**, *2008*, 5798–5804.



*Chapter one references begin on page 86*

(130) Xiang, S.-K.; Zhang, L.-H.; Jiao, N. sp–$sp^3$ C–C Bond Formation via $Fe(OTf)_3$/TfOH Cocatalyzed Coupling Reaction of Terminal Alkynes with Benzylic Alcohols. *Chem. Commun.* **2009**, 6487.

(131) Zhang, X.; Rao, W.; Sally; Chan, P. W. H. Iron(III) Chloride-Catalysed Direct Nucleophilic α-Substitution of Morita-Baylis-Hillman Alcohols with Alcohols, Arenes, 1,3-Dicarbonyl Compounds, and Thiols. *Org. Biomol. Chem.* **2009**, *7*, 4186.

(132) Shushizadeh, M. R.; Kiany, M. Solvent-Free Alkylation of Dimethyl Malonate Using Benzyl Alcohols Catalyzed by $FeCl_3/SiO_2$. *Chin. Chem. Lett.* **2009**, *20*, 1068–1072.

(133) Biswas, S.; Maiti, S.; Jana, U. New and Efficient Iron Halide Mediated Synthesis of Alkenyl Halides through Coupling of Alkynes and Alcohols. *Eur. J. Org. Chem.*, **2009**, 2354–2359.

(134) Bandini, M.; Tragni, M. π-Activated Alcohols: An Emerging Class of Alkylating Agents for Catalytic Friedel–Crafts Reactions. *Org. Biomol. Chem.* **2009**, *7*, 1501.

(135) Bandini, M,; Umani-Ronchi, A. Catalytic Asymmetric Friedel–Crafts Alkylations. Wiley June 24, 2009.

(136) Rueping, M.; Nachtsheim, B. J. A Review of New Developments in the Friedel–Crafts Alkylation – From Green Chemistry to Asymmetric Catalysis. *Beilstein J. Org. Chem.* **2010**, *6*.

(137) Groves, J. K. The Friedel–Crafts Acylation of Alkenes. *Chem. Soc. Rev.* **1972**, *1*, 73–97.

(138) Heravi, M. M.; Zadsirjan, V.; Saedi, P.; Momeni, T. Applications of Friedel–Crafts Reactions in Total Synthesis of Natural Products. *RSC Adv.* **2018**, *8*, 40061–40163.

(139) Choudhury, J.; Podder, S.; Roy, S. Cooperative Friedel−Crafts Catalysis in Heterobimetallic Regime: Alkylation of Aromatics by π-Activated Alcohols. *J. Am. Chem. Soc.* **2005**, *127*, 6162–6163.

(140) Roy, S.; Podder, S.; Choudhury, J. Ir/Sn Dual-Reagent Catalysis towards Highly Selective Alkylation of Arenes and Heteroarenes with Benzyl Alcohols. *J. Chem. Sci.* **2008**, *120*, 429–439.

(141) Podder, S.; Choudhury, J.; Roy, S. Secondary Benzylation with Benzyl Alcohols Catalyzed by A High-Valent Heterobimetallic Ir−Sn Complex. *J. Org. Chem.* **2007**, *72*, 3129–3132.



*Chapter one references begin on page 86*

(142) Chatterjee, P. N.; Roy, S. Alkylation of 1,3-Dicarbonyl Compounds with Benzylic and Propargylic Alcohols Using Ir–Sn Bimetallic Catalyst: Synthesis of Fully Decorated Furans and Pyrroles. *Tetrahedron* **2011**, *67*, 4569–4577.

(143) Chatterjee, P. N.; Roy, S. Allylic Activation across an Ir–Sn Heterobimetallic Catalyst: Nucleophilic Substitution and Disproportionation of Allylic Alcohol. *Tetrahedron* **2012**, *68*, 3776–3785.

(144) Maity, A. K.; Chatterjee, P. N.; Roy, S. Multimetallic Ir–$Sn_3$-Catalyzed Substitution Reaction of π-Activated Alcohols with Carbon and Heteroatom Nucleophiles. *Tetrahedron* **2013**, *69*, 942–956.

(145) Das, D.; Pratihar, S.; Roy, U. K.; Mal, D.; Roy, S. First Example of a Heterobimetallic 'Pd–Sn' Catalyst for Direct Activation of Alcohol: Efficient Allylation, Benzylation and Propargylation of Arenes, Heteroarenes, Active Methylenes and Allyl-Si Nucleophiles. *Org. Biomol. Chem.* **2012**, *10*, 4537.

(146) Ben Othman, R.; Affani, R.; Tranchant, M.-J.; Antoniotti, S.; Dalla, V.; Duñach, E. *N*-acyliminium Ion Chemistry: Highly Efficient and Versatile Carbon–Carbon Bond Formation by Nucleophilic Substitution of Hydroxy Groups Catalyzed by $Sn(NTf_2)_4$. *Angew. Chem. Int. Ed.*, **2010**, *49*, 776–780.

(147) Kubo, R.; Yamamoto, H.; Nakata, K. Diastereoconvergent Dehydrative Nucleophilic Substitutions of Diastereomeric Diarylmethanols with 1,3-dicarbonyls Catalyzed by $SnBr_4$. *Eur. J. Org. Chem.*, **2019**, *2019*, 7394–7398.

(148) Liu, L.-Y.; Zhang, Y.; Huang, K.-M.; Chang, W.-X.; Li, J. 1,3-Dichloro-tetra-*n*-butyl-distannoxane: A New Application for Catalyzing the Direct Substitution of 9*H*-xanthen-9-ol at Room Temperature. *Appl. Organomet. Chem.* **2012**, *26*, 9–15.

(149) Masuyama, Y.; Hayashi, M.; Suzuki, N. $SnCl_2$-catalyzed Propargylic Substitution of Propargylic Alcohols with Carbon and Nitrogen Nucleophiles. *Eur. J. Org. Chem.*, **2013**, *2013*, 2914–2921.

(150) Suzuki, N.; Tsuchihashi, S.; Nakata, K. SnBr4-Promoted Friedel–Crafts Type Dehydrative Alkylation Reaction of Diarylmethanols with 2-Naphthol Derivatives. *Tetrahedron Lett.* **2016**, *57*, 1456–1459.

(151) Liang, D.; Wang, M.; Bekturhun, B.; Xiong, B.; Liu, Q. One-pot Synthesis of Polyfunctionalized 4*H*-chromenes and Dihydrocoumarins Based on Copper(II) Bromide-



*Chapter one references begin on page 86*

catalyzed C–C Coupling of Benzylic Alcohols with Ketene Dithioacetals. *Adv. Synth. Catal.* **2010**, *352*, 1593–1599.

(152) Shibata, M.; Ikeda, M.; Motoyama, K.; Miyake, Y.; Nishibayashi, Y. Enantioselective Alkylation of *β*-Keto Phosphonates by Direct Use of Diaryl Methanols as Electrophiles. *Chem. Commun.* **2012**, *48*, 9528.

(153) Zhang, L.; Zhu, Y.; Yin, G.; Lu, P.; Wang, Y. 3-Alkenylation or 3-Alkylation of Indole with Propargylic Alcohols: Construction of 3,4-Dihydrocyclopenta[*b*]Indole and 1,4-Dihydrocyclopenta[*b*]Indole in the Presence of Different Catalysts. *J. Org. Chem.* **2012**, *77*, 9510–9520.

(154) Huang, G.-B.; Wang, X.; Pan, Y.-M.; Wang, H.-S.; Yao, G.-Y.; Zhang, Y. Atom-Economical Chemoselective Synthesis of 1,4-Enynes from Terminal Alkenes and Propargylic Alcohols Catalyzed by $Cu(OTf)_2$. *J. Org. Chem.* **2013**, *78*, 2742–2745.

(155) Trillo, P.; Baeza, A. Copper-catalyzed Asymmetric Allylic Alkylation of β-keto Esters with Allylic Alcohols. *Adv. Synth. Catal.* **2017**, *359*, 1735–1741.

(156) Trillo, P.; Baeza, A.; Nájera, C. Copper-catalyzed Asymmetric Alkylation of β-keto Esters with Xanthydrols. *Adv. Synth. Catal.* **2013**, *355*, 2815–2821.

(157) Shcherbinin, V. A.; Shpuntov, P. M.; Konshin, V. V.; Butin, A. V. $CuBr_2$ Catalyzed Synthesis of 3-Furylphthalides. *Tetrahedron Lett.* **2016**, *57*, 1473–1475.

(158) Xu, C.-F.; Xu, M.; Yang, L.-Q.; Li, C.-Y. Synthesis of Allenes via Gold-Catalyzed Intermolecular Reaction of Propargylic Alcohols and Aromatic Compounds. *J. Org. Chem.* **2012**, *77*, 3010–3016.

(159) Mastandrea, M. M.; Mellonie, N.; Giacinto, P.; Collado, A.; Nolan, S. P.; Miscione, G. P.; Bottoni, A.; Bandini, M. Gold(I)-assisted α-allylation of Enals and Enones with Alcohols. *Angew. Chem. Int. Ed.*, **2015**, *54*, 14885–14889.

(160) Naveen, N.; Koppolu, S. R.; Balamurugan, R. Silver Hexafluoroantimonate-catalyzed Direct α-alkylation of Unactivated Ketones. *Adv. Synth. Catal.* **2015**, *357*, 1463–1473.

(161) Quillian, B.; Fields, A. E.; Chace, D.; Murrell Vickery, A.; Sharma, M.; Zurwell, D.; Bazemore, J. G.; Phan, L.; Thomas, D.; Padgett, C. W. Silver Triflate Mediated Dehydration of Benzylic Alcohols and Vinyl Hydrovinylation of Styrene. *Inorganica Chim. Acta* **2019**, *489*, 224–229.



*Chapter one references begin on page 86*

(162) Pennell, M. N.; Turner, P. G.; Sheppard, T. D. Gold- and Silver-catalyzed Reactions of Propargylic Alcohols in the Presence of Protic Additives. *Chem. Eur. J.* **2012**, *18*, 4748–4758.

(163) Hikawa, H.; Suzuki, H.; Azumaya, I. Au(III)/TPPMS-Catalyzed Benzylation of Indoles with Benzylic Alcohols in Water. *J. Org. Chem.* **2013**, *78*, 12128–12135.

(164) Hikawa, H.; Suzuki, H.; Yokoyama, Y.; Azumaya, I. Chemoselective Benzylation of Unprotected Anthranilic Acids with Benzhydryl Alcohols by Water-Soluble Au(III)/TPPMS in Water. *J. Org. Chem.* **2013**, *78*, 6714–6720.

(165) Debleds, O.; Gayon, E.; Vrancken, E.; Campagne, J.-M. Gold-Catalyzed Propargylic Substitutions: Scope and Synthetic Developments. *Beilstein J. Org. Chem.* **2011**, *7*, 866–877.

(166) Qin, Q.; Xie, Y.; Floreancig, P. E. Diarylmethane Synthesis through $Re_2O_7$-Catalyzed Bimolecular Dehydrative Friedel–Crafts Reactions. *Chem. Sci.* **2018**, *9*, 8528–8534.

(167) Nallagonda, R.; Rehan, M.; Ghorai, P. Chemoselective C-Benzylation of Unprotected Anilines with Benzyl Alcohols Using $Re_2O_7$ Catalyst. *J. Org. Chem.* **2014**, *79*, 2934–2943.

(168) Umeda, R.; Takahashi, Y.; Nishiyama, Y. Rhenium Complex-Catalyzed Coupling Reaction of Enol Acetates with Alcohols. *Tetrahedron Lett.* **2014**, *55*, 6113–6116.

(169) Umeda, R.; Takahashi, Y.; Yamamoto, T.; Iseki, H.; Osaka, I.; Nishiyama, Y. Rhenium-Catalyzed α-Alkylation of Enol Acetates with Alcohols or Ethers. *J. Organomet. Chem.* **2018**, *877*, 92–101.

(170) Capdevila, M. G.; Benfatti, F.; Zoli, L.; Stenta, M.; Cozzi, P. G. Merging Organocatalysis with an Indium(III)-mediated Process: A Stereoselective α-alkylation of Aldehydes with Allylic Alcohols. *Chem. Eur. J.* **2010**, *16*, 11237–11241.

(171) Sinisi, R.; Vita, M. V.; Gualandi, A.; Emer, E.; Cozzi, P. G. $S_N1$-type Reactions in the Presence of Water: Indium(III)-promoted Highly Enantioselective Organocatalytic Propargylation of Aldehydes. *Chem. Eur. J.* **2011**, *17*, 7404–7408.

(172) Guiteras Capdevila, M.; Emer, E.; Benfatti, F.; Gualandi, A.; Wilson, C. M.; Cozzi, P. G. Indium(III)-promoted Organocatalytic Enantioselective *α*-alkylation of Aldehydes with Benzylic and Benzhydrylic Alcohols. *Asian J. Org. Chem.* **2012**, *1*, 38–42.



*Chapter one references begin on page 86*

(173) Wu, C.; Wang, Z.; Hu, Z.; Zeng, F.; Zhang, X.-Y.; Cao, Z.; Tang, Z.; He, W.-M.; Xu, X.-H. Direct Synthesis of Alkenyl Iodides *via* Indium-Catalyzed Iodoalkylation of Alkynes with Alcohols and Aqueous HI. *Org. Biomol. Chem.* **2018**, *16*, 3177–3180.

(174) Xiao, J. Merging Organocatalysis with Transition Metal Catalysis: Highly Stereoselective α-Alkylation of Aldehydes. *Org. Lett.* **2012**, *14*, 1716–1719.

(175) Wu, L.; Jiang, R.; Yang, J.-M.; Wang, S.-Y.; Ji, S.-J. $In(OTf)_3$ Catalyzed C3-Benzylation of Indoles with Benzyl Alcohols in Water. *RSC Adv.* **2013**, *3*, 5459.

(176) Jadhav, A. P.; Ali, A.; Singh, R. P. Vinylogous Nucleophilic Substitution of the Hydroxy Group in Diarylmethanols with 3-propenyl-2-silyloxyindoles: Towards the Synthesis of *α*-alkylidene-*δ*-diaryl-2-oxindoles. *Adv. Synth. Catal.* **2017**, *359*, 1508–1514.

(177) Li, M.-M.; Zhang, Q.; Yue, H.-L.; Ma, L.; Ji, J.-X. Efficient $Fe/I_2$/NaI Mediated Synthesis of Alkenyl Iodides through Direct Coupling of Alcohols and Alkynes. *Tetrahedron Lett.* **2012**, *53*, 317–319.

(178) Yang, C.; Shen, C.; Li, H.; Tian, S. Ferric Chloride-Catalyzed Decarboxylative Alkylation of *β*-Keto Acids with Benzylic Alcohols. *Chin. Sci. Bull.* **2012**, *57*, 2377–2381.

(179) Pan, X.; Li, M.; Gu, Y. $Fe(OTf)_3$-catalyzed α-benzylation of Aryl Methyl Ketones with Electrophilic Secondary and Aryl Alcohols. *Chem. Asian J.* **2014**, *9*, 268–274.

(180) Che, G.; Bi, X.; Li, Q.; Wang, Y.; Fang, Z.; Liao, P.; Barry, B.-D. Iron(III)-Catalyzed Dehydration $C(sp^2)$-$C(sp^2)$ Coupling of Tertiary Propargyl Alcohols and α-Oxo Ketene Dithioacetals: A New Route to Gem-Bis(Alkylthio)-Substituted Vinylallenes. *Synthesis* **2013**, *45*, 609–614.

(181) Bu, X.; Hong, J.; Zhou, X. Synthesis of Substituted Indenes through Iron-catalyzed Annulation of Benzylic Alcohols with Alkynes. *Adv. Synth. Catal.* **2011**, *353*, 2111–2118.

(182) Khera, R. A.; Ullah, I.; Ahmad, R.; Riahi, A.; Hung, N. T.; Sher, M.; Villinger, A.; Fischer, C.; Langer, P. Synthesis of Functionalized Triarylmethanes by Combination of $FeCl_3$-Catalyzed Benzylations of Acetylacetone with [3+3] Cyclocondensations. *Tetrahedron* **2010**, *66*, 1643–1652.

(183) Liu, Z.-Q.; Zhang, Y.; Zhao, L.; Li, Z.; Wang, J.; Li, H.; Wu, L.-M. Iron-Catalyzed Stereospecific Olefin Synthesis by Direct Coupling of Alcohols and Alkenes with Alcohols. *Org. Lett.* **2011**, *13*, 2208–2211.



*Chapter one references begin on page 86*

(184) Liébert, C.; Brinks, M. K.; Capacci, A. G.; Fleming, M. J.; Lautens, M. Diastereoselective Intramolecular Friedel–Crafts Alkylation of Tetralins. *Org. Lett.* **2011**, *13*, 3000–3003.

(185) Sarkar, S.; Maiti, S.; Bera, K.; Jalal, S.; Jana, U. Highly Efficient Synthesis of Polysubstituted Fluorene via Iron-Catalyzed Intramolecular Friedel–Crafts Alkylation of Biaryl Alcohols. *Tetrahedron Lett.* **2012**, *53*, 5544–5547.

(186) Kazakova, A. N.; Iakovenko, R. O.; Muzalevskiy, V. M.; Boyarskaya, I. A.; Avdontceva, M. S.; Starova, G. L.; Vasilyev, A. V.; Nenajdenko, V. G. Trifluoromethylated Allyl Alcohols: Acid-Promoted Reactions with Arenes and Unusual 'Dimerization.' *Tetrahedron Lett.* **2014**, *55*, 6851–6855.

(187) Kazakova, A. N.; Iakovenko, R. O.; Boyarskaya, I. A.; Nenajdenko, V. G.; Vasilyev, A. V. Acid-Promoted Reaction of Trifluoromethylated Allyl Alcohols with Arenes. Stereoselective Synthesis of $CF_3$-Alkenes and $CF_3$-Indanes. *J. Org. Chem.* **2015**, *80*, 9506–9517.

(188) Thirupathi, P.; Kim, S. S. $Fe(ClO_4)_3 \cdot \times H_2O$-Catalyzed Direct C–C Bond Forming Reactions between Secondary Benzylic Alcohols with Different Types of Nucleophiles. *Tetrahedron* **2010**, *66*, 2995–3003.

(189) Peng, S.; Wang, L.; Wang, J. Iron-Catalyzed Ene-Type Propargylation of Diarylethylenes with Propargyl Alcohols. *Org. Biomol. Chem.* **2012**, *10*, 225–228.

(190) Trillo, P.; Baeza, A.; Nájera, C. Direct Nucleophilic Substitution of Free Allylic Alcohols in Water Catalyzed by $FeCl_3 \cdot 6H_2O$: Which Is the Real Catalyst? *ChemCatChem* **2013**, *5*, 1538–1542.

(191) Nokami, T.; Yamane, Y.; Oshitani, S.; Kobayashi, J.-K.; Matsui, S.-I.; Nishihara, T.; Uno, H.; Hayase, S.; Itoh, T. The *β*-Silyl Effect on the Memory of Chirality in Friedel–Crafts Alkylation Using Chiral *α*-Aryl Alcohols. *Org. Lett.* **2015**, *17*, 3182–3185.

(192) Fujihara, R.; Nakata, K. Chiral Inductive Diastereoconvergent Allylation Reactions of Allyltrimethylsilane and Diastereomixtures of Diarylmethanols Catalyzed by $FeCl_3$. *Eur. J. Org. Chem.*, **2018**, *2018*, 6566–6573.

(193) Li, Y.; Zhang, L.; Zhang, Z.; Xu, J.; Pan, Y.; Xu, C.; Liu, L.; Li, Z.; Yu, Z.; Li, H.; Xu, L. Regio- and Stereoselective Synthesis of 1,2,3-trisubstituted Indanes from



*Chapter one references begin on page 86*

Diarylmethanols and Allylamides through Iron(III) Chloride Hexahydrate. *Adv. Synth. Catal.* **2016**, *358*, 2148–2155.

(194) Chang, M.-Y.; Chen, Y.-H.; Cheng, Y.-C. $Fe(OTf)_3$-Mediated Synthesis of Sulfonyl Dihydropyrans. *Tetrahedron* **2016**, *72*, 518–524.

(195) Chanda, R.; Kar, A.; Das, A.; Chakraborty, B.; Jana, U. Iron-Catalyzed Carboarylation of Alkynes *via* Activation of π-Activated Alcohols: Rapid Synthesis of Substituted Benzofused Six-Membered Heterocycles. *Org. Biomol. Chem.* **2021**, *19*, 5155–5160.

(196) Chanda, R.; Chakraborty, B.; Rana, G.; Jana, U. Iron-catalyzed Functionalization of 3-benzylideneindoline through Tandem $Csp^2$–$Csp^3$ Bond Formation/Isomerization with π-activated Alcohols. *Eur. J. Org. Chem.*, **2020**, 61–65.

(197) Gandhi, S.; Baire, B. Fe(III)-catalyzed, Cyclizative Coupling between 2-alkynylbenzoates and Carbinols: Rapid Generation of Polycyclic Isocoumarins and Phthalides and Mechanistic Study. *Adv. Synth. Catal.* **2020**, *362*, 2651–2657.

(198) Wang, S.; Chai, Z.; Zhou, S.; Wang, S.; Zhu, X.; Wei, Y. A Novel Lewis Acid Catalyzed [3 + 3]-Annulation Strategy for the Syntheses of Tetrahydro-β-Carbolines and Tetrahydroisoquinolines. *Org. Lett.* **2013**, *15*, 2628–2631.

(199) Šolić, I.; Seankongsuk, P.; Loh, J. K.; Vilaivan, T.; Bates, R. W. Scandium as a Precatalyst for the Deoxygenative Allylation of Benzylic Alcohols. *Org. Biomol. Chem.* **2018**, *16*, 119–123.

(200) Ohta, K.; Kobayashi, T.; Tanabe, G.; Muraoka, O.; Yoshimatsu, M. Scandium-Catalyzed Propargylation of 1,3-Diketones with Propargyl Alcohols Bearing Sulfur or Selenium Functional Groups: Useful Transformation to Furans and Pyrans. *Chem. Pharm. Bull.* **2010**, *58*, 1180–1186.

(201) He., Y.; Tang, Z.; Hong, G.; Hu, C.; Zhou, C.; Wang, L. Scandium(III) Trifluoromethanesulfonate Catalyzed Reactions of 9-aryl-9-fluorenols with 1,1-diarylethylenes. *ChemistrySelect* **2020**, *5*, 6178–6181.

(202) Zhu, Y.; Colomer, I.; Thompson, A. L.; Donohoe, T. J. HFIP Solvent Enables Alcohols to Act as Alkylating Agents in Stereoselective Heterocyclization. *J. Am. Chem. Soc.* **2019**, *141*, 6489–6493.



*Chapter one references begin on page 86*

(203) Aynetdinova, D.; Jacques, R.; Christensen, K. E.; Donohoe, T. J. Alcohols as Efficient Intermolecular Initiators for a Highly Stereoselective Polyene Cyclisation Cascade. *Chem. Eur. J.* **2023**, *29*, e202203732.

(204) Cox, L.; Zhu, Y.; Smith, P. J.; Christensen, K. E.; Sidera Portela, M.; Donohoe, T. J. Alcohols as Alkylating Agents in the Cation-induced Formation of Nitrogen Heterocycles. *Angew. Chem. Int. Ed.*, **2022**, *61*, e202206800.

(205) Fan, G.-P.; Liu, Z.; Wang, G.-W. Efficient $ZnBr_2$-Catalyzed Reactions of Allylic Alcohols with Indoles, Sulfamides and Anilines under High-Speed Vibration Milling Conditions. *Green Chem.* **2013**, *15*, 1659.

(206) Wang, S.; Chai, Z.; Wei, Y.; Zhu, X.; Zhou, S.; Wang, S. Lewis Acid Catalyzed Cascade Reaction to Carbazoles and Naphthalenes via Dehydrative [3 + 3]-Annulation. *Org. Lett.* **2014**, *16*, 3592–3595.

(207) He, T.; Klare, H. F. T.; Oestreich, M. Catalytically Generated Meerwein's Salt-Type Oxonium Ions for Friedel–Crafts $C(sp^2)$–H Methylation with Methanol. *J. Am. Chem. Soc.* **2023**, *145*, 3795–3801.

(208) Jiang, R.; Yuan, C.-X.; Xu, X.-P.; Ji, S.-J. Nucleophilic Substitution of Ferrocenyl Alcohols Catalyzed by Bismuth(III) in Aqueous Medium at Room Temperature. *Appl. Organomet. Chem.* **2012**, *26*, 62–66.

(209) Dhiman, S.; Ramasastry, S. S. V. Taming Furfuryl Cations for the Synthesis of Privileged Structures and Novel Scaffolds. *Org. Biomol. Chem.* **2013**, *11*, 4299.

(210) Nammalwar, B.; Bunce, R. A. Friedel–Crafts Cyclization of Tertiary Alcohols Using Bismuth(III) Triflate. *Tetrahedron Lett.* **2013**, *54*, 4330–4332.

(211) Kolsi, L. E.; Yli-Kauhaluoma, J.; Moreira, V. M. Catalytic, Tunable, One-Step Bismuth(III) Triflate Reaction with Alcohols: Dehydration versus Dimerization. *ACS Omega* **2018**, *3*, 8836–8842.

(212) Chandra Sau, M.; Mandal, S.; Bhattacharjee, M. Monoallylation and Benzylation of Dicarbonyl Compounds with Alcohols Catalysed by a Cationic Cobalt(III) Compound. *RSC Adv.* **2021**, *11*, 9235–9245.

(213) Donald, C. P.; Boylan, A.; Nguyen, T. N.; Chen, P.-A.; May, J. A. Quaternary and Tertiary Carbon Centers Synthesized via Gallium-Catalyzed Direct Substitution of



*Chapter one references begin on page 86*

Unfunctionalized Propargylic Alcohols with Boronic Acids. *Org. Lett.* **2022**, *24*, 6767–6771.

(214) Zhang, X.; Qiu, R.; Zhou, C.; Yu, J.; Li, N.; Yin, S.; Xu, X. Synthesis and Structure of an Air-Stable Bis(Isopropylcyclopentadienyl) Zirconium Perfluorooctanesulfonate and Its Catalyzed Benzylation of 1,3-Dicarbonyl Derivatives with Alcohols. *Tetrahedron* **2015**, *71*, 1011–1017.

(215) Yang, G.-P.; Dilixiati, D.; Yang, T.; Liu, D.; Yu, B.; Hu, C.-W. Phosphomolybdic Acid as a Bifunctional Catalyst for Friedel–Crafts Type Dehydrative Coupling Reaction. *Appl. Organomet. Chem.* **2018**, *32*, 9.

(216) Zhou, F.; Cao, Z.-Y.; Zhang, J.; Yang, H.-B.; Zhou, J. A Highly Efficient Friedel–Crafts Reaction of 3-hydroxyoxindoles and Aromatic Compounds to 3,3-diaryl and 3-alkyl-3-aryloxindoles Catalyzed by $Hg(ClO_4)_2 \cdot 3H_2O$. *Chem. Asian J.* **2012**, *7*, 233–241.

(217) Wu, Y.-C.; Li, H.-J.; Liu, L.; Demoulin, N.; Liu, Z.; Wang, D.; Chen, Y.-J. Hafnium Triflate as an Efficient Catalyst for Direct Friedel–Crafts Reactions of Chromene Hemiacetals. *Adv. Synth. Catal.* **2011**, *353*, 907–912.

(218) Geiseler, O.; Müller, M.; Podlech, J. Synthesis of the Altertoxin III Framework. *Tetrahedron* **2013**, *69*, 3683–3689.

(219) Silveira, C. C.; Mendes, S. R.; Martins, G. M. Propargylation of Aromatic Compounds Using $Ce(OTf)_3$ as Catalyst. *Tetrahedron Lett.* **2012**, *53*, 1567–1570.

(220) Tsoung, J.; Krämer, K.; Zajdlik, A.; Liébert, C.; Lautens, M. Diastereoselective Friedel–Crafts Alkylation of Hydronaphthalenes. *J. Org. Chem.* **2011**, *76*, 9031–9045.

(221) Gohain, M.; Marais, C.; Bezuidenhoudt, B. C. B. An $Al(OTf)_3$-Catalyzed Environmentally Benign Process for the Propargylation of Indoles. *Tetrahedron Lett.* **2012**, *53*, 4704–4707.

(222) Croft, R. A.; Mousseau, J. J.; Choi, C.; Bull, J. A. Structurally Divergent Lithium Catalyzed Friedel–Crafts Reactions on Oxetan-3-ols: Synthesis of 3,3-diaryloxetanes and 2,3-dihydrobenzofurans. *Chem. Eur. J.* **2016**, *22*, 16271–16276.

(223) Hikawa, H.; Matsuura, Y.; Kikkawa, S.; Azumaya, I. Platinum(II)-Catalyzed Dehydrative C3-Benzylation of Electron-Deficient Indoles with Benzyl Alcohols. *Org. Chem. Front.* **2019**, *6*, 3150–3157.



*Chapter one references begin on page 86*

(224) Kinthada, L. K.; Ghosh, S.; Babu, K. N.; Sharique, M.; Biswas, S.; Bisai, A. Friedel–Crafts Alkylations of Electron-Rich Aromatics with 3-Hydroxy-2-Oxindoles: Scope and Limitations. *Org. Biomol. Chem.* **2014**, *12*, 8152–8173.

(225) Ghosh, S.; Kinthada, L. K.; Bhunia, S.; Bisai, A. Lewis Acid-Catalyzed Friedel–Crafts Alkylations of 3-Hydroxy-2-Oxindole: An Efficient Approach to the Core Structure of Azonazine. *Chem. Commun.* **2012**, *48*, 10132.

(226) Kinthada, L. K.; Ghosh, S.; De, S.; Bhunia, S.; Dey, D.; Bisai, A. Acid-Catalyzed Reactions of 3-Hydroxy-2-Oxindoles with Electron-Rich Substrates: Synthesis of 2-Oxindoles with All-Carbon Quaternary Center. *Org. Biomol. Chem.* **2013**, *11*, 6984.

(227) Uchuskin, M. G.; Makarov, A. S.; Butin, A. V. Catalytic Alkylation of Furans by π-Activated Alcohols. *Chem. Heterocycl. Compd.* **2014**, *50*, 791–806.

(228) Gualandi, A.; Mengozzi, L.; Cozzi, P. Stereoselective $S_N1$-Type Reaction of Enols and Enolates. *Synthesis* **2017**, *49*, 3433–3443.

(229) Qian, H.; Huang, D.; Bi, Y.; Yan, G. 2-Propargyl Alcohols in Organic Synthesis. *Adv. Synth. Catal.* **2019**, *361*, 3240–3280.

(230) Mhasni, O.; Elleuch, H.; Rezgui, F. Direct Nucleophilic Substitutions of Allylic Alcohols with 1,3-Dicarbonyl Compounds: Synthetic Design, Mechanistic Aspects and Applications. *Tetrahedron* **2022**, *111*, 132732.

(231) Nagao, K.; Ohmiya, H. Carbocation Generation by Organophotoredox Catalysis. *J. Synth. Org. Chem. Japan* **2021**, *79*, 1005–1012.

(232) Cozzi, P. G.; Gualandi, A.; Mengozzi, L.; Manoni, E.; Wilson, C. M. Direct Nucleophilic Substitution of Alcohols by Brønsted or Lewis Acids Activation: An Update. In *Methods in Pharmacology and Toxicology*; Springer New York: New York, NY, 2022; pp 123–154.

(233) Moran, J.; Dryzhakov, M.; Richmond, E. Recent Advances in Direct Catalytic Dehydrative Substitution of Alcohols. *Synthesis* **2016**, *48*, 935–959.

(234) Miyaura, N.; Yamada, K.; Suzuki, A. A New Stereospecific Cross-Coupling by the Palladium-Catalyzed Reaction of 1-Alkenylboranes with 1-Alkenyl or 1-Alkynyl Halides. *Tetrahedron Lett.* **1979**, *20*, 3437–3440.



*Chapter one references begin on page 86*

(235) Cao, Z.-C.; Yu, D.-G.; Zhu, R.-Y.; Wei, J.-B.; Shi, Z.-J. Direct Cross-Coupling of Benzyl Alcohols to Construct Diarylmethanes via Palladium Catalysis. *Chem. Commun.* **2015**, *51*, 2683–2686.

(236) Rao, H. S. P.; Rao, A. V. B. Copper-Mediated Arylation with Arylboronic Acids: Facile and Modular Synthesis of Triarylmethanes. *Beilstein J. Org. Chem.* **2016**, *12*, 496–504.

(237) Akkarasamiyo, S.; Margalef, J.; Samec, J. S. M. Nickel-Catalyzed Suzuki-Miyaura Cross-Coupling Reaction of Naphthyl and Quinolyl Alcohols with Boronic Acids. *Org. Lett.* **2019**, *21*, 4782–4787.

(238) Zhao, C.; Zha, G.-F.; Fang, W.-Y.; Rakesh, K. P.; Qin, H.-L. Construction of Di(Hetero)Arylmethanes through Pd-catalyzed Direct Dehydroxylative Cross-coupling of Benzylic Alcohols and Aryl Boronic Acids Mediated by Sulfuryl Fluoride ($SO_2F_2$). *Eur. J. Org. Chem.* **2019**, 1801–1807.

(239) Toupalas, G.; Thomann, G.; Schlemper, L.; Rivero-Crespo, M. A.; Schmitt, H. L.; Morandi, B. Pd-Catalyzed Direct Deoxygenative Arylation of Non-π-Extended Benzyl Alcohols with Boronic Acids via Transient Formation of Non-Innocent Isoureas. *ACS Catal.* **2022**, *12*, 8147–8154.

(240) Zhou, P.; Li, Y.; Xu, T. Molybdenum-Catalyzed Cross-Coupling of Benzyl Alcohols: Direct C–OH Bond Transformation via [2 + 2]-Type Addition and Elimination. *Org. Lett.* **2022**, *24*, 4218–4223.

(241) Kabalka, G. W.; Dong, G.; Venkataiah, B. Rhodium-Catalyzed Cross-Coupling of Allyl Alcohols with Aryl- and Vinylboronic Acids in Ionic Liquids. *Org. Lett.* **2003**, *5*, 893–895.

(242) Miura, T.; Takahashi, Y.; Murakami, M. Rhodium-Catalysed Substitutive Arylation of Cis-Allylic Diols with Arylboroxines. *Chem. Commun.* **2007**, 595–597.

(243) Gendrineau, T.; Genet, J.-P.; Darses, S. Rhodium-Catalyzed Functionalization of Sterically Hindered Alkenes. *Org. Lett.* **2010**, *12*, 308–310.

(244) Tsukamoto, H.; Sato, M.; Kondo, Y. Palladium(0)-catalyzed direct cross-coupling reaction of allyl alcohols with aryl- and vinyl-boronic acids. *Chem Commun.* **2004**, 1200-1201.



*Chapter one references begin on page 86*

(245) Manabe, K.; Nakada, K.; Aoyama, N.; Kobayashi, S. Cross–Coupling Reactions of Allylic Alcohols in Water. *Adv. Synth. Catal.* **2005**, *347*, 1499–1503.

(246) Kayaki, Y.; Koda, T.; Ikariya, T. A Highly Effective (Triphenyl Phosphite)Palladium Catalyst for a Cross−Coupling Reaction of Allylic Alcohols with Organoboronic Acids. *Eur. J. Org. Chem.*, **2004**, 4989–4993.

(247) Tsukamoto, H.; Uchiyama, T.; Suzuki, T.; Kondo, Y. Palladium(0)-Catalyzed Direct Cross-Coupling Reaction of Allylic Alcohols with Aryl- and Alkenylboronic Acids. *Org. Biomol. Chem.* **2008**, *6*, 3005.

(248) Jiménez-Aquino, A.; Ferrer Flegeau, E.; Schneider, U.; Kobayashi, S. Catalytic Intermolecular Allyl–Allyl Cross-Couplings between Alcohols and Boronates. *Chem. Commun.* **2011**, *47*, 9456.

(249) Nazari, S. H.; Bourdeau, J. E.; Talley, M. R.; Valdivia-Berroeta, G. A.; Smith, S. J.; Michaelis, D. J. Nickel-Catalyzed Suzuki Cross Couplings with Unprotected Allylic Alcohols Enabled by Bidentate *N*-Heterocyclic Carbene (NHC)/Phosphine Ligands. *ACS Catal.* **2018**, *8*, 86–89.

(250) Zhang, Y.; Yin, S.-C.; Lu, J.-M. N-Heterocyclic Carbene-Palladium(II)-1-Methylimidazole Complex Catalyzed Allyl-Aryl Coupling of Allylic Alcohols with Arylboronic Acids in Neat Water. *Tetrahedron* **2015**, *71*, 544–549.

(251) Vanelle, P.; Tabélé, C.; Curti, C.; Primas, N.; Kabri, Y.; Remusat, V. An Efficient Method for the Synthesis of 2-Methylallyl Alkenes by Cross-Coupling Reactions. *Synthesis* **2015**, *47*, 3339–3346.

(252) Tabélé, C.; Curti, C.; Kabri, Y.; Primas, N.; Vanelle, P. Cross-Coupling Synthesis of Methylallyl Alkenes: Scope Extension and Mechanistic Study. *Molecules* **2015**, *20*, 22890–22899.

(253) Wang, G.; Gan, Y.; Liu, Y. Nickel-catalyzed Direct Coupling of Allylic Alcohols with Organoboron Reagents. *Chin. J. Chem.* **2018**, *36*, 916–920.

(254) Wang, Y.-B.; Liu, B.-Y.; Bu, Q.; Dai, B.; Liu, N. In Situ Ring-closing Strategy for Direct Synthesis of *N*-heterocyclic Carbene Nickel Complexes and Their Application in Coupling of Allylic Alcohols with Aryl Boronic Acids. *Adv. Synth. Catal.* **2020**, *362*, 2930–2940.



*Chapter one references begin on page 86*

(255) Tran, H. N.; Nguyen, C. M.; Koeritz, M. T.; Youmans, D. D.; Stanley, L. M. Nickel-Catalyzed Arylative Substitution of Homoallylic Alcohols. *Chem. Sci.* **2022**, *13*, 11607–11613. Kinetic Resolution of Morita–Baylis–Hillman Adducts Achieved by N–Ar Axially Chiral Pd-Complexes Catalyzed Asymmetric Allylation. *Chem. Commun.* **2011**, *47*, 12813.

(256) Ye, J.; Zhao, J.; Xu, J.; Mao, Y.; Zhang, Y. J. Pd-Catalyzed Stereospecific Allyl–Aryl Coupling of Allylic Alcohols with Arylboronic Acids. *Chem. Commun.* **2013**, *49*, 9761.

(257) Wu, H.-B.; Ma, X.-T.; Tian, S.-K. Palladium-Catalyzed Stereospecific Cross-Coupling of Enantioenriched Allylic Alcohols with Boronic Acids. *Chem. Commun.* **2014**, *50*, 219–221.

(258) Roggen, M.; Carreira, E. M. Enantioselective Allylic Etherification: Selective Coupling of Two Unactivated Alcohols. *Angew. Chem. Int. Ed.*, **2011**, *50*, 5568–5571.

(259) Hamilton, J. Y.; Sarlah, D.; Carreira, E. M. Iridium-Catalyzed Enantioselective Allylic Vinylation. *J. Am. Chem. Soc.* **2013**, *135*, 994–997.

(260) Hamilton, J. Y.; Sarlah, D.; Carreira, E. M. Iridium-catalyzed Enantioselective Allylic Alkynylation. *Angew. Chem. Int. Ed.*, **2013**, *52*, 7532–7535.

(261) Zheng, Y.; Yue, B.-B.; Wei, K.; Yang, Y.-R. Iridium-Catalyzed Enantioselective Allyl–Allyl Cross-Coupling of Racemic Allylic Alcohols with Allylboronates. *Org. Lett.* **2018**, *20*, 8035–8038.

(262) Guo, J.; Ma, H.-R.; Xiong, W.-B.; Fan, L.; Zhou, Y.-Y.; Wong, H. N. C.; Cui, J.-F. Iridium-Catalyzed Enantioselective Alkynylation and Kinetic Resolution of Alkyl Allylic Alcohols. *Chem. Sci.* **2022**, *13*, 13914–13921.

(263) Qu, J.-P.; Helmchen, G.; Yang, Z.-P.; Zhang, W.; You, S.-L. Iridium-Catalyzed, Enantioselective, Allylic Alkylations with Carbon Nucleophiles. *Organic Reactions*. Wiley July 26, **2019**, pp 423–632.

(264) Cheng, Q.; Tu, H.-F.; Zheng, C.; Qu, J.-P.; Helmchen, G.; You, S.-L. Iridium-Catalyzed Asymmetric Allylic Substitution Reactions. *Chem. Rev.* **2019**, *119*, 1855–1969.

(265) Sawano, T.; Takeuchi, R. Recent Advances in Iridium-Catalyzed Enantioselective Allylic Substitution Using Phosphoramidite-Alkene Ligands. *Catal. Sci. Technol*. **2022**, *12*, 4100–4112.



*Chapter one references begin on page 86*

(266) Yoshida, M.; Gotou, T.; Ihara, M. Palladium-Catalyzed Direct Coupling Reaction of Propargylic Alcohols with Arylboronic Acids. *Tetrahedron Lett.* **2004**, *45*, 5573–5575.

(267) Al-Jawaheri, Y.; Kimber, M. C. Synthesis of 1,3-Dienes via a Sequential Suzuki–Miyaura Coupling/Palladium-Mediated Allene Isomerization Sequence. *Org. Lett.* **2016**, *18*, 3502–3505.

(268) Green, N. J.; Willis, A. C.; Sherburn, M. S. Direct Cross-couplings of Propargylic Diols. *Angew. Chem. Int. Ed.*, **2016**, *55*, 9244–9248.

(269) Qin, A.; Qian, H.; Chen, Q.; Ma, S. Palladium-catalyzed Coupling of Propargylic Alcohols with Boronic Acids under Ambient Conditions. *Chin. J. Chem.* **2020**, *38*, 372–382.

(270) Liu, T.; Liu, Y.; Guo, W. Alkynyl-Induced Construction of Stereodefined Polysubstituted Conjugated Enynes *via* Pd-Catalyzed Allylic Arylations. *Org. Chem. Front.* **2022**, *9*, 3312–3316.

(271) Liu, N.; Zhi, Y.; Yao, J.; Xing, J.; Lu, T.; Dou, X. Rhodium(I)-catalyzed Arylation/Dehydroxylation of *Tert*-propargylic Alcohols Leading to Tetrasubstituted Allenes. *Adv. Synth. Catal.* **2018**, *360*, 642–646.

(272) Xing, J.; Zhu, Y.; Lin, X.; Liu, N.; Shen, Y.; Lu, T.; Dou, X. Rhodium-catalyzed Arylative Transformations of Propargylic Diols: Dual Role of the Rhodium Catalyst. *Adv. Synth. Catal.* **2018**, *360*, 1595–1599.

(273) Liu, N.; Yao, J.; Yin, L.; Lu, T.; Tian, Z.; Dou, X. Rhodium-Catalyzed Expeditious Synthesis of Indenes from Propargyl Alcohols and Organoboronic Acids by Selective 1,4-Rhodium Migration over β-Oxygen Elimination. *ACS Catal.* **2019**, *9*, 6857–6863.

(274) Zhu, H.; Zhou, Q.; Liu, N.; Xing, J.; Yao, W.; Dou, X. Relay Rhodium(I)/Acid Catalysis for Rapid Access to Benzo-2*H*-pyrans and Benzofurans. *Adv. Synth. Catal.* **2022**, *364*, 1162–1167.

(275) Yoshida, M.; Gotou, T.; Ihara, M. Palladium-Catalysed Coupling Reaction of Allenic Alcohols with Aryl- and Alkenylboronic Acids. *Chem. Commun.* **2004**, 1124.

(276) Yoshida, M.; Shoji, Y.; Shishido, K. Total Syntheses of Enokipodins A and B Utilizing Palladium-Catalyzed Addition of an Arylboronic Acid to an Allene. *Org. Lett.* **2009**, *11*, 1441–1443.



*Chapter one references begin on page 86*

(277) Liu, T.; Dong, J.; Cao, S.-J.; Guo, L.-C.; Wu, L. Suzuki–Miyaura Coupling of Phosphinoyl-α-Allenic Alcohols with Arylboronic Acids Catalyzed by a Palladium Complex "on Water": An Efficient Method to Generate Phosphinoyl 1,3-Butadienes and Derivatives. *RSC Adv.* **2014**, *4*, 61722–61726.

(278) Miura, T.; Shimizu, H.; Igarashi, T.; Murakami, M. Stereoselective Synthesis of Vinyl-Substituted (*Z*)-Stilbenes by Rhodium-Catalysed Addition of Arylboronic Acids to Allenic Alcohols. *Org. Biomol. Chem.* **2010**, *8*, 4074.

(279) Yu, D.-G.; Wang, X.; Zhu, R.-Y.; Luo, S.; Zhang, X.-B.; Wang, B.-Q.; Wang, L.; Shi, Z.-J. Direct Arylation/Alkylation/Magnesiation of Benzyl Alcohols in the Presence of Grignard Reagents via Ni-, Fe-, or Co-Catalyzed $sp^3$ C–O Bond Activation. *J. Am. Chem. Soc.* **2012**, *134*, 14638–14641.

(280) Yang, B.; Wang, Z.-X. Nickel-Catalyzed Alkylation or Reduction of Allylic Alcohols with Alkyl Grignard Reagents. *J. Org. Chem.* **2020**, *85*, 4772–4784.

(281) Yang, B.; Wang, Z.-X. Nickel-Catalyzed Cross-Coupling of Allyl Alcohols with Aryl- or Alkenylzinc Reagents. *J. Org. Chem.* **2017**, *82*, 4542–4549.

(282) He, X.-Y.; Wang, Z.-X. Synthesis of 1,4-Enynes *via* Nickel-Catalyzed Cross-Coupling of Allylic Alcohols with Alkynylzinc Reagents. *Chem. Commun.* **2021**, *57*, 11988–11991.

(283) Hamilton, J. Y.; Hauser, N.; Sarlah, D.; Carreira, E. M. Iridium-catalyzed Enantioselective Allyl–Allylsilane Cross-coupling. *Angew. Chem. Int. Ed.*, **2014**, *53*, 10759–10762.

(284) Ackerman, L. K. G.; Anka-Lufford, L. L.; Naodovic, M.; Weix, D. J. Cobalt Co-Catalysis for Cross-Electrophile Coupling: Diarylmethanes from Benzyl Mesylates and Aryl Halides. *Chem. Sci.* **2015**, *6*, 1115–1119.

(285) Ma, W.-Y.; Han, G.-Y.; Kang, S.; Pang, X.; Liu, X.-Y.; Shu, X.-Z. Cobalt-Catalyzed Enantiospecific Dynamic Kinetic Cross-Electrophile Vinylation of Allylic Alcohols with Vinyl Triflates. *J. Am. Chem. Soc.* **2021**, *143*, 15930–15935.

(286) Suga, T.; Ukaji, Y. Nickel-Catalyzed Cross-Electrophile Coupling between Benzyl Alcohols and Aryl Halides Assisted by Titanium Co-Reductant. *Org. Lett.* **2018**, *20*, 7846–7850.



*Chapter one references begin on page 86*

(287) Suga, T.; Takahashi, Y.; Ukaji, Y. One-shot Radical Cross Coupling between Benzyl Alcohols and Alkenyl Halides Using Ni/Ti/Mn System. *Adv. Synth. Catal.* **2020**, *362*, 5622–5626.

(288) Sumiyama, K.; Toriumi, N.; Iwasawa, N. Use of Isopropyl Alcohol as a Reductant for Catalytic Dehydoxylative Dimerization of Benzylic Alcohols Utilizing Ti−O Bond Photohomolysis. *Eur. J. Org. Chem.*, **2021**, 2474–2478.

(289) Peng, J.-B.; Wang, L.-C.; Wu, X.-F. Palladium-Catalyzed Carbonylative/Decarboxylative Cross-Coupling of α-Bromo-Ketones with Allylic Alcohols to γ,δ-Unsaturated Ketones. *Tetrahedron Lett.* **2019**, *60*, 150991.

(290) Zhou, X.; Zhang, G.; Huang, R.; Huang, H. Palladium-Catalyzed Allyl–Allyl Reductive Coupling of Allylamines or Allylic Alcohols with $H_2$ as Sole Reductant. *Org. Lett.* **2021**, *23*, 365–369.

(291) Jia, X.-G.; Guo, P.; Duan, J.; Shu, X.-Z. Dual Nickel and Lewis Acid Catalysis for Cross-Electrophile Coupling: The Allylation of Aryl Halides with Allylic Alcohols. *Chem. Sci.* **2018**, *9*, 640–645.

(292) Guo, P.; Wang, K.; Jin, W.-J.; Xie, H.; Qi, L.; Liu, X.-Y.; Shu, X.-Z. Dynamic Kinetic Cross-Electrophile Arylation of Benzyl Alcohols by Nickel Catalysis. *J. Am. Chem. Soc.* **2021**, *143*, 513–523.

(293) Shu, X.-Z.; Pan, F.-F.; Guo, P.; Huang, X. Synthesis of Dibenzyls by Nickel-Catalyzed Homocoupling of Benzyl Alcohols. *Synthesis* **2021**, *53*, 3094–3100.

(294) Kumar Chenniappan, V.; Peck, D.; Rahaim, R. Nickel Catalyzed Deoxygenative Cross-Coupling of Benzyl Alcohols with Aryl-Bromides. *Tetrahedron Lett.* **2020**, *61*, 151729.

(295) Gan, Y.; Hu, H.; Liu, Y. Nickel-Catalyzed Homo- and Cross-Coupling of Allyl Alcohols via Allyl Boronates. *Org. Lett.* **2020**, *22*, 4418–4423.

(296) Selander, N.; Szabó, K. J. Single-Pot Triple Catalytic Transformations Based on Coupling of in Situ Generated Allyl Boronates with in Situ Hydrolyzed Acetals. *Chem. Commun.* **2008**, 3420.

(297) Tercenio, Q. D.; Alexanian, E. J. Stereospecific Nickel-Catalyzed Reductive Cross-Coupling of Alkyl Tosylate and Allyl Alcohol Electrophiles. *Org. Lett.* **2021**, *23*, 7215–7219.



*Chapter one references begin on page 86*

(298) Wang, H.; Yang, M.; Wang, Y.; Man, X.; Lu, X.; Mou, Z.; Luo, Y.; Liang, H. Nickel-Catalyzed Reductive $Csp^2$–$Csp^3$ Cross Coupling Using Phosphonium Salts. *Org. Lett.* **2021**, *23*, 8183–8188.

(299) Yu, H.; Wang, Z.-X. Nickel-Catalyzed Cross-Electrophile Coupling of Aryl Chlorides with Allylic Alcohols. *Org. Biomol. Chem.* **2021**, *19*, 9723–9731.

(300) Liu, J.; Ye, Y.; Sessler, J. L.; Gong, H. Cross-Electrophile Couplings of Activated and Sterically Hindered Halides and Alcohol Derivatives. *Acc. Chem. Res.* **2020**, *53*, 1833–1845.

(301) Nicholas, K. M.; Bandari, C. Deoxygenative Transition-Metal-Promoted Reductive Coupling and Cross-Coupling of Alcohols and Epoxides. *Synthesis* **2021**, *53*, 267–278.

(302) Lee, D.-H.; Kwon, K.-H.; Yi, C. S. Selective Catalytic C–H Alkylation of Alkenes with Alcohols. *Science* **2011**, *333*, 1613–1616.

(303) Poater, A.; Vummaleti, S. V. C.; Polo, A.; Cavallo, L. Clean and Selective Catalytic C–H Alkylation of Alkenes with Environmental Friendly Alcohols. *Mol. Catal.* **2017**, *435*, 69–75.

(304) Poater, A.; Vummaleti, S. V. C.; Polo, A.; Cavallo, L. Mechanistic Insights of a Selective C–H Alkylation of Alkenes by a Ru-Based Catalyst and Alcohols. *ChemistySelect* **2016**, *1*, 4218–4228.

(305) Lee, D.-H.; Kwon, K.-H.; Yi, C. S. Dehydrative C–H Alkylation and Alkenylation of Phenols with Alcohols: Expedient Synthesis for Substituted Phenols and Benzofurans. *J. Am. Chem. Soc.* **2012**, *134*, 7325–7328.

(306) Kim, J.; Lee, D.-H.; Kalutharage, N.; Yi, C. S. Selective Catalytic Synthesis of Unsymmetrical Ethers from the Dehydrative Etherification of Two Different Alcohols. *ACS Catal.* **2014**, *4*, 3881–3885.

(307) Kalutharage, N.; Yi, C. S. Chemoselective Formation of Unsymmetrically Substituted Ethers from Catalytic Reductive Coupling of Aldehydes and Ketones with Alcohols in Aqueous Solution. *Org. Lett.* **2015**, *17*, 1778–1781.

(308) Lee, H.; Yi, C. S. Catalytic Synthesis of Substituted Indoles and Quinolines from the Dehydrative C–H Coupling of Arylamines with 1,2- and 1,3-Diols. *Organometallics* **2016**, *35*, 1973–1977.



*Chapter one references begin on page 86*

(309) Zheng, X.; Dai, X.-J.; Yuan, H.-Q.; Ye, C.-X.; Ma, J.; Huang, P.-Q. Umpolung of Hemiaminals: Titanocene-catalyzed Dehydroxylative Radical Coupling Reactions with Activated Alkenes. *Angew. Chem. Int. Ed.*, **2013**, *52*, 3494–3498.

(310) Li, Z.; Sun, W.; Wang, X.; Li, L.; Zhang, Y.; Li, C. Electrochemically Enabled, Nickel-Catalyzed Dehydroxylative Cross-Coupling of Alcohols with Aryl Halides. *J. Am. Chem. Soc.* **2021**, *143*, 3536–3543.

(311) Lin, Q.; Ma, G.; Gong, H. Ni-Catalyzed Formal Cross-Electrophile Coupling of Alcohols with Aryl Halides. *ACS Catal.* **2021**, *11*, 14102–14109.

(312) Chi, B. K.; Widness, J. K.; Gilbert, M. M.; Salgueiro, D. C.; Garcia, K. J.; Weix, D. J. In-Situ Bromination Enables Formal Cross-Electrophile Coupling of Alcohols with Aryl and Alkenyl Halides. *ACS Catal.* **2022**, *12*, 580–586.

(313) Xie, H.; Guo, J.; Wang, Y.-Q.; Wang, K.; Guo, P.; Su, P.-F.; Wang, X.; Shu, X.-Z. Radical Dehydroxylative Alkylation of Tertiary Alcohols by Ti Catalysis. *J. Am. Chem. Soc.* **2020**, *142*, 16787–16794.

(314) Xie, H.; Wang, S.; Wang, Y.; Guo, P.; Shu, X.-Z. Ti-Catalyzed Reductive Dehydroxylative Vinylation of Tertiary Alcohols. *ACS Catal.* **2022**, *12*, 1018–1023.

(315) McCombie, S. W.; Motherwell, W. B.; Tozer, M. J. The Barton-McCombie Reaction. *Organic Reactions*. Wiley January 25, **2012**, pp 161–432.

(316) Guo, H.-M.; He, B.-Q.; Wu, X. Direct Photoexcitation of Xanthate Anions for Deoxygenative Alkenylation of Alcohols. *Org. Lett.* **2022**, *24*, 3199–3204.

(317) Li, X.; Si, W.; Liu, Z.; Qian, H.; Wang, T.; Leng, S.; Sun, J.; Jiao, Y.; Zhang, X. Visible-Light-Promoted Desulfurative Alkylation of Alkyl Thianthrenium Salts with Activated Olefins. *Org. Lett.* **2022**, *24*, 4070–4074.

(318) Guo, H.-M.; Wu, X. Selective Deoxygenative Alkylation of Alcohols via Photocatalytic Domino Radical Fragmentations. *Nat. Commun.* **2021**, *12*, 5365.

(319) Nanjo, T.; Matsugasako, T.; Maruo, Y.; Takemoto, Y. Photocatalytic C–O Bond Cleavage of Alcohols Using Xanthate Salts. *Org. Lett.* **2022**, *24*, 359–363.

(320) Cai, A.; Yan, W.; Liu, W. Aryl Radical Activation of C–O Bonds: Copper-Catalyzed Deoxygenative Difluoromethylation of Alcohols. *J. Am. Chem. Soc.* **2021**, *143*, 9952–9960.



*Chapter one references begin on page 86*

(321) Dong, Z.; MacMillan, D. W. C. Metallaphotoredox-Enabled Deoxygenative Arylation of Alcohols. *Nature* **2021**, *598*, 451–456.

(322) Sakai, H. A.; MacMillan, D. W. C. Nontraditional Fragment Couplings of Alcohols and Carboxylic Acids: C($sp^3$)–C($sp^3$) Cross-Coupling via Radical Sorting. *J. Am. Chem. Soc.* **2022**, *144*, 6185–6192.

(323) Wang, J. Z.; Sakai, H. A.; MacMillan, D. W. C. Alcohols as Alkylating Agents: Photoredox-catalyzed Conjugate Alkylation via in Situ Deoxygenation. *Angew. Chem. Int. Ed.*, **2022**, *61*, e202207150.

(324) Intermaggio, N. E.; Millet, A.; Davis, D. L.; MacMillan, D. W. C. Deoxytrifluoromethylation of Alcohols. *J. Am. Chem. Soc.* **2022**, *144*, 11961–11968.

(325) Döben, N.; Reimler, J.; Studer, A. Cooperative NHC/Photoredox Catalysis: Three Component Radical Coupling of Aroyl Fluorides, Styrenes and Alcohols. *Adv. Synth. Catal.* **2022**, *364*, 3348–3353.

(326) Ma, X.; Wang, Q.; Wu, J.; Zhang, L.; Sun, A.; Wang, Z. NHC–Alcohol Adduct-Mediated Photocatalytic Deoxygenation for the Synthesis of 6-Phenanthridine Derivatives. *Org. Biomol. Chem.* **2022**, *20*, 5393–5396.

(327) Jefferies, L. R.; Cook, S. P. Iron-Catalyzed Arene Alkylation Reactions with Unactivated Secondary Alcohols. *Org. Lett.* **2014**, *16*, 2026–2029.

(328) Pan, A.; Chojnacka, M.; Crowley, R.; Göttemann, L.; Haines, B. E.; Kou, K. G. M. Synergistic Brønsted/Lewis Acid Catalyzed Aromatic Alkylation with Unactivated Tertiary Alcohols or Di-*Tert*-Butylperoxide to Synthesize Quaternary Carbon Centers. *Chem. Sci.* **2022**, *13*, 3539–3548.

(329) Eisch, J. J.; Hallenbeck, L. E.; Lucarelli, M. A. Desulphurization and Denitrogenation of SRC Liquids by Transition Metals on Solid Supports. *Fuel* **1985**, *64*, 440–442.

(330) (a) DeVor, R.; Carvalho-Knighton, K.; Aitken, B.; Maloney, P.; Holland, E.; Talalaj, L.; Elsheimer, S.; Clausen, C. A.; Geiger, C. L. Mechanism of the Degradation of Individual PCB Congeners Using Mechanically Alloyed Mg/Pd in Methanol. *Chemosphere* **2009**, *76*, 761–766. (b) Wu, B.-Z.; Chen, H.-Y.; Wang, S. J.; Wai, C. M.; Liao, W.; Chiu, K. Reductive Dechlorination for Remediation of Polychlorinated Biphenyls. *Chemosphere* **2012**, *88*, 757–768. (c) Ido, A.; Ishihara, S.; Kume, A.;



*Chapter one references begin on page 86*

Nakanishi, T.; Monguchi, Y.; Sajiki, H.; Nagase, H. Practical Method for PCB Degradation Using Pd/C–$H_2$–Mg System. *Chemosphere* **2013**, *90*, 57–64.

(331) (a) Robinson, A. M.; Hensley, J. E.; Medlin, J. W. Bifunctional Catalysts for Upgrading of Biomass-Derived Oxygenates: A Review. *ACS Catal.* **2016**, *6*, 5026–5043. (b) Chatterjee, C.; Pong, F.; Sen, A. Chemical Conversion Pathways for Carbohydrates. *Green Chem.* **2015**, *17*, 40–71. (c) Wan Azelee, N. I.; Mahdi, H. I.; Cheng, Y.-S.; Nordin, N.; Illias, R. M.; Rahman, R. A.; Shaarani, S. M.; Bhatt, P.; Yadav, S.; Chang, S. W.; Ravindran, B.; Ashokkumar, V. Biomass Degradation: Challenges and Strategies in Extraction and Fractionation of Hemicellulose. *Fuel* **2023**, *339*, 126982. (d) Liu, X.; Bouxin, F. P.; Fan, J.; Budarin, V. L.; Hu, C.; Clark, J. H. Recent Advances in the Catalytic Depolymerization of Lignin towards Phenolic Chemicals: A Review. *ChemSusChem* **2020**, *13*, 4296–4317.

(332) Modak, A.; Maiti, D. Metal Catalyzed Defunctionalization Reactions. *Org. Biomol. Chem.* **2016**, *14*, 21–35.

(333) (a) Brown, H. C.; Krishnamurthy, S. Forty Years of Hydride Reductions. *Tetrahedron* **1979**, *35*, 567–607. (b) Lopez, R. M.; Hays, D. S.; Fu, G. C. $Bu_3$SnH-Catalyzed Barton−McCombie Deoxygenation of Alcohols. *J. Am. Chem. Soc.* **1997**, *119*, 6949–6950. (c) McCombie, S. W.; Motherwell, W. B.; Tozer, M. J. The Barton-McCombie Reaction. *Organic Reactions*. Wiley January 25, 2012, pp 161–432. (d) Brown, W. G. Reductions by Lithium Aluminum Hydride. *Organic Reactions*. Wiley March 15, 2011, pp 469–510.

(334) Johannes G. de Vries, Cornelis J. Elsevier, eds. *The Handbook of Homogeneous Hydrogenation*. Wiley-VCH, Weinheim, 2007.

(335) Wolff, L. Chemischen Institut Der Universität Jena: Methode Zum Ersatz Des Sauerstoffatoms Der Ketone Und Aldehyde Durch Wasserstoff. [Erste Abhandlung.]. *Justus Liebigs Ann. Chem.* **1912**, *394*, 86–108.

(336) Clemmensen, E. Reduktion von Ketonen Und Aldehyden Zu Den Entsprechenden Kohlenwasserstoffen Unter Anwendung von Amalgamiertem Zink Und Salzsäure. *Ber. Dtsch. Chem. Ges.* **1913**, *46*, 1837–1843.

(337) (a) Fang, H.; Oestreich, M. Defunctionalisation Catalysed by Boron Lewis Acids. *Chem. Sci.* **2020**, *11*, 12604–12615. (b) Hackel, T.; McGrath, N. A.



*Chapter one references begin on page 86*

Tris(Pentafluorophenyl)Borane-Catalyzed Reactions Using Silanes. Molecules 2019, 24, 432. (c) Lawson, J. R.; Melen, R. L. Tris(Pentafluorophenyl)Borane and beyond: Modern Advances in Borylation Chemistry. *Inorg. Chem.* **2017**, *56*, 8627–8643.

(338) Cram, D. J.; Sahyun, M. R. V. Room Temperature Wolff-Kishner Reduction and Cope Elimination Reactions. *J. Am. Chem. Soc.* **1962**, *84*, 1734–1735.

(339) Caglioti, L.; Magi, M. The Reaction of Tosylhydrazones with Lithium Aluminium Hydride. *Tetrahedron* **1963**, *19*, 1127–1131.

(340) Furrow, M. E.; Myers, A. G. Practical Procedures for the Preparation of *N-Tert*-Butyldimethylsilylhydrazones and Their Use in Modified Wolff−Kishner Reductions and in the Synthesis of Vinyl Halides and *gem*-Dihalides. *J. Am. Chem. Soc.* **2004**, *126* (17), 5436–5445

(341) Gui, R.; Li, C.-J. Ruthenium(II)-Catalyzed Deoxygenation of Ketones. *Chem. Commun.* **2022**, *58*, 10572–10575.

(342) Campagne, J.-M.; Dal Zotto, C.; Virieux, D. $FeCl_3$-Catalyzed Reduction of Ketones and Aldehydes to Alkane Compounds. *Synlett* **2009**, *2*, 276–278.

(343) Dong, Z.; Yuan, J.; Xiao, Y.; Mao, P.; Wang, W. Room Temperature Chemoselective Deoxygenation of Aromatic Ketones and Aldehydes Promoted by a Tandem Pd/$TiO_2$ + $FeCl_3$ Catalyst. *J. Org. Chem.* **2018**, *83*, 11067–11073.

(344) Rahaim, R. J., Jr; Maleczka, R. E., Jr. C−O Hydrogenolysis Catalyzed by Pd-PMHS Nanoparticles in the Company of Chloroarenes. *Org. Lett.* **2011**, *13*, 584–587.

(345) Wang, H.; Li, L.; Bai, X.-F.; Shang, J.-Y.; Yang, K.-F.; Xu, L.-W. Efficient Palladium-catalyzed C-O Hydrogenolysis of Benzylic Alcohols and Aromatic Ketones with Polymethylhydrosiloxane. *Adv. Synth. Catal.* **2013**, *355*, 341–347.

(346) Volkov, A.; Gustafson, K. P. J.; Tai, C.-W.; Verho, O.; Bäckvall, J.-E.; Adolfsson, H. Mild Deoxygenation of Aromatic Ketones and Aldehydes over Pd/C Using Polymethylhydrosiloxane as the Reducing Agent. *Angew. Chem. Int. Ed.*, **2015**, *54*, 5122–5126.

(347) Fernandes, T. A.; Bernardo, J. R.; Fernandes, A. C. Direct Reductive Deoxygenation of Aryl Ketones Catalyzed by Oxo-rhenium Complexes. *ChemCatChem* **2015**, *7*, 1177–1183.



*Chapter one references begin on page 86*

(348) Sousa, S. C. A.; Fernandes, T. A.; Fernandes, A. C. Highly Efficient Deoxygenation of Aryl Ketones to Arylalkanes Catalyzed by Dioxidomolybdenum Complexes. *European J. Org. Chem.* **2016**, *2016*, 3109–3112.

(349) Argouarch, G. Mild and Efficient Rhodium-Catalyzed Deoxygenation of Ketones to Alkanes. *New J Chem* **2019**, *43*, 11041–11044.

(350) Guyon, C.; Baron, M.; Lemaire, M.; Popowycz, F.; Métay, E. Commutative Reduction of Aromatic Ketones to Arylmethylenes/Alcohols by Hypophosphites Catalyzed by Pd/C under Biphasic Conditions. *Tetrahedron* **2014**, *70*, 2088–2095.

(351) Kalutharage, N.; Yi, C. S. Scope and Mechanistic Analysis for Chemoselective Hydrogenolysis of Carbonyl Compounds Catalyzed by a Cationic Ruthenium Hydride Complex with a Tunable Phenol Ligand. *J. Am. Chem. Soc.* **2015**, *137*, 11105–11114.

(352) Zhou, X.-Y.; Chen, X. Recyclable Pd/C Catalyzed One-Step Reduction of Carbonyls to Hydrocarbons under Simple Conditions without Extra Base. *Tetrahedron Lett.* **2020**, *61*, 151447.

(353) Yang, Z.; Zhu, X.; Yang, S.; Cheng, W.; Zhang, X.; Yang, Z. Iridium-catalysed Reductive Deoxygenation of Ketones with Formic Acid as Traceless Hydride Donor. *Adv. Synth. Catal.* **2020**, *362*, 5496–5505.

(354) van Duzee, E. M.; Adkins, H. Hydrogenation and Hydrogenolysis of Ethers. *J. Am. Chem. Soc.* **1935**, *57*, 147–151.

(355) Álvarez-Bercedo, P.; Martin, R. Ni-Catalyzed Reduction of Inert C−O Bonds: A New Strategy for Using Aryl Ethers as Easily Removable Directing Groups. *J. Am. Chem. Soc.* **2010**, *132*, 17352–17353.

(356) Tobisu, M.; Yamakawa, K.; Shimasaki, T.; Chatani, N. Nickel-Catalyzed Reductive Cleavage of Aryl–Oxygen Bonds in Alkoxy- and Pivaloxyarenes Using Hydrosilanes as a Mild Reducing Agent. *Chem. Commun.* **2011**, *47*, 2946.

(357) Sergeev, A. G.; Hartwig, J. F. Selective, Nickel-Catalyzed Hydrogenolysis of Aryl Ethers. *Science* **2011**, *332*, 439–443.

(358) (a) Kelley, P.; Lin, S.; Edouard, G.; Day, M. W.; Agapie, T. Nickel-Mediated Hydrogenolysis of C–O Bonds of Aryl Ethers: What Is the Source of the Hydrogen? *J. Am. Chem. Soc.* **2012**, *134*, 5480–5483. (b) Ren, Y.; Yan, M.; Wang, J.; Zhang, Z. C.; Yao, K. Selective Reductive Cleavage of Inert Aryl C-O Bonds by an Iron Catalyst. *Angew. Chem.*



*Chapter one references begin on page 86*

*Int. Ed.*, **2013**, *52*, 12674–12678. (c) Sergeev, A. G.; Webb, J. D.; Hartwig, J. F. A Heterogeneous Nickel Catalyst for the Hydrogenolysis of Aryl Ethers without Arene Hydrogenation. *J. Am. Chem. Soc.* **2012**, *134*, 20226–20229.

(359) Yasuda, M.; Onishi, Y.; Ueba, M.; Miyai, T.; Baba, A. Direct Reduction of Alcohols: Highly Chemoselective Reducing System for Secondary or Tertiary Alcohols Using Chlorodiphenylsilane with a Catalytic Amount of Indium Trichloride. *J. Org. Chem.* **2001**, *66*, 7741–7744.

(360) Nishibayashi, Y.; Shinoda, A.; Miyake, Y.; Matsuzawa, H.; Sato, M. Ruthenium-catalyzed Propargylic Reduction of Propargylic Alcohols with Silanes. *Angew. Chem. Int. Ed.* **2006**, *45*, 4835–4839.

(361) Mirza-Aghayan, M.; Boukherroub, R.; Rahimifard, M. A Simple and Efficient Hydrogenation of Benzyl Alcohols to Methylene Compounds Using Triethylsilane and a Palladium Catalyst. *Tetrahedron Lett.* **2009**, *50*, 5930–5932.

(362) Wang, J.; Huang, W.; Zhang, Z.; Xiang, X.; Liu, R.; Zhou, X. $FeCl_3 \cdot 6H_2O$ Catalyzed Disproportionation of Allylic Alcohols and Selective Allylic Reduction of Allylic Alcohols and Their Derivatives with Benzyl Alcohol. *J. Org. Chem.* **2009**, *74*, 3299–3304.

(363) Kim, S.; Chan, L.; Lim, J. Iron-Catalyzed Reductive Dehydroxylation of Benzylic Alcohols Using Polymethylhydrosiloxane (PMHS). *Synlett* **2011**, *2011*, 2862–2866.

(364) Narayana Kumar, G. G. K. S.; Laali, K. K. Facile Coupling of Propargylic, Allylic and Benzylic Alcohols with Allylsilane and Alkynylsilane, and Their Deoxygenation with $Et_3SiH$, Catalyzed by $Bi(OTf)_3$ in [BMIM][$BF_4$] Ionic Liquid (IL), with Recycling and Reuse of the IL. *Org. Biomol. Chem.* **2012**, *10*, 7347.

(365) Meyer, V. J.; Niggemann, M. Highly Chemoselective Calcium-catalyzed Propargylic Deoxygenation. *Chem. Eur. J.* **2012**, *18*, 4687–4691.

(366) Dang, H.; Cox, N.; Lalic, G. Copper-catalyzed Reduction of Alkyl Triflates and Iodides: An Efficient Method for the Deoxygenation of Primary and Secondary Alcohols. *Angew. Chem. Int. Ed.*, **2014**, *53*, 752–756.

(367) Yang, Z.; Kumar, R. K.; Liao, P.; Liu, Z.; Li, X.; Bi, X. Chemo- and Regioselective Reductive Deoxygenation of 1-En-4-Yn-Ols into 1,4-Enynes through $FeF_3$ and TfOH Co-Catalysis. *Chem. Commun.* **2016**, *52*, 5936–5939.

(368) Kasner, G. R.; Boucher-Jacobs, C.; Michael McClain, J.; Nicholas, K. M. Oxo-Rhenium Catalyzed Reductive Coupling and Deoxygenation of Alcohols. *Chem. Commun.* **2016**, *52*, 7257–7260.

(369) Dai, X.-J.; Li, C.-J. En Route to a Practical Primary Alcohol Deoxygenation. *J. Am. Chem. Soc.* **2016**, *138*, 5433–5440.

(370) Li, C.-J.; Huang, J.; Dai, X.-J.; Wang, H.; Chen, N.; Wei, W.; Zeng, H.; Tang, J.; Li, C.; Zhu, D.; Lv, L. An Old Dog with New Tricks: Enjoin Wolff–Kishner Reduction for Alcohol Deoxygenation and C–C Bond Formations. *Synlett* **2019**, *30*, 1508–1524.

(371) Yang, S.; Tang, W.; Yang, Z.; Xu, J. Iridium-Catalyzed Highly Efficient and Site-Selective Deoxygenation of Alcohols. *ACS Catal.* **2018**, *8*, 9320–9326.

(372) Sai, M. An Efficient $Ga(OTf)_3$/Isopropanol Catalytic System for Direct Reduction of Benzylic Alcohols. *Adv. Synth. Catal.* **2018**, *360*, 4330–4335.

(373) Isomura, M.; Petrone, D. A.; Carreira, E. M. Coordination-Induced Stereocontrol over Carbocations: Asymmetric Reductive Deoxygenation of Racemic Tertiary Alcohols. *J. Am. Chem. Soc.* **2019**, *141*, 4738–4748.



*Chapter one references begin on page 86*

# **Chapter Two**: Deoxygenative Reduction of Diverse Carbon–Oxygen Bond Bearing Functional Groups

*"If you build it, he will come."*

- *"the Voice", Field of Dreams, 1989.*



*Chapter two references begin on page 204; experimental details begin on page 198*

## 2.1. Chapter Outlook

As outlined in Section 1.5 of this dissertation, the deoxygenative reduction of oxo-functional groups including esters, ketones, and alcohols is an important but still challenging family of transformations. Classical methods for deoxygenative reduction involve the use of pressurized gasses or specialized, often problematic reagents that limit the practicality, scope and selectivity of these transformations. Chapter two will aim to provide a potential resolution to this challenge, describing the development of a unified nickel-catalyzed platform for the deoxygenative reduction of oxo-functional groups (Figure 2.1).

The first part of this chapter will discuss the development of a one-step procedure to directly reduce aryl esters into their corresponding tolyl-derivatives (Section 2.3). The second part of this chapter will discuss how this work was expanded towards the reduction of esters, ketones, aldehydes, epoxides, ethers, and alcohols (Section 2.4). In both cases, 1,1,3,3-tetramethyldisiloxane (TMDSO) was used as a hydride source alongside a nickel/NHC catalyst. Numerous applications of this methodology are explored, including catalytic deuteration, benzyl-ether deprotection, biomass degradation and chemoselective C($sp^3$)–O bond scission. Various aspects of the reaction mechanism were explored to shed light on what reactive intermediates are present *en route* from starting material to product.

**Figure 2.1.** Nickel-catalyzed deoxygenative reduction of various oxo-functional groups

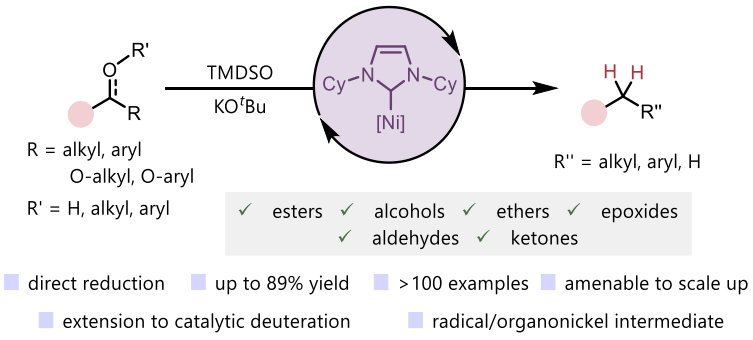




*Chapter two references begin on page 204; experimental details begin on page 198*

## 2.2. Reuse permissions and contributions

The content presented in this chapter is derived from a series of publications currently in print. Part A (Section 2.3) is adapted with permission from the manuscript "Exhaustive Reduction of Esters Enabled by Nickel Catalysis" by Adam Cook, Sekar Prakash, Yan-Long Zheng and Stephen G. Newman, published in *J. Am. Chem. Soc.* **2020**, *142*, 8109-8115. Copyright 2020 American Chemical Society. The dissertation author is a co-lead author of this manuscript. To supplement the original publication, additional relevant data has been incorporated into the text:

- Sections 2.3.1 and 2.3.6. are reproduced directly from the literature with minor modifications to aid in the flow and direction of this dissertation.
- Section 2.3.2, 2.3.3 and 2.3.4 were reproduced from the literature, with select optimization details, substrate scope examples and mechanistic details that were originally present in the supporting information incorporated into the text and expanded upon for clarity. Minor modifications were made to aid in the flow of this dissertation.
- Section 2.3.4.4 and 2.3.5 are original and present exclusively within this dissertation.

Part B (Section 2.4) is adapted with permission from the manuscript "Nickel-Catalyzed Reductive Deoxygenation of Diverse C–O Bond-Bearing Functional Groups" by Adam Cook, Haydn Maclean, Piers St. Onge and Stephen G. Newman, published in *ACS Catalysis* **2021**, *11*, 13337-13347. Copyright 2021 American Chemical Society. The dissertation author is the lead author of this manuscript. To supplement the original publication additional relevant data has been incorporated into the text:

- Section 2.4.1 and 2.4.7 were reproduced directly from the literature with minor modifications, particularly to the graphics, to aid in the flow of this dissertation.

- Section 2.4.2, 2.4.3, 2.4.4 and 2.4.5 were reproduced from the literature, with select substrate scope examples and mechanistic details that were originally present in the supporting information incorporated into the text and expanded upon for clarity. Minor modifications were made to the graphics to aid in the flow of this dissertation.
- Section 2.4.5.7 and 2.4.6 are original and present exclusively within this dissertation.

Further, Section 2.5.2. features an excerpt adapted with permission from the manuscript "Nickel-Catalyzed Desulfonylative Olefination of *β*-Hydroxysulfones" by Adam Cook, Maxwell Bezaire and Stephen G. Newman, published in *Organic Chemistry Frontiers* **2023**, *10*, 1339-1404. The dissertation author is the lead author of this manuscript. Otherwise, Section 2.5, as well as Section 2.1 are found exclusively within this dissertation. The experimental section (Section 2.6) is reproduced directly from the literature.

## Contributions

The reaction described in Part A was discovered by Yan-Long. Prakash led the optimization campaign with assistance from the author of this dissertation, and both Prakash and the author of this dissertation conducted the scope expansion. Haydn assisted in the optimization of the ketone deoxygenation presented in Part B. Piers assisted in the reproduction of experiments conducted in Part B. Otherwise, experiments were conducted by the author of this dissertation.



*Chapter two references begin on page 204; experimental details begin on page 198*

## 2.3. Part A: Exhaustive Reduction of Esters Enabled by Nickel Catalysis

### 2.3.1. Introductory theory and background information

The reduction of carboxylic acids, as well as their derivatives such as esters and amides, is of fundamental importance in organic synthesis.[1] This is most commonly achieved by the action of aggressive metal hydride reducing agents, enabling the formation of the corresponding alcohol product.[2] Exhaustive reduction – that is, reduction all the way to the methyl oxidation state – is less readily achieved. Reasons why one may seek to perform this reaction include the profound effects of methyl groups on bioactivity, [3a-b] the ability to exploit the electronic effects of an ester group prior to reduction,[3c] or its ability to create deuterium-labelled tolyl derivatives.[3d-e] In rare cases, single step transformation of an aromatic ester into a methyl group can be realized,[4] for example by the use of excess lithium aluminum hydride in refluxing ethereal solvent (Figure 2.2a).[5] More often, this transformation is carried out by a three-step sequence via initial reduction to the alcohol, functional group interconversion to an alkyl halide, and further reduction to the methyl product (Figure 2.2b).[6] Alternatively, catalytic hydrogenolysis can be used to reduce an alcohol to the methyl oxidation state (Figure 2.2c).[7]

**Figure 2.2.** Contemporary methods to achieve the ester-to-methyl transformation

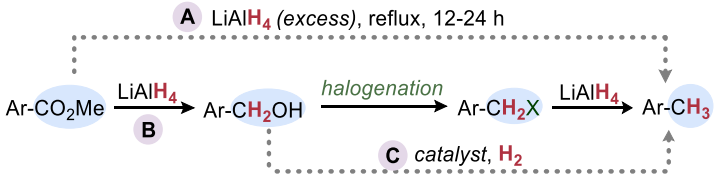


The Newman group and others have recently demonstrated that nickel catalysts are capable of the catalytic activation of methyl esters, presumably initiated by oxidative addition into the



Chapter two references begin on page 204; experimental details begin on page 198

C(acyl)–O bond.[8] In the course of these studies, it was hypothesized that useful catalytic reductions of these esters may be achievable using a similar strategy. Related work from the Martin lab for reducing anisoles to arenes (Scheme 2.1a),[9] the Rueping lab on the reduction of phenyl esters to arenes (Scheme 2.1b),[10] and the Garg lab on transforming amides to amines (Scheme 2.1c),[11] among others,[12] served as inspiration that silane reagents could act as mild hydride donors in nickel-catalyzed reactions. With this precedent in mind, a study was initiated on the reaction of silanes with methyl esters in the presence of nickel. When using 1,1,3,3-tetramethyldisiloxane (TMDSO)[13] as a reducing agent in the presence of $Ni(cod)_2$, 1,3-dicyclohexylimidazolium tetrafluoroborate salt (ICy•$HBF_4$), and potassium *tert*-butoxide, the major product was the corresponding tolyl derivative (Scheme 2.1d). Given the absence of general, functional group tolerant methods to achieve this transformation in a single step, this reaction was further explored.

**Scheme 2.1.** Nickel-catalyzed reductions mediated by organosilane reducing agents.

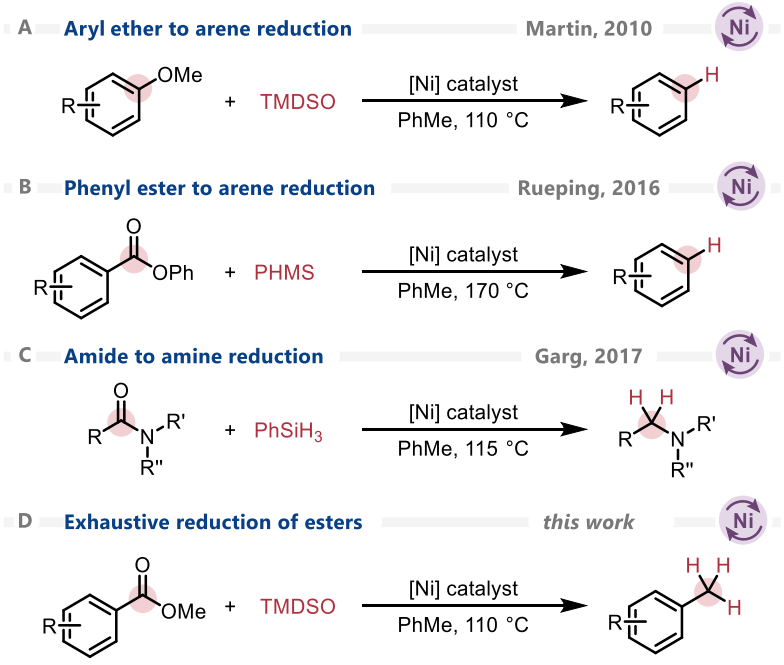




*Chapter two references begin on page 204; experimental details begin on page 198*

### **2.3.2**. Discovery and optimization: Synopsis

The nickel-catalyzed exhaustive reduction of aromatic methyl esters to the corresponding tolyl derivative was optimized using *N*-methyl indole **2.1**. Heating the substrate at 110 °C in toluene in the presence of $Ni(cod)_2$ (10 mol%), ICy•$HBF_4$ (20 mol%), TMDSO (2 equiv), and KO$^t$Bu (1 equiv) afforded methyl-bearing indole **2.2** in 84% yield (Table 2.1, entry 1). Running the reaction in the absence of either KO$^t$Bu or siloxane resulted in no conversion (entry 2). However, removing just the $Ni(cod)_2$ led to complete consumption of **2.1**, with the corresponding benzyl alcohol as the only major identifiable product after working the reaction up with TBAF (entry 3). Using this alcohol as a starting material in the presence of the nickel catalyst resulted in efficient formation of **2.2**, suggesting that the reaction proceeds through a non-catalyzed reduction to a silylated alcohol[14] followed by catalytic reduction of this species to form the alkane (entry 4). Further experiments on benzyl-alcohol derived species confirm its viability as an intermediate (Section 2.3.4.1). Alternative ligands (entry 5, 6), bases (entry 7, 8) and organosilane reducing agents (entry 9, 10) were all less efficient. Despite being highly reducing conditions, nickel(II) precatalysts such as $NiCl_2$ (entry 11) or $NiBr_2$·glyme (entry 12) gave poor yields. The addition of 0.2 equiv Mn gave a moderate improvement to 35% (entry 13), while 1 equivalent of Mn gave 78% yield (entry 14), providing a viable alternative set of conditions that can be performed without the use of a glovebox. Applying these conditions in the absence of TMDSO resulted in no formation of **2.2** (entry 15), suggesting that TMDSO is ultimately responsible for the substrate reduction.



*Chapter two references begin on page 204; experimental details begin on page 198*

**Table 2.1**. Optimization of ester reduction reaction

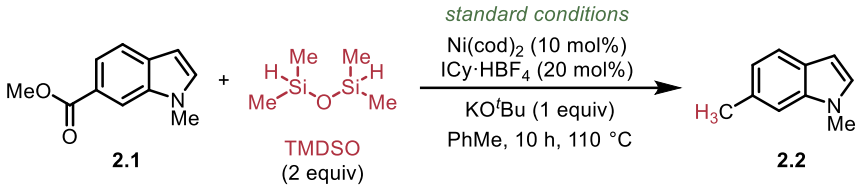


| entry | deviation from standard reaction conditions | % yield, 2.2 |
|---|---|---|
| **1** | none | 84 |
| **2** | no base or no siloxane | 0 |
| **3** | no nickel | 0[b] |
| **4** | alcohol as starting material *instead of ester* | 73 |
| **5** | IPr•HCl *instead of ICy•HBF4* | 70 |
| **6** | Xantphos *instead of ICy•HBF4* | 35 |
| **7** | KOH *instead of KO$^t$Bu* | 12 |
| **8** | KOEt *instead of KO$^t$Bu* | 51 |
| **9** | $Et_3SiH$ (4.0 equiv) | 42 |
| **10** | $(EtO)_3SiH$ (4.0 equiv) | 20 |
| **11** | $NiCl_2$ *instead of Ni(cod)2* | 4 |
| **12** | $NiBr_2$·glyme *instead of Ni(cod)2* | 7 |
| **13** | $NiBr_2$·glyme + Mn (0.2 equiv) *instead of Ni(cod)2* | 35 |
| **14** | $NiBr_2$·glyme + Mn (1.0 equiv) *instead of Ni(cod)2* | 78 |
| **15** | $NiBr_2$·glyme + Mn (1.0 equiv) *instead of Ni(cod)2, no TMDSO* | 0 |

Reactions ran on a 0.20 mmol scale. Yields determined by NMR using 1,3,5-trimethoxybenzene as internal standard. [b]Alcohol (1-methyl-*1H*-indol-6-yl)methanol observed as major product after work-up with TBAF.

### **2.3.2.1.** Investigating alternative bases and hydride sources

A range of bases were explored for use in this chemistry (Table 2.2). While potassium *tert*-butoxide was identified as the optimal base, sodium *tert*-butoxide was similarly effective. However, lithium *tert*-butoxide only afforded trace amounts of product. This deviation could be due to solubility differences between the bases under the general reaction conditions or due to the



*Chapter two references begin on page 204; experimental details begin on page 198*

ability of sodium- and potassium *tert*-butoxide to participate in single electron chemistry. Potassium ethoxide and sodium methoxide also afforded synthetically viable yields of product; however, all other tested bases led to sluggish formation of product.

**Table 2.2**. Examining alternative bases in this reductive deoxygenation

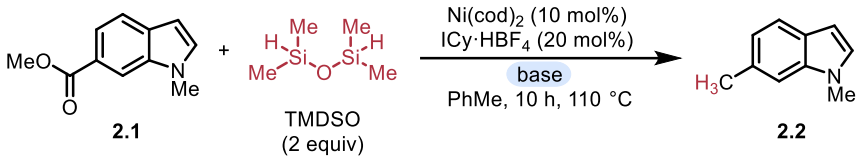


| entry | base | % yield, 2.2 |
|---|---|---|
| **1** | NaOH (1.0 eq) | 4 |
| **2** | LiOH (1.0 eq) | 0 |
| **3** | KOH (1.0 eq) | 12 |
| **4** | $Et_3N$ (1.0 eq) | 0 |
| **5** | $Cs_2CO_3$ (1.0 eq) | 0 |
| **6** | $K_2CO_3$ (1.0 eq) | 3 |
| **7** | $NMe_4OH{\cdot}5H_2O$ (1.0 eq) | 37 |
| **8** | $KHF_2$ (1.0 eq) | 0 |
| **9** | NaOMe (1.0 eq) | 56 |
| **10** | KOEt (1.0 eq) | 51 |
| **11** | Li$O^tBu$ (1.0 eq) | trace |
| **12** | Na$O^tBu$ (1.0 eq) | 75 |
| **13** | K$O^tBu$ (1 eq) | 78 |
| **14** | K$O^tBu$ (0.5 eq) | 69 |
| **15** | K$O^tBu$ (1.5 eq) | 74 |
| **16** | K$O^tBu$ (2.0 eq) | 68 |



*Chapter two references begin on page 204; experimental details begin on page 198*

In contrast, while only a select few bases permitted arylation, a range of different hydride sources could be employed including silanes (Table 2.3, entry 1-3) and siloxanes (entry 6-8). PMHS did not afford product, likely due to solubility reasons and triphenylsilane also did not afford product.

**Table 2.3.** Examining alternative organosilanes in this reductive deoxygenation

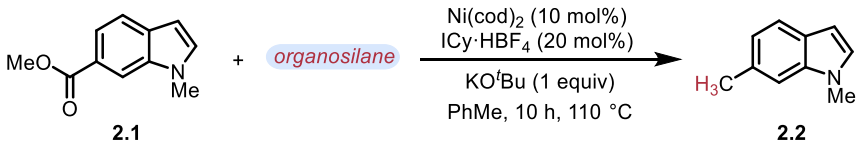


| entry | organosilane | % yield, 2.2 |
|---|---|---|
| **1** | $Et_3SiH$ (4.0 equiv) | 42 |
| **2** | $^{i}Pr_3SiH$ (4.0 equiv) | 5 |
| **3** | $(EtO)_3SiH$ (4.0 equiv) | 20 |
| **4** | PMHS (10.0 equiv) | trace |
| **5** | $PhSiH_3$ (2.0 equiv) | trace |
| **6** | $[(Me_3SiO)_2SiHMe]$ (4.0 equiv) | 48 |
| **7** | $[(CH_3)_2SiHO)_2Si(CH_3)_2]$ (4.0 equiv) | 65 |
| **8** | TMDSO (1.0 equiv) | 52 |
| **9** | TMDSO (1.5 equiv) | 76 |
| **10** | TMDSO (2.0 equiv) | 84 |
| **11** | TMDSO (2.5 equiv) | 74 |

### 2.3.2.2. Investigating alternative catalyst systems

Evaluating different precatalysts revealed that, while $Ni(cod)_2$ is optimal, this transformation could proceed in the presence of a range of other nickel sources (Table 2.4).



*Chapter two references begin on page 204; experimental details begin on page 198*

Further, this transformation could proceed when employing palladium, platinum, iridium, and ruthenium catalysts, albeit in diminished yields. Lower yields observed in the presence of alternative metals may be due to nickels proficiency at cleaving carbon-oxygen bonds.

**Table 2.4.** Examining alternative metal sources in this reductive deoxygenation

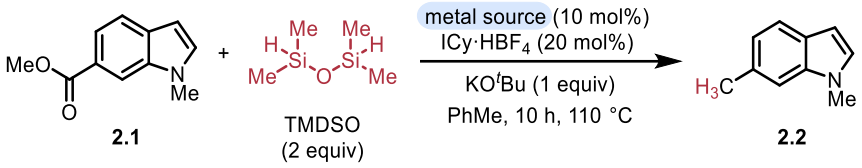


| entry | metal source | % yield, 2.2 |
|---|---|---|
| **1** | $Ni(cod)_2$ | 84 |
| **2** | $NiCl_2$ | 4 |
| **3** | $Ni(P(OPh)_3)_4$ | 0 |
| **4** | $NiCl_2(PCy_3)_2$ | 67 |
| **5** | $Ni(OAc)_2$ | trace |
| **6** | $Ni(OTf)_2$ | 5 |
| **7** | $NiBr_2$·glyme | 7 |
| **8** | $PdCl_2$ | 29 |
| **9** | $Pd(OAc)_2$ | 28 |
| **10** | $Pd_2dba_3$ | 34 |
| **11** | $RhCl(PPh_3)_3$ | trace |
| **12** | Pt/C | 11 |
| **13** | $Ir(cod)_2Cl_2$ | 13 |
| **14** | $[Ru(p\text{-cymene})Cl_2]_2$ | 7 |
| **15** | CuI | 0 |
| **16** | $FeCl_3$ | 0 |
| **17** | $Ni(cod)_2$ (5 mol%) | 62 |



*Chapter two references begin on page 204; experimental details begin on page 198*

| | | |
|---|---|---|
| **18** | $Ni(cod)_2$ (20 mol%) | 86 |
| **19** | $Ni(cod)_2$ (30 mol%) | 82 |

Similarly, while a range of ligands could be utilized in this transformation alongside $Ni(cod)_2$, ICy•$HBF_4$ proved optimal (Table 2.5). Mono- and bidentate phosphines could be employed, with monodentate $PCy_3$ affording yields up to 53%. Except for the case of IMes•HCl, all the tested NHCs afforded moderate-to-high yields, with ICy•$HBF_4$ providing slightly higher yields than IPr•HCl and ICy•HCl.

**Table 2.5.** Examining alternative ligands in this reductive deoxygenation

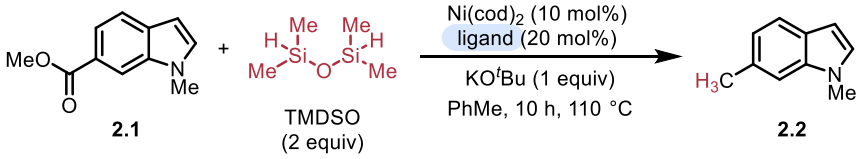


| entry | ligand | % yield, 2.2 |
|---|---|---|
| **1** | $PCy_3$ | 53 |
| **2** | $PPh_3$ | 15 |
| **3** | JohnPhos | 16 |
| **4** | Xantphos | 35 |
| **5** | *N*-Xantphos | 29 |
| **6** | dppf | 27 |
| **7** | dcype | 44 |
| **8** | dppent | 35 |
| **9** | IMes•HCl | 3 |
| **10** | SIPr•HCl | 53 |
| **11** | IPr•HCl | 70 |
| **12** | ICy•HCl | 77 |



*Chapter two references begin on page 204; experimental details begin on page 198*

| | | |
|---|---|---|
| **13** | ICy•$HBF_4$ | 84 |
| **14** | I$^t$Bu•$HBF_4$ | 73 |
| **15** | ICyp•$HBF_4$ | 60 |

### 2.3.2.3. Control experiments

Control experiments were performed in the reduction of compound **2.1** (Table 2.6). These experiments revealed the synergistic impact of base, TMDSO and the nickel catalyst in this chemistry as no product was observed in any case where they were excluded. Interestingly, alcohol **2.3** was recovered upon excluding the nickel catalyst and working the reaction up with TBAF. Further, exposure to only nickel catalyst led towards the quantitative recovery of starting material. Taken together, these data suggest that the reduction reaction first proceeds through TMDSO/KO$^t$Bu assisted reduction into the alcohol oxidation state followed by nickel-catalyzed deoxygenative reduction to the methyl oxidation state. The two-step nature of this protocol will be discussed in more depth within Section 2.3.4.1.

**Table 2.6.** Control experiments for this reductive deoxygenation

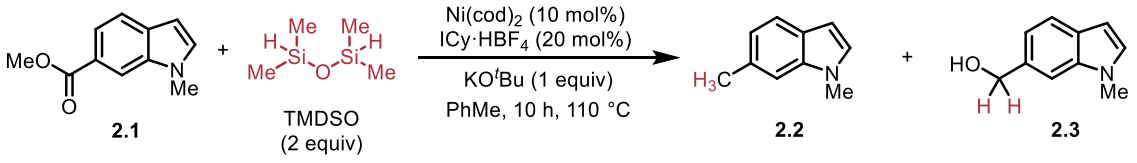


| entry | deviation from standard conditions | % yield, 2.2 | % yield, 2.3 |
|---|---|---|---|
| **1** | no deviation | 84 | 0 |
| **2** | *remove* KO$^t$Bu | 0 | 0 |
| **3** | *remove* TMDSO | 0 | 0 |



*Chapter two references begin on page 204; experimental details begin on page 198*

| | | | |
|---|---|---|---|
| **4** | *remove* $Ni(cod)_2$ | trace | 52 |
| **5** | *remove* $ICy•HBF_4$ | 14 | 0 |
| **6** | *remove all except* TMDSO and $KO^tBu$ | trace | 66 |
| **7** | *remove all except* $Ni(cod)_2$ | 0 | 0 |
| **8** | room temperature | 14 | 61 |
| **9** | 1 h | 13 | 67 |

### 2.3.3. Substrate scope

#### 2.3.3.1. Substrate scope overview

With optimized conditions in hand, attention was turned towards an evaluation of the reaction scope (Scheme 2.2). Electron-neutral and rich methyl arenes **2.4-2.8** were formed from their corresponding esters in 73–86% yield. Subjecting a styrene-bearing methyl ester to the conditions led to partial reduction of the olefin; however, slightly milder conditions enabled **2.9** to be selectivity formed in 74% yield. Slightly milder conditions also allowed recovery of stilbene **2.10** in similar yields. In contrast with prior work on nickel-catalyzed hydrogenolysis of anisoles and related compounds,[9a,12c-f] no C(aryl)–O cleavage was observed when using ethereal or phenol-containing substrates (**2.11**–**2.16**). Further, carboxylic acid-bearing esters (**2.17**) could also be tolerated, provided that an extra equivalent of base was used.

In many classical heterocycle-forming reactions, ester-containing starting materials like malonates or propiolates are used to facilitate cyclizations, thus making the ester-containing products more accessible than the corresponding methyl analogs. With this in mind, it was exciting to see that many heterocycles were tolerated, including pyridines (**2.18**–**2.21**), morpholines (**2.22, 2.23**), piperidines (**2.24, 2.25**), indoles (**2.26-2.30**), carbazoles (**2.31**–**2.33**), an indazole (**2.34**),



*Chapter two references begin on page 204; experimental details begin on page 198*

quinoline (**2.35**), benzofuran (**2.36**), and dibenzofuran (**2.37**). Derivatization of commercial pharmaceuticals bifendatatum (used to treat hepatitis B) and probenecid (a uricosuric used to treat certain forms of arthritis) successfully formed reduction products **2.38** and **2.39**, respectively. Reduction of a lactone proceeded smoothly to form alcohol-bearing tolyl-derivative **2.40** upon quenching with TBAF.

Certain functional groups such as alkynes and organofluorines were found to decompose under the standard reaction conditions. By using potassium fluoride (KF) as the stoichiometric base, fluoro (**2.41**), triflurotolyl (**2.42**), nitro (**2.43**), alkyne (**2.44**), and furan-bearing (**2.45**) substrates, as well an *α,β*-unsaturated ester (**2.46**) could be successfully reduced. Glovebox-free conditions using $NiBr_2$·glyme were also studied with a range of substrates. These conditions were observed to give synthetically viable yields, albeit with slightly lower efficiency than when using $Ni(cod)_2$. Lastly, a gram scale reaction was performed in a 50 mL heavy-walled pressure tube, providing **7** in 71% yield. Gratifyingly, product **2.8** was obtained in similar yields at the gram scale while reducing the catalyst loading to 3% nickel/ 6% ICy•$HBF_4$.



*Chapter two references begin on page 204; experimental details begin on page 198*

**Scheme 2.2**. Scope of substrates tolerated in the methyl ester reduction

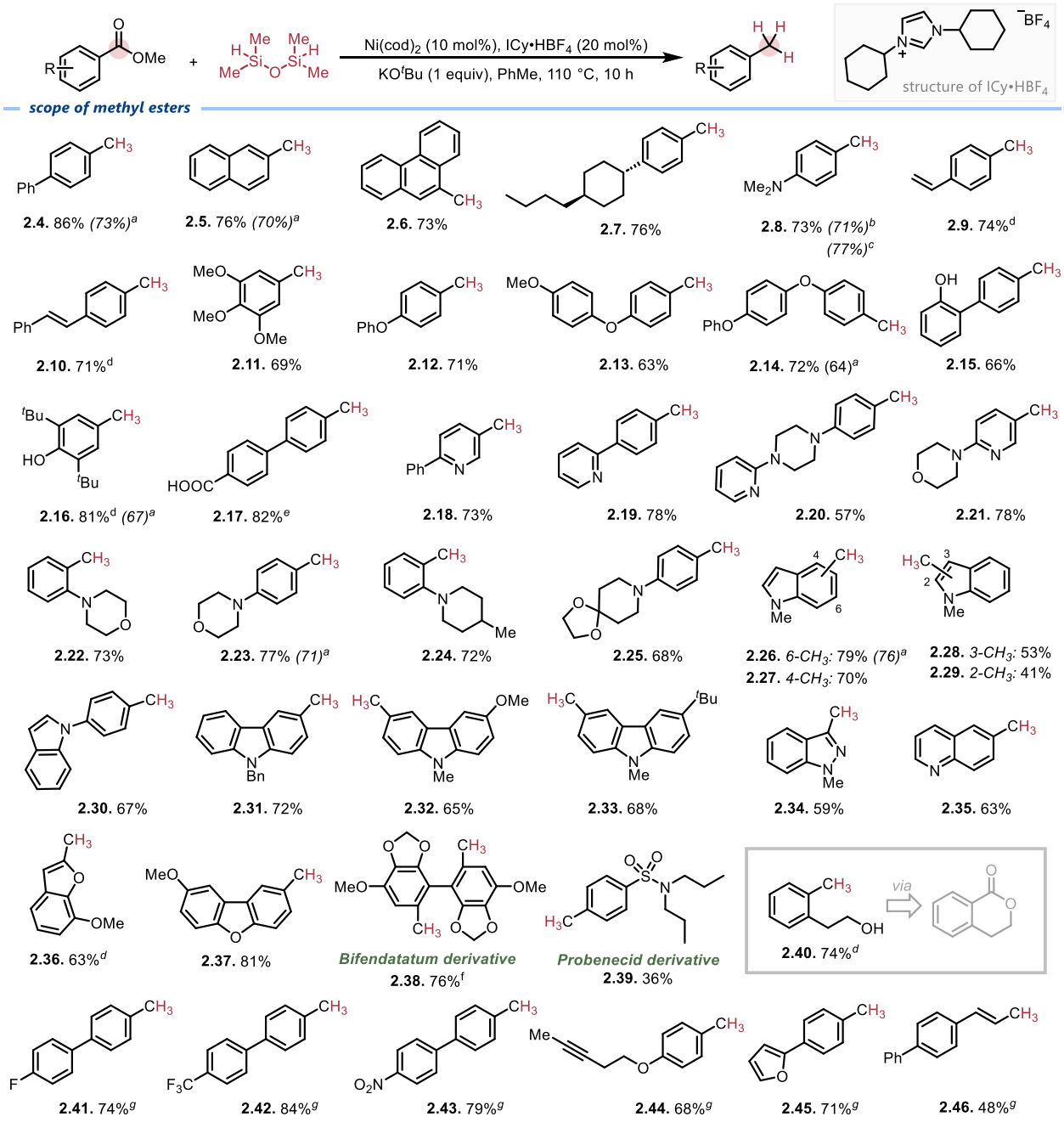


General reaction conditions: ester (0.20 mmol), TMDSO (0.40 mmol), KO$^t$Bu (0.20 mmol), ICy•$HBF_4$ (20 mol%), $Ni(cod)_2$ (0.02 mmol) in toluene (0.8 mL), 110 °C for 10 h. [*a*] $NiBr_2$·glyme (0.02 mmol) and Mn (0.20 mmol) used instead of $Ni(cod)_2$; reactions setup without use of a glovebox. [*b*] Yield obtained upon reacting 5.58 mmol (1 g) of starting material using 3 mol% Ni, 6 mol% ICy•$HBF_4$. [*c*] TMDSO (0.30



*Chapter two references begin on page 204; experimental details begin on page 198*

mmol), 90 °C for 6 h. [*d*] KO$^t$Bu (0.44 mmol) [*e*] TMDSO (0.80 mmol), KO$^t$Bu (0.40 mmol). [*f*] KF (0.20 mmol) and KO$^t$Bu (20 mol%) used instead of KO$^t$Bu (0.20 mmol).

Benzyl, isopropyl, phenyl and *tert*-butyl esters could also be reduced (Figure 2.3). Both ester-bearing naphthalenes (**2.47**-**2.49**) and ester-bearing indoles (**2.50**-**2.52**) were tested, each of which afforded the desired product in moderate-to-high yields.

**Figure 2.3.** Alternative esters that could be reduced

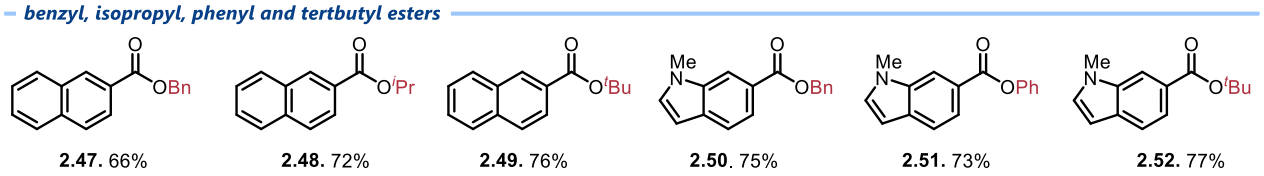


### 2.3.3.2. Unsuccessful scope examples

Several substrates, particularly those with free N–H bonds (**2.53**-**2.59**), were found to be inert to the reaction conditions, instead affording recovery of starting material (Figure 2.4a). Substrates with other carbonyl functionalities such as aldehydes (**2.60, 2.61**) and ketones (**2.62, 2.63**) were found to over-reduce to the corresponding methyl or methylene-containing products (Figure 2.4b). Further, substrates bearing aliphatic esters (**2.64**-**2.68**), rather than aryl esters, were only found to reduce to the alcohol oxidation state (Figure 2.4c). Lastly, esters bearing carbon-halogen bonds (**2.69**-**2.72**), carbon-sulfur bonds (**2.73**) and nitriles (**2.74**) were found to give intractable mixtures of products (Figure 2.4d).



*Chapter two references begin on page 204; experimental details begin on page 198*

**Figure 2.4.** Unsuccessful substrates

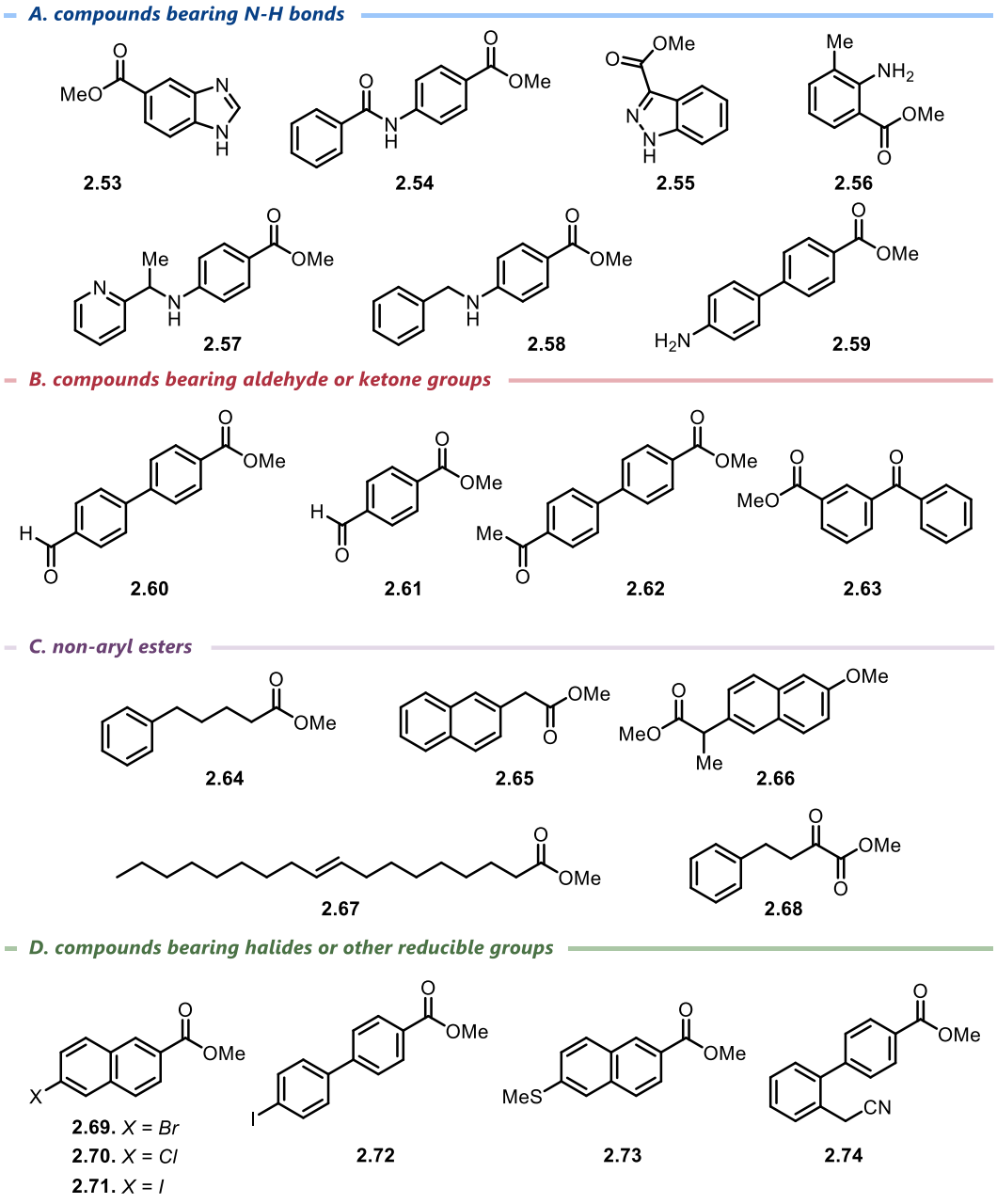




Chapter two references begin on page 204; experimental details begin on page 198

### **2.3.3.3.** Controlling selectivity: Ester vs. ether reduction

The conditions which Martin and co-workers used to reduce anisoles[9a] were very similar to the conditions that are used in this work to reduce esters. As such, a deeper comparison of these two sets of conditions was warranted. Notably, these methods differ primarily in the choice of ligand and the presence of base. To directly probe the selectivity, esters **2.75, 2.78, 2.81** and **2.84** were subjected to both sets of reaction conditions (Scheme 2.3). Using a nickel/ICy catalyst in the presence of KO$^t$Bu resulted in chemoselective formation of the ester reduction products **2.76, 2.79, 2.82** and **2.85** in 54–82% yield. Using base-free conditions with a nickel/$PCy_3$ catalyst resulted in a complete switch, cleaving of the ethereal bond while leaving the methyl ester untouched in products **2.77, 2.80, 2.83** and **2.86**. The nickel/$PCy_3$ system has been proposed by Martin and colleagues to act via a nickel(I)–$SiR_3$ active catalyst;[9b] the contrasting chemoselectivity in the system used to reduce esters suggests that both a different active catalyst and different mechanistic pathway are operative.



*Chapter two references begin on page 204; experimental details begin on page 198*

**Scheme 2.3.** Controlling selectivity between esters and ethers

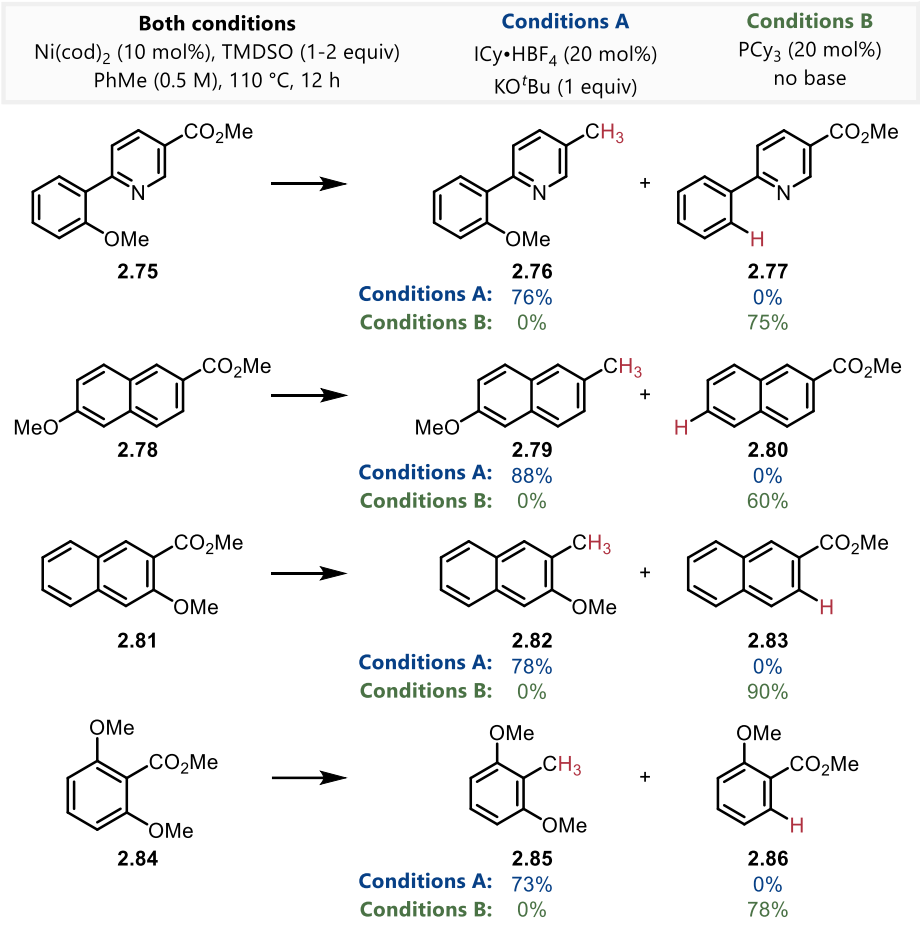


### 2.3.3.4. Extension to catalytic deuteration

Given the importance of deuterated molecules in the study of reaction mechanisms, pharmaceuticals, and as tools for understanding metabolic pathways,[15] the potential of this exhaustive reduction to synthetically introduce $-CD_3$ groups was investigated (Scheme 2.4a). While the development of methods to perform this transformation is of contemporary interest,[16] they are commonly achieved by using scarcely-available and prohibitively expensive $LiAlD_4$ or $LiEt_3BD$ as a reducing agent in the three-step procedure described in Figure 2.2.[6f-k] For instance, Salvadori and co-workers used a three-step, three-day procedure to synthesize $CD_3$-containing 2,5-



*Chapter two references begin on page 204; experimental details begin on page 198*

dimethoxy-$d_3$-toluene (**2.87**) towards the preparation of $d_3$-δ-tocopherol.[17] Reduction of the corresponding ester (**2.91**) to alcohol (**2.92**) with $LiAlD_4$, halogenation with $PBr_3$ (**2.93**), and a second $LiAlD_4$ reduction afforded product in an overall yield of 69% (Scheme 2.4b). Subjecting the same starting material to this transformation, using $d_2$-TMDSO[18] alongside $Ni(cod)_2$, gave incomplete deuterium incorporation. However, the use of $NiBr_2$·glyme/$d_2$-TMDSO/Mn in toluene-$d_8$ resulted in an efficient 73% yield with >95%D incorporation. This procedure was found to be general, enabling the synthesis of several $CD_3$-containing molecules in good yield and high deuterium incorporation (**2.87-2.90**). Experiments in non-deuterated toluene gave ~5-10% reduced deuterium incorporation.

**Scheme 2.4.** Applications of exhaustive reduction of esters

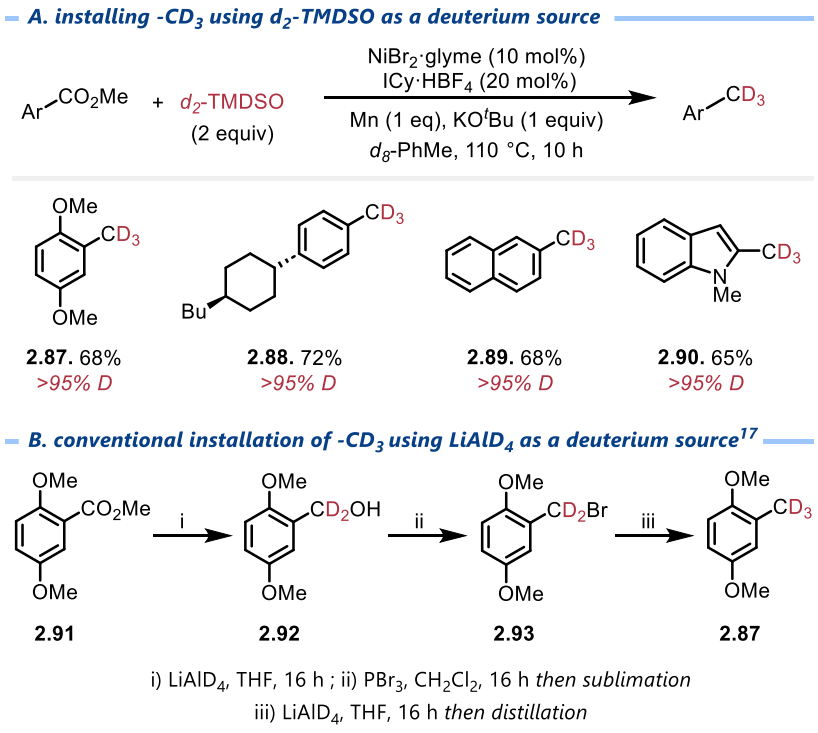




Chapter two references begin on page 204; experimental details begin on page 198

### 2.3.4. Preliminary mechanistic investigation

#### 2.3.4.1. Investigating potential reaction intermediates

Mechanistic investigations began by examining the nature and reactivity of reactive intermediates. From control experiments performed in the absence of nickel catalyst, exposure to TMDSO/KO$^t$Bu led towards the reduction of esters to the alcohol oxidation state. Nickel-catalyzed hydrogenolysis was then proposed to lead towards the generation of tolyl derivatives. In effect the transformation was proceeding through benzyl alcohol intermediates.

To probe the catalytic reaction of benzyl alcohols, various indole-bearing alcohol derivatives were subjected to the reducing conditions to determine if this step of the reaction behaved differently in isolation (Table 2.7). Using 1.0 equivalents of TMDSO provided indole **2.2** in 58% yield (entry 1). Use of 0.6 equivalents TMDSO (formally 1.2 equivalents of hydride) gave a slightly lower yield (entry 2). As was the case in the direct reduction starting from the ester, both nickel and KO$^t$Bu were required for conversion (entries 3, 4). Removing the base from the reaction mixture failed to afford product (entry 5), however base was only required in catalytic quantity to afford product (entry 6), contrasting the results when the ester was used as starting material. Replacing KO$^t$Bu with KF failed to afford product (entry 7). Adding 20 mol% of KO$^t$Bu restored reactivity (entry 8), as did substituting KOH as the base (entry 9). Reactions performed using -TBS, -TMS, -Me and -Ph protected alcohols led to a higher yield than that which was obtained when using the unprotected analog (entries 10-19). These species are more analogous to the mixture of silyl-alcohol species that are believed to form in situ via ester hydrosilylation. Finally, the corresponding aldehyde underwent reduction upon exposure to the reaction conditions, confirming it as a viable intermediate in this reaction (entry 20).

**Table 2.7.** Reduction of proposed intermediates

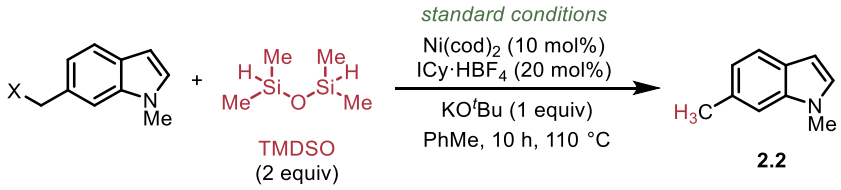


| entry | X | deviation from standard conditions | % yield, 2.2 |
|---|---|---|---|
| **1** | X = OH | none | 53 |
| **2** | X = OH | 0.6 equiv TMDSO *instead of 2.0 equiv* | 41 |
| **3** | X = OH | 0.3 equiv TMDSO *instead of 2.0 equiv* | 18 |
| **4** | X = OH | no $Ni(cod)_2$ | 0 |
| **5** | X = OH | ICy (free), no base *instead of ICy•HBF4* | 0 |
| **6** | X = OH | 20 mol% $KO^tBu$ *instead of 1.0 equiv* | 24 |
| **7** | X = OH | KF (1.0 equiv) *instead of $KO^tBu$* | trace |
| **8** | X = OH | KF (1.0 equiv) + 20 mol% $KO^tBu$ | 47 |
| **9** | X = OH | KOH (1.0 equiv) *instead of $KO^tBu$* | 31 |
| **10** | X = OTBS | KF (1.0 equiv) *instead of $KO^tBu$* | trace |
| **11** | X = OTBS | KF (1.0 equiv) + 20 mol% $KO^tBu$ | 74 |
| **12** | X = OTBS | none | 74 |
| **13** | X = OTBS | 0.6 equiv TMDSO *instead of 2.0 equiv* | 63 |
| **14** | X = OTBS | No $Ni(cod)_2$ | 0 |
| **15** | X = OTBS | ICy (free), no base *instead of ICy•HBF4* | 0 |
| **16** | X = OTMS | none | 71 |
| **17** | X = OMe | none | 77 |
| **18** | X = OMe | KF (1.0 eq) + 20 mol% KOtBu *instead of $KO^tBu$* | 70 |
| **19** | X = OPh | none | 51 |
| **20** | - | aldehyde as starting material | 73 |



*Chapter two references begin on page 204; experimental details begin on page 198*

Time-course studies (i.e. tracking product evolution vs. time) were performed to learn more about the fate of the methyl ester as it passes through the alcohol intermediate. Three separate reactions were examined: ester (**2.94**) to methyl (**2.5**), alcohol (**2.95**) to methyl (**2.5**) and ester (**2.94**) to alcohol (**2.95**). The time-course diagrams for each of the three transformations suggest that the ester-to-methyl transformation kinetically mirrors the alcohol-to-methyl transformation, while the initial ester-to-alcohol transformation occurs rapidly (Scheme 2.5).



*Chapter two references begin on page 204; experimental details begin on page 198*

**Scheme 2.5.** Time-course diagrams for the reduction of methyl-2-napthoate (**2.94**) and napthalene-2-methanol (**2.95**)

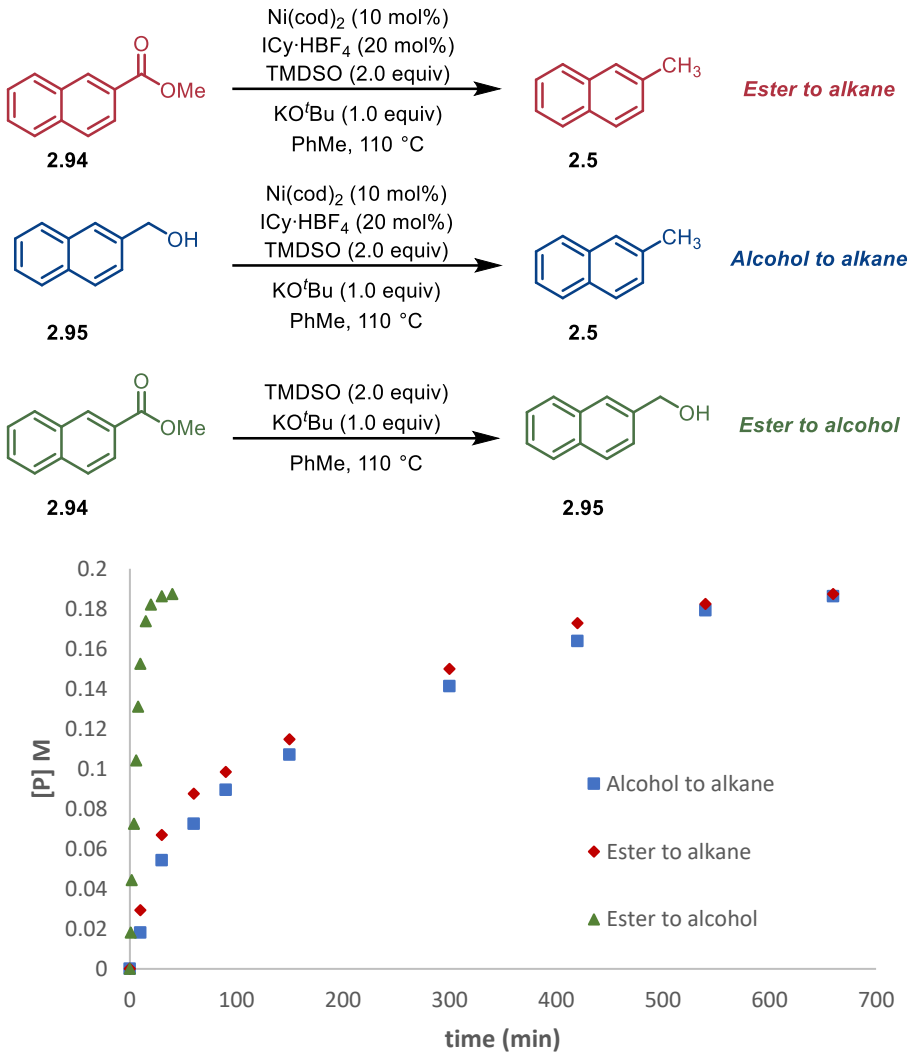


## 2.3.4.2. Variable time normalization analysis

Variable time normalization analysis, developed by Burés and coworkers, is a modern method of kinetic analysis that uses a variable normalization of the time scale of a reaction-progress diagram to enable the extraction of the kinetic parameters of a reaction through a visual comparison.[19] This technique is useful as it allows the rapid determination of approximate rate orders for components in a reaction, obviating the increased number of experiments required by



*Chapter two references begin on page 204; experimental details begin on page 198*

traditional kinetic evaluations. The benefits of variable time normalization analysis include its ease of use, its obtaining of kinetic information under synthetically relevant conditions and that it provides information for the entirety of a reaction.

To gain further mechanistic information pertaining to the exhaustive reduction of esters, the method of variable time normalization analysis was applied to the reduction of methyl naphthoate **2.94** (Scheme 2.6).[19] Positive apparent first order kinetics were observed for the nickel catalyst, substrate, siloxane, and base. While the exact nature of reducing agent is not clear, the rate dependency on the base and literature precedent both support a hypervalent O$^t$Bu-siloxane species being involved in the key hydrogen transfer.[20]

**Scheme 2.6.** Apparent rate law determination by variable time normalization kinetic analysis

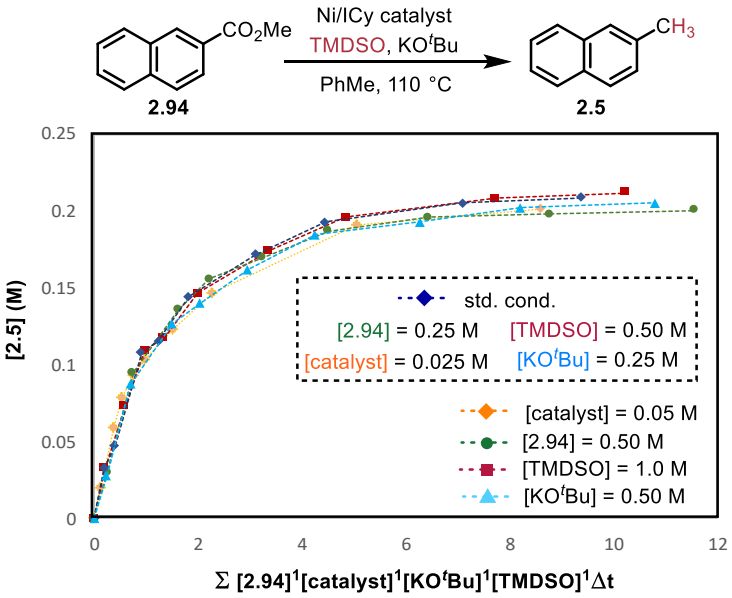


All individual kinetics experiments were performed according to the standard reaction conditions. Ten reactions were set up in parallel and stopped after 10 min, 20 min, 30 min, 1 h, 2 h, 3 h, 5 h, 7 h, 9 h and 10 h. Yields were obtained via $^1$H-NMR using 1,3,5-trimethoxybenzene as internal standard. Standard reaction conditions were 0.25 M 2-methyl naphthoate (**2.94**), 0.25 M



*Chapter two references begin on page 204; experimental details begin on page 198*

KO$^t$Bu, 0.50 M TMDSO, 0.025 M Ni(cod)$_2$ and 0.05 M ICy•HBF$_4$. Figure 2.5 was generated by setting [catalyst] (Ni(cod)$_2$ + ICy•HBF$_4$, 1:2 ratio) to 0.025 M (standard conditions), 0.050 M and 0.075 M. Figure 2.6 was generated by varying [TMDSO], setting it to 0.50 M (standard conditions), 0.75 M, and 1.0 M. Figure 2.7 was generated by varying [**2.94**], setting it to 0.25 M (standard conditions), 0.5 M and 0.75 M. Figure 2.8 was generated by varying [KO$^t$Bu], setting it to 0.025 M (standard conditions), 0.038 M and 0.050 M.



*Chapter two references begin on page 204; experimental details begin on page 198*

**Figure 2.5**. Variation in catalyst: VTNA plots suggest first order dependence

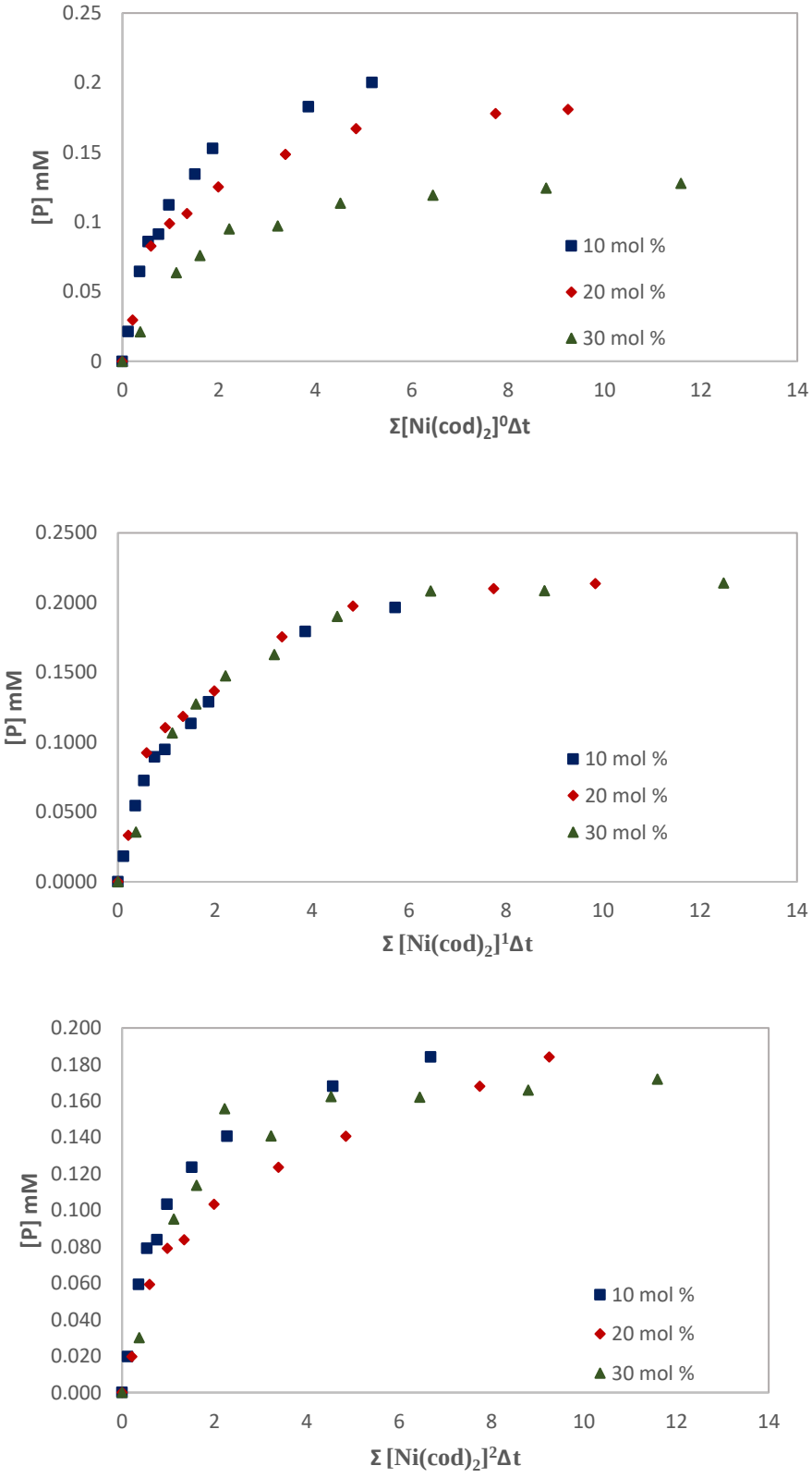




*Chapter two references begin on page 204; experimental details begin on page 198*

**Figure 2.6.** Variation in TMDSO: VTNA plots suggest first order dependence

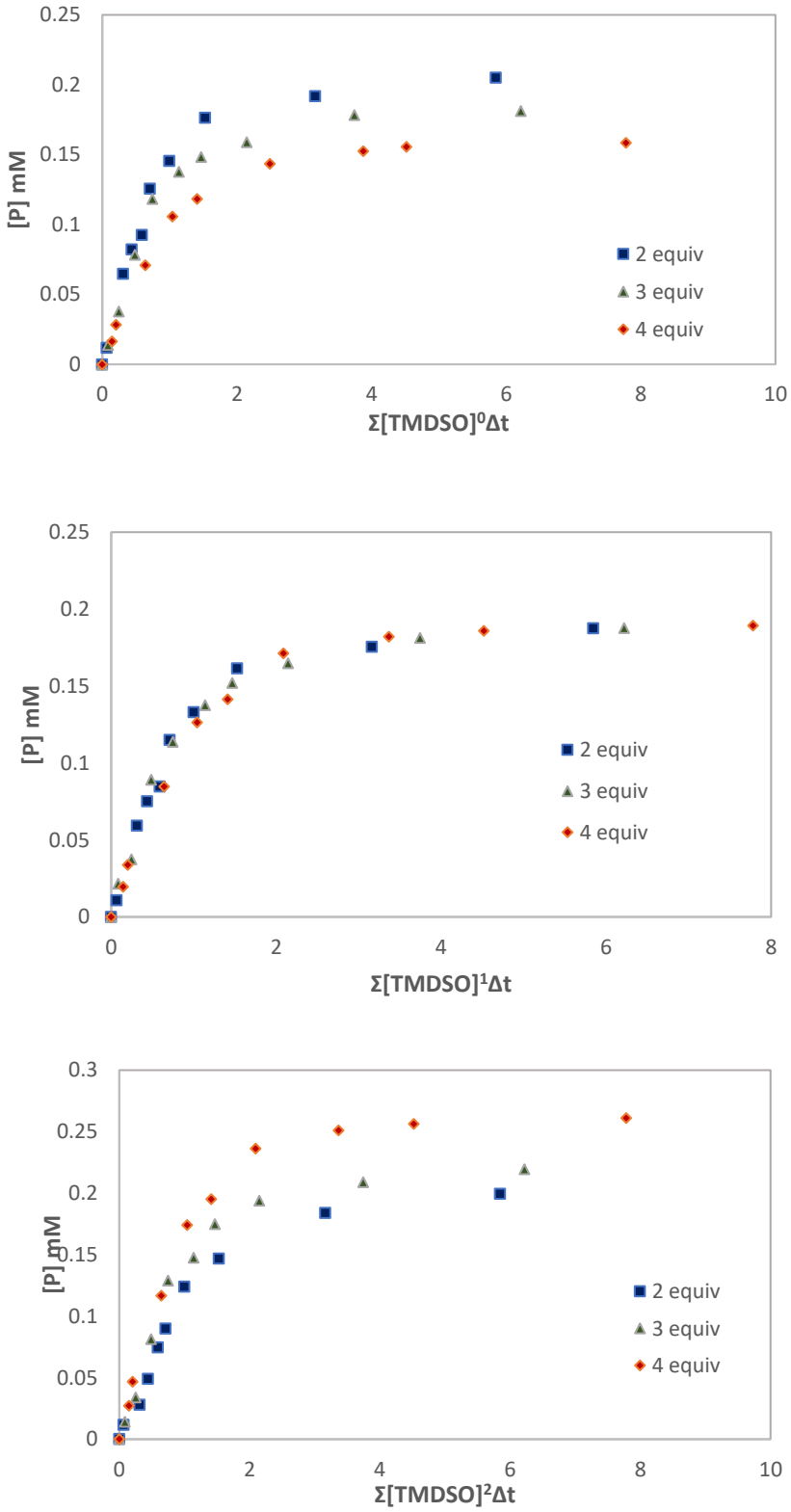




*Chapter two references begin on page 204; experimental details begin on page 198*

**Figure 2.7**. Variation in [**2.94**]: VTNA plots suggest first order dependence

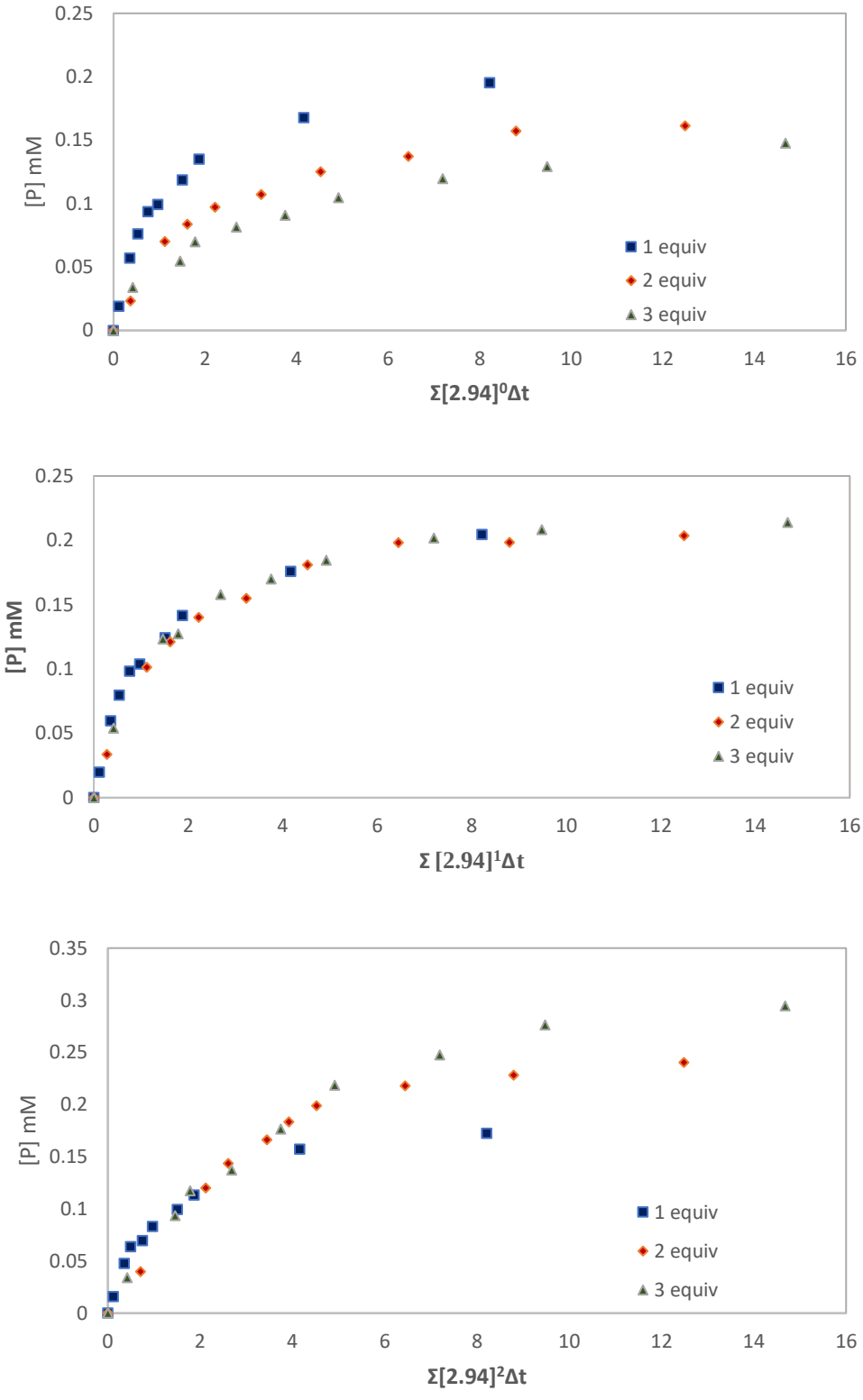




*Chapter two references begin on page 204; experimental details begin on page 198*

**Figure 2.8**. Variation in KO$^t$Bu: VTNA plots suggest first order dependence

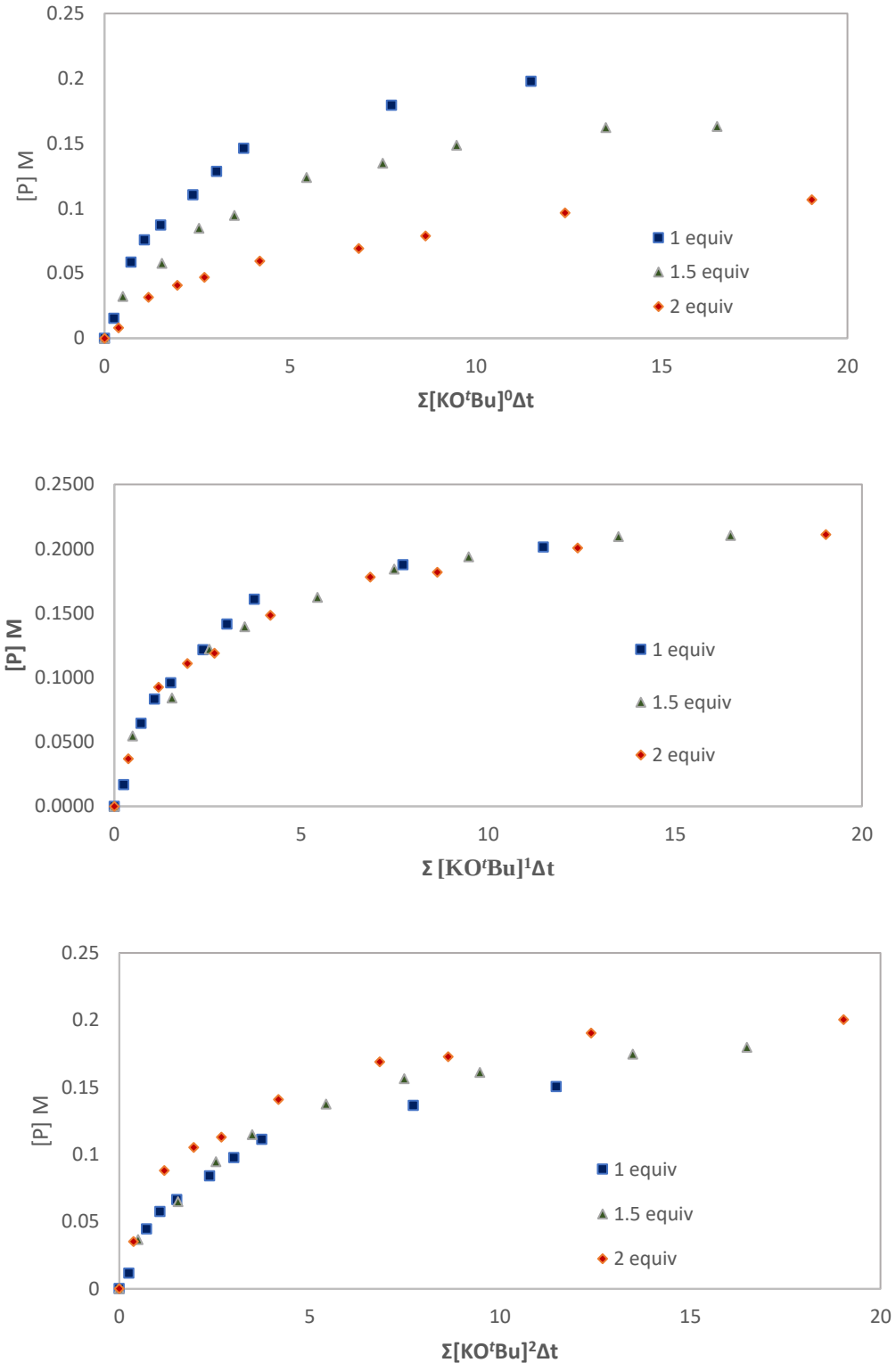




*Chapter two references begin on page 204; experimental details begin on page 198*

### 2.3.4.3. Kinetic isotope effect

In order to determine the kinetic isotope effects of the reduction reaction, two parallel reductions of napthalene-2-methanol (**2.95**) were set up, one with commercial TMDSO and one with $d_2$-TMDSO (Scheme 2.7). Aliquots of each of these reactions were taken after 5, 10, 15, 30 and 60 minutes and subsequently analyzed by GC-FID. Product formation vs. time data was plotted and the initial rates were measured to determine a kinetic isotope effect of 2.24. In this study, **2.95** was chosen as a starting material rather than the corresponding ester (**2.94**) so as to ensure that the results of these experiments reflected the proposed nickel-catalyzed hydrogenolysis step rather than the initial ester-to-alcohol reduction.

**Scheme 2.7**. Initial reaction progress in the presence of TMDSO or $d_2$-TMDSO

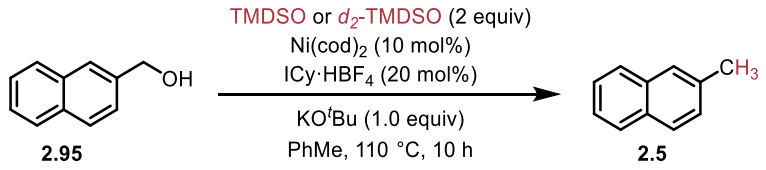


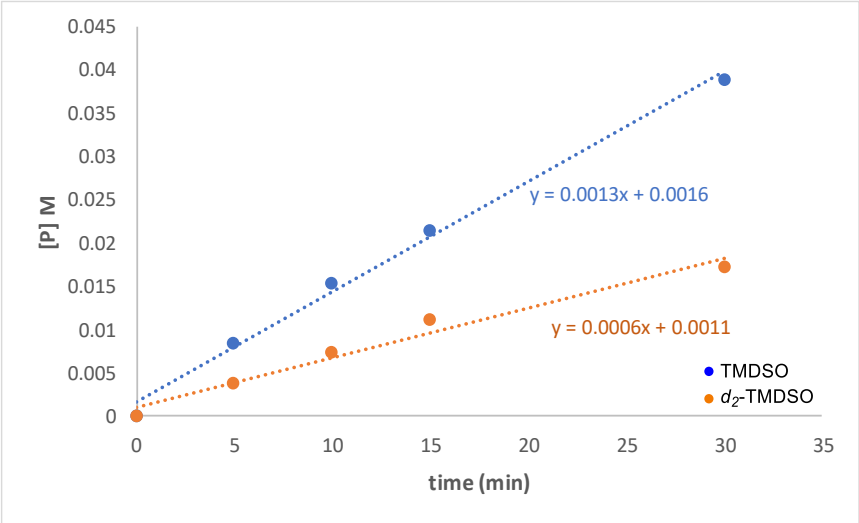




*Chapter two references begin on page 204; experimental details begin on page 198*

Comparable results were obtained by intermolecular competition kinetic-isotope experiments performed using a 50:50 ratio of TMDSO to $d_2$-TMDSO (Scheme 2.16). These experiments resulted in 27% deuterium incorporation in the methyl reduction product (**2.5**), providing further evidence for a primary-kinetic isotope effect.

**Scheme 2.8**. Competition experiments to determine deuterium incorporation

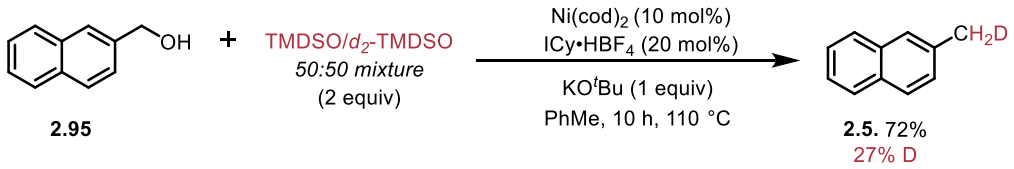


**2.95**

**2.5.** 72%
27% D

### **2.3.4.4.** Speculative reaction mechanism and commentary

While the results obtained thus far warranted publication, more information would be required to derive an accurate mechanistic picture of this transformation. The evidence gathered to this point suggested that elucidating the details of this nickel-catalyzed carbon–oxygen bond reduction would be no facile feat. As such, this paper was submitted with the caveat that follow-up works would focus heavily on exploring the mechanism of this reductive deoxygenation.

Summarizing the data obtained so far in this chapter, a visual time normalization analysis of the kinetic data associated with this reaction suggested a complex interaction at the time of the transition state, and an observed primary kinetic isotope effect suggested that hydride transfer played a key role.[21] From the literature, it was known that the combination of siloxanes and potassium *tert*-butoxide could lead towards the formation of a hypervalent silicate complex,[20d] some variation of which was likely acting as the hydride donor in this reaction. Differing chemoselectivity and reactivity between this transformation and related transformations that are proposed to proceed through nickel(I) intermediates[9] suggested that a different mechanism was at

play in this work. Perhaps the most important observation, however, was that the exhaustive reduction of esters appeared to proceed through two steps, a non-nickel catalyzed reduction of esters into the alcohol oxidation state followed by a nickel-catalyzed hydrogenolysis. With all of this being known, a speculative reaction mechanism could be proposed (Figure 2.9). In the first step of the transformation, hypervalent silicate species **2.A**, formed in situ through a reaction between TMDSO and KO$^t$Bu, is proposed to reduce ester **2.B** into silyl ether **2.C**. Subsequently, nickel(0) oxidatively adds into the C–O bond to form a benzylic intermediate (**2.D**) that is reduced by a second equivalent of the silicate species to generate exhaustively reduced product (**2.E**).

**Figure 2.9.** Speculative reaction mechanism

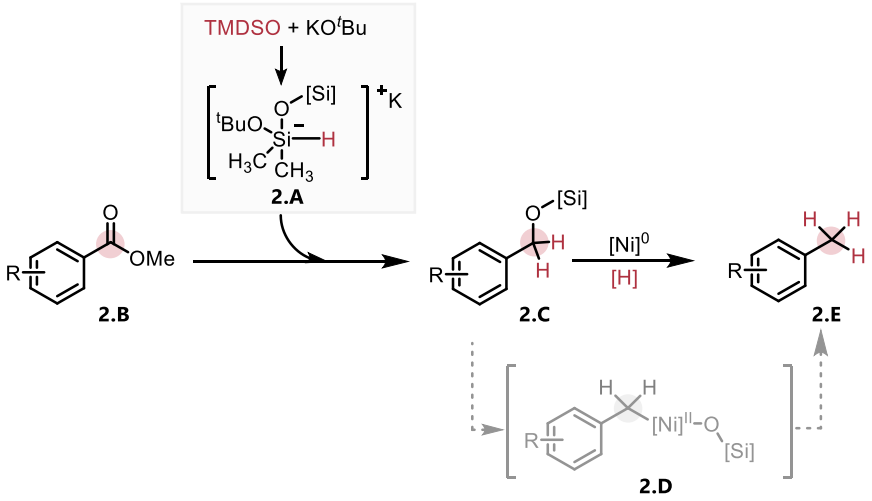


The reduction of esters into the alcohol oxidation state is a well-known transformation,[22] however the reduction of alcohols and their derivatives (as explored briefly in Table 2.7) is less understood. As such, it was determined that future efforts for this project would be best directed towards elucidating and understanding the nickel-catalyzed reduction of compounds in the alcohol oxidation state (e.g. alcohols, ethers). A foremost goal of these future directions would be to gain an understanding of how the strong carbon-oxygen bond within these alcohol derivatives was



*Chapter two references begin on page 204; experimental details begin on page 198*

cleaved. Answers to questions such as “what reactive intermediates are present upon carbon-oxygen bond cleavage”, “how is nickel involved in the bond scission”, and “what other types of oxo-functional groups can be reduced by this catalytic system” will form the basis of Section 2.4.

### **2.3.5.** Failed directions

Esters are an electron withdrawing group, and this method allows them to be transformed into electron donating methyl groups. As such, two ideas were explored in an attempt to utilize this reduction as a method to employ esters as “masked” methyl groups. The first idea considered the application of this idea towards the Diels-Alder reaction, as the electron-withdrawing nature of esters is known to facilitate rapid reactivity when they are present on the dienophile.[23] It was envisioned that methyl propiolate could be reacted with a suitable diene (e.g. 1,4-butadiene) to forge a new six-membered ring that could be oxidized to an arene and subsequently reduced via this exhaustive reduction in a one-pot procedure (Scheme 2.9a). Unfortunately, these experiments did not prove fruitful, instead leading to an intractable mixture of products.

Next, it was envisioned that aryl esters could be used as *meta*-directing functional groups prior to reducing them to methyl groups, noting that this would lead to the generation of 1,3-tolyl derivatives (Scheme 2.9b). While some success was observed when performing Friedel-Crafts acylations on methyl benzoate to afford a 1,3-substituted keto-ester, subjecting this species to the reduction conditions led to a mixture of over-reduced and partially reduced products. Ultimately, neither of these directions was deemed to be worth pursuing as an application of this method, instead favouring the pursuit of conditions that permitted catalytic deuteration.

**Scheme 2.9.** Attempts to exploit esters as 'masked' methyl groups

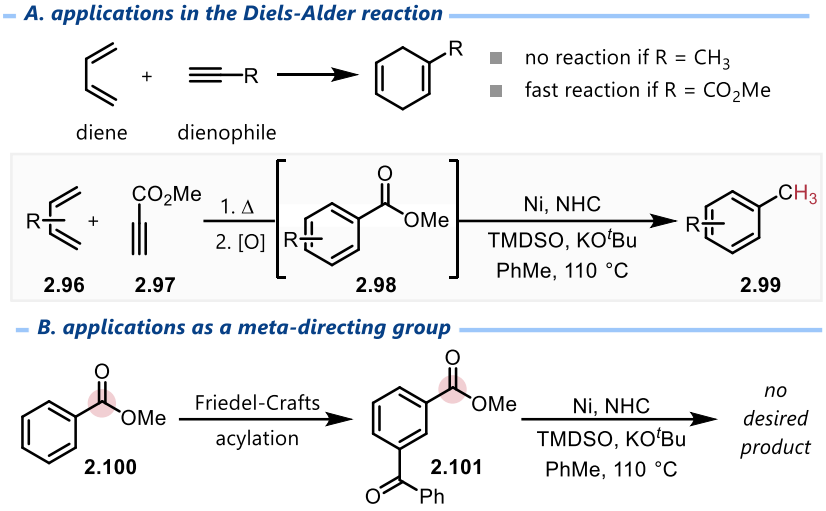


Another failed direction of this project was its attempted extension towards the reduction of carboxylic acids. Exposing compound **2.102** to the standard reaction conditions led to exclusive recovery of starting material, tentatively believed to be a result of catalyst inhibition by the native carboxylic acid (Scheme 2.10). Should this project be pursued further, then the possibility of in situ activation could be pursued to remediate this problem by performing the transformation in the presence of known carboxylic acid activating reagents such as dimethyldicarbonate (DMDC), dimethyl oxalate (DMO), diisopropylcarbodiimide (DIC), hexafluorophosphate azabenzotriazole tetramethyl uronium (HATU) or tetramethylfluoroformamidinium hexafluorophosphate (TFFH).

**Scheme 2.10.** Attempted extension to carboxylic acid reduction

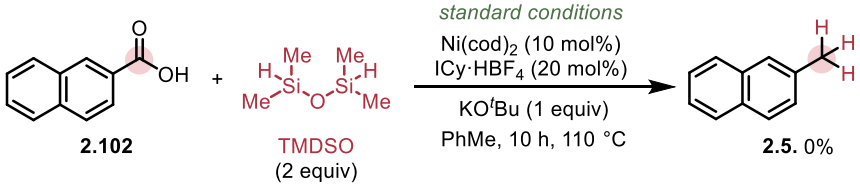




*Chapter two references begin on page 204; experimental details begin on page 198*

Interestingly, this entire project was born out of another hypothesis. Initially it was believed that reacting a methyl ester in the presence of nickel and a hydride source would allow for the selective reduction of esters into aldehydes. Conventional methods for the ester-to-aldehyde reduction employ DIBAL-H as a hydride source, which – while effective – often necessitates cryogenic conditions and difficult work-up conditions while only being moderately compatible with other functional groups (Scheme 2.11a).[24] Darcel and colleagues demonstrated in 2013 that this transformation could be achieved in the presence of an iron-NHC catalyst and hydrosilane reductant (Scheme 2.11b),[25] although the substrate scope was limited and ultraviolet irradiation was required. In the years since, cobalt,[26] manganese,[27] rhenium,[27] and iridium[28] have been used alongside hydrosilanes to perform the same transformation. A thorough overview of transition metal-catalyzed methods to reduce esters to aldehydes were documented in a review article published by Yang in 2018.[29]

**Scheme 2.11.** Reduction of esters into aldehydes

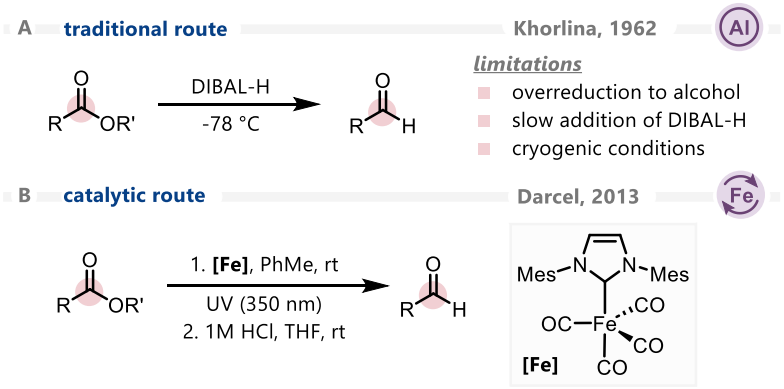


Seeking to identify nickel-catalyzed conditions for this transformation, ester **2.1** was reacted with $Ni(cod)_2$ for 12 hours at room temperature in the presence of $ICy•HBF_4$, TMDSO and $KO^tBu$ in PhMe. An analysis of the resulting reaction mixture led to the observation of 38%



*Chapter two references begin on page 204; experimental details begin on page 198*

aldehyde product (**2.103**), and a combined 29% of over-reduced species (**2.3, 2.2**), with the rest of the mass balance proving intractable. Select optimization experiments were conducted, varying the equivalents of hydride and the reaction time, however they did not prove fruitful. A small substrate screen proved this reaction to work on multiple esters, albeit in low yields (**2.104**-**2.107**); tests conducted on aliphatic esters did not afford product (**2.108**) (Scheme 2.12). While this project was abandoned, future directions may seek to explore alternative ligands, hydride sources and reaction temperatures in hopes of selectively reducing esters to aldehydes.

**Scheme 2.12.** Nickel-catalyzed reduction of esters into aldehydes

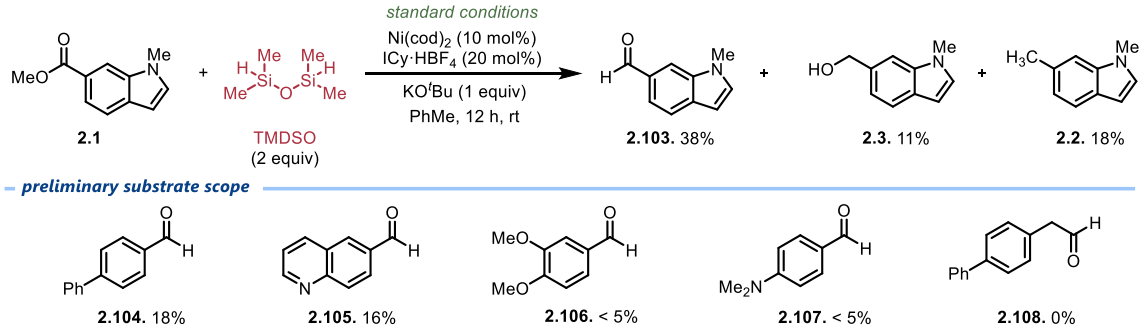


## 2.3.6. Part A: Conclusions

In summary, Section 2.3 details the development of a novel method to convert methyl esters into the corresponding tolyl derivative. In contrast to established multi-step sequences for this transformation, the reaction takes place under a single set of conditions, comprised of a rapid, non-catalyzed siloxane-mediated reduction to a silylated alcohol followed by subsequent nickel-catalyzed reduction to the corresponding $–CH_3$ group. It is believed that this reaction will be particularly useful in the synthesis of methyl-bearing heterocycles, where the corresponding esters are more readily abundant, as well as in reductive deuteration as a method to install $–CD_3$ groups. This transformation sharply contrasts previous reports of nickel-catalyzed reductions with



*Chapter two references begin on page 204; experimental details begin on page 198*

siloxanes of, e.g., amides, ethers, and phenyl esters; the inclusion of a KO$^t$Bu is proposed to be a key feature, which generates a more aggressive siloxane reducing agent in situ. Tentatively, it is proposed that a hypervalent siloxane rapidly reduces the ester into a silylated alcohol. The resultant alcohol reacts with a nickel(0) catalyst by a reversible, endothermic oxidative addition to form a benzylic nickel(II) intermediate, which is reduced by the activated siloxane in a rate-determining hydride transfer.

## 2.4. Part B: Reductive Deoxygenation of Diverse C–O Bond Bearing Functional Groups

### 2.4.1. Introductory theory and background information

Accessing complex molecules from simple starting materials is central to organic synthesis. However, there is also value in chemical reactions that decrease overall complexity by selectively removing certain functional groups. For instance, methods for late-stage defunctionalization of bioactive molecules,[30] reduction of biomass-derived compounds,[31] and removal of protecting or directing groups[32] have great utility in certain situations. Reactions that reductively remove C–O bonds have particularly diverse applications (Figure 2.10a). Alcohol deoxygenation can be done via the corresponding xanthate intermediate in the Barton-McCombie reaction.[33] Ketones and aldehydes can also be converted into the corresponding alkane, for instance through a hydrazone intermediate in the Wolff-Kishner reduction.[34] Hydrogenolysis reactions using heterogeneous transition metal catalysts provides another powerful strategy to cleave C–O bonds.[35]

Recently, good progress has been made to improve the step economy and functional group tolerance of deoxygenation reactions through the use of powerful catalysts.[36] For instance, use of $B(C_6F_5)_3$ alongside a silane hydride donor has proven to be powerful for the deoxygenation of ketones,[37] aldehydes,[37a-c, 38] alcohols,[37a, 39] amides,[40] and other C–O bond-containing functional groups.[41] However, applications of this highly Lewis acidic, air-sensitive catalyst system to the deoxygenation of complex molecules such as those bearing nitrogen-containing heterocycles is limited. Several other promising methods using the combination of a Brønsted or Lewis acid catalyst alongside a mild hydride source have also been reported.[42] Other modern deoxygenation strategies include merging catalysis with Wolff-Kishner reductions,[43] cross-coupling-like approaches,[44] and beyond.[45] Despite this progress, there is still a need for more universal, chemoselective deoxygenation reactions that work directly on unactivated C–O bond-containing starting materials.

**Figure 2.10.** Methods for reductive deoxygenation

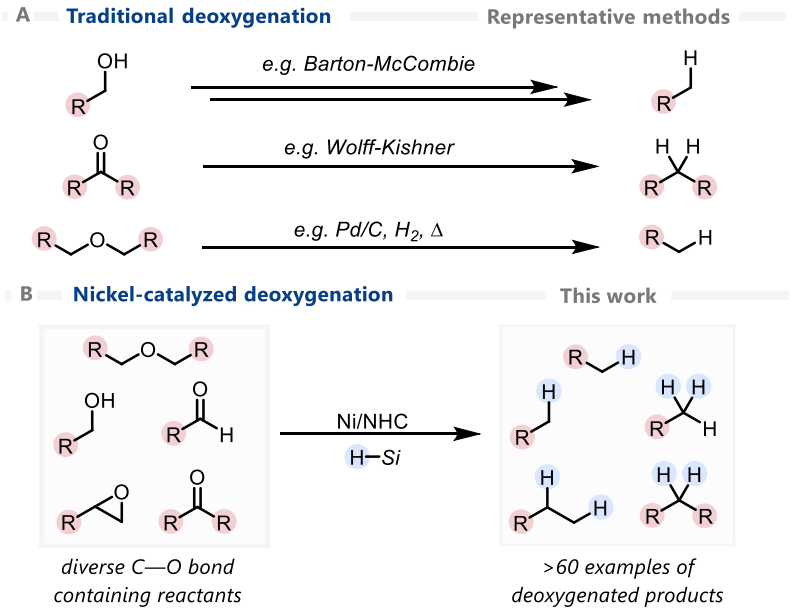




Chapter two references begin on page 204; experimental details begin on page 198

Homogeneous nickel catalysts have recently proven themselves to be particularly useful for hydrodeoxygenation reactions. For instance, reductive cleavage of C($sp^2$)–O bonds in aryl ethers has been reported using organosilanes[46] and hydrogen gas,[47] as well as other reagents.[48] Nickel-catalyzed arene defunctionalization to make benzenes,[49] amide deoxygenation to make amines,[50] and carboxylic acid reduction to make aldehydes[51] have also been reported. Recently, the Newman group discovered a method for the exhaustive reduction of unactivated esters using a nickel(0) precatalyst in the presence of a siloxane reducing agent to form the corresponding methyl group.[52] It was hypothesized that the corresponding aldehyde and silylated alcohol were reactive intermediates, suggesting that the conditions may have broad implications beyond ester reduction. Disclosed herein are studies on expanding the breadth of substrates that can be readily deoxygenated by nickel catalysis (Figure 2.10b). Examples of aldehyde, ketone, alcohol, epoxide, and ether reduction are provided, selectively forming the corresponding methyl, methylene, or methine-containing products.

## **2.4.2.** Development of reaction conditions

### **2.4.2.1**. Overview

This study began by exploring the deoxygenation of carbonyl-containing molecules with dibenzyl ketone **2.109** as a model compound. Treatment of **2.109** with 1.2 equivalents of 1,1,3,3-tetramethyldisiloxane (TMDSO; net 2.4 equivalents of hydride) in toluene at 70 °C for 5 h in the presence of $NiBr_2$·glyme (10 mol%), ICy•$HBF_4$ (20 mol%), Mn (0.3 equiv), and KO$^t$Bu (1.0 equiv) afforded reduced hydrocarbon **2.110** in 86% yield (Table 2.8, entry 1). Notably, these conditions are substantially milder than was required for ester reduction,[52] and the reactions can be set up without a glovebox. Manganese was required for obtaining good yields when using this



*Chapter two references begin on page 204; experimental details begin on page 198*

nickel(II) precatalyst (entry 2), but not if nickel(0) is used (entry 3), suggesting its role is to first reduce nickel(II) to its active oxidation state. Product is also formed when using zinc as an alternative reducing agent (entry 4), further corroborating this hypothesis. No product was obtained upon removing base or siloxane from the reaction mixture (entry 5), highlighting the importance of their roles in this reaction. Alternative silane reducing agents including $Et_3SiH$ and PMHS were less effective than TMDSO (entries 6, 7). While most bases used led to poor conversion, potassium fluoride proved to be a viable alternative provided that enough KO$^t$Bu was included in the reaction mixture to deprotonate the ICy•$HBF_4$ (entries 8, 9). The identity of the ligand proved to play a significant role in the facilitation of this reaction. Other NHCs including IPr (entry 10) and IMes (entry 11) provided substantial yield, while phosphine (entries 12, 13) and nitrogen (entry 14) ligands were less effective. Omission of $NiBr_2$·glyme from the reaction mixture provided no hydrocarbon **2.110** (entry 15). However, the starting ketone was completely assumed, and 1,3-diphenyl-2-propanol could be recovered after treatment of the crude mixture with tetrabutylammonium fluoride.

**Table 2.8.** Optimization of the ketone reduction reaction

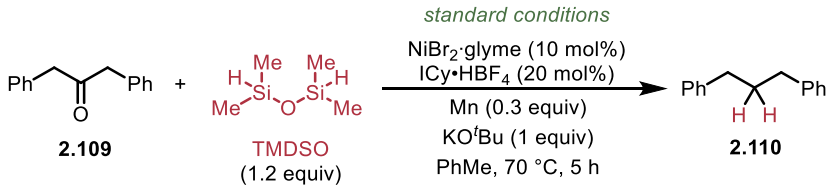


| entry | deviation from standard conditions | % yield, 2.110[a] |
|---|---|---|
| **1** | none | 86 |
| **2** | $NiBr_2$·glyme (10 mol%) *without Mn* | 14 |
| **3** | $Ni(cod)_2$ (10 mol%) *without Mn* | 84 |
| **4** | Zn (0.3 equiv) *instead of Mn* | 68 |
| **5** | no base or no TMDSO | 0 |
| **6** | $Et_3SiH$ (2.4 equiv) *instead of TMDSO* | 43 |



*Chapter two references begin on page 204; experimental details begin on page 198*

| | | |
|---|---|---|
| **7** | PMHS *instead of TMDSO* | 17 |
| **8** | KF (1.0 equiv) *instead of KO$^t$Bu* | 17 |
| **9** | KF (1.0 equiv) + KO$^t$Bu (20 mol%) | 82 |
| **10** | IPr•HCl *instead of ICy•HBF$_4$* | 74 |
| **11** | IMes•HCl *instead of ICy•HBF$_4$* | 71 |
| **12** | PCy$_3$ *instead of ICy•HBF$_4$* | 49 |
| **13** | dcype *instead of ICy•HBF$_4$* | 19 |
| **14** | 1,10-phenanthroline *instead of ICy•HBF$_4$* | 33 |
| **15** | no NiBr$_2$·glyme | 0[b] |

General reaction conditions: 0.20 mmol starting material, 0.24 mmol TMDSO, 0.20 mmol KO$^t$Bu, 0.02 mmol NiBr$_2$·diglyme, 0.04 mmol ICy•HBF$_4$, 0.06 mmol Mn in 0.8 mL PhMe (0.33 M). [a] yields acquired by GC-FID using 1,3,5-trimethoxybenzene as internal standard [b] 1,3-diphenyl-2-propanol obtained as product with an 83% yield after work-up with TBAF.

### **2.4.2.2.** Time-course study of ketone deoxygenation

To confirm that alcohol **2.111** is a viable reactive intermediate, the progress of the reaction was monitored over time (Scheme 2.13). Within the first hour, full conversion of the starting ketone **2.109** was observed with alcohol **2.111** providing the majority of the mass balance. Over the following 4 hours, alcohol **2.111** slowly converted into **2.110**; this confirms that ketone **2.109** is initially reduced in a stoichiometric reaction with the TMDSO/KO$^t$Bu reducing agent to the alcohol oxidation state which is subsequently engaged in a catalytic alcohol or silyl ether reductive deoxygenation. Independently subjecting alcohol **2.111** to the same reaction conditions led to the efficient production of alkane **2.110** through initial conversion into an oligomeric mixture of silyl ethers. Ultimately, it is believed that the fate of the cleaved oxygen to be incorporated into a complex mixture of silane oligomers that are detected by GC-MS in all studied reactions.

**Scheme 2.13.** Time-course diagram for the deoxygenation of model substrate **2.109**

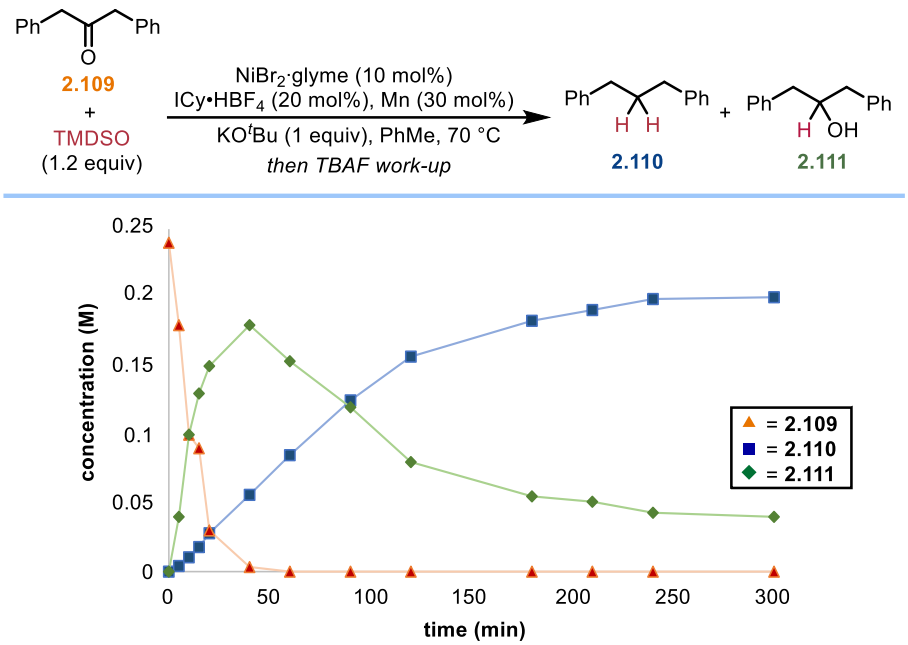


## 2.4.3. Substrate scope

### 2.4.3.1. Substrate scope for alcohol deoxygenation

With knowledge that these reaction conditions were effective both for reducing carbonyls and for reductively cleaving C($sp^3$)–O bonds, the reaction scope was investigated. A variety of unprotected alcohols were first studied (Scheme 2.14). Primary benzyl alcohols (**2.112a**), secondary benzyl alcohols (**2.112b-e**), tertiary benzyl alcohols (**2.113**, **2.114**), and diverse allylic alcohols (**2.115**–**2.117**) all smoothly converted into the corresponding hydrocarbon in yields ranging from 60–87%. Several non-benzylic or allylic alcohols were also efficiently reduced; for instance, tertiary alcohol **2.118** was deoxygenated to afford a 71% yield.

A series of phenethyl alcohol derivatives were next reduced to understand the effect of substitution patterns on the target carbon. Generally, increasing the substitution led to a decrease in yields (**2.119a-c**), corroborating the same observation that was made when reducing benzylic



*Chapter two references begin on page 204; experimental details begin on page 198*

alcohols **2.112a-c**. Functional group tolerance was also investigated. Amine-containing **2.119d**, alkene-containing **2.119e**, phenol-containing **2.119f**, and anisole-containing **2.119g** all provided similar yields of the deoxygenation product with complete chemoselectivity.

Substrates bearing C–F (**2.119h**) bonds provided mixtures of products using the standard reaction conditions but could be cleanly reduced by using potassium fluoride as an alternative base. Furan (**2.120**) and indole (**2.121**) bearing alcohols were also tolerated, and 1 gram of pyridine (**2.122**) bearing alcohol could be deoxygenated with 3 mol% of the nickel catalyst in 66% yield, confirming scalability and the ability to reduce catalyst loading. Knowing that the reaction is tolerant of heterocycles, C($sp^2$)–O bonds, amines, and olefins, quinine **2.123** was subjected to the reaction conditions. Chemoselective reduction of the benzylic alcohol was observed in 63% yield, providing an appealing alternative to other methods for the reduction of quinine motifs.[53]

Notably, most successfully reduced substrates feature a nearby π-system which appears to be important for reactivity. While benzyl alcohol **2.112a** and homobenzyl alcohol **2.119a** afford high yields, placing the target C–O bond three-carbons away from the π-system leads to lower yields. For instance, alcohol **2.124** reduces sluggishly to provide the corresponding hydrocarbon product in 54% yield. Simple alcohols bearing no nearby π-bonds such as tertiary alcohol **2.125**, menthol **2.126** and 4-phenyl-1-butanol **2.127** only afforded silylated products upon exposure to the reaction conditions without evidence of reduction.



*Chapter two references begin on page 204; experimental details begin on page 198*

**Scheme 2.14.** Substrate scope for alcohol deoxygenation

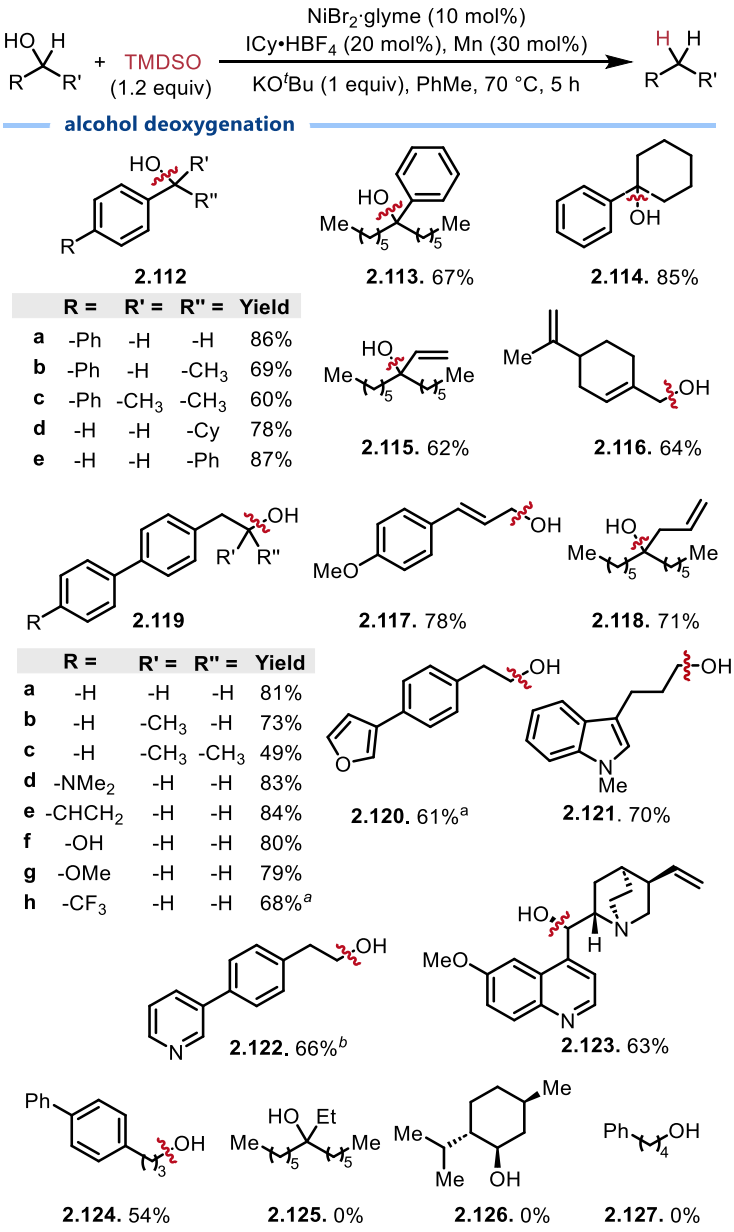


| | R = | R' = | R'' = | Yield |
|---|---|---|---|---|
| a | -Ph | -H | -H | 86% |
| b | -Ph | -H | $-CH_3$ | 69% |
| c | -Ph | $-CH_3$ | $-CH_3$ | 60% |
| d | -H | -H | -Cy | 78% |
| e | -H | -H | -Ph | 87% |

| | R = | R' = | R'' = | Yield |
|---|---|---|---|---|
| a | -H | -H | -H | 81% |
| b | -H | $-CH_3$ | -H | 73% |
| c | -H | $-CH_3$ | $-CH_3$ | 49% |
| d | $-NMe_2$ | -H | -H | 83% |
| e | $-CHCH_2$ | -H | -H | 84% |
| f | -OH | -H | -H | 80% |
| g | -OMe | -H | -H | 79% |
| h | $-CF_3$ | -H | -H | 68%a |

Reaction conditions: 0.20 mmol starting material, 0.24 mmol TMDSO, 0.20 mmol KO$^t$Bu, 0.02 mmol $NiBr_2$·diglyme, 0.04 mmol ICy•$HBF_4$, 0.06 mmol Mn in 0.8 mL PhMe (0.33 M). Reactions set up outside of the glovebox; yields are isolated. [*a*] KF (0.20 mmol) + KO$^t$Bu (0.02 mmol) used instead of KO$^t$Bu (0.20 mmol) [*b*] yield obtained upon reacting 5.91 mmol (1 g) of starting material using 3% Ni + 6% ICy•$HBF_4$.



*Chapter two references begin on page 204; experimental details begin on page 198*

### 2.4.3.2. Substrate scope for ketone and aldehyde deoxygenation

Next, an investigation into the deoxygenation of ketones and aldehydes was conducted (Scheme 2.15). Generally, the yields and functional group tolerance observed were analogous to the alcohol deoxygenation scope. Aryl ketones **2.128a-h** were reduced with similar efficiency regardless of the steric environment or presence of potentially sensitive functional groups.

Multifunctional bioactive ketone **2.129**, *β*-tetralone **2.130**, and *α,β*-unsaturated ketones **2.131** and **2.132** were chemoselectively reduced in 70–77% yield. Notably, the deoxygenation of cholestenone-bearing **2.133** was achieved, providing an alternative to contemporary methods for steroid deoxygenation.[54] Nonsteroidal anti-inflammatory drugs (NSAIDs) zaltoprofen **2.134** and ketoprofen **2.135** could also be effectively reduced by a slightly modified procedure, leaving the C–S bonds and carboxylic acids untouched. Consistent with the results presented in Scheme 2.14 on alcohol deoxygenation, ketones without a nearby arene ring could not be deoxygenated. Phenyl-2-pentanone **2.136**, decanone **2.137** and dicyclohexylketone **2.138** converted to the corresponding alcohol with no evidence of hydrocarbon formation. Aldehydes featuring a conjugated (**2.139**) or non-conjugated (**2.140**) aromatic ring, as well as an *α,β*-unsaturated aldehyde (**2.141**) could also be readily deoxygenated in good yield.

**Scheme 2.15.** Substrate scope for ketone & aldehyde deoxygenation

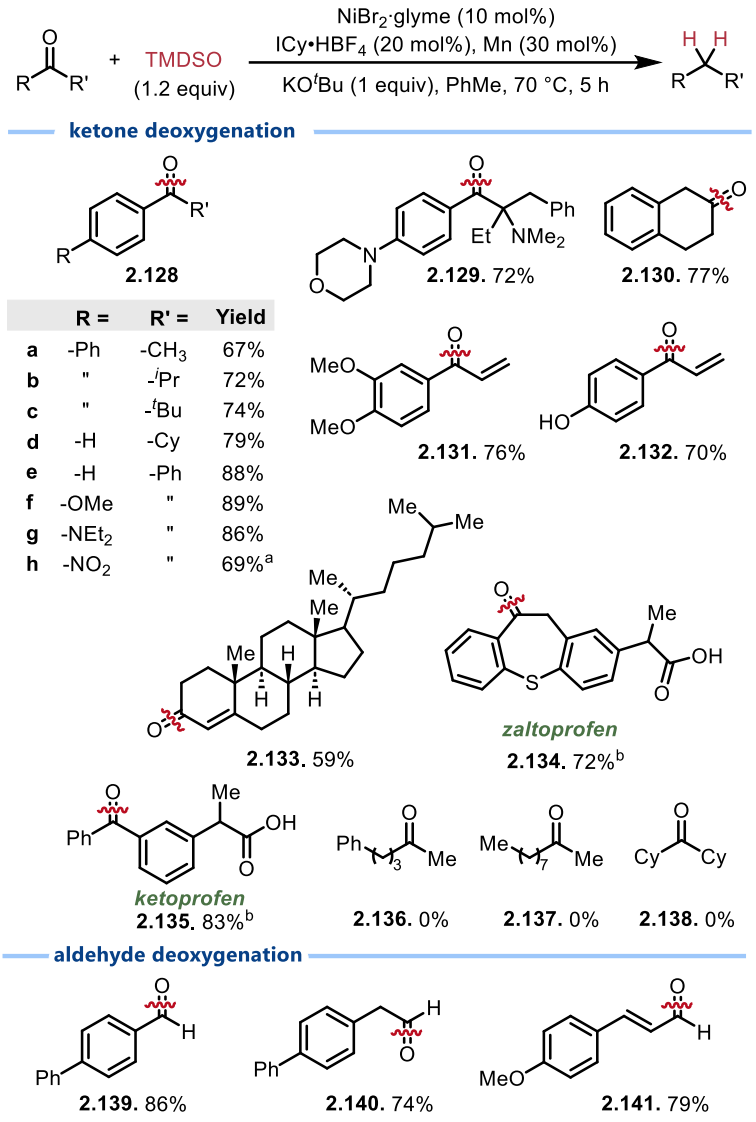


| | R = | R' = | Yield |
|---|---|---|---|
| a | -Ph | $-CH_3$ | 67% |
| b | " | $-^{i}Pr$ | 72% |
| c | " | $-^{t}Bu$ | 74% |
| d | -H | -Cy | 79% |
| e | -H | -Ph | 88% |
| f | -OMe | " | 89% |
| g | $-NEt_2$ | " | 86% |
| h | $-NO_2$ | " | 69%[a] |

Reaction conditions: 0.20 mmol starting material, 0.24 mmol TMDSO, 0.20 mmol KO$^{t}$Bu, 0.02 mmol $NiBr_2$·diglyme, 0.04 mmol ICy•$HBF_4$, 0.06 mmol Mn in 0.8 mL PhMe (0.33 M). Reactions set up outside of the glovebox; yields are isolated. [*a*] KF (0.20 mmol) + KO$^{t}$Bu (0.02 mmol) used instead of KO$^{t}$Bu (0.20 mmol) [*b*] KO$^{t}$Bu (0.40 mmol) used instead of KO$^{t}$Bu (0.20 mmol)



*Chapter two references begin on page 204; experimental details begin on page 198*

### 2.4.3.3. Substrate scope for ether and epoxide deoxygenation

Hypothesizing that all reactions discussed thus far proceed by deoxygenation of a silyl ether, the deoxygenation of ethers and related substrates was investigated next (Scheme 2.16). Methyl and isopropyl ether analogs of compound **2.142** could be efficiently reduced to provide diphenylmethane **2.143** in high yields. Seeking to demonstrate chemoselective cleavage of C($sp^3$)–O bonds in the presence of C($sp^2$)–O bonds, methyl ether **2.144** was subjected to the general reaction conditions to afford **2.145** in 79% yield without observation of compound **2.146**. Subjecting the same ether to conditions known to cleave C($sp^2$)–O bonds[46a] led to exclusive formation of **2.146**. In addition to providing useful orthogonal selectivity, this also suggests that a distinct catalytic cycle is operative in this method compared to established deoxygenation procedures that are generally limited to C(aryl)–O or activated C(alkyl)–O cleavages.[46-48]

Beyond simple ethers, TBS-protected alcohol **2.147** could also be reduced to hydrocarbon **2.148** in 79% yield. Interestingly, both C–O bonds of epoxides **2.149** and **2.151** could be cleaved, leading to deoxygenated products **2.150** and **2.152**, respectively.[55]



*Chapter two references begin on page 204; experimental details begin on page 198*

**Scheme 2.16.** Substrate scope for ether and epoxide deoxygenation

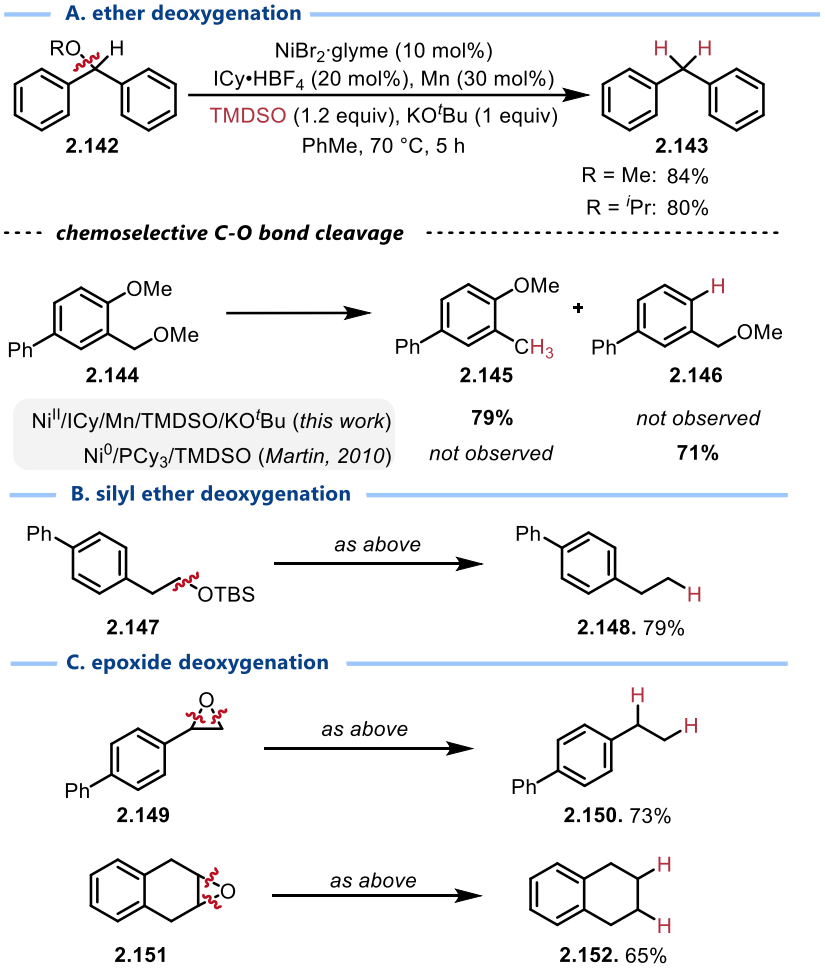


### 2.4.3.4. Multi-site deoxygenation

Lastly, an investigation was undertaken to see if multi-site deoxygenation was possible (Scheme 2.17). Indeed, subjecting **2.153** to the standard reaction conditions with excess TMDSO led to cleavage of all four distinct C–O bonds, providing hydrocarbon **2.154** in 76% yield. Similarly, reacting bis-oxygenated flavanone **2.155** led to deoxygenation at each of the benzylic positions to form product **2.156** while leaving the remaining C($sp^2$)–O bond untouched.



*Chapter two references begin on page 204; experimental details begin on page 198*

**Scheme 2.17.** Substrate scope for multi-site deoxygenation

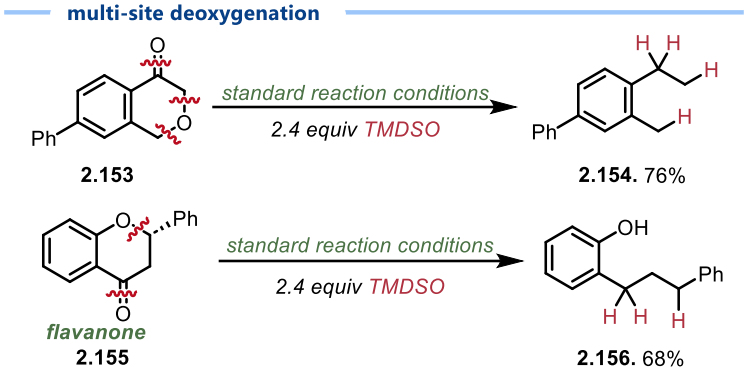


### 2.4.3.5. Unsuccessful scope examples

Multiple compounds were not reducible upon subjection to the standard reaction conditions (Figure 2.11). The attempted reduction of primary alcohols **2.157**-**2.159** led to exclusive recovery of starting material, as did the attempted reduction of secondary alcohols (**2.160, 2.161**) and tertiary alcohols (**2.162, 2.163**). C($sp^2$)–O bonds also evaded reduction upon subjection to the standard reaction conditions (**2.164**). The attempted reduction of a propargylic alcohol (**2.165**) led to the unidentified decomposition products.

**Figure 2.11**. Unsuccessful substrates in the deoxygenation of C–O bonds

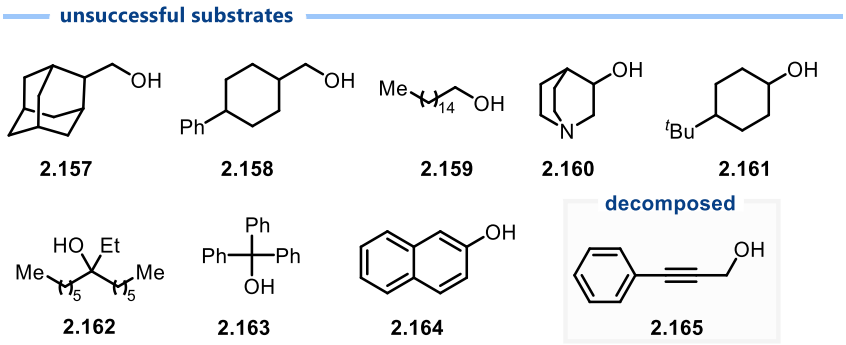




*Chapter two references begin on page 204; experimental details begin on page 198*

Knowing that the reaction proceeds through an initial Si–O bond forming event to form a silylated alcohol followed by a catalytic deoxygenation step, an investigation into which of these two steps was problematic for the above-mentioned substrates was warranted (Scheme 2.18). Upon reacting substrates **2.126** and **2.159** in the absence of the nickel-NHC catalyst, rapid formation of an oligomeric mixture of siloxanes was observed. Synthesizing the corresponding TBS-protected ethers of these species (**2.166**, **2.167**) for subjection to the standard reaction conditions led to the recovery of starting material in both cases. This suggests that, for the failed substrates detailed above in situ silylation is feasible and it is the subsequent C–O bond cleavage step that does not occur.

**Scheme 2.18.** Unsuccessful reduction of silyl ethers.

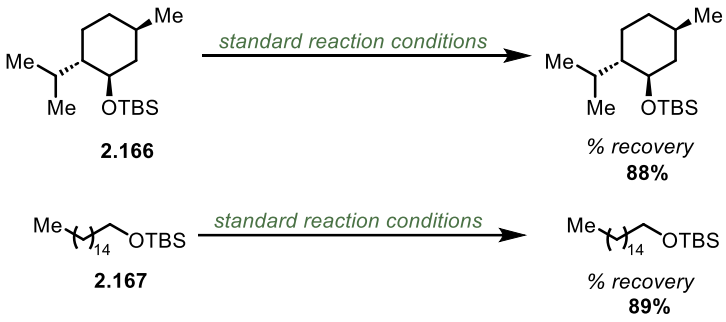


## 2.4.4. Applications of this transformation

### 2.4.4.1. Catalytic deuteration

Next, attention was turned towards applications of this deoxygenation procedure. Reductions and other functional-group removal reactions have been demonstrated to be particularly useful for isotopically labeling molecules.[56] To this end, several substrates were subjected to the reduction conditions using $d_2$-TMDSO[57] as the reducing agent (Scheme 2.19). Alcohol starting materials smoothly converted into the corresponding reduction products with



Chapter two references begin on page 204; experimental details begin on page 198

slightly reduced yields relative to when protic TMDSO was used (**2.168**, **2.169**). Similar trends were observed when using ketones; while somewhat lower yields were obtained, the corresponding bis-deuterated products were isolated with >95% deuterium incorporation (**2.170**-**2.173**). In all cases, deuterium was incorporated selectively into the position that formerly bore a C–O bond without evidence of remote deuteration. Unfortunately, commercially available $Et_3SiD$ was not found to be a viable alternative to *d*$_2$-TMDSO due to moderate yields and low deuterium incorporation.

**Scheme 2.19.** Catalytic deuteration of ketones and alcohols

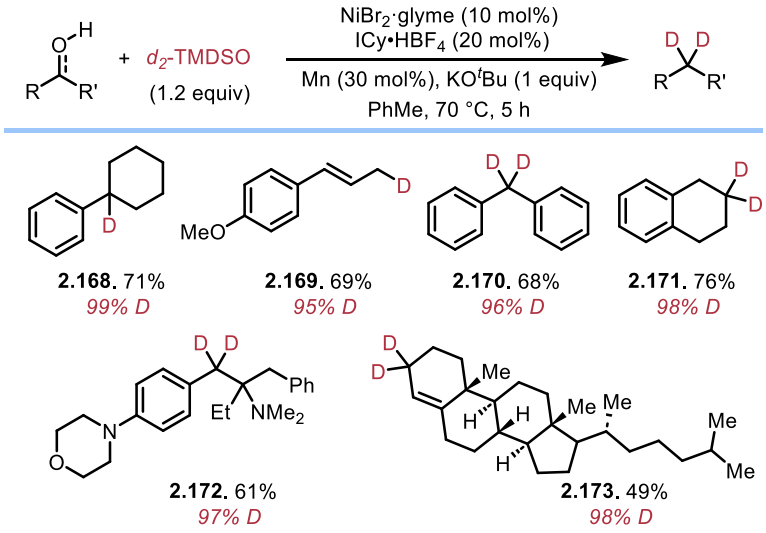


## 2.4.4.2. Deprotection of benzyl-protected alcohols

Another common application of C($sp^3$)–O cleavage is in the reductive removal of benzyl ether protecting groups to reveal the corresponding deprotected alcohol. This is most commonly carried out using a heterogeneous catalyst such as palladium/carbon, either under hydrogen gas or in the presence of an alternative hydride donor.[58] While efficient, chemoselectivity issues can arise in the presence of other reducible functional groups such as alkenes or heterocycles. Accordingly,



*Chapter two references begin on page 204; experimental details begin on page 198*

a range of other conditions have been developed for deprotecting benzyl alcohols, each with its own strengths and limitations.[59] It was hypothesized that the high selectivity of this reaction towards benzylic C($sp^3$)–O bond cleavage may provide a viable alternative to traditional deprotection conditions (Scheme 2.20). Indeed, subjecting benzyl-protected menthol to the nickel/TMDSO system resulted in exclusive cleavage of the ether at the benzylic position, providing menthol **2.174** in 91% yield. Similarly, benzylated eugenol and magnolol could be deprotected to form **2.175** and **2.176** in high yields without any cleavage of the C($sp^2$)–O ethereal linkage or reduction of the alkene, confirming this approach has utility compared to traditional heterogeneous hydrogenolysis. Further, this method was successful in the deprotection of *para*-methoxy benzyl (PMB) protected ethers, affording the same products in high yields.

**Scheme 2.20.** Deprotection of benzyl-protected alcohols

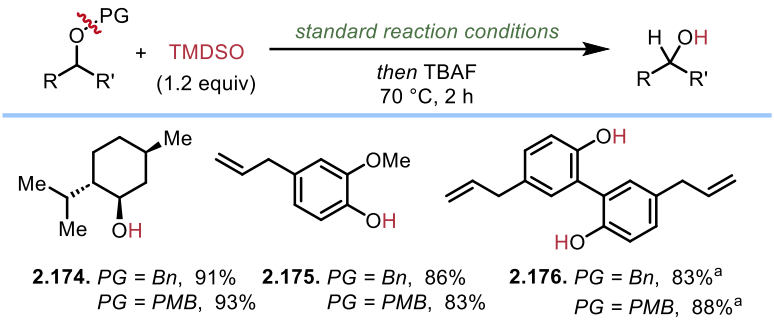


**2.174.** *PG* = *Bn*, 91% *PG* = *PMB*, 93% **2.175.** *PG* = *Bn*, 86% *PG* = *PMB*, 83% **2.176.** *PG* = *Bn*, 83%[a] *PG* = *PMB*, 88%[a]

### 2.4.4.3. Degradation of biomass-derived molecules

Ethereal linkages are also prominently featured in lignin and other biomass-derived molecules. Selective hydrogenolysis of such molecules towards the access of value-added deoxygenated products is an important step in the bioeconomy.[60] Substrate **2.177** is a useful model compound for the α-*O*-4 linkage found in lignin; of the eight distinct C–O bonds present in this substrate, the benzylic position could be selectively cleaved to reveal the two arene products **2.178**



*Chapter two references begin on page 204; experimental details begin on page 198*

and **2.179** in 86% and 81% yield, respectively (Scheme 2.21). Tannins are another class of naturally abundant aromatic biomolecule that may serve as useful substrates in the bioeconomy.[60] Exposing polyoxygenated tannin (-)-epicatechin **2.180** to this protocol allowed for the recovery of product **2.181** upon employing KF as a base rather than KO$^t$Bu.

**Scheme 2.21.** Biomass-derived molecule degradation

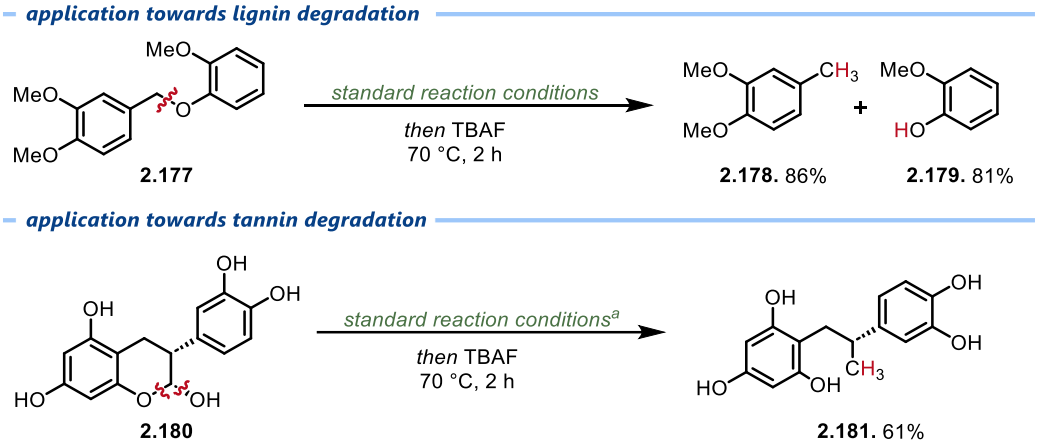


## 2.4.5. Mechanistic evaluation

### 2.4.5.1. Kinetic isotope effect and plausible intermediates

The importance of KO$^t$Bu as a stoichiometric additive in this reaction is consistent with previous studies concerning the reduction of esters that suggest that the active reducing agent is a hypervalent silicate species.[52,61] Further, the selective incorporation of deuterium in experiments with $d_2$-TMDSO (Scheme 2.30) confirms a reductive mechanism in which TMDSO is the source of the hydride that gets transferred to the substrate. The independently studied rate for the reduction of **2.182** to form **2.183** was significantly slower when using deuterated TMDSO. A kinetic isotope effect of 2.68 was observed (Scheme 2.22a), suggesting transfer of hydrogen to the substrate or to the nickel catalyst occurs at or prior to the rate-determining step of the reaction. Once more, this



Chapter two references begin on page 204; experimental details begin on page 198

observation is in line with results observed in previous studies on the reduction of esters.[52] Several potential reactive intermediates can be envisioned that may react with the hydride source, such as an olefin (**2.184**), carbocation (**2.185**), carbon-centered radical (**2.186**), or organonickel species (**2.187**) (Scheme 2.22b).

**Scheme 2.22**. Kinetic isotope effect study and plausible reactive intermediates

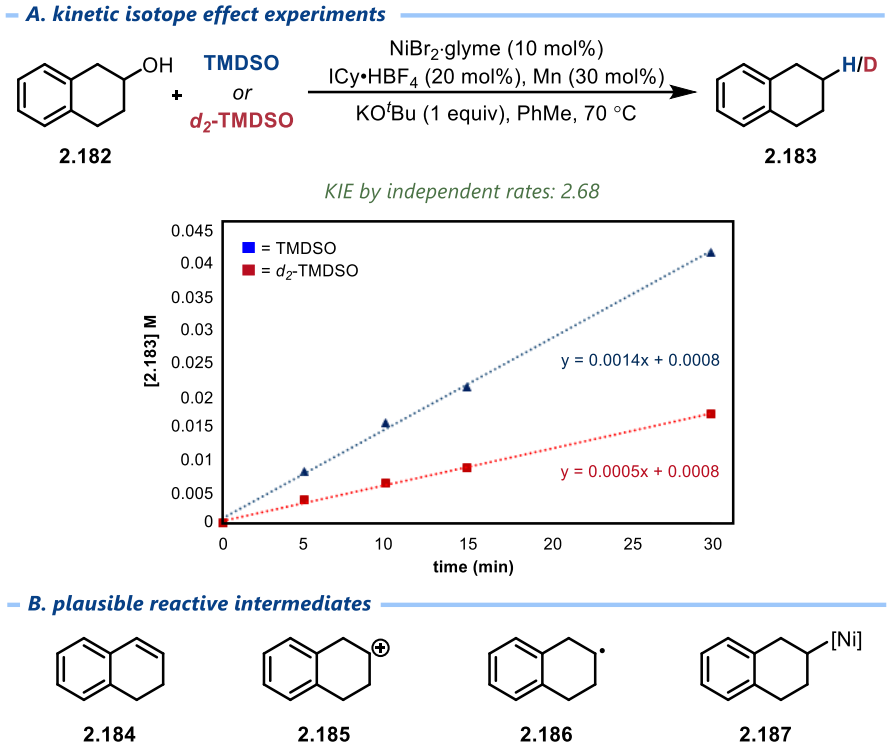


## 2.4.5.2. Investigating potential olefin intermediate

Initial dehydration to an olefin and subsequent hydrogenation is a commonly proposed mechanism for alcohol hydrodeoxygenation, particularly when using heterogeneous catalysts and elevated temperatures.[62] The tolerance of the present reaction to olefins makes this pathway unlikely. For example, while phenethyl alcohol derivative **2.119a** undergoes clean reduction to alkane **2.188**, the corresponding dehydrated starting material (**2.189**) is inert to the reaction



*Chapter two references begin on page 204; experimental details begin on page 198*

conditions (Scheme 2.23). To further refute mechanisms that involve formation of olefin intermediates, deuterated alcohol **2.190** was prepared and subjected to the general reaction conditions. The corresponding hydrocarbon **2.191** formed in 76% yield without any loss of deuterium in the benzylic or homobenzylic positions.

**Scheme 2.23**. Evidence against an olefin intermediate

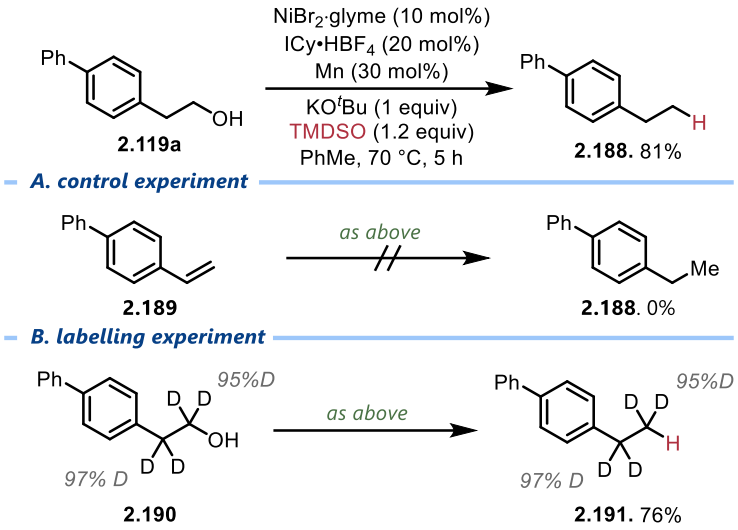


## 2.4.5.3. Investigating potential carbocation intermediate

Lewis and Brønsted acid-catalyzed C($sp^3$)–O bond reductions can proceed by the formation of a carbocation or other highly electrophilic intermediate that can be subsequently trapped by a mild hydride source.[42] A distinguishing feature in this mechanistic pathway is that the carbocation intermediates are prone to rearrangement. For instance, reduction of alcohol **2.192** by treatment with trifluoroacetic acid and triethylsilane provides rearrangement product **2.193** in 73% yield, along with **2.194** in 4% yield (Scheme 2.24). In contrast, performing the reduction with the described nickel catalyst system provides only **2.194** in 71% yield with no evidence of rearrangement, suggesting a carbocation intermediate is not likely present.



*Chapter two references begin on page 204; experimental details begin on page 198*

**Scheme 2.24**. Evidence against a carbocation intermediate

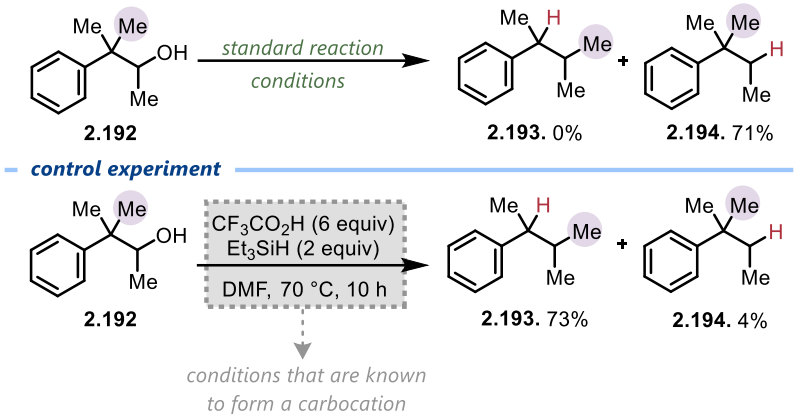


### 2.4.5.4. Investigating radical and organonickel intermediates

Next, to probe the possibility of a radical pathway, a selection of substrates that may be prone to radical-induced rearrangement were subjected to the reduction. When allyl alcohol **2.195** was reduced using the nickel/TMDSO catalyst system, the unrearranged product **2.196** was formed in 72% yield, along with 11% of the isomerized product **2.197** (Scheme 2.25a). When performing the same reaction on the corresponding xanthate using Barton-McCombie deoxygenation conditions that are known to proceed via a radical intermediate,[33] a near 1:1 ratio of the two products was observed. A second rearrangement-prone substrate, cyclopropyl-substituted alcohol **2.198**, was also reduced (Scheme 2.25b). The only product observed was the ring opened alkene **2.199**, with no evidence of the non-rearranged product **2.200**. While the ring opening of cyclopropane-bearing substrates is frequently explored in free radical chemistry,[63] the enhanced stability of the cyclopropylbenzyl radical has been shown to thermodynamically favour the ring-closed species.[64] Indeed, reacting the corresponding xanthate ester under Barton-McCombie conditions exclusively gave the ring closed product **2.200**. Taken together, these results show a significant disparity between the operative mechanism for the nickel-catalyzed system and that

which operates under purely radical conditions. Lastly, benzyl alcohol **2.201** bearing a tethered olefin was reduced (Scheme 2.25c). Using the standard conditions, a 59% yield of cyclized product **2.202** was observed, along with 9% yield of uncyclized product **2.203**. Notably, this result could support either a radical or organonickel-mediated mechanism. It was hypothesized that the radical and organonickel-mediated pathway for this 5-exo cyclization could be distinguished by observing the effect different ligands had on this project ratio. When using the NHC ligand ICy, formation of the uncyclized product **2.203** was suppressed. In contrast, use of the phosphine ligand $PCy_3$ provided 2:1 selectivity for the uncyclized product **2.203**, supporting the active involvement of nickel in the reaction mechanism and providing evidence against an exclusively free-radical pathway.

**Scheme 2.25.** Evidence against an exclusively free-radical pathway

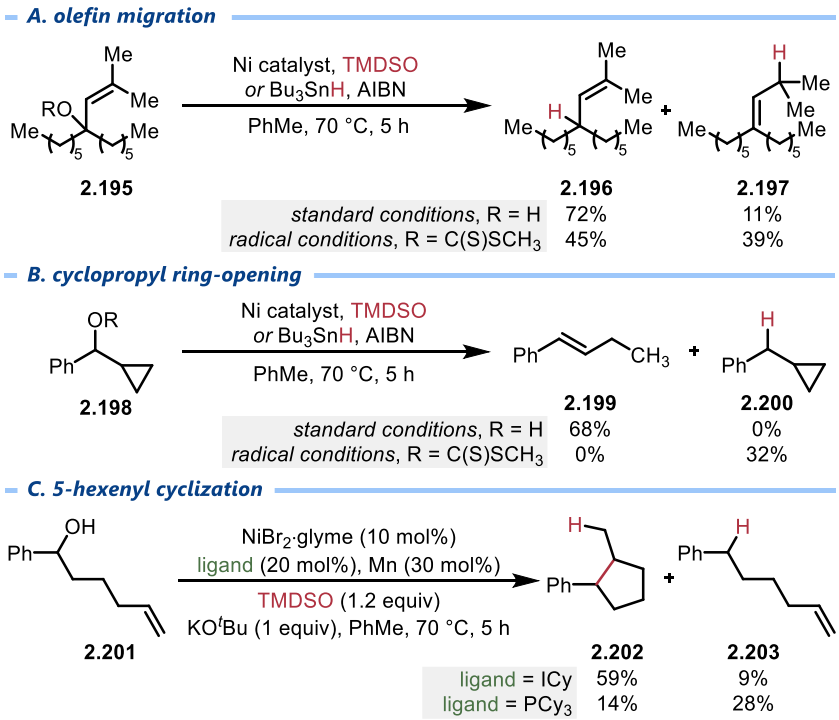




*Chapter two references begin on page 204; experimental details begin on page 198*

Recent studies from Jarvo and co-workers illustrate that nickel(0) catalysts are capable of stereospecific cleavage of C($sp^3$)–O bonds, enabled by a concerted oxidative addition step that proceeds with inversion of configuration to form a nickel(II) species.[65] To probe this mechanistic possibility for the key C–O bond cleavage step, camphor-derivatives **2.204a** and **2.204b** were prepared and subjected to the deoxygenation conditions (Scheme 2.26a).[66] When either a 10:1 mixture or a 1:1 mixture of the two starting materials were reduced, the same 1:1 ratio of diastereomeric reduction products **2.205a** and **2.205b** were obtained. This loss of stereochemical information is suggestive of a different mechanistic pathway than related benzylic activations; further, the reaction must proceed by an intermediate that is prone to epimerization.

The reaction between nickel and alkyl halides is often proposed to proceed by a two-step oxidative addition process, with initial formation of a carbon-centered radical and nickel halide that rapidly recombine.[67] Organonickel complexes have also been proposed to undergo homolysis, forming a transient radical that can lead to the loss of stereochemical information.[68] Towards further probing the possibility of a short-lived radical intermediate, $\beta$-sulfonyl alcohol **2.206** was prepared (Scheme 2.26b). Carbon-centered radicals are known to lead to rapid elimination of sulfone groups.[69] Subjecting **2.206** to the nickel/TMDSO catalyst system led to the formation of olefin **2.207** as the only identifiable product in 73% yield without observation of **2.208**. With this information, it was proposed that the reaction primarily proceeds by an organometallic mechanism, with a transient carbon-centered radical present either in the catalytic cycle or as an off-cycle species.



*Chapter two references begin on page 204; experimental details begin on page 198*

**Scheme 2.26**. Evidence against a non-radical nickel(0)/nickel(II) mechanistic pathway

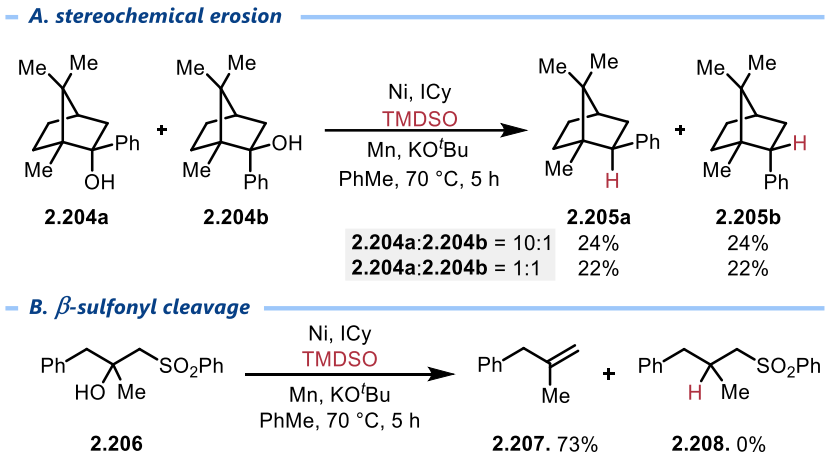


## 2.4.5.5. Effect of chain length on reactivity

While the reduction reaction presented herein displays a useful scope that goes beyond activated benzylic and allylic systems, the observation was made throughout that the target C–O bond required a nearby π-system to be successfully reduced. To probe this observation, a systematic study was performed to investigate the effects of chain-length on the outcome of this reaction (Figure 2.12). While there was little difference between the benzylic and homobenzylic positions (**2.112a** vs. **2.119a**), a substantial drop in yield was noted upon placing the target C–O bond three carbons away from the aryl ring (**2.124**). Further, moving the target bond four carbons over resulted in no product (**2.127**).



*Chapter two references begin on page 204; experimental details begin on page 198*

**Figure 2.12**. Systematic investigation into the effect of chain length on product yield

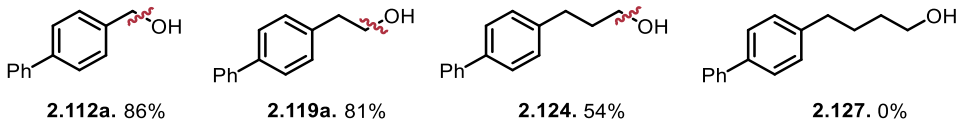


**2.112a.** 86% **2.119a.** 81% **2.124.** 54% **2.127.** 0%

To further probe this phenomenon, alcohols **2.209a-e** were prepared with varying electronics on the remote arene ring (Scheme 2.27). All five substrates were smoothly deoxygenated within five hours (**2.210a-e**), with substrates bearing more electron-rich arene rings affording higher yields. A Hammett study revealed the same relationship with the reaction rate: the more electron deficient the arene ring, the slower the reduction occurred. A linear relationship was observed between the electronics of the aryl ring and the reaction rate, suggesting that the aryl ring is involved in the rate-determining step of this deoxygenation reaction. Given the distance between the reactive alcohol and the aromatic ring as well as the KIE effect observed above, it is speculated that the origin of this effect comes from the arene acting as a directing group, stabilizing a nickel-hydride catalyst and bringing it into proximity of the reactive C–O bond.[70] This directing effect appears to diminish with increasing chain length between the alcohol and arene. Alternative groups that may serve as directing groups have not yet been identified.



*Chapter two references begin on page 204; experimental details begin on page 198*

**Scheme 2.27.** Hammett study of *para*-substituted alcohols

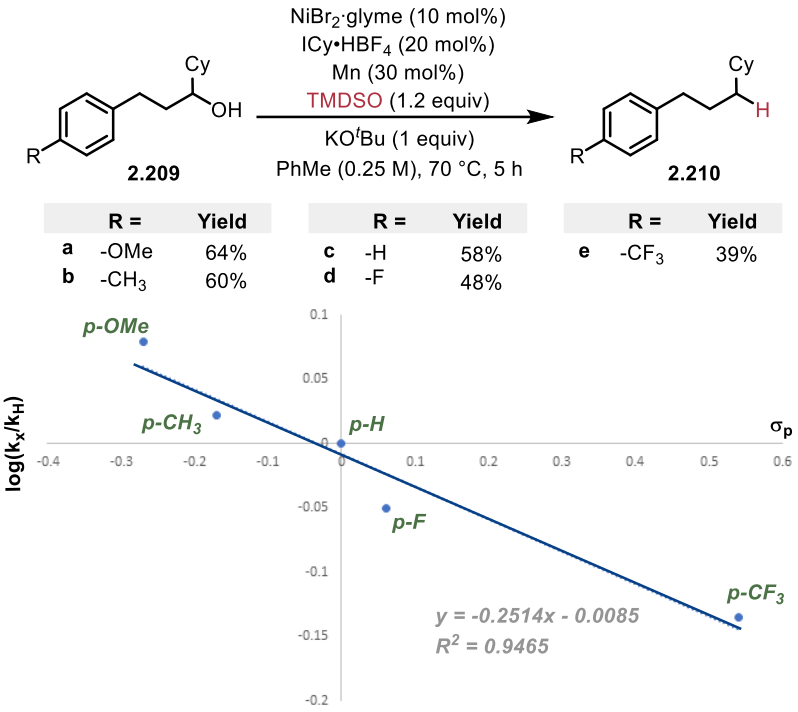


## 2.4.5.6. Effect of drop-in additives

A series of drop-in additives were included in the reaction mixture in order to prod various mechanistic hypotheses. First, substrate **2.111** was subjected to the standard reaction conditions in the presence of radical scavenging reagent TEMPO. A suppressed yield of product **2.110** provides evidence supporting radical involvement in the reaction mechanism. A suppressed yield of product **2.110** was also observed upon adding radical scavenger galvinoxyl. However, this evidence cannot be considered concrete as it is also possible that the radical-scavenging reagents acted to poison the active catalyst (Scheme 2.28).



*Chapter two references begin on page 204; experimental details begin on page 198*

**Scheme 2.28**. Radical scavenging experiments

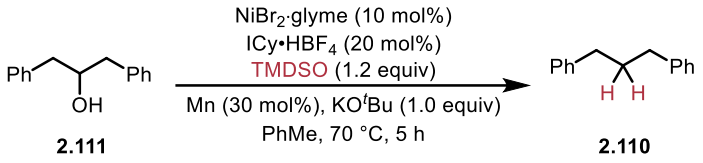


| additive | % yield, **2.110** |
|---|---|
| TEMPO (1.1 equiv) | 8% |
| galvinoxyl (1.1 equiv) | 11% |

Next, 1,3-diphenylpropanol (**2.111**) was reduced according to modified standard reaction conditions wherein 10 eq of mercury was added to the reaction mixture (Scheme 2.41). The reaction was stirred at 70 °C for 5 h before being filtered and analyzed by GC-FID. When employing $Ni(cod)_2$ as the precatalyst, a negligible loss in yield was observed. This provides evidence to support the argument of homogenous catalysis. Employing $NiBr_2$·glyme as the precatalyst along with 0.3 equivalents of manganese led to a loss in yield, presumably due to the abundance of insoluble Mn within the reaction mixture.

**Scheme 2.29**. Investigating the nature of the C–O bond reduction through Hg-poisoning experiments

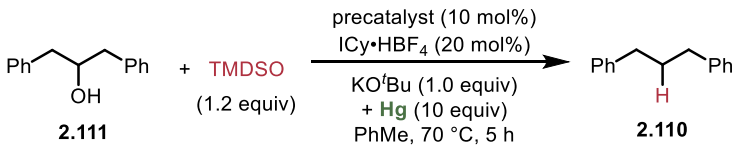


| entry | precatalyst | % yield, **2.110** |
|---|---|---|
| 1 | $Ni(cod)_2$ | 76% |
| 2 | $NiBr_2$·glyme + Mn (30 mol%) | 14% |



*Chapter two references begin on page 204; experimental details begin on page 198*

### 2.4.5.7. Tentative mechanistic hypothesis

With all of the above being known, a speculative mechanism for this transformation could be proposed (Figure 2.13). Both nickel(0) and nickel(II) precatalysts could enable reactivity, however nickel(II) precatalysts could only do so in the presence of a reducing agent such as manganese or zinc. This observation, in combination with notable differences in reactivity from related transformations,[9,65] prompted the idea that the first step of the transformation involves reduction of nickel(II) to nickel(0) (**2.F**). Also known in the literature is that the combination of a siloxane and potassium *tert*-butoxide can react with one another to form a hypervalent silicate species that is capable of reducing ketones, aldehydes and esters into silyl ethers.[61a] Thus, it is proposed that a hypervalent silicate species formed upon reaction between TMDSO and KO$^t$Bu reduces ketones/aldehydes/esters into silyl ethers (**2.G**) prior to entry into the catalytic cycle. Substantial evidence was gathered in support of the existence of a carbon-centered radical, thus it is proposed that the subsequent step involves scission of the C($sp^3$)–O bond of silyl ethers to reveal a carbon-centered radical (**2.H**) that is trapped by nickel(0) to generate a nickelated intermediate (**2.I**). This intermediate is proposed to react with a hypervalent silicate species that will donate a hydride to generate nickel(II) intermediate **2.J**, which is proposed to undergo C–H bond-forming reductive elimination to yield reduced product (**2.K**) alongside regenerated nickel(0) catalyst (**2.F**).

**Figure 2.13.** Tentative mechanistic hypothesis

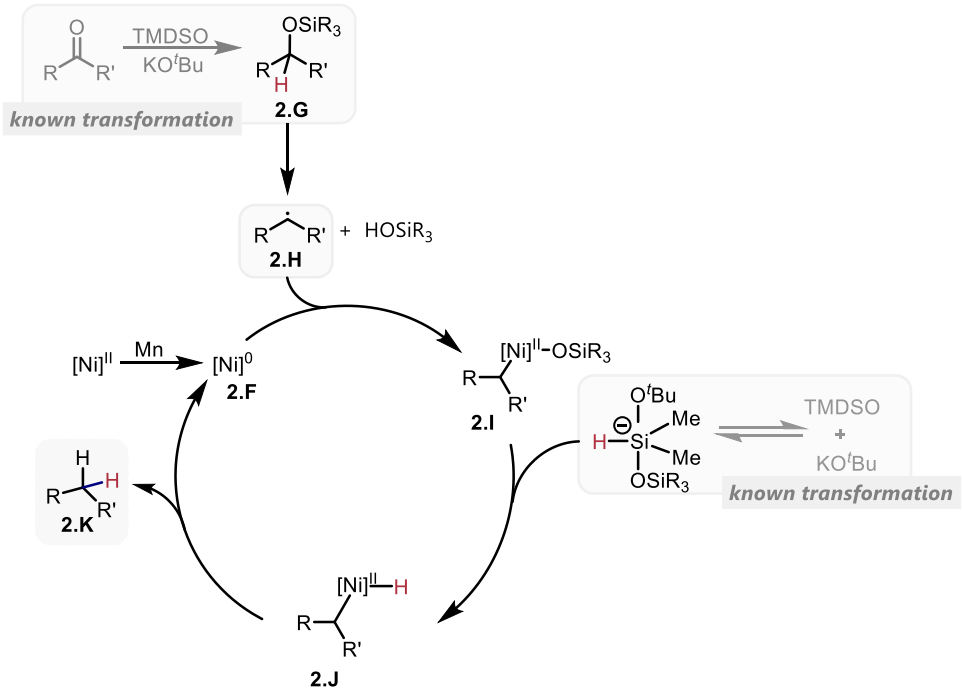


While this mechanistic depiction is plausible, there are a number of reasons that prevented it from being depicted within the published manuscript. Most notably, is that information is lacking regarding the key C($sp^3$)–O bond scission step. While evidence invokes confidence in proposing the existence of a radical intermediate, it is uncertain as to whether nickel plays a role in this step. If nickel is involved, it is unknown what its role may be. Further, little evidence has been gathered in support of the proposed nickelated intermediates **2.I** and **2.J**. Future work may consider analyzing this transformation via $^1$H NMR spectroscopy as characteristic nickel-hydride peaks may evolve over the course of the reaction. Analogously, EPR experiments could be conducted in hopes of observing a nickel(I) intermediate. Thus, as this project concluded, many aspects of this mechanism that remained unknown. However, previous reports of chemistry utilizing similar reagents (ex. KO$^t$Bu, TMDSO, nickel),[46-49, 61a, 65] along with the unique aspects of this transformation, suggest that a complex mechanism is at play that may take years to fully resolve.



*Chapter two references begin on page 204; experimental details begin on page 198*

### **2.4.6.** Additional commentary

The work detailed within Section 2.4 provides a significant expansion upon the work detailed within Section 2.3. It expands the classes of reducible functional groups from one (esters) to six (ketones, aldehydes, alcohols, ethers, epoxides, esters) while also providing a more thorough and detailed investigation into the mechanism and nature of the reactivity. Practically, the reaction conditions developed in Section 2.4 are milder than those detailed in Section 2.3, permitting reactivity at lower temperature outside of the glovebox. Most notably, the original report detailed in Section 2.3 was restricted to aryl-substituted esters, while the work disclosed in Section 2.4 was not exclusively limited to benzylic C($sp^3$)–O bond cleavage. Applications were demonstrated towards reductive deuteration, late stage defunctionalization, deprotection and, in general, the replacement of traditionally aggressive deoxygenation chemistry such as Wolff-Kishner, Barton McCombie or Clemmensen reductions. This method is operationally simple, general and represents a substantial step towards expanding the field of carbon-oxygen bond activation away from activated substrates such as triflates and pivalates towards unprotected, unactivated and native functional groups.

This project was revisited in the spring semester of 2023, when the author of this dissertation welcomed and mentored two high-school students inside the laboratory for a week's worth of chemistry as a part of the Verna J. Kirkness Indigenous Scholar's Program. The goal of this project was to utilize high-throughput chemistry to evaluate whether this reductive deoxygenation could be extended towards the site-selective reduction of a carbohydrate model compound, **2.211** to form reduced product **2.212**. Unfortunately, testing a range of catalyst combinations did not yield product, instead leading towards the recovery of starting material (Figure 2.14).



*Chapter two references begin on page 204; experimental details begin on page 198*

**Figure 2.14.** Attempted reduction of carbohydrate model compound **2.211**

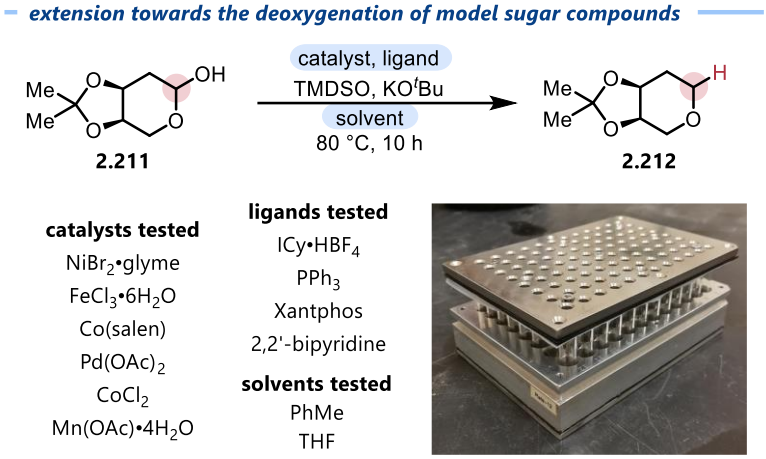


## 2.4.7. Part B: Conclusions

Part B of this chapter describes a nickel-catalyzed method for the direct deoxygenation of carbon–oxygen bonds using an abundant organosilane reducing agent. The transformation directly cleaves the C($sp^3$)–O bonds present in alcohols, ethers, and epoxides, and can similarly reduce ketones and aldehydes via an initial reduction step to form a silylated alcohol intermediate. C($sp^2$)–O bonds, olefins, amines, heterocycles, and organofluorides are resistant to cleavage, demonstrating appealing chemoselectivity compared to analogous hydrogenolysis methods. Applications for the mono- and bis-deuteration of alcohols and ketones are demonstrated, as is selective deprotection of benzyl ethers at the C(benzyl)–O linkage. Mechanistic studies suggest the reaction pathway is distinct from related reductions that proceed via C($sp^3$)–O bond dehydration or carbocation formation, and most strongly support an organometallic mechanism with an organonickel species acting as a key reactive intermediate. Studies towards elucidating the nature of the active catalyst and the details of the C–O bond cleavage step are underway.

## 2.5. Conclusion, impact, future work and considerations

### 2.5.1. Conclusion

Collectively, the works presented in Sections 2.3 and 2.4 detail the development of a catalytic system consisting of nickel, ICy•$HBF_4$, KO$^t$Bu and TMDSO that can permit the deoxygenative reduction of esters, ketones, aldehydes, epoxides, ethers and alcohols. Between the two works, over 100 substrates were reduced, including complex molecules such as NSAIDs, cholesterol, and quinine as well as lignin and tannin model compounds. This nickel-catalyzed transformation was applied towards the catalytic deuteration of a variety of compounds, providing a strategy for the selective installation of up to three deuterium atoms with greater than 95% deuterium incorporation. This reaction could be reliably scaled up, with products obtained in yields reflective of optimized conditions even when halving the catalyst loading. Strong chemoselectivity was observed, with this reaction selectively targeting C($sp^3$)–O bonds in the presence of C($sp^2$)–O bonds, amines, nitro groups, phenols, carboxylic acids, olefins, and alkynes.

Further, the mechanism of this transformation was investigated. The KO$^t$Bu/TMDSO-assisted reduction of unsaturated functional groups including esters, ketones and aldehydes proceeds in the absence of nickel catalyst to afford silyl ethers. Mechanistic evidence was gathered to suggest that cleavage of the C($sp^3$)–O bond of the silyl ether occurs to yield a radical intermediate that was likely sequestered by nickel, generating an organonickel intermediate. Evidence was gathered that suggests a stark contrast between the mechanism of this transformation and analogous methods for nickel-catalyzed reductive deoxygenation.

### **2.5.2.** Impact and collaborations

Ultimately, this work represents a unified pathway to reduce a wide range of carbon-oxygen bonds. Accordingly, these works have been cited over forty times at the time of the writing of this dissertation. Notable extensions of this work are detailed below.

Wu and colleagues developed a titanium-catalyzed exhaustive reduction of carboxylic acid derivatives and other oxo-chemicals (alcohols, aldehydes, ketones, lactones) in 2022 (Scheme 2.30a).[71] The authors utilized $NH_3{\cdot}BH_3$ as a reductant in this work, proposing that it reacts with the titanium catalyst to form a $Ti^{III}$–H species in situ. While this work provides a notable advance in terms of functional group tolerance and in the ability to exhaustively reduce free carboxylic acids, it remains hampered by the restriction for the target C($sp^3$)–O bond to be present in a benzylic position. The exhaustive reduction of esters, carboxylic acids and carbamates was further explored by Mejia and colleagues in 2023 (Scheme 2.30b).[72] Metal-free catalysis was achieved in this case, with the authors utilizing boronic acids as catalysts and $NH_3{\cdot}BH_3$ as a reductant. Once more, while carboxylic acids could be exhaustively reduced according to this protocol, the scope of carboxylates remained limited to those in benzylic positions. A similar catalytic system as that described within this chapter, featuring a nickel(II) catalyst, NHC ligand, hydrosilane and sodium *tert*-butoxide, was observed to lead towards the reduction of alkenes by Qiu and colleagues in 2022 (Scheme 2.30c).[73]



*Chapter two references begin on page 204; experimental details begin on page 198*

**Scheme 2.30.** Extensions of the exhaustive reduction of esters

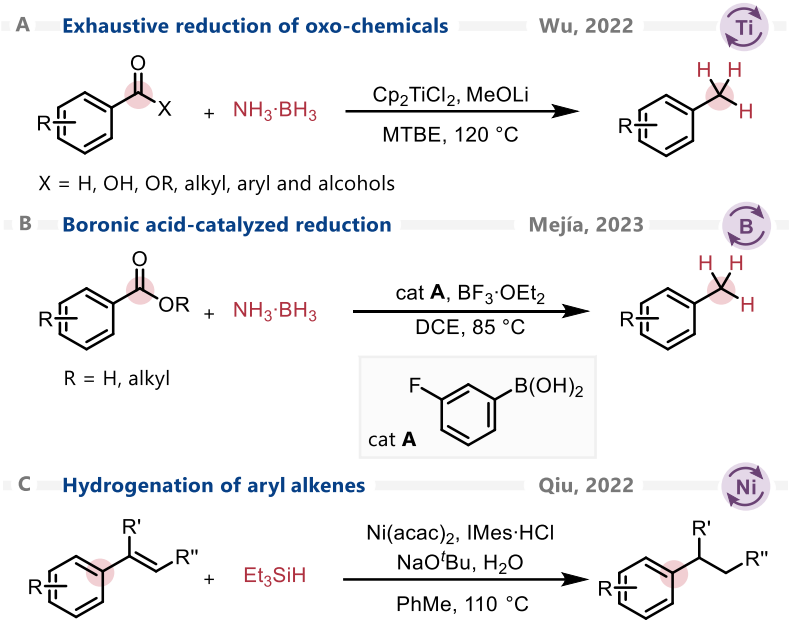


Shu and colleagues explored the titanium-catalyzed deoxygenative reduction of alcohols using a hydrosilane reductant in 2022 (Scheme 2.31a).[74] Using this catalyst, the authors were able to activate tertiary non-π-activated alcohols. The catalytic hydrodefluorination was achieved by Ogoshi using a similar catalyst system as was described within this chapter, consisting of a nickel catalyst, NHC ligand, hydrosilane and base (Scheme 2.31b).[75] Similar to the deoxygenative conditions developed in this chapter, Ogoshi and colleagues depict a potential mechanism involving arene coordination to the nickel catalyst that can permit homobenzylic activation. The iridium-catalyzed deoxygenative reduction of benzyl alcohols was demonstrated by Chen, Yang and colleagues in 2023 (Scheme 2.31c).[76] The authors demonstrate excellent chemoselectivity for C($sp^3$)–O cleavage in the presence of C($sp^2$)–O bonds while also providing evidence in the form of a kinetic isotope effect to suggest *β*-hydride elimination is involved in the rate-limiting step. Others have also explored the deoxygenative reduction of alcohols, employing photocatalysis,[77]



*Chapter two references begin on page 204; experimental details begin on page 198*

electrocatalysis,[78] nanoparticles,[79] or other transition metals such as iridium,[80] rhenium,[81] and titanium.[82]

**Scheme 2.31.** Selected extensions of the reductive deoxygenation of alcohols

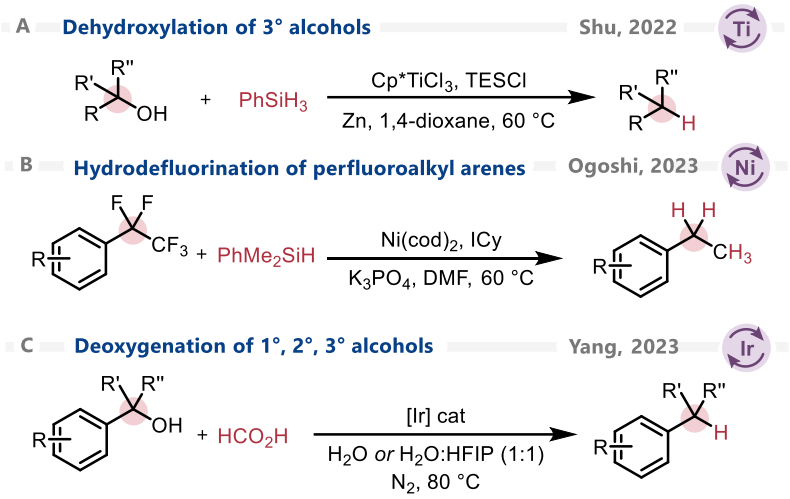


The work described within this chapter also led to collaborations and ongoing projects within the Newman group. While studying the nickel/TMDSO/KO$^t$Bu system, carbon-carbon bond scission was observed in select trifluorotolylpyridines by a colleague, Piers St. Onge. This work was published in the article "Reductive Cleavage of C($sp^2$)–$CF_3$ Bonds in Trifluoromethylpyridines" by Piers St. Onge, Shajia I. Khan, Adam Cook and Stephen G. Newman, published in *Organic Letters*, **2023**, *25*, 1030-1034 (Scheme 2.32). The author of this dissertation acted as third author on this manuscript, having been responsible for conducting variable time normalization analysis experiments that revealed approximate first order dependence on substrate, TMDSO and base. A range of compounds could be de-trifluoromethylated including those bearing chlorines (**2.213**), diverse heterocycles (**2.214-2.217**) and ortho-substitution patterns (**2.218**). The TMDSO/KO$^t$Bu system has continued to be exploited within the Newman group,



*Chapter two references begin on page 204; experimental details begin on page 198*

with Piers St. Onge exploiting it towards the development of a yet-to-be-published method for the hydroalkylation of alkenes.

**Scheme 2.32.** TMDSO/KO$^t$Bu as a platform for the reductive cleavage of C($sp^2$)–$CF_3$ bonds in trifluoromethylpyridines

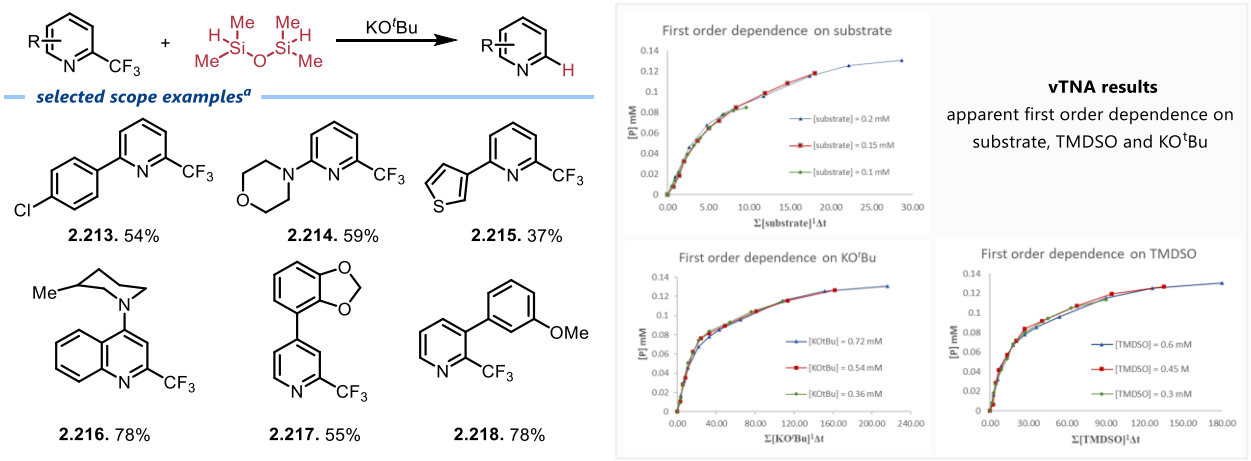


[a]Reactions performed and yields obtained by Piers St. Onge and Shajia I. Khan

The mechanistic probe discussed in Scheme 2.26b, wherein nickel-catalyzed reduction of a *β*-hydroxysulfone was observed, led directly towards a spin-off publication, "Nickel-Catalyzed Desulfonylative Olefination of *β*-Hydroxysulfones" by Adam Cook, Maxwell Bezaire and Stephen G. Newman, published in *Organic Chemistry Frontiers*, **2023**, *10*, 1339-1404, on which the author of this dissertation acted as lead author. This work expanded upon the aforementioned example, establishing a protocol that permits the desulfonylative olefination of *β*-hydroxy, *β*-keto and *β*-ethereal sulfones through the activity of a Ni-NHC catalyst, generating products with a range of functionality (**2.219-2.224**) (Scheme 2.33). Employing this method allowed for the reliable synthesis of both nonconjugated and conjugated olefins with mono-, di-, tri- or tetrasubstitution patterns. A brief mechanistic exploration of this reaction provided evidence to support the existence of both radical and organonickel intermediates *en route* to form product.



*Chapter two references begin on page 204; experimental details begin on page 198*

**Scheme 2.33.** Nickel-catalyzed desulfonylative olefination of *β*-hydroxysulfones

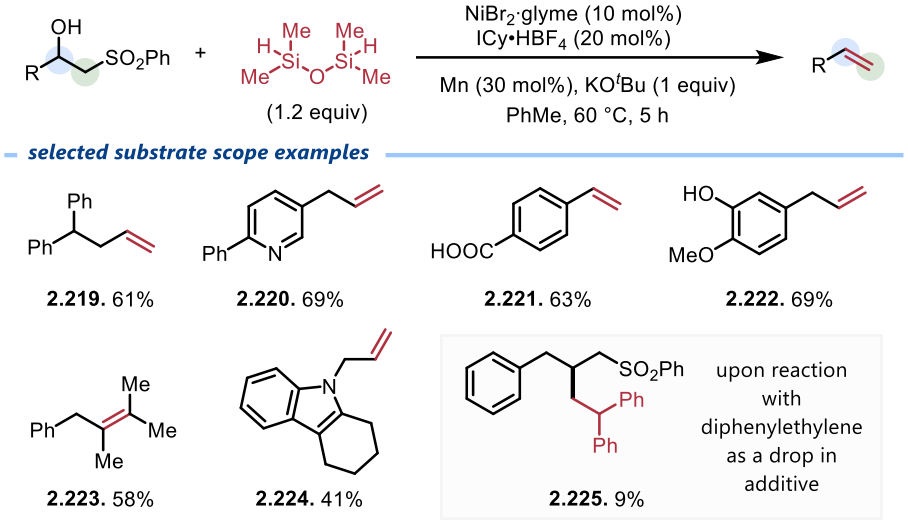


## 2.5.3. Future work and considerations

While this chapter has emphasized the strengths of the disclosed works, they are not without their faults. Firstly, while ICy•$HBF_4$ can be prepared in a few synthetic steps, it costly to purchase ($475 CAD/5 g, Sigma Aldrich). Further, catalyst/ligand loading is high at 10 mol% catalyst and 20 mol% ligand. There are several notable scope limitations, with this reaction failing to produce product in the presence of free N–H bonds, select heterocycles and halides. Further, the restriction to benzyl, homobenzyl and bis-homobenzyl C($sp^3$)–O bonds poses a severe and not yet to be fully understood limitation. Mechanistically, while an understanding of the rate-limiting step and the potential intermediates has been obtained, the nature of the active catalyst and how it interacts with the organic intermediate that forms upon C($sp^3$)–O cleavage is yet to be understood.

Future work may proceed in a number of directions. First, a collaboration with a group that focuses on computational chemistry should be undertaken so that more can be learned about the mechanism of this reaction. Specifically, it would be valuable to gain a better understanding of the



*Chapter two references begin on page 204; experimental details begin on page 198*

restrictions of this work. Why does it only work with benzyl/homobenzyl/bishomobenzyl C–O bonds? Why is it chemoselective for C($sp^3$)–O bonds over C($sp^2$) bonds? How does the active catalyst interact with the reactive intermediate that forms after C–O cleavage?

As a synthetic extension of this method, one may consider evaluating the extent to which the nickel/TMDSO/KO$^t$Bu system can reduce other bonds, such as those between carbon and iodine, chlorine or bromine, as there still remains a limited number of methods to selectively reduce such species in homobenzylic, bishomobenzylic and tertiary positions. Lastly, there is room for expanding upon the two notable applications of this method that were illustrated, the degradation of biomass and catalytic deuteration. Applications towards biomass degradation could seek to determine the extent of compounds that can be degraded. For instance, can these conditions be optimized towards the reduction of carbohydrates? Alternatively, applications towards biomass degradation could focus on finding the most energetically efficient conditions that permit the degradation of a specific compound, for instance, lignin. Applications towards catalytic deuteration could focus on developing the most efficient conditions for the late stage deuteration of a range of complex, biorelevant compounds. Given the beneficial effect of both deuteration and installing methyl groups on pharmaceuticals, a collaboration could be established with a group capable of testing biological activity and medicinal relevance of the resulting products that could prove fruitful.

## 2.6. Experimental

### 2.6.1. General details

Unless otherwise indicated, reactions were conducted under an atmosphere of nitrogen in 8 mL screw capped vials that were oven dried (120 °C). Column chromatography was either performed manually using Silicycle F60 40−63 μm silica gel or by using a Combiflash Rf+ automated chromatography system with commercially available Biotage normal-phase Silica Flash columns (35−70 μm). Analytical thin layer chromatography (TLC) was conducted with aluminum-backed EMD Millipore Silica Gel 60 F254 pre-coated plates. Unless otherwise noted, visualization of developed plates was performed under UV light (254 nm) and/or using $KMnO_4$ stain.

### 2.6.2. Instrumentation

$^{1}H$ NMR and $^{13}C$ NMR were recorded on a Bruker AVANCE 400 MHz spectrometer. $^{1}H$ NMR spectra were internally referenced to the residual solvent signal (e.g., $CDCl_3$ = 7.27 ppm). $^{13}C$ NMR spectra were internally referenced to the residual solvent signal (e.g., $CDCl_3$ = 77.00 ppm). Data for $^{1}H$ NMR are reported as follows: chemical shift (δ ppm), multiplicity (s = singlet, d = doublet, t = triplet, q = quartet, quin = quintet, m = multiplet), coupling constant (Hz), integration. NMR yields for optimization studies were obtained by $^{1}H$ NMR analysis of the crude reaction mixture using 1,3,5-trimethoxybenzene as an internal standard. GC data was obtained via a 5-point calibration curve using FID analysis on an Agilent Technologies 7890B GC with 30 m x 0.25 mm HP-5 column. Accurate mass data (EI) was obtained from an Agilent 5977A GC/MSD using MassWorks 4.0 from CERNO Bioscience.

### **2.6.3**. Materials

Organic solvents were purified by rigorous degassing with nitrogen before passing through a PureSolv solvent purification system. Low water content was confirmed by Karl Fischer titration (<20 ppm for all solvents). Unless otherwise noted, starting materials were obtained commercially from Sigma Aldrich, Alfa Aesar or Combi-Blocks and used as received. $d_8$-Toluene was purchased from Sigma Aldrich (99 %D). $Ni(cod)_2$ was purchased from Sigma Aldrich. $Ni(OTf)_2$ (96% purity) was purchased from Alfa Aesar. $NiBr_2$·glyme (97% purity) was purchased from Sigma Aldrich. Granulated Mn was purchased from Alfa Aesar (99.6% purity, < 10 micron). $D_2$ (g) was purchased as a 458 mL cylinder from Sigma Aldrich (99.8% D). $Ni(OAc)_2$ (98% purity) was purchased from Sigma Aldrich. $NiBr_2$·glyme (97% purity) was purchased from Sigma Aldrich. $Ni(PPh_3)_2(CO)_2$ (97% purity) was purchased from Alfa Aesar. $PdCl_2$ was purchased from Sigma Aldrich. $[Pd(cinnamyl)(Cl)]_2$ (95% purity) was purchased from Sigma Aldrich. $Ir(cod)_2Cl_2$ (98% purity) was purchased from Alfa Aesar. $Fe(acac)_3$ was purchased from Sigma Aldrich. $CrCl_2$ (99.4% purity) was purchased from Sigma Aldrich. *N*,*N*′-Bis(salicylidene)ethylenediaminocobalt (99% purity) was purchased from Sigma Aldrich. $Rh(cod)_2Cl_2$ (98% purity) was purchased from Sigma Aldrich. Granulated Mn was purchased from Alfa Aesar (99.6% purity, < 10 micron). The synthesis of starting materials, products and all other experimental details are fully described and all original spectra are available in the freely-available Supporting Information files (https://pubs.acs.org/doi/10.1021/jacs.0c02405 for data discussed in Section 2.3, https://pubs.acs.org/doi/abs/10.1021/acscatal.1c03980 for data discussed in Section 2.4).

### **2.6.4**. General procedures

***Procedure A – Glovebox conditions for deoxygenative reduction (Part A)***: To an oven dried 8 mL screw-top test-tube, 0.20 mmol of methyl ester starting material is added alongside an oven dried micro-stir bar. The screw-top test-tube is subsequently brought into a nitrogen-filled glovebox. Once under the inert atmosphere, 0.04 mmol ICy•$HBF_4$, 0.02 mmol $Ni(cod)_2$ and 0.20 mmol of $KO^tBu$ are added. 0.8 mL of toluene is added to the test-tube, followed by 0.40 mmol of 1,1,3,3-tetramethyldisiloxane. The reaction vessel is quickly sealed with a Teflon-septum equipped cap and brought outside of the glovebox, where it is stirred inside of a mineral-oil bath at 600 rpm for 10 hours at 110 °C. After 10 hours, the reaction vessel is allowed to come to room temperature before being opened to the atmosphere. 0.80 mmol of tetra-n-butylammonium fluoride is added slowly as a 1.0 M solution in tetrahydrofuran and the resulting solution is heated to 65 °C and stirred for 2 hours. The crude reaction solution is subsequently added directly to a 10 g Biotage SNAP silica-packed column where it is purified on a CombiFlash Rf+ automated chromatography instrument using a mixture of ethyl acetate in hexanes.

***Procedure B – Glovebox-free conditions for deoxygenative reduction (Part B)***: To an oven-dried 8 mL screw-top test-tube, 0.20 mmol starting material is added alongside a micro stir bar. 0.06 mmol Mn, 0.02 mmol $NiBr_2$·glyme, 0.04 mmol ICy•$HBF_4$ and 0.20 mmol of $KO^tBu$ are subsequently added. 0.8 mL of toluene is introduced to the test-tube, followed by 0.24 mmol of 1,1,3,3-tetramethyldisiloxane. The reaction vessel is quickly sealed with a Teflon-septum equipped cap, purged with $N_2$ (g) and stirred inside of a mineral-oil bath at 650 RPM for 5 hours at 70 °C. After 5 hours, the reaction vessel is allowed to cool to room temperature before being opened to the atmosphere. To aid in purification, non-polar siloxane oligomers can optionally be degraded: 0.48 mmol of tetrabutylammonium fluoride is added slowly as a 1.0 M solution in

tetrahydrofuran and the resulting solution is stirred for 2 more hours at 70 °C. The crude reaction solution is diluted with EtOAc and passed through a short silica plug via suction filtration. Solvent is evacuated in vacuo and the subsequent residue is dissolved in dichloromethane. A small amount of $SiO_2$ is added to the resulting solution and the solvent is subsequently removed in vacuo. The resulting solid is loaded directly on to a 10 g Biotage SNAP silica-packed column where after it is purified on a CombiFlash Rf+ automated chromatography instrument using a mixture of ethyl acetate in hexanes.

***Procedure C – Glovebox-free conditions for reduction of esters (Part A):*** To an 8 mL screw-top test-tube, 0.20 mmol of methyl ester starting material is added alongside a micro-stir bar. 0.20 mmol Mn, 0.02 mmol $NiBr_2$·glyme, 0.04 mmol ICy·$HBF_4$ and 0.20 mmol of KO$^t$Bu are subsequently added. 0.8 mL of toluene is introduced to the test-tube, followed by 0.40 mmol of 1,1,3,3-tetramethyldisiloxane. The reaction vessel is quickly sealed with a Teflon-septum equipped cap and stirred inside of a mineral-oil bath at 600 rpm for 10 hours at 110 °C. After 10 hours, the reaction vessel is allowed to come to room temperature before being opened to the atmosphere. 0.80 mmol of tetra-n-butylammonium fluoride is added slowly as a 1.0 M solution in tetrahydrofuran and the resulting solution is heated to 65 °C and stirred for 2 hours. The crude reaction solution is subsequently added directly to a 10 g Biotage SNAP silica-packed column where it is purified on a CombiFlash Rf+ automated chromatography instrument using a mixture of ethyl acetate in hexanes.

***Procedure D – Deuteration of alcohols or ketones (Part B):*** To an 8 mL screw-top test tube is added one micro stir bar alongside 0.2 mmol of starting material, 0.02 mmol $NiBr_2$·glyme, 0.04 mmol ICy•$HBF_4$, 0.06 mmol Mn, 0.2 mmol KO$^t$Bu and 0.24 mmol of $d_2$-TMDSO (prepared according to the literature).[34] 0.8 mL of anhydrous PhMe is added to the reaction vessel which is



*Chapter two references begin on page 204; experimental details begin on page 198*

then is capped and purged with $N_2$ (g) before being left to stir at 650 RPM for 5 h at 70 °C. The resulting reaction solution is quenched with 5 mL of distilled water and diluted in 10 mL of EtOAc. It is washed twice with saturated $NaHCO_3$, once with saturated NaCl (aq) before being dried over $MgSO_4$ and filtered via suction filtration. Solvent is evacuated in vacuo to reveal crude product that is subsequently purified via column-chromatography to provide pure product.

***Procedure E – Reduction of C($sp^2$)–O bonds (Part A):*** To an oven dried 8 mL screw-top test-tube, 0.20 mmol of starting material is added alongside an oven dried micro-stir bar. The screw-top test-tube is subsequently brought into a nitrogen-filled glovebox. Once under the inert atmosphere, 0.04 mmol $PCy_3$ and 0.02 mmol $Ni(cod)_2$ are added. 0.4 mL of toluene is added to the test-tube, followed by 0.20 mmol of 1,1,3,3-tetramethyldisiloxane. The reaction vessel is quickly sealed with a Teflon-septum equipped cap and brought outside of the glovebox, where it is stirred inside of a mineral-oil bath at 600 rpm for 12 hours at 110 °C. After 12 hours, the reaction vessel is allowed to come to room temperature before being opened to the atmosphere. 0.80 mmol of tetra-n-butylammonium fluoride is added slowly as a 1.0 M solution in tetrahydrofuran and the resulting solution is heated to 65 °C and stirred for 2 hours. The crude reaction solution is subsequently added directly to a 10 g Biotage SNAP silica-packed column where it is purified on a CombiFlash Rf+ automated chromatography instrument using a mixture of ethyl acetate in hexanes, affording products **58-60**.

## **2.6.5**. Characterization data of synthesized products

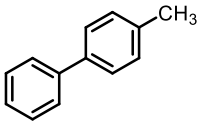


**4-Methyl-1,1'-biphenyl (2.4)** was prepared according to general procedure A. Purification was performed using a gradient of 1→5% ethyl acetate in hexanes to afford (**2.4**) as a yellow liquid (30 mg, 86% yield). The reaction was repeated according to general procedure B (24 mg, 73% yield). Characterization data matched those previously reported.[83] **$^{1}$H NMR** (400 MHz, $CDCl_3$): δ 7.62-7.60 (d, *J* = 7.8 Hz, 2H), 7.54-7.42 (t, *J* = 8.4 Hz, 2H), 7.37-7.33 (d, *J* = 7.8 Hz, 2H), 7.29-7.27 (d, *J* = 7.8 Hz, 2H), 7.25 (m, 1H) 2.47 (s, 3 H); **$^{13}$C NMR** (100 MHz, $CDCl_3$): 141.1, 138.3, 136.9, 129.4, 127.6, 126.9, 126.8, 126.9, 21.0.

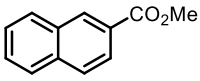


**Methyl-2-napthoate (2.83)** was prepared according to general procedure E to afford (**2.83**) (28 mg, 79% yield [90% yield via $^{1}$H-NMR]). Characterization data matched those previously reported.[84] **$^{1}$H NMR** (400 MHz, $CDCl_3$): *δ* 8.62 (s, 1H), 8.08-8.04 (dd, *J* = 8.6, 1.6 Hz, 1H), 7.58-7.53 (m, 2H), 3.98 (s, 3H); **$^{13}$C NMR** (100 MHz, $CDCl_3$): 167.1, 135.3, 132.4, 129.2, 128.0, 127.7, 126.3, 124.8, 51.7.

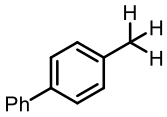


**4-Methyl-biphenyl** (*from alcohol* **2.112a**) was prepared according to general procedure B. Column chromatography was performed using a gradient of 1→5% ethyl acetate in hexanes to afford product as an off-white solid (36 mg, 86% yield). The reaction was repeated on 4-biphenylaldehyde (**2.139**), the corresponding aldehyde, to afford product (37 mg, 86% yield). Characterization data matched those previously reported.[85] **$^{1}$H NMR** (400 MHz, $CDCl_3$): δ 7.68-7.65 (m, 2H), 7.60-7.58 (m, 2H), 7.53-7.49 (m, 2H), 7.43-7.39 (m, 1H), 7.35-7.33 (m, 2H), 2.48 (s, 3H); **$^{13}$C NMR** (100 MHz, $CDCl_3$): 141.1, 138.3, 137.0, 129.5, 128.7, 126.97, 126.95, 126.89, 21.1.

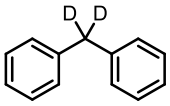


**(*d*$_2$)-Diphenylmethane (2.170)** was prepared according to general procedure D. Column chromatography was performed using a gradient of 1→5% ethyl acetate in hexanes to afford product as a yellow liquid (23 mg, 68% yield). The reaction was repeated on diphenylmethanol, the corresponding alcohol (24 mg, 73% yield). Characterization data matched those previously reported.[86] **$^{1}$H NMR** (400 MHz, $CDCl_3$): δ 7.51-7.44 (m, 5H), 7.41-7.33 (m, 5H), 4.12 (s, 0.04H).



*Chapter two references begin on page 204; experimental details begin on page 198*

## 2.7. References

(1) (a) Pritchard, J.; Filonenko, G. A.; van Putten, R.; Hensen, E. J.; Pidko, E. A. Heterogeneous and Homogeneous Catalysis for the Hydrogenation of Carboxylic Acid Derivatives: History, Advances and Future Directions. *Chem. Soc. Rev*. **2015**, *44*, 3808–3833. (b) Magano, J.; Dunetz, J. R. Large-Scale Carbonyl Reductions in the Pharmaceutical Industry. *Org. Process Res. Dev*. **2012**, *16*, 1156–1184. (c) Addis, D.; Das, S.; Junge, K.; Beller, M. Selective Reduction of Carboxylic Acid Derivatives by Catalytic Hydrosilylation. *Angew. Chem. Int. Ed.* **2011**, *50*, 6004–6011.

(2) (a) Berk, S. C.; Kreutzer, K. A.; Buchwald, S. L. A Catalytic Method for the Reduction of Esters to Alcohols. *J. Am. Chem. Soc.* **1991**, *113*, 5093–5095. (b) Turek, D.; Trimm, D.; Cant, N. W. The Catalytic Hydrogenolysis of Esters to Alcohols. *Catal. Rev. - Sci. Eng.* **1994**, *36*, 645–683. (c) Krishnamurthy, S.; Brown, H. C. Forty Years of Hydride Reductions. *Tetrahedron*. **1979**, *35*, 567–607. (d) Zheng, J., Darcel, C., Sortais, J. P. A Convenient Nickel-catalyzed Hydrosilylation of Carbonyl Derivatives. *Catal. Sci. Technol.* **2012**, *3*, 81–84.

(3) (a) Barreiro, E. J.; Kümmerle, A. E.; Fraga, C. A. M. The Methylation Effect in Medicinal Chemistry. *Chem. Rev*. **2011**, *111*, 5215–5246. (b) Schönherr, H.; Cernak, T. Profound Methyl Effects in Drug Discovery and a Call for New C–H Methylation Reactions. *Angew. Chem. Int. Ed*. **2013**, *52*, 12256–12267. (c) Shnurch, M. et al. A Comprehensive Overview of Directing Groups Applied in Metal-catalyzed C-H Functionalization Chemistry. *Chem. Soc. Rev.* **2018**, *47*, 6603–6743. (d) Pirali, T.; Serafini, M.; Cargnin, S.; Genazzani, A.A. Applications of Deuterium in Medicinal Chemistry. *J. Med. Chem.* **2019**, *62*, 5276–5297 (e) Liu, J. F. et al. Chapter Fourteen – A Decade of Deuteration in Medicinal Chemistry. *Annu. Rep. Med. Chem.* **2017**, *50*, 519–542.

(4) (a) Yamamoto, Y.; Bajracharya, G. B.; Nogami, T.; Jin, T.; Matsuda, K.; Gevorgyan, V. Reduction of Carbonyl Function to a Methyl Group. *Synthesis.* **2004**, *2*, 308–311 (b) Yamamoto, Y.; Liu, J.; Rubin, M.; Gevorgyan, V. A Direct Reduction of Aliphatic Aldehyde, Acyl chloride and Carboxylic Functions into a Methyl Group. *J. Org. Chem.* **2001**, *66*, 1672–1675. (c) Okita, T.; Muto, K.; Yamaguchi, J. Decarbonylative Methylation of Aromatic Esters by a Nickel Catalyst. *Org. Lett*. **2018**, *20*, 3132−3135.

(5) (a) Zhang, J.; Kohlbouni, S. T.; Borhan, B. Cu-Catalyzed Oxidation of $C_2$ and $C_3$ Alkyl-Substituted Indole via Acyl Nitroso Reagents. *Org. Lett.* **2019**, *21*, 14–17. (b) Zhang, Z.; Ji, C. L.;

Yang, C.; Chen, J.; Hong, X.; Xia, J. B. Nickel Catalyzed Kumada Coupling of boc-Activated Aromatic Amines via Nondirected Selective Aryl C–N bond Cleavage. *Org. Lett.* **2019**, *21*, 1226–1231. (c) Borger, C.; Knolker, H. J. A General Approach to 1,6-Dioxygenated Carbazole Alkaloids – First Total Synthesis of Clausine G, Clausine I and Clausine Z. *Synlett*. **2008**, *11*, 1698–1702. (d) Conover, L.H.; Tarbell, D.S. Hydrogenolysis of Certain Substituted Aromatic Acids and Carbonyl Compounds by Lithium Aluminum Hydride. *J. Am. Chem. Soc.* **1950**, *72*, 3586-3588.

(6) (a) Fuchs, B.; Zizuashvili, J.; Abramson, S. Geometrically Biased Homoconjugated Ketones. Synthetic Avenues to 1-acyl-2,4-cyclohexadienes. *J. Org. Chem.* **1982,** *47*, 3474–3477. (b) Beckwith, A.; Gerba, S. The Stereochemistry of Ring Closure of Some Monosubstituted *o*-(but-3-enyl)phenyl Radicals. *J. Aus. Chem.* **1992**, *45*, 289–308. (c) Kanomata, N.; Sakaguchi, R.; Sekine, K.; Yamashita, S.; Tanaka, H. Enantioselective Cyclopropanation Reactions with Planar-Chiral Pyridinium Ylides: a Substituent Effect and a Remote Steric Effect. *Adv. Synth. & Cat.* **2010,** *352*, 2966–2978. (d) Robaa, D.; Enzensperger, C.; Abulazm, S. E.; M. Hefnawy, M.; I. El-Subbagh, H.; A. Wani, T.; Lehmann, J. Chiral Indole [3,2-f][3]benzecine-type Dopamine Receptor Antagonists: Synthesis and Activity of Racemic and Enantiopure Derivatives. *J. Med. Chem.* **2011,** *54*, 7422–7426. (e) Crockett, Marc, et al. Preparation of Phenolics from Biomass. Nederlandse Organisatie voor Toegepast-Natuurwetenschappeljik Onderzoek TNO, Neth. *WO 2016114668*. 21 July **2016**. (f) Pollack, S.K.; Raine, B.C.; Hehre, W.J. Determination of the Heats of Formation of the Isomeric Xylylenes by Ion Cyclotron Double-Resonance Spectroscopy. *J. Am. Chem. Soc.* **1981,** *103*, 6308–6313. (g) Holland, H.L.; Brown, F.M.; Conn, M. Side Chain Hydroxylation of Aromatic Compounds by Fungi. Influence of the para Substituent on Kinetic Isotope Effects During Benzylic Hydroxylation by Mortierella isabelline. *J. Chem. Soc. Perkin Trans. 2* **1990**, *10*, 1651–1655. (h) Hanzlik, R. P.; Schaefer, A. R.; Moon, J. B.; Judson, C. M. Primary and Secondary Kinetic Deuterium Isotope Effects and Transition-state Structures for Benzylic Chlorination and Bromination of Toluene. *J. Am. Chem. Soc.* **1987**, *109*, 4926–4930. (i) Koshiyama, T.; Hirai, K.; Tomioka, H. Generation, Reactions, and Kinetics of Di(naphthyl)carbenes: Effects of the Methyl Group. *The Journal of Physical Chemistry A.* **2002**, *106*, 10261–10274. (j) Hayama, T.; Baldridge, K. K.; Wu, Y.-T.; Linden, A.; Siegel, J. S. Steric Isotope Effects Gauged by the Bowl-Inversion Barrier in Selectively Deuterated Pentaarylcorannulenes. *J. Am. Chem. Soc*. **2008**, *130*, 1583–1591. (k) Courchay, F. C.; Sworen, J. C.; Ghiviriga, I.; Abboud, K. A.; Wagener, K. B.

Understanding Structural Isomerization During Ruthenium-Catalyzed Olefin Metathesis: A Deuterium Labelling Study. *Organometallics*. **2006**, *25*, 6074–6086.

(7) (a) Barfield, M.; Collins, M. J.; Gready, J. E.; Sternhell, S.; Tansey, C. W. Bond-order Dependence o Orthobenzylic Coupling Constants Involving a Methyl Group. *J. Am. Chem. Soc.* **1989**, *111*, 4285–4290. (b) Maj, A. M.; Suisse, I.; Hardouin, C.; Agbossou-Niedercorn, F. Synthesis of New Chiral 2-functionalized-1,2,3,4-tetrahydroquinoline Derivatives via Asymmetric Hydrogenation of Substituted Quinolines. *Tetrahedron* **2013**, *69*, 9322–9328. (c) Sorella, G. L.; Sperni, L.; Canton, P.; Coletti, L.; Fabris, F.; Strukul, G.; Scarso, A. Selective Hydrogenations and Dechlorinations in Water Mediated by Anionic Surfactant-Stabilized Pd Nanoparticles. *J. Org. Chem.* **2018,** *83*, 7438–7446. (d) Shiraishi, Y.; Fujiwara, K.; Sugano, Y.; Ichikawa, S.; Hirai, T. N-Monoalkylation of Amines with Alcohols by Tandem Photocatalytic and Catalytic Reactions on $TiO_2$ Loaded with Pd Nanoparticles. *ACS Catal.* **2013,** *3*, 312–320. (e) He, J.; Zhao, C.; Lercher, J. A. Ni-Catalyzed Cleavage of Aryl Ethers in the Aqueous Phase. *J. Am. Chem. Soc.* **2012,** *134*, 20768–20775. (f) Covert, L. W.; Connor, R.; Adkins, H. Use of Nickel as a Catalyst for Hydrogenation. *J. Am. Chem. Soc.* **1932,** *54*, 1651–1663. (g) Baltzly, R.; Buck, J. S. Catalytic Debenzylation. The Effect of Substitution on the Strength of the *O*-Benzyl and *N*-Benzyl Linkages. *J. Am. Chem. Soc.* **1943,** *65*, 1984–1992.

(8) (a) Ben Halima, T.; Masson-Makdissi, J.; Newman, S. G. Nickel Catalyzed Amide Bond Formation from Methyl Esters. *Angew. Chemie. Int. Ed.* **2018**, *57*, 12925–12929. (b) Zheng, Y.-L.; Newman, S. G. Methyl esters as cross-coupling electrophiles: Direct Synthesis of Amide Bonds. *ACS Catal.* **2019**, *9*, 4426–4433. (c) Hie, L.; Fine Nathel, N. F.; Hong, X.; Yang, Y.-F.; Houk, K. N.; Garg, N. K. Nickel-Catalyzed Activation of Acyl C−O Bonds of Methyl Esters. *Angew. Chemie. Int. Ed*. **2016**, *55*, 2810–2814. (d) Yue, H.; Zhu, C.; Rueping, M. Catalytic Ester to Stannane Functional Group Interconversion via Decarbonylative Cross-Coupling of Methyl Esters. *Org. Lett.* **2018**, *20*, 385–388. (e) Rosen, B. M.; Quasdorf, K. W.; Wilson, D. A.; Zhang, N.; Resmerita, A. M.; Garg, N. K.; Percec, V. Nickel-Catalyzed Cross-Couplings Involving Carbon–Oxygen Bonds. *Chem. Rev.* **2011**, *111*, 1346–1416. (f) Walker, J. A., Jr; Vickerman, K. L.; Humke, J. N.; Stanley, L. M. Ni-Catalyzed Alkene Carboacylation via Amide C–N Bond Activation. *J. Am. Chem. Soc.* **2017**, *139*, 10228– 10231.

(9) (a) Alvarez-Bercedo, P.; Martin, R. Ni-Catalyzed Reduction of Inert-C–O Bonds: A New Strategy for Using Aryl Ethers as Easily Removable Directing Groups. *J. Am. Chem. Soc.* **2010**, *132*, 17352–17353. (b) Cornella, J.; Gómez-Bengoa, E.; Martin, R. Combined Experimental and Theoretical Study on the Reductive Cleavage of Inert C–O Bonds with Silanes: Ruling out a Classical Ni(0)/Ni(II) Catalytic Couple and Evidence for Ni(I) Intermediates. *J. Am. Chem. Soc.* **2013**, *135*, 1997–2009.

(10) Yue, H.; Guo, L.; Lee, S.-C.; Liu, X.; Rueping, M. Selective Reductive Removal of Ester and Amide Groups from Arenes and Heteroarenes through Nickel-Catalyzed C−O and C−N Bond Activation. *Angew. Chem. Int. Ed.* **2017**, *129*, 4030–4034.

(11) Simmons, B. J.; Hoffmann, M.; Hwang, J.; Jackl, M. K.; Garg, N. K. Nickel-Catalyzed Reduction of Secondary and Tertiary Amides. *Org. Lett.* **2017**, *19*, 1910–1913.

(12) (a) Ritleng, V.; Henrion, M.; Chetcuti, M. J. Nickel *N*-Heterocyclic Carbene-Catalyzed C–Heteroatom Bond Formation, Reduction, and Oxidation: Reactions and Mechanistic Aspects. *ACS Catal*. **2016**, *6*, 890–906. (b) Dey, A.; Sasmal, S.; Seth, K.; Lahiri, G. K.; Maiti, D. Nickel-Catalyzed Deamidative Step-Down Reduction of Amides to Aromatic Hydrocarbons. *ACS Catal*. **2016**, *7*, 433–437. (c) Tobisu, M.; Morioka, T.; Ohtsuki, A.; Chatani, N. Nickel-Catalyzed Reductive Cleavage of Aryl Alkyl Ethers to Arenes in Absence of External Reductant. *Chem. Sci.* **2015**, *6*, 3410–3414. (d) Sergeev, A.; Webb, J.; Hartwig, J. F. A Heterogenous Nickel Catalyst for the Hydrogenation of Ethers without Arene Hydrogenation. *J. Am. Chem. Soc*. **2012**, *134*, 20226–20229. (e) Sergeev, A.; Hartwig, J. F. Selective Nickel-Catalyzed Hydrogenolysis of Ethers. *Science* **2011**, *332*, 439–443. (f) Tobisu, M.; Yamakawa, K.; Shimasaki, T.; Chatani, N. Nickel-Catalyzed Reductive Cleavage of Aryl-Oxygen Bonds in Alkoxy and Pivaloxyarenes using Hydrosilanes as a Mild Reducing Agent. *Chem. Comm.* **2011**, *47*, 2946–2948. (g) Iosub, A.V.; Moravcik, S.; Wallentin, C.-J.; Bergman, J. Nickel-Catalyzed Selective Reduction of Carboxylic Acids to Aldehydes. *Org. Lett.* **2019**, 10.1021/acs.orglett.9b02779.

(13) Pesti, J.; Larson, G. L. Tetramethyldisiloxane: A Practical Organosilane Reducing Agent. *Org. Process Res. Dev*. **2016**, *20*, 1164–1181.

(14) The combination of base and organosilanes are known to form species capable of reducing carbonyl groups. For examples, see: (a) Kobayashi, Y.; Takahisa, E.; Nakano, M.; Watatani, K. Reduction of Carbonyl Compounds by using Polymethylhydro-Siloxane: Reactivity and

Selectivity. *Tetrahedron* **1997**, *53*, 1627–1634 (b) Fernández-Salas, J. A.; Manzini, S.; Nolan, S. P. Facile and Efficient KOH-Catalysed Reduction of Esters and Tertiary Amides. *Chem. Comm*. **2013**, *49*, 9758–9760. (c) Hojo, M.; Murakami, C.; Fujii, A.; Hosomi, A. New Reactivity of Methoxyhydridosilane in the Catalytic Activation System. *Tetrahedron Lett.* **1999**, *40*, 911–914. (d) Beller, M. et al. Hydrosilylation of Ketones: From Metal-Organic Frameworks to Simple Base Catalysts. *Chem. Asian J.* **2010**, *5*, 2341–2345. (e) Hosomi, A.; Hayashida, H.; Kohra, S; Tominaga, Y. Pentacoordinate Silicon Compounds in Synthesis: Chemo- and Stereo-selective Reduction of Carbonyl Compounds using Trialkoxy-substituted Silanes and Alkali Metal Alkoxides. *J. Chem. Soc. Chem. Commun.* **1986**, *18*, 1411–1412.

(15) (a) Mullard, A. Deuterated Drugs Draw Heavier Backing. *Nat. Rev. Drug Discov*, **2016**, *15*, 219–221. (b) Pirali, T.; Serafini, M.; Cargnin, S.; Genazzani, A. A. Applications of Deuterium in Medicinal Chemistry. *J. Med. Chem.* **2019,** *62*, 5276–5297. (c) Tung, R. D. Deuterium Medicinal Chemistry Comes of Age. *Future Med. Chem.* **2016**, *8*, 491–494.

(16) (a) Shen, Z.; Shang, S.; Geng, H.; Wang, J.; Zhang, X.; Zhou, A.; Yao, C.; Chen, X.; Want, W. Trideuteromethylation Enabled by a Sulfoxonium Metathesis Reaction. *Org. Lett*. **2019**, *21*, 448–452. (b) He, Z.-T.; Li, H.; Haydl, A.; Whiteker, G.; Hartwig, J. F. Trimethylphosphate as a Methylating Agent for Cross Coupling: A Slow-Release Mechanism for the Methylation of Arylboronic Esters. *J. Am. Chem. Soc.* **2018**, *140*, 17197–17202. (c) Han, X.; Yuan, Y.; Shi, Z. Rhodium-Catalyzed Selective C−H Trideuteromethylation of Indole at C7 Position Using Acetic-$d_6$ Anhydride. *J. Org. Chem.* **2019**, *84*, 12764-12772. (d) Hu, L.; Liu, X.; Liao, X. Nickel-Catalyzed Methylation of Aryl Halides with Deuterated Methyl Iodide. *Angew. Chem. Int. Ed*. **2016**, *55*, 9743–9747.

(17) Mazzini, F.; Alpi, E.; Salvadori, P.; Netscher, T. First Synthesis of (8-$^2H_3$)-(all-*rac*)-δ-Tocopherol. *Eur. J. Org. Chem*. **2003**, *15*, 2840–2844.

(18) (a) Smart, K. A.; Mothes-Martin, E.; Annaka, T.; Grellier, M.; Sabo-Etienne, S. Silane Deuteration Catalyzed by Ruthenium Bis(dihydrogen) Complexes or Simple Metal Salts. *Adv. Synth. Catal*. **2014**, *356*, 759–764. (b) Zhou, R.; Li, J.; Cheo, H. W.; Chua, R.; Zhan, G.; Hou, Z.; Wu, J. Visible-Light Mediated Deuteration of Silanes with Deuterium Oxide. *Chem. Sci*. **2019**, *10*, 7340–7344.

(19) (a) Burés, J. Variable Time Normalization Analysis: General Graphical Elucidation of Reaction Orders from Concentration Profiles. *Angew. Chem. Int. Ed.* **2016**, *55*, 16084–16087. (b) Neilsen, D.-T. C.; Burés, J. Visual Kinetic Analysis. *Chem. Sci.* **2019**, *10*, 348–353.

(20) (a) L. Larson, G.; L. Fry, J. Ionic and Organometallic-Catalyzed Organosilane Reductions. In Organic Reactions, (Ed.). doi: 10.1002/0471264180.or071.01 (b) Rendler, S.; Oestreich, M. Hypervalent Silicon as a Reactive Site in Selective Bond-Forming Processes. *Synthesis*. **2005**, *11*, 1727–1747. (c) Dieters, J. A.; Holmes, R. R. Enhanced Reactivity of Pentacoordinated Silicon Species. An ab Initio Approach. *J. Am. Chem. Soc.* **1990**, *112*, 7197–7202. (d) Revunova, K.; Nikonov, G. I. Base-Catalyzed Hydrosilylation of Ketones and Esters and Insight into the Mechanism. *Chem. Eur. J.* **2013**, *20*, 839–845. (e) Drew, M. D.; Lawrence, N. J.; Fontaine, D.; Sehkri, D.; Bowles, S. A.; Watson, W. A Convenient Procedure for the Reduction of Esters, Carboxylic Acids, Ketones and Aldehydes using Tetrabutylammonium Fluoride and Polymethylhydrosiloxane. *Synlett.* **1997**, *8*, 989–911. (f) Brook, M. A. Silicon in Organic, Organometallic, and Polymer Chemistry; Interscience Publisher, Inc.: New York, **2000**, Chap. 4, 97.

(21) Simmons, E. M.; Hartwig, J. F. On the Interpretation of Deuterium Kinetic Isotope Effects in C-H Bond Functionalizations by Transition-metal Complexes. *Angew. Chem. Int. Ed.*, **2012**, *51*, 3066–3072.

(22) Smith, M.B.; March, J. Oxidations and reductions. In *March's Advanced Organic Chemistry*; John Wiley and Sons, Inc.: Hoboken, NJ, USA, 2006; pp. 1703–1869.

(23) Smith, M.B.; March, J. Diels-Alder reaction. In *March's Advanced Organic Chemistry*; John Wiley and Sons, Inc.: Hoboken, NJ, USA, 2006; pp. 1194–1208.

(24) Zakharkin, L. I.; Khorlina, I. M. Reduction of Esters of Carboxylic Acids into Aldehydes with Diisobutylaluminium Hydride. *Tetrahedron Lett.* **1962**, *3*, 619–620.

(25) Li, H.; Misal Castro, L. C.; Zheng, J.; Roisnel, T.; Dorcet, V.; Sortais, J.-B.; Darcel, C. Selective Reduction of Esters to Aldehydes under the Catalysis of Well-defined NHC–Iron Complexes. *Angew. Chem. Int. Ed.*, **2013**, *52*, 8045–8049.

(26) (a) Rysak, V.; Descamps-Mandine, A.; Simon, P.; Blanchard, F.; Burylo, L.; Trentesaux, M.; Vandewalle, M.; Collière, V.; Agbossou-Niedercorn, F.; Michon, C. Selective Ligand-Free

Cobalt-Catalysed Reduction of Esters to Aldehydes or Alcohols. *Catal. Sci. Technol.* **2018**, *8*, 3504–3512. (b) Pattanaik, S.; Gunanathan, C. Cobalt-Catalysed Selective Synthesis of Aldehydes and Alcohols from Esters. *Chem. Commun.,* **2020**, *56*, 7345–7348.

(27) Wei, D.; Buhaibeh, R.; Canac, Y.; Sortais, J.-B. Manganese and Rhenium-Catalyzed Selective Reduction of Esters to Aldehydes with Hydrosilanes. *Chem. Commun.,* **2020**, *56*, 11617–11620.

(28) Corre, Y.; Rysak, V.; Capet, F.; Djukic, J.-P.; Agbossou-Niedercorn, F.; Michon, C. Selective Hydrosilylation of Esters to Aldehydes Catalysed by Iridium(III) Metallacycles through Trapping of Transient Silyl Cations. *Chemistry* **2016**, *22*, 14036–14041.

(29) Yang, Z. Partial Reductions of Carboxylic Acids and Their Derivatives to Aldehydes. *Org. Chem. Front.* **2022**, *9*, 3908–3931.

(30) (a) Modak, A.; Maiti, D. Metal Catalyzed Defunctionalization Reactions. *Org. Biomol. Chem*. **2016**, *14*, 21-35. (b) Dominiquez-Huerta, A.; Dai, X.-J.; Zhou, F.; Querard, P.; Qiu, Z.; Ung, S.; Liu, W.; Li, J.; Li, C.-J. Exploration of New Reaction Tools for Late-Stage Functionalization of Complex Chemicals. *Can. J. Chem*. **2019**, *97*, 67-85. (c) Hong, B.; Luo, T.; Lei, X. Late-Stage Diversification of Natural Products. *ACS Cent. Sci.* **2020,** *6*, 622-635.

(31) (a) Sun, Z.; Fridrich, B.; de Santi, A.; Elangovan, S.; Barta, K. Bright Side of Lignin Depolymerization: Toward New Platform Chemicals. *Chem. Rev*. **2018**, *118*, 614-678. (b) Feghali, E.; Cantat, T. Unprecedented Organocatalytic Reduction of Lignin Model Compounds to Phenols and Primary Alcohols using Hydrosilanes. *Chem. Commun*. **2014**, *50*, 862-865. (c) Li, X.-Y.; Shang, R.; Fu, M.-C.; Fu, Y. Conversion of Biomass-Derived Fatty Acids and Derivatives into Hydrocarbons using a Metal-Free Hydrodeoxygenation Process. *Green Chem.* **2015**, *17*, 2790-2793.

(32) (a) Rousseau, G.; Breit, B. Removable Directing Groups in Organic Synthesis and Catalysis. *Angew. Chem. Int. Ed.* **2011**, *50*, 2450-2494. (b) Luo, J.; Preciado, S.; Larrosa, I. Overriding Ortho-Para Selectivity via a Traceless Directing Group Relay Strategy: The Meta-Selective Arylation of Phenols. *J. Am. Chem. Soc.* **2014**, *136*, 4109-4112. (c) Zhang, F.; Spring, D. R. Arene C-H Functionalisation Using a Removable/Modifiable or a Traceless Directing Group Strategy. *Chem. Soc. Rev*. **2014**, *43*, 6906-6919.

(33) (a) McCombie, S. W.; Motherwell, W. B.; Tozer, M. J. The Barton-McCombie Reaction. *Organic Reactions,* **2012**, *77*, 161-432. (b) Barton, D. H. R.; McCombie, S. W. A New Method for

the Deoxygenation of Secondary Alcohols. *J. Chem. Soc., Perkin Trans.* **1975**, *16*, 1574−1585. (c) Heravi, M. M.; Bakhtiari, A.; Faghihi, Z. Applications of Barton-McCombie Reaction in Total Syntheses. *Curr. Org. Synth.* **2014**, *11*, 787−823.

(34) (a) Szmant, H. H.; Harmuth, C. M. The Wolff-Kishner Reaction of Hydrazones. *J. Am. Chem. Soc*. **1964**, *86*, 2909-2914. (b) Lewis, D. L. The Wolff-Kishner Reduction and Related Reactions: Discovery and Development. **2019**, *Elsevier*. doi: 10.1016/C2017-0-03849-1. (c) Furrow, M. E.; Myers, A. G. Practical Procedures for the Preparation of *N-tert*-Butyldimethylsilylhydrazones and Their Use in Modified Wolff-Kishner Reductions and in the Synthesis of Vinyl Halides and gem-Dihalides. *J. Am. Chem. Soc*. **2004**, *126*, 5436-5445.

(35) (a) Ooi, X. Y.; Gao, W.; Ong, H. C.; Lee, H. V.; Juan, J. C.; Chen, W. H.; Lee, K. T. Overview on Catalytic Deoxygenation for Biofuel Synthesis using Metal Oxide Supported Catalysts. *Renew. Sust. Energ. Rev.* **2019**, *112*, 834-852. (b) Lup, A. N. K.; Abnisa, F.; Daud, W. M. A. W.; Aroura, M. K. A Review on Reactivity and Stability of Heterogeneous Metal Catalysts for Deoxygenation of Bio-Oil Model Compounds. *J. Ind. Eng. Chem*. **2017**, *56*, 1-34. (c) Volkov, A.; Gustafson, K. P. J.; Tai, C.-W.; Verho, O.; Backvall, J.-E.; Adolfsson, H. Mild Deoxygenation of Aromatic Ketones and Aldehydes over Pd/C Using Polymethylhydrosiloxane as the Reducing Agent. *Angew. Chem. Int. Ed.* **2015**, *54*, 5122-5126. (d) Lonsky, W.; Traitler, H.; Kratzl, K. A Simple Method for the Removal of Phenolic Hydroxy-Groups. *J. Chem. Soc. Perkin Trans.* **1975**, *1*, 169-170.

(36) (a) Herrmann, J. M.; Konig, B. Reductive Deoxygenation of Alcohols: Catalytic Methods Beyond Barton-McCombie Deoxygenation. *Eur. J. Org. Chem.* **2013**, *2013*, 7017−7027. (b) Speckmeier, E.; Padie, C.; Zeitler, K. Visible Light Mediated Reductive Cleavage of C–O Bonds Accessing α-Substituted Aryl Ketones. *Org. Lett*. **2015**, *17*, 4818-4821. (c) Liu, J.-T.; Yang, S.; Tang, W.; Yang, Z.; Xu, J. Iridium-Catalyzed Efficient Reduction of Ketones in Water with Formic Acid as a Hydride Donor at Low Catalyst Loading. *Green Chem.* **2018**, *20*, 2118−2124. (d) Argouarch, G. Mild and Efficient Rhodium-Catalyzed Deoxygenation of Ketones to Alkanes. *New J. Chem.*, **2019**, *43*, 11041-11044. (e) Wang, H.; Li, L.; Bai, X.-F.; Shang, J.-Y.; Yang, K.-F.; Xu, L.-W. Efficient Palladium-Catalyzed C–O Hydrogenolysis of Benzylic Alcohols and Aromatic Ketones with Polymethylhydrosiloxane. *Adv. Synth. Catal.* **2013**, *355*, 341-347. (f) Dong, Z.; Yuan, J.; Xiao, Y.; Mao, P.; Wang, W. Room Temperature Chemoselective Deoxygenation of Aromatic Ketones and Aldehydes Promoted by a Tandem Pd/$TiO_2$ + $FeCl_3$ Catalyst. *J. Org. Chem.* **2018**, *83*, 11067-11073. (g) Lam, K.; Markó, I. E. Electrochemical Deoxygenation of Primary Alcohols.

*Synlett,* **2012**, *23*, 1235-1239. (h) Kalutharage, N.; Yi, C. S. Scope and Mechanistic Analysis for Chemoselective Hydrogenolysis of Carbonyl Compounds Catalyzed by a Cationic Ruthenium Hydride Complex with a Tunable Phenol Ligand. *J. Am. Chem. Soc.* **2015**, *137*, 11105-11114. (i) Magano, J.; Dunetz, J. R. Large-Scale Carbonyl Reductions in the Pharmaceutical Industry. *Org. Process Res. Dev.* **2012**, *16*, 1156–1184.

(37) (a) Chandrasekhar, S.; Reddy, C. R.; Babu, B. N. Rapid Defunctionalization of Carbonyl Group to Methylene with Polymethylhydrosiloxane-$B(C_6F_5)_3$. *J. Org. Chem.* **2002**, *67*, 9080-9082. (b) Nimmagadda, R. D.; McRae, C. A Novel Reduction Reaction for the Conversion of Aldehydes, Ketones, and Primary, Secondary and Tertiary Alcohols into Their Corresponding Alkanes. *Tetrahedron Lett.* **2006**, *47*, 5755-5758. (c) Mahdi, T.; Stephan, D. W. Facile Protocol for Catalytic Frustrated Lewis Pair Hydrogenation and Reductive Deoxygenation of Ketones and Aldehydes. *Angew. Chem. Int. Ed*. **2015**, *54*, 8511-8514.

(38) (a) Gevorgyan, V.; Rubin, M.; Liu, J.-X.; Yamamoto, Y. A Direct Reduction of Aliphatic Aldehyde, Acyl Chloride, Ester, and Carboxylic Functions into a Methyl Group. *J. Org. Chem.* **2001**, *66*, 1672-1675. (b) Bach, P.; Albright, A.; Laali, K. K. Influence of Lewis Acid and Solvent in the Hydrosilylation of Aldehydes and Ketones with $Et_3SiH$; Tris(pentafluorophenyl)borane $B(C_6F_5)_3$ versus Metal Triflates [$M(OTf)_3$; M = Sc, Bi, Ga, and Al]–Mechanistic Implications. *Eur. J. Org. Chem*. **2009**, 1961-1966.

(39) (a) Gevorgyan, V.; Liu, J.-X.; Rubin, M.; Benson, S.; Yamamoto, Y. A Novel Reduction of Alcohols and Ethers with a $HSiEt_3$ Catalytic $B(C_6F_5)_3$ System. *Tetrahedron Lett*. **1999**, *40*, 8919-8922. (b) Gevorgyan, V.; Rubin, M.; Benson, S.; Liu, J.-X.; Yamamoto, Y. A Novel $B(C_6F_5)_3$-Catalyzed Reduction of Alcohols and Cleavage of Aryl and Alkyl Ethers with Hydrosilanes. *J. Org. Chem.* **2000**, *65*, 6179-6186. (c) Adduci, L. L.; McLaughlin, M. P.; Bender, T. A.; Becker, J. J.; Gagné, M. R. Metal-Free Deoxygenation of Carbohydrates. *Angew. Chem. Int. Ed.* **2014**, *53*, 1646-1649. (d) Adduci, L. L.; Bender, T. A.; Dabrowski, J. A.; Gagné, M. R. Chemoselective Conversion of Biologically Sourced Polyols into Chiral Synthons. *Nat. Chem*. **2015**, *7*, 576–581.

(40) (a) Blondiaux, E.; Cantat, T. Efficient Metal-Free Hydrosilylation of Tertiary, Secondary and Primary Amides to Amines. *Chem. Commun.* **2014**, *50*, 9349-9352. (b) Chadwick, R. C.; Kardelis, V.; Lim, P.; Adronov, A. Metal-Free Reduction of Secondary and Tertiary *N*-Phenyl Amides by Tris(pentafluorophenyl)boron-Catalyzed Hydrosilylation. *J. Org. Chem.* **2014**, *79*, 7728-7733. (c) Huang, P.-Q.; Lang, Q.-W.; Wang, Y.-R. Mild Metal-Free Hydrosilylation of Secondary Amides to

Amines. *J. Org. Chem.* **2016**, *81*, 4235-4243. (d) Lucas, K. M.; Kleman, A. F.; Sadergaski, L. R.; Jolly, C. L.; Bollinger, B. S.; Mackesey, B. L.; McGrath, N. A. Versatile, Mild, and Selective Reduction of Various Carbonyl Groups using an Electron-Deficient Boron Catalyst. *Org. Biomol. Chem*. **2016**, *14*, 5774–5778.

(41) (a) Fang, H.; Oestrich, M. Defunctionalisation Catalysed by Boron Lewis acids. *Chem. Sci.* **2020**, *11*, 12604-12615. (b) Hackel, T.; McGrath, N. A. Tris(pentafluorophenyl)borane-Catalyzed Reactions Using Silanes. *Molecules*, **2019**, *24*, 432.

(42) (a) Corma, A.; Garcia, H. Lewis Acids: From Conventional Homogeneous to Green Homogeneous and Heterogeneous Catalysis. *Chem. Rev*. **2003**, *103*, 4307-4366. (b) Dal Zotto, C.; Virieux, D., Campagne, J.-M. $FeCl_3$-Catalyzed Reduction of Ketones and Aldehydes to Alkane Compounds. *Synlett* **2009**, *2*, 276-278. (c) Surya Prakash, G. K.; Do, C.; Mathew, T.; Olah, G. A. Reduction of Carbonyl to Methylene: Organosilane-$Ga(OTf)_3$ as an Efficient Reductant System. *Catal. Lett*. **2011**, *141*, 507-511. (d) Dieguez, H. R.; Lopez, A.; Domingo, V.; Arteaga, J. F.; Dobado, J. A.; Herrador, M. M.; Quilez del Moral, J. F.; Barrero, A. F. Weakening C-O Bonds: Ti(III), a New Reagent for Alcohol Deoxygenation and Carbonyl Coupling Olefination. *J. Am. Chem. Soc*. **2010**, *132*, 254-259. (e) Yasuda, M.; Onishi, Y.; Ueba, M.; Miyai, T.; Baba, A. Direct Reduction of Alcohols: Highly Chemoselective Reducing System for Secondary or Tertiary Alcohols Using Chlorodiphenylsilane with a Catalytic Amount of Indium Trichloride. *J. Org. Chem*. **2001**, *66*, 7741-7744. (f) West, C. T.; Donnelly, S. J.; Kooistra, D. A.; Doyle, M. P. Silane Reductions in Acidic Media. II. Reductions of Aryl Aldehydes and Ketones by Trialkylsilanes in Trifluoroacetic Acid. A Selective Method for Converting the Carbonyl Group to Methylene. *J. Org. Chem.* **1973**, *38*, 2675-2681.

(43) (a) Dai, X.-J.; Li, C.-J. En Route to a Practical Primary Alcohol Deoxygenation. *J. Am. Chem. Soc*. **2016**, *138*, 5433-5440. (b) Bauer, J. O.; Chakraborty, S.; Milstein, D. Manganese-Catalyzed Direct Deoxygenation of Primary Alcohols. *ACS Catal.* **2017**, *7*, 4462−4466. (c) Cranwell, P. B.; Russell, A. T.; Smith, C. D. Methyl Hydrazinocarboxylate as a Practical Alternative to Hydrazine in the Wolff-Kishner Reaction. *Synlett.* **2016**, *27*, 131-135.

(44) Dang, H.; Cox, N.; Lalic, G. Copper-Catalyzed Reduction of Alkyl Triflates and Iodides: An Efficient Method for the Deoxygenation of Primary and Secondary Alcohols. *Angew. Chem. Int. Ed.* **2014**, *53*, 752−756.

(45) (a) Zhang, J.; Yang, J.-D.; Cheng, J.-P. Diazaphosphinyl Radical-Catalyzed Deoxygenation of α-Carboxy Ketones: A New Protocol for Chemoselective C–O Bond Scission via Mechanism Regulation. *Chem. Sci.* **2020**, *11*, 8476-8481. (b) Mehta, M.; Holthausen, M. H.; Mallov, I.; Perez, M.; Qu, Z.-W.; Grimme, S.; Stephan, D. W. Catalytic Ketone Hydrodeoxygenation Mediated by Highly Electrophilic Phosphonium Cations. *Angew. Chem. Int. Ed*. **2015**, *54*, 8250-8254. (c) Sousa, S. C. A.; Fernandes, T. A.; Fernandes, A. C. Highly Efficient Deoxygenation of Aryl Ketones to Arylalkanes Catalyzed by Dioxidomolybdenum Complexes. *Eur. J. Org. Chem*. **2016**, *18*, 3109-3112. (d) Chambers, D. R.; Juneau, A.; Ludwig, C. T.; Frenette, M.; Martin, D. B. C. C–O Bond Cleavage of Alcohols via Visible Light Activation of Cobalt Alkoxycarbonyls. *Organometallics* **2019**, *38*, 4570-4577. (e) Fast, C. D.; Schley, N. D. Light-Promoted Transfer of an Iridium Hydride in Alkyl Ether Cleavage. *Organometallics* **2021**, *40,* 3291-3297.

(46) (a) Alvarez-Bercedo, P.; Martin, R. Ni-Catalyzed Reduction of Inert C–O Bonds: A New Strategy for Using Aryl Ethers as Easily Removable Directing Groups. *J. Am. Chem. Soc*. **2010**, *132*, 17352– 17353. (b) Cornella, J.; Gomez-Bengoa, E.; Martin, R. Combined Experimental and Theoretical Study on the Reductive Cleavage of Inert C−O Bonds with Silanes: Ruling Out a Classical Ni(0)/Ni(II) Catalytic Couple and Evidence for Ni(I) Intermediates. *J. Am. Chem. Soc.* **2013**, *135*, 1997−2009. (c) Tobisu, M.; Yamakawa, K.; Shimasaki, T.; Chatani, N. Nickel-Catalyzed Reductive Cleavage of Aryl-Oxygen Bonds in Alkoxy- and Pivaloxyarenes Using Hydrosilanes as a Mild Reducing Agent. *Chem. Commun.* **2011**, *47*, 2946-2948.

(47) (a) Sergeev, A.; Hartwig, J. F. Selective Nickel-Catalyzed Hydrogenolysis of Ethers. *Science* **2011**, *332*, 439−443. (b) Sergeev, A.; Webb, J.; Hartwig, J. F. A Heterogenous Nickel Catalyst for the Hydrogenation of Ethers Without Arene Hydrogenation. *J. Am. Chem. Soc.* **2012**, *134*, 20226−20229. (c) Kusumoto, S.; Nozaki, K. Direct and Selective Hydrogenolysis of Arenols and Aryl Methyl Ethers. *Nat. Commun*. **2015**, *6*, 6296-6302.

(48) (a) Igarashi, T.; Haito, A.; Chatani, N.; Tobisu, M. Nickel-Catalyzed Reductive Cleavage of Carbon-Oxygen Bonds in Anisole Derivatives Using Diisopropylaminoborane. *ACS Catal.* **2018**, *8*, 7475-7483. (b) Xi, X.; Chen, T.; Zhang, J.-S.; Han, L.-B. Efficient and Selective Hydrogenation of C–O Bonds with a Simple Sodium Formate Catalyzed by Nickel. *Chem. Comm*. **2018**, *54*, 1521-1524. (c) Tobisu, M.; Morioka, T.; Ohtsuki, A.; Chatani, N. Nickel-Catalyzed Reductive Cleavage of Aryl Alkyl Ethers to Arenes in Absence of External Reductant. *Chem. Sci.* **2015**, *6*, 3410-3414.

(49) (a) Yue, H.; Guo, L.; Lee, S.-C.; Liu, X.; Rueping, M. Selective Reductive Removal of Ester and Amide Groups from Arenes and Heteroarenes through Nickel-Catalyzed C–O and C–N Bond Activation. *Angew. Chem. Int. Ed.* **2017**¸ *56*, 3972-3976. (b) Dey, A.; Sasmal, S.; Seth, K.; Lahiri, G. K.; Maiti, D. Nickel-Catalyzed Deamidative Step-Down Reduction of Amides to Aromatic Hydrocarbons. *ACS Catal.* **2017**, *7*, 433-437. c) Patra, T.; Agasti, S.; Modak, A.; Maiti, D. Nickel-Catalyzed Hydrogenolysis of Unactivated Carbon–Cyano Bonds. *Chem. Commun*. **2013**, *49*, 8362-8365. d) Ohgi, A.; Nakao, Y. Selective Hydrogenolysis of Arenols with Hydrosilanes by Nickel Catalysis. *Chem. Lett.* **2016**, *45*, 45.

(50) (a) Simmons, B. J.; Hoffmann, M.; Hwang, J.; Jackl, M. K.; Garg, N. K. Nickel-Catalyzed Reduction of Secondary and Tertiary Amides. *Org. Lett.* **2017**, *19*, 1910−1913. (c) Yue, H.; Guo, L.; Lee, S.-C.; Liu, X.; Rueping, M. Selective Reductive Removal of Ester and Amide Groups from Arenes and Heteroarenes through Nickel-Catalyzed C−O and C−N Bond Activation. *Angew. Chem. Int. Ed.* **2017**, *56*, 3972−3976.

(51) Iosub, A. V.; Moravcik, S.; Wallentin, C.-J.; Bergman, J. Nickel Catalyzed Selective Reduction of Carboxylic Acids to Aldehydes. *Org. Lett.* **2019**, 21, 7804-7808.

(52) Cook, A.; Prakash, S.; Zheng, Y.-L.; Newman, S. G. Exhaustive Reduction of Esters Enabled by Nickel Catalysis. *J. Am. Chem. Soc.* **2020**, *142*, 8109-8115.

(53) (a) Alumasa, J. N.; Gorka, A. P.; Casabianca, L. B.; Comstock, E.; de Dios, A. C.; Roepe, P. D. The Hydroxyl Functionality and a Rigid Proximal N are Required for Forming a Novel Non-Covalent Quinine-Heme Complex. *J. Inorg. Biochem*. **2011**, *105*, 467-475. (b) Nakano, A.; Kawahara, S.; Akamatsu, S.; Morokuma, K.; Nakatani, M.; Iwabuchi, Y.; Takahashi, K.; Ishihara, J.; Hatakeyama, S. β-Isocupreidine-Hexafluoroisopropyl Acrylate Method for Asymmetric Baylis-Hillman Reactions. *Tetrahedron* **2006**, *62*, 381-389.

(54) (a) Yoneda, R.; Osaki, T.; Harusawa, S.; Kurihara, T. Dephosphorylation of Cyano Diethyl Phosphates by Reduction with Lithium-Liquid Ammonia: An Efficient Method for Conversion of Carbonyl Compounds into Nitriles. *J. Chem. Soc. Perkin Trans.* **1990**, *3*, 607-610. (b) Offei, S. D.; Arman, H. D.; Yoshimoto, F. K. Chemical Synthesis of 7α-Hydroxycholest-4-en-3-one, A Biomarker for Irritable Bowel Syndrome and Bile Acid Malabsorption. *Steroids* **2019**, *151*, 108449-108457. (c) Kalutharage, N.; Yi, C. S. Scope and Mechanistic Analysis for Chemoselective Hydrogenolysis of Carbonyl Compounds Catalyzed by a Cationic Ruthenium Hydride Complex with a Tunable Phenol Ligand. *J. Am. Chem. Soc*. **2015**, *137*, 11105-11114. (d)

Li, T.-S.; Li, Y.-L.; Liang, X.-T. A Facile Route for the Synthesis of 4β-Methyl-5α-Cholestane. *Chin. J. Org. Chem.* **1990**, *10*, 240-244.

(55) While reduction of both C–O bonds in an epoxide is uncommon, monoreduction to form alcohol products is easily achieved. For examples, see: (a) Chow, K. Y.-K.; Bode, J. W. Catalytic Generation of Activated Carboxylates: Direct, Stereoselective Synthesis of Beta-Hydroxyesters from Epoxyaldehydes. *J. Am. Chem. Soc*. **2004**, *126*, 8126-8127. (b) Gansauer, A.; Klatte, M.; Brandle, G. M.; Friedrich, J. Catalytic Hydrogen Atom Transfer (HAT) for Sustainable and Diastereoselective Radical Reduction. *Angew. Chem. Int. Ed*. **2012**, *51*, 8891-8894. (c) Yao, C.; Dahmen, T.; Gansauer, A.; Norton, J. Anti-Markovnikov Alcohols via Epoxide Hydrogenation Through Cooperative Catalysis. *Science* **2019**, *364*, 764-767.

(56) (a) Mullard, A. Deuterated Drugs Draw Heavier Backing. *Nat. Rev. Drug Discov.* **2016**, *15*, 219−221. (b) Pirali, T.; Serafini, M.; Cargnin, S.; Genazzani, A. A. Applications of Deuterium in Medicinal Chemistry. *J. Med. Chem.* **2019**, *62*, 5276−5297. (c) Tung, R. D. Deuterium Medicinal Chemistry Comes of Age. *Future Med. Chem.* **2016**, *8*, 491−494. (d) Zhu, N.; Su, M.; Wan, W.-M.; Li, Y, Bao, H. Practical Method for Reductive Deuteration of Ketones with Magnesium and $D_2O$. *Org. Lett*. **2020**, *22*, 991-996. (e) Rowbotham, J. S.; Ramirez, M. A.; Lenz, O.; Reeve, H. A.; Vincent, K. A. Bringing Biocatalytic Deuteration into the Toolbox of Asymmetric Isotopic Labelling Techniques. *Nat. Commun*. **2020**, *11*, 1454. (f) Ou, W.; Xiang, X.; Zou, R.; Xu, Q.; Loh, K. P.; Su, C. Room-Temperature Palladium-Catalyzed Deuterogenolysis of Carbon Oxygen Bonds Towards Deuterated Pharmaceuticals. *Angew. Chem. Int. Ed*. **2021**, *60*, 6357-6361.

(57) Smart, K. A.; Mothes-Martin, E.; Annaka, T.; Grellier, M.; Sabo-Etienne, S. Silane Deuteration Catalyzed by Ruthenium Bis(dihydrogen) Complexes or Simple Metal Salts. *Adv. Synth. Catal*. **2014**, *356*, 759–764.

(58) W. Green; P. G. M. Wuts. *Protective Groups in Organic Synthesis*, Wiley-Interscience, New York, **1999**, *76-86*, 708-711.

(59) For methods used as an alternative to Pd/C in benzyl ether deprotections: (a) Okano, K.; Okuyama, K.-I.; Fukuyama, T.; Tokuyama, H. Mild Debenzylation of Aryl Benzyl Ether with $BCl_3$ in the Presence of Pentamethylbenzene as a Non-Lewis Basic Cation Scavenger. *Synlett* **2008**, *13*, 1977-1980. (b) Alonso, E.; Ramon, D. J.; Mukaiyama, T. Reductive Deprotection of Allyl, Benzyl and Sulfonyl Substituted Alcohols, Amines and Amides using a Naphthalene-Catalyzed Lithiation. *Tetrahedron* **1997**, *53*, 14355-14368. (c) Cavedon, C.; Sletten, E. T.; Madani, A.; Niemeyer, O.;

Seeberger, P. H.; Pieber, B. Visible-Light-Mediated Oxidative Debenzylation Enables the Use of Benzyl Ethers as Temporary Protecting Groups. *Org. Lett.* **2021,** *23,* 514-518.

(60) (a) Pizzi, A. Tannins: Prospectives and Actual Industrial Applications. *Biomolecules* **2019**, *9,* 344. (b) Arbenz, A.; Avérous, L. Chemical Modification of Tannins to Elaborate Aromatic Biobased Macromolecular Architectures. *Green Chem.* **2015**, *17,* 2626-2646. (c) Zhu, H.; Li, P.; Ren, S.; Tan, W.; Fang, G. Low-Cost Ru/C-Catalyzed Depolymerization of the Polymeric Proanthocyanidin-Rich Fraction from Bark to Produce Oligomeric Proanthocyanidins with Antioxidant Activity. *ACS Omega* **2019**, *15,* 16471-16480.

(61) (a) Revunova, K.; Nikonov, G. I. Base-Catalyzed Hydrosilylation of Ketones and Esters and Insight into the Mechanism. *Chem. - Eur. J.* **2014**, *20*, 839−845. (b) Rendler, S.; Oestreich, M. Hypervalent Silicon as a Reactive Site in Selective Bond-Forming Processes. *Synthesis* **2005**, *11*, 1727−1747.

(62) (a) Atesin, A. C.; Ray, N. A.; Stair, P. C.; Marks, T. J. Etheric C-O Bond Hydrogenolysis Using a Tandem Lanthanide Triflate/Supported Palladium Nanoparticle Catalyst System. *J. Am. Chem. Soc.* **2012**, *134*, 14682-14685. (b) King, A. E.; Brooks, T. J.; Tian, T.-H.; Batista, E. R.; Sutton, A. D. Understanding Ketone hydrodeoxygenation for the Production of Fuels and Feedstocks from Biomass. *ACS Catal.* **2015**, *5*, 1223-1226. (c) Yang, X.; Jenkins, R. W.; Leal, J. H.; Moore, C. M.; Judge, E. J.; Semelsberger, T. A.; Sutton, A. D. Hydrodeoxygenation (HDO) of Biomass Derived Ketones using Supported Transition Metals in a Continuous Reactor. *ACS. Sus. Chem. Eng*. **2019**, *7*, 14521-14530.

(63) (a) Newcomb, M. Radical Kinetics and Clocks. Encyclopedia of Radicals in Chemistry, *Biology and Materials* **2012**, *1* DOI: 10.1002/9781119953678.rad007. (b) Bowry, V. W.; Lusztyk, J.; Ingold, K. U. Calibration of a New Horologery of Fast Radical Clocks. Ring-Opening Rates for Ring- and α-Alkyl-Substituted Cyclopropylcarbinyl Radicals and for the Bicyclo[2.1.0]pent-2-yl Radical. *J. Am. Chem. Soc*. **1991**, *113*, 5687-5698.

(64) (a) Halgren, T. A.; Roberts, J. D.; Horner, J. H.; Martinez, F. N.; Tronche, C.; Newcomb, M. Kinetics and Equilibrium Constants for Reactions of α-Phenyl-Substituted Cyclopropylcarbinyl Radicals. *J. Am. Chem. Soc*. **2000**, *122*, 2988-1994. (b) Bowry, V. W.; Lusztyk, J.; Ingold, K. U. Evidence for Reversible Ring-Opening of the α-Cyclopropylbenzyl Radical. *J. Chem. Soc., Chem. Comm*. **1990**, *13*, 923-925.

(65) (a) Harris, M. R.; Hanna, L. E.; Greene, M. A.; Moore, C. E.; Jarvo, E. R. Retention or Inversion in Stereospecific Nickel-Catalyzed Cross-Coupling of Benzylic Carbamates with Arylboronic Esters: Control of Absolute Stereochemistry with an Achiral Catalyst. *J. Am. Chem. Soc.* **2013**, *135*, 3303-3306. (b) Zhang, S.; Taylor, B. L. H.; Ji, C.; Gao, Y.; Harris, M. R.; Hanna, L. E.; Jarvo, E. R.; Houk, K. N.; Hong, X. Mechanism and Origins of Ligand-Controlled Stereoselectivity of Ni-Catalyzed Suzuki-Miyaura Coupling with Benzylic Esters: A Computational Study. *J. Am. Chem. Soc.* **2017**, *139*, 12994-13005.

(66) Dimitrov, V.; Bratovanov, S.; Simova, S.; Kostova, K. Cerium (III) Chloride as Catalytic and Stoichiometric Promotor of the Quantitative Addition of Organometallic Reagents to (+)-Camphor and (-)-Fenchone. *Tetrahedron Lett*. **1994**, *35*, 6713-6716.

(67) (a) Diccianni, J. B.; Diao, T. Mechanisms of Nickel-Catalyzed Cross-Coupling Reactions. *Trends Chem*. **2019**, *1*, 830-844. (b) Choi, J.; Fu, G. C. Transition Metal-Catalyzed Alkyl-Alkyl Bond Formation: Another Dimension in Cross-Coupling Chemistry. *Science* **2017**, *356*, eaaf7230. (c) Fu, G. C. Transition-Metal Catalysis of Nucleophilic Substitution Reactions: A Radical Alternative to $S_N1$ and $S_N2$ Processes. *ACS Cent. Sci*. **2017**, *3*, 692-700. (d) Tellis, J. C.; Primer, D. N.; Molander, G. A. Single-Electron Transmetalation in Organoboron Cross-Coupling by Photoredox/Nickel Dual Catalysis. *Science* **2014**, *345*, 433-436.

(68) (a) He, Y.; Liu, C.; Yu, L.; Zhu, S. Enantio- and Regioselective NiH-Catalyzed Reductive Hydroarylation of Vinylarenes with Aryl Iodides. *Angew. Chem. Int. Ed.* **2020**, *59*, 21530-21534. (b) Gutierrez, O.; Tellis, J. C.; Primer, D. N.; Molander, G. A.; Kozlowski, M.C. Nickel-Catalyzed Cross-Coupling of Photoredox-Generated Radicals: Uncovering a General Manifold for Stereoconvergence in Nickel-Catalyzed Cross Couplings. *J. Am. Chem. Soc.* **2015**, *137*, 4896-4899. (c) Anthony, D.; Lin, Q.; Baudet, J.; Diao, T. Nickel-Catalyzed Asymmetric Reductive Diarylation of Vinylarenes. *Angew. Chem. Int. Ed.* **2019**, *58*, 3198-3202.

(69) (a) Chu, X.Q.; Ge, D.; Cui, Y.-Y.; Shen, Z.-L.; Li, C.-J. Desulfonylation via Radical Process: Recent Developments in Organic Synthesis. *Chem. Rev.* **2021**, *121*, 12548-12680. (b) Alonso, D. A.; Ajera, C. N. Desulfonylation Reactions. *Organic Reactions* **2009,** DOI: 10.1002/0471264180.or072.02.

(70) For observations related to the importance of non-covalent interactions with arene rings in Ni-catalyzed reactions, see: (a) Saito, B.; Fu, G. C. Enantioselective Alkyl-Alkyl Suzuki Cross-Couplings of Unactivated Homobenzylic Halides. *J. Am. Chem. Soc.* **2008**, *130*, 6694-6695. (b)

Saper, N. I.; Ohgi, A.; Small, D. W.; Semba, K.; Nakao, Y.; Hartwig, J. F. Nickel-Catalysed anti-Markovnikov Hydroarylation of Unactivated Alkenes with Unactivated Arenes Facilitated by Non-Covalent Interactions. *Nature Chem.* **2020**, *12*, 276-283. (c) Zheng, Y.-L.; Xie, P.-P.; Daneshfar, O.; Houk, K. N.; Hong, X.; Newman, S. G. Direct Synthesis of Ketones from Methyl Esters by Nickel-Catalyzed Suzuki-Miyaura Coupling. *Angew. Chem. Int. Ed.* **2021**, 133, 13476-13483.

(71) Han, B.; Ren, C.; Jiang, M.; Wu, L. Titanium-catalyzed Exhaustive Reduction of Oxo-chemicals. *Angew. Chem. Int. Ed.,* **2022**, *61*, e202209232.

(72) Guo, X.; Zuo, Y.; Alvarez, G. A.; Mejía, E. Exhaustive Reduction of Esters, Carboxylic Acids and Carbamates to Methyl Groups Catalyzed by Boronic Acids. *European J. Org. Chem.* **2023**, *26*, e202300904.

(73) Wang, H.; Lu, L.; Xiong, B.; Ling, Y.; Zeng, X.; Qiu, X. Nickel-catalyzed Transfer Hydrogenation of Unactivated Aryl Alkenes with Hydrosilane as Hydrogen Source. *Asian J. Org. Chem.* **2023**, *12*, e202200590.

(74) Lin, Q.; Tong, W.; Shu, X.-Z.; Chen, Y. Ti-Catalyzed Dehydroxylation of Tertiary Alcohols. *Org. Lett.* **2022**, *24*, 8459–8464.

(75) Doi, R.; Yasuda, M.; Kajita, N.; Koh, K.; Ogoshi, S. Nickel-Catalyzed Exhaustive Hydrodefluorination of Perfluoroalkyl Arenes. *J. Am. Chem. Soc.* **2023**, *145*, 11449–11456.

(76) Wang, J.; Wang, T.; Du, H.; Chen, N.; Xu, J.; Yang, Z. Accessing *Para*-Alkylphenols via Iridium-Catalyzed Site-Specific Deoxygenation of Alcohols. *J. Org. Chem.* **2023**, *88*, 12572–12584.

(77) (a) Williams, O. P.; Chmiel, A. F.; Mikhael, M.; Bates, D. M.; Yeung, C. S.; Wickens, Z. K. Practical and General Alcohol Deoxygenation Protocol. *Angew. Chem. Int. Ed.,* **2023**, *62, e202300178.* (b) He, B.-Q.; Wu, X. Deuterium- and Electron-Shuttling Catalysis for Deoxygenative Deuteration of Alcohols. *Org. Lett.* **2023**, *25*, 6571–6576.

(78) (a) Sun, Z.; Ji, R.; Wu, J.; Zhao, J.; Fang, F.; Wang, F.; Jiang, C.; Liu, Z.-Q. Electrochemical Deoxygenative Hydrogenation and Deuteration of Aldehydes/Ketones by Protic Acids in Water. *Adv. Synth. Catal.* **2023**, *365*, 476–481. (b) Villo, P.; Lill, M.; Alsaman, Z.; Soto Kronberg, A.; Chu, V.; Ahumada, G.; Agarwala, H.; Ahlquist, M.; Lundberg, H. Electroreductive

Deoxygenative C−H and C−C Bond Formation from Non-derivatized Alcohols Fueled by Anodic Borohydride Oxidation. *ChemElectroChem* **2023**, *10*, e202300420.

(79) Han, S.; Gao, R.; Sun, M.-S.; Zhou, Y.; Chen, W.-T.; Liu, X.; Qin, J.; Tao, D.-J.; Zhang, Z. Synergistic Roles of Single Co Atoms and Co Nanoparticles for the Hydrodeoxygenation and Ring Hydrogenation Reactions. *J. Phys. Chem. C Nanomater. Interfaces* **2023**, *127*, 14185–14196.

(80) Wang, T.; Chen, Y.; Chen, N.; Xu, J.; Yang, Z. Iridium-Catalyzed Highly Stereoselective Deoxygenation of Tertiary Cycloalkanols: Stereoelectronic Insights and Synthetic Applications. *Org. Biomol. Chem.* **2021**, *19*, 9004–9011.

(81) Nishiyama, Y.; Xu, S.; Hanatani, Y.; Tsuda, S.; Umeda, R. Rhenium Complex-Catalyzed Deoxygenation and Silylation of Alcohols with Hydrosilane. *Tetrahedron Lett.* **2022**, *99*, 153839.

(82) (a) Lin, Q.; Tong, W.; Shu, X.-Z.; Chen, Y. Ti-Catalyzed Dehydroxylation of Tertiary Alcohols. *Org. Lett.* **2022**, *24*, 8459–8464. (b) Căciuleanu, A.; Vöhringer, F.; Fleischer, I. Titanium-Catalysed Deoxygenation of Benzylic Alcohols and Lignin Model Compounds. *Org. Chem. Front.* **2023**, *10*, 2927–2935.

(83) Yamada, M.; Shio, Y.; Akiyama, T.; Honma, T.; Ohki, Y.; Takahashi, N.; Murai, K.; Arisawa, M. Ligand-free Suzuki–Miyaura coupling reaction of an aryl chloride using a continuous irradiation type microwave and a palladium nanoparticle catalyst: effect of a co-existing solid. *Green. Chem.* **2019**, *21*, 4541–4549.

(84) Frost, J. R.; Cheong, C. B.; Donohoe, T. J. Iridium-Catalyzed C4-Alkylation of 2,6-Di-tert-butylphenol by Using Hydrogen-Borrowing Catalysis. *Synthesis* **2017**, *49*, 910–916.

(85) Bandari, R.; Hoeche, T.; Prager, A.; Dirnberger, K.; Buchmeiser, M. R. Ring-Opening Metathesis Polymerization Based Pore-Size-Selective Functionalization of Glycidyl Methacrylate Based Monolithic Media: Access to Size-Stable Nanoparticles for Ligand-Free Metal Catalysis. *Chem. - Eur. J.* **2010**, *16*, 4650-4658.

(86) Milstein, D.; Stille, J. K. Palladium-catalyzed coupling of tetraorganotin compounds with aryl and benzyl halides. Synthetic utility and mechanism. *J. Am. Chem. Soc.* **1979**, *101*, 4992–4998.

# **Chapter Three**. Deoxygenative Suzuki-Miyaura arylation of tertiary alcohols through silyl ether intermediates

*"All I can say is what I've always said: If you break your leg, stop thinking about dancing and start decorating the cast."*

- *Warren Zevon, 1947-2003.*



*Chapter three references begin on page 276; experimental details begin on page 272*

## 3.1. Chapter outlook

Chapter two focussed on the discussion of a nickel catalyzed method for deoxygenative *defunctionalization*, methods that replace a carbon-oxygen bond with a carbon-hydrogen bond. On the other side of the coin exists deoxygenative *functionalization* reactions, those that replace a carbon-oxygen bond with a carbon-carbon bond (or, a carbon-heteroatom bond). Chapter three will discuss the development of a deoxygenative Suzuki-Miyaura arylation.

As discussed in the introduction Sections 1.3 and 1.4, Suzuki-Miyaura couplings are amongst the most utilized reactions in the chemical industry. This is despite the frequently encountered limitation for use primarily upon $sp^2$-hybridized (pseudo)halides. This chapter demonstrates how Lewis acid/transition metal dual catalysis can be used as a technique to resolve this limitation. A bismuth-based Lewis acid is used in synergy with a nickel-based transition metal catalyst to enable the Suzuki-Miyaura arylation of a diverse range of unprotected tertiary alcohols (Figure 3.1).

**Figure 3.1.** Lewis acid/transition metal dual catalyzed deoxygenative Suzuki-Miyaura arylation of tertiary alcohols

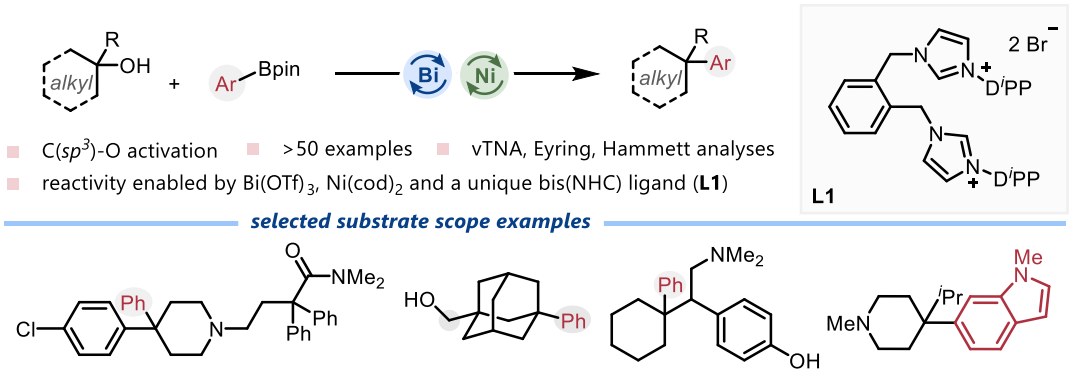




*Chapter three references begin on page 276; experimental details begin on page 272*

## 3.2. Reuse permissions and contributions

The data presented in this chapter is adapted with permission from the manuscript "Deoxygenative Suzuki-Miyaura Arylation of Tertiary Alcohols Through Silyl Ethers" by Adam Cook, Piers St. Onge and Stephen G. Newman, published in *Nature Synthesis*, **2023**, *2*, 663-669. Copyright 2023 Springer Nature. The dissertation author is the lead author of this manuscript. To supplement the original publication, additional relevant data has been incorporated into the text:

- Section 3.3 is reproduced directly from the literature. Minor modifications were made to the graphics to aid in the flow of this dissertation.
- Sections 3.4, 3.5 and 3.6 are reproduced directly from the literature, with select optimization details, control experiments, substrate scope examples and mechanistic details that were originally present in the supporting information incorporated into the text and expanded upon for clarity. Minor modifications were made to the graphics to aid in the flow of this dissertation.
- Sections 3.7 and 3.8 are original and are found exclusively within this thesis, although they feature some details that are found within the supporting information of the aforementioned article.

### Contributions

Unless otherwise indicated, all work presented within this chapter was conducted by the author of this dissertation. Piers St. Onge assisted in reproducing certain scope examples and in conducting the work presented in Schemes 3.19 and 3.20. Dr. Yan-Long Zheng is credited with synthesizing the first batch of **L1**, the ligand that would prove optimal in this transformation.

## 3.3. Introductory theory and background information

Cross-coupling reactions are among the most utilized reactions in the contemporary pharmaceutical industry, with Suzuki-Miyaura coupling standing out primarily due to the ease of handling, commercial availability, and mildness of organoboron reactants.[1, 2] With aryl halides and pseudohalides as the most common and reliable electrophilic coupling partners,[3, 4] there is demand for better methods to engage C($sp^3$)-hybridized electrophiles[5, 6] and for the use of surrogates for halides, such as C–O bonds.[7, 8]

In recent years, several strategies have emerged to enable alcohols to participate in cross-coupling chemistry. For example, unprotected alcohols bearing a nearby π-electron system such as phenols,[9, 10] benzyl alcohols[11-13] and allylic alcohols[14] have been shown to be sufficiently activated to undergo catalytic arylation. Towards reacting aliphatic alcohols, stoichiometric activation of the C($sp^3$)–O bond to provide a reactive intermediate that may either be isolated or formed in situ has emerged as a powerful strategy. For instance, oxalates[15], thiocarbamates[16], and NHC-alcohol adducts[17] have all been demonstrated to participate in deoxygenative arylation chemistry, [18-20] while electrochemical activation,[21] oxazolium salts,[22] or triphenylphosphonium anhydride[23] have been demonstrated to enable alcohol coupling by in situ halogenation and subsequent arylation (Figure 3.2a). Notably, radical-mediated dehydroxylative C–C bond forming reactions have also been recently disclosed.[24,25]



*Chapter three references begin on page 276; experimental details begin on page 272*

**Figure 3.2**. Contemporary strategies for cross-coupling of unprotected alcohols.

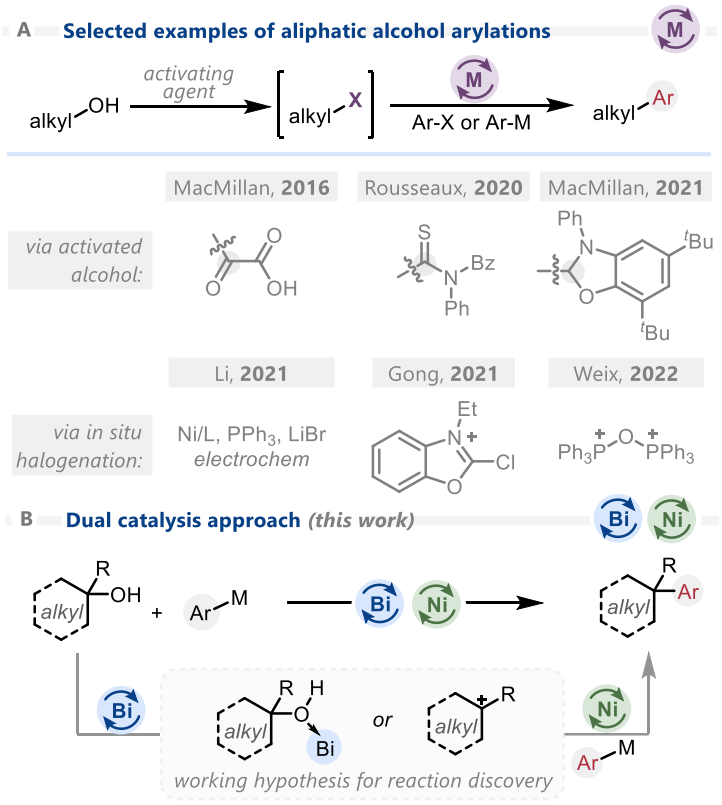


Lewis acid catalysis is another powerful strategy to facilitate activation and derivatization of alcohols via an $S_N1$-type pathways.[26-29] While this approach is primarily documented with traditional nucleophiles, it was speculated that a similar approach may enable direct alcohol arylation by trapping with a transition metal catalyst and organoboron reagent. Disclosed herein are efforts towards this goal, culminating in a general method for arylating cyclic tertiary alcohols to form quaternary carbon centers (Figure 3.2b).



*Chapter three references begin on page 276; experimental details begin on page 272*

## 3.4. Discovery, optimization and further investigations into the reaction conditions

### 3.4.1. Discovery and optimization synopsis

With the working hypothesis that a dual transition metal/Lewis acid dual catalyst system may enable direct alcohol arylation, a high-throughput screening campaign was carried out to investigate different metals, ligands, Lewis acids, and organometallic nucleophiles.[30] A hit was identified when using a combination of nickel(0), an atypical ligand bearing two NHC units (**L1**),[31] $Bi(OTf)_3$ as a mild Lewis acid,[32] and PhBpin, which enabled the functionalization of tertiary piperidinol **3.1** to provide arylated product **3.2** in 16% yield (Table 3.1, entry 1). While several reports detail the arylation of tertiary carbon atoms with cross-coupling chemistry,[33-36] the relative straightforwardness of this approach appeared promising to pursue. Among all tested Lewis acids, $Bi(OTf)_3$ consistently outperformed alternatives. Lewis acid-catalyzed activation of alcohols has often been facilitated by the addition of organosilane reagents.[37-40] In this reaction, introducing dimethyldichlorosilane ($Me_2SiCl_2$) – an inexpensive and abundant chlorosilane – led to an increased yield of 34% (entry 2). Pre-mixing the alcohol with the organosilane to first form the intermediate silyl ether led to a further increase in the yield to 73% (entry 3). The nature of the NHC ligand proved important, with more common ligands than **L1**, like IPr and ICy, being ineffective (entries 4, 5). Running the reaction in the absence of either the nickel or $Bi(OTf)_3$ provided no evidence of arylation, confirming the importance of the dual catalytic conditions.

**Table 3.1**. Reaction Optimization

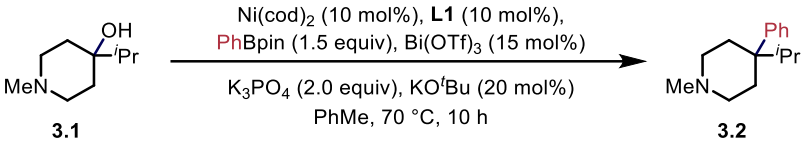


| entry | deviation from initial conditions | % yield, 3.2[a] |
|---|---|---|
| 1 | none | 16% |
| 2 | with 1 equiv $Me_2SiCl_2$ | 34% |
| 3 | with 1 equiv $Me_2SiCl_2$ *pre-mixed*[b] | 77% |
| 4 | as in entry 3, IPr•HCl *instead of NHC* | 6% |
| 5 | as in entry 3, ICy•$HBF_4$ *instead of NHC* | 9% |
| 6 | as in entry 3, no $Bi(OTf)_3$ or no $Ni(cod)_2$ | 0% |

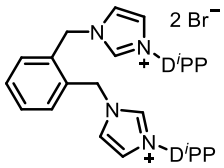

L1

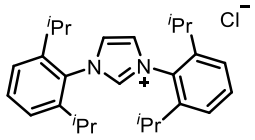

IPr•HCl

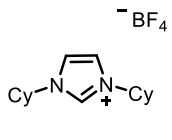

ICy•$HBF_4$

General reaction conditions: 0.20 mmol starting material, 0.02 mmol $Ni(cod)_2$, 0.02 mmol **L1**, 0.30 mmol PhBpin, 0.03 mmol $Bi(OTf)_3$, 0.20 mmol $Me_2SiCl_2$, 0.40 mmol $K_3PO_4$, 0.04 mmol KO$^t$Bu in 0.8 mL PhMe. [a]yields acquired by GC-FID using 1,3,5-trimethoxybenzene as internal standard. [b]starting material (0.20 mmol) stirred with $Me_2SiCl_2$ (0.20 mmol) and $K_3PO_4$ (0.40 mmol) in 0.4 mL PhMe at rt for 30 minutes before adding other reagents. [c]reactions performed with 20 mol% of ligand rather than 10 mol%.



*Chapter three references begin on page 276; experimental details begin on page 272*

### 3.4.2. Ligand investigation

Among the most interesting observations arising from the high-throughput discovery campaign was the observation that only a small subset of tested ligands (Figure 3.3) could permit reactivity. Specifically, only NHC-type ligands bearing multiple potential coordination sites afforded yields greater than 9%. Among these ligands, bis(NHC) **L1** afforded the highest yields (Table 3.2).

**Table 3.2**. Ligand Optimization

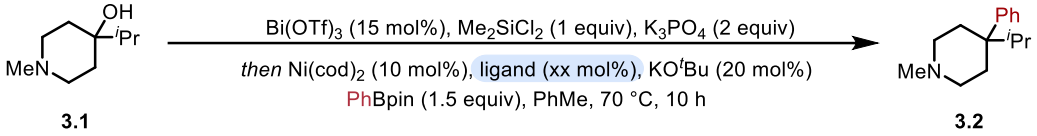


3.1 3.2

| entry | ligand | % yield, 3.2 |
|---|---|---|
| **1** | *no ligand* | 0 |
| **2** | IPr•HCl (20 mol%) | 6 |
| **3** | IPr•HCl (10 mol%) | 4 |
| **4** | IMes•HCl (20 mol%) | 3 |
| **5** | IMes•HCl (10 mol%) | 0 |
| **6** | SIPr•HCl (20 mol%) | 0 |
| **7** | ICy•$HBF_4$ (20 mol%) | 9 |
| **8** | ICy•$HBF_4$ (10 mol%) | 4 |
| **9** | **L1** (10 mol%) | 73 |
| **10** | **L1** (20 mol%) | 68 |
| **11** | **L2** (10 mol%) | 27 |
| **12** | **L3** (10 mol%) | 43 |
| **13** | **L4** (10 mol%) | 4 |
| **14** | $PCy_3$ (20 mol%) | 3 |



*Chapter three references begin on page 276; experimental details begin on page 272*

| | | |
|---|---|---|
| **15** | $PPh_3$ (20 mol%) | 0 |
| **16** | JohnPhos (20 mol%) | 0 |
| **17** | Xantphos (20 mol%) | 0 |
| **18** | dppf (20 mol%) | 0 |
| **19** | dcype (20 mol%) | 4 |
| **20** | dppent (20 mol%) | 0 |
| **21** | $P(^tBu)_3$ (20 mol%) | 0 |
| **22** | 1,10-phenanthroline (20 mol%) | 8 |
| **23** | bipyridine (20 mol%) | 6 |
| **24** | $(P^{Cy}N^{Ph})_2$ (20 mol%) | 0 |
| **25** | $(P^{Cy}N^{Bn})_2$ (20 mol%) | 0 |



*Chapter three references begin on page 276; experimental details begin on page 272*

**Figure 3.3.** Structures of ligands used in this optimization

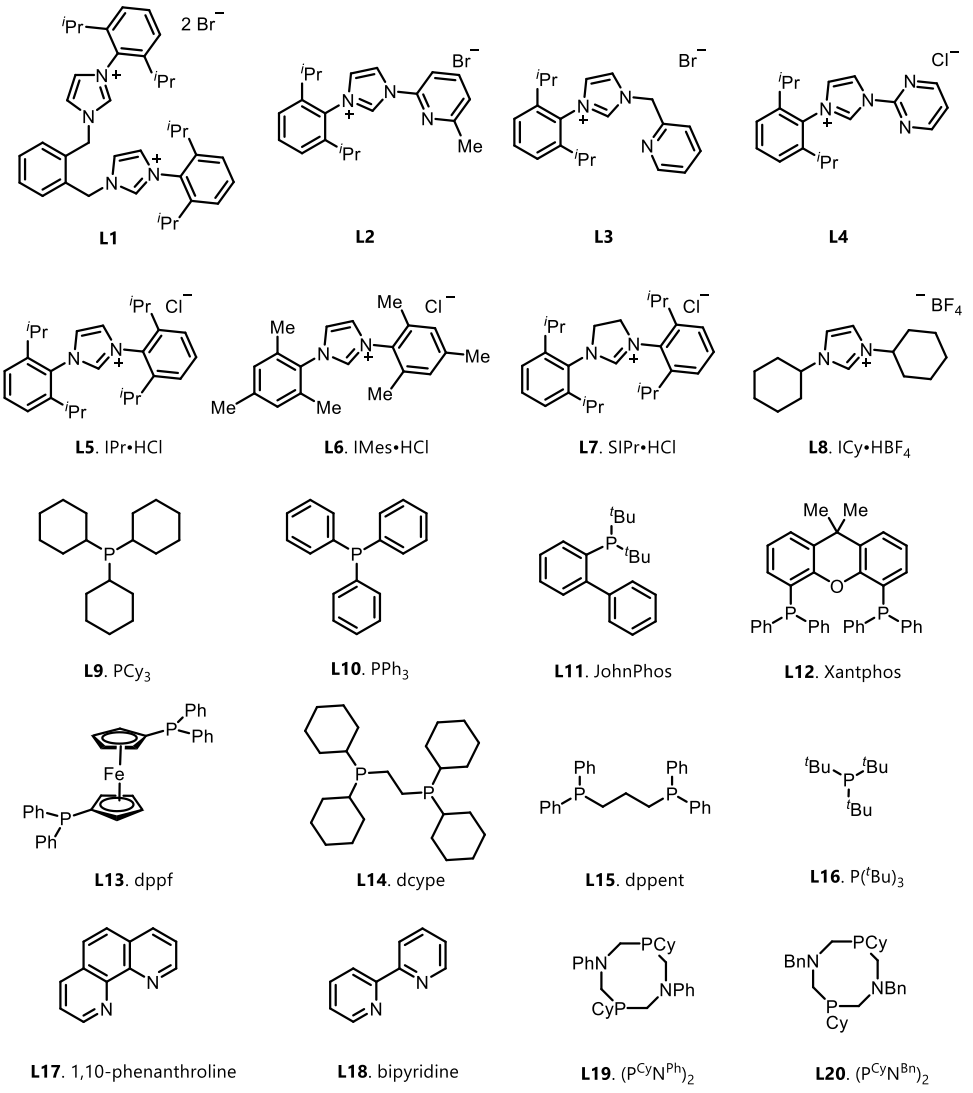


While there is an abundance of precedence concerning the use of bis(NHC) ligands in catalysis,[41] bis(NHC) **L1** has not seen limited use in catalysis.[42-44] To this author's knowledge, the first report of **L1** was in the early 2000s by Danopolous and colleagues, who characterized **L1** alongside a range of other bis(NHC) ligands.[31] The first batch of **L1** that was utilized in the high-throughput study was synthesized by Dr. Yan-Long Zheng, a former postdoctoral researcher in the Newman group, for evaluation in the optimization of a protocol for the amidation of methyl



*Chapter three references begin on page 276; experimental details begin on page 272*

esters.[45] It was synthesized through a five-step procedure from 2,6-diisopropylaniline (Scheme 3.1); subsequent batches have been synthesized by the author of this dissertation according to the same protocol.

**Scheme 3.1.** Synthesis of **L1**

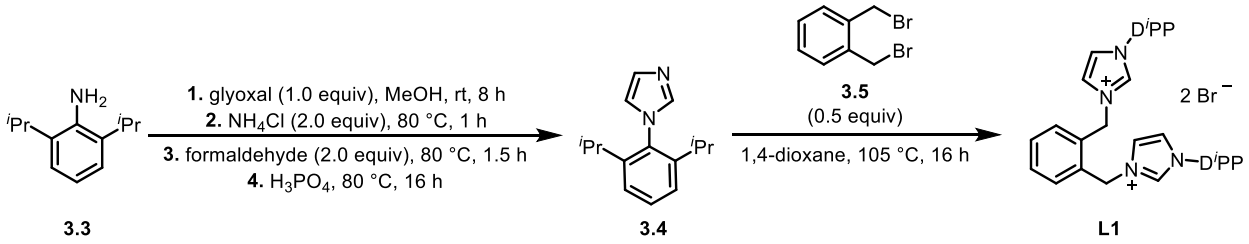


### 3.4.3. Investigations into the role of $Bi(OTf)_3$

Control experiments indicate that the inclusion of $Bi(OTf)_3$ was essential for product formation (Table 3.1, entry 6). Notably, $Bi(OTf)_3$ has been demonstrated to be capable of acting as either a Lewis acid or a Brønsted acid through the in situ formation of triflic acid.[32] Thus, further knowledge was sought as to the exact role of $Bi(OTf)_3$ in this arylation protocol. A series of control experiments were performed to investigate the role of $Bi(OTf)_3$ and other Lewis acid additives in this reaction, the results of which are summarized below (Table 3.3).



*Chapter three references begin on page 276; experimental details begin on page 272*

**Table 3.3**. Control experiments investigating the role of $Bi(OTf)_3$ in this arylation protocol

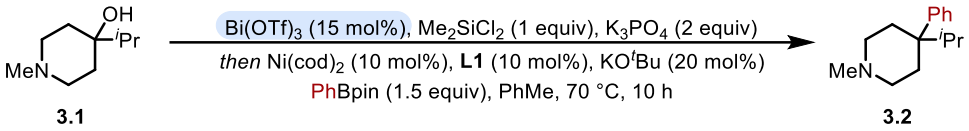


| entry | deviation from above conditions | % yield, 3.2 |
|---|---|---|
| **1** | *none* | 73 |
| **2** | + triflic acid (15 mol%) | 0 |
| **3** | + triflic acid (15 mol%), *no $Bi(OTf)_3$* | 0 |
| **4** | + DTBMP (1 equiv) | 75 |
| **5** | $BiCl_3$ *instead of $Bi(OTf)_3$* | 17 |
| **6** | $CrCl_3$ *instead of $Bi(OTf)_3$* | 31 |
| **7** | $I_2$ (15 mol%) *instead of $Bi(OTf)_3$* | 0 |
| **8** | $Fe(OTf)_3$ (15 mol%) *instead of $Bi(OTf)_3$* | 0 |
| **9** | $La(OTf)_3$ (15 mol%) *instead of $Bi(OTf)_3$* | 0 |
| **10** | $Gd(OTf)_3$ (15 mol%) *instead of $Bi(OTf)_3$* | 0 |
| **11** | $Sc(OTf)_3$ (15 mol%) *instead of $Bi(OTf)_3$* | 0 |
| **12** | $Dy(OTf)_3$ (15 mol%) *instead of $Bi(OTf)_3$* | 0 |
| **13** | $Yt(OTf)_3$ (15 mol%) *instead of $Bi(OTf)_3$* | 0 |
| **14** | $Sn(OTf)_3$ (15 mol%) *instead of $Bi(OTf)_3$* | 0 |
| **15** | $Sm(OTf)_3$ (15 mol%) *instead of $Bi(OTf)_3$* | 0 |
| **16** | $Er(OTf)_3$ (15 mol%) *instead of $Bi(OTf)_3$* | 0 |

No product was obtained upon the inclusion of triflic acid into the reaction mixture, both in the presence of $Bi(OTf)_3$ or upon excluding it, suggesting that $Bi(OTf)_3$ is not acting as a source of triflic acid under these reaction conditions (entries 2, 3). Further, employing 2,6-di-tertbutyl-4-



*Chapter three references begin on page 276; experimental details begin on page 272*

methylpyridine (DTBMP) as a stoichiometric additive to this reaction did not lead to an appreciable loss in yield, further suggesting that a Brønsted acid is not facilitating product formation (entry 4). Finally, product could be obtained – albeit in diminished yields – upon employing alternative Lewis acid catalysts such as $BiCl_3$ or $CrCl_3$ in place of $Bi(OTf)_3$ (entries 5, 6). Each of these observations suggest that $Bi(OTf)_3$ is acting as a Lewis acid in this arylation protocol. A range of alternative Lewis acids did not afford product (entries 6-16).

Next, the evolution of product **3.2** was monitored as a function of the amount of $Bi(OTf)_3$ added to the reaction. Product yield increased as the loading of $Bi(OTf)_3$ was increased, with an apparent plateau being reached as catalyst loading approached 15% (Scheme 3.2).

**Scheme 3.2.** Dependence of product yield on $Bi(OTf)_3$ catalyst loading

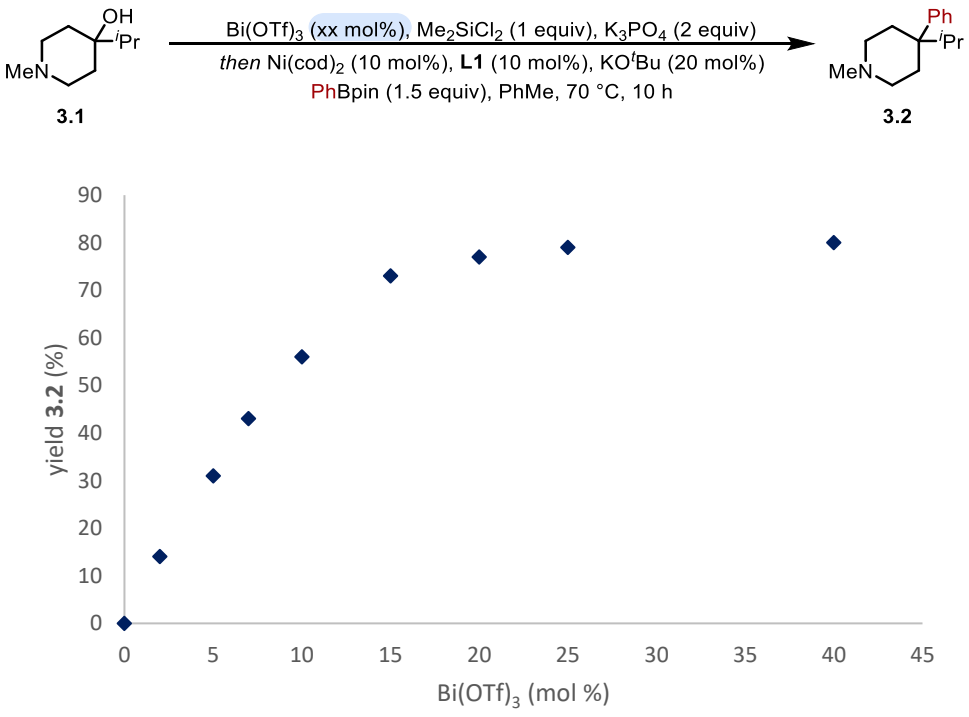




*Chapter three references begin on page 276; experimental details begin on page 272*

### 3.4.4. Investigations into the role of chlorosilane additive

Over the course of this study, it was discovered that the addition of a chlorosilane into the reaction mixture drastically increased reaction yield; while the inclusion of other silyl additives also led to product formation, chlorosilanes consistently performed the strongest (Table 3.4, entries 1-6). Further, a substantial increase in reaction yield occurred upon pre-stirring the alcohol starting material with a chlorosilane additive and base before dosing in the catalytic complex and nucleophilic coupling partner (entries 7-9).

**Table 3.4.** Varying silane additive and pre-stirring conditions

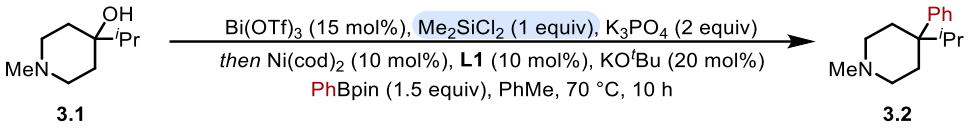


| entry | deviation from above conditions | % yield, 3.2 |
|---|---|---|
| **1** | *none* | 73 |
| **2** | $Me_3SiCl$ *instead of* $Me_2SiCl_2$ | 27 |
| **3** | $MeSiCl_3$ *instead of* $Me_2SiCl_2$ | 75 |
| **4** | $Ph_2SiCl_2$ *instead of* $Me_2SiCl_2$ | 79 |
| **5** | $^iPr_3SiH$ *instead of* $Me_2SiCl_2$ | 14 |
| **6** | TMDSO *instead of* $Me_2SiCl_2$ | 21 |
| **7** | no pre-mixing of alcohol/$Me_2SiCl_2$/$K_3PO_4$/$Bi(OTf)_3$ | 17 |
| **8** | stirring for 1 min *prior* to catalyst addition | 21 |
| **9** | stirring for 15 min *prior* to catalyst addition | 62 |

It was hypothesized that this observation may be due to the in situ formation of a silyl ether intermediate. Validating this hypothesis, stirring alcohol **3.1** with $Me_2SiCl_2$ (1 equiv), $Bi(OTf)_3$



*Chapter three references begin on page 276; experimental details begin on page 272*

and $K_3PO_4$ (2 equiv) in a solution of PhMe for 30 minutes at room temperature led to the formation of chlorosilylether **3.6**, which was isolated and characterized (Table 3.5, entry 1). $Bi(OTf)_3$ could be removed from this reaction mixture without notable loss in yield (entry 2), suggesting that it is not required in the silylation step. Conversely, the exclusion of base was found to be detrimental for the formation of chlorosilylether **3.6** (entry 3). Changing reaction time, temperature, or equivalents of $Me_2SiCl_2$ did not have a substantial effect on reaction outcome (entries 4-7).

**Table 3.5**. Investigating the reaction of free alcohol to form a chlorosilylether intermediate

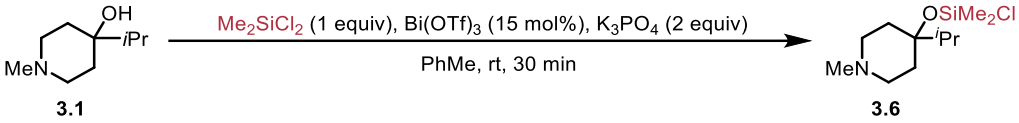


3.1 3.6

| entry | deviation from above conditions | % yield, 3.6 |
|---|---|---|
| **1** | *none* | 78 |
| **2** | no $Bi(OTf)_3$ | 76 |
| **3** | no $K_3PO_4$ | 11 |
| **4** | *time* = 15 min | 61 |
| **5** | *time* = 45 min | 76 |
| **6** | *temperature* = 40 °C | 86 |
| **7** | $Me_2SiCl_2$ (2.0 equiv) | 75 |

Further control experiments were performed on various ethereal analogs, including the isolated chlorosilylether intermediate **3.6** (Table 3.6). Various silyl ethers could be successfully arylated according to the general reaction conditions (entries 1-3), with chlorosilylether **3.6** affording the highest yield. Control experiments performed in the absence of $Bi(OTf)_3$ or $Ni(cod)_2$ failed to afford product, suggesting their synergistic importance in the arylation step of this



*Chapter three references begin on page 276; experimental details begin on page 272*

protocol (entries 4, 5). Methyl and benzyl ethers did not undergo arylation (entries 6, 7). Carrying out the reaction with the corresponding alkyl (pseudo)halides (entries 8-10) also gave no product, suggesting that in situ halogenation is an unlikely mechanistic pathway.

**Table 3.6**. Control experiments pertaining to the arylation step

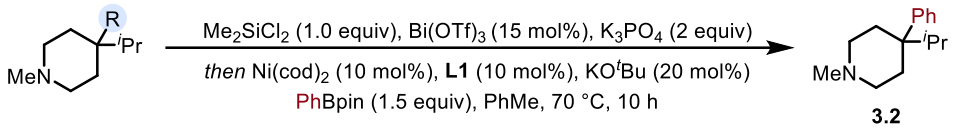


**3.2**

| entry | deviation from standard conditions | % yield, 3.2 |
|---|---|---|
| **1** | R = OTBS, *no $Me_2SiCl_2$* | 61 |
| **2** | R = OTMS, *no $Me_2SiCl_2$* | 42 |
| **3** | R = $OSiMe_2Cl$, *no $Me_2SiCl_2$* | 75 |
| **4** | R = $OSiMe_2Cl$, *no $Bi(OTf)_3$ or $Me_2SiCl_2$* | 0 |
| **5** | R = $OSiMe_2Cl$, *no Ni-**L1** or $Me_2SiCl_2$* | 0 |
| **6** | R = OMe | 0 |
| **7** | R = OBn | 0 |
| **8** | R = Br | 0 |
| **9** | R = Cl | 0 |
| **10** | R = OTf | 0 |

To further verify that silyl ethers are viable intermediates in this transformation, time-course data was obtained and compared for the arylation of unprotected alcohol **3.1** and the arylation of its corresponding TBS-protected alcohol **3.7** (Scheme 3.3). The product evolution vs. time plot for each of these reactions was found to be similar, showing significant visual overlay. This data suggests that silyl-protected alcohols behave in a manner similar to unprotected alcohols



*Chapter three references begin on page 276; experimental details begin on page 272*

upon exposure to the general reaction conditions, while also suggesting that the initial silylation step in the overall transformation of alcohol to arylated product is completed prior to the addition of Ni-**L1** catalyst.

**Scheme 3.3**. Comparing the rate of arylation for free alcohol **3.1** vs. TBS-protected alcohol **3.7**

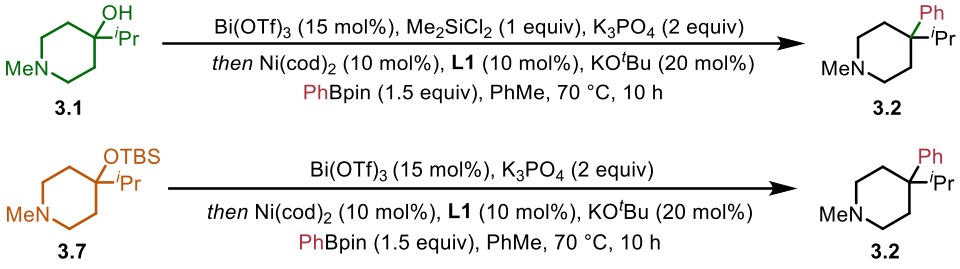


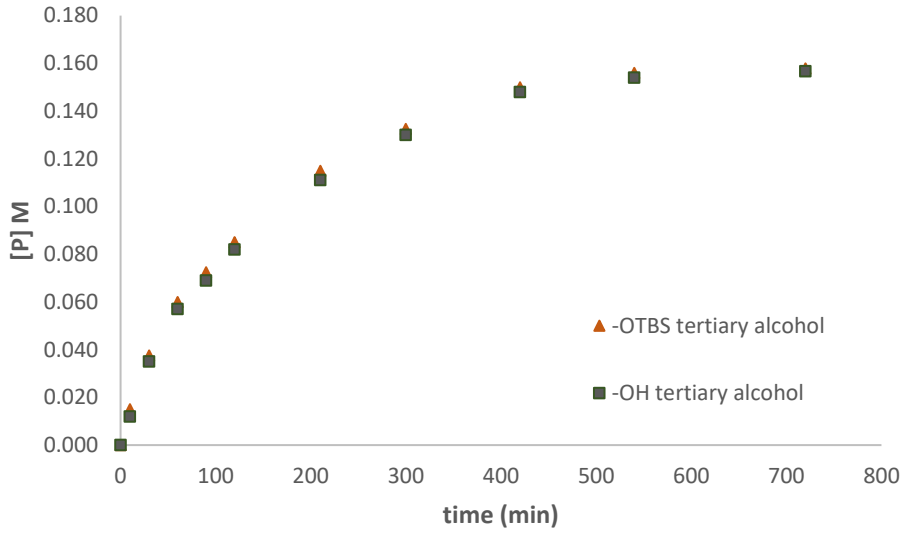




*Chapter three references begin on page 276; experimental details begin on page 272*

### 3.4.5. Control reactions with drop-in additives

To elucidate more information about the reaction mechanism, chlorosilylether **3.6** was exposed to the general reaction conditions alongside a series of drop-in additives (Table 3.7). The yield of the reaction was suppressed in the presence of dibenzocyclooctatetraene (dct), a known inhibitor of homogeneous catalysts (entry 2). Conversely, no depletion in yield was observed upon conducting the reaction in the presence of Hg, a known inhibitor of heterogeneous catalysis (entry 3). The reaction was also conducted in the presence of a series of different radical scavenging reagents (entries 4, 5, 6). No significant depletion in yield was observed in any of the three cases, suggesting that a radical intermediate is unlikely to be present in the reaction mechanism.

**Table 3.7**. Effect of drop-in additives on the arylation reaction

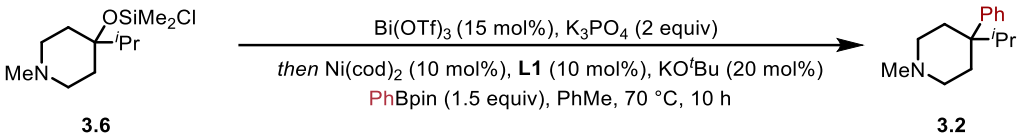


**3.6** **3.2**

| entry | deviation from above conditions | % yield, 3.2 |
|---|---|---|
| **1** | *none* | 73 |
| **2** | + dct (2 equiv) | 0 |
| **3** | + Hg (10 equiv) | 71 |
| **4** | + TEMPO (1 equiv) | 75 |
| **5** | + galvinoxyl (1 equiv) | 71 |
| **6** | + diphenylethylene (1 equiv) | 69 |



*Chapter three references begin on page 276; experimental details begin on page 272*

### 3.4.6. Observed byproducts

When subjecting piperidinol **3.1** to the standard reaction conditions, a significant amount of species **3.8** could be observed alongside arylated product **3.2**. To investigate whether species **3.8** was a reactive intermediate or a byproduct of this transformation, a series of control reactions were performed (Scheme 3.4). While **3.8** was observed in the absence of Ni-**L1**, it was not observed in the absence of $Bi(OTf)_3$, suggesting that the presence of a Lewis acid is essential to its formation. Subjecting **3.8** to the standard reaction conditions led to no evidence of cross-coupled product **3.2**, instead leading only towards the recovery of starting material. Collectively, these observations suggest that **3.8** is a byproduct of this transformation rather than a reactive intermediate.

**Scheme 3.4.** Investigating the observed byproduct

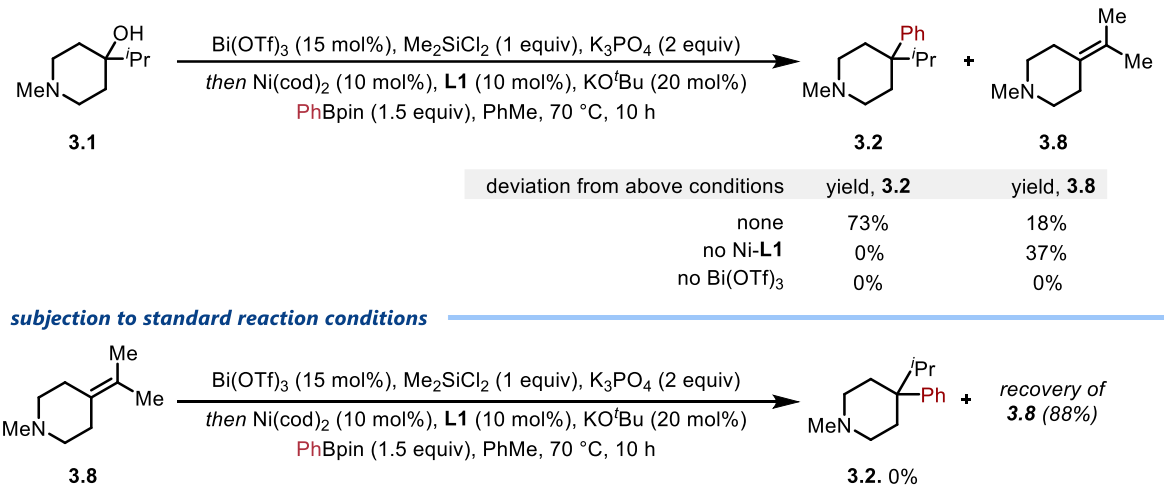




Chapter three references begin on page 276; experimental details begin on page 272

## 3.5. Substrate scope

### 3.5.1. Substrate scope overview

To explore the scope of this deoxygenative arylation, a range of *N*-methyl-piperidinyl scaffolds were first examined (Scheme 3.5). Variously sized substitutions adjacent to the alcohol were tolerated with larger groups generally providing higher yields (**3.9-12**). A vinyl group (**3.13**) and an allyl group (**3.14**) were also tolerated with no evidence of isomerization or rearrangement. Heterocyclic substituents including pyridine (**3.15**) and furan (**3.16**) were tolerated, albeit in low yields. No product was obtained upon placing an electron-withdrawing group adjacent to the reactive center (**3.17**) or upon subjecting a secondary alcohol (**3.18**) to this methodology.

An assortment of cyclic hydrocarbon rings ranging in size from 4-10 carbons were next arylated (**3.19-3.24**), as was 1-adamantanol (**3.25**), a tetrahydropyran (**3.26**) and a cyclohexenol (**3.27**). The arylation of various bioactive scaffolds was also evaluated, enabling the preparation of derivatives of desmethylvenlafaxine (**3.28**), loperamide (**3.29**) and cedrol (**3.30**). While tertiary cyclic alcohols were privileged substrates in this reaction,[46] primary (**3.31, 3.32**) and secondary (**3.33**) alcohols could also be arylated provided they were located adjacent to a π-system.

Functional group compatibility was further investigated by varying the structure of the boronate ester coupling partner (**3.34-3.50**). Notable examples demonstrate tolerance of unprotected O–H groups (**3.36**, **3.37**, **3.44**), halogens (**3.39**, **3.42**, **3.47**), and heterocycles (**3.43-3.50**). A gram-scale reaction was performed at reduced catalyst loading to reveal indole **3.45** in yields reflective of the optimized conditions. Lastly, the chemoselective coupling of diols was investigated. Using 3 equivalents of chlorosilane, cyclic tertiary alcohols bearing a primary (**3.51**), secondary (**3.53**), or tertiary acyclic (**3.55**) alcohol provided good yields of the monoarylated products (**3.42**, **3.54**, **3.56**) after work-up with TBAF.



*Chapter three references begin on page 276; experimental details begin on page 272*

**Scheme 3.5**. Reaction scope of arylation reaction

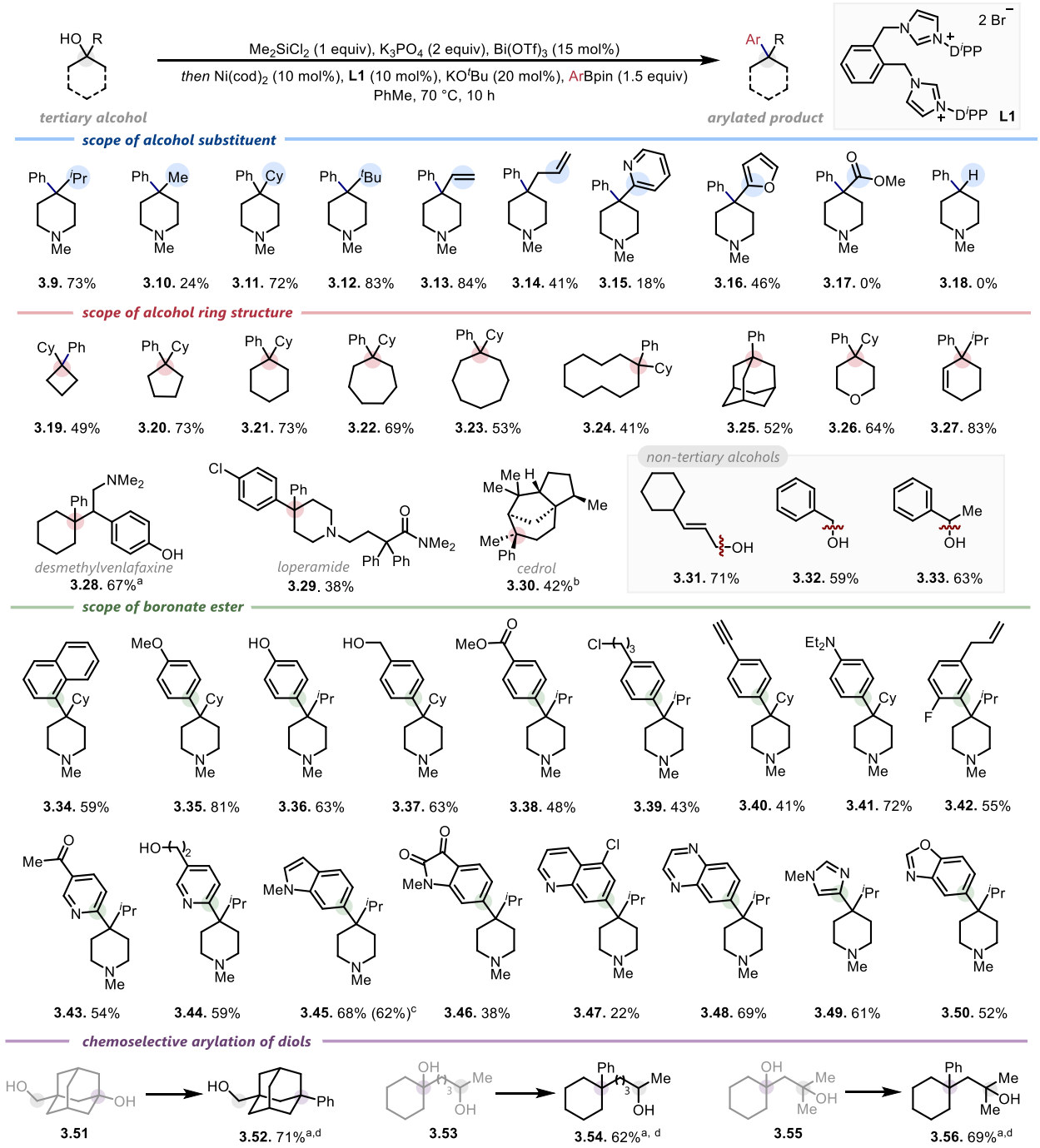


General reaction conditions: 0.20 mmol starting material, 0.02 mmol $Ni(cod)_2$, 0.02 mmol **L1**, 0.30 mmol PhBpin, 0.03 mmol $Bi(OTf)_3$, 0.20 mmol $Me_2SiCl_2$, 0.40 mmol $K_3PO_4$, 0.04 mmol $KO^tBu$ in 0.8 mL PhMe. [a]0.60 mmol $K_3PO_4$. [b]*d.r.* 2.6:1. [c]Yield obtained upon reacting 1.0 g (6.37

mmol) of substrate; 0.64 mmol $Ni(cod)_2$, 0.64 mmol **L1**, 1.28 mmol $KO^tBu$. [d]0.60 mmol $Me_2SiCl_2$; 0.40 mmol TBAF added upon reaction completion.

### **3.5.2.** Unsuccessful scope examples

Multiple compounds proved unreactive upon subjection to the standard reaction conditions. The most significant limitation of this arylation procedure is the restriction to use on tertiary cyclic alcohols and π-activated alcohols. Primary, secondary, and tertiary acyclic alcohols showed little or no reactivity in the absence of a nearby π-electron system (**3.57**-**3.66**) (Figure 3.4a). The reaction also failed to afford the arylation product when tertiary cyclic alcohols were substituted with esters (**3.67**, **3.68**), ketones (**3.69**) or amides (**3.70**) (Figure 3.4b). Further, ethers were not suitable substrates under these reaction conditions (**3.71**-**3.73**) (Figure 3.4c). Finally, various functionalized (**3.74**-**3.85**) and heterocyclic (**3.86**-**3.91**) boronate esters failed to produce the desired product upon subjection to the standard reaction conditions with 1-methyl-4-isopropylpiperid-4-ol (**3.1**) (Figure 3.4d).



*Chapter three references begin on page 276; experimental details begin on page 272*

**Figure 3.4**. Unsuccessful alcohol and boronate ester coupling partners

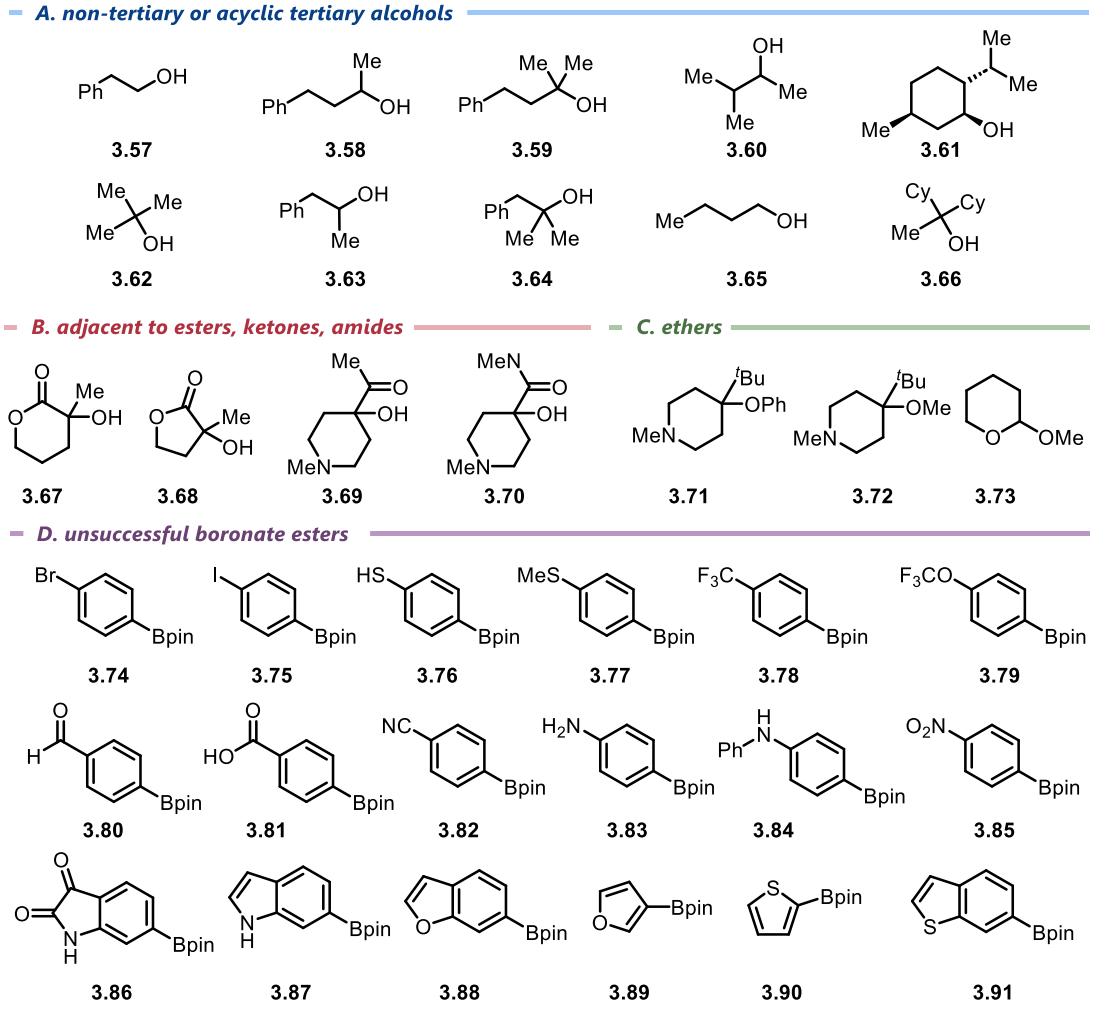




*Chapter three references begin on page 276; experimental details begin on page 272*

## 3.6. Mechanistic investigations

Armed with an adequate knowledge of the reaction scope and functional group tolerance, attention was turned towards gaining mechanistic insight. The silane additive was confirmed to silylate the alcohol under the reaction conditions and various silyl ethers (where R = $SiMe_3$, $SiMe_2{}^tBu$, $SiMe_2Cl$) were shown to undergo arylation without the need for additional chlorosilane, confirming that the silyl ether is a viable reactive intermediate (see Table 3.6, entries 1-5). In situ chlorination of alcohols in the presence of bismuth(III) reagents and chlorosilanes is a known transformation (Scheme 3.7);[47] however, subjection of the corresponding alkyl chlorides to the standard reaction conditions did not lead to the formation of product (see Table 3.6, entry 9), suggesting that the in situ halogenation mechanism is not operative.[21-23]

**Scheme 3.7.** Bismuth-catalyzed chlorination of alcohols

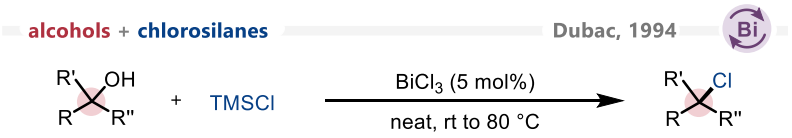


### 3.6.1. Investigating olefin and radical intermediates

During the reaction discovery and screening efforts, a mechanism in which a reactive carbocation intermediate was generated and intercepted was envisioned. An alternative plausible pathway involves dehydration to the olefin and subsequent metal-catalyzed hydroarylation.[48, 49] Indeed, olefins such as compound **3.8** were commonly observed in the crude reaction mixture. However, subjecting **3.8** directly to the standard reaction conditions did not afford arylated product, suggesting it is a side-product rather than a reactive intermediate (Scheme 3.8a). Another alternative plausible pathway may involve formation of a carbon-centered radical, as is commonly proposed in the coupling of alkyl halides.[50, 51] However, this arylation of compound **3.1** to form



*Chapter three references begin on page 276; experimental details begin on page 272*

was found to be unaffected by the presence of TEMPO or other radical scavenging reagents; further, cyclopropane (**3.92**)[52] and 5-hexenyl (**3.95**)[53] bearing substrates were arylated to form products **3.93** and **3.96** without evidence of rearrangement products **3.94** and **3.97**, which would be expected if a carbon-centered radical was formed (Scheme 3.8b).

**Scheme 3.8.** Summarizing evidence against olefin and radical intermediates

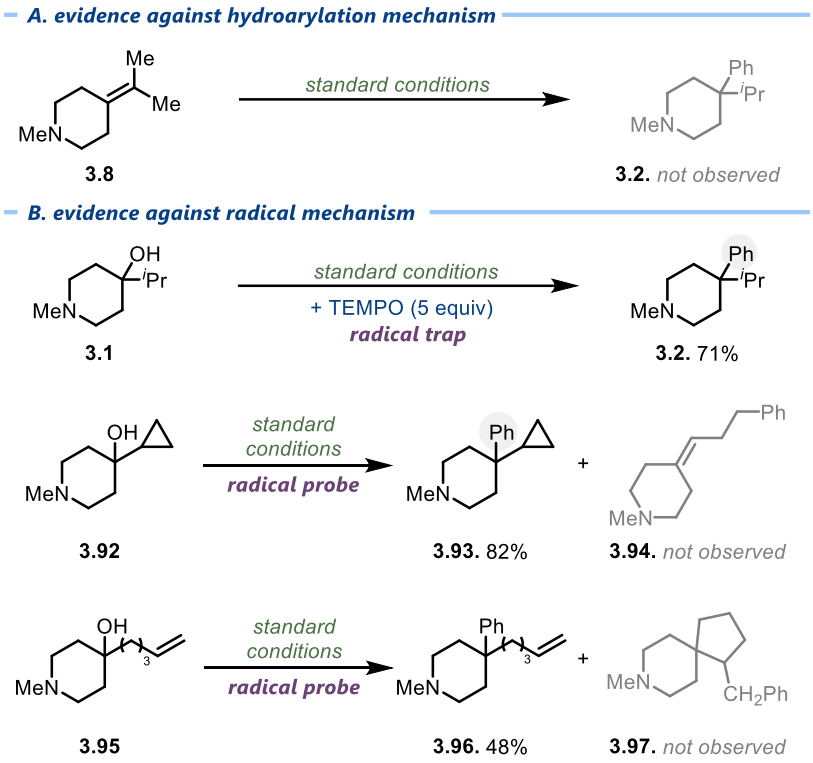


## 3.6.2. Hammett analysis

Towards exploring the plausibility of a carbocation intermediate, a Hammett study was carried out on a series of silylated alcohols with varying electronic properties (Scheme 3.9).[54] As the -OSiMe$_2$Cl ethers that formed in situ were found to be of modest stability, these kinetic studies were performed on -OTBS ethers to ensure that substrate decomposition would not interfere with the kinetic analysis (for a comparison of -OTBS ether reactivity to -OH reactivity, refer to Scheme



Chapter three references begin on page 276; experimental details begin on page 272

3.5). Silyl ethers **3.98a-e** were found to be smoothly arylated under the reaction conditions to afford piperidines **3.99a-e** with the lowest yields resulting from the more electron-deficient alcohols. The same trend was observed when studying the reaction kinetics; more electron-deficient alcohols led to slower rates of reaction. A linear relationship was observed upon plotting the normalized rate constants against the $\sigma_p^+$ parameter, with a $\rho$ value of -1.18 suggesting a substantial buildup of positive charge in the transition state in this particular benzylic example.[55]

**Scheme 3.9.** Investigating the effects of *p*-substitution on reactivity

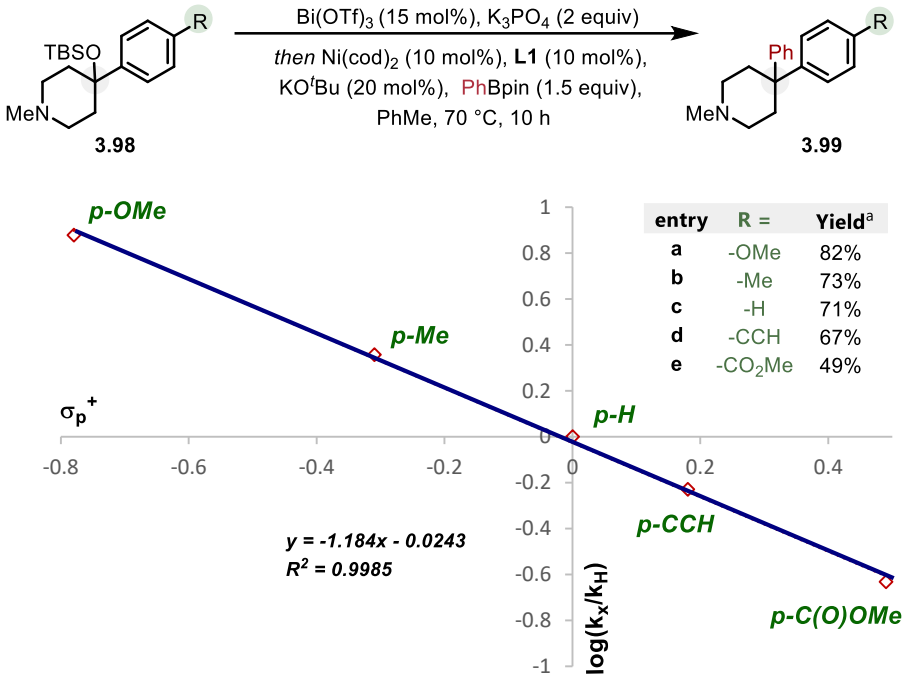


### 3.6.3. Carbocation rearrangements

Carbocations are prone to undergo 1,2-alkyl shift reactions to generate more stable carbocations. Preparing alcohol **3.100** and subjecting it to the standard conditions led to the formation of rearranged product **3.101** (Scheme 3.10). This observed 1,2-alkyl shift provides evidence supporting a carbocation or carbocation-like intermediate.



*Chapter three references begin on page 276; experimental details begin on page 272*

**Scheme 3.10.** Evidence supporting a 1,2-alkyl shift

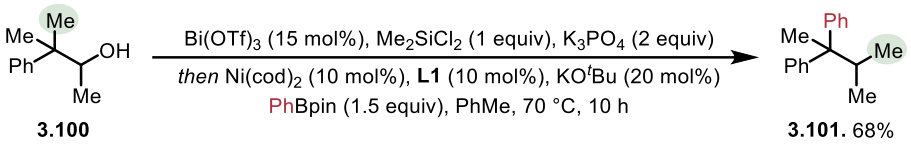


Carbocations are similarly prone to undergo 1,2-hydride shift. Subjecting substrate **3.102$_H$** to the standard reaction conditions led to the formation of rearranged product **3.103$_H$** (Scheme 3.11). Subjecting the corresponding deuterated analog **3.102$_D$** to the standard reaction conditions afforded the product of a 1,2-deuteride shift (**3.103$_D$**), albeit in lower yield, suggesting a more sluggish migration of deuterium. Placing the target C($sp^3$)–O bond one carbon further from the dibenzyl system, as in compound **3.104**, did not lead to any product formation upon subjection to the standard reaction conditions.

**Scheme 3.11.** Evidence supporting a 1,2-hydride shift

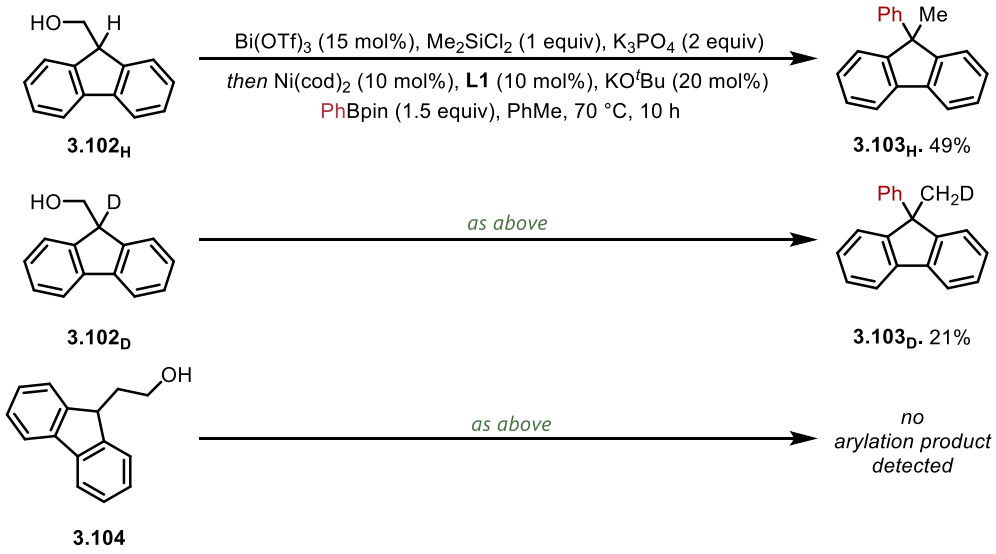




*Chapter three references begin on page 276; experimental details begin on page 272*

### 3.6.4. Stereochemical erosion

To test whether the reaction occurs with retention, inversion, or loss of stereochemical information, a Grignard addition between 4-phenylcyclohexanone and isopropyl magnesium bromide was conducted, leading to the recovery of a 1:1 mixture of diastereomers **3.105a** and **3.105b**. Arylation of this mixture according to the standard reaction conditions afforded a 1:1 mixture of the corresponding diastereomeric products **3.106a** and **3.106b** (Scheme 3.12a). A diastereomerically pure sample of **3.105a** was then isolated and subjected to the standard reaction conditions, also affording a 1:1 mixture of diastereomeric products **3.106a** and **3.106b**. This apparent loss of stereochemical information suggests that the transformation proceeds via a reactive intermediate that has lost its stereochemical identity, such as a carbocation. To probe this observation further, a Friedel-Crafts arylation (which, presumably proceeds via a carbocation intermediate) was performed on substrate **3.105a**, also leading to the recovery of a 1:1 mixture of diastereomeric products **3.106a** and **3.106b** (Scheme 3.12b).[56]

**Scheme 3.12.** Erosion of stereochemical information in alcohol **3.105** occurs in both the standard reaction conditions and with Friedel–Crafts conditions.

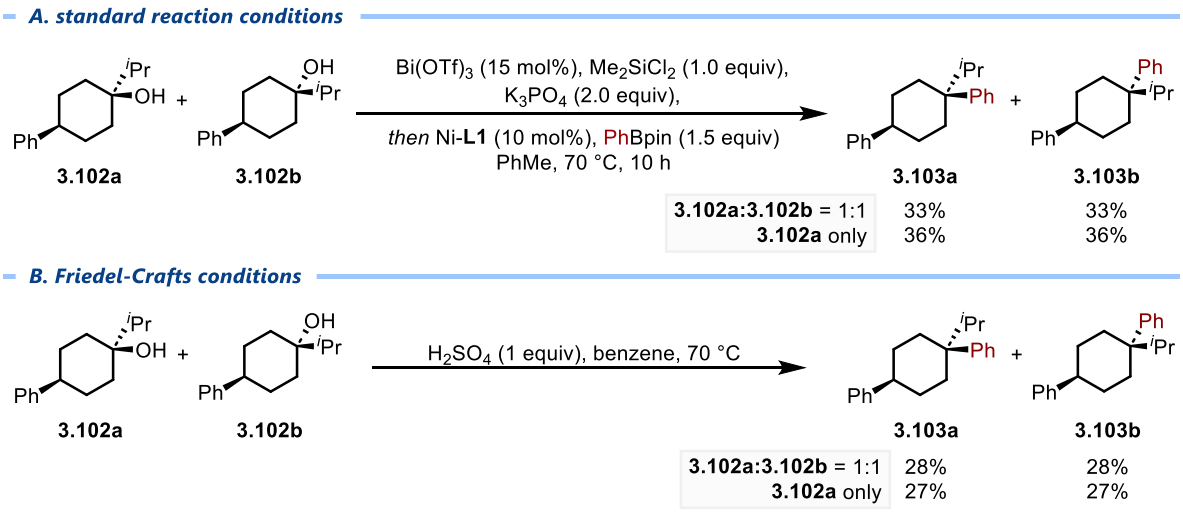




Chapter three references begin on page 276; experimental details begin on page 272

### 3.6.5. Variable time normalization analysis

A kinetic analysis was performed on alcohols **3.98b** and **3.106** according to the variable time–normalization analysis method (Scheme 3.13).[57] In each case, the corresponding -OTBS protected silyl ether was utilized as a substrate so as to ensure that the monitored kinetics reflected that of the arylation step rather than the initial silylation.

**Scheme 3.13.** Arylation of a benzylic (**3.98b**) and non-benzylic (**3.106**) silyl ether

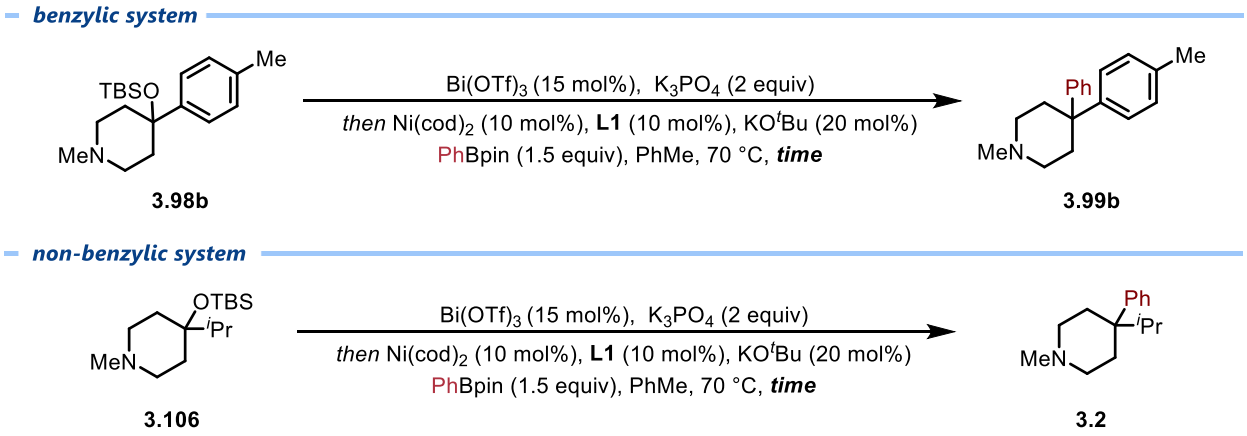


For tertiary aliphatic alcohol **3.106**, results suggest positive, apparent first order involvement of the substrate, Ni-**L1** catalyst and $Bi(OTf)_3$ at the transition state of this reaction and zeroth order dependence on PhBpin (Figures 3.5-3.8). In contrast, tertiary benzylic silyl ether **3.98b** exhibited first-order dependence on *only* the substrate and $Bi(OTf)_3$ and zeroth order dependence on Ni-**L1** catalyst and PhBpin (Figure 3.9-3.112). While all data thus far was supportive of the presence of an $S_N1$-type pathway, it was surprising to observe the suggested rate dependence of nickel in the arylation of **3.106**. Tentatively, this is proposed to be due to nickel assisting in the generation of a carbocation or carbocation-like intermediate in this specific case.



*Chapter three references begin on page 276; experimental details begin on page 272*

Additionally, the lack of dependence on the concentration of Ni-**L1** catalyst for substrate **3.97b**, suggests this substrate may be arylated directly via a carbocation. However, control experiments performed to investigate this possibility demonstrated no product formation, instead leading to starting material recovery and the observation of significant amounts of olefin byproduct (**3.107**) (Scheme 3.14). Thus, although the arylation of substrate **3.98b** may show a zeroth order dependence on Ni-**L1**, it is still required in order to afford product.

**Scheme 3.14.** No arylation in the absence of nickel catalyst

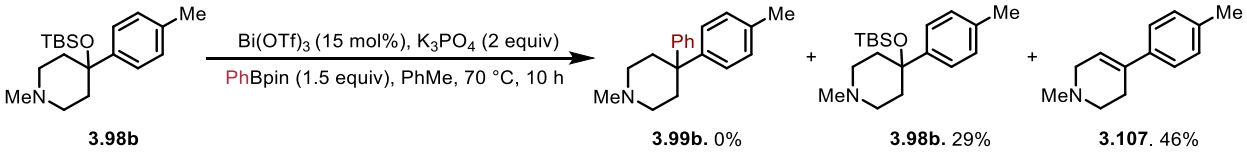


**3.98b** **3.99b.** 0% **3.98b.** 29% **3.107**. 46%



*Chapter three references begin on page 276; experimental details begin on page 272*

**Figure 3.5**. Variation in [Ni-**L1**] catalyst for the arylation of substrate **3.106**: Variable time normalization plots illustrate positive order dependency.

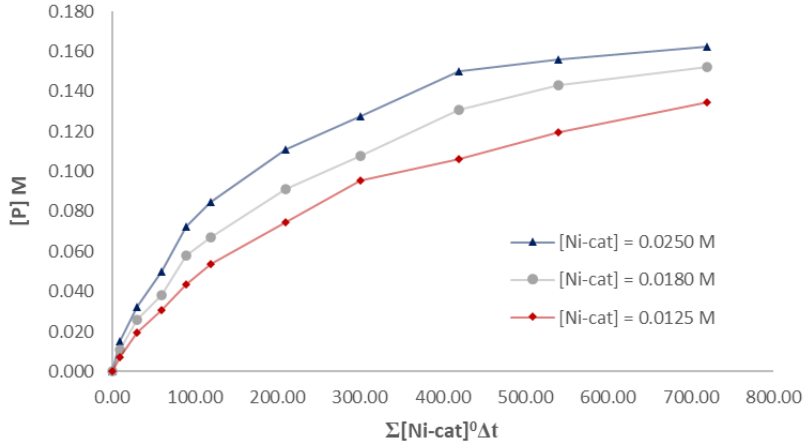


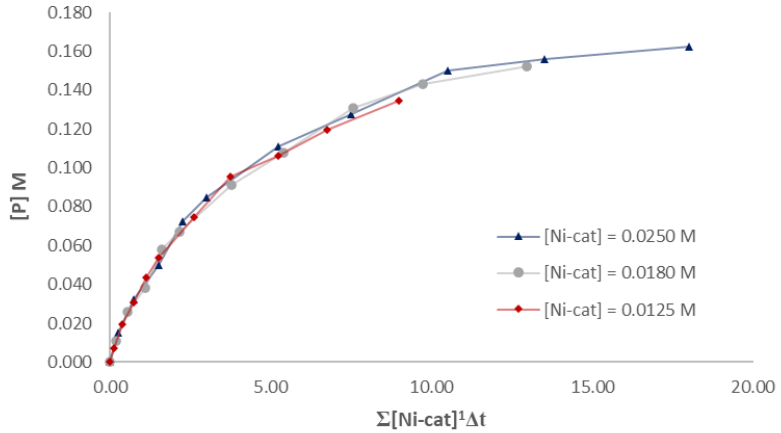


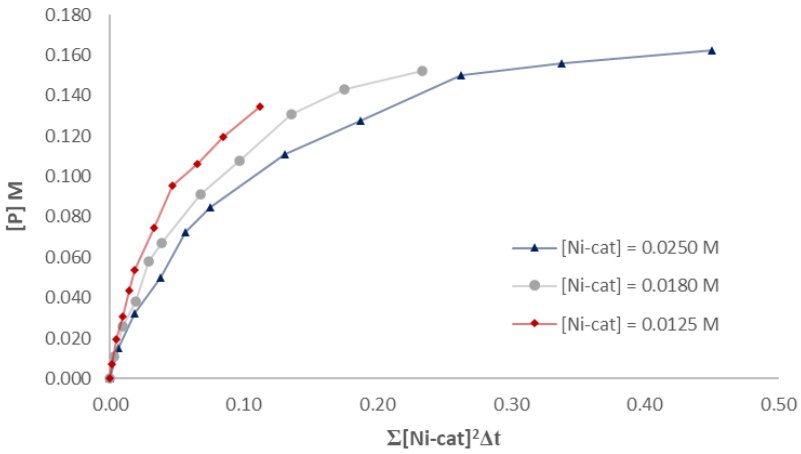




*Chapter three references begin on page 276; experimental details begin on page 272*

**Figure 3.6.** Variation in [PhBpin] for the arylation of substrate **3.106**: Variable time normalization plots illustrate positive order dependency.

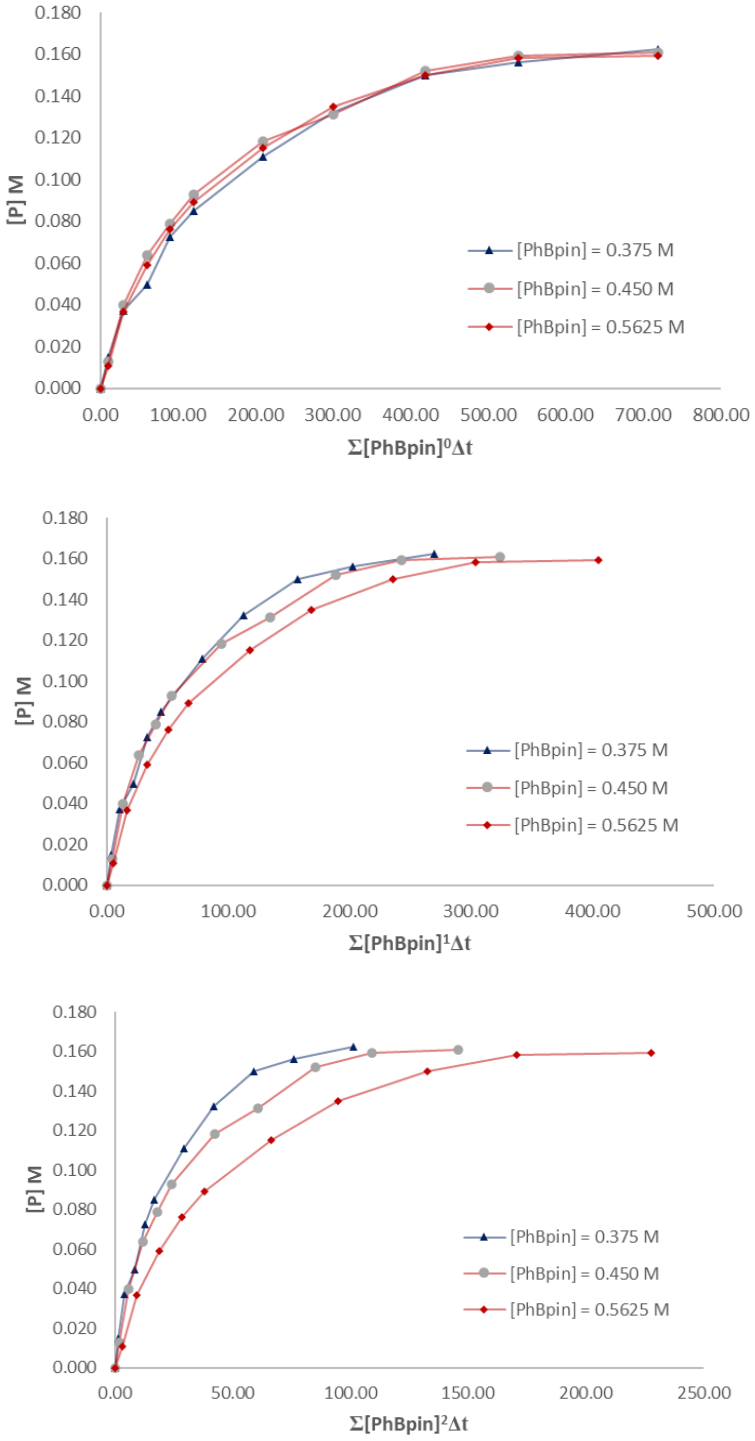




*Chapter three references begin on page 276; experimental details begin on page 272*

**Figure 3.7**. Variation in [substrate] for the arylation of substrate **3.106**: Variable time normalization plots illustrate positive order dependency.

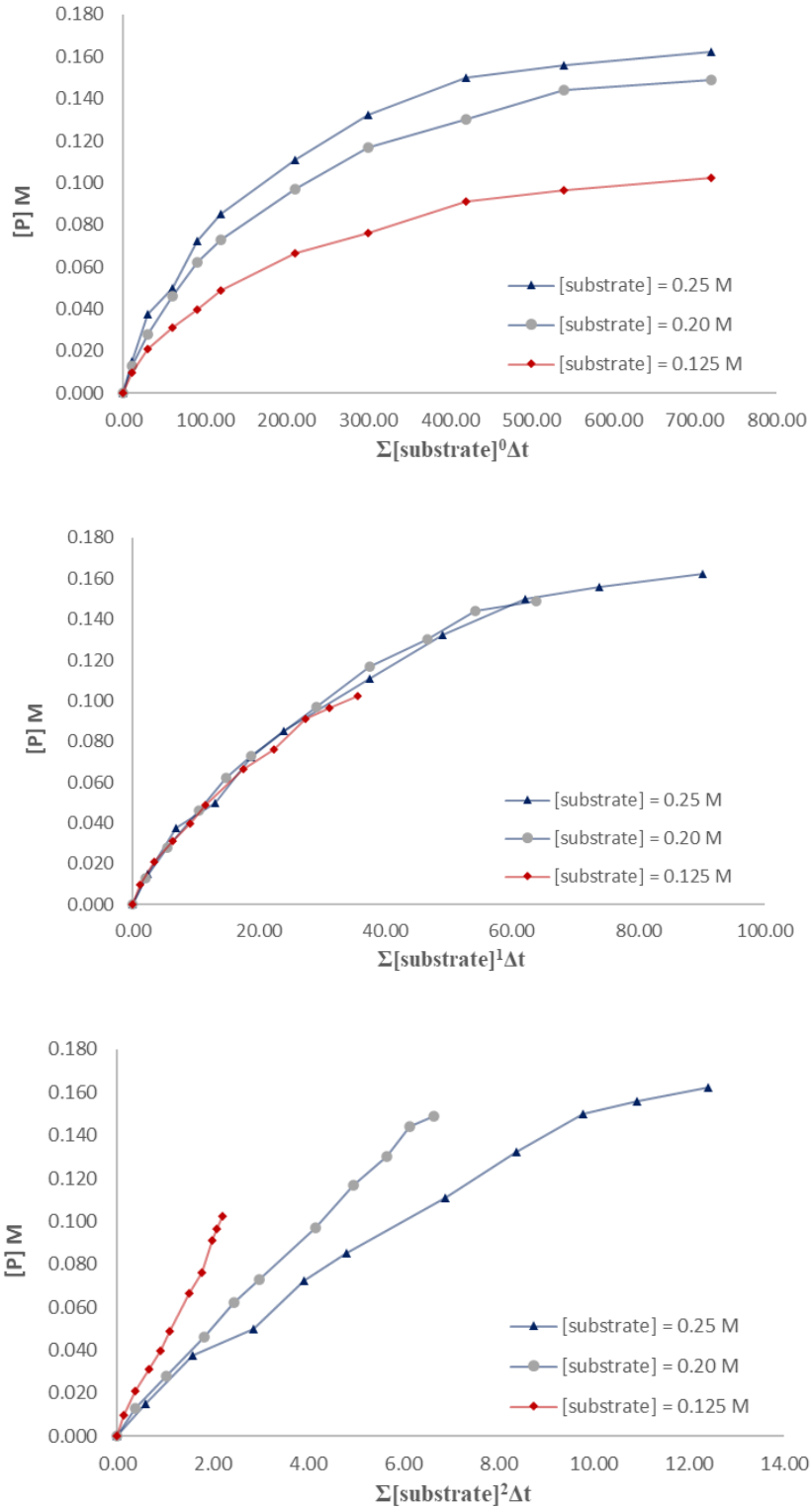




*Chapter three references begin on page 276; experimental details begin on page 272*

**Figure 3.8**. Variation in [Bi(OTf)$_3$] for the arylation of substrate **3.106**: Variable time normalization plots illustrate positive order dependency.

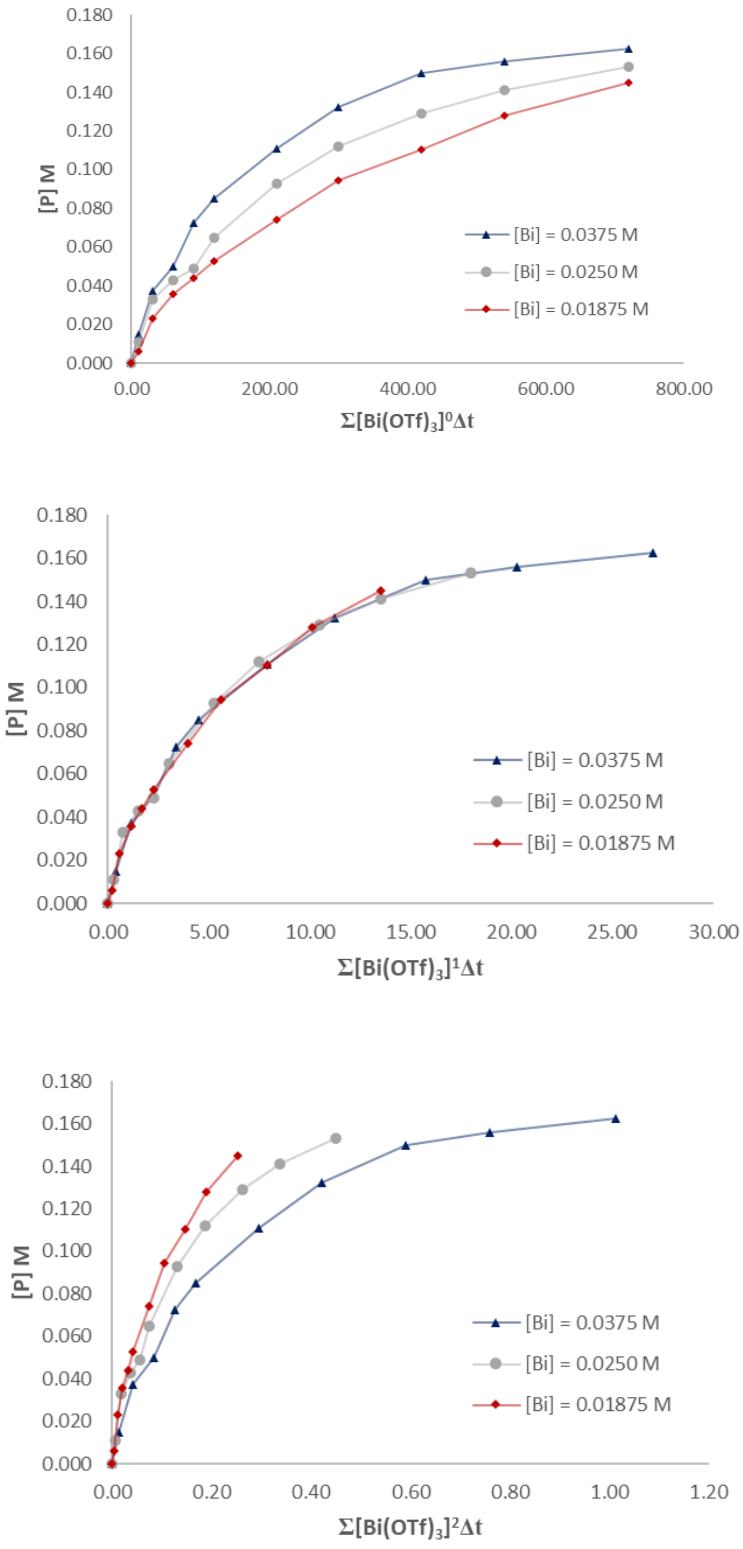




*Chapter three references begin on page 276; experimental details begin on page 272*

**Figure 3.9**. Variation in [Ni-**L1**] for the arylation of substrate **3.98b**: Variable time normalization plots illustrate positive order dependency.

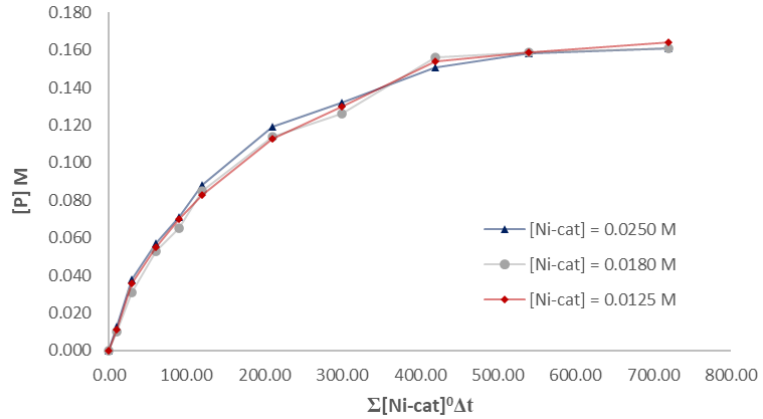


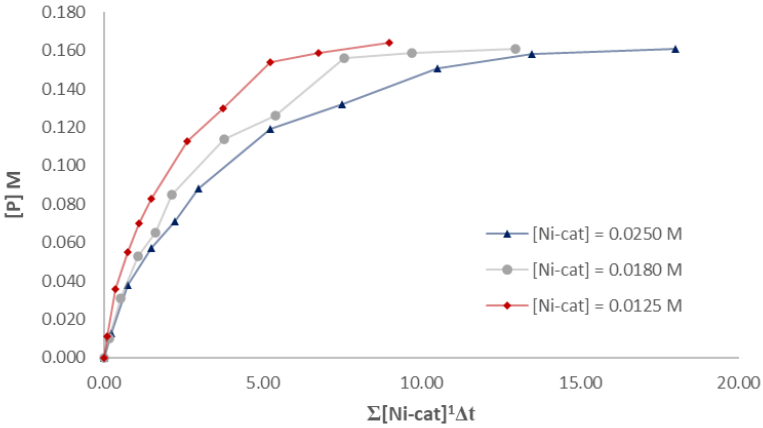


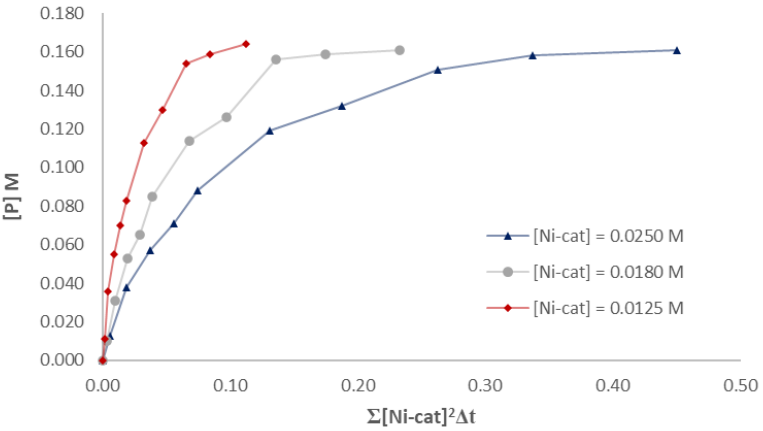




*Chapter three references begin on page 276; experimental details begin on page 272*

**Figure 3.10**. Variation in [PhBpin] for the arylation of substrate **3.98b**: Variable time normalization plots illustrate positive order dependency.

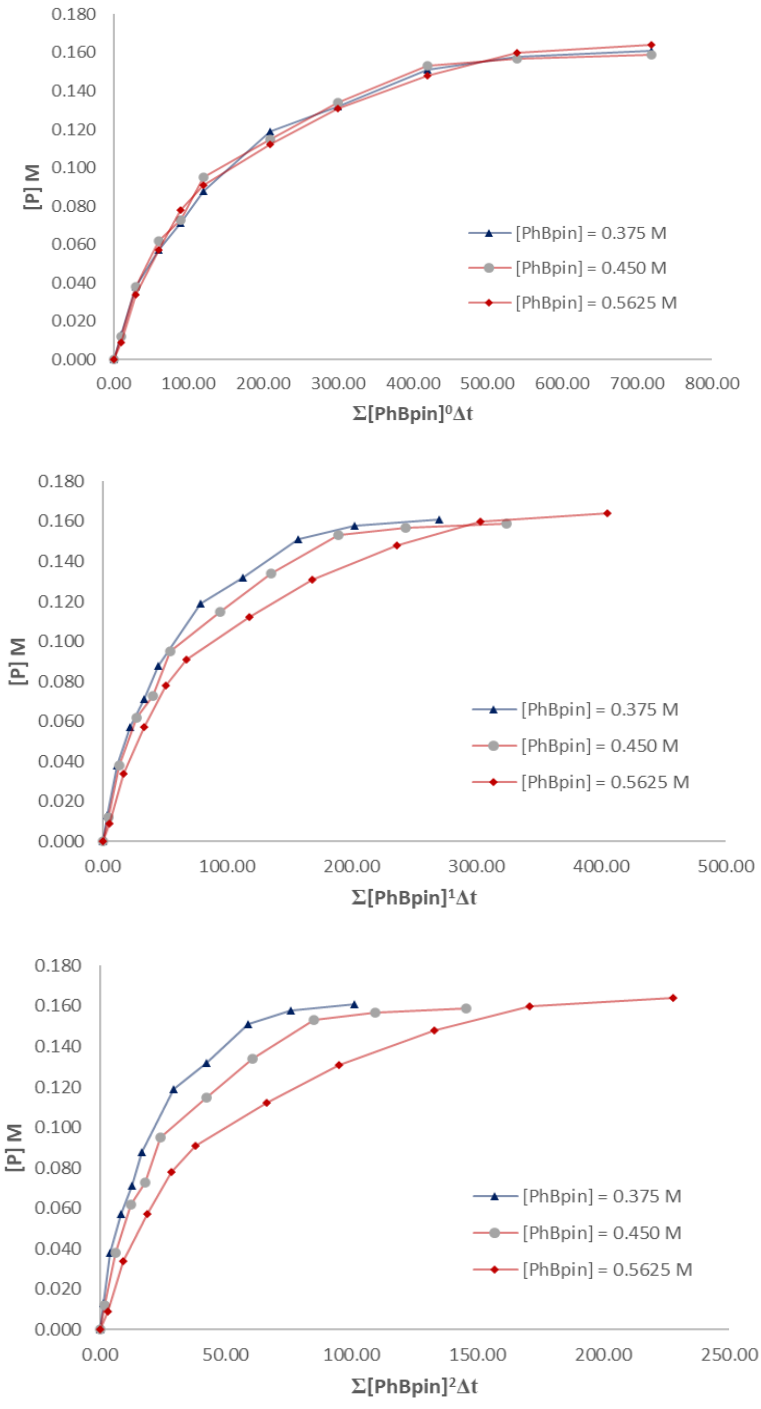




*Chapter three references begin on page 276; experimental details begin on page 272*

**Figure 3.11**. Variation in [substrate] for the arylation of substrate **3.98b**: Variable time normalization plots illustrate positive order dependency.

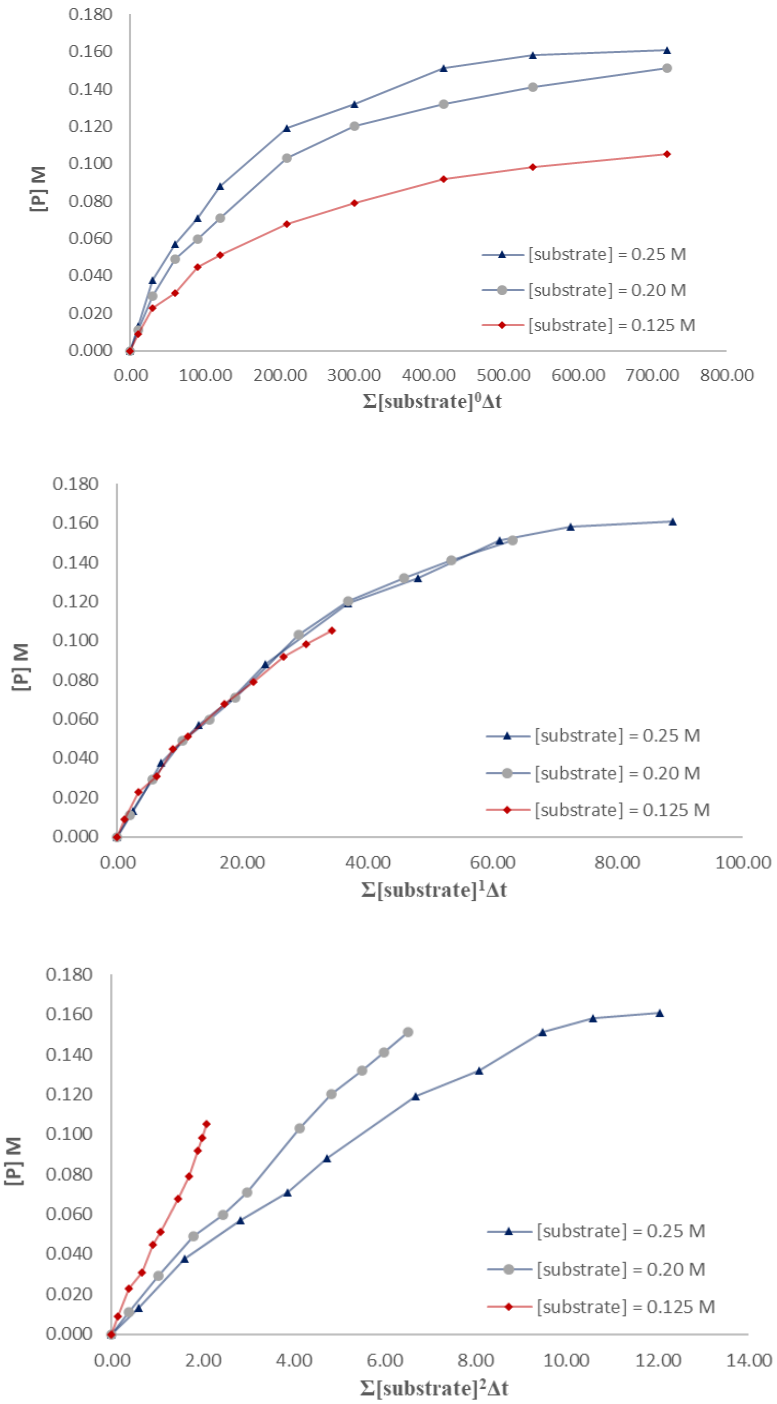




*Chapter three references begin on page 276; experimental details begin on page 272*

**Figure 3.12**. Variation in [Bi(OTf)$_3$] for the arylation of substrate **3.98b**: Variable time normalization plots illustrate positive order dependency.

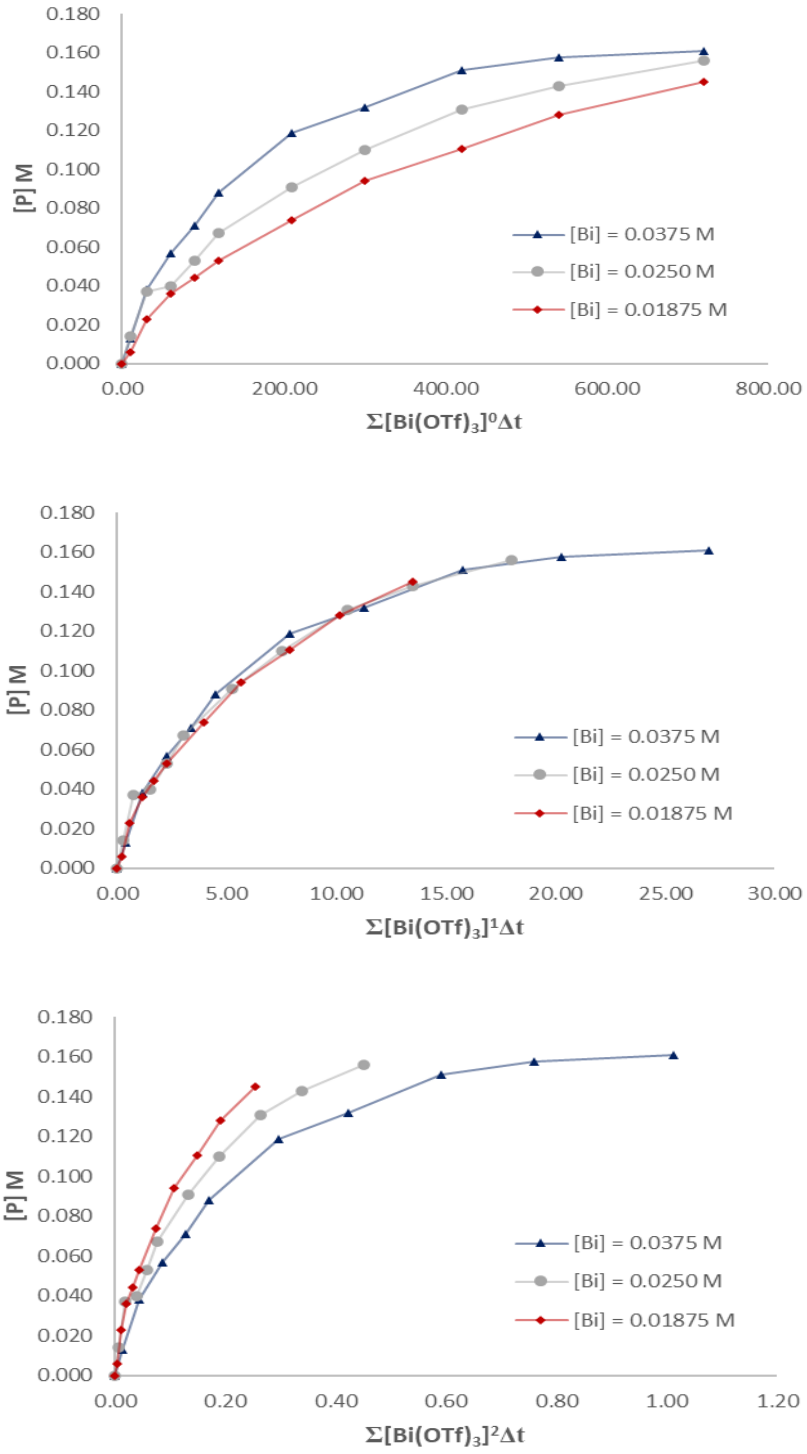




*Chapter three references begin on page 276; experimental details begin on page 272*

### **3.6.6.** Eyring analysis

To probe the observation of differing reaction kinetics for benzylic and non-benzylic systems, an Eyring analysis[58,59] was conducted on both substrate **3.98b** (Scheme 3.15) and on substrate **3.106** (Scheme 3.16). For isopropyl-substituted alcohol **3.106**, the entropy of activation was -7 cal $mol^{-1}$ $K^{-1}$ and the enthalpy of activation was calculated to be 22 kcal $mol^{-1}$. For tolyl-substituted alcohol **3.98b**, the entropy of activation was calculated to be 6 cal $mol^{-1}$ $K^{-1}$ and the enthalpy of activation was calculated to be 26 kcal $mol^{-1}$. The different entropies of activations for each substrate further corroborates the different rate equations observed in the kinetic analysis. Collectively, this data suggests that cleavage of the C–O bond in benzylic alcohol **3.98b** may proceed via a carbocation in an $S_N1$-like process with Lewis acid catalysis alone, while the nickel-catalyst may be involved in the cleavage of the C–O bond of the aliphatic alcohol **3.106**. [60-62] It must be noted, however, that activation parameters calculated through an Eyring analysis must be taken with a grain of salt as they are prone to substantial errors. Calculated values for the entropy of activation of a reaction are particularly error prone as they are calculated from extrapolating data to the y-intercept of the Eyring plot. In contrast, calculated values for the enthalpy of activation of a reaction are less error prone as they are calculated from the slope of the Eyring plot. In order to increase the accuracy of these data, multiple trials should have been conducted so as to gauge the error bars on the calculated activation parameters.



*Chapter three references begin on page 276; experimental details begin on page 272*

**Scheme 3.15.** Eyring plot for the arylation of compound **3.106**

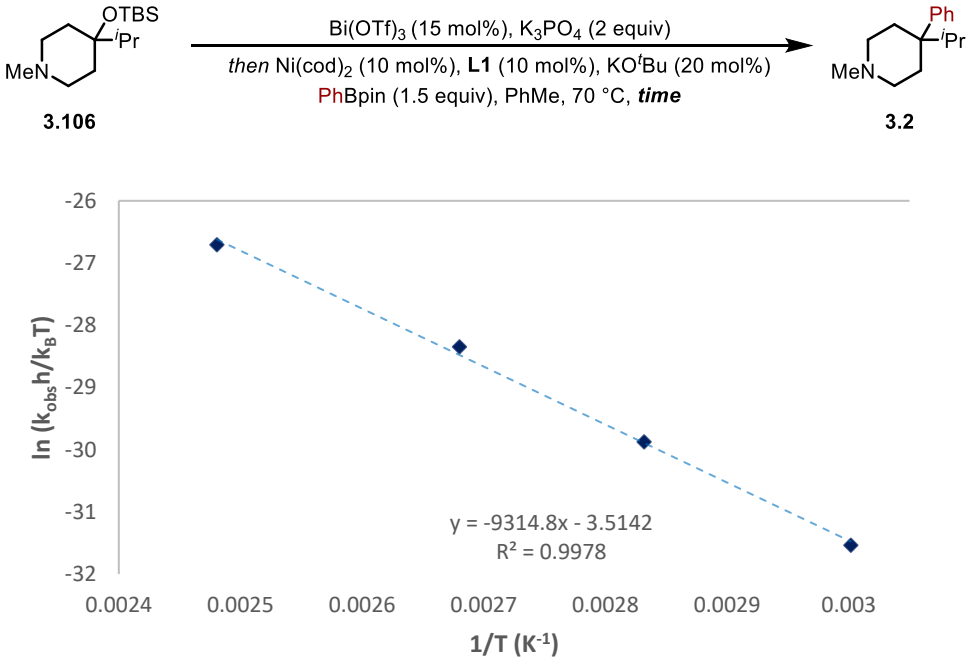


**Scheme 3.16.** Eyring plot for the arylation of compound **3.98b**

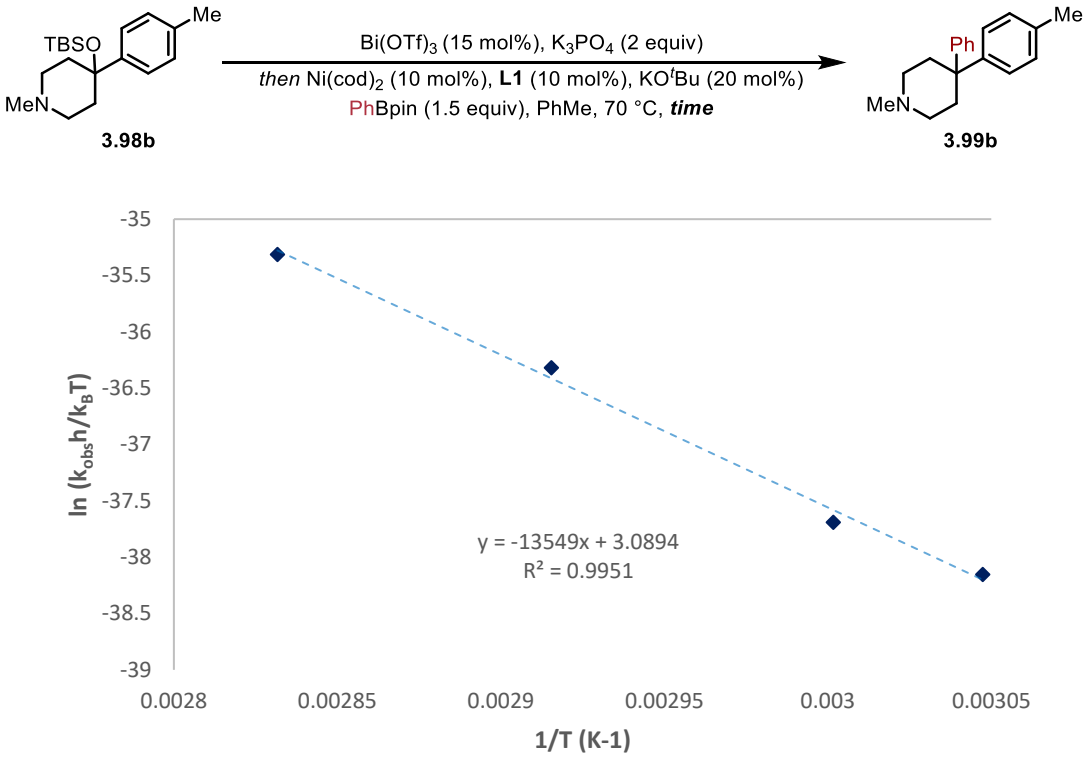




*Chapter three references begin on page 276; experimental details begin on page 272*

### **3.6.7.** Preliminary mechanistic hypothesis

While more extensive mechanistic studies are needed to fully elucidate the activation pathway for the alcohol and the catalytic cycle, a working mechanistic hypothesis can be proposed that explains many of the observations made over the course of this study (Figure 3.12). In situ silylation of **3.A** is strongly supported, as the resulting silyl ether **3.B** can be isolated and directly used in the arylation procedure. The evidence of formation of carbocation **3.C** is primarily supported by kinetic studies, the observation of carbocation rearrangement reactions, and stereochemical erosion of diastereomerically pure starting material. However, confidence in the existence of a carbocation intermediate is weakened by the differing rate equations observed with a benzyl (R = Ar) vs aliphatic (R = $^{i}$Pr) substrate. Specifically, while VTNA analysis of the benzylic substrate suggests the rate is only proportional to the substrate and Lewis acid, with the aliphatic substrate, the reaction is also first order in nickel. The dependence on nickel does not preclude the formation of a carbocation, instead only suggesting that it may be involved in its formation. Moreover, attempted trappings of the presumed carbocation intermediate with traditional nucleophiles via an $S_N1$ process have been unsuccessful (to be discussed in Section 3.7).

**Figure 3.12.** Proposed reaction mechanism and related evidence

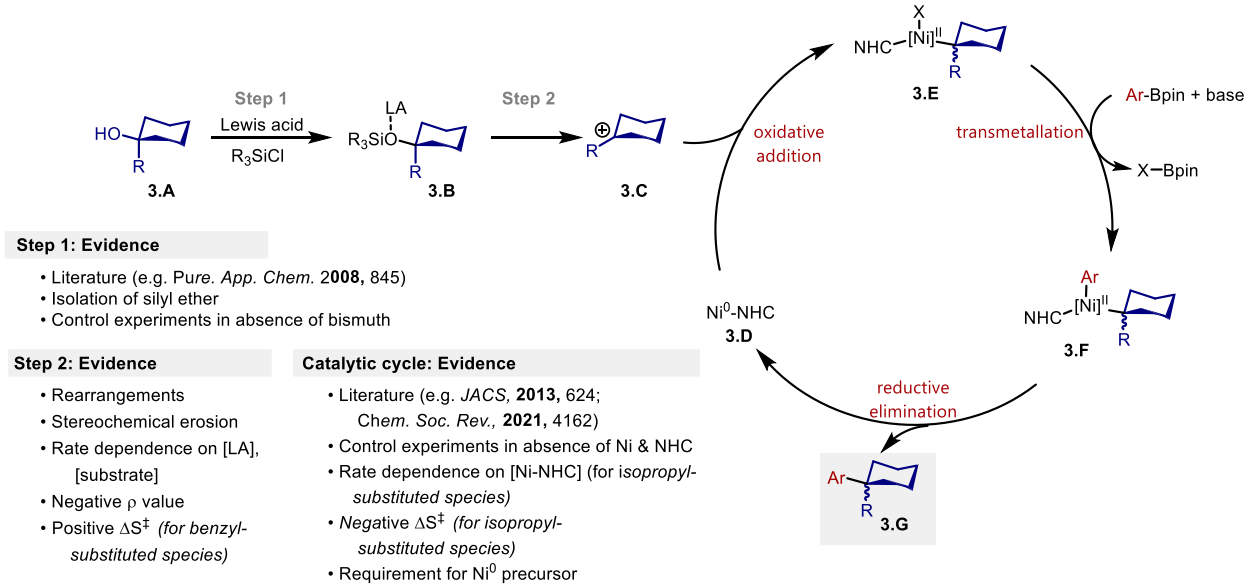


The carbocation (or carbocation-like intermediate) may engage with the nickel catalyst **3.D** to initiate a cross-coupling catalytic cycle, proceeding through formal oxidative addition complex **3.E** and transmetallated complex **3.F**, ultimately resulting in the regeneration of **3.D** and the formation of product **3.G**, presumably through reductive elimination. The absence of any radical rearrangement products suggest that this mechanism proceeds exclusively by two-electron processes. Given the requirement for a nickel(0) pre-cursor, it is proposed this is a nickel(0)/nickel(II) cycle, though the possibility of nickel(I) and/or nickel(III) cannot be eliminated. To this author's knowledge, the trapping of a carbocation with nickel(0) to make cationic nickel(II) has not yet been proposed, and hindered tertiary alkyl oxidative addition complexes such as the one proposed are not well precedented. Thus, ongoing research is actively investigating other possible mechanistic hypotheses beyond this traditional cross-coupling pathway.



*Chapter three references begin on page 276; experimental details begin on page 272*

## 3.7. Failed directions and additional commentary

At the outset of this project, three substantial obstacles that had to be overcome to permit the use of alcohols in Suzuki-Miyaura arylation were identified: (*i*) the strong C($sp^3$)–O bond must be sufficiently weakened so as to allow for transition metal insertion into the bond, (*ii*) alkoxide formation, which may inhibit the active nickel catalyst, must be subdued, and (*iii*) undesired competing *β*-hydride elimination pathways must be supressed.[69]

Three important discoveries were made over the course of the optimization campaign that aided in the resolution to these obstacles. First, the addition of $Me_2SiCl_2$ was found to form a silyl ether in situ. Not only did this activate the C–O bond towards bond cleavage, but the strong O–Si bond strength likely prevented the formation of alkoxides in situ. It is possible that the reason yields plummeted when obviating the pre-mixing step of the transformation was due to catalyst inhibition by way of alkoxide formation. The second important discovery was that $Bi(OTf)_3$ was required to afford product. The addition of this Lewis acid likely aided in weakening the strong C–O bond of the alcohol (or of the silyl ether), thus permitting bond cleavage.

The third significant discovery was that **L1** appeared to be privileged in attaining high yields of product. It has been proposed that ligands with large bite angles favour reductive elimination over *β*-hydride elimination,[70] therefore it can be speculated that **L1** possesses a large bite angle when bound to nickel which leads to its enhanced ability to couple aliphatic alcohols. In hopes of exploring this hypothesis, significant time was invested in learning more about the active nickel-**L1** catalyst, particularly as previous studies of this ligand with palladium have demonstrated it to act via *cis*-bidentate, *trans*-bidentate or multi-metallic coordination to the metal center.[41,71]



*Chapter three references begin on page 276; experimental details begin on page 272*

Unfortunately, in this author's hands the observation and isolation of a ligated nickel-**L1** species had remained elusive at the time of publication of this work. Stoichiometric experiments with the free carbene of **L1** and $Ni(cod)_2$ reliably formed a dark green, catalytically active solution (Scheme 3.17). This species rapidly decomposed into a brown, catalytically inactive material when attempting crystallization or solvent evaporation, preventing efforts at drawing a clear conclusion about the nature of the catalyst.

**Scheme 3.17.** Attempts to isolate a nickel-**L1** complex

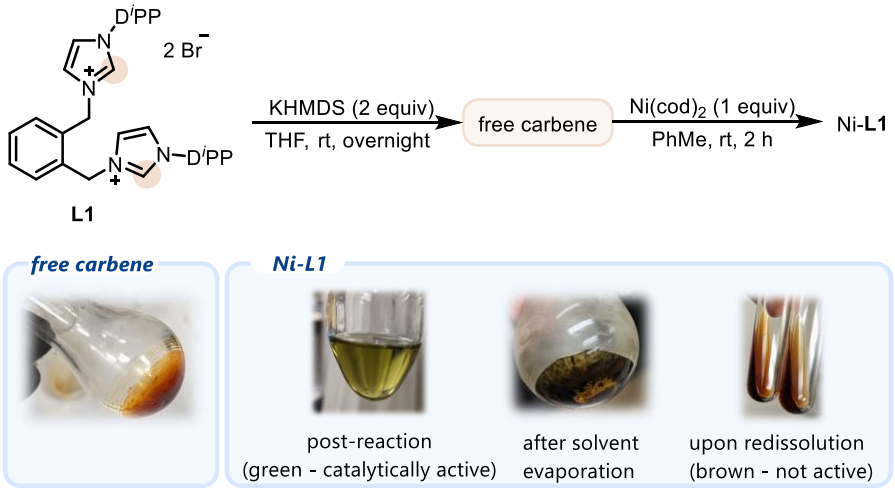


While most of the reactions conducted during the high throughput campaign launched at the outset of this project led to fruitless results, two interesting results were observed while evaluating different ligands in the absence of a Lewis acid co-catalyst. Firstly, the deoxygenative coupling of 1-octanol (**3.107**) was observed, coupling it with phenylboronic acid to afford product **3.108** in the presence of $Ni(cod)_2$, KO$^t$Bu and the NHC ligand IAd·HCl, albeit only in trace yields (Scheme 3.18a). Unfortunately, attempts to reproduce this transformation at the 0.2 mmol scale were unsuccessful. Next, the oxidative coupling of **3.107** with phenylboronic acid in the presence



*Chapter three references begin on page 276; experimental details begin on page 272*

of $Ni(cod)_2$, $KO^tBu$ and the NHC ligand IPent·$HBF_4$ was observed, resulting in the generation of ketone **3.109** in 8% yield (Scheme 3.18b). Including *sec*-butanol (*s*-BuOH) as an additive in this transformation improved the yield to 17%. This hit was not pursued further as the discovery of the bismuth/nickel dual catalytic conditions was made soon after.

**Scheme 3.18.** Other productive results from the high-throughput campaign

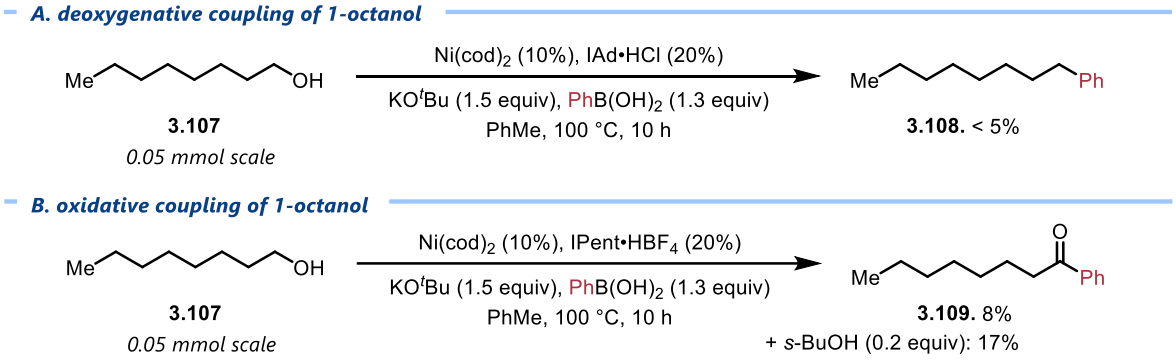


While expanding the scope of the deoxygenative arylation reaction, the coupling of chiral alcohols was tested. Unfortunately, the limitations associated with the substrate scope of this arylation reaction (i.e. the restriction to only cyclic, tertiary alcohols) substantially limited the pool of substrates that could be used. Eventually, the second author on this work, Piers St. Onge, obtained chiral alcohols **3.110** and **3.111**. Unfortunately, subjection of these alcohol to the standard reaction conditions did not lead to arylated products (Scheme 3.19), which is hypothesized to be due to steric build up which restricts nickel-coordination to the already-bulky tertiary carbon. Due to difficulties associated with the synthesis and purification of these chiral alcohol starting materials, this direction was abandoned.



*Chapter three references begin on page 276; experimental details begin on page 272*

**Scheme 3.19.** Attempted arylation of chiral alcohols

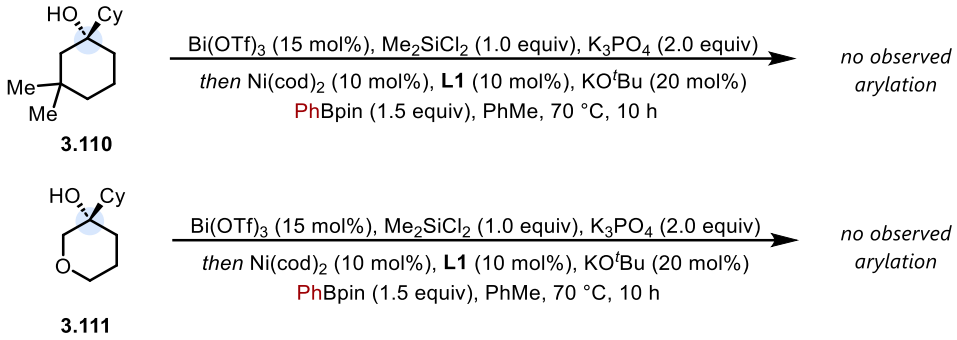


While searching for evidence that this transformation proceeded via a carbocation intermediate, it was theorized that – if a carbocation intermediate was being formed – then it could be trapped by a range of species. Unfortunately, attempts to trap the formed carbocation with a range of known carbocation traps including a malonate (**3.112**), benzene (**3.113**), anisole (**3.114**), benzyl alcohol (**3.115**), indole (**3.116**) and *N*-methylindole (**3.117**) did not result in the recovery of trapped species (Scheme 3.20), instead leading to the recovery of starting material alongside olefin byproduct.

**Scheme 3.20.** Attempted trapping of carbocation intermediate

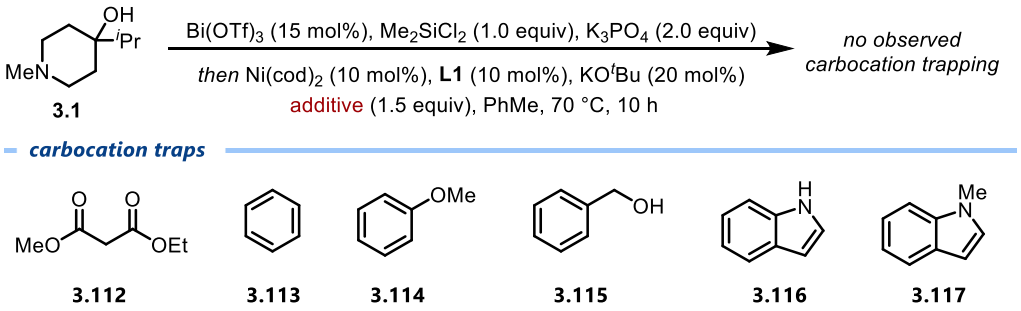




*Chapter three references begin on page 276; experimental details begin on page 272*

## 3.8. Conclusion, impact, future work and considerations

### 3.8.1. Conclusions

In summary, this chapter described a straightforward method to arylate tertiary alcohols with boronate esters. A nickel(0) catalyst was used in concert with a mild Lewis acid, which enabled the coupling of a broad scope of arenes including those bearing heterocyclic rings, carbonyl groups, halides, and more. Chemoselectivity was demonstrated for polyols, wherein arylation occurred selectively on tertiary cyclic alcohols. The observation of rearranged products, stereochemical erosion, a strong Hammett relationship, and first order rate dependance on substrate and Lewis acid were consistent with an $S_N1$-like alcohol activation process, which to this author's knowledge is a largely undeveloped strategy for facilitating cross-coupling reactions with bulky aliphatic coupling partners. However, conflicting results arose upon comparing the reaction kinetics of benzyl and non-benzyl substituted alcohols. Further efforts are underway to further understand the nature of the key C–O bond cleavage step, the origin for high selectivity towards tertiary cyclic alcohols, and how the reactive carbocation-like intermediate may react with the nickel catalyst and boronate ester to form new C–C bonds.

### 3.8.2. Impact

Ultimately, this work represents the first example of non-π-activated alcohols being utilized as substrates in Suzuki-Miyaura arylations. Conventional Suzuki-Miyaura arylations generally require (pseudo)halogenated – or similarly activated – substrates, and even then, are commonly restricted to C($sp^2$)-hybridized substrates. This nickel-catalyzed transformation obviates both of these limitations. Further, mechanistic experiments provide evidence to support an $S_N1$-like activation pathway, which has scarcely been reported as a strategy to mediate cross-



*Chapter three references begin on page 276; experimental details begin on page 272*

coupling reactions. Thus, this reaction not only provides a novel, effective method for generating complex, medicinally-relevant structures from accessible materials– it contributes to the fundamental development of how reaction mechanisms are thought about in cross-coupling chemistry.

This work served as the inspiration for unpublished collaborations within the Newman group, undertaken by PhD candidate Aref Vaezghaemi, wherein the deoxygenative arylation of ketones can be achieved through in situ pivalation (Scheme 3.21a). The discovery that bis(NHC)s appear to be privileged ligands for the activation of aliphatic species, particularly aliphatic alcohols, has also inspired other colleagues in the Newman group to routinely include them while screening for ligands that can be used to achieve novel reactivity. In fact, an undergraduate researcher, Carlos Barbery, pursued the synthesis and evaluation of bis(NHC) ligands in the winter semester of 2023 (Scheme 3.21b). To this end, the entirety of this work served as a valuable starting point for the research that will be discussed in chapter four concerning the arylation of *β*-hydroxysilanes.

**Scheme 3.21.** Extensions of this project within the Newman Lab

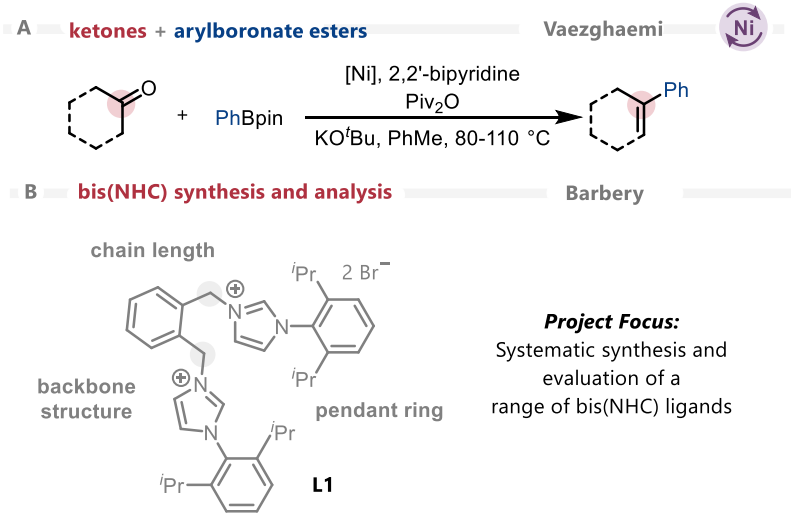




*Chapter three references begin on page 276; experimental details begin on page 272*

Around the same time as this transformation was being investigated, MacMillan and colleagues began to disclose the development of a series of deoxygenative functionalization reactions of alcohols under metallaphotoredox-conditions. MacMillan's work represents a substantial contribution to the field of non-π-activated alcohol activation, having been demonstrated to work in a range of transformations on primary, secondary and tertiary alcohol scaffolds.[72-78] A significant difference between the work of MacMillan and that explored within this chapter is that MacMillan's work inherently relies on single electron pathways, using photochemistry and/or single-electron transfer to facilitate the formation and subsequent trapping of alkyl radicals (Scheme 3.22). While the work that has been described within this chapter is still lacking a complete picture of the catalytic cycle, the gathered evidence for an $S_N1$-type mechanism potentially presents an alternative and, to this author's knowledge, underexplored pathway towards the coupling of alkyl substrates.

**Scheme 3.22.** Key mechanistic steps of MacMillan's deoxygenative arylation

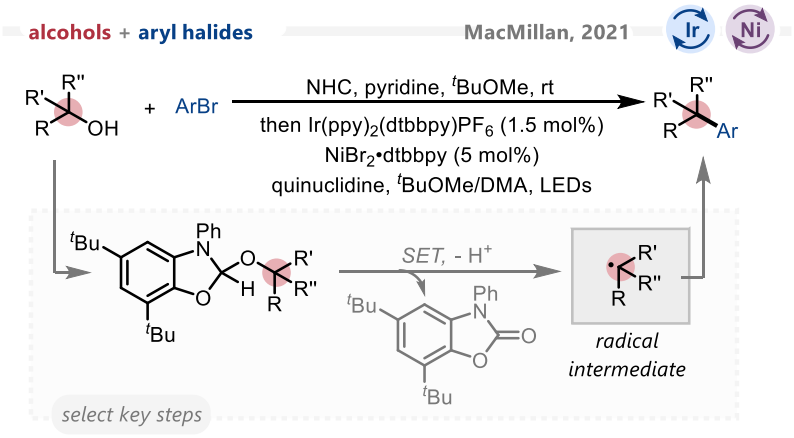




*Chapter three references begin on page 276; experimental details begin on page 272*

### **3.8.3.** Future work and considerations

Upon the completion of this work, many avenues were illuminated for future exploration. Broadly, these avenues fall under one of two umbrellas: mechanistic exploration or synthetic exploration (Scheme 3.23).

One conclusion that can be drawn from this work is that it represents a novel catalytic system for activating cyclic tertiary alcohols. While this chapter has described in detail the application of this catalytic system towards Suzuki-Miyaura arylations, one may still wonder as to what other transformations this catalytic system can enable. What about extending this work towards C($sp^3$)–C($sp^3$) bond forming reactions by employing alkyl boron species as coupling partners alongside cyclic tertiary alcohols? What about employing alkylzinc species, or alkyl Grignards? Effectively, this avenue for exploration asks the question: What other coupling partners can be enabled by this catalytic system to react with alcohols?

Alternatively, one may seek to explore and expand upon the scaffold limitations of this transformation. For instance, this chapter has described how cyclic tertiary alcohols can be effectively arylated, but how can one extend this reactivity beyond cyclic tertiary alcohols? A potential answer to this question will be described within chapter four, detailing how the carbocation-stabilizing phenomenon of the β-silicon effect could be exploited to extend the scope of this transformation beyond cyclic tertiary alcohols, but one may seek to investigate other ways to do so. This avenue would explore the question: How can reactivity be extended beyond cyclic tertiary systems?

**Scheme 3.23.** Further investigations into this deoxygenative arylation: Selected unanswered questions

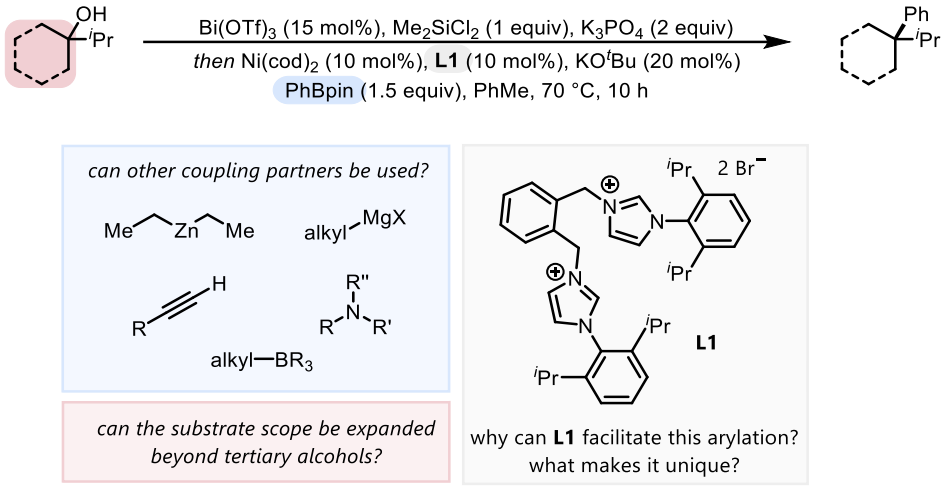


Under the umbrella of mechanism, one may seek to gain an understanding as to why this transformation works the way that it does. Why is **L1** a privileged scaffold for this transformation? How does it bind to the nickel catalyst? Why is $Bi(OTf)_3$ uniquely capable of leading this transformation towards high yields of product? Is the nickel catalyst involved in the rate-determining carbon-oxygen bond cleavage, and if so, what is its role? If not, then why do only nickel precatalysts work in this chemistry? If one were to seek an answer to many of these questions, it is suggested that the first steps would involve initiating a collaboration with a computational chemist who can model this system in hopes of gaining a better understanding of the mechanistic underpinnings of the transformation. In the same vein, one could enlist an inorganic chemist to assist in the synthesis, isolation and characterization of nickel-**L1** catalytic complexes. Through performing stoichiometric experiments with these complexes, one would be able to gain a deeper understanding and appreciation of why this transformation works the way that it does.



*Chapter three references begin on page 276; experimental details begin on page 272*

## 3.9. Experimental

### 3.9.1. General details

Unless otherwise indicated, reactions were conducted under an atmosphere of nitrogen in oven dried (120 °C) 8 mL screw capped vials. Column chromatography was either performed manually using Silicycle F60 40−63 μm silica gel or by using a Combiflash Rf+ automated chromatography system with commercially available Biotage normal-phase Silica Flash columns (35−70 μm). Analytical thin layer chromatography (TLC) was conducted with aluminum-backed EMD Millipore Silica Gel 60 F254 pre-coated plates. Unless otherwise noted, visualization of developed plates was performed under UV light (254 nm) and/or using $KMnO_4$ stain.

### 3.9.2. Instrumentation

$^{1}H$ NMR and $^{13}C$ NMR were recorded on a Bruker AVANCE 400 MHz spectrometer. $^{1}H$ NMR spectra were internally referenced to the residual solvent signal (e.g., $CDCl_3$ = 7.27 ppm, $CD_3OD$ = 4.28 ppm). $^{13}C$ NMR spectra were internally referenced to the residual solvent signal (e.g., $CDCl_3$ = 77.00 ppm). Data for $^{1}H$ NMR are reported as follows: chemical shift (δ ppm), multiplicity (s = singlet, d = doublet, t = triplet, q = quartet, quin = quintet, m = multiplet), coupling constant (Hz), integration. NMR yields for optimization studies were obtained by $^{1}H$ NMR analysis of the crude reaction mixture using 1,3,5-trimethoxybenzene as an internal standard. GC data was obtained via a 5-point calibration curve using FID analysis on an Agilent Technologies 7890B GC with a 30 m x 0.25 mm HP-5 column. Accurate mass data (EI) was obtained from an Agilent 5977A GC/MSD using MassWorks 4.0 from CERNO Bioscience.[79]

### 3.9.3. Materials

Organic solvents were purified by rigorous degassing with nitrogen before passing through a PureSolv solvent purification system. Low water content was confirmed by Karl Fischer titration (<20 ppm for all solvents). Unless otherwise noted, starting materials were obtained commercially from Sigma Aldrich, Alfa Aesar or Combi-Blocks and used as received. $Ni(cod)_2$ was purchased from Sigma-Aldrich. $Bi(OTf)_3$ was purchased from Strem Chemicals. $Me_2SiCl_2$ was purchased from Sigma-Aldrich. PhBpin was purchased from Combi-Blocks and other pinacol boronic esters were synthesized from the corresponding chloride[80] or boronic acid[81] according to the literature. The NHC ligand that proved optimal for this arylation reaction, **L1**, was prepared as described in Section 2.1, while other *N*-heterocyclic carbenes were prepared according to the literature.[82] The synthesis of ligands, starting materials, products and all other experimental details are fully described and all original spectra are available in the freely-available Supporting Information files (https://doi.org/10.1038/s44160-023-00275-w).

### 3.9.4. General procedures

***Procedure A – Conditions for the arylation of tertiary alcohols:*** An oven-dried 8 mL screw-top test-tube was equipped with an oven-dried micro-stir bar and brought into a nitrogen-filled glovebox. This reaction vessel was charged with alcohol (1.0 equivalent, 0.20 mmol), $K_3PO_4$ (2.0 equivalent, 0.40 mmol), $Bi(OTf)_3$ (0.15 equivalent, 0.03 mmol), $Me_2SiCl_2$ (1.0 equivalent, 0.20 mmol) and PhMe (0.4 mL). This mixture was left to stir for 30 min at room temperature. After 30 min, a premixed solution of $Ni(cod)_2$ (0.10 equivalent, 0.02 mmol), **L1** (0.10 equivalent, 0.02 mmol) and $KO^tBu$ (0.20 equivalent, 0.04 mmol) in PhMe (0.4 mL) was added to the stirring alcohol solution, followed by PhBpin (1.5 equivalent, 0.30 mmol), before the reaction vessel was

sealed with a Teflon-septum equipped cap and brought outside of the glovebox to be stirred within a mineral-oil bath at 800 rpm for 10 hours at 70 ˚C. After 10 hours, the reaction vessel was allowed to come to room temperature. The crude reaction solution was quenched with sat. KOH (5 mL) and diluted with EtOAc before being transferred into a separatory funnel. KOH was removed via liquid-liquid extraction with EtOAc (3 x 10 mL); the resulting organic phases were combined in the separatory funnel before being washed twice with sat. $NaHCO_3$ and once with sat. NaCl. The organic phase was dried with $MgSO_4$ before being passed through a short plug composed of $SiO_2$ and celite in a 50:50 mixture. Solvent was evacuated by rotary evaporation and the subsequent residue was purified by column chromatography.

***General Procedure B – Conditions for the arylation of diols:*** An oven dried 8 mL screw-top test-tube was equipped with an oven-dried micro-stir bar and brought into a nitrogen-filled glovebox. The reaction vessel was charged with alcohol (1.0 equivalent, 0.20 mmol), $K_3PO_4$ (2.0 equivalent, 0.40 mmol), $Bi(OTf)_3$ (0.15 equivalent, 0.03 mmol), $Me_2SiCl_2$ (3.0 equivalent, 0.60 mmol) and PhMe (0.4 mL). The mixture was left to stir for 30 min at room temperature. After 30 min, a premixed solution of $Ni(cod)_2$ (0.10 equivalent, 0.02 mmol), **L1** (0.10 equivalent, 0.02 mmol) and $KO^tBu$ (0.20 equivalent, 0.04 mmol) in PhMe (0.4 mL) was added to the stirring alcohol solution, followed by PhBpin (1.5 equivalent, 0.30 mmol), before the reaction vessel was sealed with a Teflon-septum equipped cap. The reaction vessel was brought outside of the glovebox and stirred within a mineral-oil bath at 800 rpm for 10 hours at 70 ˚C. After 10 hours, the reaction vessel was allowed to come to room temperature, after which it was uncapped and charged with tetrabutylammonium fluoride (2.0 equivalent, 0.40 mmol). The resulting mixture was stirred at 800 rpm for 2 h at 70 ˚C. This solution was quenched with sat. KOH (5 mL) and diluted with EtOAc before being transferred into a separatory funnel. KOH was removed via liquid-liquid

extraction with EtOAc (3 x 10 mL); the resulting organic phases were combined in the separatory funnel before being washed twice with sat. $NaHCO_3$ and once with sat. NaCl. The organic phase was dried with $MgSO_4$ before being passed through a short plug composed of $SiO_2$ and celite in a 50:50 mixture. Solvent was evacuated by rotary evaporation and the subsequent residue was dissolved in dichloromethane. A small amount of $SiO_2$ was added to the resulting solution and the solvent was once more removed via rotary evaporation. The resulting solid was loaded directly on to a 10 g Biotage SNAP silica-packed column and purified on a CombiFlash Rf+ automated chromatography instrument.

### **3.9.6**. Characterization data of synthesized products

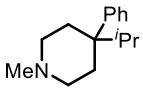


**1-Methyl-4-phenyl-4-isopropylpiperidine (3.2)** was prepared from **3.1** according to general procedure A. Column chromatography was performed using a gradient of 1→10% ethyl acetate in hexanes to afford product as a yellow liquid (31.2 mg, 73% yield). **$^1$H NMR** (400 MHz, $CD_3OD$): δ 7.20-7.11 (m, 3H), 7.06-7.02 (m, 2H), 2.82-2.74 (m, 1H), 2.65-2.63 (m, 4H), 2.40-2.35 (m, 4H), 2.30 (s, 3H), 1.16 (d, $J$ = 6.4 Hz, 6H); **$^{13}$C NMR** (100 MHz, $CDCl_3$): 137.4, 128.6, 128.5, 128.3, 55.3, 46.2, 45.4, 45.2, 41.1, 22.8. **Accurate mass (EI)**: Theoretical: 217.1830. Found: 217.1828. Spectral Accuracy: 98.6%. **FT-IR**: $\nu$ ($cm^{-1}$) 3120, 3049, 2984, 2845, 2801, 2630, 2230, 1495, 1420, 1139.

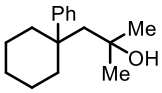


**α,α-Dimethyl-1-phenyl-cyclohexaneethanol (3.56)** was prepared from the corresponding alcohol according to general procedure B. Column chromatography was performed using a gradient of 1→15% ethyl acetate in hexanes to afford product as a yellow liquid (32.1 mg, 69% yield). **$^1$H NMR** (400 MHz, $CDCl_3$): δ 7.31-7.27 (m, 3H), 7.26-7.24 (m, 2H), 1.57-1.33 (m, 10H), 1.24 (s, 2H), 1.12-1.10 (s, 6H); **$^{13}$C NMR** (100 MHz, $CDCl_3$): 137.4, 128.6, 128.5, 128.3, 71.1, 46.2, 39.4, 36.3, 25.6, 22.6, 8.6. **Accurate mass (EI)**: Theoretical: 232.1827. Found: 232.1822. Spectral Accuracy: 98.6%. **FT-IR**: $\nu$ ($cm^{-1}$) 3601, 3084, 2934, 2881, 2740, 1480, 1423, 1389.

## 3.10. References

(1) Brown, D. G.; Boström, J. Analysis of past and present synthetic methodologies on medicinal chemistry: Where have all the new reactions gone? *J. Med. Chem.* **2016**, *59*, 4443–4458.

(2) Buskes, M. J.; Blanco, M.-J. Impact of cross-coupling reactions in drug discovery and development. *Molecules* **2020**, *25*, 3493.

(3) Miyaura, N.; Suzuki, A. Palladium-catalyzed cross-coupling reactions of organoboron compounds. *Chem. Rev.* **1995**, *95*, 2457-2483.

(4) Koshvandi, A. T. K.; Heravi, M. M.; Momeni, T. Current applications of Suzuki-Miyaura coupling reaction in the total synthesis of natural products: An update. *App. Organomet. Chem.* **2018**, *32*, e4210.

(5) Glasspoole, B. W.; Crudden, C. M. Cross-coupling: The final frontier. *Nat. Chem.* **2011**, *3*, 912-913.

(6) Choi, J.; Fu, G. C. Transition metal-catalyzed alkyl-alkyl bond formation: Another dimension in cross-coupling chemistry. *Science* **2017**, *356*, eaaf7230.

(7) Yu, D.-G.; Li, B.-J.; Shi, Z.-J. Exploration of new C−O electrophiles in cross-coupling reactions. *Acc. Chem. Res*. **2010**, *43*, 1486-1495.

(8) Zhou, T.; Szostak, M. Palladium-catalyzed cross-couplings by C−O bond activation. *Catal. Sci. Technol*. **2020**, *10*, 5702-5739.

(9) Yu, D.-G.; Li, B.-J.; Zheng, S.-F.; Guan, B.-T.; Wang, B.-Q.; Shi, Z.-J. Direct application of phenolic salts to nickel-catalyzed cross-coupling reactions with aryl Grignard reagents. *Angew. Chem. Int. Ed*. **2010**, *49*, 4566-4570.

(10) Zeng, H.; Qiu, Z.; Domíngues-Huerta, A.; Hearne, Z.; Chen, Z.; Li, C.-J. An adventure in sustainable cross-coupling of phenols and derivatives via carbon-oxygen bond cleavage. *ACS Catal*. **2017**, *7*, 510-519.

(11) Yu, D.-G.; Wang, X.; Zhu, R.-Y.; Luo, S.; Zhang, X.-B.; Wang, B.-Q.; Wang, L.; Shi, Z.-J. Direct arylation/alkylation/magnesiation of benzyl alcohols in the presence of Grignard

reagents via Ni-, Fe- or Co- catalyzed sp3 C−O bond activation. *J. Am. Chem. Soc*. **2012**, *134*, 14638-14641.

(12) Guo, P.; Wang, K.; Jin, W.-J.; Qi, L.; Liu, X.-Y.; Shu, X.-Z. Dynamic kinetic cross-electrophile arylation of benzyl alcohols by nickel catalysis. *J. Am. Chem. Soc*. **2021**, *143*, 513-523.

(13) Suga, T.; Ukaji, Y. Nickel-catalyzed cross-electrophile coupling between benzyl alcohols and aryl halides assisted by titanium co-reductant. *Org. Lett*. **2018**, *20*, 7846-7850.

(14) Nazari, S. H.; Bourdeau, J. E.; Talley, M. R.; Valdivia-Berroeta, G. A.; Smith, S. J.; Michaelis, D. J. Nickel-catalyzed Suzuki cross couplings with unprotected allylic alcohols enabled by bidentate *N*-heterocyclic carbene (NHC)/phosphine ligands. *ACS Catal*. **2018**, *8*, 85-89.

(15) Zhang, X.; MacMillan, D. W. C. Alcohols as latent coupling fragments for metallaphotoredox catalysis: $sp^3$-$sp^2$ cross-coupling of oxalates with aryl halides. *J. Am. Chem. Soc*. **2016**, *138*, 13862-13865.

(16) Mills, R. J.; Monteith, J. J.; dos Passos Gomes, G.; Aspuru-Guzik, A.; Rousseaux, S. A. L. The cyclopropane ring as a reporter of radical leaving-group reactivity for Ni-catalyzed C($sp^3$)−O arylation. *J. Am. Chem. Soc*. **2020**, *142*, 13246-13254.

(17) Dong, Z.; MacMillan, D. W. C. Metallaphotoredox-enabled deoxygenative arylation of alcohols. *Nature* **2021**, *598*, 451-456.

(18) Lackner, G. L.; Quasdorf, K. W.; Overman, L. E. Direct construction of quaternary carbons from tertiary alcohols via photoredox-catalyzed fragmentation of *tert*-alkyl *N*-phthalimidoyl oxalates. *J. Am. Chem. Soc*. **2013**, *135*, 15342−15345.

(19) Kariofillis, S.; Jiang, S.; Żuranski, A.; Gandhi, S.; Martinez Alvarado, J.; Doyle, A. Using data science to guide aryl bromide substrate scope analysis in a Ni/photoredox-catalyzed cross-coupling with acetals as alcohol-derived radical sources. *J. Am. Chem. Soc*. **2022**, *144*, 1045-1055.

(20) Ye, Y.; Chen, H.; Sessler, J. L.; Gong, H. Zn-mediated fragmentation of tertiary alkyl oxalates enabling formation of alkylated and arylated quaternary carbon centers. *J. Am. Chem. Soc.* **2019**, *141*, 820−824.

(21) Li, Z.; Sun, W.; Wang, X.; Li, L.; Zhang, Y.; Li, C. Electrochemically enabled, nickel-catalyzed dehydroxylative cross-coupling of alcohols with aryl halides. *J. Am. Chem. Soc.* **2021**, *143*, 3535-3543.

(22) Lin, Q.; Ma, G.; Gong, H. Ni-catalyzed formal cross-electrophile coupling of alcohols with aryl halides. *ACS Catal*. **2021**, *11*, 14102-14109.

(23) Chi, B. K.; Widness, J. K.; Gilbert, M. M.; Salgueiro, D. C.; Garcia, K. J.; Weix, D. J. In-situ bromination enables formal cross-electrophile coupling of alcohols with aryl and alkenyl halides. *ACS Catal*. **2022**, *12*, 580-586.

(24) Xie, H.; Guo, J.; Wang, Y.-Q.; Wang, K.; Guo, P.; Su, P.-F.; Wang, X.; Shu, X.-Z. Radical dehydroxylative alkylation of tertiary alcohols by Ti Catalysis. *J. Am. Chem. Soc*. **2020**, *142*, 16787-16794.

(25) Sakai, H. A.; MacMillan, D. W. C. Nontraditional fragment couplings of alcohols and carboxylic acids: C($sp^3$)-C($sp^3$) cross-coupling via radical sorting. *J. Am. Chem. Soc*. **2022**, *144*, 6185-6192.

(26) Emer, E.; Sinisi, R.; Capdevila, M. G.; Petruzziello, D.; De Vincentiis, F.; Cozzi, P. G. Direct nucleophilic $S_N1$-type reactions of alcohols. *Eur. J. Org. Chem*. **2011**, 647-667.

(27) Yasuda, M.; Somyo, T.; Baba, A. Direct carbon-carbon bond formation from alcohols and active methylenes, alkoxyketones, or indoles catalyzed by indium trichloride. *Angew. Chem. Int. Ed.* **2006**, *45*, 793-796.

(28) Jia, X.-G.; Guo, P.; Duan, J.; Shu, X.-Z. Dual nickel and Lewis acid catalysis for cross-electrophile coupling: The allylation of aryl halides with allylic alcohols. *Chem. Sci.* **2018**, *9*, 640-645.

(29) Liu, X.; Hsiao, C.-C.; Kalvet, I.; Leiendecker, M.; Guo, L.; Schoenebeck, F.; Rueping, M. Lewis-acid assisted nickel-catalyzed cross-coupling of aryl methyl ethers by C−O bond-

cleaving alkylation: Prevention of undesired β-hydride elimination. *Angew. Chem. Int. Ed.* **2016**, *55*, 6093-6098.

(30) Isbrandt, E. S.; Sullivan, R. J.; Newman, S. G. High-throughput strategies for the discovery and optimization of catalytic reactions. *Angew. Chem. Int. Ed.* **2019**, *58*, 7180-7191.

(31) Tulloch, A. A. D.; Danopoulos, A. A.; Winston, S.; Kleinhenz, S.; Eastham, G. N-functionalized heterocyclic carbene complexes of silver. *J. Chem. Soc., Dalton Trans.* **2000**, *24*, 4499-4506.

(32) Kolsi, L. E.; Yli-Kauhaluoma, J.; Moreira, V. M. Catalytic, tunable, one-step bismuth (III) triflate reaction with alcohols: Dehydration versus dimerization. *ACS Omega* **2018**, *3*, 8836-8842.

(33) Zultanski, S. L.; Fu, G. C. Nickel-catalyzed carbon-carbon bond-forming reactions of unactivated tertiary alkyl halides: Suzuki arylations. *J. Am. Chem. Soc.* **2013**, *135*, 624-627.

(34) Qin, T.; Cornella, J.; Li, C.; Malins, L. R.; Edwards, J. T.; Kawamura, S.; Maxwell, B. D.; Eastgate, M. D.; Baran, P. S. A general alkyl-alkyl cross-coupling enabled by redox-active esters and alkylzinc reagents. *Science* **2016**, *352*, 801-805.

(35) Primer, D. N.; Molander, G. A. Enabling the cross-coupling of tertiary organoboron nucleophiles through radical-mediated alkyl transfer. *J. Am. Chem. Soc.* **2017**, *139*, 9847-9850.

(36) Dorsheimer, J. R.; Ashley, M. A.; Rovis, T. Dual nickel/photoredox-catalyzed deaminative cross-coupling of sterically hindered primary amines. *J. Am. Chem. Soc.* **2021**, *143*, 19294-19299.

(37) Dryzhakov, M.; Hellal, M.; Wolf, E.; Falk, F. C.; Moran, J. Nitro-assisted Brønsted acid catalysis: Application to a challenging catalytic azidation. *J. Am. Chem. Soc.* **2015**, *137*, 9555-9558.

(38) Baba, A.; Yasuda, M.; Nishimoto, Y.; Saito, T.; Onishi, Y. Reaction of alcohols and silyl ethers in the presence of an indium/silicon-based catalyst system: Deoxygenation and allyl substitution. *Pure. App. Chem.* **2008**, *80*, 845-854.

(39) Wiensch, E.; Todd, D.; Montgomery, J. Silyloxyarenes as versatile coupling substrates enabled by nickel-catalyzed C−O bond cleavage. *ACS Catal.* **2017**, *7*, 5568−5571.

(40) Yasuda, M.; Yamasaki, S.; Onishi, Y.; Baba, A. Indium-catalyzed direct chlorination of alcohols using chlorodimethylsilane-benzil as a selective and mild system. *J. Am. Chem. Soc.* **2004**, *126*, 7186-7187.

(41) Gardiner, M. G.; Ho, C. C. Recent Advances in Bidentate Bis(*N*-Heterocyclic Carbene) Transition Metal Complexes and Their Applications in Metal-Mediated Reactions. *Coord. Chem. Rev.* **2018**, *375*, 373–388.

(42) Baker, M. V.; Brown, D. H.; Simpson, P. V.; Skelton, B. W.; White, A. H.; Williams, C. C. Palladium, Rhodium and Platinum Complexes of Ortho-Xylyl-Linked Bis-*N*-Heterocyclic Carbenes: Synthesis, Structure and Catalytic Activity. *J. Organomet. Chem.* **2006**, *691*, 5845–5855.

(43) Biffis, A.; Tubaro, C.; Buscemi, G.; Basato, M. Highly Efficient Alkyne Hydroarylation with Chelating Dicarbene Palladium(II) and Platinum(II) Complexes. *Adv. Synth. Catal.* **2008**, *350*, 189–196.

(44) Biffis, A.; Gazzola, L.; Gobbo, P.; Buscemi, G.; Tubaro, C.; Basato, M. Alkyne Hydroarylations with Chelating Dicarbene Palladium(II) Complex Catalysts: Improved and Unexpected Reactivity Patterns Disclosed upon Additive Screening. *European J. Org. Chem.* **2009**, *2009*, 3189–3198.

(45) Zheng, Y.-L.; Newman, S. G. Methyl Esters as Cross-Coupling Electrophiles: Direct Synthesis of Amide Bonds. *ACS Catal.* **2019**, *9*, 4426–4433.

(46) Jefferies, L. R.; Cook, S. P. Iron-catalyzed arene alkylation reactions with unactivated secondary alcohols. *Org Lett.* **2014**, *16*, 2026-2029.

(47) Labrouillère, M.; Le Roux, C.; Gaspard-Iloughmane, H.; Dubac, J. Bismuth(III) chloride-catalyzed chlorination of alcohols by chlorosilanes. *Synlett* **1994**, *9*, 723-724.

(48) Xiao, L.-J.; Cheng, L.; Feng, W.-M.; Li, M.-L.; Xie, J.-H.; Zhou, Q.-L. Nickel(0)-catalyzed hydroarylation of styrenes and 1,3-dienes with organoboron compounds. *Angew. Chem. Int. Ed.* **2017**, 57, 461-464.

(49) Lv, H.; Xiao, L.-J.; Zhao, D.; Zhou, Q.-L. Nickel(0)-catalyzed linear-selective hydroarylation of unactivated alkenes and styrenes with aryl boronic acids. *Chem. Sci.* **2018**, *9*, 6839-6843.

(50) Zultanski, S. L.; Fu, G. C. Nickel-catalyzed carbon-carbon bond-forming reactions of unactivated tertiary alkyl halides: Suzuki arylations. *J. Am. Chem. Soc.* **2013**, *135*, 624-627.

(51) Diccianni, J. B.; Diao, T. Mechanisms of nickel-catalyzed cross-coupling reactions. *Trends in Chem.* **2019**, *9*, 830-844.

(52) Bowry, V. W.; Lusztyk, J.; Ingold, K. U. Calibration of a new horologery of fast radical clocks. Ring-opening rates for ring- and α-alkyl-substituted cyclopropylcarbinyl radicals and for the bicyclo[2.1.0]pent-2-yl radical. *J. Am. Chem. Soc.* **1991**, *113*, 5687-5698.

(53) Walling, C.; Cioffari, A. Cyclization of 5-hexenyl radicals. *J. Am. Chem. Soc*. **1972**, *94*, 6059-6064.

(54) Hammett, L. P. Some relations between reaction rates and equilibrium constants. *Chem. Rev*. **1935**, *17*, 125-136.

(55) Hansch, C.; Leo, A.; Taft, R. W. A survey of Hammett substituent constants and resonance and field parameters. *Chem. Rev*. **1991**, *91*, 165-195.

(56) Vives, G.; Gonzalez, A.; Jaud, J.; Launay, J.-P.; Rapenne, G. Synthesis of molecular motors incorporating para-phenylene-conjugated or bicyclo[2.2.2]octane-insulated electroactive groups. *Chem. Eur. J*. **2007**, *13*, 5622-5631.

(57) Burés, J. A simple graphical method to determine the order in catalyst. *Angew. Chem. Int. Ed*. **2016**, *55*, 2028-2031.

(58) Eyring, H. The activated complex in chemical reactions. *J. Chem. Phys*. **1935**, *3*, 107-115.

(59) Otomo, T.; Suzuki, H.; Iida, R.; Takayanagi, T. $S_N1$ Reaction Mechanisms of *Tert*-Butyl Chloride in Aqueous Solution: What Can Be Learned from Reaction Path Search Calculations and Trajectory Calculations for Small Hydrated Clusters? *Comput. Theor. Chem.* **2021**, *1201*, 113278.

(60) Phan, T. B.; Nolte, C.; Kobayashi, S.; Ofial, A. R.; Mayr, H. Can one predict changes from $S_N1$ to $S_N2$ mechanisms? *J. Am. Chem. Soc.* **2009**, *131*, 11392-11401.

(61) Winstein, S.; Grunwald, E.; Jones, H. W. The correlation of solvolysis rates and the classification of solvolysis reactions into mechanistic categories. *J. Am. Chem. Soc*. **1951**, *73*, 2700-2707.

(62) Krumper, J. R.; Salamant, W. A.; Woerpel, K. A. Continuum of mechanisms for nucleophilic substitution of cyclic acetals. *Org. Lett.* **2008**, *10*, 4907-4910.

(63) Ben Halima, T.; Zhang, W.; Yalaoui, I.; Hong, X.; Yang, Y.-F.; Houk, K. N.; Newman, S. G. Palladium-Catalyzed Suzuki–Miyaura Coupling of Aryl Esters. *J. Am. Chem. Soc.* **2017**, *139*, 1311–1318.

(64) Ben Halima, T.; Vandavasi, J. K.; Shkoor, M.; Newman, S. G. A Cross-Coupling Approach to Amide Bond Formation from Esters. *ACS Catal.* **2017**, *7*, 2176–2180.

(65) Vandavasi, J. K.; Hua, X.; Halima, H. B.; Newman, S. G. A Nickel-catalyzed carbonyl-Heck Reaction. *Angew. Chem. Int. Ed.* **2017**, *56* (48), 15441–15445.

(66) Ben Halima, T.; Masson-Makdissi, J.; Newman, S. G. Nickel-catalyzed Amide Bond Formation from Methyl Esters. *Angew. Chem. Int. Ed.* **2018**, *57*, 12925–12929.

(67) Verheyen, T.; van Turnhout, L.; Vandavasi, J. K.; Isbrandt, E. S.; De Borggraeve, W. M.; Newman, S. G. Ketone Synthesis by a Nickel-Catalyzed Dehydrogenative Cross-Coupling of Primary Alcohols. *J. Am. Chem. Soc.* **2019**, *141*, 6869–6874.

(68) Beddoe, R. H.; Andrews, K. G.; Magné, V.; Cuthbertson, J. D.; Saska, J.; Shannon-Little, A. L.; Shanahan, S. E.; Sneddon, H. F.; Denton, R. M. Redox-Neutral Organocatalytic Mitsunobu Reactions. *Science* **2019**, *365*, 910–914.

(69) Yu, D.-G.; Li, B.-J.; Shi, Z.-J. Exploration of New C−O Electrophiles in Cross-Coupling Reactions. *Acc. Chem. Res.* **2010**, *43*, 1486–1495.

(70) Hayashi, T.; Konishi, M.; Kobori, Y.; Kumada, M.; Higuchi, T.; Hirotsu, K. Dichloro[1,1'-Bis(Diphenylphosphino)Ferrocene]-Palladium(II): An Effective Catalyst for Cross-Coupling

of Secondary and Primary Alkyl Grignard and Alkylzinc Reagents with Organic Halides. *J. Am. Chem. Soc.* **1984**, *106*, 158–163.

(71) Danopoulos, A. A.; Tulloch, A. A. D.; Winston, S.; Eastham, G.; Hursthouse, M. B. Chelating and 'pincer' dicarbene complexes of palladium; Synthesis and structural studies. *Dalton Trans*. **2003**, *5*, 1009-1015.

(72) Sakai, H. A.; MacMillan, D. W. C. Nontraditional Fragment Couplings of Alcohols and Carboxylic Acids: C($sp^3$)–C($sp^3$) Cross-Coupling via Radical Sorting. *J. Am. Chem. Soc.* **2022**, *144*, 6185–6192.

(73) Wang, J. Z.; Sakai, H. A.; MacMillan, D. W. C. Alcohols as Alkylating Agents: Photoredox-catalyzed Conjugate Alkylation via in situ Deoxygenation. *Angew. Chem. Int. Ed.* **2022**, *61* (35).

(74) Intermaggio, N. E.; Millet, A.; Davis, D. L.; MacMillan, D. W. C. Deoxytrifluoromethylation of Alcohols. *J. Am. Chem. Soc.* **2022**, *144*, 11961–11968.

(75) Lyon, W. L.; MacMillan, D. W. C. Expedient Access to Underexplored Chemical Space: Deoxygenative C($sp^3$)–C($sp^3$) Cross-Coupling. *J. Am. Chem. Soc.* **2023**, *145*, 7736–7742.

(76) Gould, C. A.; Pace, A. L.; MacMillan, D. W. C. Rapid and Modular Access to Quaternary Carbons from Tertiary Alcohols via Bimolecular Homolytic Substitution. *J. Am. Chem. Soc.* **2023**, *145*, 16330–16336.

(77) Bissonnette, N. B.; Bisballe, N.; Tran, A. V.; Rossi-Ashton, J. A.; MacMillan, D. W. C. Development of a General Organophosphorus Radical Trap: Deoxyphosphonylation of Alcohols. *ChemRxiv*, **2023**. https://doi.org/10.26434/chemrxiv-2023-65m0v.

(78) Carson, W. P., II; Sarver, P. J.; Goudy, N. S.; MacMillan, D. W. C. Photoredox Catalysis-Enabled Sulfination of Alcohols and Bromides. *J. Am. Chem. Soc.* **2023**, *145*, 20767–20774.

(79) Wang, Y.; Gu, M. The Concept of Spectral Accuracy for MS. *Anal. Chem*. **2010**, *82*, 7055–7062.

(80) Ishiyama, T.; Murata, M.; Miyaura, N. Palladium(0)-Catalyzed Cross-Coupling Reaction of Alkoxydiboron with Haloarenes: A Direct Procedure for Arylboronic Esters. *J. Org. Chem.* **1995**, *60*, 7508–7510.

(81) Iwamoto, T.; Okuzono, C.; Adak, L.; Jin, M.; Nakamura, M. Iron-Catalyzed Enantioselective Suzuki-Miyaura Coupling of Racemic Alkyl Bromides. *Chem. Commun.* **2019**, *55*, 1128–1131.

(82) Hans, M.; Lorkowski, J.; Demonceau, A.; Delaude, L. Efficient Synthetic Protocols for the Preparation of Common *N*-Heterocyclic Carbene Precursors. *Beilstein J. Org. Chem.* **2015**, *11*, 2318–2325.

# **Chapter Four**: An $S_N1$-approach to cross-coupling: Deoxygenative arylation facilitated by the $\beta$-silicon effect.

*"Tomorrow, when I wake, or think I do, what shall I say of today? That with my friend, at this place, until the fall of night, I waited?"*

- *Waiting for Godot, Samuel Beckett, 1906-1989.*



*Chapter four references begin on page 364; experimental details begin on page 331*

## 4.1. Chapter outlook

Chapter three of this dissertation sought to illustrate the advantages, and challenges, of developing methods to directly utilize alcohols as coupling partners in Suzuki-Miyaura coupling. This work resulted in the successful development of a method for the deoxygenative arylation of tertiary alcohols. However, three significant limitations remained unresolved upon the conclusion of this work: (*i*) only cyclic, tertiary alcohols could be arylated, (*ii*) there was not enough concrete evidence to be able to fully support the existence of a carbocation intermediate, and (*iii*) there was limited understanding as to why the optimal ligand enabled reactivity.

Chapter four will aim to resolve each of these limitations as it describes a method for arylating primary, secondary, and tertiary alcohols through exploiting the carbocation-stabilizing properties of the *β*-silicon effect (Figure 4.1). Within this chapter is a systematic study of bis-imidazolium ligands, culminating in the synthesis, isolation, and characterization of a range of novel nickel-NHC complexes with ligand **L2**. Lastly, evidence is gathered through various kinetic studies that supports the existence of a carbocation, or carbocation-like, intermediate.

**Figure 4.1.** Graphical outlook for chapter four

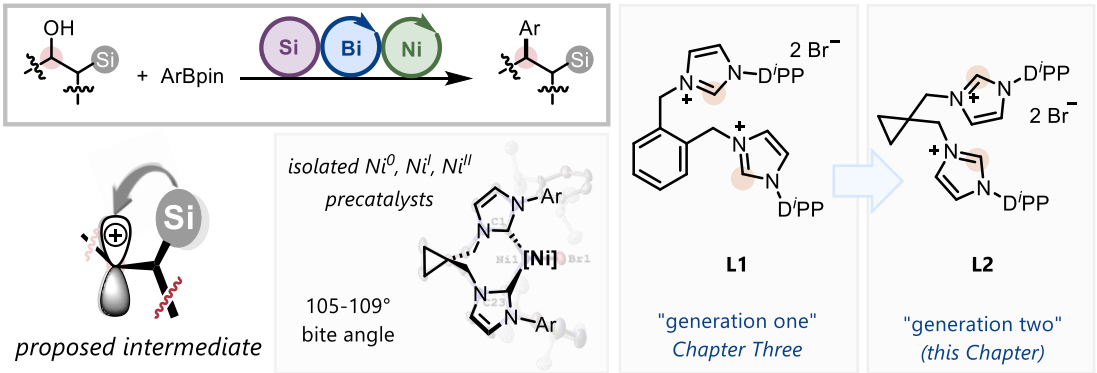




*Chapter four references begin on page 364; experimental details begin on page 331*

## 4.2. Reuse permissions and contributions

The data presented in this chapter is derived from the manuscript "An $S_N1$-approach to cross-coupling: Deoxygenative arylation facilitated by the *β*-silicon effect" by Adam Cook, Aisha Kassymbek, Aref Vaezghaemi, Carlos Barbery, and Stephen G. Newman, currently submitted for publication in a peer-reviewed journal. The dissertation author is the lead author of this manuscript. To supplement the original publication, additional relevant data has been incorporated:

- Section 4.3 is reproduced directly from the literature. Minor modifications were made to the graphics, along with the text, to aid in the flow of this dissertation.
- Sections 4.4, 4.5 and 4.6 are reproduced directly from the literature, with select optimization details, control experiments, substrate scope examples and mechanistic details that were originally present in the supporting information incorporated into the text and expanded upon for clarity. Minor modifications were made to the graphics to aid in the flow and direction of this dissertation.
- Sections 4.7 and 4.8 are original and found exclusively within this thesis.

### Contributions

Unless otherwise noted, the experiments presented within this chapter were conducted by the author of this dissertation. The bis(NHC) ligands that were used in this project were initially synthesized by Carlos. In particular, Carlos was the first to synthesize **L2**, the ligand that was found to be optimal for reactivity. Section 4.6.1, concerning the synthesis and characterization of Ni-**L2** complexes, was primarily conducted by Aisha with experimental assistance by the author of this dissertation. It is included for clarity due to its importance in understanding the nature of the catalyst described within this chapter.



*Chapter four references begin on page 364; experimental details begin on page 331*

## 4.3. Introductory theory and background information

The Suzuki-Miyaura cross-coupling reaction has emerged as a favorite of chemists who seek to rapidly diversify accessible compounds using readily available organoboron nucleophiles.[1] While aryl halides have been the most commonly used electrophiles in this transformation, major efforts have been made to harness C–O bonds such as those found in phenols and their derivatives as pseudohalides. [2] Another substantial goal in cross-coupling chemistry has been to develop methods that can better harness aliphatic coupling partners to allow access to flexible $sp^3$-hybridized carbon linkages.[3]

The union of these two research directions – the cross-coupling of aliphatic alcohols – is still in its infancy.[4] Contemporary strategies for this transformation are predominantly limited to the use of substrates bearing an adjacent π-electron system.[5] The coupling of simple aliphatic alcohols generally requires stoichiometric reagents to first convert the alcohol into an activated intermediate prior to functionalization.[6] Lewis acid/transition metal dual catalysis has recently emerged as an alternative strategy, obviating the necessity of undesirable activating agents.[7] In the previous chapter of this dissertation, a method was detailed that allowed the Suzuki-Miyaura arylation of aliphatic alcohols, facilitated through nickel and bismuth dual catalysis.[8] High-throughput screening revealed bis(NHC) ligands to be essential, though little understanding was gained regarding the role and behaviour of this underexplored class of ligand in this transformation. Unfortunately, this reaction was limited to the functionalization of tertiary alcohols and the mechanism for substrate activation was ambiguous; while the possibility of a carbocation intermediate was speculated, kinetic data was inconclusive.

A key step in all Suzuki-Miyaura cross-coupling reactions is oxidative addition. Common pathways include concerted additions occurring via three-center transition states, $S_N2$-type



*Chapter four references begin on page 364; experimental details begin on page 331*

pathways, and radical mechanisms.[9] In contrast, oxidative addition to a C–X bond (where X = I, Br, Cl, F, OR) by $S_N1$-type mechanisms is seldom considered a possibility, though some related heteroatomic species, including iminium, pyridinium and oxocarbenium ions, have been speculated to react with transition metal catalysts via this type of pathway.[10]

To expand the range of alcohols that can participate in this deoxygenative arylation reaction as well as to probe the viability of an $S_N1$-like oxidative addition, exploitation of the $\beta$-silicon effect was considered. This phenomenon describes the enhanced stability of a carbocation when positioned $\beta$ to a silicon atom,[11] and has recently been exploited in the stabilization of positively charged intermediates in the functionalization of alkynes,[12] aryl systems[13] and C–H bonds[14] (Scheme 4.1a). These reports, alongside disclosures regarding the incorporation of silicon into medicinally active agents,[15] agrochemicals[16] and materials,[17] led to the realization that the inclusion of silicon atoms within a chemical framework may present an underutilized strategy for generating chemical diversity (Scheme 4.1b).



*Chapter four references begin on page 364; experimental details begin on page 331*

**Scheme 4.1.** Silicon as a synthetically and industrially useful heteroatom

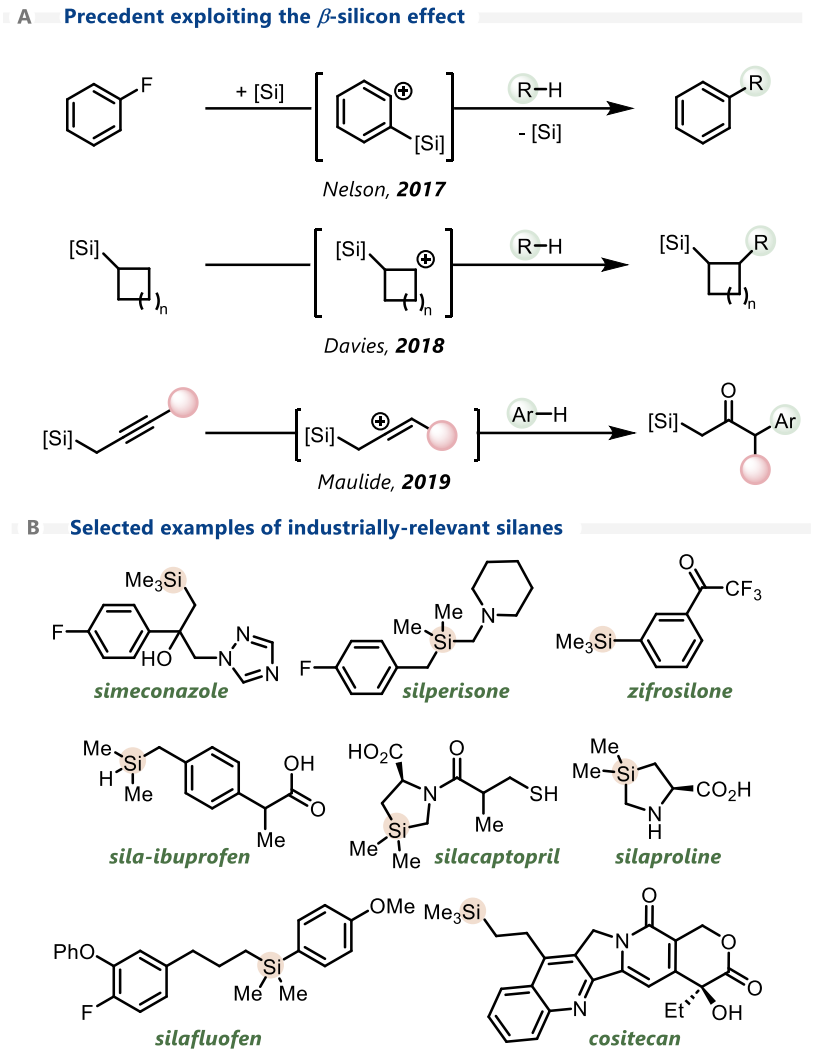


Herein, the development of a method that harnesses the *β*-silicon effect to permit the Suzuki-Miyaura cross-coupling reaction of unprotected primary, secondary and tertiary alcohols is detailed (Figure 4.2). A dual nickel/bismuth catalyst system is shown to be effective. Dimethyldichlorosilane ($Me_2SiCl_2$), an abundant and inexpensive silane, is used as the only stoichiometric activating agent, generating a reactive silyl ether intermediate upon premixing with the substrate. The reaction is found to be facilitated by a novel bis(NHC) ligand. Characterization of nickel(0)-, nickel(I)- and nickel(II)-NHC complexes suggest that these bis(NHC) ligands act as



*Chapter four references begin on page 364; experimental details begin on page 331*

bidentate ligands with relatively large bite angles compared to related complexes. Further, mechanistic studies including kinetic isotope effect experiments, rate equation determination, and an Eyring analysis are all consistent with the formation of a carbocation as a reactive intermediate, providing evidence suggesting that a rare $S_N1$-type oxidative addition might be operative.

**Figure 4.2**. Exploiting the *β*-silicon effect in the arylation of *β*-hydroxysilanes

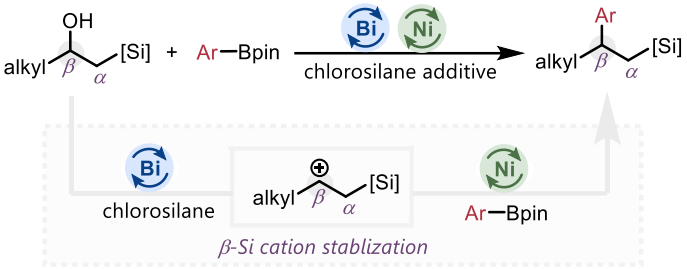


## 4.4. Discovery and optimization of reaction conditions

### 4.4.1. Discovery and optimization synopsis

This study commenced by investigating the Suzuki-Miyuara coupling between phenylboronic acid pinacol ester (PhBpin) and alcohol **4.1**, which features an appropriately positioned silicon atom that can potentially stabilize a carbocation intermediate that might form upon C–O cleavage. The experimental procedure which was identified as optimal involved pre-stirring this alcohol in the presence of $Bi(OTf)_3$, $Me_2SiCl_2$, and $K_3PO_4$ for 15 min at room temperature followed by addition of a nickel catalyst mixture and PhBpin, then heating at 70 °C (Scheme 4.2). The novel bis(NHC) **L2** was found to be optimal, providing the arylated product **4.2** in 86% yield. This ligand was easily recrystallized from isopropanol, allowing the isolation of crystals suitable for X-ray analysis.



*Chapter four references begin on page 364; experimental details begin on page 331*

Both Ni($^t$Bu-stb)$_3$ and NiBr$_2$•glyme could be used as alternative air-stable precatalysts, albeit in lower yield. Control reactions performed both with palladium and in the absence of transition metal catalyst resulted in no conversion. Diverse silanes could also be used, although $Me_2SiCl_2$ consistently outperformed all tested alternatives. The reaction gave 17% yield of **4.2** when no chlorosilane additive was used, suggesting that it increases the yield but that chlorosilanes are not fundamentally necessary in the reaction mechanism. Upon screening Lewis acids, only those derived from bismuth were active, with Bi(OTf)$_3$ affording the highest yields of product.

**Scheme 4.2.** Optimizing Lewis acid, precatalyst and silane in this arylation

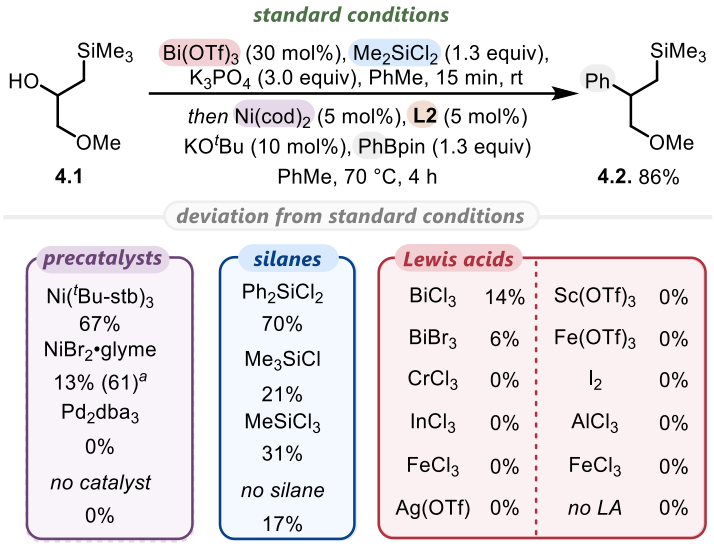


Standard reaction conditions: 0.20 mmol starting material, 0.26 mmol $Me_2SiCl_2$, 0.26 mmol PhBpin, 0.60 mmol $K_3PO_4$, 0.06 mmol Bi(OTf)$_3$, 0.01 mmol Ni(cod)$_2$, 0.01 mmol **L2**, 0.02 mmol KO$^t$Bu in 0. 8 mL PhMe (concentration of overall reaction solution: 0.25 M). Yields acquired by GC-FID using 1,3,5-trimethoxybenzene as internal standard. (*a*) NiBr$_2$·glyme (0.01 mmol) + Mn (0.20 mmol) instead of NiBr$_2$·glyme (0.01 mmol). LA, Lewis acid.



*Chapter four references begin on page 364; experimental details begin on page 331*

The deoxygenative arylation of tertiary alcohols, as disclosed in chapter three of this dissertation, was achieved using bis(NHC) **L1**, which was originally identified by high throughput screening and found to be broadly superior to conventional NHC ligands.[8] In the present work, better understanding and optimization of this ligand scaffold was desired. All phosphines and pyridyl ligands screened were ineffective, while the NHC IPr provided **4.2** in 14% yield (Scheme 4.3). In contrast, **L1** proved moderately effective, permitting the synthesis of **4.2** in a 49% yield. Further investigation was performed on the tether length between the two imidazolium units (**L3**-**L7**), revealing that a three carbon linker was ideal. Introduction of a methyl group on to the backbone (**L8**) increased the yield to 69%. It was hypothesized that these bis-imidazolium scaffolds bound to nickel in a bidentate fashion, thus this increase in yield was attributed to an enforcement of the Thorpe-Ingold effect. This hypothesis ultimately inspired the synthesis of the optimal ligand **L2** which bears a cyclopropyl ring in the backbone. Notably, cyclopropyl groups have been found to be useful when introduced on to the backbone of other bidentate ligands, such as bis-oxazolines and phosphines, where their unique rigidity is proposed to affect the likelihood of bidentate binding to the transition metal catalyst.[18]



*Chapter four references begin on page 364; experimental details begin on page 331*

**Scheme 4.3.** Optimizing ligands in this arylation

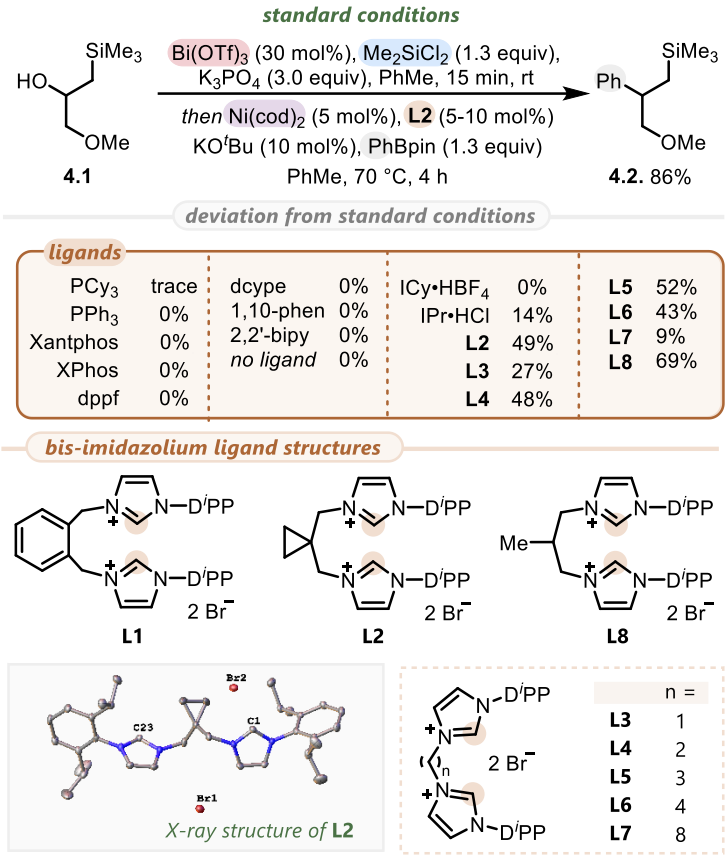


Standard conditions: *As per the footnote of Scheme 4.2*

## 4.4.2. Detailed ligand investigation

A range of ligands were tested over the course of this study (Figure 4.3). Throughout, only NHC ligands afforded any product (Table 4.1). Moreover, only NHC ligands possessing two imidazolium rings [i.e. bis(NHC)s], provided yields in excess of 15%. In the arylation of compound **4.1**, product **4.2** was obtained in 6% yield when using IMes•HCl, 14% yield when using IPr•HCl and 7% when using ligand **L9**.



*Chapter four references begin on page 364; experimental details begin on page 331*

**Table 4.1.** Phosphine, pyridyl and other ligands tested in this arylation

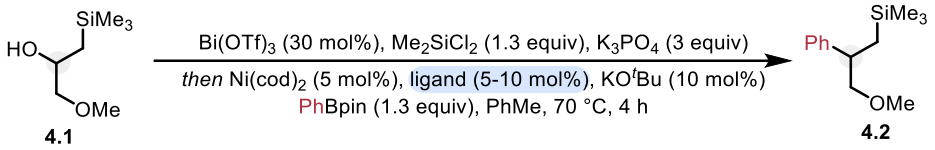


| entry | ligand | % yield, 4.2 |
|---|---|---|
| **1** | *no ligand* | 0 |
| **2** | IPr•HCl (10 mol%) | 14 |
| **3** | IMes•HCl (10 mol%) | 6 |
| **4** | SIPr•HCl (10 mol%) | 0 |
| **5** | ICy•$HBF_4$ (10 mol%) | 0 |
| **6** | **L2** (10 mol%) | 84 |
| **7** | **L2** (5 mol%) | 86 |
| **8** | **L1** (5 mol%) | 49 |
| **9** | **L3** (5 mol%) | 27 |
| **10** | **L4** (5 mol%) | 48 |
| **11** | **L5** (5 mol%) | 52 |
| **12** | **L6** (5 mol%) | 43 |
| **13** | **L7** (5 mol%) | 9 |
| **14** | **L8** (5 mol%) | 69 |
| **15** | **L9** (10 mol%) | 7 |
| **16** | $PPh_3$ (10 mol%) | 0 |
| **17** | $PCy_3$ (10 mol%) | trace |
| **18** | Xantphos (10 mol%) | 0 |
| **19** | dppf (10 mol%) | 0 |
| **20** | dppp (10 mol%) | 0 |



*Chapter four references begin on page 364; experimental details begin on page 331*

| | | |
|---|---|---|
| **21** | XPhos (10 mol%) | 0 |
| **22** | 1,10-phenanthroline (10 mol%) | 0 |
| **23** | 2,2'-bipyridine (10 mol%) | 0 |

**Figure 4.3.** Structures of ligands used in this optimization

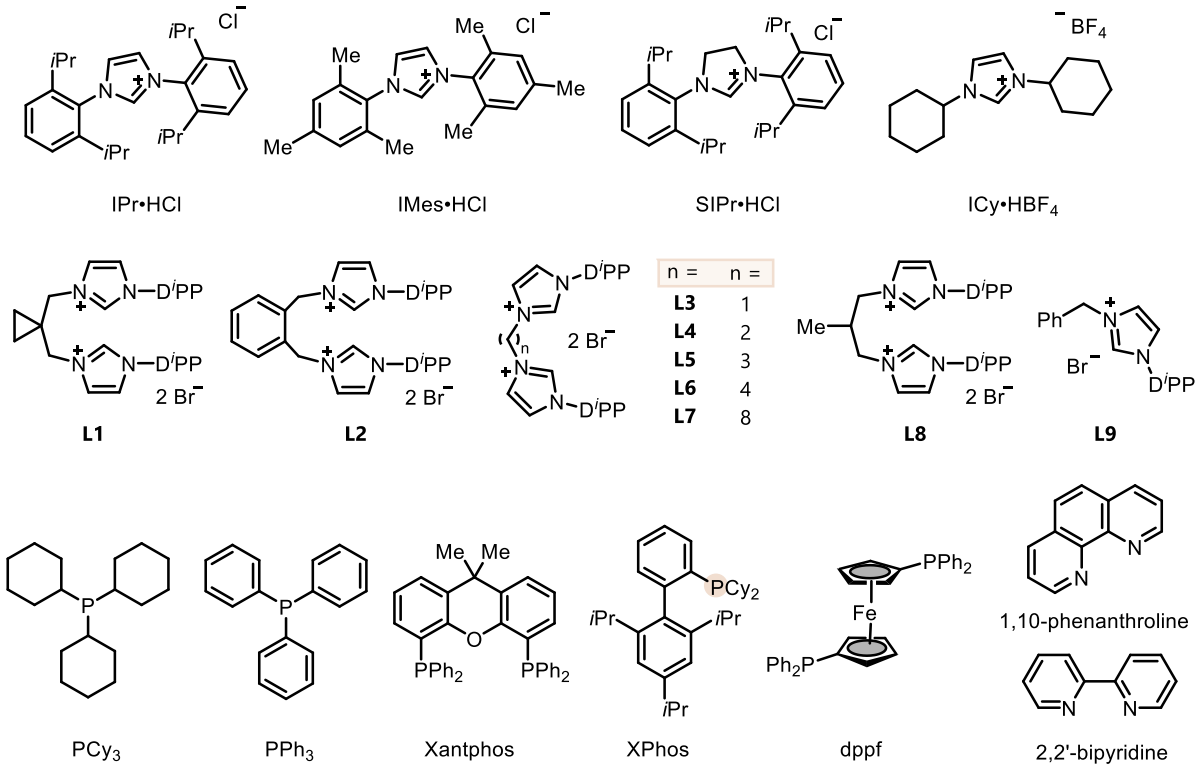


Noting the privileged reactivity of bis(NHC)s, a library of such species was synthesized with the goal of discovering what structural features of the ligand had the largest impact on reactivity. Using **L1** as the model ligand, three distinct features were identified as those that could affect reactivity: the aryl system on the imidazolium, the chain length between imidazolium rings, and the backbone structure (Figure 4.4).



*Chapter four references begin on page 364; experimental details begin on page 331*

**Figure 4.4.** Dissecting the structure of bis(NHC)s.

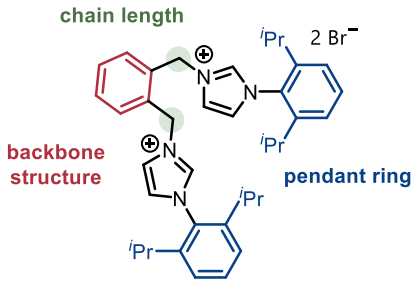


Ultimately, a library of thirteen bis(NHC)s were synthesized and tested in the arylation of *β*-hydroxysilanes (Scheme 4.4). The relationship between chain length and chain substitution was discussed within Scheme 4.3, wherein chain lengths of three, alongside increased substitution, were optimal. Further, incorporating cyclohexyl (**L10**) or quinazoline (**L11**) rings into the backbone of the ligand shut down reactivity. Altering the aryl system on the pendant ring had a small impact on reactivity (**L12**, **L13**), while switching the aryl system for an *N*-butyl group led to a substantial decrease in yield (**L14**).



*Chapter four references begin on page 364; experimental details begin on page 331*

**Scheme 4.4.** Systematic investigation into the effect of NHC structures on reactivity

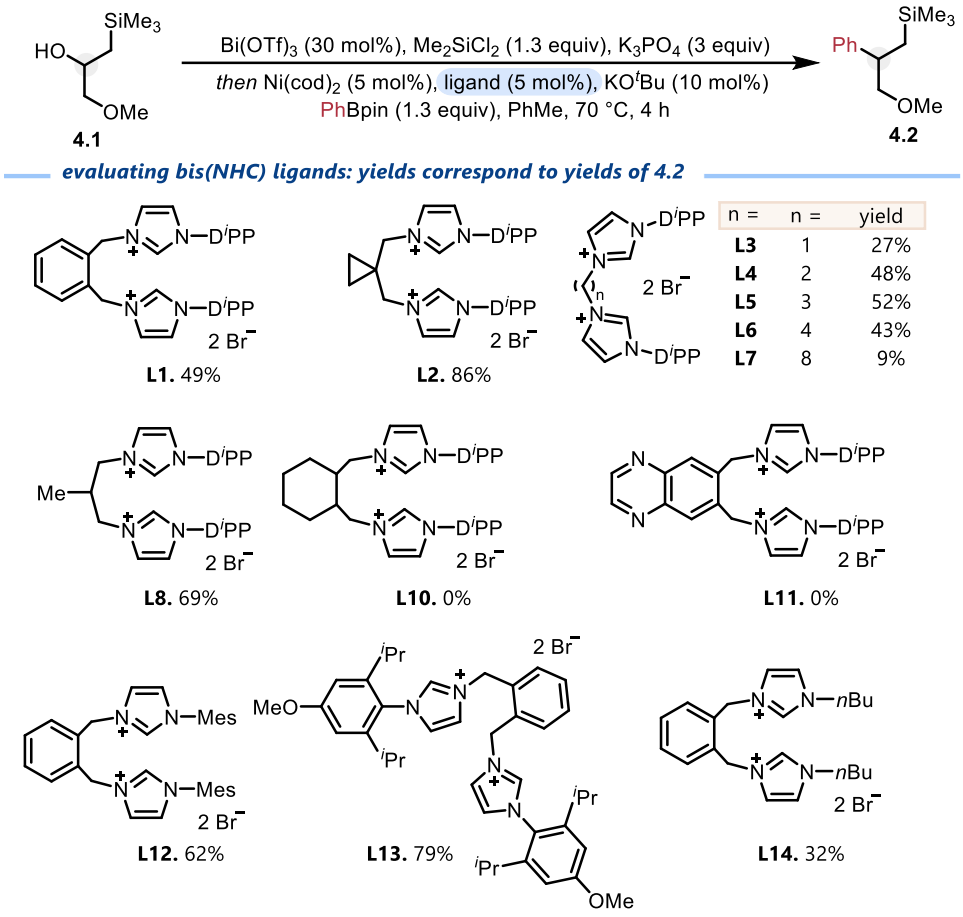


A 2018 review article details advances made in the synthesis and applications of bis(NHC) ligands, focusing specifically on their applications in transition metal mediated transformations.[19] Within, authors note that the overwhelming majority of bis(NHC)s possess five-membered imidazole-2-ylidene rings. This is common within all of the ligands that were studied within this chapter. A range of strategies exist for the synthesis of bis(NHC)s. The strategy employed to synthesize **L2**, as well as the majority of other ligands tested in this arylation, involves the *N*-substitution of pre-synthesized imidazoles with a dihaloalkane.[20] Relative to the ligands studied in this work, it is of note that most examples of bis(NHC)s with linkers greater than two carbons in



*Chapter four references begin on page 364; experimental details begin on page 331*

length bear -$CH_3$, -*n*Bu or -$^t$Bu *N*-substitutents. In fact, the authors of the aforementioned review article[19] note that examples of *N*-aryl bis(NHC)s are frequently encountered as dinuclear upon complexing with a metal, with the bis(NHC) ligand in a bridging binding mode, speculating that this is due to the high strains associated with forming chelate rings around a metal center.

### **4.4.3.** Synthesis of *β*-hydroxysilanes

Amongst the most general methods to introduce an activating silane moiety this moiety *β*- to the target C–O bond – and the method used in the synthesis of most silanes examined in this chapter – is via a conventional Grignard addition with commercially available $Me_3SiCH_2MgCl$ ($227 CAD/100 mL as a 1.0 M solution in diethyl ether from Sigma Aldrich) (Scheme 4.5). A diverse range of chloromethylsilanes (i.e. silanes of the general form $R_3SiCH_2Cl$) are also available that can be transformed into their corresponding Grignard reagents in house.

**Scheme 4.5.** Synthesis of *β*-hydroxysilanes

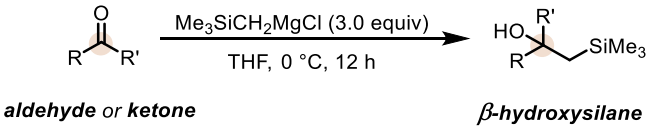




Chapter four references begin on page 364; experimental details begin on page 331

## 4.5. Substrate scope

### 4.5.1. Substrate scope overview

With optimized conditions identified, attention was towards the scope of this reaction. A range of *β*-hydroxysilanes could be arylated (Scheme 4.6). Secondary (**4.2-4.7**), tertiary (**4.8**) and primary (**4.9, 4.10**) scaffolds were readily arylated in 73-92% yield. Heterocycle-containing alcohols were also tolerated (**4.11-4.13**). Attempting the reaction on an alcohol in the absence of a silyl activating group did not afford product (**4.14**); this alcohol was chosen as it is the carbon analog of the *β*-hydroxysilane that was arylated to yield product **4.3**. Varying the boronate ester coupling partner revealed that the reaction succeeds regardless of the electronic or steric properties of this coupling partner (**4.15-4.24**). Heterocycle-containing boronate esters including a benzothiophene (**4.25**), benzofuran (**4.26**), benzodioxole (**4.27**), pyridine (**4.28**), morpholine (**4.29**) and carbazole (**4.30**) were also efficient, albeit with slightly lower yields than non-heterocyclic variants. A benzyl boronate pinacol ester could also be employed, demonstrating this method to be successful in the synthesis of C($sp^3$)–C($sp^3$) bonds (**4.31**). While most of the scope was evaluated with a trimethylsilyl group, this was not a limitation as the reaction proved similarly effective in the presence of triethyl (**4.32**), phenyldimethyl (**4.33**) and tertbutyldimethyl (**4.34**) silanes. Silyl ethers (**4.35**, **4.36**) were also effective starting materials, enabling the reaction to proceed without the initial pre-mixing step with $Me_2SiCl_2$. However, use of benzyl ether **4.37** provided only recovery of starting material, further suggesting that silicon plays an important role in the reaction's success.

The reaction was also found to work with $NiBr_2$·glyme as a catalyst in the presence of manganese, obviating the strict requirement for air sensitive $Ni(cod)_2$ in the synthesis of **4.2**, **4.4**,



*Chapter four references begin on page 364; experimental details begin on page 331*

**4.7**, **4.31**, and **4.32**. Moreover, this reaction was found successfully scaled up to the gram scale, synthesizing product **4.9** in 82% yield even upon reducing the catalyst loading to 2.5%.

**Scheme 4.6.** Substrate scope

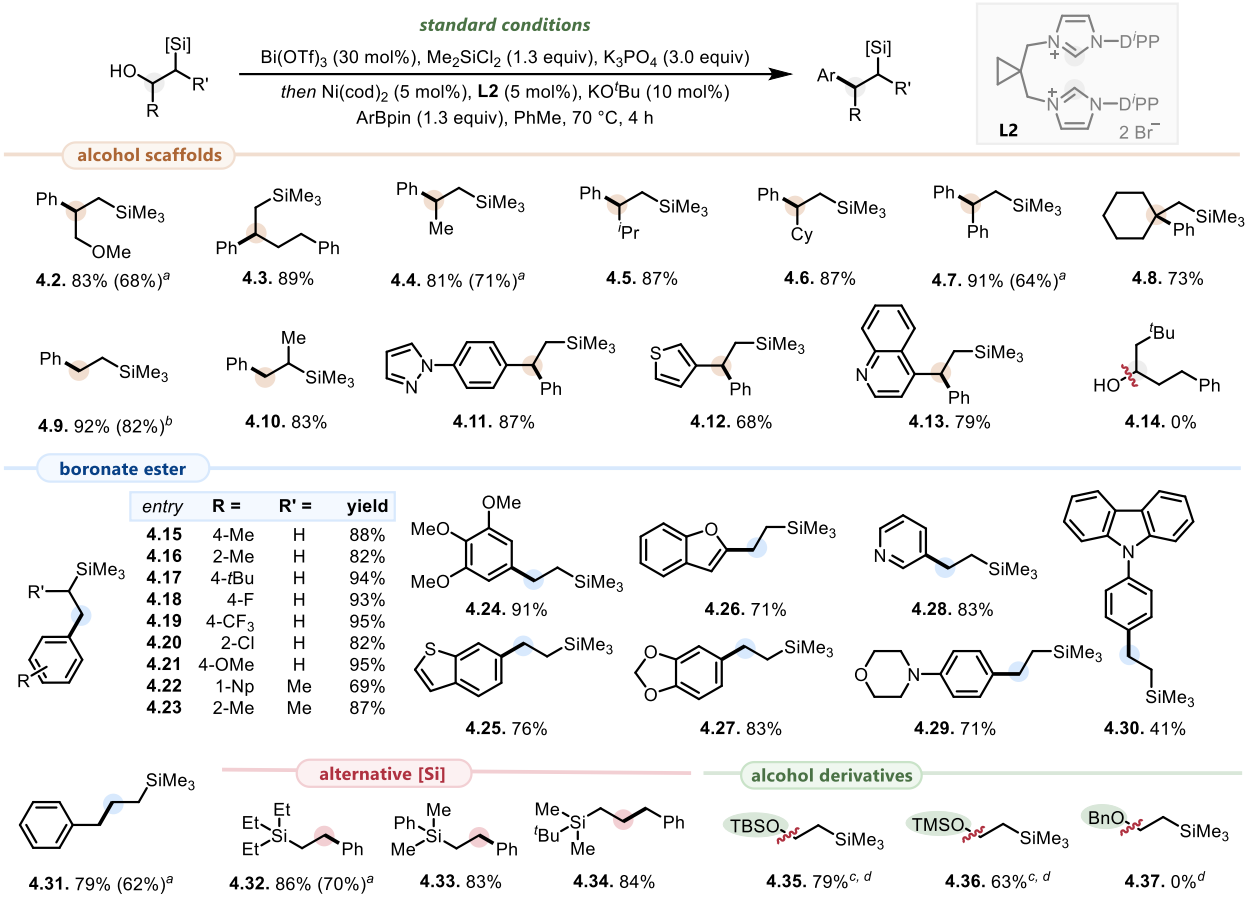


Standard reaction conditions: 0.20 mmol starting material, 0.26 mmol $Me_2SiCl_2$, 0.26 mmol PhBpin, 0.60 mmol $K_3PO_4$, 0.06 mmol $Bi(OTf)_3$, 0.01 mmol $Ni(cod)_2$, 0.01 mmol **L2**, 0.02 mmol KO$^t$Bu in 0.8 mL PhMe. Yields are isolated. (a) $NiBr_2$·glyme (0.01 mmol) + Mn (0.20 mmol) instead of $Ni(cod)_2$. (b) Yield obtained upon reacting 1.0 g (8.47 mmol) of substrate; 0.42 mmol $Ni(cod)_2$, 0.42 mmol **L2**, 0.84 mmol KO$^t$Bu. (c) Reaction performed in the absence of $Me_2SiCl_2$.



*Chapter four references begin on page 364; experimental details begin on page 331*

### 4.5.2. Derivatization of products

Lastly, while there are many instances where the inclusion of silicon in these arylated products is desirable, an investigation of methods to derivatize these materials was conducted. The oxidation method developed by Matsunaga (Scheme 4.7a)[21] was applied to different products to confirm that the silicon atom can be a useful synthetic handle (**4.38, 4.39**). It was serendipitously found that treating silane **4.2** with $Et_3SiH$ and TFA at 85 °C resulted in the formation of protodesilylation product **4.40**; this reactivity was extended to the protodesilylation of compounds **4.6** and **4.8** to form **4.41** and **4.42**, respectively (Scheme 4.7b). Protodesilylation of benzyl, allyl, and aryl silanes is well established,[22] while alkyl silanes generally require extremely harsh conditions for C–Si bond-cleavage.[23] The neighbouring Ph ring likely plays a key role in facilitating the protodesilylation. Further evaluation of this reaction, including mechanism, generality, optimization, and scope, are underway in the Newman lab.

**Scheme 4.7.** Derivatization of product compounds

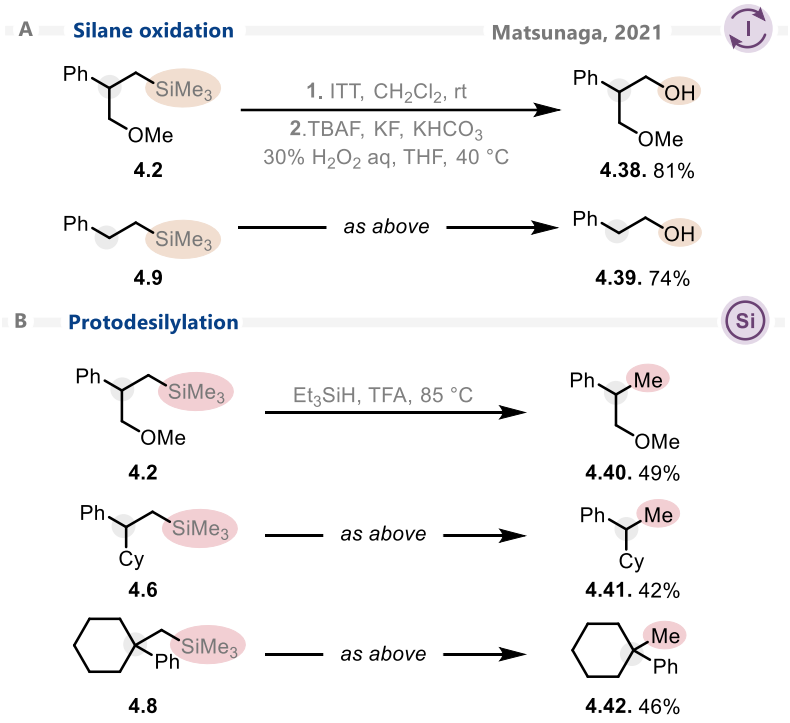




*Chapter four references begin on page 364; experimental details begin on page 331*

### **4.5.3**. Unsuccessful scope examples

Numerous compounds were found to be unreactive upon subjection to the general reaction conditions (Figure 4.5). The foremost limitation of this method is the restriction to $\beta$-hydroxysilanes. In the absence of a silane group, no product was observed (**4.43**). The reaction also failed to afford product if $\alpha$-hydroxysilanes or $\gamma$-hydroxysilanes were utilized (**4.44, 4.45**). Ethers or other protected analogs of $\beta$-hydroxysilanes were not suitable substrates under the standard reaction conditions (**4.46, 4.37, 4.47**). Geometrically constrained $\beta$-hydroxysilanes were not arylated (**4.48**). Finally, variously functionalized boronate esters (**4.49**-**4.58**) failed to produce the desired product upon subjection to the general reaction conditions with 1-methoxy-3-(trimethylsilyl)propan-2-ol (**4.1**).

**Figure 4.5**. Unsuccessful substrates

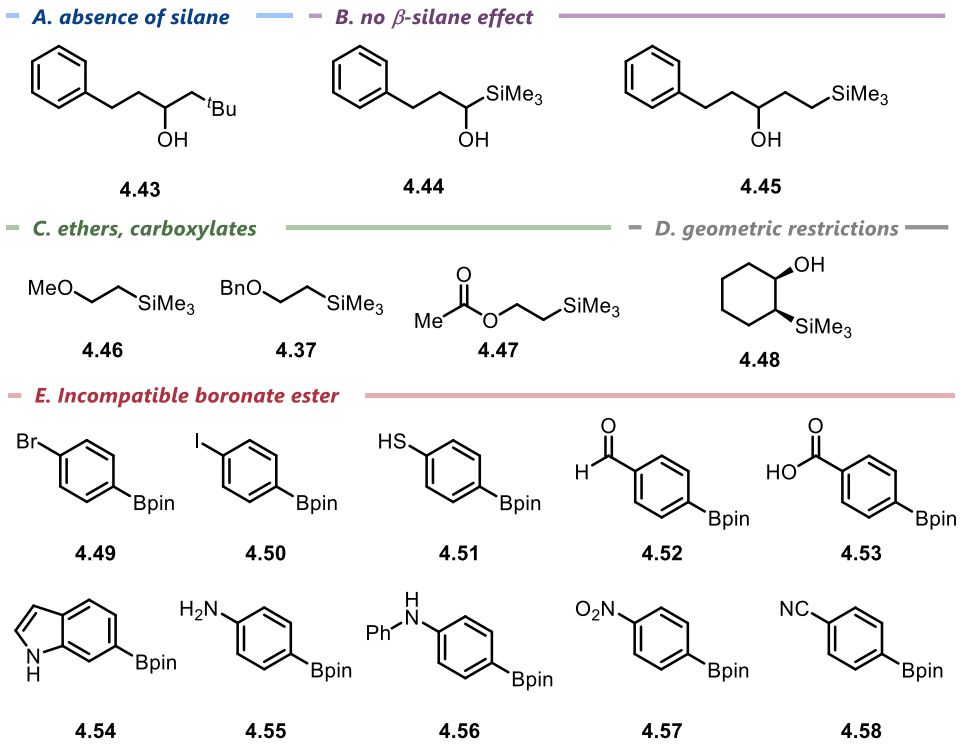




*Chapter four references begin on page 364; experimental details begin on page 331*

## 4.6. Mechanistic investigations

### 4.6.1. Investigating nickel-**L2** complexes

Throughout this study, the apparently distinct ability of bis(NHC)s to promote reactivity stimulated intrigue. While bis(NHC) ligands with one carbon linker between imidazolium rings, as in **L3**, are well-studied,[24] the use of longer linkers is relatively rare, especially when bearing *N*-aryl substituents.[25,26] Previous reports concerning bis(NHC) ligands have demonstrated that they may coordinate to metal centers in a *cis*-bidentate, *trans*-bidentate or multi-metallic fashion.[19, 25g] To gain deeper insight into the binding mode and role of **L2** in this transformation, attention was turned towards the preparation of well-defined nickel-**L2** complexes

Initial attempts to prepare a nickel(0) complex from $Ni(cod)_2$ and the bis(NHC) **L2** resulted in the unexpected formation of a nickel(II) peroxo complex (**4.59**) (Scheme 4.8).[27] Repeating this reaction in the presence of dry oxygen enabled the clean isolation of **4.59**, with crystals suitable for X-ray analysis being grown from concentrated THF. The monometallic, bidentate nature of the bis(NHC) ligand was confirmed, and the nickel center was found to adopt a distorted square planar geometry with Ni-C1 and Ni-C23 bond lengths of 1.912(5) Å and 1.924(5) Å, respectively, and a C1-Ni1-C23 bond angle of 105.39(19)°. The peroxo character of the dioxygen was suggested by the observed bond distance of 1.458(5).[28]



*Chapter four references begin on page 364; experimental details begin on page 331*

**Scheme 4.8.** Preparation and solid state structure of nickel(II)-peroxo complex **4.59**

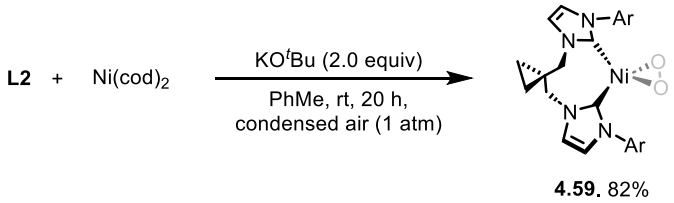


**4.59.** 82%

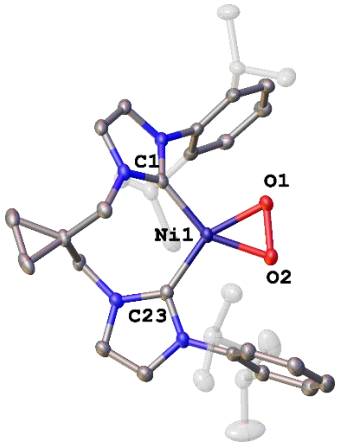


A nickel(I) complex was unexpectedly obtained by treatment of a mixture of **L2** and $NiBr_2$•glyme with three equivalents of KO$^t$Bu, affording **L2**-nickel(I) bromide (**4.60**) (Scheme 4.9).[29] Notably, the isolation and characterization of such nickel(I) species is scarce in the literature,[30] and this author is unaware of any reports of isolated nickel(I) complexes with bis(NHC) ligands. Analysis of the crystal structure of **4.60** revealed Ni-C1 and Ni-C23 bond lengths of 1.933(9) Å and 1.925(10) Å, respectively, and a C1-Ni1-C23 bond angle of 109.6(4)°. $^1$H NMR analysis of the isolated complex reveals the existence of a single paramagnetic species.



*Chapter four references begin on page 364; experimental details begin on page 331*

**Scheme 4.9.** Preparation and solid state structure of nickel(I)-bromide complex **4.60**

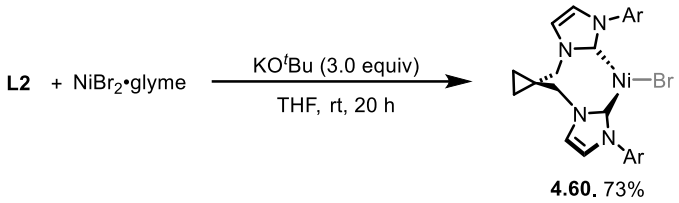


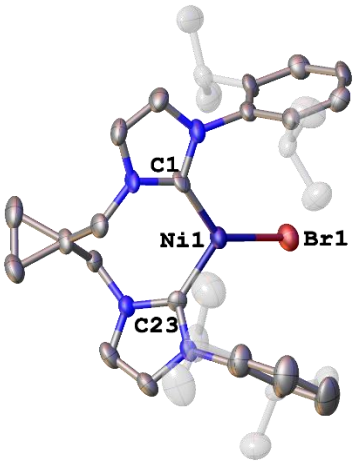


Towards accessing a nickel(0) species, a a mixture of $Ni(cod)_2$, **L2** and KO$^t$Bu was treated with one equivalent of 3,3'-bistrifluoromethylstilbene,[31] affording **L2**-nickel(0) complex **4.61** (Scheme 4.10). While the crystals obtained were weakly diffracting, providing a low resolution structure, the observation of connectivity was permitted, which confirmed that *p*-$CF_3$ stilbene is coordinated in an $\eta^2$ fashion, with a $^1$H NMR signal of stilbene appearing at 2.98 ppm.[32] A second nickel(0) complex was obtained as a mixture of isomers (**4.62**, **4.63**) through the simple reaction of $Ni(cod)_2$ with **L2** in the presence of KO$^t$Bu (Scheme 4.11). Analysis of the crystal structure of this species revealed Ni-C1 and Ni-C23 bond lengths of 1.880(2) Å and 1.905(3) Å, respectively, and a C1-Ni1-C23 bond angle of 108.39(1)° in complex **4.62** and Ni-C1 and Ni-C23 bond lengths of 1.888(2) Å and 1.893(2) Å, respectively, and a C1-Ni1-C23 bond angle of 106.56(10)° in complex **4.63**.



*Chapter four references begin on page 364; experimental details begin on page 331*

**Scheme 4.10**. Preparation and solid state structure of nickel(0)-stilbene complex **4.61**

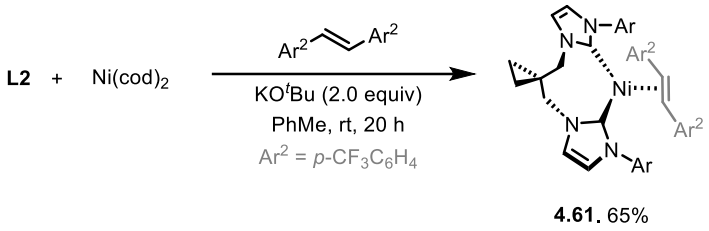


**4.61.** 65%

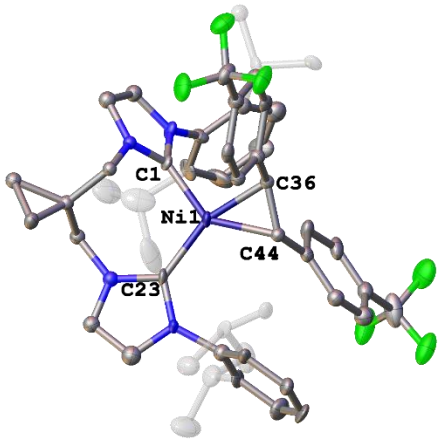


**Scheme 4.11**. Preparation and solid state structure of nickel(0)-cod complexes **4.62** and **4.63**

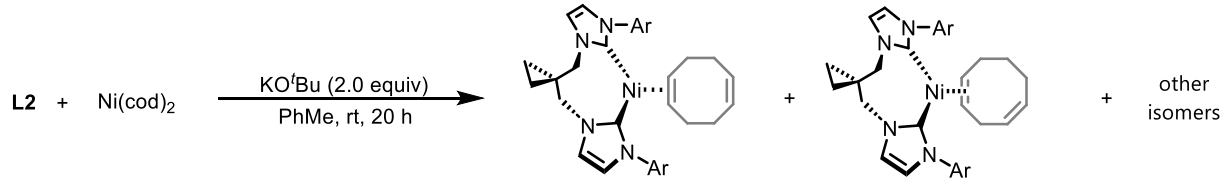


**4.62** **4.63**

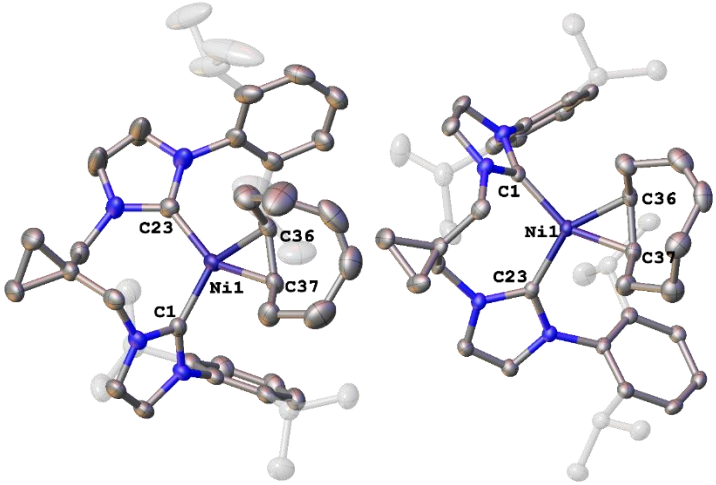




*Chapter four references begin on page 364; experimental details begin on page 331*

Notably, all these isolated nickel-**L2** complexes are monometallic, featuring bidentate coordination with relatively wide bite angles (105-109°) compared to well-established complexes with one-carbon linkers (91-94°).[24] These bite angles are consistent with common phosphine bite angles. For example, the one-carbon linker bis(NHC)s are comparable to bisphosphines that make 6-membered ring chelates, such as dppp (bite angle = 87°), while longer chain linkers, as in **L2**, give bite angles more comparable to bisphosphines that make 8-membered ring chelates such as DPEphos (102-104°) or Xantphos (108-111°).[33] Wider bite angles in bidentate phosphines have been shown to promote reductive elimination over β-hydride elimination.[34] For instance, in a 1984 report from Hayashi and colleagues, a direct correlation was observed in the coupling of aryl halides (**4.64**) with alkyl-hybridized organometallic coupling partners (**4.65**) between the bite angle of phosphine ligands and the branched (**4.66**) to linear (**4.67**) product ratio (Scheme 4.12).[34a] A similar concept may be operative in this nickel-catalyzed arylation in facilitating the cross-coupling of aliphatic alcohols.

**Scheme 4.12.** Effect of bite angle on reactivity for a series of phosphine ligands

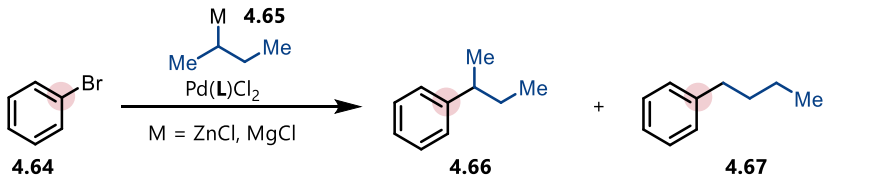


| L | bite angle | yield of branched product |
|---|---|---|
| dppf | 99.1° | 95% |
| dmpe | 90.6° | 43% |
| dppe | 85.8° | <5% |

To evaluate the reactivity of these novel complexes, they were used as catalysts in the deoxygenative arylation of silylated alcohol **4.35** (Scheme 4.13). Nickel(0) catalysts afforded both



Chapter four references begin on page 364; experimental details begin on page 331

the fastest initial reaction rates and, after 4 hours, the highest yields, with nickel(0) complex **4.61** slightly outperforming free **L2** alongside $Ni(cod)_2$. Nickel(II) complex **4.59** as well as the in situ formed catalyst from $NiBr_2$•glyme and **L2** were each inactive in the absence of Mn reductant, but became catalytically active in the presence of Mn after a brief induction period. Lastly, nickel(I) complex **4.60** reacted sluggishly, affording less than 50% yield of product **4.9** in the presence or absence of manganese. Overall, these data suggest that the active catalyst is likely nickel(0) and that nickel(II) is a viable precursor provided that a reductant is included to facilitate generation of the active catalyst.

**Scheme 4.13.** Reactivity of different nickel species

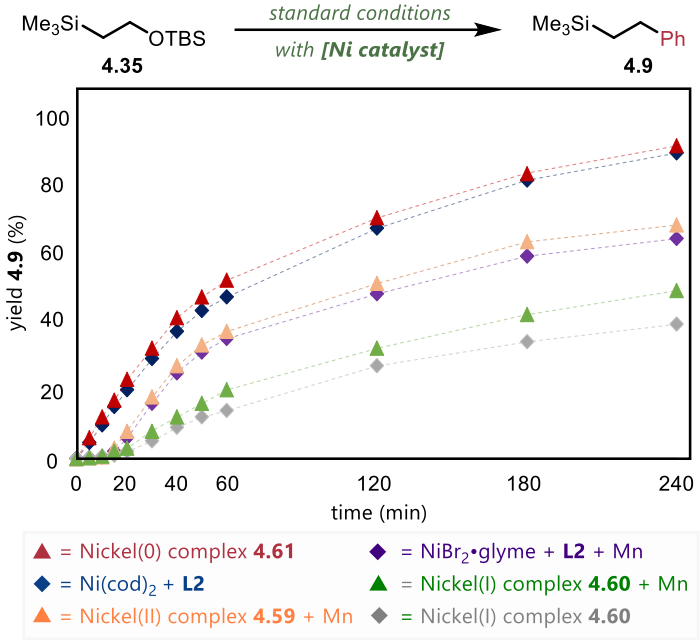




*Chapter four references begin on page 364; experimental details begin on page 331*

## **4.6.2.** Kinetic evaluation of reaction mechanism

### 4.6.2.1. Variable time normalization analysis

With knowledge of the nickel-**L2** catalyst in hand, an investigation was launched to probe if the reaction might be proceeding through an $S_N1$-type pathway as was originally speculated. A kinetic analysis was performed according to the variable time-normalization analysis method (Scheme 4.14).[35] A silyl ether (**4.68**) was chosen for this analysis to directly study the key C–O bond-cleaving step independent of the silylation step. A first-order dependence on both Lewis acid (Figure 4.6) and substrate (Figure 4.7) was observed, alongside a zeroth order dependence on ArBPin (Figure 4.8) and the nickel-**L2** catalyst (Figure 4.9). These results are consistent with a rate-determining step involving the Lewis acid-catalyzed generation of a carbocation intermediate.

**Scheme 4.14.** Kinetic data was obtained for the arylation of compound **4.68**.

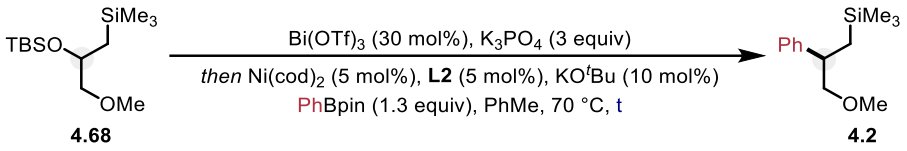




*Chapter four references begin on page 364; experimental details begin on page 331*

**Figure 4.6.** Investigating the rate dependence on $[Bi(OTf)_3]$

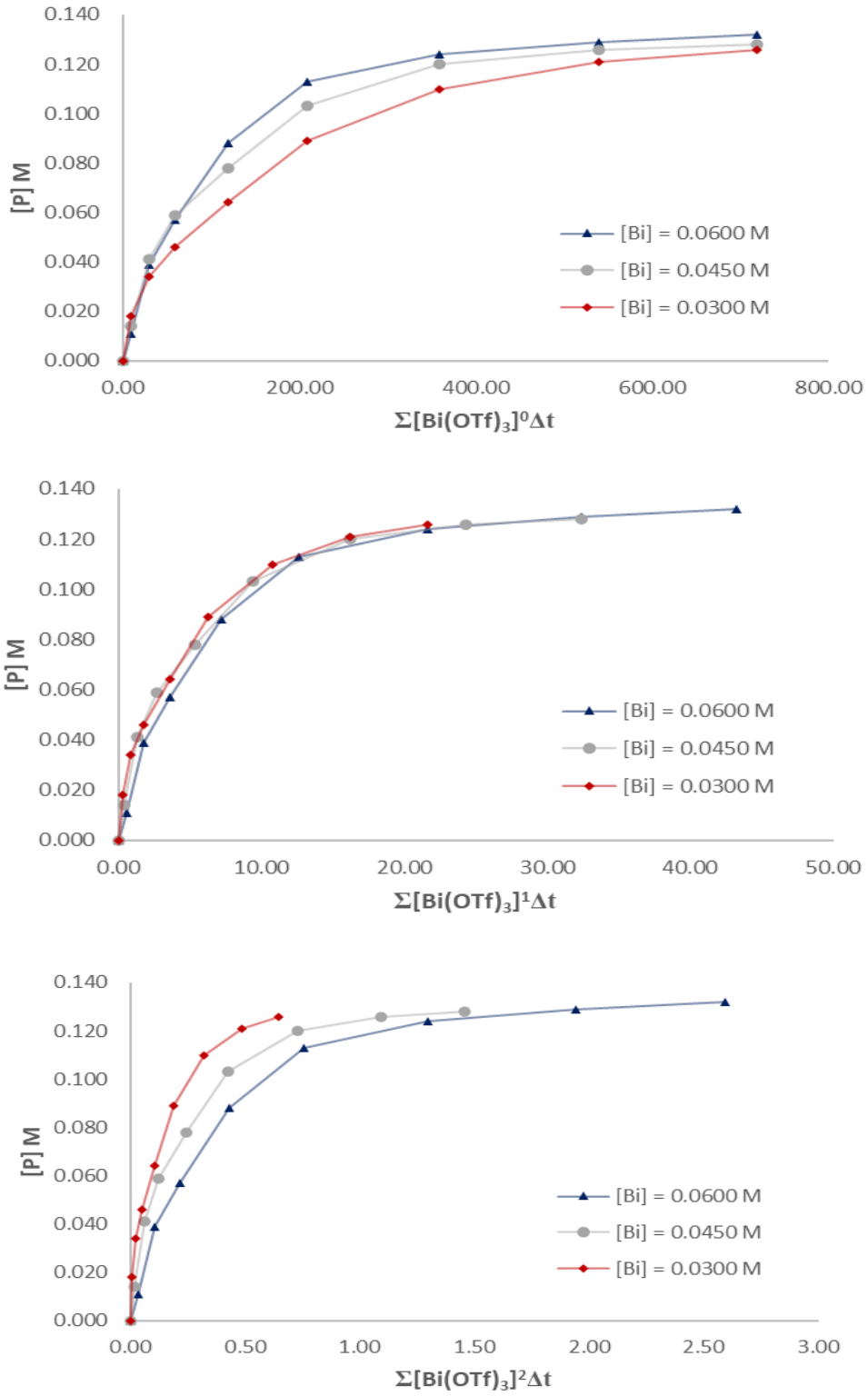




*Chapter four references begin on page 364; experimental details begin on page 331*

**Figure 4.7.** Investigating the rate dependence on [substrate]

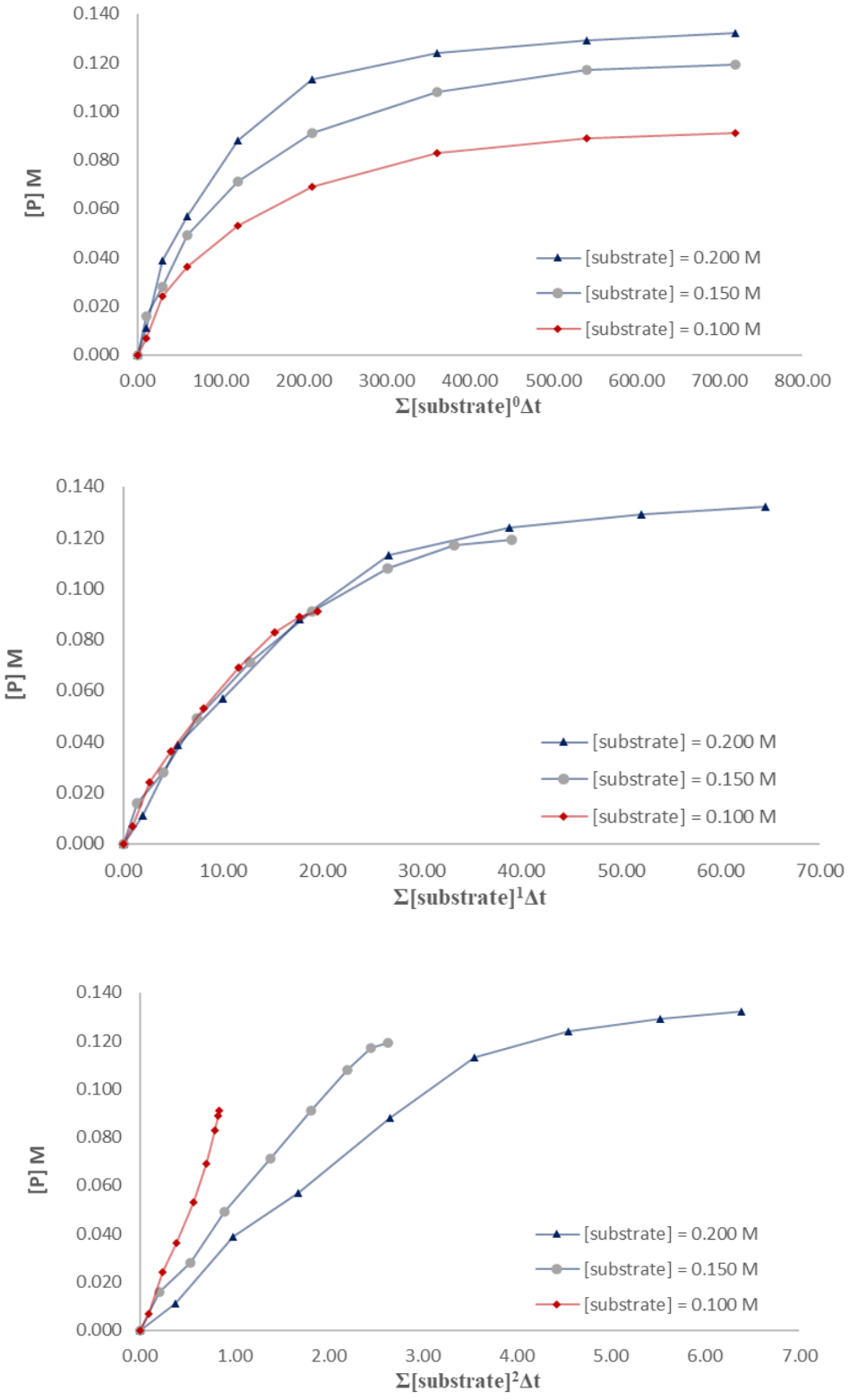




*Chapter four references begin on page 364; experimental details begin on page 331*

**Figure 4.8.** Investigating the rate dependence on [PhBpin]

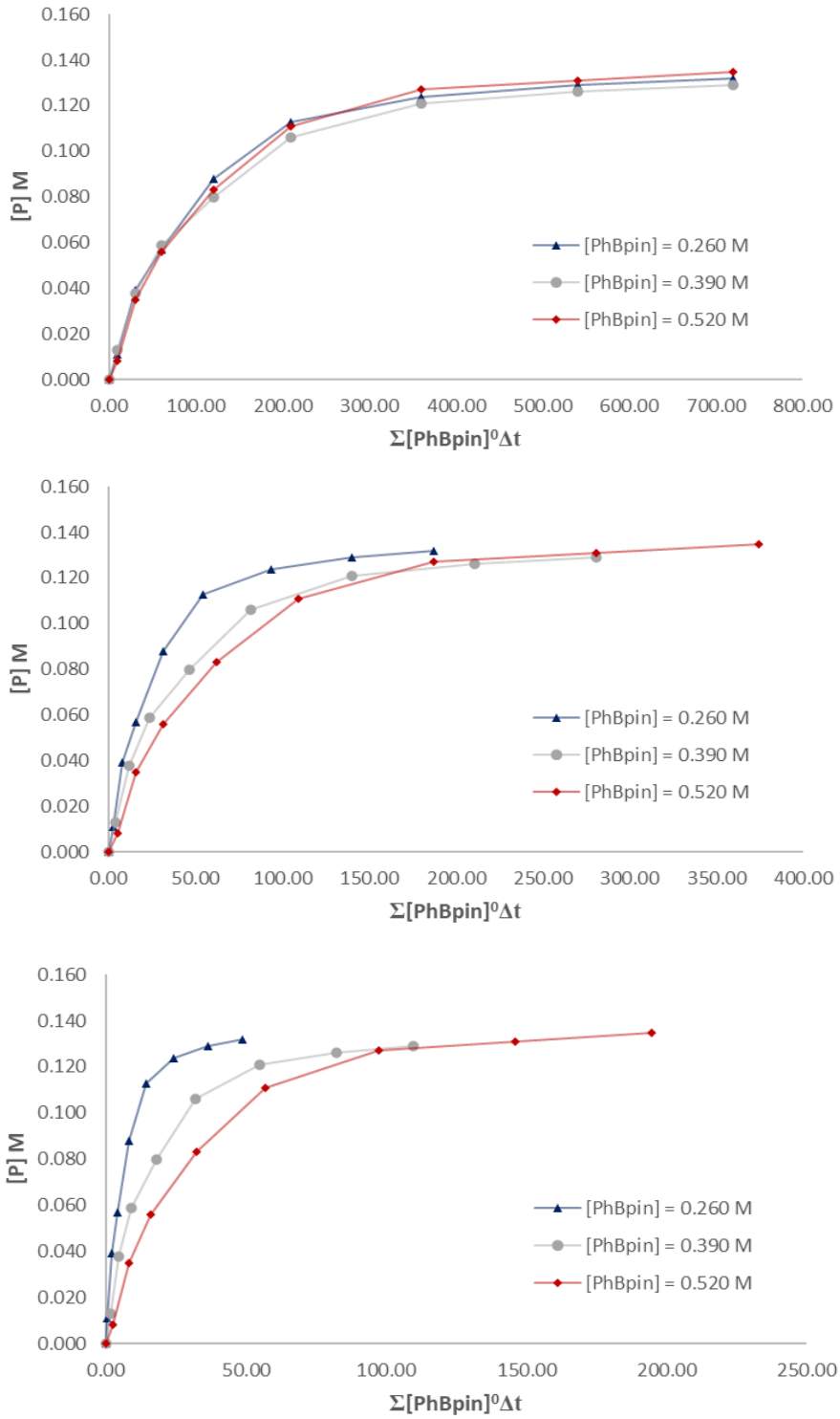




*Chapter four references begin on page 364; experimental details begin on page 331*

**Figure 4.9.** Investigating the rate dependence on [Ni-**L2**] catalyst

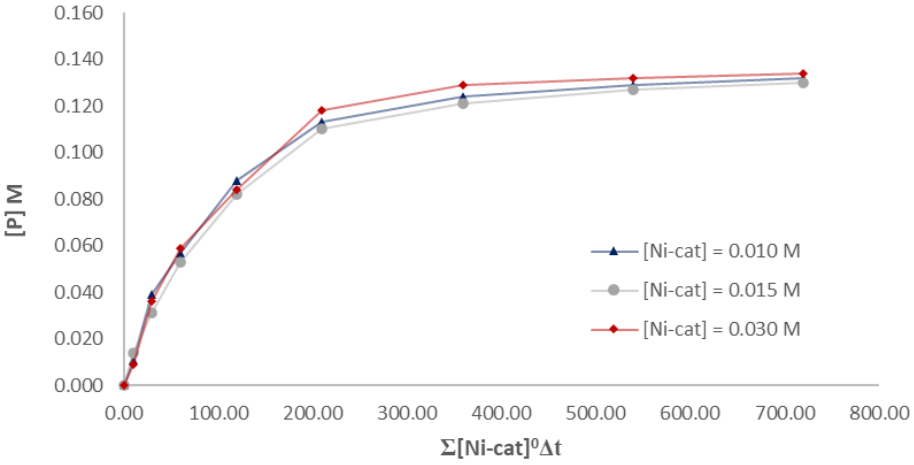


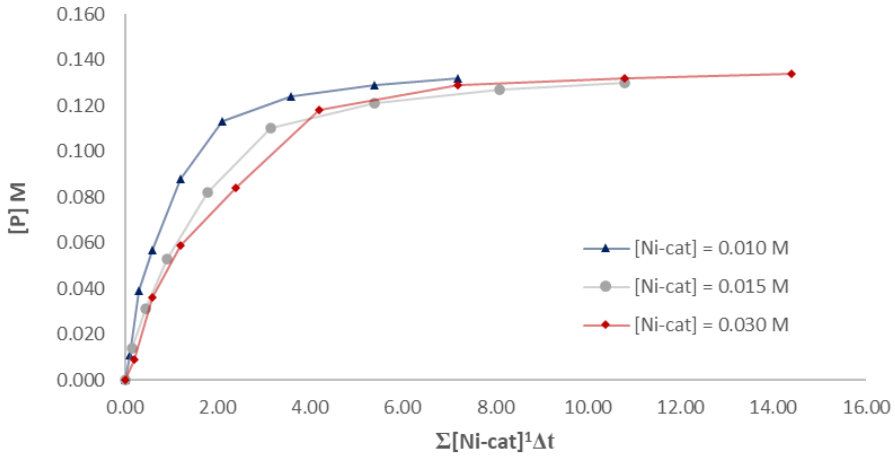


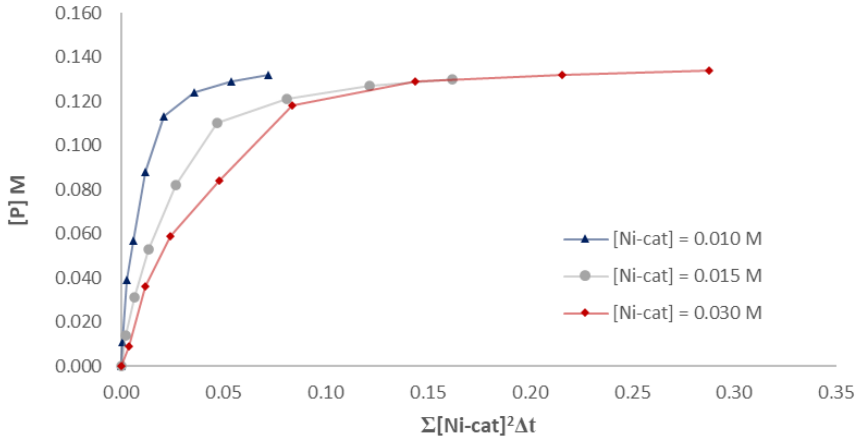




*Chapter four references begin on page 364; experimental details begin on page 331*

### 4.6.2.2. Eyring analysis

To determine the activation parameters for this transformation, an Eyring analysis was conducted with respect to the arylation of compound **4.68**. Plotting the rate constant data obtained at a range of different temperatures according to the Eyring equation revealed a linear plot (Scheme 4.15). Entropies of activation ($\Delta S^{\ddagger}$) were calculated by multiplying the value of the calculated intercept by R (universal gas constant), and enthalpies of activation ($\Delta H^{\ddagger}$) were calculated by multiplying the inverse slope of each of the Eyring plots by R (universal gas constant). Ultimately, this analysis revealed significant bond cleavage ($\Delta H^{\ddagger}$ = 29.9 kcal mol$^{-1}$) along with an increase in entropy ($\Delta S^{\ddagger}$ = 15.2 cal mol$^{-1}$ K$^{-1}$) at the time of the transition state.[36] Once more, the values of activation parameters as calculated from Eyring analyses, particularly the entropy of activation, are error prone. To increase the accuracy of this analysis, kinetic experiments should have been conducted in triplicate.

**Scheme 4.15.** Eyring analysis for the arylation of compound **4.68**

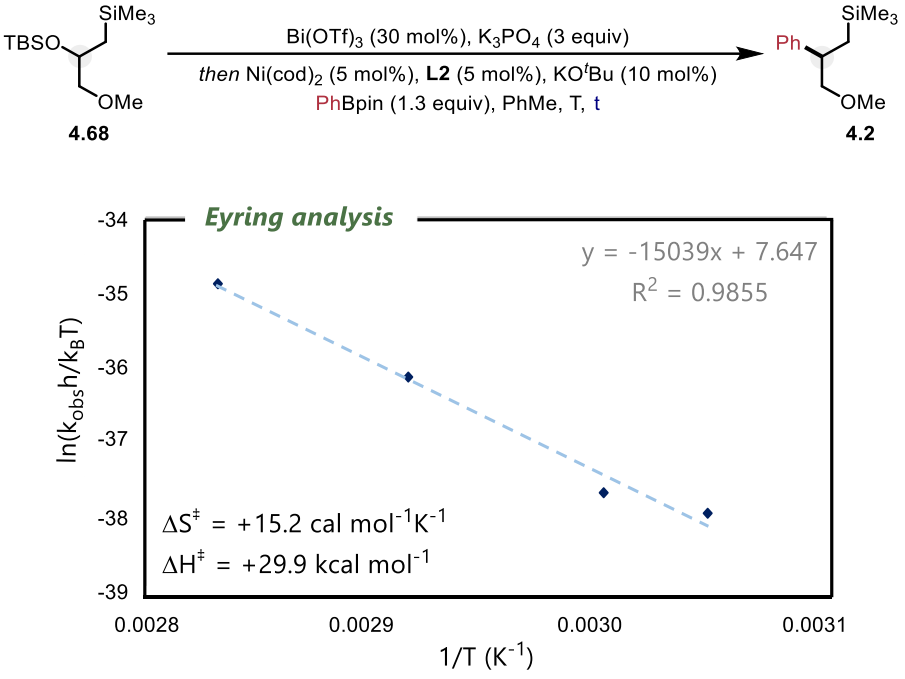




*Chapter four references begin on page 364; experimental details begin on page 331*

### 4.6.2.3. Kinetic isotope effect

The initial rate kinetics for substrate **4.68$_H$** were examined alongside its deuterated analog **4.68$_D$** in order to investigate the kinetic isotope effects of this reaction (Scheme 4.16). This experiment was repeated in triplicate to ensure accuracy. The average of the approximate rate constants of the arylation of **4.68$_H$** was determined to be 0.001358 and the average of the approximate rate constants of the arylation of **4.68$_D$** was determined to be 0.001066. These values were divided (i.e. $k_H/k_D$) to determine a kinetic isotope effect of **1.27**. This kinetic isotope suggests that the hybridization of the deuterated carbon atom changes from $sp^3$ to $sp^2$ at the time of the transition state of this reaction; this is consistent with a mechanism proceeding via the generation of a carbocation.

**Scheme 4.16.** Results of the kinetic isotope effect experiments

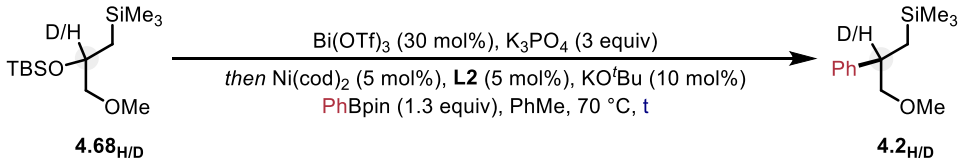


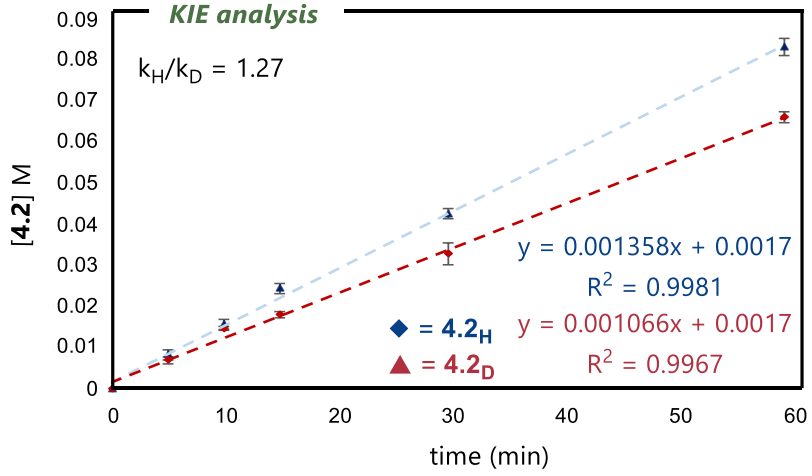




*Chapter four references begin on page 364; experimental details begin on page 331*

### 4.6.2.4. Time-course diagram comparison with different ligands

During this study, interest was garnered regarding the fate of the starting material upon exposure to the standard reaction conditions in the presence of different ligands (Scheme 4.17). In the presence of **L2**, the arylation of **4.35** led to the observation of 92% of the expected product **4.9**, 2% of starting material and 4% of the vinyl silane **4.69**, which is believed to be the product of an elimination reaction. Utilizing **L7** instead of **L2** afforded the desired product in 12% yield alongside 8% recovery of starting material and 63% of the vinyl silane byproduct. Utilizing dppp as a ligand instead of **L2** did not lead to the formation of product, instead allowing observation of 7% unreacted starting material and 70% of the vinyl silane byproduct.

**Scheme 4.17**. Comparing the mass balance of the reaction in the presence of three different ligands: **L2**, **L7** and dppp

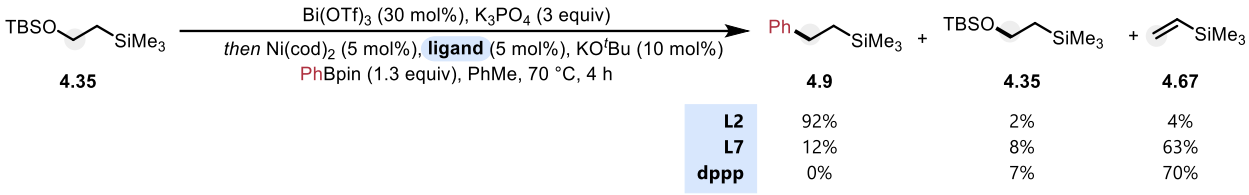


| | 4.9 | 4.35 | 4.67 |
|---|---|---|---|
| **L2** | 92% | 2% | 4% |
| **L7** | 12% | 8% | 63% |
| **dppp** | 0% | 7% | 70% |

Following these experiments, time-course data was collected for the arylation of silyl ether **4.35** in the presence of each of these three ligands (Figure 4.10). For the reaction in the presence of **L2**, it was found, generally, that consumption of starting material **4.35** was mirrored by the appearance of product **4.9** over the course of the 4 hour reaction time. Small amounts of **4.67** were produced as well. For the reaction in the presence of **L7**, starting material consumption occurred at similar rates as it did with ligand **L2**, however **4.67** formed in significant amounts over the course of the first two hours of the reaction. Small amounts of product **4.9** evolved as well over the course of the reaction. For the reaction in the presence of dppp, starting material was again



*Chapter four references begin on page 364; experimental details begin on page 331*

consumed at approximately the same rate as with ligands **L2** and **L7**, however **4.67** formed rapidly with the reaction being complete during the first hour of the reaction.

**Figure 4.10**. Time-course data for arylation in the presence of **L2**, **L7**, and dppp

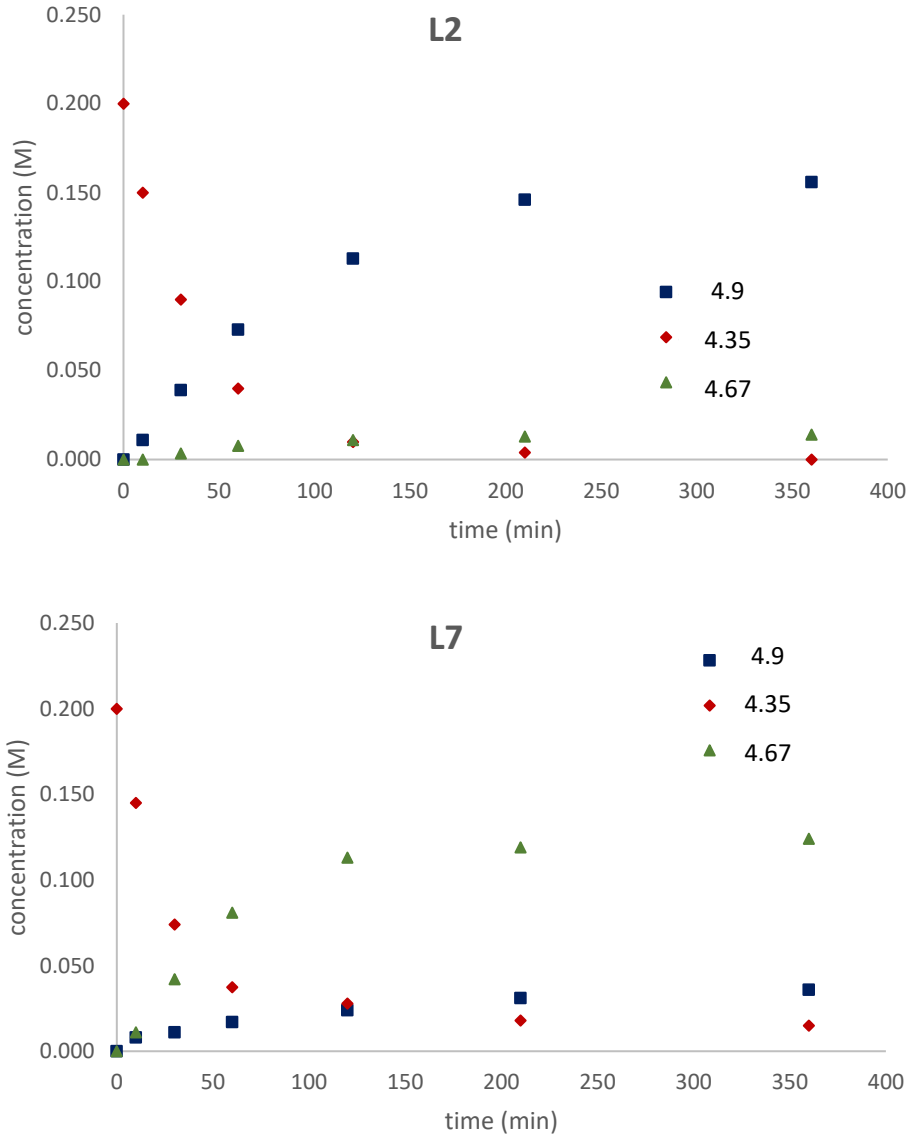




*Chapter four references begin on page 364; experimental details begin on page 331*

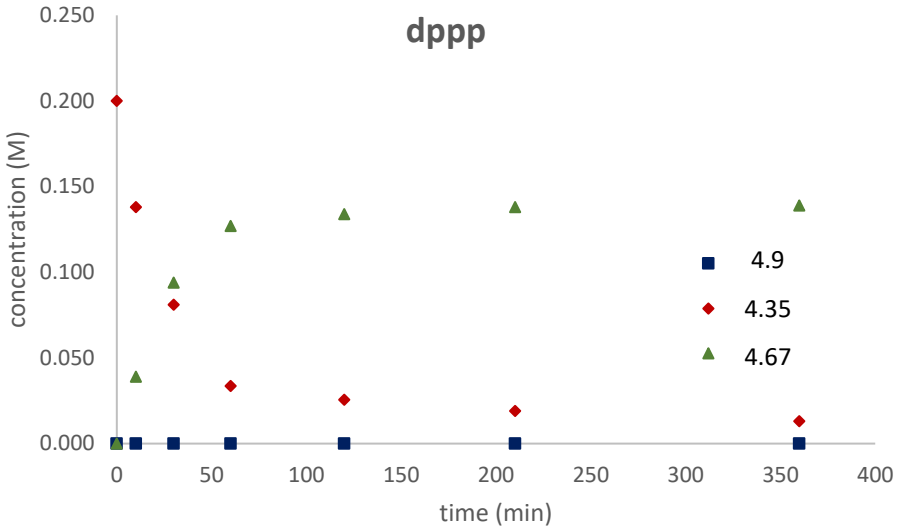


### **4.6.3.** Miscellaneous mechanistic experiments

***Testing for radical reactivity***

While these kinetic experiments are supportive of an $S_N1$-type pathway, the activation of $sp^3$ hybridized electrophiles such as alkyl halides is often proposed to proceed through a radical pathway in nickel-catalyzed cross-couplings.[38] To probe if similar intermediates may be present, an alcohol bearing an adjacent cyclopropane ring (**4.68**) and a tethered olefin (**4.71**) were prepared, both of which may undergo rearrangements if the reaction proceeds via a carbon-centered radical intermediate (Scheme 4.18). In both cases, direct substitution products (**4.69**, **4.72**) were observed, with no evidence of rearranged species (**4.70**, **4.73**) that would have been indicative of long-lived carbon-centered radical intermediates.

Further, the inclusion of radical-scavenging reagents, such as TEMPO, diphenylethylene and galvinoxyl, did not inhibit the formation of product **4.72**. To ensure that this effect was not substrate dependent, the arylation of compound **4.1** was performed in the presence of the same

radical scavenging reagents. In each case, arylated product **4.2** was obtained in yields reflective of the optimized reaction conditions. Together, these data suggest that the reaction does not proceed via a radical intermediate.

**Scheme 4.18.** Experiments refuting the existence of radical intermediates

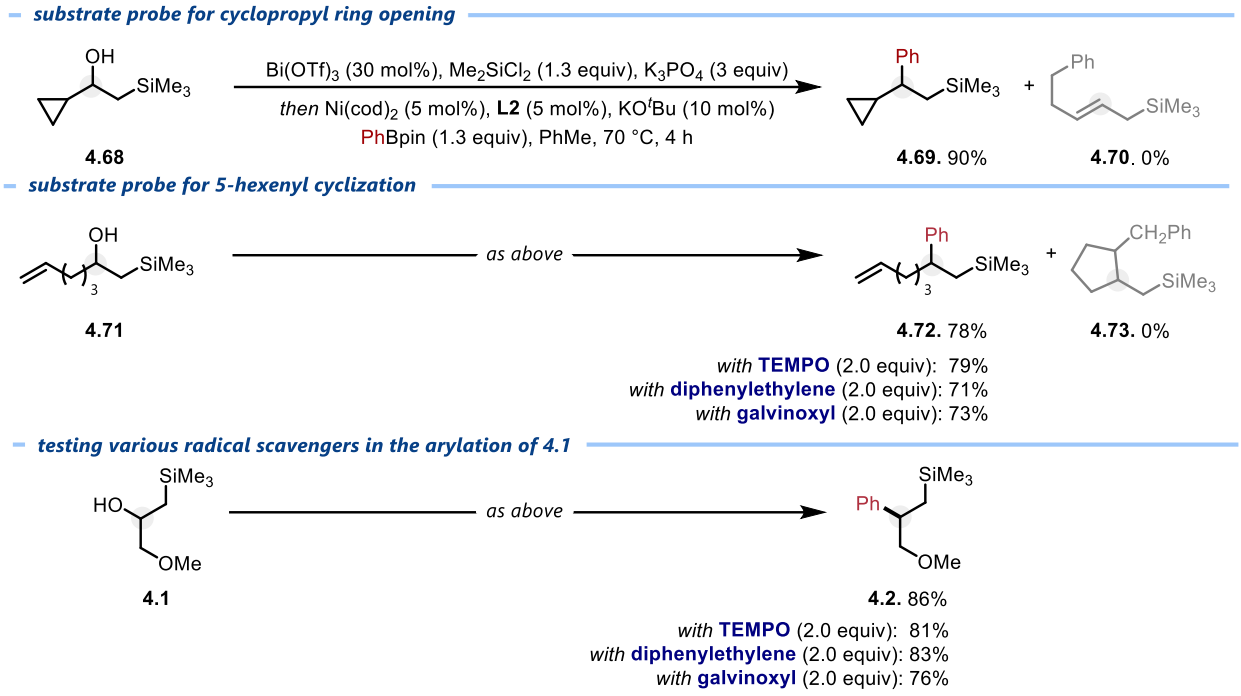


### *Testing a cyclic β-hydroxysilane*

To clarify the role that the *β*-silicon atom plays in the success of this deoxygenative arylation, two diastereomers of cyclic *β*-hydroxysilane **4.74** were prepared.[11c] The *β*-silicon effect is most commonly proposed to arise from the ability of the C–Si bond to stabilize adjacent carbocations by hyperconjugation, requiring an anti-periplanar bond angle that **4.74**$_{\mathbf{anti}}$ can adopt but **4.74**$_{\mathbf{syn}}$ cannot.[11b] Indeed, **4.74**$_{\mathbf{anti}}$ resulted in successful cross-coupling to give **4.75**$_{\mathbf{anti}}$ in 68% yield while **4.74**$_{\mathbf{syn}}$ gave no identifiable arylated products (Scheme 4.19). Together, these results suggest that anti-periplanar overlap is required for reactivity.



*Chapter four references begin on page 364; experimental details begin on page 331*

**Scheme 4.19.** Investigating the effects of substrate stereochemistry on reactivity

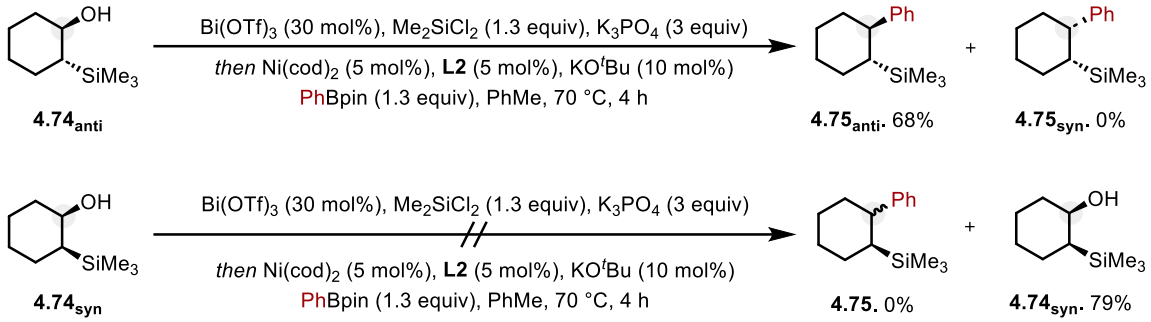


***Testing the effects of drop-in additives***

A number of hypotheses were tested through the introduction of drop-in additives in the arylation of substrate **4.1** (Table 4.2). Firstly, pre-mixing of hydroxysilane **4.1** with $Bi(OTf)_3$, $Me_2SiCl_2$ and $K_3PO_4$ is necessary in order to attain high yields (entry 1); performing the reaction without premixing (entry 2) leads to depleted product formation. This observation is in line with previous work.[8] Secondly, the yield of the reaction was suppressed in the presence of dibenzocyclooctatetraene (dct), a known inhibitor of homogeneous catalysts (entry 3). Conversely, no depletion in yield was observed upon conducting the reaction in the presence of Hg, a known inhibitor of heterogeneous catalysis (entry 4). These observations suggest that arylation proceeds via homogeneous catalysis.

Additionally, the inclusion of $Bi(OTf)_3$ was essential for product formation. As $Bi(OTf)_3$ has been demonstrated to act as either a Lewis or Brønsted acid through the in situ formation of triflic acid (TfOH),[39] an investigation into its behaviour in this arylation was warranted. Upon including triflic acid into the reaction mixture, no product was formed (entries 5, 6). Further, including 2,6-ditertbutyl-4-methylpyridine (DTBMP), a proton scavenging reagent, into the



*Chapter four references begin on page 364; experimental details begin on page 331*

reaction mixture did not lead to a decrease in yield (entry 7). Each of these observations provide support against Brønsted acid behaviour of $Bi(OTf)_3$ in this protocol.

**Table 4.2.** Testing variables, including drop in additives, in this arylation

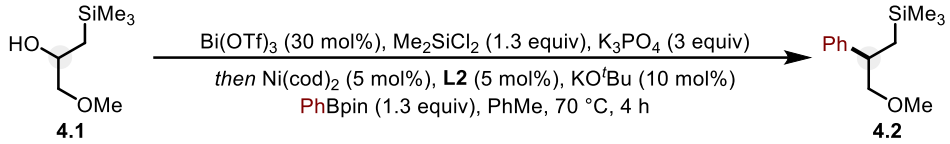


| entry | deviation from above conditions | % yield, 4.2 |
|---|---|---|
| **1** | *none* | 86 |
| **2** | *no pre-mixing* | 28 |
| **3** | + dct (2 equiv) | 0 |
| **4** | + Hg (10 equiv) | 81 |
| **5** | + TfOH (30 mol%) | 0 |
| **6** | + TfOH (30 mol%), no $Bi(OTf)_3$ | 0 |
| **7** | + DTBMP (1 equiv) | 82 |

### **4.6.4.** Mechanistic hypothesis

The aforementioned results, alongside kinetic studies, suggest that the *β*-silicon effect is indeed operative in this chemistry, facilitating the formation of a carbocation intermediate that acts as an electrophile in nickel-catalyzed Suzuki-Miyaura coupling. Accordingly, a plausible catalytic cycle is proposed (Figure 4.11). *β*-Hydroxysilane **4.A** is first converted into silyl ether **4.B**. The resulting intermediate may undergo a Lewis acid-assisted rate-limiting C($sp^3$)–O bond cleavage to yield *β*-Si stabilized carbocation **4.C** that may be intercepted by a nickel(0)-NHC catalyst[8,10,40] **4.D** to generate oxidative addition complex **4.E.** Subsequent transmetalation with the boronate ester would give complex **4.F**, which may undergo reductive elimination to afford arylated product **4.G**.



*Chapter four references begin on page 364; experimental details begin on page 331*

**Figure 4.11.** Tentative reaction mechanism

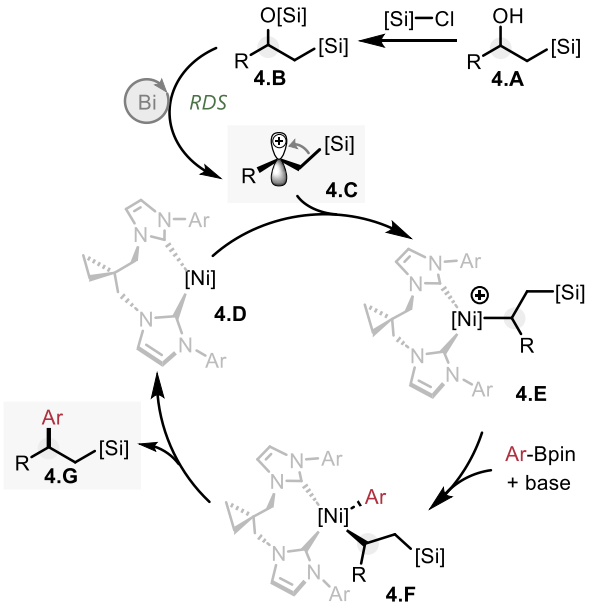


While the evidence that has been collected during this project lends evidence to support the plausible reaction mechanism presented in Figure 4.11, more work could still be done in order to inspire more confidence in this proposal. For instance, while it is speculated that the Ni(0) catalyst might react directly with the stabilized carbocation via an $S_N1$-type oxidative addition, alternative mechanistic interpretations, such as the existence of a transient organo(pseudo)halide intermediate, cannot be excluded. While the isolation of various nickel-**L2** complexes was successful, the isolation and characterization of complexes on the catalytic cycle, for instance oxidative addition complexes, has proved elusive, thus limiting confidence in the exact steps of the catalytic cycle. Secondly, given the apparent rate dependence on only Lewis acid and substrate, it is unusual for the reaction to have such a drastic dependence on the identity of the ligand as it does not appear in the rate law of the reaction. While it can be imagined that this is due to the ligands preference for participating in reductive elimination rather than $\beta$-hydride elimination,[34] this remains speculation. Thirdly, while substantial evidence supports the existence of a



*Chapter four references begin on page 364; experimental details begin on page 331*

carbocation intermediate that is formed in the absence of nickel catalyst, efforts to trap the hypothesized carbocation have proved futile, instead leading towards the recovery of silyl ether and small amounts of elimination product.

## 4.7. Additional commentary

Initially, this reaction was discovered, optimized, and explored with **L1**, the ligand which was found to be optimal in the work described in chapter three of this dissertation (Scheme 4.20). However, moderate yields were obtained. Early in 2023 a range of newly-synthesized bis(NHC) ligands were screened in this reaction in hope of obviating this limitation, wherein **L2** was superior to **L1** in the coupling of both secondary (**4.1**) and primary (**4.76**) *β*-hydroxysilanes. As such, the reaction optimization, scope expansion and further exploration was conducted with **L2**.

**Scheme 4.20.** Comparing **L1** vs **L2** in the arylation of primary and secondary alcohols

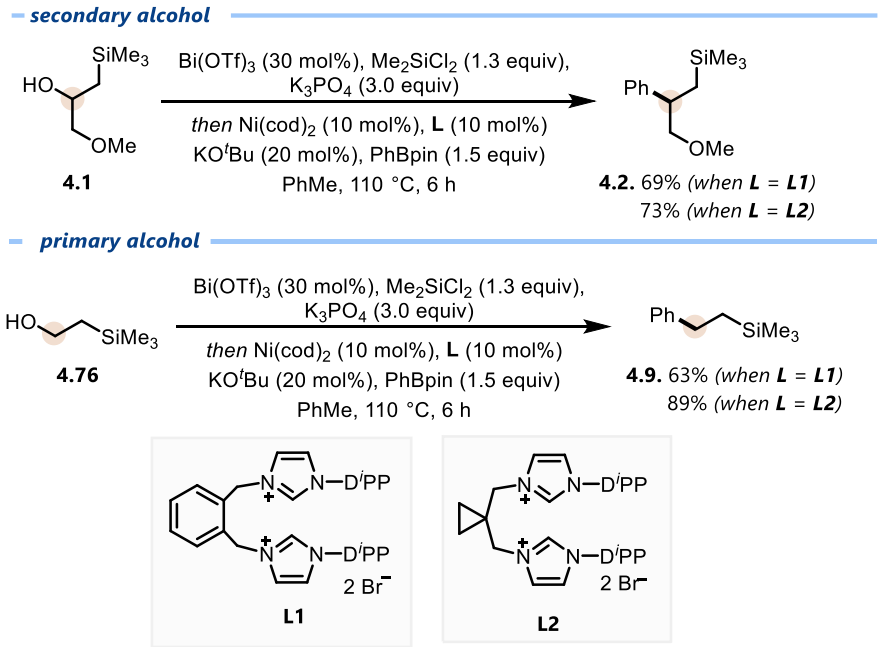


A significant difficulty when pursuing this project was that many *β*-hydroxysilanes were observed to be unstable, decomposing rapidly upon storage under ambient conditions. While



Chapter four references begin on page 364; experimental details begin on page 331

decomposition generally led towards the formation of an intractable mixture of species, it is speculated that decomposition is largely due to a Brook rearrangement wherein the silane on the *β*-hydroxysilane **4.77** migrated on to the oxygen atom to generate silyl ether **4.78** (Scheme 4.21).[41] To resolve this problem, substrates were synthesized and subjected to the arylation conditions in the same day, most often mere hours after synthesis. Certain *β*-hydroxysilanes, such as **4.35**, proved to be stable for extended periods of time; this is a substantial reason that **4.35** was chosen as the substrate to test the scope of boronate ester coupling partner in Scheme 4.6.

**Scheme 4.21.** Brook rearrangement

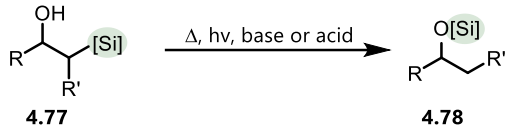


**4.77** **4.78**

The *β*-silicon effect requires anti-periplanar overlap in order to stabilize carbocations.[11] This effect was exploited in the example presented in Scheme 4.19. It was theorized that this idea could be extended towards the stereoretentive arylation of allylic *β*-hydroxysilanes. To this end, substrate **4.79** was prepared according to a method published by Rousch and colleagues.[42] Unfortunately, subjecting compound **4.79** to the standard reaction conditions did not lead towards arylation, instead leading to the generation of an intractable mixture of compounds (Scheme 4.22). It is speculated that this could either be due to steric factors preventing favourable interaction with the nickel catalyst or due to substrate decomposition upon exposure to the standard reaction conditions.

**Scheme 4.22.** Attempts at stereoretentive arylation

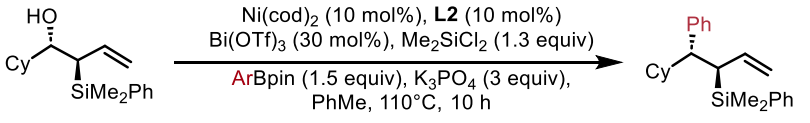


**4.79** **4.80.** *not observed*



*Chapter four references begin on page 364; experimental details begin on page 331*

## 4.8. Conclusion, impact, future work and considerations

### 4.8.1. Conclusion

In summary, this chapter details the arylation of β-hydroxysilanes via a Suzuki-Miyaura coupling to forge new C($sp^3$)–C($sp^2$) bonds. A dual metal catalyzed system is used, featuring bismuth as a Lewis acid alongside a novel nickel/NHC cross-coupling catalyst. Crystallographic analysis of nickel(0), nickel(I), and nickel(II) species reveals that the long-chain bis(NHC) ligand **L2** acts as a bidentate ligand with a large bite angle. Kinetic studies on the arylation reaction are consistent with a reaction that proceeds through an $S_N1$-like pathway, representing a rare example of a Suzuki-Miyaura reaction featuring a carbocation intermediate. The resulting *β*-arylsilanes may be immediately useful due to the growing interest in silicon-containing molecules, or the silicon may be used as a synthetic handle to prepare derivatives via oxidation, C–H borylation or protodesilylation. Research is underway within the Newman lab to understand the scope of coupling partners and activating groups that may be further exploited in this integration of transition-metal catalyzed cross-coupling and Lewis acid activation of alcohols.

### 4.8.2. Impact, future work and considerations

As in previous work, Suzuki-Miyaura transformations are a practical, highly utilized method to forge carbon-carbon bonds that is commonly restricted towards the use of $sp^2$-hybridized organo(pseudo)halides as coupling partners.[1] Further, the overwhelming majority of Suzuki-Miyaura arylations that do utilize alcohols as coupling partners require them to be preactivated or π-activated.[4] As in previous work, the reaction discussed within this chapter represents numerous practical advantages over conventional methods, allowing the arylation of



*Chapter four references begin on page 364; experimental details begin on page 331*

non-π-activated, unprotected alcohols in a single step. However, this work represents a practical extension of the previous work as it obviates the strict restriction for use only on cyclic tertiary alcohols, as was noted previously. While it does require an activating silane group, it was demonstrated in Section 4.4.3 that this group can be introduced via a facile Grignard addition onto carbonyl-containing compounds and it is demonstrated in Section 4.5.2 that this silane group can be further functionalized – or removed entirely – after the arylation reaction is conducted.

Beyond the practical aspects of this work, this transformation is also interesting – and important – to the fundamental way that cross-coupling mechanisms are thought about in catalysis. Mechanistically, this transformation represents a rare, and to this author's knowledge, unexplored, example of a carbocation being intercepted by a transition metal catalyst to generate a "formal oxidative addition" complex. Conventional methods for oxidative addition often involve two-electron insertions of transition metals into C–X bonds or, more commonly for alkyl-hybridized coupling partners, single electron chemistry.[9] For example, photoredox catalysis has emerged as a useful method to permit the cross-coupling of alkyl halides, carboxylates and more. Inherently, these methods rely on the generation of radical intermediates. Carbocations are a frequently explored, well understood reactive intermediate. The ability to enable them as precursors in cross-coupling chemistry presents a modernized alternative to conventional Friedel-Crafts-type transformations.

## Future work

The work presented within this chapter may serve as a source of inspiration for a range of projects in the future. Perhaps the most obvious spin-off projects would involve varying the nucleophilic coupling partner (Scheme 4.23a). While Suzuki-Miyaura arylation has been thoroughly explored, can this same set of reaction conditions enable the coupling of *β*-



*Chapter four references begin on page 364; experimental details begin on page 331*

hydroxysilanes with other nucleophiles such as organobismuths (**4.81**), organozincs (**4.82**), Grignard reagents (**4.83**), alkynes (**4.84**) or amines (**4.85**)? This hypothesis could be explored via a high-throughput approach. For instance, a 96-well plate could be envisioned that tests up to 96 different nucleophilic coupling partners. Not only would each of these methods be useful, but they would allow insight into the utility of the newly-discovered bis(NHC) ligand **L2**.

**Scheme 4.23.** Extending this transformation towards other cross-couplings.

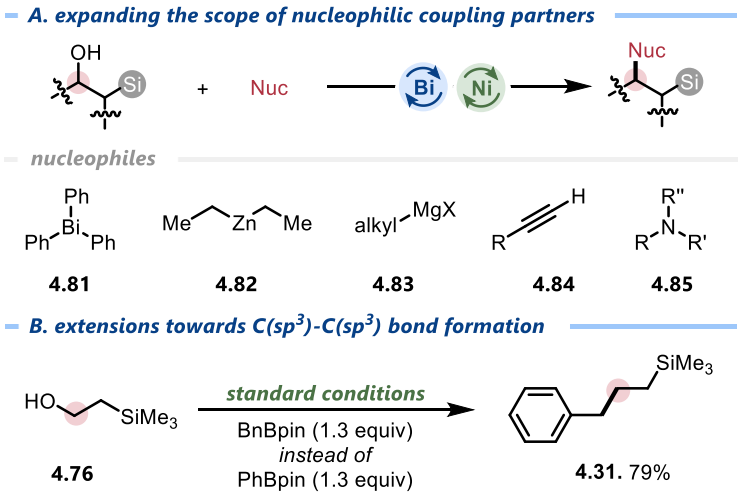


An interesting observation made over the course of this study was that compound **4.31** could be obtained upon reacting a benzyl boronate ester with **4.76**, thereby forging a new C($sp^3$)–C($sp^3$) bond (Scheme 4.23b). Methods to forge these types of bonds are significantly limited through cross-coupling approaches and this example suggests that this arylation reaction could be extended towards the coupling of two C($sp^3$)-hybridized compounds. Thus, an extension of the present work could consider evaluating the range of alkyl boronate esters that can be used in this chemistry: What are the scope limitations of benzyl boronic esters? What about alkyl-9-BBN species? What about dialkylzincs, alkylaluminiums or alkyl Grignards?



*Chapter four references begin on page 364; experimental details begin on page 331*

A key feature of this transformation is the requirement of an activating silane group. While it is believed that this is due to the carbocation-stabilizing properties of the β-silicon effect, it is not unreasonable to view this as a neighbouring-group interaction. If so, then it may be possible that other atoms and chemical moieties could be used in place of the silicon atom. For instance, this reaction is likely to be extendable to alkylgermanes as they are known to share many chemical properties with alkyl silanes. While alkylgermanes may be the "low-hanging fruit", other neighbouring groups such as amines could be biased towards these types of interactions as well (Figure 4.12).

**Figure 4.12.** Exploring non-silicon based neighbouring groups.

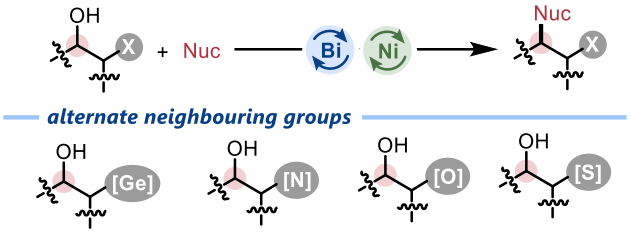


Finally, ligand **L2** has been demonstrated to be the optimal ligand for this reaction, however a range of bis(NHC) scaffolds was observed to afford product in synthetically valuable yields. The synthesis of these ligands was discussed in the previous chapter of this manuscript (Scheme 3.1). In some cases, such as in the synthesis of **L10**, the precursor to the ligand was synthesized through the dibromination of commercially available 1,2-cyclohexane diol. A large number of diols are commercially available, and a potential direction for this project could seek to synthesize a library of bis(NHC)s for evaluation in other transformations. In particular, chiral diol **4.86** is commercially available at a moderate price. It is feasible to imagine that a pool of chiral



*Chapter four references begin on page 364; experimental details begin on page 331*

analogs of **L2**, such as **L15**, could be synthesized and utilized in this chemistry as a method to achieve enantioselective cross-couplings of alcohols (Figure 4.13).

**Figure 4.13.** Extending this transformation towards stereocontrolled syntheses

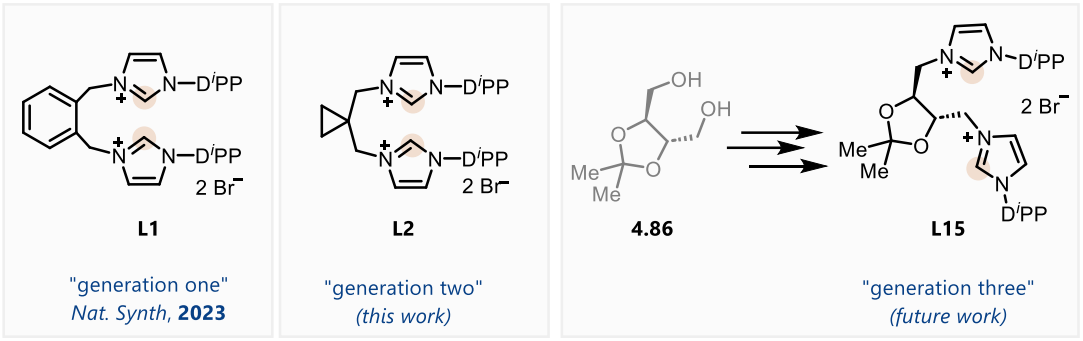




*Chapter four references begin on page 364; experimental details begin on page 331*

## 4.9. Experimental

### 4.9.1. General details

Unless otherwise indicated, reactions were conducted under an atmosphere of nitrogen in 8 mL screw-capped vials that were oven-dried (120 °C). Column chromatography was either performed manually using Silicycle F60 40−63 μm silica gel or by using a Combiflash Rf+ automated chromatography system with Biotage normal-phase Silica Flash columns (35−70 μm). Analytical thin layer chromatography (TLC) was conducted with aluminum-backed EMD Millipore Silica Gel 60 F254 pre-coated plates. Visualization of developed plates was performed under UV light (254 nm) and/or using $KMnO_4$ stain.

### 4.9.2. Instrumentation

$^{1}H$ NMR and $^{13}C$ NMR were recorded on a Bruker AVANCE II 400 MHz spectrometer, a Bruker AVANCE III HD 500 MHz spectrometer, or a Bruker AVANCE III HD 600 MHz spectrometer. $^{1}H$ NMR spectra were internally referenced to the residual solvent signal (e.g., $CDCl_3$ = 7.27 ppm). $^{13}C$ NMR spectra were internally referenced to the residual solvent signal (e.g., $CDCl_3$ = 77.00 ppm). Data for $^{1}H$ NMR are reported as follows: chemical shift (δ ppm), multiplicity (s = singlet, d = doublet, t = triplet, q = quartet, quin = quintet, m = multiplet), coupling constant (Hz), integration. NMR yields for optimization studies were obtained by $^{1}H$ NMR analysis of the crude reaction mixture using 1,3,5-trimethoxybenzene as an internal standard. GC data was obtained via a 5-point calibration curve using FID analysis on an Agilent Technologies 7890B GC with a 30 m x 0.25 mm HP-5 column. Accurate mass data (EI) was obtained from an Agilent 5977A GC/MSD using MassWorks 4.0 from CERNO Bioscience.[43]

### 4.9.3. Materials

Organic solvents were purified by rigorous degassing with nitrogen before passing through a PureSolv solvent purification system. Low water content was confirmed by Karl Fischer titration (<20 ppm for all solvents). Unless otherwise noted, starting materials were obtained commercially from Sigma Aldrich, Alfa Aesar or Combi-Blocks and used as received. (Trimethylsilyl)methylmagnesium chloride ($Me_3SiCH_2MgCl$) was purchased from Sigma Aldrich (1.0 M in diethyl ether). $Ni(cod)_2$ was purchased from Sigma Aldrich. $Bi(OTf)_3$ was purchased from Combi-Blocks. $Me_2SiCl_2$ was purchased from Sigma Aldrich. PhBpin was purchased from Combi-Blocks and other pinacol boronic esters were synthesized from the corresponding chloride[44] or boronic acid[45] according to the literature. **L1** was prepared as described in a previous work,[46] while other *N*-heterocyclic carbenes were prepared according to the literature.[47] 1-(Trimethylsilyl)-2-propanol, 2-(trimethylsilyl)-1-propanol, 2-(trimethylsilyl)ethanol, α-(2,2-dimethylpropyl)benzanemethanol), 2-(triethylsilyl)ethanol, 2-(dimethylphenylsilyl)ethanol and 2-[(1,1-dimethylethyl)dimethylsilyl]ethanol were used from commercial sources.

### 4.9.4. General procedures

***General Procedure A – Grignard reaction to synthesize β-hydroxysilanes:*** *β*-Hydroxysilane starting materials were prepared from the corresponding aldehyde or ketone according to a literature procedure.[48] An oven-dried 100 mL round bottom flask was equipped with a magnetic stir bar. Anhydrous THF (16 mL) was added to the round bottom flask and purged for 10 min with a positive pressure of argon. A solution of aldehyde/ketone (1.0 equivalents, 2.0 mmol) in 3.0 mL anhydrous THF was added to the round bottom flask. After cooling for 10 min at 0 °C using an ice bath, (trimethylsilyl)methylmagnesium chloride (1.5 equivalents, 1.0 M in THF, 3 mL) was added dropwise to the stirring solution at 0 °C. After the addition was complete,

the flask was removed from the ice bath and the reaction was stirred for 10 h at room temperature. The reaction solution was quenched with sat. $NH_4Cl$, diluted with EtOAc, and the organic layer was washed twice with $H_2O$ followed by sat. NaCl. The organic fractions were combined and dried with $MgSO_4$ before being passed through a short plug composed of $SiO_2$ and celite in a 50:50 mixture. Solvent was evacuated by rotary evaporation and the subsequent residue was purified via column chromatography. *Note:* In general, *β*-hydroxysilanes were found to be of moderate stability. It is recommended that they are used directly after synthesis. If stored in a freezer, their purity should be checked by $^1H$ NMR prior to use.

***General Protocol B – Arylation of β-hydroxysilanes:*** An oven-dried 8 mL screw-top test-tube was equipped with an oven-dried micro-stir bar and brought into a nitrogen-filled glovebox. This reaction vessel was charged with *β*-hydroxysilane (1.0 equiv, 0.20 mmol), $K_3PO_4$ (3.0 equiv, 127.2 mg, 0.60 mmol), $Bi(OTf)_3$ (0.30 equiv, 39.4 mg, 0.06 mmol), $Me_2SiCl_2$ (1.3 equiv, 31.3 µL, 0.26 mmol) and PhMe (0.4 mL). This mixture was capped and left to stir inside the glovebox for 15 min at room temperature. After 15 min a premixed solution of $Ni(cod)_2$ (0.05 equiv, 2.75 mg, 0.01 mmol), **L2** (0.05 equiv, 7.20 mg, 0.01 mmol) and KO$^t$Bu (0.10 equiv, 2.25 mg, 0.02 mmol) in PhMe (0.4 mL) was added to the stirring solution, followed by ArBpin (1.3 equiv, 0.26 mmol), before the reaction vessel was sealed with a Teflon-septum equipped cap and brought outside of the glovebox to be stirred within a mineral-oil bath at 800 rpm for 4 hours at 70 ˚C. After 4 hours, the reaction vessel was removed from heat and allowed to come to room temperature. The crude reaction solution was then quenched with 15% KOH (5 mL) and diluted with EtOAc before being transferred into a separatory funnel. Liquid-liquid extraction was done with EtOAc (3 x 10 mL); the resulting organic phases were combined in the separatory funnel before being washed twice with sat. $NaHCO_3$ and once with sat. NaCl. The organic phase was dried with $MgSO_4$ before being



*Chapter four references begin on page 364; experimental details begin on page 331*

passed through a short plug composed of $SiO_2$ and celite in a 50:50 ratio. Solvent was removed via rotary evaporation and the subsequent residue was dissolved in dichloromethane. A small amount of $SiO_2$ was added to the resulting solution and the solvent was once more removed via rotary evaporation. The resulting mixture was purified using column chromatography.

*Note: All NMR spectra and associated data for chapter four is present in the Appendix, Section 7.*

### **4.9.5.** Characterization details of β-hydroxysilane starting materials

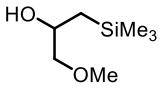


**1-Methoxy-3-(trimethylsilyl)propan-2-ol (4.1)** was prepared from methoxyacetaldehyde according to general procedure A. Column chromatography was performed using a gradient of 1→15% ethyl acetate in hexanes to afford product as a clear liquid (156.8 mg, 49% yield). **$^1$H NMR** (400 MHz, $CDCl_3$): δ 33.92-3.84 (m, 1H), 3.30 (s, 3H), 3.29-3.13 (m, 2H), 2.31 (br, 1H), 1.07-1.05 (m, 2H), 0.18 (s, 9H); **$^{13}$C NMR** (100 MHz, $CDCl_3$): 78.2, 66.3, 58.9, 18.6, -1.2. **Accurate mass (EI)**: Theoretical: 162.1076. Found: 162.1067. Spectral Accuracy: 98.4%.

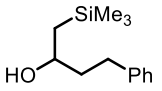


**4-Phenyl-1-(trimethylsilyl)butan-2-ol (4.87)** was prepared from 3-phenylpropanal according to general procedure A. Column chromatography was performed using a gradient of 0→15% ethyl acetate in hexanes to afford product as a clear liquid (200.2 mg, 45% yield). Spectral data matched that found within the literature.[49] **$^1$H NMR** (400 MHz, $CDCl_3$): δ 7.34-7.29 (m, 2H), 7.24-7.21 (m, 3H), 3.89-3.83 (m, 1H), 2.87-2.65 (m, 2H), 1.86-1.76 (m, 2H), 0.93 (dd, *J* = 7.0, 1.4 Hz, 2H), 0.07 (s, 9H); **$^{13}$C NMR** (100 MHz, $CDCl_3$): 142.1, 128.4, 128.3, 125.7, 69.6, 42.4, 32.2, 26.7, -0.7.



*Chapter four references begin on page 364; experimental details begin on page 331*

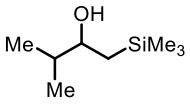


**2-Methyl-4-(trimethylsilyl)butan-3-ol (4.88)** was prepared from isobutyraldehyde according to general procedure A. Column chromatography was performed using a gradient of 0→10% diethyl ether in pentane to afford product as a clear liquid (263.1 mg, 82% yield). **$^{1}$H NMR** (400 MHz, $CDCl_3$): δ 3.58 (ddd, *J* = 9.4, 4.8, 4.7 Hz, 1H), 1.59 (sept, *J* = 4.7 Hz, 1H), 1.23 (br s, 1H), 0.92-0.90 (m, 6H), 0.87-0.77 (m, 2H), 0.05 (s, 9H); **$^{13}$C NMR** (100 MHz, $CDCl_3$): 74.7, 35.9, 22.4, 18.7, 16.8, -0.8. **Accurate mass (EI)**: Theoretical: 160.1278. Found: 160.1210. Spectral Accuracy: 97.2%.

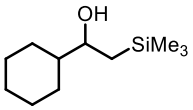


**1-Cyclohexyl-2-(trimethylsilyl)ethan-1-ol (4.89)** was prepared from cyclohexane carboxaldehyde according to general procedure A. Column chromatography was performed using a gradient of 0→20% ethyl acetate in hexanes to afford product as a clear liquid (304.8 mg, 76% yield). Spectral data matched that found within the literature.[49] **$^{1}$H NMR** (400 MHz, $CDCl_3$): δ 3.53 (ddd, *J* = 9.5, 4.8, 4.6 Hz, 1H), 1.88-1.59 (m, 5H), 1.32-0.89 (m, 7H), 0.82 (dd, *J* = 14.7, 4.6 Hz, 1H), 0.72 (dd, *J* = 14.7, 9.5 Hz, 1H), 0.02 (s, 9H); **$^{13}$C NMR** (100 MHz, $CDCl_3$): 74.3, 46.2, 29.4, 27.3, 26.6, 26.4, 26.2, 22.6, -0.8.

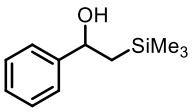


**1-Phenyl-2-(trimethylsilyl)ethan-1-ol (4.90)** was prepared from benzaldehyde according to general procedure A. Column chromatography was performed using a gradient of 1→20% ethyl acetate in hexanes to afford product as a clear liquid (357.5 mg, 92% yield). Spectral data matches those within the literature.[49] **$^{1}$H NMR** (400 MHz, $CDCl_3$): δ 7.36-7.30 (m, 4H), 7.26-7.23 (m, 1H), 4.82 (t, *J* = 7.4 Hz, 1H), 1.81 (br s, 1H), 1.26 (dd, *J* = 14.3, 7.4 Hz, 1H), 1.17 (dd, *J* = 14.3, 7.4 Hz, 1H), -0.09 (s, 9H); **$^{13}$C NMR** (100 MHz, $CDCl_3$): 146.4, 128.5, 127.6, 125.8, 72.9, 28.4, -1.1.



*Chapter four references begin on page 364; experimental details begin on page 331*

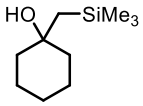


**1-[Trimethylsilyl)methyl]cyclohexanol (4.91)** was prepared from cyclohexanone according to general procedure A. Column chromatography was performed using a gradient of 1→10% diethyl ether in hexanes to afford the product as a clear liquid (130.4 mg, 35% yield). Spectral data matches that within the literature.[50] **$^{1}$H NMR** (400 MHz, $CDCl_3$): δ 1.59-1.41 (m, 10H), 0.96 (s, 2H), 0.06 (s, 9H); **$^{13}$C NMR** (100 MHz, $CDCl_3$): 68.7, 40.5, 29.5, 26.6, 25.8, 22.1, -1.5. **Accurate mass (EI)**: Theoretical: 186.1434. Found: 186.1395. Spectral Accuracy: 98.9%.

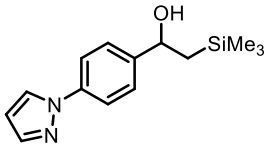


**1-[4-(1*H*-pyrazol-1-yl)phenyl]-2-(trimethylsilyl)ethan-1-ol (4.92)** was prepared from 4-(*1H*-pyrazol-1-yl)benzaldehyde according to general procedure A. Column chromatography was performed using a gradient of 1→30% ethyl acetate in hexanes to afford product as a white solid (447.9 mg, 86% yield). **$^{1}$H NMR** (400 MHz, $CDCl_3$): δ 7.93 (d, *J* = 2.8 Hz, 1H), 7.72-7.68 (m, 1H), 7.65 (d, *J* = 8.6 Hz, 2H), 7.41 (d, *J* = 8.6 Hz, 2H), 6.44 (dd, *J* = 2.8, 1.6 Hz, 1H), 4.84 (m, 1H), 1.98 (br s, 1H), 1.26 (dd, *J* = 14.3, 7.4 Hz, 1H), 1.17 (dd, *J* = 14.3, 7.4 Hz, 1H), -0.06 (s, 9H); **$^{13}$C NMR** (100 MHz, $CDCl_3$): 144.9, 140.9, 139.2, 126.8, 126.7, 119.1, 107.5, 72.1, 28.4, -1.1. **Accurate mass (EI)**: Theoretical: 260.1339. Found: 260.1317. Spectral Accuracy: 97.2%. Melting point: 94 - 96 °C.

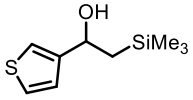


**α-[(Trimethylsilyl)methyl]-3-thiophenemethanol (4.93)** was prepared from 3-thiophenecarboxaldehyde according to general procedure A. Column chromatography was performed using a gradient of 1→20% ethyl acetate in hexanes to afford product as a clear liquid (312.6 mg, 78% yield). Spectral data matches that found within the literature.[51] **$^{1}$H NMR** (400 MHz, $CDCl_3$): δ 7.24 (dd, *J* = 5.0, 1.4 Hz, 1H), 6.97 (dd, *J* = 3.5, 1.4 Hz, 1H), 6.94 (dd, *J* = 5.0, 3.5 Hz, 1H), 5.12 (td, *J* = 7.5, 2.8 Hz, 1H), 1.98 (br s, 1H), 1.37 (dd, *J* = 14.3, 7.5 Hz, 1H), 1.31 (dd, *J* = 14.3, 7.5 Hz, 1H), -0.02 (s, 9H); **$^{13}$C NMR** (100 MHz, $CDCl_3$): 151.0, 126.4, 124.5, 123.3, 68.3, 28.9, -1.3. **Accurate mass (EI)**: Theoretical: 200.0686. Found: 200.0691. Spectral Accuracy: 98.0%.



*Chapter four references begin on page 364; experimental details begin on page 331*

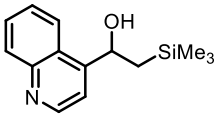


**α-[(Trimethylsilyl)methyl]-5-quinolinemethanol (4.94)** was prepared from cyclohexane carboxaldehyde according to general procedure A. Column chromatography was performed using a gradient of 1→20% ethyl acetate in hexanes to afford the product as a white solid (454.4 mg, 92% yield). **$^{1}$H NMR** (400 MHz, $CDCl_3$): δ 8.68 (d, *J* = 4.5 Hz, 1H), 8.02 (d, *J* = 8.4 Hz, 1H), 7.99 (d, *J* = 8.4 Hz, 1H), 7.63 (ddd, *J* = 8.4, 6.8, 1.4 Hz, 1H), 7.51-7.46 (m, 2H), 5.56 (dd, *J* = 8.8, 5.4 Hz, 1H), 3.23 (br s, 1H), 1.24-1.21 (m, 2H), 0.05 (s, 9H); **$^{13}$C NMR** (100 MHz, $CDCl_3$): 153.1, 150.3, 148.1, 130.0, 129.0, 126.3, 125.2, 123.1, 116.7, 68.2, 27.7, -0.9. **Accurate mass (EI)**: Theoretical: 245.1230. Found: 245.1242. Spectral Accuracy: 97.3%. Melting point 103 - 105 °C.

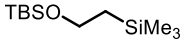


**[2-[[(1,1-Dimethylethyl)dimethylsilyl]oxy]ethyl]trimethylsilane (4.35)** was prepared according to a modified literature procedure.[58] In an oven dried 25 mL round bottom flask charged with a magnetic stir bar, 2-trimethylsilylethanol (1.0 equiv., 2.0 mmol, 286 μL), imidazole (3.0 equiv., 6 mmol, 408 mg), *tert*-butyldimethylsilyl chloride (1.1 equiv., 2.2 mmol, 331 mg), and iodine (2.5 equiv., 5.0 mmol, 634 mg) were dissolved in 6mL of dichloromethane. The reaction was stirred overnight at room temperature. Afterwards, the solvent was removed under reduced pressure, and the residue was dissolved in ethyl acetate, and extracted by a concentrated solution of $Na_2S_2O_3$. The combined organic phase was dried over $MgSO_4$, concentrated in reduced pressure and purified by column chromatography using a gradient of 1→10% ethyl acetate in hexanes to afford the product as a colourless liquid (223.2 mg, 48% yield). **$^{1}$H NMR** (300 MHz, $CDCl_3$): δ 3.71 (dt, *J* = 8.0, 7.2 Hz, 2H), 0.94-0.85 (m, 11H), 0.05 (s, 6H), 0.01 (s, 9H); **$^{13}$C NMR** (126 MHz, $CDCl_3$) 60.5, 26.2, 22.0, 18.5, -1.1, -5.0. **Accurate mass (EI)**: Theoretical: 232.1679. Found: 232.1678. Spectral Accuracy: 97.8%.

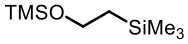


**Trimethyl[2-(trimethylsilyl)ethoxy]silane (4.36)** was prepared from 2-trimethylsilylethanol according to a literature procedure; analytical data matched those in the literature.[59] **$^{1}$H NMR** (400 MHz, $CDCl_3$): δ 3.71 (dt, *J* = 7.7, 7.1 Hz, 2H), 0.92 (dt, *J* = 8.2, 7.4 Hz, 2H), 0.11 (s, 9H), 0.01 (s, 9H); **$^{13}$C NMR** (100 MHz, $CDCl_3$): 59.8, 21.9, -0.2, -1.2.

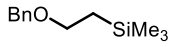

**Benzyl-2-(trimethylsilyl)ethyl ether (4.37)** was prepared according to a modified literature procedure using benzyl bromide and 2-trimethylsilylethanol.[60] Column chromatography was performed using a gradient of 1→5% ethyl acetate in hexanes to afford the product as a colourless liquid (36.7 mg, 79% yield). **$^1$H NMR** (400 MHz, $CDCl_3$): δ 7.38-7.24 (m, 5H), 4.48 (s, 2H), 3.57 (dt, *J* = 8.0, 7.4 Hz, 2H), 0.99 (dt, *J* = 8.0, 7.4 Hz, 2H), 0.01 (s, 9H). **$^{13}$C NMR** (100 MHz, $CDCl_3$): 138.8, 128.4, 128.3, 127.8, 127.6, 127.4, 72.4, 67.7, 18.3, -1.3. **Accurate mass (EI)**: Theoretical: 232.1679. Found: 232.1678. Spectral Accuracy: 97.8%.

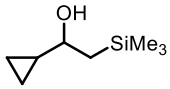

**1-Cyclopropyl-2-(trimethylsilyl)ethan-1-ol (4.68)** was prepared from cyclopropyl carboxaldehyde according to general procedure A. Column chromatography was performed using a gradient of 0→10% diethyl ether in pentane to afford the product as a clear liquid (285.1 mg, 90% yield). **$^1$H NMR** (400 MHz, $CDCl_3$): δ 3.09-3.04 (td, J = 7.9, 6.4 Hz, 1H), 1.55 (br s, 1H), 1.04-0.89 (m, 3H), 0.54-0.47 (m, 2H), 0.30-0.19 (m, 2H), 0.02 (s, 9H); **$^{13}$C NMR** (100 MHz, $CDCl_3$): 74.8, 26.1, 20.8, 3.4, 3.1, -0.7. **Accurate mass [M–$CH_3$]$^+$ (EI):** Theoretical: 143.0918. Found: 143.0945

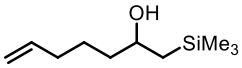

**1-Trimethylsilyl-6-hepten-2-ol (4.71)** was prepared from hexenal according to General Procedure A. Column chromatography was performed using a gradient of 1→20% ethyl acetate in hexanes to afford product as a clear liquid (226.9 mg, 61% yield). **$^1$H NMR** (400 MHz, $CDCl_3$): δ 6.00-5.91 (m, 1H), 5.18-5.09 (m, 2H), 3.57-3.54 (m, 2H), 2.24-2.19 (m, 2H), 2.07-1.97 (m, 2H), 1.62-1.56 (m, 1H), 1.11-1.08 (m, 2H), 0.17 (s, 9H); **$^{13}$C NMR** (100 MHz, $CDCl_3$): 138.6, 114.6, 60.1, 33.8, 33.5, 32.6, 22.1, -1.4. **Accurate mass (EI)**: Theoretical: 186.1440. Found: 186.1437. Spectral Accuracy: 98.4%.



*Chapter four references begin on page 364; experimental details begin on page 331*

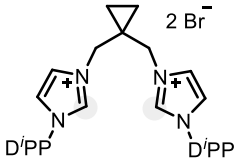


**1,1'-Di(2,6-diisopropylphenyl)-3,3'-(2-cyclopropyl)propylenediimidazolium dibromide** (**L2**) was prepared from 1-(2',6'-diisopropylphenyl)imidazole and dibromomethylcyclopropane according to the procedure detailed in Section 3.9.5, revealing product as a beige solid that was utilized without further purification (198 mg, 58% yield). **$^{1}$H NMR** (400 MHz, $d_6$-DMSO): δ 9.85 (t, *J* = 1.3 Hz, 2H), 8.26 (dt, *J* = 14.8, 1.7 Hz, 4H), 7.66 (t, *J* = 7.8 Hz, 2H), 7.49 (d, *J* = 7.8 Hz, 4H), 4.39 (s, 4H), 2.26 (sept, *J* = 6.7 Hz, 4H), 1.15 (d, *J* = 6.5 Hz, 12 H), 1.13 (d, *J* = 6.5 Hz, 12 H), 1.08-1.04 (s, 4H); **$^{13}$C NMR** (100 MHz, $d_6$-DMSO): 145.1, 137.9, 131.5, 130.5, 125.2, 124.5, 124.0, 53.2, 28.1, 23.8, 21.7, 11.3. **Accurate mass (ESI+):** m/z calc'd for $[H_{48}C_{35}N_4]^{2+}$ Theoretical: 262.1939. Found: 262.1941. Melting point: 243-246 °C.

Crystals suitable for X-ray were grown by slow evaporation of isopropanol solution of **L2** (Figure 4.14).

**Figure 4.14.** X-ray crystal structure of **L2**. Thermal ellipsoids are shown at 30% probability. Hydrogen atoms co-crystallized solvent molecules are omitted for clarity.

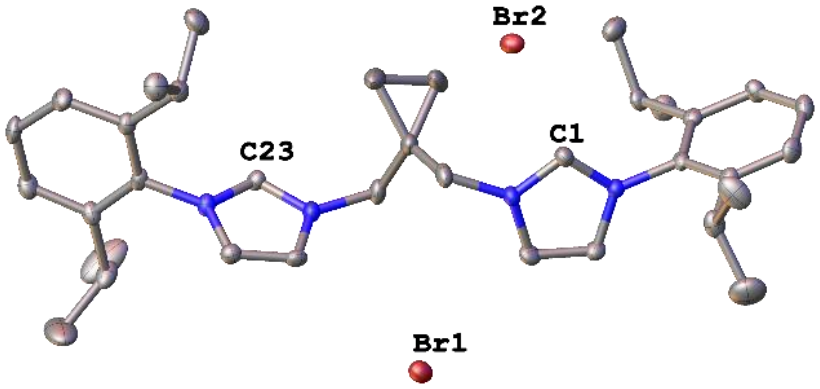




*Chapter four references begin on page 364; experimental details begin on page 331*

### **4.9.6.** Characterization details of products

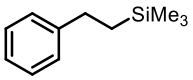


**[2-(Trimethylsilyl)ethyl]benzene (4.9)** was prepared from 2-trimethylsilylethanol and phenylboronic acid pinacol ester according to general procedure B. Column chromatography was performed using a gradient of 1→5% ethyl acetate in hexanes to afford product as a colourless liquid (22.4 mg, 92% yield). Analytical data matched those in the literature.[52] **$^{1}$H NMR** (400 MHz, $CDCl_3$): δ 7.31-7.28 (m, 2H), 7.23-7.16 (m, 3H), 2.66-2.62 (m, 2H), 0.91-0.87 (m, 2H), 0.03 (s, 9H); **$^{13}$C NMR** (100 MHz, $CDCl_3$): 145.3, 128.3, 127.8, 125.4, 30.0, 18.7, -1.8.

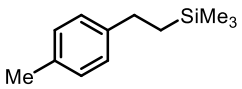


**1-Methyl-4-[2-(trimethylsilyl)ethyl]-benzene (4.15)** was prepared from 2-trimethylsilylethanol and 4-methylphenylboronic acid pinacol ester according to general procedure B. Column chromatography was performed using a gradient of 1→5% ethyl acetate in hexanes to afford product as a colourless liquid (38.4 mg, 88% yield). Analytical data matched those in the literature.[53] **$^{1}$H NMR** (400 MHz, $CDCl_3$): δ 7.13-7.01 (m, 4H), 2.63-2.58 (m, 2H), 2.34 (s, 3H), 0.89-0.85 (m, 2H), 0.03 (s, 9H); **$^{13}$C NMR** (100 MHz, $CDCl_3$): 142.3, 134.8, 128.9, 127.6, 29.6, 21.0, 18.8, -1.8.

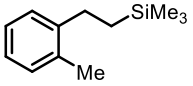


**1-Methyl-2-[2-(trimethylsilyl)ethyl]benzene (4.16)** was prepared from 2-trimethylsilylethanol and 2-methylphenylboronic acid pinacol ester according to general procedure B. Column chromatography was performed using a gradient of 1→5% ethyl acetate in hexanes to afford product as a colourless liquid (31.5 mg, 82% yield). Analytical data matched those in the literature.[54] **$^{1}$H NMR** (400 MHz, $CDCl_3$): δ 7.19-7.07 (m, 4H), 2.61-2.57 (m, 2H), 2.31 (s, 3H), 0.83-0.79 (m, 2H), 0.06 (s, 9H); **$^{13}$C NMR** (100 MHz, $CDCl_3$): 143.5, 135.3, 130.1, 127.9, 126.0, 125.6, 27.4, 19.1, 17.5, -1.8.



*Chapter four references begin on page 364; experimental details begin on page 331*

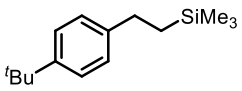


**1-(1,1-Dimethylethyl)-4-[2-(trimethylsilyl)ethyl]benzene (4.17)** was prepared from 2-trimethylsilylethanol and 4-*tert*-butylphenylboronic acid pinacol ester according to general procedure B. Column chromatography was performed using a gradient of 1→5% ethyl acetate in hexanes to afford product as a colourless liquid (44.1 mg, 94% yield). Analytical data matched those in the literature.[53] **$^{1}$H NMR** (400 MHz, $CDCl_3$): δ 7.32-7.30 (m, 2H), 7.17-7.14 (m, 2H), 2.63-2.58 (m, 2H), 1.32 (s, 9H), 0.90-0.85 (m, 2H), 0.03 (s, 9 H); **$^{13}$C NMR** (100 MHz, $CDCl_3$): 148.2, 142.3, 127.4, 125.1, 34.3, 31.4, 29.4, 18.6, -1.8.

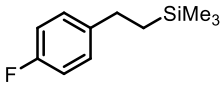


**1-Fluoro-4-[2-(trimethylsilyl)ethyl]benzene (4.18)** was prepared from 2-trimethylsilylethanol and 4-fluorophenylboronic acid pinacol ester according to general procedure B. Column chromatography was performed using a gradient of 1→5% ethyl acetate in hexanes to afford product as a colourless liquid (36.5 mg, 93% yield). Analytical data matched those in the literature.[53] **$^{1}$H NMR** (400 MHz, $CDCl_3$): δ 7.17-7.13 (m, 2H), 6.98-6.94 (m, 2H), 2.63-2.58 (m, 2H), 0.88-0.83 (m, 2H), 0.02 (s, 9H); **$^{13}$C NMR** (100 MHz, $CDCl_3$): 161.0 (d, $J$ = 242.4 Hz), 140.8, 129.1 (d, $J$ = 7.6 Hz), 115.0 (d, $J$ = 20.8 Hz), 29.3, 18.8, -1.8. **$^{19}$F NMR** (376 MHz, $CDCl_3$): $\delta$ -114.23.

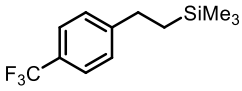


**1-(Trifluoromethyl)-4-[2-(trimethylsilyl)ethyl]benzene (4.19)** was prepared from 2-trimethylsilylethanol and 4-trifluoromethylphenylboronic acid pinacol ester according to general procedure B. Column chromatography was performed using a gradient of 1→5% ethyl acetate in hexanes to afford product as a colourless liquid (46.7 mg, 95% yield). **$^{1}$H NMR** (400 MHz, $CDCl_3$): δ 7.53 (d, $J$ = 8.0 Hz, 2H), 7.31 (d, $J$ = 8.0 Hz, 2H), 2.70-2.66 (m, 2H), 0.90-0.86 (m, 2H), 0.04 (s, 9H); **$^{13}$C NMR** (100 MHz, $CDCl_3$): 149.5 (d, J = 1.2 Hz), 128.1, 125.2 (q, $J$ = 3.9 Hz), 123.4 (q, $J$ = 272.4 Hz), 30.1, 18.5, -1.8. **$^{19}$F NMR** (376 MHz, $CDCl_3$): $\delta$ -63.42. **Accurate mass (EI)**: Theoretical: 246.1052. Found: 246.1049. Spectral Accuracy: 98.4%.



*Chapter four references begin on page 364; experimental details begin on page 331*

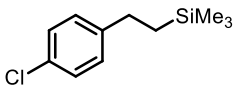


**1-Chloro-4-[2-(trimethylsilyl)ethyl]benzene (4.20)** was prepared from 2-trimethylsilylethanol and 4-chlorophenylboronic acid pinacol ester according to general procedure B. Column chromatography was performed using a gradient of 1→5% ethyl acetate in hexanes to afford product as a yellow liquid (34.8 mg, 82% yield). Analytical data matched those in the literature.[53] **$^{1}$H NMR** (400 MHz, $CDCl_3$): δ 7.36-7.31 (m, 1H), 7.21-7.17 (m, 1H), 7.15-7.09 (m, 2H), 2.74-2.69 (m, 2H), 0.88-0.83 (m, 2H), 0.06 (s, 9H); **$^{13}$C NMR** (100 MHz, $CDCl_3$): 145.3, 128.3, 127.8, 125.4, 30.0, 18.7, -1.8.

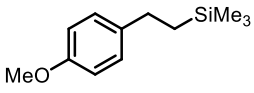


**1-Methoxy-4-[2-(trimethylsilyl)ethyl]benzene (4.21)** was prepared from 2-trimethylsilylethanol and 4-methoxyphenylboronic acid pinacol ester according to general procedure B. Column chromatography was performed using a gradient of 1→5% ethyl acetate in hexanes to afford product as a colourless liquid (39.5 mg, 95% yield). Analytical data matched those in the literature.[55] **$^{1}$H NMR** (400 MHz, $CDCl_3$): δ 7.13 (d, *J* = 8.4 Hz, 2H), 6.83 (d, *J* = 8.4 Hz, 2H), 3.80 (s, 3H), 2.62-2.57 (m, 2H), 0.89-0.84 (m, 2H), 0.02 (s, 9H); **$^{13}$C NMR** (100 MHz, $CDCl_3$): 157.5, 137.4, 128.6, 113.7, 55.3, 29.1, 18.9, -1.7.

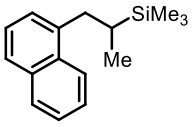


**1-[2-(Trimethylsilyl)propyl]naphthalene (4.22)** was prepared from 2-trimethylsilyl-1-propanol and 2-napthylboronic acid pinacol ester according to general procedure B. Column chromatography was performed using a gradient of 1→5% ethyl acetate in hexanes to afford product as a colourless liquid (33.4 mg, 69% yield). **$^{1}$H NMR** (400 MHz, $CDCl_3$): δ 7.83-7.77 (m, 3H), 7.60-7.59 (m, 1H), 7.48-7.40 (m, 2H), 7.33 (dd, *J* = 8.3, 1.6 Hz, 1H), 3.03 (dd, *J* = 13.7, 3.9 Hz, 1H), 2.41 (dd, *J* = 13.7, 11.4 Hz, 1H), 1.12-1.02 (m, 1H), 0.86 (d, *J* = 7.3 Hz, 3H), 0.05 (s, 9H); **$^{13}$C NMR** (100 MHz, $CDCl_3$): 140.3, 133.5, 131.9, 127.6, 127.5, 127.4, 126.9, 125.8, 124.9, 38.1, 21.9, 13.6, -3.3. **Accurate mass (EI)**: Theoretical: 242.1491. Found: 242.1490. Spectral Accuracy: 98.4%.



*Chapter four references begin on page 364; experimental details begin on page 331*

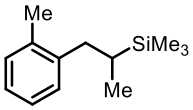


**1-(2-Methylphenyl)-2-methyl-2-trimethylsilylethane (4.23)** was prepared from 2-trimethylsilyl-1-propanol and 2-methylphenylboronic acid pinacol ester according to general procedure B. Column chromatography was performed using a gradient of 1→5% ethyl acetate in hexanes to afford product as a colourless liquid (33.4 mg, 87% yield). **$^{1}$H NMR** (400 MHz, $CDCl_3$): δ 7.13-7.09 (m, 4H), 2.86 (dd, *J* = 13.6, 4.4 Hz, 1H), 2.30 (s, 3H), 2.2 (dd, *J* = 13.6, 11.6 Hz, 1H), 0.94-0.88 (m, 1H), 0.86 (d, *J* = 7.3 Hz, 3H), 0.04 (s, 9H); **$^{13}$C NMR** (100 MHz, $CDCl_3$): 140.6, 136.0, 130.2, 129.8, 125.6, 125.4, 39.9, 20.4, 19.4, 13.5, -3.4. **Accurate mass (EI)**: Theoretical: 206.1491. Found: 206.1486. Spectral Accuracy: 98.6%.

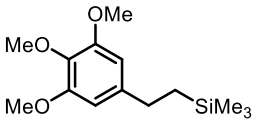


**1,2,3-Trimethoxy-5-[2-(trimethylsilyl)ethyl]-benzene (4.24)** was prepared from 2-trimethylsilylethanol and 3,4,5-trimethoxyphenylboronic acid pinacol ester according to general procedure B. Column chromatography was performed using a gradient of 1→10% ethyl acetate in hexanes to afford product as a colourless liquid (48.8 mg, 91% yield). Analytical data matched those in the literature.[54] **$^{1}$H NMR** (400 MHz, $CDCl_3$): δ 6.43 (s, 2H), 3.86 (s, 6H), 3.83 (s, 3H), 2.60-2.56 (m, 2H), 0.89-0.85 (m, 2H), 0.04 (s, 9H); **$^{13}$C NMR** (100 MHz, $CDCl_3$): 153.0, 141.1, 135.8, 104.5, 60.8, 56.0, 30.4, 18.6, -1.8.

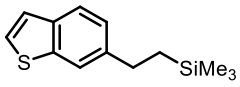


**5-[2-(Trimethylsilyl)ethyl]benzo[*b*]thiophene (4.25)** was prepared from 2-trimethylsilylethanol and 6-thiophenylboronic acid pinacol ester according to general procedure B. Column chromatography was performed using a gradient of 1→10% ethyl acetate in hexanes to afford product as a yellow liquid (35.6 mg, 76% yield). **$^{1}$H NMR** (400 MHz, $CDCl_3$): δ 9.05 (s, 1H), 8.22 (d, *J* = 8.6 Hz, 1H), 8.03 (d, *J* = 8.6 Hz, 1H), 7.57 (t, *J* = 8.4 Hz, 1H), 7.50 (t, *J* = 8.4 Hz, 1H) 3.80-3.77 (m, 2H), 1.02-0.99 (m, 2H), 0.07 (s, 9H); **$^{13}$C NMR** (100 MHz, $CDCl_3$): 140.4, 140.1, 133.3, 128.7, 127.7, 126.9, 125.8, 124.2, 44.7, 33.2, -1.2. **Accurate mass (EI)**: Theoretical: 234.0898. Found: 234.0895. Spectral Accuracy: 98.6%.



*Chapter four references begin on page 364; experimental details begin on page 331*

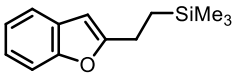

**2-[2-(Trimethylsilyl)ethyl]benzofuran (4.26)** was prepared from 2-trimethylsilylethanol and 2-benzofuranylboronic acid pinacol ester according to general procedure B. Column chromatography was performed using a gradient of 1→10% ethyl acetate in hexanes to afford product as a yellow liquid (31.0 mg, 71% yield). **$^{1}$H NMR** (400 MHz, $CDCl_3$): δ 7.49-7.39 (m, 2H), 7.22-7.16 (m, 2H), 6.39 (s, 1H), 2.80-2.76 (m, 2H), 1.02-0.97 (m, 2H), 0.05 (s, 9H); **$^{13}$C NMR** (100 MHz, $CDCl_3$): 147.5, 145.3, 139.3, 120.3, 108.3, 108.0, 100.7, 29.8, 19.0, -1.8**Accurate mass (EI)**: Theoretical: 218.1127. Found: 218.1128. Spectral Accuracy: 97.0%.

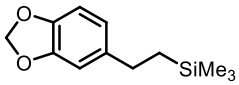

**5-[1-(Trimethylsilyl)ethyl]-1,3-benzodioxole (4.27)** was prepared from 2-trimethylsilylethanol and 5-(1,3-benzodioxole)boronic acid pinacol ester according to general procedure B. Column chromatography was performed using a gradient of 1→10% ethyl acetate in hexanes to afford product as a yellow liquid (36.9 mg, 83% yield). **$^{1}$H NMR** (400 MHz, $CDCl_3$): δ 6.74-6.64 (m, 3H), 5.92 (s, 2H), 2.58-2.54 (m, 2H), 0.86-0.82 (m, 2H), 0.02 (s, 9H); **$^{13}$C NMR** (100 MHz, $CDCl_3$): 147.5, 145.3, 139.3, 120.3, 108.3, 108.0, 100.7, 29.8, 19.0, -1.8. **Accurate mass (EI)**: Theoretical: 222.1076. Found: 222.1078. Spectral Accuracy: 97.8%.

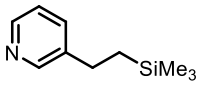

**3-[2-(Trimethylsilyl)ethyl]pyridine (4.28)** was prepared from 2-trimethylsilylethanol and 3-pyridylboronic acid pinacol ester according to general procedure B. Column chromatography was performed using a gradient of 1→10% ethyl acetate in hexanes to afford product as a yellow liquid (29.7 mg, 83% yield). **$^{1}$H NMR** (400 MHz, $CDCl_3$): δ 8.46-8.40 (m, 2H), 7.52-7.49 (m, 1H), 7.21-7.17 (m, 1H), 2.64-2.60 (m, 2H), 0.88-0.84 (m, 2H), 0.02 (s, 9H); **$^{13}$C NMR** (100 MHz, $CDCl_3$): 149.5, 147.0, 140.3, 135.2, 123.2, 27.3, 18.4, -1.8. **Accurate mass (EI)**: Theoretical: 179.1130. Found: 179.1124. Spectral Accuracy: 97.0%.



*Chapter four references begin on page 364; experimental details begin on page 331*

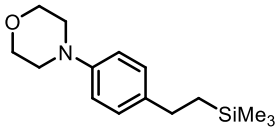

**4-[4-[2-(Trimethylsilyl)ethyl]phenyl]morpholine (4.29)** was prepared from 2-trimethylsilylethanol and 4-(4-morpholino)phenylboronic acid pinacol ester according to general procedure B. Column chromatography was performed using a gradient of 1→30% ethyl acetate in hexanes to afford product as a yellow liquid (37.3 mg, 71% yield). Analytical data matched those in the literature.[54] **$^1$H NMR** (400 MHz, $CDCl_3$): δ 7.13 (d, *J* = 8.5 Hz, 2H), 6.86 (d, *J* = 8.5 Hz, 2H), 3.88-3.86 (m, 4H), 3.14-3.12 (m, 4H), 2.59-2.55 (m, 2H), 0.87-0.82 (m, 2H), 0.01 (s, 9H); **$^{13}$C NMR** (100 MHz, $CDCl_3$): 149.3, 137.1, 128.4, 116.0, 67.0, 49.9, 29.0, 18.7, -1.7.

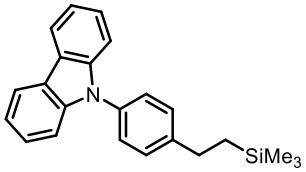

**9-[4-[2-(Trimethylsilyl)ethyl]phenyl]-9*H*-carbazole (4.30)** was prepared from 2-trimethylsilylethanol and 4-[9-(*9H*-carbazolyl)]phenylboronic acid pinacol ester according to general procedure B. Column chromatography was performed using a gradient of 1→10% ethyl acetate in hexanes to afford product as a yellow liquid (28.1 mg, 41% yield). Analytical data matched those in the literature.[54] **$^1$H NMR** (400 MHz, $CDCl_3$): δ 8.15 (d, *J* = 7.9 Hz, 2H), 7.45-7.40 (m, 8H), 7.30-7.27 (m, 2H), 2.79-2.75 (m, 2H), 1.01-0.97 (m, 2H), 0.08 (s, 9H); **$^{13}$C NMR** (100 MHz, $CDCl_3$): 141.1, 129.2, 127.0, 125.8, 123.2, 120.2, 119.7, 109.8, 29.8, 18.7, -1.7.

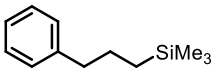

**[3-(Trimethylsilyl)propyl]benzene (4.31)** was prepared from 2-trimethylsilylethanol and benzylboronic acid pinacol ester according to general procedure B. Column chromatography was performed using a gradient of 1→5% ethyl acetate in hexanes to afford product as a colourless liquid (30.3 mg, 79% yield). The same product was recovered (23.8 mg, 62% yield) upon subjecting 2-trimethylsilylethanol and benzylboronic acid pinacol ester to a modified general procedure B, employing $NiBr_2$·glyme (5 mol%, 6.1 mg) as a precatalyst alongside Mn (30 mol%, 1.6 mg) rather than $Ni(cod)_2$. Analytical data matched those in the literature.[56] **$^1$H NMR** (400 MHz, $CDCl_3$): δ 7.32-7.27 (m, 2H), 7.21-7.17 (m, 3H), 2.63 (t, *J* = 15.8 Hz, 2H), 1.62 (ddt, *J* = 15.8, 7.7, 3.1 Hz, 2H), 0.57-0.53 (m, 2H), -0.02 (s, 9H); **$^{13}$C NMR** (100 MHz, $CDCl_3$): 142.8, 128.5, 128.2, 125.6, 39.9, 26.1, 16.6, -1.7.



*Chapter four references begin on page 364; experimental details begin on page 331*

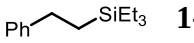 **1-Phenyl-2-triethylsilylethane (4.32)** was prepared from 2-triethylsilylethanol and phenylboronic acid pinacol ester according to general procedure B. Column chromatography was performed using a gradient of 1→10% ethyl acetate in hexanes to afford product as a colourless liquid (37.8 mg, 86% yield). The same product was recovered (30.8 mg, 70% yield) upon subjecting 2-triethylsilylethanol and phenylboronic acid pinacol ester to a modified general procedure B, employing $NiBr_2$·glyme (5 mol%, 6.1 mg) as a precatalyst alongside Mn (30 mol%, 1.6 mg) rather than $Ni(cod)_2$. Analytical data matched those in the literature.[57] **$^1$H NMR** (400 MHz, $CDCl_3$): δ 7.33-7.29 (m, 2H), 7.25-7.18 (m, 3H), 2.67-2.63 (m, 2H), 1.01-0.95 (m, 9H), 0.93-0.90 (m, 2H), 0.62-0.54 (m, 6H); **$^{13}$C NMR** (100 MHz, $CDCl_3$): 145.6, 128.3, 127.7, 125.5, 30.0, 13.6, 7.4, 3.3. **Accurate mass (EI)**: Theoretical: 220.1647. Found: 220.1643. Spectral Accuracy: 97.8%.

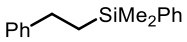 **[Dimethyl(2-phenylethyl)silyl]benzene (4.33)** was prepared from 2-(dimethylphenylsilyl)ethanol and phenylboronic acid pinacol ester according to general procedure B. Column chromatography was performed using a gradient of 1→10% ethyl acetate in hexanes to afford product as a yellow liquid (39.8 mg, 83% yield). **$^1$H NMR** (400 MHz, $CDCl_3$): δ 7.70-7.68 (m, 2H), 7.52-7.50 (m, 3H), 7.42-7.39 (m, 2H), 7.33-7.30 (m, 3H), 2.81-2.77 (m, 2H), 1.30-1.27 (m, 2H), 0.44 (s, 6H); **$^{13}$C NMR** (100 MHz, $CDCl_3$): 144.9, 139.0, 133.6, 128.9, 128.3, 127.8, 127.7, 125.5, 29.9, 17.7, -3.1. **Accurate mass (EI)**: Theoretical: 240.1334. Found: 240.1331. Spectral Accuracy: 98.2%.

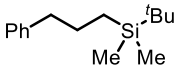 **[3-[(1,1-Dimethylethyl)dimethylsilyl]propyl]benzene (4.34)** was prepared from 2-[(1,1-dimethylethyl)dimethylsilyl]ethanol and benzylboronic acid pinacol ester according to general procedure B. Column chromatography was performed using a gradient of 1→10% ethyl acetate in hexanes to afford product as a yellow liquid (39.3 mg, 84% yield). **$^1$H NMR** (400 MHz, $CDCl_3$): δ 7.31-7.28 (m, 2H), 7.24-7.18 (m, 3H), 3.38 (t, *J* = 6.6 Hz, 2H), 2.77 (t, *J* = 7.4 Hz, 2H), 2.19-2.12 (m, 2H), 0.97 (s, 9H), 0.36 (s, 6H); **$^{13}$C NMR** (100 MHz, $CDCl_3$): 140.5, 128.53, 128.47, 126.1, 34.0, 33.1, 30.9, 25.3, 19.0, -1.6. **Accurate mass (EI)**: Theoretical: 234.1804. Found: 234.1802. Spectral Accuracy: 97.6%.



*Chapter four references begin on page 364; experimental details begin on page 331*

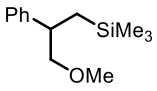


**1-Methoxy-2-phenyl-3-(trimethylsilyl)propane (4.2)** was prepared from **4.1** and phenylboronic acid pinacol ester according to general procedure B. Column chromatography was performed using a gradient of 1→5% ethyl acetate in hexanes to afford product as a colourless liquid (36.7 mg, 83% yield). The same product was recovered (30.1 mg, 68% yield) upon subjecting **4.1** and phenylboronic acid pinacol ester to a modified general procedure B, employing $NiBr_2$·glyme (5 mol%, 6.1 mg) as a precatalyst alongside Mn (30 mol%, 1.6 mg) rather than $Ni(cod)_2$. **$^1$H NMR** (400 MHz, $CDCl_3$): δ 7.49-7.46 (m, 2H), 7.26-7.19 (m, 3H), 3.49-3.46 (m, 1H), 3.46 (s, 3H), 1.77-1.70 (m, 2H), 0.59-0.54 (m, 2H), -0.02 (s, 9H);**$^{13}$C NMR** (100 MHz, $CDCl_3$): 131.5, 130.0, 126.9, 122.5, 50.8, 48.0, 27.7, 14.3, -1.8. **Accurate mass (EI)**: Theoretical: 222.1440. Found: 222.1437. Spectral Accuracy: 98.6%.

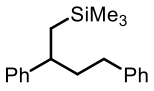


**1,3-Diphenyl-4-trimethylsilylbutane (4.3)** was prepared from the corresponding alcohol and phenylboronic acid pinacol ester according to general procedure B. Column chromatography was performed using a gradient of 1→5% ethyl acetate in hexanes to afford product as a clear liquid (50.2 mg, 89% yield). Analytical data matched those in the literature.[54] **$^1$H NMR** (400 MHz, $CDCl_3$): δ δ 7.32-7.24 (m, 2H), 7.24-7.21 (m, 2H), 7.19-7.16 (m, 4H), 7.12-7.09 (m, 2H), 2.68 (ddd, *J* = 14.8, 8.6, 6.2 Hz, 1H), 2.42 (dt, *J* = 14.8, 8.6 Hz, 2H), 1.98-1.88 (m, 2H), 0.98-0.96 (m, 2H), -0.20 (s, 9H); **$^{13}$C NMR** (100 MHz, $CDCl_3$): 147.2, 142.6, 128.34, 128.28, 128.2, 127.6, 126.0, 125.5, 42.6, 41.7, 34.0, 25.4, -1.1.

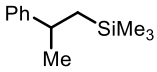


**[1-Methyl-2-(trimethylsilyl)ethyl]benzene (4.4)** was prepared from 2-trimethylsilyl-2-propanol and phenylboronic acid pinacol ester according to general procedure B. Column chromatography was performed using a gradient of 1→5% ethyl acetate in hexanes to afford product as a colourless liquid (31.1 mg, 81% yield). The same product was recovered (27.3 mg, 71% yield) upon subjecting 2-trimethylsilyl-2-propanol to a modified general procedure B, employing $NiBr_2$·glyme (5 mol%, 6.1 mg) as a precatalyst alongside Mn (30 mol%, 1.6 mg) rather than $Ni(cod)_2$. Analytical data matches those within the literature.[52] **$^1$H NMR** (400 MHz, $CDCl_3$): δ 7.37-7.30 (m, 3H), 7.26-7.19 (m, 2H), 2.93 (q, *J* = 7.1 Hz, 1H), 1.33 (d, *J* = 7.1 Hz, 3H), 1.04 (dd, J = 14.9, 8.5 Hz, 1H), 0.94 (dd, *J* = 14.9, 8.5 Hz, 1H), -0.06 (s, 9H); **$^{13}$C NMR** (100 MHz, $CDCl_3$): 149.8, 128.3, 126.6, 125.7, 36.4, 27.0, 26.4, -1.0.



*Chapter four references begin on page 364; experimental details begin on page 331*

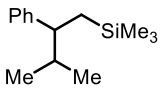


**[2-Methyl-3-phenyl-4-(trimethylsilyl)]butane (4.5)** was prepared from the corresponding alcohol and phenylboronic acid pinacol ester according to general procedure B. Column chromatography was performed using a gradient of 1→5% ethyl acetate in hexanes to afford product as a yellow liquid (38.7 mg, 88% yield). **$^{1}$H NMR** (500 MHz, $CDCl_3$): δ 7.25-7.22 (m, 2H), 7.18-7.11 (m, 3H), 2.39 (sept, *J* = 3.6 Hz, 1H), 1.72 (ddd, *J* = 13.5, 6.8, 6.8 Hz, 1H), 0.92 (d, *J* = 6.8 Hz, 3H), 0.87-0.84 (m, 2H), 0.71 (d, *J* = 6.8 Hz, 3H), -0.26 (s, 9H); **$^{13}$C NMR** (126 MHz, $CDCl_3$): 128.6, 127.8, 125.7, 48.9, 36.1, 29.7, 20.8, 20.3, -1.2. **Accurate mass (EI)**: Theoretical: 220.1647. Found: 220.1649. Spectral Accuracy: 97.2%.

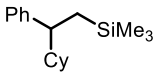


**(2-Cyclohexyl-2-phenylethyl)trimethylsilane (4.6)** was prepared from the corresponding alcohol and phenylboronic acid pinacol ester according to general procedure B. Column chromatography was performed using a gradient of 1→10% ethyl acetate in hexanes to afford product as a yellow liquid (45.2 mg, 87% yield). **$^{1}$H NMR** (500 MHz, $CDCl_3$): δ 7.32-7.29 (m, 2H), 7.22-7.14 (m, 3H), 2.48-2.43 (m, 1H), 1.99-1.95 (m, 1H), 1.80-1.76 (m, 1H), 1.69-1.64 (m, 2H), 1.50-1.31 (m, 3H), 1.19-1.06 (m, 3H), 0.95-0.87 (m, 2H), 0.83-0.74 (m, 1H), -0.23 (s, 9H); **$^{13}$C NMR** (126 MHz, $CDCl_3$): 146.0, 128.6, 127.8, 125.7, 48.1, 45.9, 43.7, 31.3, 30.7, 26.7, 26.6, 20.6, -1.2. **Accurate mass (EI)**: Theoretical: 260.1960. Found: 260.1954. Spectral Accuracy: 97.4%.

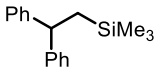


**(2,2-Diphenylethyl)trimethylsilane (4.7)** was prepared from the corresponding alcohol and phenylboronic acid pinacol ester according to general procedure B. Column chromatography was performed using a gradient of 1→5% ethyl acetate in hexanes to afford product as a yellow liquid (46.3 mg, 91% yield). The same product was recovered (32.5 mg, 64% yield) upon subjecting the corresponding alcohol and phenylboronic acid pinacol ester to a modified general procedure B, employing $NiBr_2$·glyme (5 mol%, 6.1 mg) as a precatalyst alongside Mn (30 mol%, 1.6 mg) rather than $Ni(cod)_2$. Analytical data matches those within the literature.[61] **$^{1}$H NMR** (400 MHz, $CDCl_3$): δ 7.29-7.22 (m, 8H), 7.15-7.11 (m, 2H), 4.06 (t, *J* = 8.0 Hz, 1H), 1.39 (d, *J* = 8.0 Hz, 2H), -0.20 (s, 9H); **$^{13}$C NMR** (100 MHz, $CDCl_3$): 147.1, 128.3, 127.5, 125.9, 47.3, 24.2, -1.2.



*Chapter four references begin on page 364; experimental details begin on page 331*

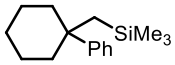


**Trimethyl[(1-phenylcyclohexyl)methyl)]silane (4.8)** was prepared from the corresponding alcohol and phenylboronic acid pinacol ester according to general procedure B. Column chromatography was performed using a gradient of 1→5% ethyl acetate in hexanes to afford product as a colourless liquid (35.9 mg, 73% yield). **$^{1}$H NMR** (400 MHz, $CDCl_3$): δ 7.49-7.46 (m, 2H), 7.28-7.20 (m, 3H), 3.43-3.41 (m, 2H), 1.77-1.63 (m, 5H), 1.48-1.44 (m, 1H), 1.29-1.10 (m, 3H), 0.94-0.86 (m, 2H), 0.02 (s, 9H); **$^{13}$C NMR** (100 MHz, $CDCl_3$): 148.1, 128.3, 126.8, 125.8, 44.6, 34.5, 26.9, 26.2, 3.3, 1.9. **Accurate mass (EI)**: Theoretical: 246.1804. Found: 246.1802. Spectral Accuracy: 97.4%.

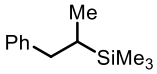


**1-(Phenyl)-2-methyl-2-trimethylsilylethane (4.10)** was prepared from 2-trimethylsilyl-1-propanol and phenylboronic acid pinacol ester according to general procedure B. Column chromatography was performed using a gradient of 1→5% ethyl acetate in hexanes to afford product as a colourless liquid (31.9 mg, 83% yield). **$^{1}$H NMR** (500 MHz, $CDCl_3$): δ 7.29-7.24 (m, 2H), 7.19-7.15 (m, 3H), 2.85 (dd, *J* = 13.6, 4.1 Hz, 1H), 2.25 (dd, *J* = 13.6, 11.4 Hz, 1H), 0.99-0.93 (m, 1H), 0.84 (d, *J* = 7.2 Hz, 3H), 0.00 (s, 9H); **$^{13}$C NMR** (126 MHz, $CDCl_3$): 142.7, 128.8, 128.1, 125.5. 38.0, 22.1, 13.6, -3.4. **Accurate mass (EI)**: Theoretical: 192.1334. Found: 192.1329. Spectral Accuracy: 97.8%.

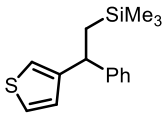


**2-[2-Trimethylsilyl)-1-phenethyl]-thiazole (4.12)** was prepared from the corresponding alcohol and phenylboronic acid pinacol ester according to general procedure B. Column chromatography was performed using a gradient of 1→5% ethyl acetate in hexanes to afford product as a colourless liquid (35.4 mg, 68% yield). **$^{1}$H NMR** (400 MHz, $CDCl_3$): δ 7.31-7.24 (m, 3H), 7.19-7.15 (m, 2H), 7.09-7.07 (m, 1H), 6.88-6.84 (m, 1H), 6.81-6.79 (m, 1H), 4.29-4.25 (m, 1H), 1.48-1.35 (m, 2H), -0.19 (s, 9H); **$^{13}$C NMR** (100 MHz, $CDCl_3$): 140.4, 140.1, 133.3, 128.7, 127.7, 126.9, 125.7, 124.2, 44.7, 33.2, -1.2. **Accurate mass (EI)**: Theoretical: 260.1055. Found: 260.1057. Spectral Accuracy: 97.0%.



*Chapter four references begin on page 364; experimental details begin on page 331*

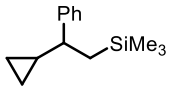


**1-Cyclopropyl-1-phenyl-2-trimethylsilylethane (4.69)** was prepared from **4.68** and phenylboronic acid pinacol ester according to general procedure B. Column chromatography was performed using a gradient of 1→5% ethyl acetate in hexanes to afford product as a colourless liquid (39.2 mg, 90% yield). **$^{1}$H NMR** (400 MHz, $CDCl_3$): δ 7.31-7.28 (m, 2H), 7.21-7.14 (m, 3H), 1.91 (dt, *J* = 9.1, 7.7 Hz, 1H), 1.10 (d, *J* = 7.7 Hz, 2H), 1.04-0.98 (m, 1H), 0.60-0.53 (m, 1H), 0.39-0.0.34 (m, 1H), 0.23-0.17 (m, 1H), 0.14-0.09 (m, 1H), -0.18 (s, 9H): **$^{13}$C NMR** (100 MHz, $CDCl_3$): 147.5, 128.7, 128.1, 127.5, 127.4, 125.9, 47.3, 24.7, 21.2, 5.8, 4.5, -1.1. **Accurate mass (EI)**: Theoretical: 218.1491. Found: 218.1487. Spectral Accuracy: 97.4%.

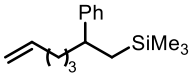


**1-[(Trimethylsilyl)-6-heptenyl]benzene (4.72)** was prepared from **4.71** and phenylboronic acid pinacol ester according to general procedure B. Column chromatography was performed using a gradient of 1→5% ethyl acetate in hexanes to afford product as a yellow liquid (38.4 mg, 78% yield). **$^{1}$H NMR** (400 MHz, $CDCl_3$): δ 7.50-7.47 (m, 2H), 7.27-7.20 (m, 3H), 5.82-5.74 (ddt, *J* = 16.9, 10.2, 6.6 Hz, 1H), 5.02-4.93 (m, 2H), 3.41-3.38 (m, 2H), 2.05 (m, 2H), 1.86 (quin, *J* = 6.8 Hz, 2H), 1.46-1.39 (m, 3H), 0.03 (s, 9H); **$^{13}$C NMR** (100 MHz, $CDCl_3$): 139.2, 137.8, 129.0, 128.8, 128.4, 114.1, 33.53, 33.48, 31.1, 22.2, 13.9, -2.5. **Accurate mass (EI)**: Theoretical: 246.1804. Found: 246.1801. Spectral Accuracy: 98.4%.



*Chapter four references begin on page 364; experimental details begin on page 331*

## **4.9.7.** Diversification of silane handle in reaction products

### 4.9.7.1. Procedure for oxidation of -$SiMe_3$ into -OH

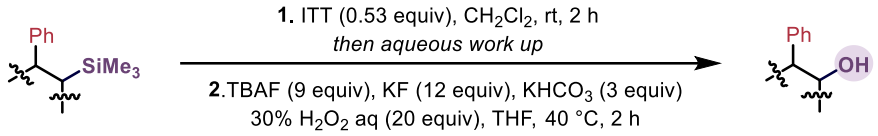


This reaction procedure was adapted from the literature.[21] An oven-dried 8 mL screw-top test-tube was equipped with an oven-dried micro-stir bar and brought into a nitrogen-filled glovebox. This reaction vessel was charged with iodine tris(trifluoroacetate) (*ITT*; 0.53 equivalent, 0.106 mmol) and dichloromethane (0.5 mL). To this mixture was added a solution of silane (1.0 equivalent, 0.20 mmol) in dichloromethane (0.4 mL). The reaction mixture was capped and brought out of the glovebox before being stirred at room temperature for 2 h. After 2 h, a mixture of aqueous $Na_2S_2O_3$ (5%, 2 mL) and saturated $NaHCO_3$ aqueous solution (2 mL) was added. The reaction mixture was extracted into dichloromethane (3 x 5 mL); the organic layers were combined, washed with sat. NaCl and dried over $Na_2SO_4$. Filtration and evaporation via rotary evaporation revealed the crude product as an oil which was directly used in the subsequent step.

To the crude product was added tetrabutyl ammonium fluoride (*TBAF*; 1.0 M in THF; 9.0 equivalent, 1.8 mmol), KF (12 equivalent, 2.4 mmol), $KHCO_3$ (3 equivalent, 0.60 mmol) and hydrogen peroxide (30% in $H_2O$; 20 equivalent, 4.0 mmol). The reaction mixture was capped and stirred at 40 ˚C for 2 h. After 2 h, the reaction mixture was allowed to cool to room temperature before being quenched with $Na_2S_2O_3$ (5%, 10 mL). The resulting mixture was extracted with EtOAc (3 x 5 mL), and the organic layers were combined, washed with sat. NaCl and dried over anhydrous $Na_2SO_4$. Solvent was evacuated via rotary evaporation and the subsequent residue was dissolved in dichloromethane. A small amount of $SiO_2$ was added to the resulting solution and the



*Chapter four references begin on page 364; experimental details begin on page 331*

solvent was once more removed via rotary evaporation. The resulting mixture was purified via column chromatography.

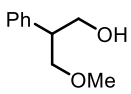


**3-Methoxy-2-phenylpropan-1-ol (4.38)** was prepared from **4.2** according to the above procedure. Column chromatography was performed using a gradient of 1→10% ethyl acetate in hexanes to afford product as a colourless liquid (26.9 mg, 81% yield). Analytical data matched those in the literature.[62] **$^1$H NMR** (400 MHz, $CDCl_3$): δ 7.26-7.14 (m, 5H), 3.83 (dd, *J* = 10.8, 7.2 Hz, 1H), 3.72 (dd, *J* = 10.8, 5.5 Hz, 1H), 3.65 (dd, *J* = 9.4, 7.2 Hz, 1H), 3.59 (dd, *J* = 9.4, 5.5 Hz, 1H), 3.27 (s, 3H), 3.08-3.02 (m, 1H), 3.00 (br s, 1H); **$^{13}$C NMR** (100 MHz, $CDCl_3$): 139.7, 128.2, 127.7, 126.6, 75.2, 65.3, 47.5, 13.8.

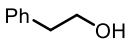


**Phenylethanol (4.39)** was prepared from **4.9** according to the above procedure. Column chromatography was performed using a gradient of 1→10% ethyl acetate in hexanes to afford product as a colourless liquid (18.1 mg, 74% yield). Analytical data matched those within the literature.[63] **$^1$H NMR** (400 MHz, $CDCl_3$): δ 7.36-7.31 (m, 2H), 7.26-7.22 (m, 3H), 3.80 (t, *J* = 6.8 Hz, 2H), 2.85 (t, *J* = 6.8 Hz, 2H), 2.57 (br, 1H); **$^{13}$C NMR** (100 MHz, $CDCl_3$): 138.5, 128.9, 128.3, 126.2, 63.4, 39.0.

### 4.9.7.2. Procedure for protodesilylation of -$SiMe_3$ to -H

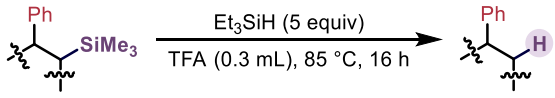


An oven-dried 8 mL screw-top test-tube was equipped with an oven-dried micro-stir bar and brought into a nitrogen-filled glovebox. This reaction vessel was charged with silane (1.0 equivalent, 0.20 mmol) and triethylsilane (*$Et_3SiH$*; 5 equiv, 1.0 mmol). Trifluoroacetic acid (*TFA*; 0.3 mL) was added dropwise to the stirring reaction mixture before the reaction vessel was sealed



*Chapter four references begin on page 364; experimental details begin on page 331*

with a Teflon-septum equipped cap and brought outside of the glovebox to be stirred within a mineral-oil bath at 800 rpm for 16 hours at 85 ˚C. After 16 hours, the reaction vessel was allowed to come to room temperature. The crude reaction solution was quenched slowly with 15% KOH (5 mL) and diluted with EtOAc before being transferred into a separatory funnel. KOH was removed via liquid-liquid extraction with EtOAc (3 x 10 mL); the resulting organic phases were combined in the separatory funnel before being washed twice with sat. $NaHCO_3$ and once with sat. NaCl. The organic phase was dried with $MgSO_4$ before being passed through a short plug composed of $SiO_2$ and celite in a 50:50 ratio. Solvent was evacuated via rotary evaporation and the subsequent residue was dissolved in dichloromethane. A small amount of $SiO_2$ was added to the resulting solution and the solvent was once more removed via rotary evaporation. The resulting mixture was purified via column chromatography.

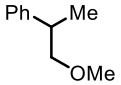


**(2-Methoxy-1-methylethyl)benzene (4.40)** was prepared from **4.2** according to the above procedure. Column chromatography was performed using a gradient of 1→5% ethyl acetate in hexanes to afford product as a colourless liquid (14.7 mg, 49% yield). Analytical data matched those found within the literature.[64] **$^1$H NMR** (400 MHz, $CDCl_3$): δ 7.40-7.36 (m, 2H), 7.32-7.26 (m, 3H), 3.59 (dd, *J* = 9.2, 6.6 Hz, 1H), 3.50 (dd, *J* = 9.2, 6.6 Hz, 1H), 3.40 (s, 3H), 3.11 (dt, *J* = 7.0, 7.0 Hz, 1H), 1.37 (d, *J* = 7.0 Hz, 3H); **$^{13}$C NMR** (100 MHz, $CDCl_3$): 144.3, 128.3, 127.1, 126.2, 78.6, 58.6, 39.8, 18.3.



*Chapter four references begin on page 364; experimental details begin on page 331*

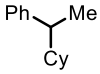


**1-Cyclohexyl-1-phenylethane (4.41)** was prepared from **4.6** according to the above procedure. Column chromatography was performed using a gradient of 1→5% ethyl acetate in hexanes to afford product as a colourless liquid (15.8 mg, 42% yield). Analytical data match those within the literature.[65] **$^1$H NMR** (400 MHz, $CDCl_3$): δ 7.33-7.29 (m, 2H), 7.23-7.17 (m, 3H), 2.48 (dq, *J* = 7.2, 7.0 Hz, 1H), 1.95-1.90 (m, 1H), 1.81-1.76 (m, 1H), 1.69-1.64 (m, 2H), 1.50-1.40 (m, 1H), 1.32-1.29 (m, 1H), 1.27 (d, *J* = 7.0 Hz, 3H), 1.20-1.11 (m, 2H), 1.03-0.82 (m, 3H); **$^{13}$C NMR** (100 MHz, $CDCl_3$): 147.1, 128.0, 127.7, 125.6, 45.9, 44.2, 31.5, 30.6, 29.7, 26.6, 26.5, 18.8.

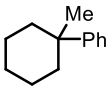


**Trimethyl(phenethyl)silane (4.42)** was prepared from **4.8** according to the above procedure. Column chromatography was performed using a gradient of 1→5% ethyl acetate in hexanes to afford product as a colourless liquid (16.0 mg, 46% yield). Analytical data matched those in the literature.[66] **$^1$H NMR** (400 MHz, $CDCl_3$): δ 7.48-7.17 (m, 4H), 2.08-1.97 (m, 2H), 1.72-1.37 (m, 8H), 1.23 (s, 3H); **$^{13}$C NMR** (100 MHz, $CDCl_3$): 128.3, 128.2, 125.9, 125.5, 38.0, 37.9, 37.3, 26.44, 26.40, 22.68, 22.66.

### **4.9.8.** Other experimental details and procedures

#### *Variable time normalization analysis procedure*

All individual kinetics experiments with silyl ether **4.68** were performed according to a modified General Procedure B, excluding $Me_2SiCl_2$ from the pre-mixing step. Eight reactions were set up in parallel and stopped after 10 min, 30 min, 60 min, 120 min, 210 min, 360 min, 540 min and 720 min. Yields were obtained via $^1$H-NMR using 1,3,5-trimethoxybenzene as internal standard. Variable time normalization analysis was conducted on the obtained time vs. yield data based on the method described by Burés and co-workers[35] to determine the observed rate equation.

Standard reaction conditions were 0.200 M silyl ether (**4.68**), 0.260 M PhBpin, 0.0100 M Ni-**L2** catalyst, 0.0600 M $Bi(OTf)_3$ and 0.600 M $K_3PO_4$. Figure 4.9 was generated by setting



*Chapter four references begin on page 364; experimental details begin on page 331*

[catalyst] ($Ni(cod)_2$ + **L2** + KO$^t$Bu, 1:1:2 ratio) to 0.0100 M (standard conditions), 0.0200 M or 0.0150 M while keeping all else constant. Figure 4.8 was generated by varying [PhBpin], setting it to 0.260 M (standard conditions), 0.520 M or 0.390 M while keeping all else constant. Figure 4.7 was generated by varying [substrate], setting it to 0.200 M (standard conditions), 0.150 M or 0.100 M while keeping all else constant. Figure 4.6 was generated by varying [$Bi(OTf)_3$], setting it to 0.0600 M (standard conditions), 0.0450 M or 0.0300 M while keeping all else constant.

### *Kinetic isotope analysis procedure*

The initial rate kinetics for substrate **4.68$_H$** were examined alongside its deuterated analog **4.68$_D$** in order to investigate the kinetic isotope effects of this reaction. Arylation reactions of substrates **4.68$_H$** and **4.68$_D$** were conducted in parallel according to a modified General Procedure B, excluding the $Me_2SiCl_2$ additive and stopping the reaction after 5, 10, 15, 30 and 60 minutes. Product formation vs. time was plotted, with the rate constant for each reaction being proportional to the change in product concentration divided by the change in time (i.e. $\Delta[P]/\Delta[t]$). This experiment was repeated in triplicate to ensure accuracy.

### *Eyring analysis procedure*

To determine the activation parameters for this transformation, an Eyring analysis was conducted with respect to the arylation of compound **4.68**. Compound **4.68** was subjected to a modified General Procedure B, excluding the $Me_2SiCl_2$ additive, to afford arylated product **4.2** while using the initial-rates method to obtain rate constant values at four different temperatures: 55 °C, 60 °C, 70 °C and 80 °C Plotting the rate constant data according to the Eyring equation[36]



*Chapter four references begin on page 364; experimental details begin on page 331*

revealed a linear plot (Scheme 4.15). Entropies of activation ($\Delta S^{\ddagger}$) were calculated by multiplying the value of the calculated intercept by R (universal gas constant), and enthalpies of activation ($\Delta H^{\ddagger}$) were calculated by multiplying the inverse slope of each of the Eyring plots by R (universal gas constant).

Reaction vials were brought into a glovebox. To each of the reaction vials was added **4.68** (1.0 equivalent, 0.50 mmol), $K_3PO_4$ (3.0 equivalent, 1.5 mmol), $Bi(OTf)_3$ (0.30 equivalent, 0.150 mmol) and PhMe (1.5 mL) – these solutions were allowed to stir for 30 min at room temperature. After 30 min, a pre-mixed solution of $Ni(cod)_2$ (0.05 equivalent, 0.025 mmol), **L2** (0.05 equivalent, 0.025 mmol) and KO$^t$Bu (0.10 equivalent, 0.05 mmol) in PhMe (0.5 mL) was added, followed by PhBpin (1.3 equivalent, 0.65 mmol), and the vials were capped, removed from the glovebox and placed in an oil bath at a variable temperature: 55 °C, 60 °C, 70 °C or 80 °C. Each vial was quenched with EtOAc at a variable amount of time: 5 min, 10 min, 20 min, 30 min, 45 min, 60 min or 80 min. The subsequent solution was washed twice with $NaHCO_3$ (aq) and once with saturated NaCl (aq) before being filtered through a silica-celite (50:50 mixture) plug into a round bottom flask. Solvent was removed via rotary evaporation to reveal product. Yields were obtained via $^1$H NMR using 1,3,5-trimethoxybenzene as an internal standard.

### *Scale up procedure*

An oven-dried 50 mL pressure-tube was equipped with an oven-dried stir bar and brought into a nitrogen-filled glovebox. This reaction vessel was charged with trimethylsilylethanol (1.0 equiv, 8.47 mmol), $K_3PO_4$ (3.0 equiv, 25.4 mmol), $Bi(OTf)_3$ (0.30 equiv, 2.54 mmol), $Me_2SiCl_2$ (1.3 equiv, 11.0 mmol) and PhMe (17 mL). This mixture was capped and left to stir inside the glovebox for 15 min at room temperature. After 15 min a premixed solution of $Ni(cod)_2$ (0.025

equiv, 0.21 mmol), **L2** (0.025 equiv, 0.21 mmol) and KO$^t$Bu (0.05 equiv, 0.42 mmol) in PhMe (17 mL) was added to the stirring solution, followed by ArBpin (1.3 equiv, 11.0 mmol), before the reaction vessel was sealed and brought outside of the glovebox to be stirred within a mineral-oil bath at 800 rpm for 4 hours at 70 ˚C. After 4 hours, the reaction vessel was removed from heat and allowed to come to room temperature. The crude reaction solution was then quenched with 15% KOH and diluted with EtOAc before being transferred into a separatory funnel. Liquid-liquid extraction was done with EtOAc; the resulting organic phases were combined in the separatory funnel before being washed twice with sat. $NaHCO_3$ and once with sat. NaCl. The organic phase was dried with $MgSO_4$ before being passed through a short plug composed of $SiO_2$ and celite in a 50:50 ratio. Solvent was removed via rotary evaporation and the subsequent residue was dissolved in dichloromethane. A small amount of $SiO_2$ was added to the resulting solution and the solvent was once more removed via rotary evaporation. The resulting mixture was purified using column chromatography.

### **4.9.9.** Synthesis of nickel-**L2** complexes

Synthesis and characterization of nickel(II)-**L2**, **4.59**

An oven-dried 10 mL Schlenk flask was equipped with a stir bar and transferred into a nitrogen-filled glovebox. To the flask was added 1,1'-di(2,6-diisopropylphenyl)-3,3' (cyclopropyl)propylenediimidazolium dibromide (**L2**) (1 equiv, 0.1 mmol), KO$^t$Bu (2 equiv, 0.2 mmol), and $Ni(cod)_2$ (1 equiv, 0.1 mmol). The mixture was dissolved in dry THF (0.2 M, 0.5 mL) and taken out of the glovebox. Dry compressed air was added to a flask via ballon and reaction was stirred for 20 h at room temperature. After 20 h, the volatiles were removed under reduced pressure and the flask was transferred into glovebox. The red residue was dissolved in THF and

filtered through fine-frit filter. The resulting solution was concentrated under reduced pressure and triturated with pentane to provide an orange solid (42.5 mg, 68% yield). Suitable crystals for X-ray diffraction were grown from concentrated THF solution of **4.59** (Figure 4.15)**.**

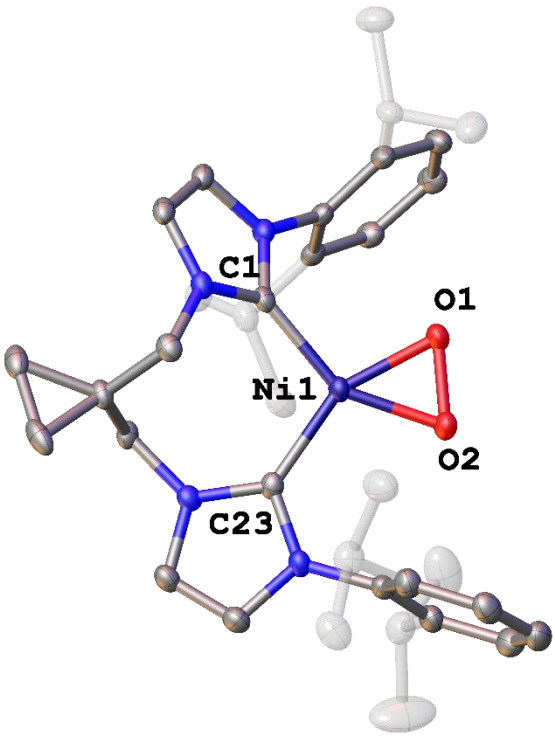


**Figure 4.15**. X-ray crystal structure of **4.59**. Thermal ellipsoids are shown at 50% probability. Hydrogen atoms co-crystallized solvent molecules are omitted for clarity. Selected bond lengths (Å) and angles (°): Ni1-O1 1.829(3), Ni1-O2 1.838(3), Ni1-C1 1.926(5), Ni1-C23 1.910(5), O1-O2 1.457(5); O1-Ni1-O2 46.81(14), C23-Ni1-C1 105.48(19).

Synthesis and characterization of nickel(I)-**L2**, **4.60**

An oven-dried 8 mL reaction vial equipped with a stir bar and transferred into a nitrogen-filled glovebox. Ta the vial was added 1,1'-di(2,6-diisopropylphenyl)-3,3' (cyclopropyl)propylenediimidazolium dibromide (**L2**) (1 equiv, 0.1 mmol), KO$^t$Bu (3 equiv, 0.3 mmol), and $NiBr_2 \cdot$glyme (1 equiv, 0.1 mmol). The mixture was dissolved in dry THF (0.2 M, 0.5



*Chapter four references begin on page 364; experimental details begin on page 331*

mL) and stirred for 20 h at room temperature. After 20 h, the yellow mixture was filtered through fine-frit filter. The resulting solution was concentrated under reduced pressure and triturated with pentane to afford **4.60** as yellow solid (48.1 mg, 73% yield). Suitable crystals for X-ray diffraction were grown from concentrated THF solution of **4.60** (Figure 4.16).

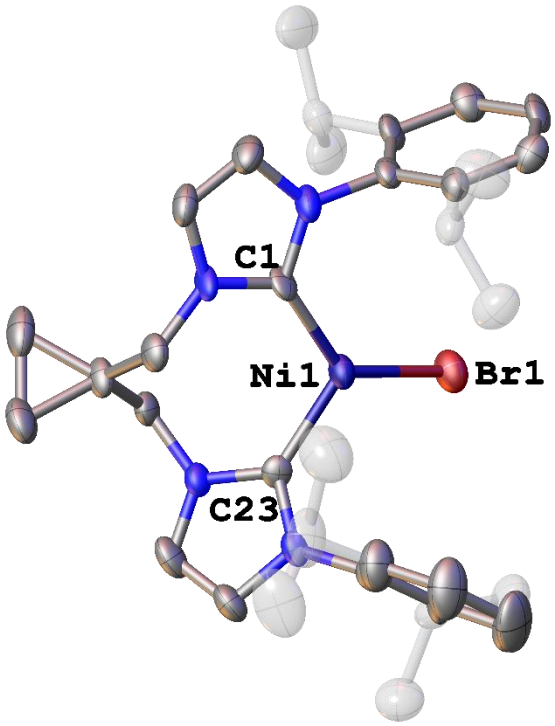


**Figure 4.16.** X-ray crystal structure of **4.60**. Thermal ellipsoids are shown at 50% probability. Hydrogen atoms co-crystallized solvent molecules are omitted for clarity. Selected bond lengths (Å) and angles (°): Br1-Ni1 2.3267(15), Ni1-C1 1.933(9), Ni1-C23 1.925(10); C23-Ni1-C1 109.6(4).

Synthesis and characterization of nickel(0)-**L2**, **4.61**

An oven-dried 8 mL reaction vial equipped with a stir bar and transferred into a nitrogen-filled glovebox. To the vial was added 1,1'-di(2,6-diisopropylphenyl)-3,3'



*Chapter four references begin on page 364; experimental details begin on page 331*

(cyclopropyl)propylenediimidazolium dibromide (**L2**) (1 equiv, 0.2 mmol), KO$^t$Bu (2 equiv, 0.4 mmol), Ni(cod)$_2$ (1 equiv, 0.2 mmol), and 3,3'-bistrifluoromethyl stilbene (1 equiv, 0.2 mmol). The mixture was dissolved in dry toluene (0.2 M, 1 mL) and stirred for 20 h at room temperature. After 20 h, the dark red viscous mixture was filtered through a fine-frit filter and volatiles were removed under reduced pressure. The dark red residue was dissolved in a minimum amount of THF and layered with pentane. The resulting solution was stored at -30 °C upon which the dark red crystals precipitated out of solution. Suitable crystals for X-ray diffraction were selected and the rest was dried under reduced pressure to afford **4.61** as dark red powder (116.5 mg, 65% yield). **$^1$H NMR** (500 MHz, $C_6D_6$) δ 7.25 (t, *J* = 7.8 Hz, 3H), 7.19 (d, *J* = 8.1 Hz, 4H), 6.99 (d, *J* = 7.8 Hz, 2H), 6.52 (d, *J* = 8.1 Hz, 4H), 6.41 (d, *J* = 1.4 Hz, 2H), 6.08 (d, *J* = 1.4 Hz, 2H), 4.66 (d, *J* = 14.3 Hz, 2H), 3.22 (sept, *J* = 6.9 Hz, 2H), 2.98 (s, 2H), 2.72 (sept, *J* = 6.7 Hz, 2H), 1.92 (d, *J* = 14.3 Hz, 2H), 1.38 (d, *J* = 6.9 Hz, 6H), 1.05 (d, *J* = 6.9 Hz, 6H), 0.93 (d, *J* = 6.7 Hz, 6H), 0.89 (d, *J* = 6.7 Hz, 6H), 0.01 (m, 2H), -0.17 (m, 2H). **$^{19}$F NMR** (471 MHz, $C_6D_6$) δ -60.82. **$^{13}$C NMR** (126 MHz, $C_6D_6$) δ 154.4, 146.0, 145.9, 138.5, 129.5, 125.2, 124.7, 124.7, 124.4, 119.8, 53.5, 46.8, 28.9, 28.2, 26.1, 25.7, 23.7, 23.0, 22.4, 10.0.

Publication-quality data proved elusive for complex **4.61** (1.1 Å resolution) due to the rapid decomposition of **4.61** in air during sample preparation for X-ray diffraction. The connectivity of the structure was confirmed (Figure 4.17).

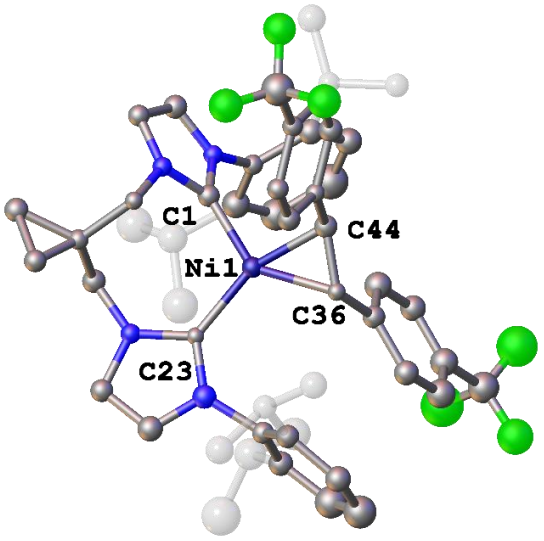


**Figure 4.17**. X-ray crystal structure of **4.61**. Thermal ellipsoids are shown at 50% probability. Hydrogen atoms co-crystallized solvent molecules are omitted for clarity.

Towards identifying an alternative Ni(0) complex that could result in high quality X-ray crystal structure data, the synthesis of **L1**-Ni(cod) was explored (Figures 4.18, 4.19). The reaction of 1,1'-di(2,6-diisopropylphenyl)-3,3'-(cyclopropyl)propylenediimidazolium dibromide (**L1**) (1 equiv 0.1 mmol), KOtBu (2 equiv, 0.2 mmol), $Ni(cod)_2$ (1 equiv, 0.1 mmol) in benzene resulted in a mixture of products which appears to be isomerized cyclooctadiene-Ni complexes. The separation of a single isomer as a pure compound proved elusive; however, crystals of 1,5-cod and 1,4-cod coordinated Ni complexes (**4.62** and **4.63**, respectively) suitable for X-ray diffraction were grown from concentrated THF solution layered with pentane stored at -30 °C. While this procedure was not deemed to be appropriate for scale-up and NMR characterization due to the formation of mixtures, this X-ray data complements structural assignment of the more reliably formed but less well crystalized Ni(0) complex **4.61**.

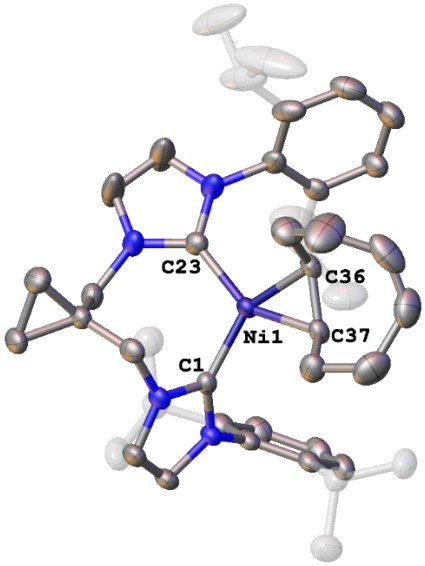


**Figure 4.18**. X-ray crystal structure of **4.62**. Thermal ellipsoids are shown at 30% probability. Hydrogen atoms and co-crystallized solvent molecules are omitted for clarity. Selected bond lengths (Å) and angles (°): Ni1-C1 1.880(2), Ni1-C23 1.905(3), Ni1-C36 1.963(2), Ni1-C37 1.960(3), C36-C37 1.427(4); C1-Ni1-C23 108.39(11).

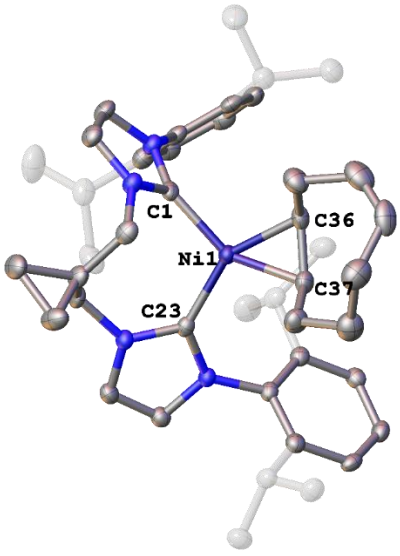


**Figure 4.19**. X-ray crystal structure of **4.63**. Thermal ellipsoids are shown at 30% probability. Hydrogen atoms co-crystallized solvent molecules are omitted for clarity. Selected bond lengths



*Chapter four references begin on page 364; experimental details begin on page 331*

(Å) and angles (°): Ni1-C1 1.888(2), Ni1-C23 1.893(2), Ni1-C36 1.959(2), Ni1-C37 1.967(2), C36-C37 1.422(3); C1-Ni1-C23 106.56(10).

Procedure for investigating the reactivity of different nickel species

An oven-dried 8 mL screw-top test-tube was equipped with an oven-dried micro-stir bar and brought into a nitrogen-filled glovebox. This reaction vessel was charged with **4.35** (1.0 equiv, 0.20 mmol), $K_3PO_4$ (3.0 equiv, 127.2 mg, 0.60 mmol), $Bi(OTf)_3$ (0.30 equiv, 39.4 mg, 0.06 mmol) and PhMe (0.4 mL). This mixture was capped and left to stir inside the glovebox for 15 min at room temperature. After 15 min a premixed solution of [Ni] catalyst[a] (0.05 equiv, 0.01 mmol) in PhMe (0.4 mL) was added to the stirring solution, followed by PhBpin (1.3 equiv, 0.26 mmol), before the reaction vessel was sealed with a Teflon-septum equipped cap and brought outside of the glovebox to be stirred within a mineral-oil bath at 800 rpm for 4 hours at 70 ˚C. A 50 µL aliquot of this reaction solution was sampled after 5 min, 10 min, 15 min, 20 min, 30 min, 40 min, 50 min, 60 min, 120 min, 180 min, and 240 min. Each time, this aliquot was filtered with EtOAc through silica; 100 µL of a 0.1 M solution of 1,3,5-trimethoxybenzene in PhMe was added to the filtrate and the mixture was subsequently analyzed by GC-FID to assess reaction yield.

[a]When employing synthesized Ni-**L2** complexes they were dissolved in PhMe and added to the reaction mixture. When employing ligand alongside the catalyst, 5 mol% ligand is dissolved alongside 5 mol% nickel catalyst in PhMe before being added to the reaction mixture. When employing Mn alongside catalyst, it is added directly as a solid after the addition of nickel/PhMe or nickel/ligand/PhMe solutions.



*Chapter four references begin on page 364; experimental details begin on page 331*

## 4.10. References

(1). (a) Miyaura, N.; Suzuki, A. Palladium-Catalyzed Cross-Coupling Reactions of Organoboron Compounds. *Chem. Rev.* **1995**, *95*, 2457-2483. (b) Johansson Seechurn, C. C. C.; Kitching, M. O.; Colacot, T. J.; Snieckus, V. Palladium-Catalyzed Cross-Coupling: A Historical Contextual Perspective to the 2010 Nobel Prize. *Angew. Chem. Int. Ed.* **2012**, *51*, 5062-5085. (c) Buskes, M. J.; Blanco, M. -J. Impact of Cross-Coupling Reactions in Drug Discovery and Development. *Molecules* **2020**, *25*, 3493.

(2) (a) Qiu, Z.; Li, C. -J. Transformations of Less-Activated Phenols and Phenol Derivatives via C–O Cleavage. *Chem. Rev.* **2020**, *120*, 10454-10515. (b) Yu, D.-G.; Li, B.-J.; Shi, Z.-J. Exploration of New C–O Electrophiles in Cross-Coupling Reactions. *Acc. Chem. Res.* **2010**, *43*, 1486-1495. (c) Zhou, T.; Szostak, M. Palladium-Catalyzed Cross-Couplings by C–O Bond Activation. *Catal. Sci. Technol.*, **2020**, *10*, 5702-5739.

(3) Kambe, N.; Iwasaki, T.; Terao, J. Pd-Catalyzed Cross-Coupling of Alkyl Halides. *Chem. Soc. Rev*., **2011**, *40*, 4937-4947.

(4) Cook, A.; Newman, S. G. Alcohols as Substrates in Transition Metal-Catalyzed Arylation, Alkylation and Related Reactions. *ChemRxiv* **2023**. doi: 10.26434/chemrxiv-2023-7k37p.

(5) For selected examples of the coupling of π-activated alcohols with organoboron nucleophiles: (a) Cao, Z.-C.; Yu, D.-G.; Zhu, R.-Y.; Wei, J.-B.; Shi, Z.-J. Direct Cross-Coupling of Benzyl Alcohols to Construct Diarylmethanes via Palladium Catalysis. *Chem. Commun.*, **2015**, *51*, 2683-2686. (b) Akkarasamiyo, S.; Margalef, J.; Samec, J. S. M. Nickel-Catalyzed Suzuki-Miyaura Cross-Coupling Reaction of Naphthyl and Quinolyl Alcohols with Boronic Acids. *Org. Lett.* **2019**, *21*, 4782-4787. (c) Zhao, C.; Zha, G.-F.; Fang, W.-Y.; Rakesh, K. P.; Qin, H.-L. Construction of Di(hetero)arylmethanes Through Pd-Catalyzed Direct Dehydroxylative Cross-Coupling of Benzylic Alcohols and Aryl Boronic Acids Mediated by Sulfuryl Fluoride ($SO_2F_2$). *Eur. J. Org. Chem.* **2019**, 1801-1807. (d) Toupalas, G.; Thomann, G.; Schlemper, L.; Rivero-Crespo, M. A.; Schmitt, H. L.; Morandi, B. Pd-Catalyzed Direct Deoxygenative Arylation of Non-π-Extended Benzyl Alcohols with Boronic Acids via Transient Formation of Non-Innocent Isoureas. *ACS Catal.*, **2022**, *12*, 8147-8154. (e) Hamilton, J. Y.; Sarlah, D.; Carreira, E. M. Iridium-Catalyzed Enantioselective Allylic Vinylation. *J. Am. Chem. Soc.* **2013**, *135*, 994-997. (f) Nazari, S. H.; Bourdeau, J. E.; Talley, M. R.; Valdivia-Berroeta, G. A.; Smith, S. J.; Michaelis, D. J. Nickel-

Catalyzed Suzuki Cross Couplings with Unprotected Allylic Alcohols Enabled by Bidentate *N*-Heterocyclic Carbene (NHC)/Phosphine Ligands. *ACS Catal*., **2018**, *8*, 85-89.

(6) For selected examples of activating reagents used for alcohols in alkylation or arylation reactions: (a) Zhang, X.; MacMillan, D. W. C. Alcohols as Latent Coupling Fragments for Metallaphotoredox Catalysis: $sp^3$-$sp^2$ Cross-Coupling of Oxalates with Aryl Halides. *J. Am. Chem. Soc*. **2016**, *138*, 13862-13865. (b) Dong, Z.; MacMillan, D. W. C. Metallaphotoredox-Enabled Deoxygenative Arylation of Alcohols. *Nature* **2021**, *598*, 451-456. (c) Lackner, G. L.; Quasdorf, K. W.; Overman, L. E. Direct Construction of Quaternary Carbons from Tertiary Alcohols via Photoredox-Catalyzed Fragmentation of Tert-Alkyl *N*-Phthalimidoyl Oxalates. *J. Am. Chem. Soc*. **2013**, *135*, 15342−15345. (d) Ye, Y.; Chen, H.; Sessler, J. L.; Gong, H. Zn-Mediated Fragmentation of Tertiary Alkyl Oxalates Enabling Formation of Alkylated and Arylated Quaternary Carbon Centers. *J. Am. Chem. Soc.* **2019**, *141*, 820−824. (e) Lin, Q.; Ma, G.; Gong, H. Ni-Catalyzed Formal Cross-Electrophile Coupling of Alcohols with Aryl Halides. *ACS Catal*., **2021**, *11*, 14102-14109. (f) Monteith, J. J.; Rousseaux, S. A. L. Ni-Catalyzed C($sp^3$)-O Arylation of α-Hydroxyesters. *Org. Lett*. **2021**, *23*, 9485-9489. (g) Desroches, J.; Champagne, P. A.; Benhassine, Y.; Paquin, J. -F. In situ Activation of Benzyl Alcohols with XtalFluor-E: Formation of 1,1-Diarylmethanes and 1,1,1-Triarylmethanes through Friedel-Crafts Benzylation. *Org. Biomol. Chem.,* **2015**, *13*, 2243-2246. (h) Zhao, C.; Zha, G.-F.; Fang, W.-Y.; Rakesh, K. P.; Qin, H. -L. Construction of Di(hetero)arylmethanes Through Pd-Catalyzed Direct Dehydroxylative Cross-Coupling Benzylic Alcohols and Aryl Boronic Acids Mediated by Sulfuryl Fluoride ($SO_2F_2$). *Eur. J. Org. Chem.* **2019**, 1801-1807. (g) Toupalas, G.; Thomann, G.; Schlemper, L.; Rivero-Crespo, M. A.; Schmitt, H. L.; Morandi, B. Pd-Catalyzed Direct Deoxygenative Arylation of Non-π-Extended Benzyl Alcohols with Boronic Acids via Transient Formation of Non-Innocent Isoureas. *ACS Catal.*, **2022**, *12*, 8147-8154. (i) Ackerman, L. K. G.; Anka-Lufford, L. L.; Naodovic, M.; Weix, D. J. Cobalt Co-Catalysis for Cross-Electrophile Coupling: Diarylmethanes from Benzyl Mesylates and Aryl Halides. *Chem. Sci.*, **2015**, *6*, 1115-1119.

(7) (a) Jia, X.-G.; Guo, P.; Duan, J.; Shu, X.-J. Dual Nickel and Lewis Acid Catalysis for Cross-Electrophile Coupling: The Allylation of Aryl Halides with Allylic Alcohols. *Chem. Sci.*, **2018**, *9*, 640. (b) Wang, H.; Yang, M.; Wang, Y.; Man, X.; Lu, X.; Mou, Z.; Luo, Y.; Liang, H. Nickel-Catalyzed Reductive $Csp^2$-$Csp^3$ Cross Coupling Using Phosphonium Salts. *Org. Lett.* **2021**, *23*, 8183-8188. (c) Nakao, Y.; Yada, A.; Ebata, S.; Hiyama, T. A Dramatic Effect of Lewis-Acid

Catalysts on Nickel-Catalyzed Carbocyanation of Alkynes *J. Am. Chem. Soc.* **2007**, *129*, 2428-2429. (d) Becica, J.; Dobereiner, G. E. The Roles of Lewis Acidic Additives in Organotransition Metal Catalysis. *Org. Biomol. Chem.* **2019**, *17*, 2055-2069.

(8) Cook, A.; St. Onge, P.; Newman, S. G. Deoxygenative Suzuki-Miyaura Arylation of Tertiary Alcohols. *Nature Synthesis*, **2023**. *2*, 663-669.

(9) Labinger, J. A. Tutorial on Oxidative Addition. *Organometallics* **2015**, *34*, 4784–4795.

(10) For examples where oxidative addition is proposed to occur by reaction of a metal to a positively charged intermediate, see: (a) Sylvester, K. T.; Wu, K.; Doyle, A. G. Mechanistic Investigation of the Nickel-Catalyzed Suzuki Reaction of *N, O*-Acetals: Evidence for Boronic Acid Assisted Oxidative Addition and an Iminium Activation Pathway. *J. Am. Chem. Soc.* **2012**, *134*, 16967-16970. (b) Jones, G. S.; Scott, W. J. Oxidative Addition of Palladium(0) to the Anomeric Center of Carbohydrate Electrophiles. *J. Am. Chem. Soc.* **1992**, *114*, 1491-1492. (c) Sepelak, D. J.; Pierpont, C. G.; Barefield, E. K.; Budz, J. T.; Poffenberger, C. A. Organometallic Chemistry of the Carbon-Nitrogen Double Bond. 1. Nickel Complexes Prepared from Iminium Cations and the X-Ray Structure of $\{C_6H_5\}_3P]Ni[CH_2N(CH_3)_2]Cl\}$. *J. Am. Chem. Soc.*, **1976**, *98*, 6178-6185. (d) Davis, J. L.; Dhawan, R.; Arndtsen, B. A. Imines in Stille-Type Cross-Coupling Reactions: A Multicomponent Synthesis of α-Substituted Amides. *Angew. Chem. Int. Ed.*, **2004**, *43*, 590-595. (e) Lu, Y.; Arndtsen, B. A. Activation of Carbon-Oxygen Bonds by Palladium: Toward a Mild, Catalytic Approach to α -Amino Acid Derivatives. *Org. Lett.* **2007**, *9*, 4395-4397. (f) Heinz, C.; Lutz, J. P.; Simmons, E. M.; Miller, M. M.; Ewing, W. R.; Doyle, A. G. Ni-Catalyzed Carbon-Carbon Bond-Forming Reductive Amination. *J. Am. Chem. Soc*. **2018**, *140*, 2292-2300.

(11) (a) Sommer, L. H.; Dorfman, E.; Goldberg, G. M.; Whitmore, F. C. The Reactivity with Alkali of Chlorine-Carbon Bonds *α*, *β* and *γ* to Silicon. *J. Am. Chem. Soc.* **1946**, *68*, 488-489. (b) Lambert, J. B.; Zhao, Y.; Emblidge, R. W.; Salvador, L. A.; Liu, X.; So, J. -H.; Chelius, E. C. The *β* Effect of Silicon and Related Manifestations of σ Conjugation. *Acc. Chem. Res.* **1999**, *32*, 183-190. (c) Lambert, J. B.; Wang, G.-T.; Finzel, R. B.; Teramura, D. H. Stabilization of Positive Charge by *β* Silicon. *J. Am. Chem. Soc.* **1987**, *109*, 7838-7845. (d) Klaer, A.; Saak, W.; Haase, D.; Muller, T. Molecular Structure of a Cyclopropyl Substituted Vinyl Cation. *J. Am. Chem. Soc.* **2008**, *130*, 14956-14957. (e) Wierschke, S. G.; Chandrasekhar, J.; Jorgensen, W. L. Magnitude and Origin of the beta.-Silicon Effect on Carbenium Ions. *J. Am. Chem. Soc.* **1985**, *107*, 1496-1500. (f) Ibrahim,

M. R.; Jorgensen, W. L. Ab Initio Investigations of the beta.-Silicon Effect on Alkyl and Cyclopropyl Carbenium Ions and Radicals. *J. Am. Chem. Soc.* **1989**, *111*, 819-824. (g) Dabbagh, H. A.; Zamani, M.; Fakhraee, S. The Nature of Resonance and Hyperconjugation for Cyclic *β*-Silyl Substituted Carbocations: NBO, NRT, EDA, and NMR Studies. *Res. Chem. Intermediates* **2013**, *39*, 2011-2033.

(12) Pons, A.; Michalland, J.; Zawodny, W.; Chen, Y.; Tona, V.; Maulide, N. Vinyl Cation Stabilization by Silicon Enables a Formal Metal-Free α-Arylation of Alkyl Ketones. *Angew. Chem. Int. Ed.* **2019**, *58*, 17303-17306.

(13) (a) Olofsson, K.; Larhed, M.; Hallberg, A. Highly Regioselective Palladium-Catalyzed Internal Arylation of Allyl Trimethylsilane with Aryl Triflates. *J. Org. Chem.* **1998**, *63*, 5076-5079. (b) Shao, B.; Bagdasarian, A. L.; Popov, S.; Nelson, H. M. Arylation of Hydrocarbons Enabled by Organosilicon Reagents and Weakly Coordinating Anions. *Science* **2017**, *355*, 1403-1407.

(14) (a) Ninomiya, R.; Arai, K.; Chen, G.; Morisaki, K.; Kawabata, T.; Ueda, Y. β-Silicon-Effect-Promoted Intermolecular Site-Selective C($sp^3$)-H Amination with Dirhodium Nitrenes. *Chem. Commun.* **2020**, *56*, 5759-5762. (b) Garlets, Z. J.; Davies, H. M. L. Harnessing the *β*-Silicon Effect for Regioselective and Stereoselective Rhodium(II)-Catalyzed C–H Functionalization by Donor/Acceptor Carbenes Derived from 1-Sulfonyl-1,2,3-Triazoles. *Org. Lett.* **2018**, *20*, 2168-2171.

(15) (a) Bains, W.; Tacke, R. Silicon Chemistry as a Novel Source of Chemical Diversity in Drug Design. *Curr. Opin. Drug Discovery Dev.* **2003**, *6*, 526-543. (b) Showell, G. A.; Mills, J. S. Chemistry Challenges in Lead Optimization: Silicon Isosteres in Drug Discovery. *Drug Discovery Today* **2003**, *8*, 551-556. (c) Franz, A. K.; Wilson, S. O. Organosilicon Molecules with Medicinal Applications. *J. Med. Chem.* **2013**, *56*, 388-405. (d) Ramesh, R.; Reddy, D. S. Quest for Novel Chemical Entities through Incorporation of Silicon in Drug Scaffolds. *J. Med. Chem.* **2018**, *61*, 3779. (e) Fujii, S.; Hashimoto, Y. Progress in the Medicinal Chemistry of Silicon: C/Si Exchange and Beyond. *Future Med. Chem* **2017**, *9*, 485-505.

(16) (a) Zhou, C.; Cheng, J.; Li, Z.; Maienfisch, P. Discovery and Optimization of Silicon-Containing Complex II Acaricides. Recent Highlights in the Disc. And Optimization of Crop Protection Products **2021**, 275-288. (b) Sieburth, S. M.; Manly, C. J.; Gammon, D. W.

Organosilane Insecticides. Part I: Biological and Physical Effects of Isosteric Replacement of Silicon for Carbon in Etofenprox and MTI 800. *Pestic. Sci.*, **1990**, *28*, 289-307. (c) Zhou, C.; Cheng, J.; Beadle, R.; Earley, F. G.; Li, Z.; Maienfisch, P. Design, Synthesis and Acaricidal Activities of Cyflumetofen Analogues Based on Carbon-Silicon Isosteric Replacement. *Bioorg. Med. Chem.* **2020**, *28*, 115509. (d) Tsuda, M.; Itoh, H.; Kato, S. Systemic Activity of Simeconazole and its Derivatives in Plants. *Pest Manage. Sci.* **2004**, *60*, 881-886.

(17) (a) Su, T. A.; Widawsky, J. R.; Li, H.; Klausen, R. S.; Leighton, J. L.; Steigerwald, M. L.; Venkataraman, L.; Nuckolls, C. Silicon Ring Strain Creates High-Conductance Pathways in Single-Molecule Circuits. *J. Am. Chem. Soc.* **2013**, *135*, 18331-18334. (b) Su, T. A.; Li, H.; Klausen, R. S.; Kim, N. T.; Neupane, M.; Leighton, J. L.; Steigerwald, M. L.; Venkataraman, L.; Nuckolls, C. Silane and Germane Molecular Electronics. *Acc. Chem. Res.* **2017**, *50*, 1088-1095. (c) Bui, R.; Brook, M. A. Thermoplastic Silicone Elastomers from Divanillin Crosslinkers in a Catalyst-Free Process. *Green Chem.* **2021**, *23*, 5600-5608. (d) Barroso, G.; Li, Q.; Bordia, R. K.; Motz, G. Polymeric and Ceramic Silicon-Based Coatings – a Review. *J. Mater. Chem.* **2019**, *7*, 1936-1963. (e) O'Lenick, A. J. Silicones – Basic Chemistry and Selected Applications. *J. Surfactants Deterg.*, **2000**, *3*, 229-236.

(18) (a) Molander, G. A.; Burke, J. P.; Carroll, P. J. Synthesis and Application of Chiral Cyclopropane-Based Ligands in Palladium-Catalyzed Allylic Alkylation. *J. Org. Chem.* **2004**, *69*, 8062–8069. (b) Davies, I. W.; Gerena, L.; Castonguay, L.; Senanayake, C. H.; Larsen, R. D.; Verhoeven, T. R.; Reider, P. J. The Influence of Ligand Bite Angle on the Enantioselectivity of Copper(II)-Catalysed Diels–Alder Reactions. *Chem. Commun.* **1996**, *15*, 1753–1754.

(19) Gardiner, M. G.; Ho, C. C. Recent Advances in Bidentate Bis(*N*-Heterocyclic Carbene) Transition Metal Complexes and Their Applications in Metal-Mediated Reactions. *Coord. Chem. Rev.* **2018**, *375*, 373–388.

(20) Cao, C.; Zhuang, Y.; Zhao, J.; Liu, H.; Geng, P.; Pang, G.; Shi, Y. Green Synthesis of Alkane Bridged Bisimidazolium Salts under Solvent-Free Conditions. *Synth. Commun.* **2012**, *42*, 380–387.

(21) Matsuoka, K.; Komami, N.; Kojima, M.; Mita, T.; Suzuki, K.; Maeda, S.; Yoshino, T.; Matsunaga, S. Chemoselective Cleavage of Si–C($sp^3$) Bonds in Unactivated Tetraalkylsilanes Using Iodine Tris(trifluoroacetate). *J. Am. Chem. Soc.* **2021**, *143*, 103-108.

(22) (a) Fleming, I.; Marchi, D.; Patel, S. K. The Mechanism of the Protodesilylation of Allylsilanes Which Are Disubstituted on C-3. *J. Chem. Soc., Perkin Trans. 1* **1981**, 2518. (b) Fleming, I.; Higgins, D. Protodesilylation of Allylsilanes for the Control of Double Bond Geometry Exocyclic to a Ring. *J. Chem. Soc., Perkin Trans. 1* **1989**, 206. (c) Radner, F.; Wistrand, L.-G. A Convenient Method for the Protodesilylation of Aryltrimethylsilanes. *Tetrahedron Lett.* **1995**, *36*, 5093–5094. (d) Yao, W.; Li, R.; Jiang, H.; Han, D. An Additive-Free, Base-Catalyzed Protodesilylation of Organosilanes. *J. Org. Chem.* **2018**, *83*, 2250–2255. (e) Kuhlmann, J. H.; Uygur, M.; García Mancheño, O. Protodesilylation of Arylsilanes by Visible-Light Photocatalysis. *Org. Lett.* **2022**, *24*, 1689–1694.

(23) Itami, K.; Terakawa, K.; Yoshina, J. -I.; Kajimoto, O. Efficient and Rapid C–Si Bond Cleavage in Supercritical Water. *J. Am. Chem. Soc.* **2003**, *125*, 6058-6059.

(24) For select examples of bis-NHCs with one-carbon linkers, see: (a) Herrmann, W. A.; Schwarz, J.; Gardiner, M. G.; Spiegler, M. Homoleptic Chelating *N*-Heterocyclic Carbene Complexes of Palladium and Nickel. *J. Organomet. Chem.* **1999**, *575*, 80–86. (b) A. Herrmann, W.; Reisinger, C.-P.; Spiegler, M. Chelating *N*-Heterocyclic Carbene Ligands in Palladium-Catalyzed Heck-Type Reactions. *J. Organomet. Chem.* **1998**, *557*, 93–96. (c) Huffer, A.; Jeffery, B.; Waller, B. J.; Danopoulos, A. A. Synthesis of Bis *N*-Heterocyclic Carbenes, Derivatives and Metal Complexes. *C. R. Chim.* **2013**, *16*, 557–565. (d) Brendel, M.; Braun, C.; Rominger, F.; Hofmann, P. Bis-NHC Chelate Complexes of Nickel(0) and Platinum(0). *Angew. Chem. Int. Ed.*, **2014**, *53*, 8741–8745.

(25) For select examples of metal complexes with bis-NHCs bearing long linkers, see: (a) Clyne, D. S.; Jin, J.; Genest, E.; Gallucci, J. C.; RajanBabu, T. V. First Chelated Chiral *N*-Heterocyclic Bis-Carbene Complexes. *Org. Lett.* **2000**, *2*, 1125–1128. (b) Lowry, R. J.; Jan, M. T.; Abboud, K. A.; Ghiviriga, I.; Veige, A. S. The next Generation of C2-Symmetric Ligands: A Di-N-Heterocyclic Carbene (NHC) Ligand and the Synthesis and X-Ray Characterization of Mono- and Dinuclear Rhodium(I) and Iridium(I) Complexes. *Polyhedron* **2010**, *29*, 553–563. (c) Kaloğlu, M.; Şahan, M. H.; Düşünceli, S. D.; Özdemir, İ. Synthesis of Quinoxaline-Linked Bis(Benzimidazolium) Salts and Their Catalytic Application in Palladium-Catalyzed Direct Arylation of Heteroarenes. *Catal. Letters* **2022**, *152*, 2012–2024. (d) Gutiérrez-Blanco, A.; Dobbe, C.; Hepp, A.; Daniliuc, C. G.; Poyatos, M.; Hahn, F. E.; Peris, E. Synthesis and Characterization

of poly-NHC-derived Silver(I) Assemblies and Their Transformation into Poly-imidazolium Macrocycles. *Eur. J. Inorg. Chem.* **2021**, 2442–2451. (e) Ahrens, S.; Zeller, A.; Taige, M.; Strassner, T. Extension of the Alkane Bridge in BisNHC−Palladium−Chloride Complexes. Synthesis, Structure, and Catalytic Activity. *Organometallics* **2006**, *25*, 5409–5415. (f) Chiu, C.-C.; Chiu, H.-T.; Lee, D.-S.; Lu, T.-J. An Efficient Class of Bis-NHC Salts: Applications in Pd-Catalyzed Reactions under Mild Reaction Conditions. *RSC Adv.* **2018**, *8*, 26407–26415. (g) Danopoulos, A. A.; Tulloch, A. A. D.; Winston, S.; Eastham, G.; Hursthouse, M. B. Chelating and 'Pincer' Dicarbene Complexes of Palladium; Synthesis and Structural studies. *Dalton Trans.* **2003**, *5*, 1009–1015.

(26) For general reviews covering NHCs bearing more than one imidazolium ring: (a) Poyatos, M.; Mata, J. A.; Peris, E. Complexes with Poly(*N*-Heterocyclic Carbene) Ligands: Structural Features and Catalytic Applications. *Chem. Rev.* **2009**, *109*, 3677–3707. (b) Biffis, A.; Baron, M.; Tubaro, C. Poly-NHC Complexes of Transition Metals. In *Advances in Organometallic Chemistry*; Elsevier, 2015; pp 203–288. (c) Gardiner, M. G.; Ho, C. C. Recent Advances in Bidentate Bis(*N*-Heterocyclic Carbene) Transition Metal Complexes and Their Applications in Metal-Mediated Reactions. *Coord. Chem. Rev.* **2018**, *375*, 373–388.

(27) Hoshimoto, Y.; Hayashi, Y.; Suzuki, H.; Ohashi, M.; Ogoshi, S. One-Pot, Single-Step, and Gram-Scale Synthesis of Mononuclear [($\eta^6$-Arene)Ni(N-Heterocyclic Carbene)] Complexes: Useful Precursors of the $Ni^0$–NHC Unit. *Organometallics* **2014**, *33*, 1276–1282.

(28) (a) Cramer, C. J.; Tolman, W. B.; Theopold, K. H.; Rheingold, A. L. Variable Character of O–O and M–O Bonding in Side-on ($\eta^2$) 1:1 Metal Complexes of $O_2$. *Proc. Natl. Acad. Sci. U. S. A.* **2003**, *100*, 3635–3640. (b) Otsuka, S.; Nakamura, A.; Tatsuno, Y. Oxygen Complexes of Nickel and Palladium. Formation, Structure, and Reactivities. *J. Am. Chem. Soc.* **1969**, *91*, 6994–6999. (c) Matsumoto, M.; Nakatsu, K. Dioxygen-Bis-(*t*-Butylisocyanide)Nickel. *Acta Crystallogr. B* **1975**, *31*, 2711–2713.

(29) For discussion on the viability of KO$^t$Bu as a single electron donor, see: (a) Barham, J. P.; Coulthard, G.; Emery, K. J.; Doni, E.; Cumine, F.; Nocera, G.; John, M. P.; Berlouis, L. E. A.; McGuire, T.; Tuttle, T.; Murphy, J. A. KO$^t$Bu: A Privileged Reagent for Electron Transfer Reactions? *J. Am. Chem. Soc.* **2016**, *138*, 7402–7410. (b) Emery, K.; Young, A.; Arokianathar, J.; Tuttle, T.; Murphy, J. KO$^t$Bu as a Single Electron Donor? Revisiting the Halogenation of Alkanes

with $CBr_4$ and $CCl_4$. *Molecules* **2018**, *23*, 1055. (c) Bhattacharyya, D.; Sarmah, B. K.; Nandi, S.; Srivastava, H. K.; Das, A. Selective Catalytic Synthesis of α-Alkylated Ketones and β-Disubstituted Ketones via Acceptorless Dehydrogenative Cross-Coupling of Alcohols. *Org. Lett.* **2021**, *23*, 869–875. (d) Madasu, J.; Shinde, S.; Das, R.; Patel, S.; Shard, A. Potassium *Tert*-Butoxide Mediated C–C, C–N, C–O and C–S Bond Forming Reactions. *Org. Biomol. Chem.* **2020**, *18*, 8346–8365.

(30) Newman-Stonebraker, S. H.; Raab, T. J.; Roshandel, H.; Doyle, A. G. Synthesis of Nickel(I)–Bromide Complexes via Oxidation and Ligand Displacement: Evaluation of Ligand Effects on Speciation and Reactivity. *J. Am. Chem. Soc.* **2023**, *145*, 19368–19377.

(31) For related Ni(0) complexes with stilbenes, see: Nattmann, L.; Saeb, R.; Nöthling, N.; Cornella, J. An Air-Stable Binary Ni(0)–Olefin Catalyst. *Nat. Catal.* **2019**, *3*, 6–13.

(32) (a) Nett, A. J.; Cañellas, S.; Higuchi, Y.; Robo, M. T.; Kochkodan, J. M.; Haynes, M. T., II; Kampf, J. W.; Montgomery, J. Stable, Well-Defined Nickel(0) Catalysts for Catalytic C–C and C–N Bond Formation. *ACS Catal.* **2018**, *8*, 6606–6611. (b) Clement, N. D.; Cavell, K. J.; Ooi, L.-L. Zerovalent *N*-Heterocyclic Carbene Complexes of Palladium and Nickel Dimethyl Fumarate: Synthesis, Structure, and Dynamic Behavior. *Organometallics* **2006**, *25*, 4155–4165.

(33) van Leeuwen, P. W. N. M.; Kamer, P. C. J.; Reek, J. N. H. The Bite Angle Makes the Catalyst. *Pure Appl. Chem.* **1999**, *71*, 1443–1452.

(34) (a) Hayashi, T.; Konishi, M.; Kobori, Y.; Kumada, M.; Higuchi, T.; Hirotsu, K. Dichloro[1,1'-Bis(Diphenylphosphino)Ferrocene]-Palladium(II): An Effective Catalyst for Cross-Coupling of Secondary and Primary Alkyl Grignard and Alkylzinc Reagents with Organic Halides. *J. Am. Chem. Soc.* **1984**, *106*, 158–163. (b) Brown, J. M.; Guiry, P. J. Bite Angle Dependence of the Rate of Reductive Elimination from Diphosphine Palladium Complexes. *Inorganica Chim. Acta* **1994**, *220*, 249–259. (c) Marcone, J. E.; Moloy, K. G. Kinetic Study of Reductive Elimination from the Complexes (Diphosphine)Pd(R)(CN). *J. Am. Chem. Soc.* **1998**, *120*, 8527–8528. (d) Culkin, D. A.; Hartwig, J. F. Carbon−Carbon Bond-Forming Reductive Elimination from Arylpalladium Complexes Containing Functionalized Alkyl Groups. Influence of Ligand Steric and Electronic Properties on Structure, Stability, and Reactivity. *Organometallics* **2004**, *23*, 3398–3416. (e) Whitehurst, W. G.; Kim, J.; Koenig, S. G.; Chirik, P. J. C($sp^3$)–C($sp^2$) Reductive Elimination versus *β*-Hydride Elimination from Cobalt(III) Intermediates in Catalytic C–H

Functionalization. *ACS Catal.* **2023**, *13*, 8700–8707. (f) Daniels, D. S. B.; Jones, A. S.; Thompson, A. L.; Paton, R. S.; Anderson, E. A. Ligand Bite Angle-dependent Palladium-catalyzed Cyclization of Propargylic Carbonates to 2-alkynyl Azacycles or Cyclic Dienamides. *Angew. Chem. Int. Ed.* **2014**, *53*, 1915–1920. (g) Cornella, J.; O'Neill, M. Retaining Alkyl Nucleophile Regiofidelity in Transition-Metal-Mediated Cross-Couplings to Aryl Electrophiles. *Synthesis* **2018**, *50*, 3974–3996.

(35) (a) Burés, J. A Simple Graphical Method to Determine the Order in Catalyst. *Angew. Chem. Int. Ed*. **2016**, *55*, 2028-2031. (b) Nelson, C. D.-T.; Burés, J. Visual Kinetic Analysis. *Chem. Sci.* **2019**, *10*, 348-353.

(36) (a) Eyring, H. The activated complex in chemical reactions. *J. Chem. Phys.*, **1935**, *3*, 107-115. (b) Otomo, T.; Suzuki, H.; Iida, R.; Takayanagi, T. $S_N1$ Reaction Mechanisms of *Tert*-Butyl Chloride in Aqueous Solution: What Can Be Learned from Reaction Path Search Calculations and Trajectory Calculations for Small Hydrated Clusters? *Comput. Theor. Chem.* **2021**, *1201*, 113278.

(38) (a) Diccianni, J. B.; Diao, T. Mechanisms of Nickel-Catalyzed Cross-Coupling Reactions. *Trends in Chem.* **2019**, *9*, 830-844.

(39) Kolsi, L. E.; Yli-Kauhaluoma, J.; Moreira, V. M. Catalytic, tunable, one-step bismuth (III) triflate reaction with alcohols: Dehydration versus dimerization. *ACS Omega* **2018**, *3*, 8836-8842.

(40) Saito, T.; Nishimoto, Y.; Yasuda, M.; Baba, A. Direct Coupling Reaction between Alcohols and Silyl Compounds: Enhancement of Lewis Acidity of $Me_3SiBr$ Using $InCl_3$. *J. Org. Chem.* **2006**, *71*, 8516–8522

(41) Brook, A. G.; Bassindale, A. R. (1980). "Chapter 9. Molecular rearrangements of organosilicon compounds". *Rearrangements in Ground and Excited States, Vol 2*. New York: Academic Press. pp. 149–221.

(42) Roush, W. R.; Pinchuk, A. N.; Micalizio, G. C. [(E)-γ-(Dimethylphenylsilyl)Allyl]Diisopinocampheylborane: A Highly Enantioselective Reagent for the Synthesis of Anti-β-Hydroxyallylsilanes. *Tetrahedron Lett.* **2000**, *41*, 9413–9417

(43) Wang, Y.; Gu, M. The Concept of Spectral Accuracy for MS. *Anal. Chem.* **2010**, *82*, 7055–7062.

(44) Ishiyama, T.; Murata, M.; Miyaura, N. Palladium(0)-Catalyzed Cross-Coupling Reaction of Alkoxydiboron with Haloarenes: A Direct Procedure for Arylboronic Esters. *J. Org. Chem.* **1995**, *60*, 7508-7510.

(45) Iwamoto, T.; Okuzono, C.; Adak, L.; Jin, M.; Nakamura, M. Iron-Catalyzed Enantioselective Suzuki-Miyaura Coupling of Racemic Alkyl Bromides. *Chem. Commun.* **2019**, *55*, 1128-1131.

(46) Cook, A.; St. Onge, P.; Newman, S. G. Deoxygenative Suzuki-Miyaura Arylation of Tertiary Alcohols. *Nature Synthesis*, **2023**. *2*, 663-669.

(47) Hans, M.; Lorkowski, J.; Demonceau, A.; Delaude, L. Efficient Synthetic Protocols for the Preparation of Common N-heterocyclic Carbene Precursors. *Beilstein. J. Org. Chem.* **2015**, *11*, 2318–2325.

(48) Ryu, J. H.; Kim, S.; Han, H. Y.; Son, H. J.; Lee, H. J.; Shin, Y. A.; Kim, J.-S.; Park, H.-G. Synthesis and Biological Evaluation of Picolinamides as Potent Inhibitors of 11β—Hydroxysteroid Dehydrogenase Type 1 (11β-HSD1). *Bioorg. Med. Chem.* **2015**, *25*, 695-700.

(49) Brown, P. A.; Bonnert, R. V.; Jenkins, P. R.; Lawrence, N. J.; Selim, M. R. Silicon-directed diene synthesis. *J. Chem. Soc., Perkin Trans. 1*, **1991**, 1893-1900

(50) Carey, F. A.; Toler, J. R. Formation of vinylsilanes and allylsilanes in thermal elimination reactions of esters of .beta.-hydroxyalkyltrimethylsilanes. *J. Org. Chem.* **1976**, *41*, 1966-1971.

(51) Nokami, T.; Yamane, Y.; Oshitani, S.; Kobayashi, J.-K.; Matsui, S.-I.; Nishihara, T.; Uno, H.; Hayase, S.; Itoh, T. The β-Silyl Effect on the Memory of Chirality in Friedel–Crafts Alkylation Using Chiral α-Aryl Alcohols. *Org. Lett.* **2015**, *17*, 3182–3185.

(52) Simonneau, A.; Oestreich, M. 3-Silylated Cyclohexa-1,4-dienes as Precursors for Gaseous Hydrosilanes: The $B(C_6F_5)_3$-catalyzed Transfer Hydrosilylation of Alkenes. *Angew. Chem. Int. Ed.*, **2013**, *52*, 11905–11907.

(53) Jia, Z.; Liu, Q.; Peng, X.-S.; Wong, H. N. C. Iron-Catalysed Cross-Coupling of Organolithium Compounds with Organic Halides. *Nat. Commun.* **2016**, *7*, 10614.

(54) Wang, X.; Yu, Z.-X.; Liu, W.-B. Formal Hydrotrimethylsilylation of Styrenes with Anti-Markovnikov Selectivity Using Hexamethyldisilane. *Org. Lett.* **2022**, *24*, 8735–8740.

(55) Li, M.-B.; Tang, X.-L.; Tian, S.-K. Cross-coupling of Grignard Reagents with Sulfonyl-activated $Sp^3$ Carbon-nitrogen Bonds. *Adv. Synth. Catal.* **2011**, *353*, 1980–1984.

(56) Dobereiner, G. E.; Yuan, J.; Schrock, R. R.; Goldman, A. S.; Hackenberg, J. D. Catalytic Synthesis of *n*-Alkyl Arenes through Alkyl Group Cross-Metathesis. *J. Am. Chem. Soc.* **2013**, *135*, 12572–12575.

(57) Li, J.; Peng, J.; Zhang, G.; Bai, Y.; Lai, G.; Li, X. Hydrosilylation Catalysed by a Rhodium Complex in a Supercritical $CO_2$/Ionic Liquid System. *New J Chem* **2010**, *34*, 1330.

(58) Stawinski, J.; Bartoszewicz, A.; Kalek, M.; Nilsson, J.; Hiresova, R. A New Reagent System for Efficient Silylation of Alcohols: Silyl Chloride-*N*-Methylimidazole-Iodine. *Synlett* **2008**, *2008*, 37–40.

(59) Chulsky, K.; Dobrovetsky, R. Metal-Free Catalytic Reductive Cleavage of Enol Ethers. *Org. Lett.* **2018**, *20*, 6804–6807.

(60) Yesilcimen, A.; Jiang, N.-C.; Gottlieb, F. H.; Wasa, M. Enantioselective Organocopper-Catalyzed Hetero Diels–Alder Reaction through in situ Oxidation of Ethers into Enol Ethers. *J. Am. Chem. Soc.* **2022**, *144*, 6173–6179.

(61) Keess, S.; Simonneau, A.; Oestreich, M. Direct and Transfer Hydrosilylation Reactions Catalyzed by Fully or Partially Fluorinated Triarylboranes: A Systematic Study. *Organometallics* **2015**, *34*, 790–799.

(62) Polidano, K.; Williams, J. M. J.; Morrill, L. C. Iron-Catalyzed Borrowing Hydrogen β-$C(sp^3)$-Methylation of Alcohols. *ACS Catal.* **2019**, *9*, 8575–8580.

(63) Dieskau, A. P.; Plietker, B. A Mild Ligand-Free Iron-Catalyzed Liberation of Alcohols from Allylcarbonates. *Org. Lett.* **2011**, *13*, 5544–5547.

(64) Li, G.; Leow, D.; Wan, L.; Yu, J.-Q. Ether-directed *Ortho*-C–H Olefination with a Palladium(II)/ Monoprotected Amino Acid Catalyst. *Angew. Chem. Int. Ed.* **2013**, *52*, 1245–1247.

(65) Monfette, S.; Turner, Z. R.; Semproni, S. P.; Chirik, P. J. Enantiopure $C_1$-Symmetric Bis(Imino)Pyridine Cobalt Complexes for Asymmetric Alkene Hydrogenation. *J. Am. Chem. Soc.* **2012**, *134*, 4561–4564.

# **Chapter Five:** High-throughput evaluation of future directions for the deoxygenative functionalization of unprotected, non-π-activated alcohols

*"Around here, however, we don't look backwards for very long.*

*We keep moving forward, opening up new doors and doing new things, because we're curious… and curiosity keeps leading us down new paths."*

- *Walt Disney, 1901-1966.*



*Chapter five references begin on page 413; experimental details begin on page 401*

## 5.1. Chapter outlook

Chapters three and four of this dissertation discussed the development of a deoxygenative Suzuki-Miyaura arylation of non-π-activated aliphatic alcohols. At the heart of this discussion was the development of a bismuth/nickel-NHC catalytic system that permitted the activation of C($sp^3$)–O bonds in alcohols. The Suzuki-Miyaura arylation, while synthetically useful, was ultimately chosen arbitrarily as a proof of concept for the ability to intercept carbocations with transition metal catalysts.

This chapter will describe the high-throughput approach that was taken towards exploring the chemical space of this discovery with a focus on examining what nucleophilic coupling partners can be employed (Figure 5.1). Successful reactivity was observed in the coupling of non-π-activated alcohols with allylsilanes, benzyl boronate esters, terminal alkynes and select nitrogen-containing heterocycles. This chapter will document the discovery and pursuit of each of these transformations, sowing the seeds of reactivity for future members in the Newman group to pursue.

**Figure 5.1.** High-throughput expansion of nucleophilic coupling partners amenable to previously discussed alcohol activation

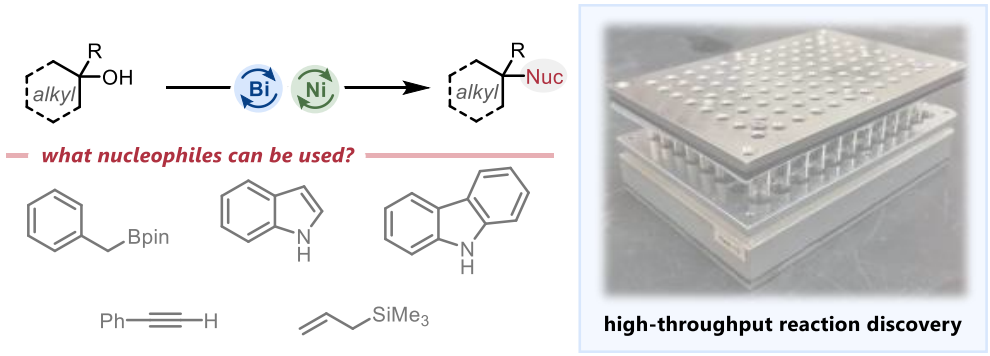




Chapter five references begin on page 413; experimental details begin on page 401

## 5.2. Reuse permissions

The work detailed within this chapter is unpublished and has been conducted solely by the author of this dissertation. Section 5.3.1. is adapted with permission from the manuscript "Reaction screening in multiwell plates: High-throughput optimization of a Buchwald-Hartwig amination" by Adam Cook, Roxanne Clément, and Stephen G. Newman. *Nature Protoc*. **2021**, *2*, 1152-1169. Copyright 2021 Springer Nature. The dissertation author is the lead author of this manuscript. Otherwise, this chapter is original and found exclusively within this dissertation.

## 5.3. Introductory theory and background information

Chemical space is vast, and chemical reactions involve the complex interplay of multiple variables. When performing even the simplest of chemical reactions, a large number of interrelated variables must be considered and selected. For instance, reaction time, concentration, temperature, stoichiometry, and solvent choice can each have a substantial impact on the outcome of an experiment. Each additional component adds an extra degree of complexity; for example, the choice and relative amount of metal, ligand, and other additives must be considered in a transition metal–catalyzed coupling reaction. The vast number of possible experimental conditions sharply contrasts with the number of experiments that a chemist can perform in a reasonable amount of time. Consequently, a sequential, one-variable-at-a-time (OVAT) approach is usually favored over a more comprehensive screen. For instance, a standard set of conditions will be selected with all variables fixed except one (e.g., choice of ligand). After identifying the best among those experiments, that variable will be fixed and the next one examined (e.g., choice of solvent).

Although this keeps the total number of experiments down, critical relationships between variables may be overlooked.

High-throughput experimentation (HTE) is the practice of using improved tools and techniques to enable a large number of experiments to be conducted and analyzed in a reasonable amount of time (Figure 5.2).[1] Although this can take many forms, the most common approach is to miniaturize each experiment and run a number of them in parallel.[2,3] For instance, performing experiments in 96-well plates enables one to simultaneously investigate all possible combinations of twelve nucleophiles, four bases, and two solvents in a catalytic cross-coupling reaction. With further miniaturization, 1,536-well plates can be used to achieve comprehensive multivariate screening on a nanomole scale.[4]

**Figure 5.2.** High-throughput experimentation as a method for the rapid generation of data

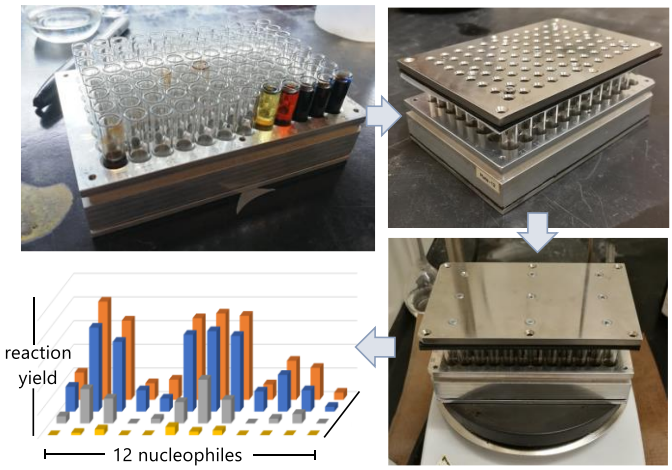


In many cases, the use of HTE may prove advantageous in comparison to traditional sequential experimentation. Routine optimization of a reaction that initially gives an unsatisfactory outcome is a particularly common application in which HTE enables rapid identification of more effective conditions.[5,6] An experiment using a single multiwell plate is often sufficient for these

modestly challenging problems. HTE provides an even bigger advantage for experiments for which there is no known reasonable starting point, for instance, in reaction discovery projects that necessitate broad exploration of discrete variables.[7–11] In addition to discovery and optimization problems, HTE can be useful for any application in which similar reactions must be repeated with minor changes in conditions. Examples include robustness screening to understand functional group tolerance,[12] building of data sets for construction of models using machine learning,[13,14] and obtainment of kinetic data,[8,15] and more.[16–20]

At present, the use of HTE to investigate chemical reactions is primarily achieved in industry[21] or within the small subset of academic institutions[22] that have invested in centralized high-throughput chemistry facilities. The heart of these facilities is generally a robotic platform that can manipulate reaction vials, measure and dose chemical reagents, acquire reaction samples, and quench experiments within multiwell plates. These systems can be programmed to reproducibly carry out these tasks at all hours of the day, seven days a week. As a consequence of the cost of high-throughput robotics, the benefits of HTE are often considered to be out of reach to labs without such resources. Allen et al.[22] argued that this should not be the case; although advanced technology is required for the most ambitious screening endeavors, most of the benefits of HTE are achievable using simple and accessible tools.

Amongst cross-coupling reactions, Buchwald-Hartwig aminations are particularly common targets for HTE as a result of their complexity. For example, a recent report from Dreher et al.[4] at Merck noted a 55% failure rate when Buchwald-Hartwig reactions were performed on the highly functionalized molecules common in drug discovery. They demonstrated that high-throughput screening of carefully chosen catalysts, bases, and ligands enables effective reaction conditions to be identified for many of these amine-forming reactions.



*Chapter five references begin on page 413; experimental details begin on page 401*

In chapters three and four, a method for the Suzuki-Miyaura arylation of non-π-activated tertiary alcohols via Lewis acid/transition metal dual catalysis was discussed.[23] This chapter will describe the results of a high-throughput study conducted to expand the scope of nucleophilic coupling partners that can react with unprotected, non-π-activated alcohols.

## 5.4. High-throughput exploration of nucleophilic coupling partners

Due to the vast range of accessible nucleophilic coupling partners, a high-throughput approach was utilized towards reaction discovery. Taking heed from previous works concerning the coupling of tertiary alcohols,[23] it was decided that the combination of $Bi(OTf)_3$ (30 mol%), $Ni(cod)_2$ (10 mol%), **L1** (10 mol%) and $Me_2SiCl_2$ (1.3 equiv.) would be kept constant. 1-Adamantanol (**5.1**) was chosen as a commercially available substrate for this transformation and the scale for this transformation was determined to be 0.05 mmol.

The variable parameters in this high-throughput experiment were chosen to be solvent, base and nucleophile; altogether, two solvents, two bases and twelve nucleophiles would be screened in a single high-throughput experiment (Figure 5.3). Toluene and *N*,*N*-dimethylformamide (DMF) were chosen as solvents to cover a range of polarity and solubilities. $K_3PO_4$ and $Cs_2CO_3$ were chosen as inorganic bases. A benzylboronic acid (**5.3**) and a benzylboronate ester (**5.4**) were incorporated as nucleophilic coupling partners into this high-throughput screen. Various classes of *N*-nucleophiles were included in this high-throughput screen, including aniline (**5.5**), *N*-methylaniline (**5.6**), morpholine (**5.7**), indole (**5.8**) and carbazole (**5.9**). Nickel-catalyzed Sonogashira reactions are attractive alternatives to their more conventional palladium-catalyzed counterparts.[24] To this end, terminal alkyne **5.10** was incorporated into the



*Chapter five references begin on page 413; experimental details begin on page 401*

screen. Lastly, thiophenol (**5.11**), allyltrimethylsilane (**5.12**), 2-methylfuran (**5.13**) and anisole (**5.14**) were chosen as coupling partners.

**Figure 5.3.** High-throughput reaction discovery: Alternative nucleophiles in the Lewis acid/transition metal catalyzed functionalization of tertiary alcohols

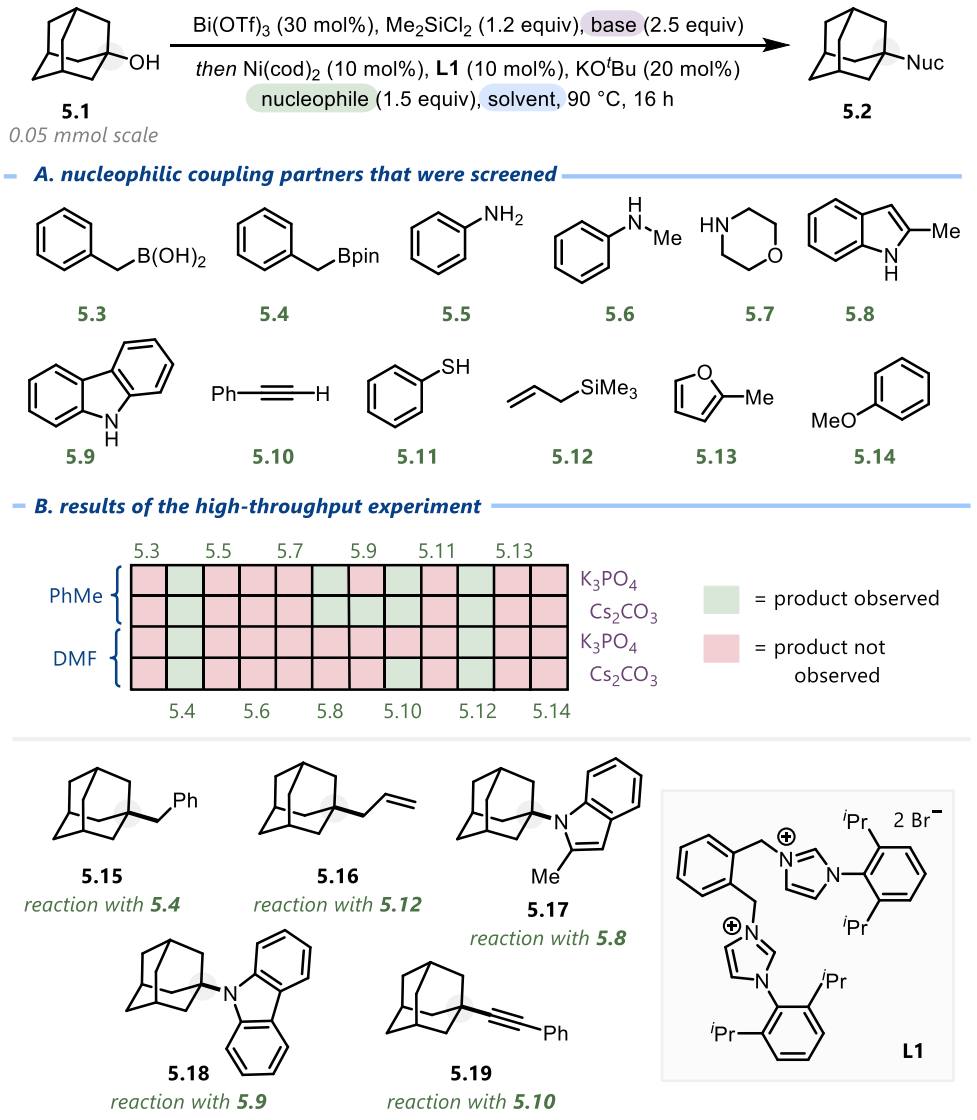


Multiple hits were obtained from this high-throughput experiment. As this was a high-throughput screen for reaction discovery, success was assessed by noting if the desired product



*Chapter five references begin on page 413; experimental details begin on page 401*

was observed by GC-MS analysis of the crude reaction mixture. Determining product yields was not a priority at this preliminary evaluation stage.

The coupling of benzylboronic acid pinacol ester **5.4** with 1-adamantanol (**5.1**) afforded product (**5.15**) in all four wells that this reaction was present in. The coupling of allyltrimethylsilane to form product **5.16** also proceeded in each of the four wells it was present within. These results suggest that the reaction between these nucleophilic coupling partners proceeds with limited dependence on solvent or base. The reaction between indole **5.8** and alcohol **5.1** afforded *N*-alkylated product **5.17** upon employing $Cs_2CO_3$ or $K_3PO_4$ in toluene, and the reaction between carbazole **5.9** and alcohol **5.1** proceeded to afford *N*-alkylated product **5.18** when using $Cs_2CO_3$ in toluene. Finally, the alkynylation of alcohol **5.1** with alkyne **5.10** proceeded to afford product **5.19** in the presence of either $K_3PO_4$ or $Cs_2CO_3$ in toluene, or with $Cs_2CO_3$ in DMF. In all other cases, no deoxygenative cross-coupling was observed.

## 5.5. Investigating C($sp^3$)–C($sp^3$) bond forming reactions

The discovery of methods to forge C($sp^3$)–C($sp^3$) bonds is a highly desirable goal of contemporary research.[25] Modern pharmacological and medicinal chemistry libraries are flooded with "flat" molecules bearing biaryl linkages because these linkages are easily forged through traditional cross-coupling chemistry. The development of reactions that form C($sp^3$)–C($sp^3$) bonds will be paramount in the "escape from flatland".[26] The coupling of alkyl boron species in Suzuki-Miyaura reactions represents an attractive strategy to forge bonds to C($sp^3$)-hybridized nucleophiles, yet efforts to reliably employ them alongside C($sp^3$)-hybridized electrophiles, particular tertiary electrophiles, are still underdeveloped.[27] Thus, the observed hit between alcohol

**5.1** and benzylboronate ester **5.4** served as an attractive starting point for an investigation into the utility of the nickel/bismuth catalytic system for reactions that form C($sp^3$)–C($sp^3$) bonds (Scheme 5.1).

**Scheme 5.1.** Initial hit: Coupling of 1-adamantanol and a benzylboronate ester

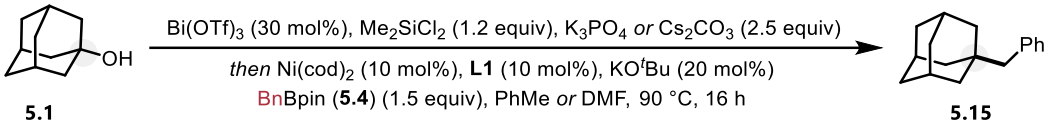


**5.1** **5.15**

Following from the initial hit, the yield of this reaction at the 0.2 mmol scale was obtained. The adamantanol scaffold is specialized amongst tertiary alcohol scaffolds as geometric restrictions make it unlikely to participate in deleterious $\beta$-hydride elimination reactions.[28] Due to this, all further experiments were conducted on pyran-bearing **5.20** to ensure that any observed reactivity was reflective of more common tertiary alcohols. Each of the four positive results observed from the high throughput investigation were ran on the 0.20 mmol scale, resulting in yields of product **5.21** between 4 and 9% (Scheme 5.2).

**Scheme 5.2.** Reproducing the hits from the high-throughput plate

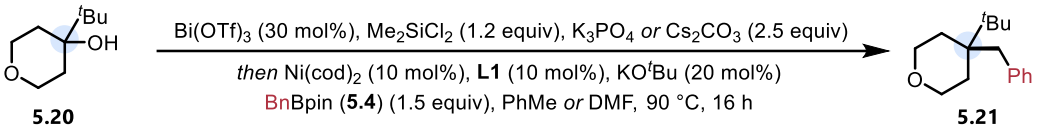


**5.20** **5.21**

| conditions | % yield, **5.21** |
|---|---|
| $K_3PO_4$, DMF | 3 |
| $K_3PO_4$, PhMe | 6 |
| $Cs_2CO_3$, DMF | 8 |
| $Cs_2CO_3$, PhMe | 9 |

Next, a brief optimization campaign was undertaken towards the benzylation of substrate **5.20** (Table 5.1). Control experiments performed in the absence of $Ni(cod)_2$, $Bi(OTf)_3$ and base afforded no product (entries 2-4), showing their synergistic importance in this transformation. Further, switching the identity of precatalyst, ligand or Lewis acid catalyst shut down reactivity



*Chapter five references begin on page 413; experimental details begin on page 401*

(entries 5-8). Varying the equivalents of BnBpin (entries 9-11) and equivalents of Lewis acid (entries 12, 13) led to a moderate increase in yield, affording product **5.21** in yields up to 21%. Lastly, screening various temperatures led to the observation that yields could be increased upon performing the reaction at heightened temperatures (entries 14-16).

**Table 5.1.** Preliminary optimization of benzylation

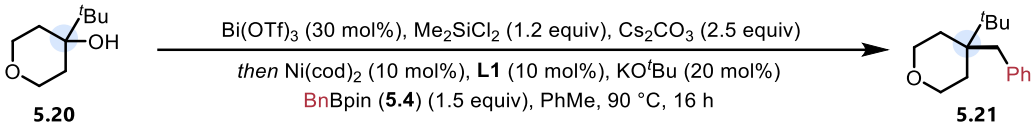


| entry | deviation from above conditions | % yield, 5.21 |
|---|---|---|
| **1** | *none* | 9 |
| **2** | no $Ni(cod)_2$ | 0 |
| **3** | no $Bi(OTf)_3$ | 0 |
| **4** | no $Cs_2CO_3$ | 0 |
| **5** | $NiBr_2$•glyme + Mn *instead of* $Ni(cod)_2$ | 0 |
| **6** | IPr•HCl, ICy•$HBF_4$, IMes•HCl *instead of* ***L1*** | 0 |
| **7** | $PPh_3$, $PCy_3$ *or* dppf *instead of* ***L1*** | 0 |
| **8** | $Sc(OTf)_3$, $InCl_3$ *or* $CrCl_3$ *instead of* $Bi(OTf)_3$ | 0 |
| **9** | BnBpin (1 equiv) | 7 |
| **10** | BnBpin (2 equiv) | 14 |
| **11** | BnBpin (3 equiv) | 13 |
| **12** | $Bi(OTf)_3$ (1 equiv), BnBpin (2 equiv) | 19 |
| **13** | $Bi(OTf)_3$ (50 mol%), BnBpin (2 equiv) | 21 |
| **14** | T = 70 °C, $Bi(OTf)_3$ (50 mol%), BnBpin (2 equiv) | 13 |
| **15** | T = 100 °C, $Bi(OTf)_3$ (50 mol%), BnBpin (2 equiv) | 20 |
| **16** | T = 120 °C, $Bi(OTf)_3$ (50 mol%), BnBpin (2 equiv) | 28 |



*Chapter five references begin on page 413; experimental details begin on page 401*

At this point, the optimization campaign for this transformation was temporarily halted in favour of investigating the other successful reactions from the high-throughput plate. At the time of writing this dissertation, this transformation has yet to have been revisited. Should this reaction be pursued in the future, a more comprehensive optimization screen may yield fruitful results. In particular, an in depth screening of ligands, specifically bis(NHC) ligands, is warranted as it is likely to result in increased yields.

## 5.6. Investigating the allylation of tertiary alcohols

As illustrated in Section 1.4 of this dissertation, the allylation of alcohols using allyltrimethylsilane is a known reaction.[29] However, the vast majority of these methods employ π-activated alcohols (i.e. allyl or benzyl alcohols) as substrates. As such, the observed coupling of 1-adamantanol **5.1** with allyltrimethylsilane **5.12** represents a transformation that warrants further pursuit.

Repeating the reaction between 1-adamantanol **5.1** and allyltrimethylsilane **5.12** at the 0.2 mmol scale led to the formation of product **5.16** in a 23% yield (Scheme 5.3). Unfortunately, no allylated product was observed upon reacting allyltrimethylsilane with pyran-bearing alcohol **5.20**, suggesting that this transformation may be substrate dependant. Performing the reaction of **5.1** with allyltrimethylsilane **5.12** in the absence of $Ni(cod)_2$ also revealed product **5.16**, albeit in decreased yields. The apparent substrate dependence and background reactivity of this transformation led to the decision to not pursue this transformation further.



*Chapter five references begin on page 413; experimental details begin on page 401*

**Scheme 5.3.** Investigating the allylation of non-π-activated tertiary alcohols.

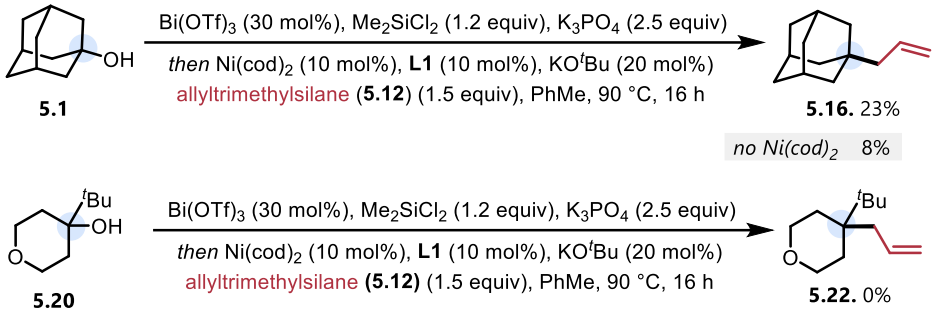


## 5.7. Investigating the alkynylation of tertiary alcohols

The Sonogashira reaction is a transition metal-catalyzed method to alkynylate chemical species.[30] Usually, Sonogashira reactions utilize a palladium/copper catalyst and they proceed through the generation of an alkynyl cuprate coupling partner. While this is an established reaction, Sonogashira reactions featuring alcohols are scarce in the literature, as are Sonogashira reactions that proceed in the absence of additional copper co-catalyst.[31] As such, the reaction between **5.1** and **5.10** that was observed in the high-throughput experiment provides a starting point for exploring the nickel-catalyzed, copper-free Sonogashira reaction of non-π-activated alcohols.

The reaction between phenylacetylene **5.10** and tertiary alcohol **5.20** was conducted at the 0.2 mmol scale under the three different reaction conditions that afforded product in the high throughput experiment (Scheme 5.4). The highest yield (74%) was obtained when the reaction was performed while employing $Cs_2CO_3$ as a base in DMF.



*Chapter five references begin on page 413; experimental details begin on page 401*

**Scheme 5.4**. Investigating the alkynylation of tertiary alcohols

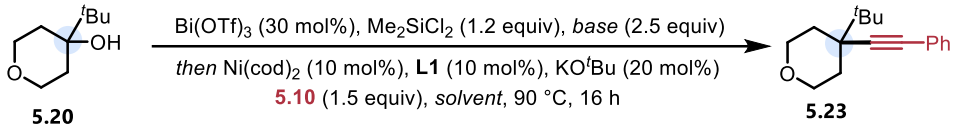


| conditions | % yield, **5.23** |
|---|---|
| $K_3PO_4$, PhMe | 68 |
| $Cs_2CO_3$, DMF | 74 |
| $Cs_2CO_3$, PhMe | 51 |

Experiments were carried out to optimize the alkynylation of substrate **5.20**. Once more, control experiments performed in the absence of $Ni(cod)_2$, $Bi(OTf)_3$ and base revealed their importance in achieving reactivity (Table 5.2, entries 2-4). In line with the optimization experiments for the coupling of BnBpin with substrate **5.20**, increasing the equivalents of nucleophile and $Bi(OTf)_3$ led to an increase in yield (entries 5-8). Further, it was realized that higher yields of product **5.23** could be achieved when increasing the reaction temperature to 120 °C (entry 9).

**Table 5.2.** Preliminary optimization of alkynylation reaction

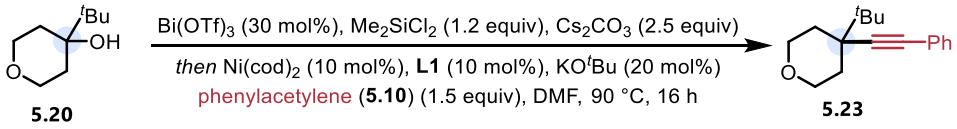


| entry | deviation from above conditions | % yield, 5.23 |
|---|---|---|
| **1** | *none* | 74 |
| **2** | no $Ni(cod)_2$ | 0 |
| **3** | no $Bi(OTf)_3$ | 0 |
| **4** | no $Cs_2CO_3$ | 0 |
| **5** | phenylacetylene (2.0 equiv) | 78 |
| **6** | phenylacetylene (2.5 equiv) | 77 |
| **7** | $Bi(OTf)_3$ (1 equiv), phenylacetylene (2.0 equiv) | 69 |



*Chapter five references begin on page 413; experimental details begin on page 401*

| | | |
|---|---|---|
| **8** | $Bi(OTf)_3$ (50 mol%), phenylacetylene (2.0 equiv) | 79 |
| **9** | T = 120 °C, $Bi(OTf)_3$ (50 mol%), phenylacetylene (2.0 equiv) | 84 |

While these results were promising, pursuit of this transformation was temporarily halted to pursue another direction in this project, the amination of tertiary alcohols (to be discussed in Section 5.8). Revisiting this Sonogashira project months later revealed significant reproducibility problems. The alkynylation of **5.20** with phenylacetylene **5.10** provided unpredictable results, yielding low-or-no product. Tentatively, it is proposed that this could be due to residual impurities on the stir bars,[32] glassware or within the reagents that were used in the reactions conducted in pursuit of this Sonogashira reaction.

## 5.8. Investigating the amination of tertiary alcohols

Amines are an important class of chemical compounds; in fact, it has been estimated that amines are present in 43% of commercial pharmaceuticals.[33] More specifically, *N*-heterocycles, including piperidines, indoles, carbazoles[34] and beyond, represent a particularly privileged scaffold.[35]

Catalytic methods to forge C($sp^2$)–N bonds are well developed. Notable cross-coupling-like approaches include Ullman-Goldberg coupling,[36] Chan-Evans-Lam coupling[37] and Buchwald-Hartwig coupling[38] (Figure 5.4a). Comparatively, methods to forge flexible C($sp^3$)–N bonds are less developed, often relying on more 'traditional' Mitsunobu,[39] hydroamination,[40] reductive amination[41] or $S_N2$-type pathways. Recently, advances in catalytic methods to forge



*Chapter five references begin on page 413; experimental details begin on page 401*

C($sp^3$)–N bonds have been developed through borrowing-hydrogen,[42] photocatalytic[43] or metal-catalyzed[44] strategies (Figure 5.4b), among others. However, methods that employ tertiary species as electrophiles have proven challenging, and methods to *N*-alkylate heterocycles remain scarce.

**Figure 5.4.** Conventional methods for amination.

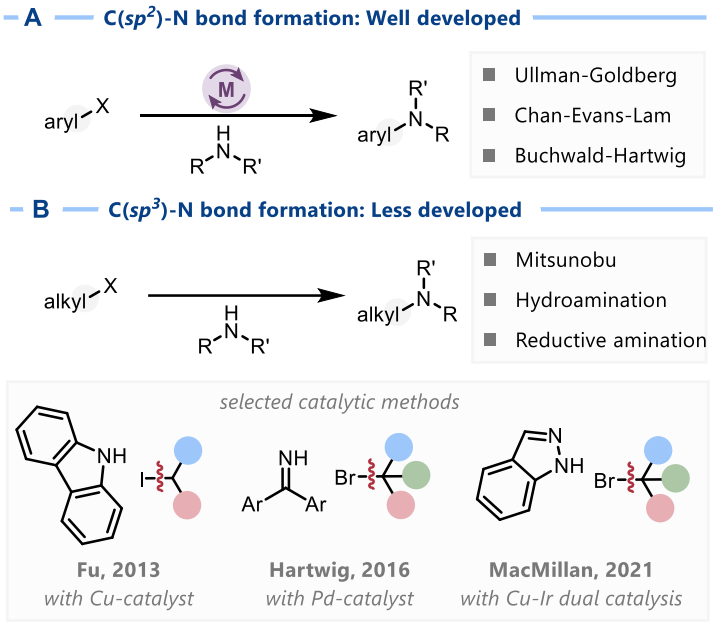


The successful deoxygenative coupling of 1-adamantanol **5.1** with both indole **5.8** and carbazole **5.9**, as observed in the high-throughput experiment (Scheme 5.4), serves as a starting point for the investigation into the use of non-π-activated alcohols as substrates in Buchwald-Hartwig-type coupling reactions. These hits were reproduced at the 0.2 mmol scale, affording product **5.18** in 23% yield and product **5.19** in a 48% yield. This reactivity could be extended towards pyran-bearing alcohol **5.20**, leading to the formation of products **5.24** and **5.25** in 33% and 68% yields, respectively (Scheme 5.5).



*Chapter five references begin on page 413; experimental details begin on page 401*

**Scheme 5.5.** Investigating the reaction of indole and carbazole with tertiary alcohols

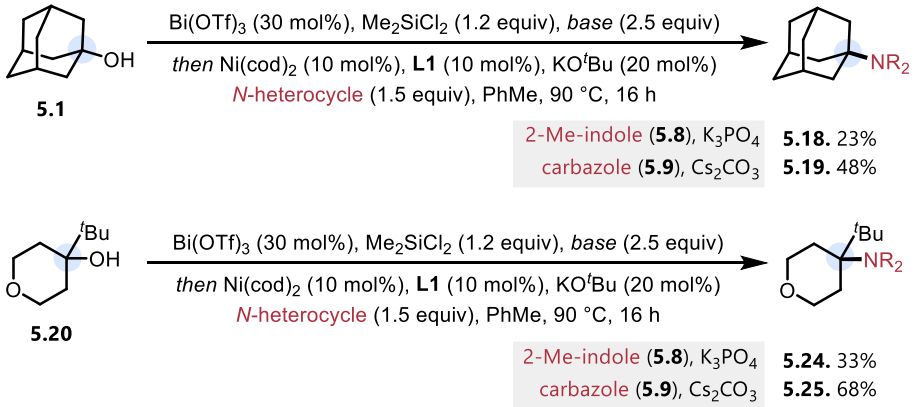


Optimization of this transformation was performed on the reaction of **5.20** with carbazole **5.9**. Control experiments revealed $Ni(cod)_2$, $Bi(OTf)_3$ and base to be essential for reactivity (Table 5.3, entries 2-4). These experiments revealed that yields could be increased by increasing the equivalents of $Bi(OTf)_3$ (entries 5, 6), increasing the equivalents of nucleophilic coupling partner (entries 7-10), increasing the equivalents of $Me_2SiCl_2$ (entries 11-14) and increasing the reaction temperature (entries 15-18). With these changes, the yield of product **5.25** increased to 82%. The yield of the reaction of indole to form product **5.24** also increased to 59% when these reaction conditions were employed. Further optimization could be performed to achieve higher yields when using indole as a coupling partner, however this has not been completed at the time of writing this dissertation.



*Chapter five references begin on page 413; experimental details begin on page 401*

**Table 5.3.** *N*-alkylation of carbazole with pyran-bearing alcohol

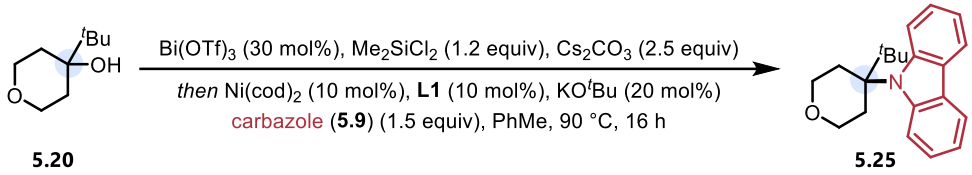


5.20 5.25

| entry | deviation from above conditions | % yield, 5.25 |
|---|---|---|
| **1** | *none* | 68 |
| **2** | no $Ni(cod)_2$ | 0 |
| **3** | no $Bi(OTf)_3$ | 0 |
| **4** | no $Cs_2CO_3$ | 0 |
| **5** | $Bi(OTf)_3$ (1 equiv) | 56 |
| **6** | $Bi(OTf)_3$ (50 mol%) | 71 |
| **7** | carbazole (2.0 equiv), $Bi(OTf)_3$ (50 mol%) | 76 |
| **8** | carbazole (2.5 equiv), $Bi(OTf)_3$ (50 mol%) | 60 |
| **9** | T = 100 °C, $Bi(OTf)_3$ (50 mol%), carbazole (2.0 equiv) | 74 |
| **10** | T = 120 °C, $Bi(OTf)_3$ (50 mol%), carbazole (2.0 equiv) | 82 |

Conventional Buchwald-Hartwig reactions tend to utilize nucleophilic amines as coupling partners.[38,45] Noting this, it was interesting that the indole **5.8** and carbazole **5.9** could be coupled successfully with tertiary alcohols while the other tested amines (**5.5-5.7**) could not. Seeking to investigate what amines were amenable to this reaction, a series of nucleophilic coupling partners were screened for reactivity using the optimized conditions established in Table 5.3 (Figure 5.5). Once more, success was assessed by noting if the desired product was observed by GC-MS analysis of the crude reaction mixture. Determining product yields was not a priority at this preliminary evaluation stage. Testing a wide variety of amines, amides and *N*-heterocycles (**5.26-**



*Chapter five references begin on page 413; experimental details begin on page 401*

**5.49**) revealed reactivity only in the case that an indole (**5.26**), carbazole (**5.27**), pyrazole (**5.33**) or oxazolidone (**5.44**) was employed as a nucleophilic coupling partner.

**Figure 5.5.** Screening of amine nucleophilic coupling partners

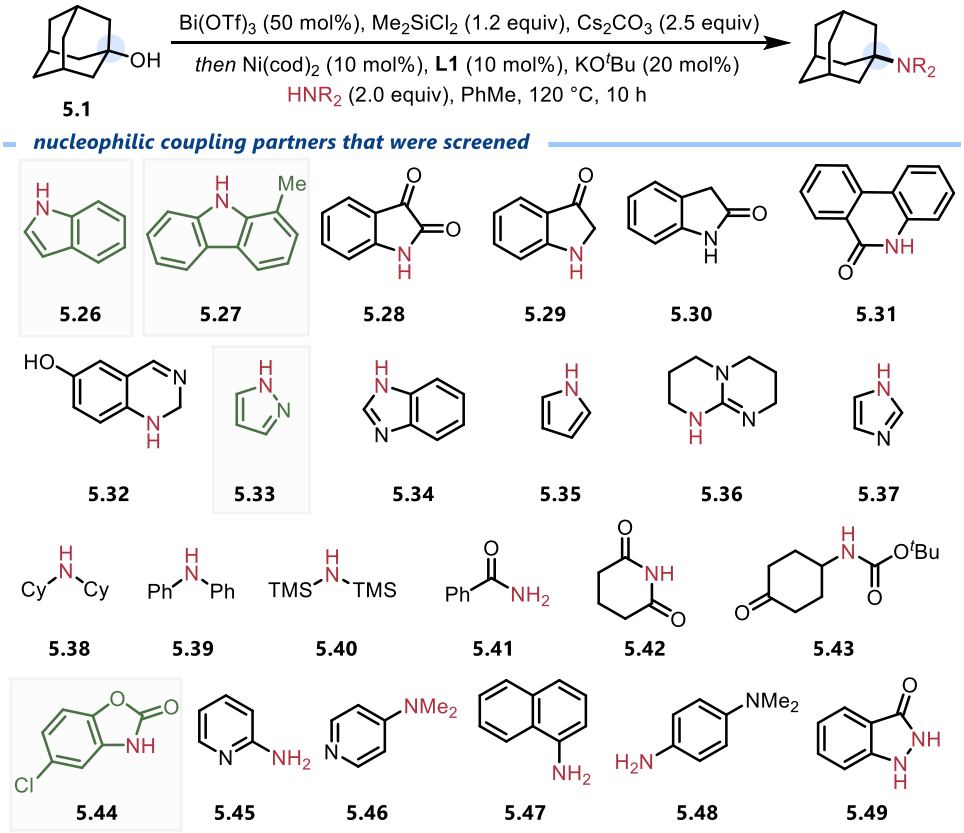


Seeking to establish a trend in reactivity, it was notable that each of the heterocycles that were successfully coupled with tertiary alcohol **5.1** (indole, pyrazole, carbazole, oxazolidone) have been reported to have a pKa in a narrow range, from 19.8 and 20.9.[46] Sigman and colleagues recently demonstrated a similar restriction in a recent report of an *N*-alkylation.[46a] As such, it is tentatively proposed that there is an 'optimal window' of N–H pKa's within which reactivity can be achieved (Figure 5.6). However, ureas, amides, hydrazones and some aliphatic amines also bear pKa's within this window. As these species are not amenable towards this *N*-alkylation according



*Chapter five references begin on page 413; experimental details begin on page 401*

to the general reaction conditions, there must be more complex interactions dictating reactivity beyond pKa.

**Figure 5.5.** 'Optimal pKa window' for this reaction

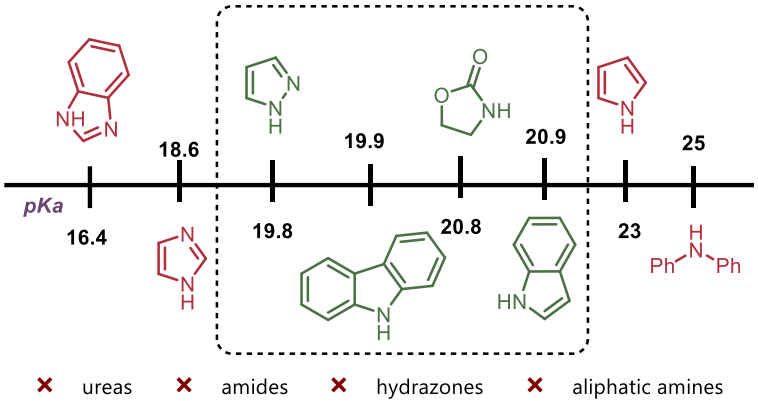


With this knowledge in hand, a preliminary substrate scope was established (Scheme 5.6). A range of indoles could act as viable coupling partners (**5.50**-**5.54**), including those bearing ester (**5.51**), bromide (**5.52**) and alcohol (**5.53**) moieties. Piperidine scaffolds could be aminated (**5.54**), and N-alkylation of oxazolidinone-bearing chloroxazone (**5.55**) could be achieved. Pyrazoles could also be alkylated with both a pyran (**5.56**) and adamantane (**5.57**) bearing alcohol. Regioselective alkylation of pyrazoles is a topic of interest in synthetic chemistry.[47] To this end, an X-ray crystal of pyrazole product **5.57** revealed binding the bond to be to the $N^1$ nitrogen of the pyrazole – no $N^2$ bonding was observed. Beyond tertiary alcohols, benzyl alcohols could also be aminated (**5.58**); however, attempts at aminating non-π-activated alcohols have thus far proven futile (**5.59**, **5.60**). Indoles are known to be nucleophilic in C-alkylation reactions at the C3 position. The fact that this transformation fails on *N*-methyl indole (**5.61**), as well as the observation of eight aromatic peaks on the $^1$H NMR spectra of product **5.50**, serve as indicators that this transformation is indeed the *N*-alkylation of indoles rather than C3-alkylation.



*Chapter five references begin on page 413; experimental details begin on page 401*

**Scheme 5.6.** Preliminary substrate scope

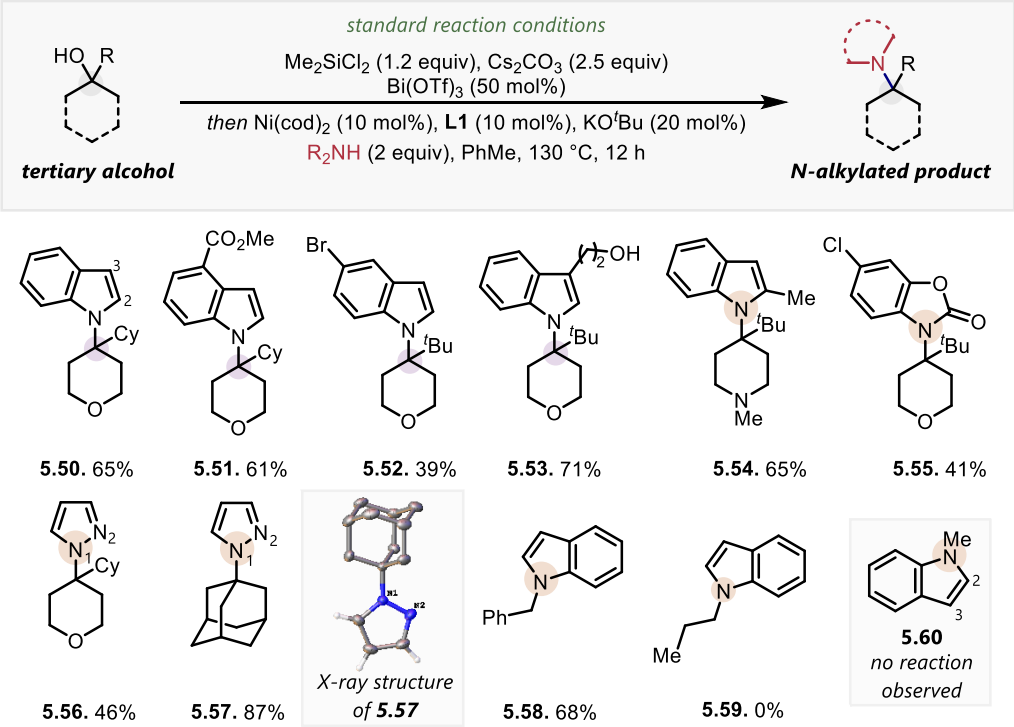


Concurrent with the investigation of the scope of this reaction were efforts towards investigating the reaction mechanism. Given the similarities between the catalytic system employed in this transformation and that that was described in chapters three and four of this dissertation, it is reasonable to assume that this transformation is proceeding through a similar mechanism. Evidence against a radical intermediate was obtained as the amination of cyclopropane-bearing compound **5.62** proceeded without observation of the ring-opened compound, instead affording **5.63** in 77% yield (Scheme 5.7a). Further, the reaction of **5.20** proceeds to afford *N*-alkylated product **5.25** in yields reflective of the optimized conditions when including radical scavenging reagents such as TEMPO, galvinoxyl, or diphenylethylene (Scheme 5.7b).



*Chapter five references begin on page 413; experimental details begin on page 401*

**Scheme 5.7**. Evidence against a radical intermediate

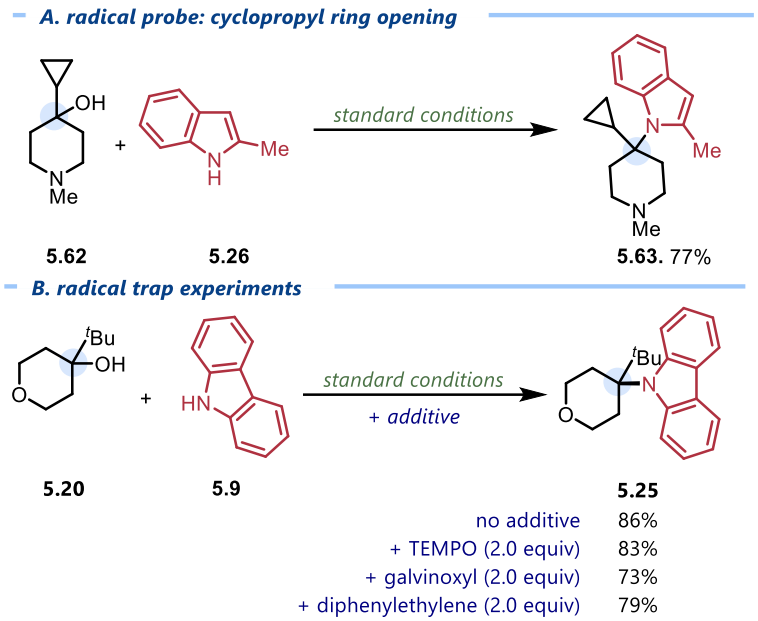


The kinetics of this transformation were briefly investigated according to the variable time normalization analysis method,[48] wherein this reaction showed an apparent first order dependence on Lewis acid and substrate and a zeroth order dependence on nickel catalyst and nucleophile (Scheme 5.8). While this result – along with that presented in Scheme 5.7 – suggests an $S_N1$-type transformation, further experiments, such as a Hammett Plot, would be required to be certain.



*Chapter five references begin on page 413; experimental details begin on page 401*

**Scheme 5.8.** Preliminary mechanistic investigation

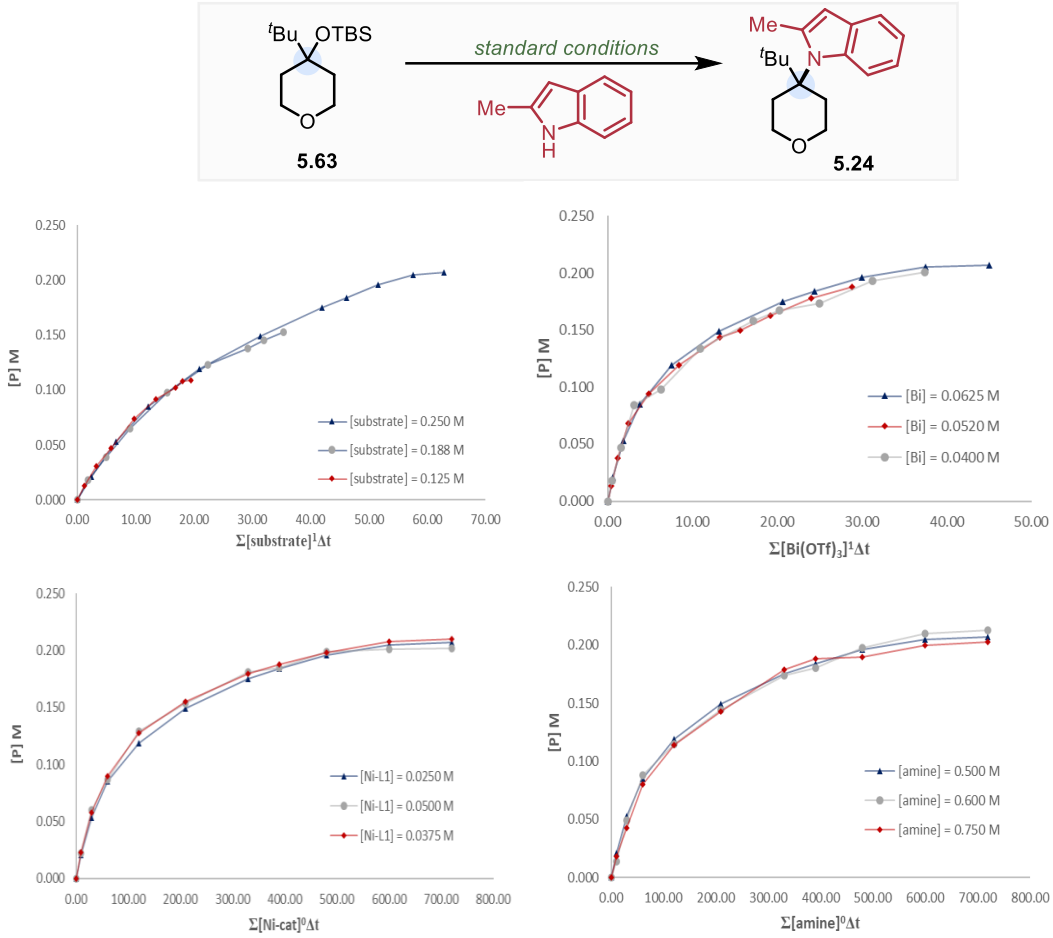


***vTNA results:*** rate $\alpha$ $[substrate]^1[Bi(OTf)_3]^1$



*Chapter five references begin on page 413; experimental details begin on page 401*

## 5.9. Conclusion, future outlook and considerations

### 5.9.1. Conclusions

The goal of this chapter was to determine whether nucleophilic coupling partners other than arylboronate esters could be used in the functionalization of non-π-activated alcohols in the presence of a nickel/bismuth dual catalyst. High-throughput experiments revealed several successful results, each of which were subsequently investigated. Specifically, four results were pursued: the coupling of tertiary alcohols with allylsilanes, benzyl boronates esters, terminal alkynes and *N*-heterocycles. Investigations into the coupling of allylsilanes with tertiary alcohols were abandoned upon realizing that the transformation was substrate dependent and occurred in the absence of nickel catalyst. Investigation into the coupling of benzylboronate esters with tertiary alcohols led to the observation of product in yields up to 28%, however this reaction was not pursued further. The coupling of tertiary alcohols with terminal alkynes afforded yields up to 84%, although reproducibility issues arose. Lastly, pursuit of the coupling of *N*-heterocycles with tertiary alcohols revealed product yields in excess of 80%. Multiple heterocycles of a similar pKa including indoles, carbazoles, pyrazoles and oxazolidones could be coupled with tertiary alcohols to reveal product; preliminary scope expansion and mechanistic investigations are also reported.

### 5.9.2. Future outlook and considerations

There are a number of directions that can be taken regarding the work presented within chapter five of this dissertation. Firstly, this work was performed prior to the discovery that ligand **L2** is superior to ligand **L1** in Suzuki-Miyaura arylations. It is reasonable to believe that **L2** may be superior to **L1** in the work presented within this chapter as well. As such, the first thing that

should be done concerning the future of these potential projects should be to revisit ligand effects and screen each of the reactions discussed in Sections 5.6, 5.7 and 5.8 with **L2** and other bis(NHC) ligands that have been synthesized in the Newman lab after the work presented in this chapter was conducted (Figure 5.7).

**Figure 5.7.** bis(NHC) ligands that could be screened in these transformations

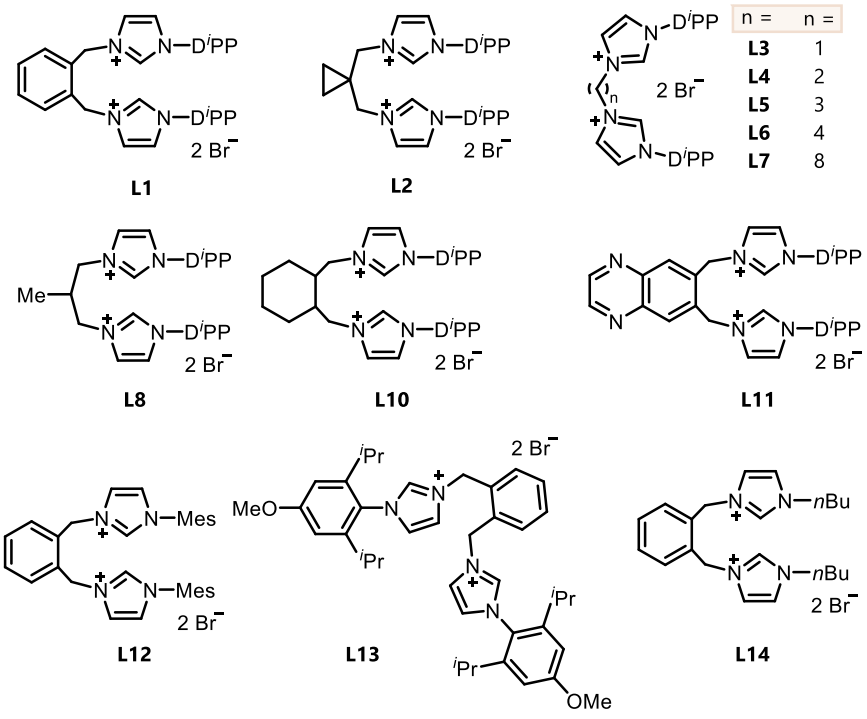


In the same vein, the limitations associated with previous chapters should be reevaluated in the transformations discussed in chapter five. For instance, it was assumed that since tertiary alcohols were the only class of alcohols that could be coupled in the Suzuki-Miyaura arylation discussed within chapter three that this restriction would carry over to the work presented in this chapter. While preliminary results support this assumption, it would be worthwhile to investigate further regarding whether primary and secondary alcohols can be employed in these



*Chapter five references begin on page 413; experimental details begin on page 401*

transformations. Similarly, it would be interesting to investigate if the reactivity presented in this chapter can be extended towards the functionalization of *β*-hydroxysilanes.

For the coupling of alcohols with benzylboronic acids, while yields reported thus far have been low, there was not a lot of time spent optimizing/investigating this transformation. Future work concerning this reaction could lead to strong results, and that the establishment of a method for the coupling of non-π-activated alcohols that forms C($sp^3$)-C($sp^3$) bonds is a desired transformation. The starting point for further evaluation of this transformation should be the screening of alternative ligands and other reaction conditions. It would also be intriguing to test other alkyl nucleophiles in this reaction, such as alkylzincs, alkylmagnesiums, or even other alkylboron species such as trifluoroborate salts or alkyl-9-borabicyclo(3.3.1)nonanes.

For the coupling of alcohols with terminal alkynes, it is not convincing that further pursuit of this project will yield fruitful results. While yields up to 84% were obtained initially, setting up the alkynylation of **5.20** with phenylacetylene in triplicate in the weeks leading up to the submission of this dissertation led to the observation of product in a mere 7% yield in one trial, a 4% yield in a second and a 0% yield in the third. Nonetheless, it would be worthwhile to revisit this reaction with alternative bis(NHC) ligands, or to attempt the transformation on alternative alcohols and β-hydroxysilanes. One possibility is that there were trace metal contaminants on the stir bars/equipment, or within the reagents, that the original reactions detailed in Section 5.7 were conducted with. To investigate this possibility, trace metals, such as copper, could be doped into the reaction mixtures in an attempt to achieve higher yields.

The coupling of alcohols with *N*-heterocycles has, thus far, afforded the most promising results. The first step for the continuation of this project would be to screen bis(NHC) ligands to ensure that the ligand employed is indeed the optimal ligand. Following this, work should continue

into expanding the scope and investigating the mechanism of transformation. Far-off-future objectives for this transformation could seek to extend reactivity towards more medicinally-relevant amines, such as amino acids. Further, extensions towards enantioselective transformations could be interesting to the chemical community. It is possible that a chiral, or increasingly rigid, bis(NHC) could be utilized towards this purpose.



*Chapter five references begin on page 413; experimental details begin on page 401*

## 5.10. Experimental

### 5.10.1. General details

Unless otherwise indicated, reactions were conducted under an atmosphere of nitrogen in 8 mL screw-capped vials that were oven-dried (120 °C). Column chromatography was either performed manually using Silicycle F60 40−63 μm silica gel or by using a Combiflash Rf+ automated chromatography system with Biotage normal-phase Silica Flash columns (35−70 μm). Analytical thin layer chromatography (TLC) was conducted with aluminum-backed EMD Millipore Silica Gel 60 F254 pre-coated plates. Visualization of developed plates was performed under UV light (254 nm) and/or using $KMnO_4$ stain.

### 5.10.2. Instrumentation

$^{1}H$ NMR and $^{13}C$ NMR were recorded on a Bruker AVANCE II 400 MHz spectrometer, a Bruker AVANCE III HD 500 MHz spectrometer, or a Bruker AVANCE III HD 600 MHz spectrometer. $^{1}H$ NMR spectra were internally referenced to the residual solvent signal (e.g., $CDCl_3$ = 7.27 ppm). $^{13}C$ NMR spectra were internally referenced to the residual solvent signal (e.g., $CDCl_3$ = 77.00 ppm). Data for $^{1}H$ NMR are reported as follows: chemical shift (δ ppm), multiplicity (s = singlet, d = doublet, t = triplet, q = quartet, quin = quintet, m = multiplet), coupling constant (Hz), integration. NMR yields for optimization studies were obtained by $^{1}H$ NMR analysis of the crude reaction mixture using 1,3,5-trimethoxybenzene as an internal standard. GC data was obtained via a 5-point calibration curve using FID analysis on an Agilent Technologies 7890B GC with a 30 m x 0.25 mm HP-5 column. Accurate mass data (EI) was obtained from an Agilent 5977A GC/MSD using MassWorks 4.0 from CERNO Bioscience.[1]

### 5.10.3. Materials

Organic solvents were purified by rigorous degassing with nitrogen before passing through a PureSolv solvent purification system. Low water content was confirmed by Karl Fischer titration (<20 ppm for all solvents). Unless otherwise noted, starting materials were obtained commercially from Sigma Aldrich, Alfa Aesar or Combi-Blocks and used as received. (Trimethylsilyl)methylmagnesium chloride ($Me_3SiCH_2MgCl$) was purchased from Sigma Aldrich (1.0 M in diethyl ether). $Ni(cod)_2$ was purchased from Sigma Aldrich. $Bi(OTf)_3$ was purchased from Combi-Blocks. $Me_2SiCl_2$ was purchased from Sigma Aldrich. PhBpin was purchased from Combi-Blocks and other pinacol boronic esters were synthesized from the corresponding chloride[2] or boronic acid[3] according to the literature. **L2** was prepared as described in a previous work,[4] while other *N*-heterocyclic carbenes were prepared according to the literature.[5]

### 5.10.4. General procedures

***High-throughput procedure***

***General considerations****:* All manipulations were performed in a glovebox under a nitrogen atmosphere. All liquids were vigorously degassed with inert gas before shipping inside the glovebox. All reactions were run at on a 0.05 mmol scale at a 0.1 M concentration. Glassware and consumables were used as received from the original packaging. Solids were dispensed using plastic scoops (TWD TradeWinds, ASPS-01, Disposable Antistatic Polypropylene Sample Transfer Scoop, 1-10 mg capacity) and liquids were dispensed using micropipettes. Plates were sealed by placing a PFA sheet (Analytical Sales and Services, cat. no. 96967) and two rubber gaskets (Analytical Sales and Services, cat. no. 96965) on top of the aluminum block followed by

screwing in the plate lid with 1.5” stainless steel screws. The sealed HTE plate was removed from the glovebox and placed in a heated tumble stirrer at 85 °C equipped with a mica deck insert (V&P Scientific, cat. no. VP 710C5-7A-CC, VP741D, VP710C5-7-2) and stirred for 16 hours. For details regarding the set up and execution of high-throughput experiments, the reader is referred to the manuscript “Reaction screening in multiwell plates: High-throughput optimization of a Buchwald-Hartwig amination” by Adam Cook, Roxanne Clément, and Stephen G. Newman. *Nature Protoc*. **2021**, *2*, 1152-1169.

***96 well-plate preparation:*** Each 96 well-plate was ran in an aluminum block assembly (Analytical Sales and Services, cat. no. 96973). Glass vials (8 × 40-mm, 1.2-mL vials; Chemglass Life Sciences, cat. no. CV-2103-0840) were loaded into the wells with a pair of clean forceps. Micro stir bars (Parylene-coated micro stir bars, VP Scientific, cat. no. VP 712-1) were dispensed into each glass vial within the 96-well plates using a stir bar dispenser (VP Scientific, cat. no. VP-711A-1S/D).

***General procedure for high-throughput experimentation***: To each vial in the 96-well plate was added the appropriate base (2.5 equivalent, 0.15 mmol), $Bi(OTf)_3$ (0.3 equivalent, 0.015 mmol) $Me_2SiCl_2$ (1.2 equivalent, 0.06 mmol), alcohol (1.0 equivalent, 0.05 mmol) and the appropriate solvent (0.2 mL). The entire plate was stirred on a Heidolph hotplate at room temperature for five minutes. Subsequently, a mixture of $Ni(cod)_2$ (10 mol%, 0.005 mmol), **L1** (10 mol%), 0.005 mmol) and $KO^tBu$ (20 mol%, 0.010 mmol) in the appropriate solvent (0.3 mL) was added to each vial, followed by the appropriate nucleophile (1.5 equiv, 0.075 mmol). The plate was subsequently sealed and the reactions were stirred at 90 C for 16 h. Subsequently, 0.025 mmol of internal standard (1,3,5-trimethoxybenzene) was added to each vial and an aliquot from each reaction vial

was separately filtered through a silica plug with EtOAc. The crude results were analyzed by GC-MS.

***General Procedure A – Alkylation of tertiary alcohol with benzyl boronate ester:*** An oven-dried 8 mL screw-top test-tube was equipped with an oven-dried micro-stir bar and brought into a nitrogen-filled glovebox. This reaction vessel was charged with alcohol (1.0 equivalent, 0.20 mmol), $Cs_2CO_3$ (2.5 equivalent, 0.50 mmol), $Bi(OTf)_3$ (0.50 equivalent, 0.10 mmol), $Me_2SiCl_2$ (1.2 equivalent, 0.24 mmol) and PhMe (0.4 mL). This mixture was left to stir for 15 min at room temperature. After 15 min, a premixed solution of $Ni(cod)_2$ (0.10 equivalent, 0.02 mmol), **L1** (0.10 equivalent, 0.02 mmol) and KO$^t$Bu (0.20 equivalent, 0.04 mmol) in PhMe (0.4 mL) was added to the stirring alcohol solution, followed by BnBpin (2.0 equivalent, 0.40 mmol), before the reaction vessel was sealed with a Teflon-septum equipped cap and brought outside of the glovebox to be stirred within a mineral-oil bath at 800 rpm for 16 hours at 120 C. After 10 hours, the reaction vessel was allowed to come to room temperature. The crude reaction solution was quenched with sat. KOH (5 mL) and diluted with EtOAc before being transferred into a separatory funnel. KOH was removed via liquid-liquid extraction with EtOAc (3 x 10 mL); the resulting organic phases were combined in the separatory funnel before being washed twice with sat. $NaHCO_3$ and once with sat. NaCl. The organic phase was dried with $MgSO_4$ before being passed through a short plug composed of $SiO_2$ and celite in a 50:50 mixture. Solvent was evacuated by rotary evaporation and the subsequent residue was purified by column chromatography.

***General Procedure B – Allylation of tertiary alcohol with allyltrimethylsilane:*** An oven-dried 8 mL screw-top test-tube was equipped with an oven-dried micro-stir bar and brought into a nitrogen-filled glovebox. This reaction vessel was charged with alcohol (1.0 equivalent, 0.20 mmol), $K_3PO_4$ (2.5 equivalent, 0.50 mmol), $Bi(OTf)_3$ (0.30 equivalent, 0.06 mmol), $Me_2SiCl_2$ (1.2 equivalent, 0.24 mmol) and PhMe (0.4 mL). This mixture was left to stir for 15 min at room temperature. After 15 min, a premixed solution of $Ni(cod)_2$ (0.10 equivalent, 0.02 mmol), **L1** (0.10 equivalent, 0.02 mmol) and KO$^t$Bu (0.20 equivalent, 0.04 mmol) in PhMe (0.4 mL) was added to the stirring alcohol solution, followed by allyltrimethylsilane (1.5 equivalent, 0.30 mmol), before the reaction vessel was sealed with a Teflon-septum equipped cap and brought outside of the glovebox to be stirred within a mineral-oil bath at 800 rpm for 16 hours at 90 C. After 10 hours, the reaction vessel was allowed to come to room temperature. The crude reaction solution was quenched with sat. KOH (5 mL) and diluted with EtOAc before being transferred into a separatory funnel. KOH was removed via liquid-liquid extraction with EtOAc (3 x 10 mL); the resulting organic phases were combined in the separatory funnel before being washed twice with sat. $NaHCO_3$ and once with sat. NaCl. The organic phase was dried with $MgSO_4$ before being passed through a short plug composed of $SiO_2$ and celite in a 50:50 mixture. Solvent was evacuated by rotary evaporation and the subsequent residue was purified by column chromatography.

***General Procedure C – Alkynylation of tertiary alcohol with phenylacetylene***: An oven-dried 8 mL screw-top test-tube was equipped with an oven-dried micro-stir bar and brought into a nitrogen-filled glovebox. This reaction vessel was charged with alcohol (1.0 equivalent, 0.20 mmol), $Cs_2CO_3$ (2.5 equivalent, 0.50 mmol), $Bi(OTf)_3$ (0.50 equivalent, 0.10 mmol), $Me_2SiCl_2$ (1.2 equivalent, 0.24 mmol) and DMF (0.4 mL). This mixture was left to stir for 15 min at room

temperature. After 15 min, a premixed solution of $Ni(cod)_2$ (0.10 equivalent, 0.02 mmol), **L1** (0.10 equivalent, 0.02 mmol) and $KO^tBu$ (0.20 equivalent, 0.04 mmol) in DMF (0.4 mL) was added to the stirring alcohol solution, followed by phenylacetylene (2.0 equivalent, 0.40 mmol), before the reaction vessel was sealed with a Teflon-septum equipped cap and brought outside of the glovebox to be stirred within a mineral-oil bath at 800 rpm for 16 hours at 120 C. After 10 hours, the reaction vessel was allowed to come to room temperature. The crude reaction solution was quenched with sat. KOH (5 mL) and diluted with EtOAc before being transferred into a separatory funnel. KOH was removed via liquid-liquid extraction with EtOAc (3 x 10 mL); the resulting organic phases were combined in the separatory funnel before being washed twice with sat. $NaHCO_3$ and once with sat. NaCl. The organic phase was dried with $MgSO_4$ before being passed through a short plug composed of $SiO_2$ and celite in a 50:50 mixture. Solvent was evacuated by rotary evaporation and the subsequent residue was purified by column chromatography.

***General Procedure D – N-alkylation of tertiary alcohols:*** An oven-dried 8 mL screw-top test-tube was equipped with an oven-dried micro-stir bar and brought into a nitrogen-filled glovebox. This reaction vessel was charged with alcohol (1.0 equivalent, 0.20 mmol), $Cs_2CO_3$ (2.5 equivalent, 0.50 mmol), $Bi(OTf)_3$ (0.50 equivalent, 0.10 mmol), $Me_2SiCl_2$ (1.2 equivalent, 0.24 mmol) and PhMe (0.4 mL). This mixture was left to stir for 15 min at room temperature. After 15 min, a premixed solution of $Ni(cod)_2$ (0.10 equivalent, 0.02 mmol), **L1** (0.10 equivalent, 0.02 mmol) and $KO^tBu$ (0.20 equivalent, 0.04 mmol) in PhMe (0.4 mL) was added to the stirring alcohol solution, followed by *N*-nucleophile (2.0 equivalent, 0.40 mmol), before the reaction vessel was sealed with a Teflon-septum equipped cap and brought outside of the glovebox to be stirred within a mineral-oil bath at 800 rpm for 16 hours at 120 C. After 10 hours, the reaction vessel was

allowed to come to room temperature. The crude reaction solution was quenched with sat. KOH (5 mL) and diluted with EtOAc before being transferred into a separatory funnel. KOH was removed via liquid-liquid extraction with EtOAc (3 x 10 mL); the resulting organic phases were combined in the separatory funnel before being washed twice with sat. $NaHCO_3$ and once with sat. NaCl. The organic phase was dried with $MgSO_4$ before being passed through a short plug composed of $SiO_2$ and celite in a 50:50 mixture. Solvent was evacuated by rotary evaporation and the subsequent residue was purified by column chromatography.

### **4.9.5.** Characterization details

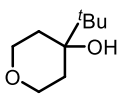


**4-(1,1-Dimethylethyl)tetrahydro-2*H*-pyran-4-ol (5.20)** was prepared via a Grignard reaction between tetrahydro-4H-pyran-4-one and *tert*-butyl magnesium bromide according to a literature procedure. Column chromatography was performed using a gradient of 1→10% ethyl acetate in hexanes to afford product as a colourless liquid (18.1 mg, 74% yield). **$^1$H NMR** (400 MHz, $CDCl_3$): δ 3.98-3.95 (m, 4H), 2.51-2.48 (m, 4H), 1.09 (s, 9H); **$^{13}$C NMR** (100 MHz, $CDCl_3$): 68.5, 67.8, 42.8, 29.5, 10.5. **Accurate mass (EI)**: Theoretical: 158.1307. Found: 158.1302. Spectral Accuracy: 98.4%.

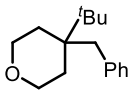


**4-Benzyl-4-(1,1-dimethylethyl)tetrahydro-2*H*-pyran (5.21)** was prepared from **5.20** according to general procedure A. Column chromatography was performed using a gradient of 1→20% ethyl acetate in hexanes to afford product as a clear liquid (312.6 mg, 78% yield). **$^1$H NMR** (400 MHz, $CDCl_3$): 7.41-7.32 (m, 3H), 7.24-7.20 (m, 2H), 4.20-4.15 (m, 2H), 3.91-3.88 (m, 4H), 2.31-2.25 (m, 4H), 0.91 (s, 9H); **$^{13}$C NMR** (100 MHz, $CDCl_3$): 140.5, 128.5, 128.4, 126.1, 67.8, 63.0, 36.4, 34.1, 33.9, 33.1. **Accurate mass (EI)**: Theoretical: 232.1827. Found: 232.1822. Spectral Accuracy: 98.3%.



*Chapter five references begin on page 413; experimental details begin on page 401*

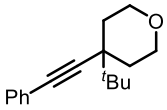


**4-Alkynyl-4-(1,1-dimethylethyl)tetrahydro-2*H*-pyran (5.23)** was prepared from **5.20** according to general procedure C. Column chromatography was performed using a gradient of 1→20% ethyl acetate in hexanes to afford product as a clear liquid (312.6 mg, 78% yield). **$^{1}$H NMR** (400 MHz, $CDCl_3$): δ 7.44-7.41 (m, 2H), 7.29-7.21 (m, 3H), 3.95-3.89 (m, 4H), 2.45-2.39 (m, 4H), 0.87 (s, 9H); **$^{13}$C NMR** (100 MHz, $CDCl_3$): 132.0, 128.6, 128.2, 122.0, 83.5, 76.6, 67.7, 57.2, 42.7, 32,7, 27.0. **Accurate mass (EI)**: Theoretical: 242.1671. Found: 242.1665. Spectral Accuracy: 97.6%.

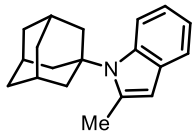


**2-Methyl-1-tricyclo[3.3.1.1$^{3,7}$]dec-1-yl-1*H*-indole (5.18)** was prepared **5.1** according to general procedure D. Column chromatography was performed using a gradient of 1→20% ethyl acetate in hexanes to afford product as a clear liquid (312.6 mg, 78% yield). **$^{1}$H NMR** (400 MHz, $CDCl_3$): δ 7.53-7.52 (m, 1H), 7.29-7.26 (m, 1H), 7.13-7.06 (m, 2H), 6.30-6.18 (m, 1H), 2.16 (s, 3H), 1.74-1.65 (m, 7H), 1.62-1.59 (m, 8H); **$^{13}$C NMR** (100 MHz, $CDCl_3$): 136.0, 135.0, 129.0, 120.8, 119.6, 119.5, 110.2, 100.3, 45.3, 36.0, 30.7, 13.7. **Accurate mass (EI)**: Theoretical: 265.1830. Found: 265.1824. Spectral Accuracy: 97.1%.

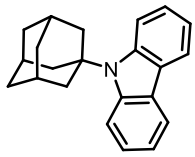


**9-Tricyclo[3.3.1.1$^{3,7}$]dec-1-yl-9*H*-carbazole (5.19)** was prepared from **5.1** according to general procedure D. Column chromatography was performed using a gradient of 1→20% ethyl acetate in hexanes to afford product as a clear liquid (312.6 mg, 78% yield). **$^{1}$H NMR** (400 MHz, $d_6$-DMSO): δ 8.19-8.17 (m, 2H), 7.58-7.55 (m, 2H), 7.48-7.44 (m, 2H), 7.25-7.21 (m, 2H), 2.50-2.39 (m, 6H), 2.13-2.11 (m, 3H), 1.76-1.74 (m, 6H); **$^{13}$C NMR** (100 MHz, $d_6$-DMSO): 139.8, 125.6, 122.5, 120.2, 118.5, 111.0, 68.4, 49.0, 34.9, 32.2. **Accurate mass (EI)**: Theoretical: 301.1830. Found: 301.1827. Spectral Accuracy: 98.4%.

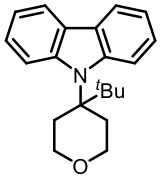


**4-(*9H*-Carbazolyl)-4-(1,1-dimethylethyl)tetrahydro-2*H*-pyran (5.25)** was prepared from **5.20** according to general procedure D. Column chromatography was performed using a gradient of 1→20% ethyl acetate in hexanes to afford product as a clear liquid (312.6 mg, 78% yield). **$^{1}$H NMR** (400 MHz, $d_6$-DMSO): δ 8.11-8.09 (m, 2H), 7.50-7.48 (m, 2H), 7.40-7.36 (m, 2H) 7.17-7.13 (m, 2H), 3.87-3.84 (m, 4H), 2.40-2.36 (m, 4H), 0.95 (s, 9H); **$^{13}$C NMR** (100 MHz, $d_6$-DMSO): 138.0, 124.7, 121.7, 119.6, 117.9, 110.2, 66.1, 56.3, 41.8, 31.7, 26.1. **Accurate mass (EI)**: Theoretical: 307.1936. Found: 307.1932. Spectral Accuracy: 98.4%.

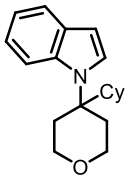


**4-Cyclohexyl-4-(*1H*-indolyl)tetrahydro-*2H*-pyran (5.50)** was prepared according from 4-cyclohexyltetrahydro-2*H*-pyran-4-ol to general procedure D. Column chromatography was performed using a gradient of 1→20% ethyl acetate in hexanes to afford product as a clear liquid (312.6 mg, 78% yield). **$^{1}$H NMR** (400 MHz, $CDCl_3$): δ 7.77-7.75 (m, 1H), 7.26-7.20 (m, 2H), 7.20-7.15 (m, 2H), 6.49-6.48 (m, 1H), 3.98-3.95 (m, 4H), 2.50-2.49 (m, 4H), 1.77-1.66 (m, 5H), 1.52-1.45 (m, 1H), 1.30-1.15 (m, 3H), 0.97-0.89 (m, 2H); **$^{13}$C NMR** (100 MHz, $CDCl_3$): 135.7, 127.7, 124.1, 121.8, 120.6, 119.6, 110.9, 102.4, 42.8, 40.4, 29.54, 29.50, 29.47, 26.5, 25.7. **Accurate mass (EI)**: Theoretical: 283.1936. Found: 283.1931. Spectral Accuracy: 97.3%.

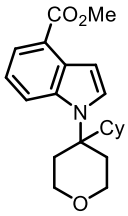


**Methyl 1-(4-cyclohexyl-tetrahydro-2*H*-pyran-4-yl)-1*H*-indole-4-carboxylate (5.51)** was prepared from 4-cyclohexyltetrahydro-2*H*-pyran-4-ol according to general procedure D. Column chromatography was performed using a gradient of 1→20% ethyl acetate in hexanes to afford product as a clear liquid (312.6 mg, 78% yield). **$^{1}$H NMR** (400 MHz, $CDCl_3$): δ 7.71-7.70 (m, 2H), 7.35-7.16 (m, 3H), 3.99-3.97 (m, 4H), 3.96 (s, 3H), 2.53-2.50 (m, 4H), 1.81-0.94 (m, 11H); **$^{13}$C NMR** (100 MHz, $CDCl_3$): 162.5, 136.9, 127.3, 127.0, 125.3, 122.5, 120.7, 111.9, 108.7, 51.9, 42.8, 40.4, 29.52, 29.48, 27.9, 26.5, 25.8. **Accurate mass (EI)**: Theoretical: 341.1991. Found: 341.1988. Spectral Accuracy: 98.6%.



*Chapter five references begin on page 413; experimental details begin on page 401*

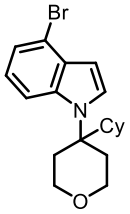


**5-Bromo-1-(4-cyclohexyl-tetrahydro-2*H*-pyran-4-yl)-1*H*-indole (5.52)** was prepared from 4-cyclohexyltetrahydro-2*H*-pyran-4-ol according to general procedure D. Column chromatography was performed using a gradient of 1→20% ethyl acetate in hexanes to afford product as a clear liquid (312.6 mg, 78% yield). **$^{1}$H NMR** (400 MHz, $CDCl_3$): δ 7.89-7.87 (m, 1H), 7.39-7.37 (m, 2H), 7.33-7.31 (m, 1H), 6.61-6.60 (m, 1H), 4.09 (m, 4H), 2.62 (m, 4H), 1.89-1.78 (m, 5H), 1.65-1.57 (m, 1H), 1.43-1.26 (m, 3H), 1.10-1.00 (m, 2H); **$^{13}$C NMR** (100 MHz, $CDCl_3$): 133.1, 129.7, 125.5, 124.7, 122.7, 112.8, 112.4, 102.7, 68.7, 67.7, 42.8, 40.4, 29.5, 26.5, 25.8. **Accurate mass (EI)**: Theoretical: 361.1041. Found: 361.1038. Spectral Accuracy: 98.3%.

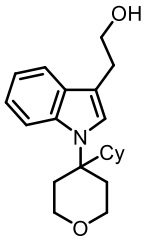


**1-(4-Cyclohexyl-tetrahydro-2*H*-pyran-4-yl)-1*H*-indolyl-2-ethanol (5.53)** was prepared from 4-cyclohexyltetrahydro-2*H*-pyran-4-ol according to general procedure D. Column chromatography was performed using a gradient of 1→20% ethyl acetate in hexanes to afford product as a clear liquid (312.6 mg, 78% yield). **$^{1}$H NMR** (400 MHz, $CDCl_3$): δ 7.73-7.70 (m, 1H), 7.47-7.43 (m, 1H), 7.35-7.25 (m, 2H), 7.19-7.13 (m, 1H), 4.04-4.00 (m, 4H), 3.99-3.97 (m, 2H), 3.13-3.10 (m, 2H), 2.57 (m, 4H), 2.01-1.89 (m, 2H), 1.84-1.75 (m, 4H), 1.60-1.53 (m, 1H), 1.39-0.97 (m, 4H); **$^{13}$C NMR** (100 MHz, $CDCl_3$): 136.1, 125.9, 122.8, 121.5, 119.9, 117.5, 113.1, 111.1, 68.6, 67.7, 62.5, 42.7, 40.4, 29.5, 29.4, 28.7, 25.7. **Accurate mass (EI)**: Theoretical: 327.2198. Found: 327.2189. Spectral Accuracy: 98.7%.

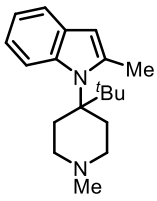


**2-Methyl-(4-tertbutyl-1-methyl-piperidinyl)-1*H*-indole (5.54)** was prepared from 4-(1,1-dimethylethyl)-1-methyl-4-piperidinol according to general procedure D. Column chromatography was performed using a gradient of 1→20% ethyl acetate in hexanes to afford product as a clear liquid (312.6 mg, 78% yield). **$^{1}$H NMR** (400 MHz, $CDCl_3$): δ 7.53-7.51 (m, 1H), 7.28-7.26 (m, 1H), 7.12-7.05 (m, 2H), 6.22-7.21 (m, 1H), 2.74-2.71 (m, 4H), 2.50-2.47 (m, 4H), 2.44 (s, 3H), 2.41 (s, 3H), 1.29 (s, 9H); **$^{13}$C NMR** (100 MHz, $CDCl_3$): 136.0, 135.0, 125.2, 120.7, 119.5, 119.4, 110.1, 100.1, 69.1, 55.3, 45.4, 41.0, 31.2, 13.6. **Accurate mass (EI)**: Theoretical: 284.2252. Found: 284.2249. Spectral Accuracy: 98.9%.



*Chapter five references begin on page 413; experimental details begin on page 401*

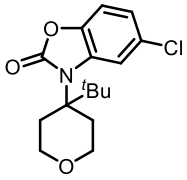

**4-(*1H*-Chlorzoxazonyl)-4-(1,1-dimethylethyl)tetrahydro-2*H*-pyran (5.55)** was prepared from **5.20** according to general procedure D. Column chromatography was performed using a gradient of 1→20% ethyl acetate in hexanes to afford product as a clear liquid (312.6 mg, 78% yield). **$^{1}$H NMR** (400 MHz, *d*$_6$-DMSO): δ 7.23-7.21 (m, 1H), 7.07-7.02 (m, 2H), 3.80-3.77 (m, 4H), 2.50-2.29 (m, 4H), 0.87 (s, 9H); **$^{13}$C NMR** (100 MHz, *d*$_6$-DMSO): 154.4, 142.2, 131.8, 127.9, 121.6, 110.9, 109.9, 55.9, 57.1, 42.4, 32.6, 26.8. **Accurate mass (EI)**: Theoretical: 309.1132. Found: 309.1130. Spectral Accuracy: 98.5%.

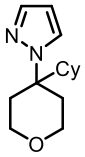

**1-(Tetrahydro-4-cyclohexyl-2*H*-pyran-4-yl)-1*H*-pyrazole (5.56)** was prepared from 4-cyclohexyltetrahydro-2*H*-pyran-4-ol according to general procedure D. Column chromatography was performed using a gradient of 1→20% ethyl acetate in hexanes to afford product as a clear liquid (312.6 mg, 78% yield). **$^{1}$H NMR** (400 MHz, $CDCl_3$): δ 7.67-7.66 (m, 2H), 6.40-6.39 (m, 1H), 4.02 (m, 4H), 2.55 (m, 4H), 1.85-1.77 (m, 5H), 1.66-1.55 (m, 1H), 1.46-1.34 (m, 3H), 1.16-0.94 (m, 2H); **$^{13}$C NMR** (100 MHz, $CDCl_3$): 133.6, 104.9, 68.5, 67.7, 42.8, 40.4, 29.51, 29.48, 25.8. **Accurate mass (EI)**: Theoretical: 234.1732. Found: 234.1726. Spectral Accuracy: 97.4%.

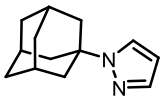

**1-Tricyclo[3.3.1.1$^{3,7}$]dec-1-yl-1*H*-pyrazole (5.57)** was prepared from **5.1** according to general procedure D. Column chromatography was performed using a gradient of 1→20% ethyl acetate in hexanes to afford product as a clear liquid (312.6 mg, 78% yield). Spectral data matches that found within the literature.[49] **$^{1}$H NMR** (400 MHz, $CDCl_3$): δ 7.56-7.52 (m, 2H), 6.25-6.24 (m, 1H), 2.25-2.23 (m, 3H), 2.19-2.18 (m, 6H), 1.78-1.77 (m, 6H); **$^{13}$C NMR** (100 MHz, $CDCl_3$): 138.4, 124.6, 104.3, 58.3, 42.9, 36.2, 29.5. Crystals suitable for X-ray analysis were grown from isopropanol.

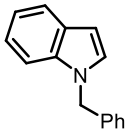


***N*-benzylindole (5.58)** was prepared from benzyl alcohol according to general procedure D. Column chromatography was performed using a gradient of 1→20% ethyl acetate in hexanes to afford product as a clear liquid (312.6 mg, 78% yield). Spectral data matches that found within the literature.[50] **$^{1}$H NMR** (400 MHz, $CDCl_3$): δ 7.75-7.69 (m, 1H), 7.35-7.30 (m, 4H), 7.23-7.13 (m, 5H), 6.61-6.60 (m, 1H), 5.36 (s, 2H); **$^{13}$C NMR** (100 MHz, $CDCl_3$): 137.5, 136.3, 128.72, 128.68, 128.2, 127.6, 126.7, 121.7, 120.9, 119.5, 109.7, 101.7, 50.0.

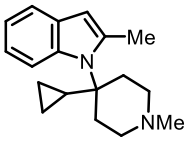


**2-Methyl-(4-cyclopropyl-1-methyl-piperidinyl)-1*H*-indole (5.63)** was prepared according to general procedure D. Column chromatography was performed using a gradient of 1→20% ethyl acetate in hexanes to afford product as a clear liquid (312.6 mg, 78% yield). **$^{1}$H NMR** (400 MHz, $CDCl_3$): δ 7.53-7.51 (m, 1H), 7.28-7.26 (m, 1H), 7.13-7.06 (m, 2H), 6.22 (m, 1H), 2.74-2.71 (m, 4H), 2.50-2.48 (m, 4H), 2.43 (s, 3H) 2.32 (s, 3H), 1.13-1.09 (m, 1H), 0.55-0.53 (m, 2H), 0.23-0.22 (m, 2H); **$^{13}$C NMR** (100 MHz, $CDCl_3$): 136.0, 135.0, 129.0, 120.7, 119.5, 119.4, 110.1, 100.1, 67.5, 55.3, 45.4, 41.0, 13.6, 13.5, 2.6. **Accurate mass (EI)**: Theoretical: 268.1939. Found: 268.1934. Spectral Accuracy: 98.5%.

## 5.11. References

(1) Shevlin, M. Practical high-throughput experimentation for chemists. *ACS Med. Chem. Lett*. **2017**, *8*, 601-607.

(2) Vries, J. G. D.; Vries, A. H. M. D. The power of high-throughput experimentation in homogeneous catalysis research for fine chemicals. *ChemInform* **2003**, *34*, 799-811.

(3) Schmink, J. R.; Bellomo, A.; Berritt, S. Scientist-led high-throughput experimentation and its utility in academia and industry. *Aldrichimica Acta* **2013**, *46*, 71-80.

(4) Dreher, S. D. et al. Nanomole-scale high-throughput chemistry synthesis of complex molecules. *Science* **2015**, *347*, 49-53.

(5) Krska, S. W.; DiRocco, D. A.; Dreher, S. D.; Shevlin, M. The evolution of chemical high-throughput experimentation to address challenging problems in pharmaceutical synthesis. *Acc. Chem. Res.* **2017**, *50*, 2976-2985.

(6) Shah, A. A.; Kelly, M. J.; Perkins, J. J. Access to unnatural α-amino acids via visible-light-mediated addition to dehydroalanine. *Org. Lett*. **2020**, *22*, 184-196.

(7) Collins, K. D.; Gensch, T.; Glorius, F. Contemporary screening approaches to reaction discovery and development. *Nature Chem.* **2014**, *6*, 859–871.

(8) Shevlin, M.; Friedfeld, M. R.; Sheng, H.; Pierson, N. A.; Hoyt, J. M.; Campeau, L.-C.; Chirik, P. J. Nickel-catalyzed asymmetric alkene hydrogenation of α,β-unsaturated esters: High-throughput experimentation-enabled reaction discovery, optimization and mechanistic elucidation. *J. Am. Chem. Soc.* **2016**, *138*, 3562-3569.

(9) Troshin, K.; Hartwig, J. F. Snap deconvolution: An informatics approach to high-throughput discovery of catalytic reactions. *Science* **2017**, *357*, 175-181.

(10) Robbins, D. W.; Hartwig, J. F. A simple, multidimensional approach to high-throughput discovery of catalytic reactions. *Science* **2011**, *333*, 1423-1427.

(11) McNally, A.; Prier, C. K.; MacMillan, D. W. C. Discovery of an α-amino C–H arylation reaction using the strategy of accelerated serendipity. *Science* **2011**, *334*, 1114-1117.

(12) Collins, K. D.; Glorius, F. A robustness screen for the rapid assessment of chemical reactions. *Nature Chem*. **2013**, *5*, 597-601.

(13) Granda, J. M.; Donina, L.; Dragone, V.; Long, D.-L.; Cronin, L. Controlling an organic synthesis robot with machine learning to search for new reactivity. *Nature* **2018**, *559*, 377-381.

(14) Ahneman, D. T.; Estrada, J. G.; Lin, S.; Dreher, S. D.; Doyle, A. G. Predicting reaction performance in C-N cross-coupling using machine learning. *Science* **2018**, *360*, 186-190.

(15) Mann, D. J. et al. High-throughput kinetic analysis for target-directed covalent ligand discovery. *Angew. Chem. Int. Ed*. **2018**, *57*, 5257-5261.

(16) Campeau, L.-C.; Hazari, N. Cross-coupling and related reactions: Connecting past successes to the development of new reactions for the future. *Organometallics* **2019**, *38*, 3-35.

(17) Hansen, E. C.; Pedro, D. J.; Wotal, A. C.; Gower, N. J.; Nelson, J. D.; Caron, S.; Weix, D. J. New ligands for nickel catalysis from diverse pharmaceutical heterocycle libraries. *Nature Chem.* **2016**, *8*, 1126-1130.

(18) Larson, H.; Schultz, D.; Kalyani, D. Ni-catalyzed C–H arylation of oxazoles and benzoxazoles using pharmaceutically relevant aryl chlorides and bromides. *J. Org. Chem*. **2019**, *84*, 13092-13103.

(19) Nelson, J. J. M.; Cheisson, T.; Rugh, H. J.; Gau, M. R.; Carroll, P. J.; Schelter, E. J. High-throughput screening for discovery of benchtop separations systems for selected rare earth elements. *Commun. Chem.* **2020**, *3*, 1-6.

(20) Herrera, B. T.; Moor, S. R.; McVeigh, M.; Roesner, E. K.; Marini, F.; Anslyn, E. V. Rapid optical determination of enantiomeric excess, diastereomeric excess, and total concentration using dynamic-covalent assemblies. A demonstration using 2-aminocyclohexanol and chemometrics. *J. Am. Chem. Soc.* **2019**, *141*, 11151-11160.

(21) Welch C. J. et al. The enabling technologies consortium (ETC): Fostering precompetitive collaborations on new enabling technologies for pharmaceutical research and development. *Org. Process Res. Dev*. **2017**, *21*, 414-419.

(22) Allen, C. L.; Leitch, D. C.; Anson, M.; Zajac, M. A. The power and accessibility of high-throughput methods for catalysis research. *Nature Catalysis* **2019**, *2*, 2-4

(23) Cook, A.; St. Onge, P.; Newman, S. G. Deoxygenative Suzuki-Miyaura Arylation of Tertiary Alcohols. *Nature Synthesis*, **2023**. *2*, 663-669.

(24) (a) Nair, P. P.; Philip, R. M.; Anilkumar, G. Nickel Catalysts in Sonogashira Coupling Reactions. *Org. Biomol. Chem.* **2021**, *19*, 4228–4242.

(25) Robbins, D. W.; Hartwig, J. F. A simple, multidimensional approach to high-throughput discovery of catalytic reactions. *Science* **2011**, *333*, 1423-1427

(26)(a) Lovering, F.; Bikker, J.; Humblet, C. Escape from Flatland: Increasing Saturation as an Approach to Improving Clinical Success. *J. Med. Chem.* **2009**, *52*, 6752–6756. (b) Lovering, F. Escape from Flatland 2: Complexity and Promiscuity. *Medchemcomm* **2013**, *4*, 515.

(27) (a) Ishiyama, T.; Abe, S.; Miyaura, N.; Suzuki, A. Palladium-Catalyzed Alkyl-Alkyl Cross-Coupling Reaction of 9-Alkyl-9-BBN Derivatives with Iodoalkanes Possessing β-Hydrogens. *Chem. Lett.* **1992**, *21*, 691–694. (b) Devasagayaraj, A.; Stüdemann, T.; Knochel, P. A New Nickel-catalyzed Cross-coupling Reaction between $Sp^3$ Carbon Centers. *Angew. Chem., Int. Ed.* **1996**, *34*, 2723–2725. (c) Netherton, M. R.; Dai, C.; Neuschütz, K.; Fu, G. C. Room-Temperature Alkyl−Alkyl Suzuki Cross-Coupling of Alkyl Bromides That Possess β Hydrogens. *J. Am. Chem. Soc.* **2001**, *123*, 10099–10100. (d) Doucet, H. Suzuki–Miyaura Cross-coupling Reactions of Alkylboronic Acid Derivatives or Alkyltrifluoroborates with Aryl, Alkenyl or Alkyl Halides and Triflates. *European J. Org. Chem.* **2008**, *2008*, 2013–2030. (e) Saito, B.; Fu, G. C. Alkyl−Alkyl Suzuki Cross-Couplings of Unactivated Secondary Alkyl Halides at Room Temperature. *J. Am. Chem. Soc.* **2007**, *129*, 9602–9603. (f) Ahmed, A.; Mushtaq, I.; Chinnam, S. Suzuki–Miyaura Cross-Couplings for Alkyl Boron Reagent: Recent Developments—a Review. *Futur. J. Pharm. Sci.* **2023**, *9*, 1. (g) El-Maiss, J.; Mohy El Dine, T.; Lu, C.-S.; Karamé, I.; Kanj, A.; Polychronopoulou, K.; Shaya, J. Recent Advances in Metal-Catalyzed Alkyl–Boron ($C(sp^3)$–$C(sp^2)$) Suzuki-Miyaura Cross-Couplings. *Catalysts* **2020**, *10*, 296.

(28) Fuse, H.; Mitsunuma, H.; Kanai, M. Catalytic Acceptorless Dehydrogenation of Aliphatic Alcohols. *J. Am. Chem. Soc.* **2020**, *142*, 4493–4499.

(29) Cook, A.; Newman, S. G. Alcohols as Substrates in Transition Metal-Catalyzed Arylation, Alkylation and Related Reactions. *ChemRxiv* **2023**. doi: 10.26434/chemrxiv-2023-7k37p.

(30) (a) Chinchilla, R.; Nájera, C. The Sonogashira Reaction: A Booming Methodology in Synthetic Organic Chemistry. *Chem. Rev.* **2007**, *107*, 874–922. (b) Chinchilla, R.; Nájera, C. Recent Advances in Sonogashira Reactions. *Chem. Soc. Rev.* **2011**, *40*, 5084. (c) Kanwal, I.; Mujahid, A.; Rasool, N.; Rizwan, K.; Malik, A.; Ahmad, G.; Shah, S. A. A.; Rashid, U.; Nasir, N.

M. Palladium and Copper Catalyzed Sonogashira Cross Coupling an Excellent Methodology for C-C Bond Formation over 17 Years: A Review. *Catalysts* **2020**, *10*, 443.

(31) Mohajer, F.; Heravi, M. M.; Zadsirjan, V.; Poormohammad, N. Copper-Free Sonogashira Cross-Coupling Reactions: An Overview. *RSC Adv.* **2021**, *11*, 6885–6925.

(32) Pentsak, E. O.; Eremin, D. B.; Gordeev, E. G.; Ananikov, V. P. Phantom Reactivity in Organic and Catalytic Reactions as a Consequence of Microscale Destruction and Contamination-Trapping Effects of Magnetic Stir Bars. *ACS Catal.* **2019**, *9*, 3070–3081.

(33) Ali, S. Z.; Budaitis, B. G.; Fontaine, D. F. A.; Pace, A. L.; Garwin, J. A.; White, M. C. Allylic C–H Amination Cross-Coupling Furnishes Tertiary Amines by Electrophilic Metal Catalysis. *Science* **2022**, *376*, 276–283.

(34) (a) Schmidt, A. W.; Reddy, K. R.; Knolker, H. -J. *Chem. Rev.* **2012**, *112*, 3193-3328. (b) Li, J.; Grimsdale, A. C. *Chem. Soc. Rev.* **2010**, *39*, 2399-2410. (c) Hirota, T.; Lee, J. W.; St. John, P.; Sawa, M.; Iwaisako, K.; Noguchi, T.; Pongsawakul, P. Y.; Sonntag, T.; Welsh, D. K.; Brenner, D. A.; Doyle III, F. J.; Schultz, P. G.; Kay, S. A. Identification of Small Molecule Activators of Cryptochrome. *Science* **2012**, *337*, 1094-1097. (d) Uoyama, H.; Goushi, K.; Shizu, K.; Nomura, H.; Adachi, C. Highly Efficient Organic Light-Emitting Diodes from Delayed Fluorescence. *Nature* **2012**, *492*, 234-238.

(35) Vitaku, E.; Smith, D. T.; Njardarson, J. T. Analysis of the Structural Diversity, Substitution Patterns and Frequency of Nitrogen Heterocycles among U.S. FDA Approved Pharmaceuticals. *J. Med. Chem.* **2014**, *57*, 10257-10274.

(36) (a) Ullmann, F.; Sponagel, P. Ueber Die Phenylirung von Phenolen. *Ber. Dtsch. Chem. Ges.* **1905**, *38*, 2211–2212. (b) D. Senra, J.; C. S. Aguiar, L.; B. C. Simas, A. Recent Progress in

Transition-Metal-Catalyzed C–N Cross-Couplings: Emerging Approaches towards Sustainability. *Curr. Org. Synth.* **2011**, *8*, 53–78. (c) Sambiagio, C.; Marsden, S. P.; Blacker, A. J.; McGowan, P. C. Copper Catalyzed Ullman Type chemistry: From Mechanistic Aspects to Modern Development. *Chem. Soc Rev*. **2014**, *43*, 3525-3550

(37) (a) West, M. J.; Fyfe, J. W. B.; Vantourout, J. C.; Watson, A. J. B. Mechanistic Development and Recent Applications of the Chan–Lam Amination. *Chem. Rev.* **2019**, *119*, 12491–12523. (b) Chen, J.-Q.; Li, J.-H.; Dong, Z.-B. A Review on the Latest Progress of Chan-Lam Coupling Reaction. *Adv. Synth. Catal.* **2020**, *362*, 3311–3331.

(38) (a) Ruiz-Castillo, P.; Buchwald, S. L. Applications of Palladium-Catalyzed C–N Cross-Coupling Reactions. *Chem. Rev.* **2016**, *116*, 12564-12649. (b) Beletskaya, I. P.; Cheprakov, A. V. The Complimentary Competitors: Palladium and Copper in C–N Cross-Coupling Reactions. *Organometallics* **2012**, *31*, 7753-7808. (c) Banwal, J.; Van der Eycken, E. C–N Bond Forming Cross-Coupling Reactions; an Overview. *Chem. Soc. Rev.* **2013**, *42*, 9283-9303.

(39) (a) Fletcher, S. The Mitsunobu Reaction in the 21st Century. *Org. Chem. Front*. **2015**, *2*, 739-752. (b) Munawar, S.; Zahoor, A. F.; Ali, S.; Javed, S.; Irfan, M.; Irfan, A.; Kotwica-Mojzych, K.; Mojzych, M. Mitsunobu Reaction: A Powerful Tool for the Synthesis of Natural Products: A Review. *Molecules* **2022**, *27*, 6953.

(40) (a) Muller, T. E.; Hulzsch, K. C.; Yus, M. Foubelo, F.; Tada, M. Hydroamination: Direct Addition of Amines to Alkenes and alkynes. *Chem. Rev*. **2008**, *108*, 3795-3892. (b) Huang, L.; Arndt, M.; Goossen, K.; Heydt, H.; Goossen, L. J. Late Transition Metal-Catalyzed hydroamination and Hydroamidation. *Chem. Rev*. **2015**, *115*, 2596-2697.

(41) (a) Abdel-Magid, A. F.; Mehrman, S. J. A Review on the Use of Sodium Triacetoxyborohydride in the Reductive Amination of Ketones and Aldehydes. *Org. Process. Res. Dev*. **2006**, *10*, 971-1031. (b) Tripathi, R. P.; Verma, S. S.; Pandey, J.; Tiwari, V. K. Recent Development on Catalytic Reductive Amination and Applications. *Curr. Org. Chem*. **2008**, *12*, 1093-1115.

(42) (a) Guillena, G.; Ramon, D. J.; Yus, M. Hydrogen Autotransfer in the *N*-Alkylation of Amines and Related Compounds using Alcohols and Amines as Electrophiles. *Chem. Rev*. **2010**, *110*, 1611-1641. (b) Leonard, J.; Blacker, A. J.; Marsden, S. P.; Jones, M. F.; Mulholland, K. R.; Newton, R. A Survey of the Borrowing Hydrogen Approach to the Synthesis of some Pharmaceutically Relevant Intermediates. *Org. Process. Res. Dev.* **2015**, *19*, 1400-1410. (c) Bähn, S.; Imm, S.; Neubert, L.; Zhang, M.; Neumann, H.; Beller, M. The Catalytic Amination of Alcohols. *ChemCatChem* **2011**, *3*, 1853–1864.

(43) (a) Bissember, A. C.; Lundgren, R. J.; Creutz, S. E.; Peters, J. C.; Fu, G. C. Transition-Metal-Catalyzed Alkylations of Amines with Alkyl Halides: Photoinduced, Copper-Catalyzed Couplings of Carbazoles. *Angew. Chem. Int. Ed.* **2013**, *52*, 5129-5133. (b) Kainz, Q. M.; Matier, C. D.; Bartoszewicz, A.; Zultanski, S. L.; Peters, J. C.; Fu, G. C. Asymmetric Copper-Catalyzed C–N Cross-Couplings Induced by Visible Light. *Science* **2016**, *351*, 681-684. (c) Dow, N. W.; Cabré, A.; MacMillan, D. W. C. A General *N*-Alkylation Platform via Copper Metallaphotoredox and Silyl Radical Activation of Alkyl Halides. Chem **2021**, 7, 1827–1842.

(44) (a) Peacock, D. M.; Roos, C. B.; Hartwig, J. F. Palladium-Catalyzed Cross Coupling of Secondary and Tertiary Alkyl Bromides with a Nitrogen Nucleophile. *ACS. Cent. Sci*. **2016**, *2*, 647-652. (b) Trowbridge, A.; Walton, S. M.; Gaunt, M. J. New Strategies for the Transition-Metal Catalyzed Synthesis of Aliphatic Amines. *Chem. Rev.* **2020,** *120*, 2613-2692.

(45) (a) Dorel, R.; Grugel, C. P.; Haydl, A. M. The Buchwald–Hartwig Amination after 25 Years. *Angew. Chem. Int. Ed.* **2019**, *58*, 17118–17129. (b) Ohtsuka, Y.; Yamamoto, T.; Miyazaki, T.; Yamakawa, T. Palladium-catalyzed Selective Amination of Aryl(Haloaryl)Amines with 9*H*-carbazole Derivatives. *Adv. Synth. Catal.* **2018**, *360*, 1007–1018.

(46) (a) Allen, J. R.; Bahamonde, A.; Furukawa, Y.; Sigman, M. S. Enantioselective *N*-Alkylation of Indoles via an Intermolecular Aza-Wacker-Type Reaction. *J. Am. Chem. Soc.* **2019**, *141*, 8670–8674. (b) Bordell pKa table, accessed February 6, 2024. https://organicchemistrydata.org/hansreich/resources/pka/ (c) Baran heterocycles notes, accessed February 6, 2024. https://baranlab.org//heterocycles/Essentials1-2009.pdf

(47) (a) Norman, N. J.; Bao, S. T.; Curts, L.; Hui, T.; Zheng, S.-L.; Shou, T.; Zeghibe, A.; Burdick, I.; Fuehrer, H.; Huang, A. Highly Selective *N*-Alkylation of Pyrazoles: Crystal Structure Evidence for Attractive Interactions. *J. Org. Chem.* **2022**, *87*, 10018–10025. (b) Wang, M.; Simon, J. C.; Xu, M.; Corio, S. A.; Hirschi, J. S.; Dong, V. M. Copper-Catalyzed Hydroamination: Enantioselective Addition of Pyrazoles to Cyclopropenes. *J. Am. Chem. Soc.* **2023**, *145*, 14573–14580.

(48) (a) Burés, J. A Simple Graphical Method to Determine the Order in Catalyst. *Angew. Chem. Int. Ed.* **2016**, *55*, 2028-2031. (b) Nelson, C. D. -T.; Burés, J. Visual Kinetic Analysis. *Chem. Sci.* **2019**, *10*, 348-353.

(49) Cabildo, P.; Claramunt, R. M.; Elguero, J. Synthesis and Reactivity of New L-(1-adamantyl)Pyrazoles. *J. Heterocycl. Chem.* **1984**, *21*, 249–251.

(50) Austin, J. F.; MacMillan, D. W. C. Enantioselective Organocatalytic Indole Alkylations. Design of a New and Highly Effective Chiral Amine for Iminium Catalysis. *J. Am. Chem. Soc.* **2002**, *124*, 1172–1173.

# **Chapter Six:** Conclusions

*"Gatsby believed in the green light, the orgastic future that year by year recedes before us. It eluded us then, but that's no matter – tomorrow we will run faster, stretch out our arms farther… and one fine morning –*

*So we beat on, boats against the current, borne back ceaselessly into the past."*

- *The Great Gatsby, F. Scott. Fitzgerald, 1896-1940.*



*Chapter six references begin on page 435*

## 6.0. Contents of this conclusion

Chapter six seeks to provide a critical overview of the material discussed in chapters two through five, touching upon both the strengths and the weaknesses of the research described therein. A holistic analysis of discoveries and developments will be provided, and potential future projects that stem from the work described within this dissertation will be proposed. Finally, this chapter will conclude with a brief commentary on the author's opinions regarding the future of the topic that ties this dissertation together, nickel-catalyzed carbon-oxygen bond activation.

As extended conclusions and commentary were provided at the end of chapters two through five of this dissertation, this chapter will be limited in size so as to not duplicate information that has already been discussed. In particular, readers are referred to the conclusions present at the end of each chapter for discussion regarding potential applications and future avenues for discovery and development.

## 6.1. Summary of the work presented within this dissertation

Each of the projects discussed within chapters two through five of this dissertation concern the development of nickel-catalyzed methods to activate carbon-oxygen bonds. Chapter two described the development of a unified method for the deoxygenative reduction of a range of oxo-functional groups, including alcohols (Figure 6.1a). Chapter three turned attention towards the functionalization of chemical compounds; described within this chapter was the discovery and development of the *first* method for the deoxygenative Suzuki-Miyaura arylation of non-π-activated tertiary alcohols (Figure 6.1b). Chapter four expanded upon this methodology, exploiting the *β*-silicon effect to allow primary and secondary alcohols to be brought into scope while also



Chapter six references begin on page 435

providing insight into the role of bis(NHC) ligands in achieving reactivity (Figure 6.1c). Collectively, chapters three and four presented mechanistic evidence in support of a scarcely explored $S_N1$-type approach towards oxidative addition. Finally, chapter five explored the catalytic system developed in chapters three and four by using high-throughput chemistry to explore nucleophilic coupling partners beyond arylboronate esters (Figure 6.1d).

**Figure 6.1.** Summarizing the contents of this dissertation

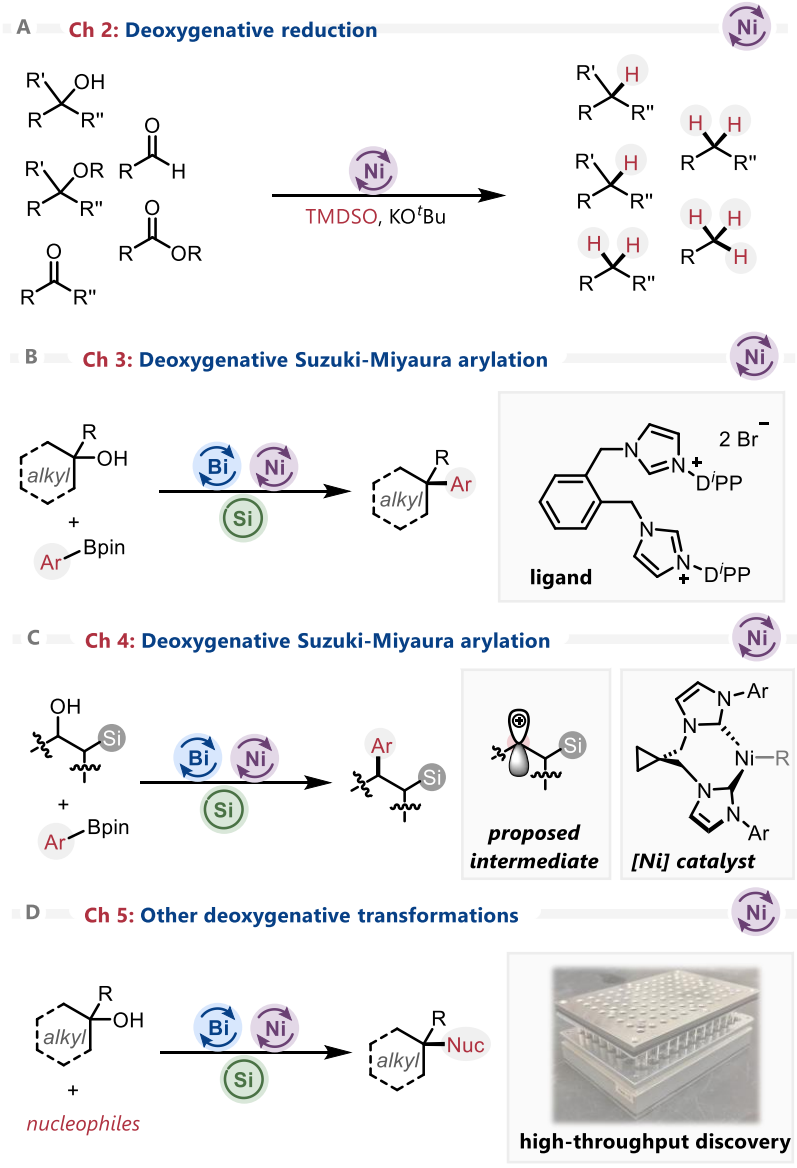




Chapter six references begin on page 435

Various themes unite the contents of this dissertation. Nickel – having been demonstrated by many to be a formidable warrior in the battlefield of carbon-oxygen bond activation[1] – is employed throughout this dissertation as the optimal catalyst. Moreover, *N*-heterocyclic carbene ligands were consistently found to be optimal in each of the studied reactions. Contemporary research points towards NHCs being privileged in numerous nickel-catalyzed transformations, such as alkene functionalization, with authors frequently citing their strong σ-donating capabilities and molecular bulk as reasons for their privileged nature.[2] Often, the difficult mechanistic step in transition metal-catalyzed carbon-oxygen activation is oxidative addition.[3] It is likely that the strong electron-donating properties of NHCs aid in the facilitation of these traditionally-difficult steps.[1b,2a]

Whether it be used as a hydride source or an in situ activation reagent, each chapter within this dissertation is also bound by the unified necessity of a silicon-containing reagent, with chapter two using TMDSO and chapters three through five using $Me_2SiCl_2$. Silanes and siloxanes are inexpensive, accessible alternatives to other hydride sources (e.g. $NaBH_4$, $LiAlH_4$)[4] or activating groups (e.g. oxalates,[5] NHCs,[6] thiocarbamates)[7] and they are particularly useful in reactions that proceed through carbon-oxygen bond activation.

Lastly, curiosity was peaked towards the mechanisms of the various transformations developed within this dissertation. In each chapter, mechanistic evidence is provided in the form of carefully chosen substrate probes or a mixture of modern and traditional kinetic experiments.

## 6.2. Critical analysis of the work presented within this dissertation

### 6.2.1. Strengths



Chapter six references begin on page 435

The contents of this dissertation bear various strengths. In all works, nickel was used as a transition metal catalyst. While the "cost of catalysis" is often driven by the enhanced cost of ligands relative to precatalysts,[8] the use of nickel is advantageous relative to the use of more expensive transition metals such as palladium and platinum. Further, each of the optimal ligands within this dissertation were synthesized in house via a short, relatively facile protocol (Scheme 6.1).[9,10] While it would have been advantageous to be able to use cheaper, commercially available ligands, the ability to synthesize these ligands reproducibly from accessible starting materials (**6.1-6.4**) will prove to be a benefit to anyone who hopes to continue researching these transformations, both inside the Newman lab and outside.

**Scheme 6.1.** Procedures used to synthesize the optimal ligands in each chapter.

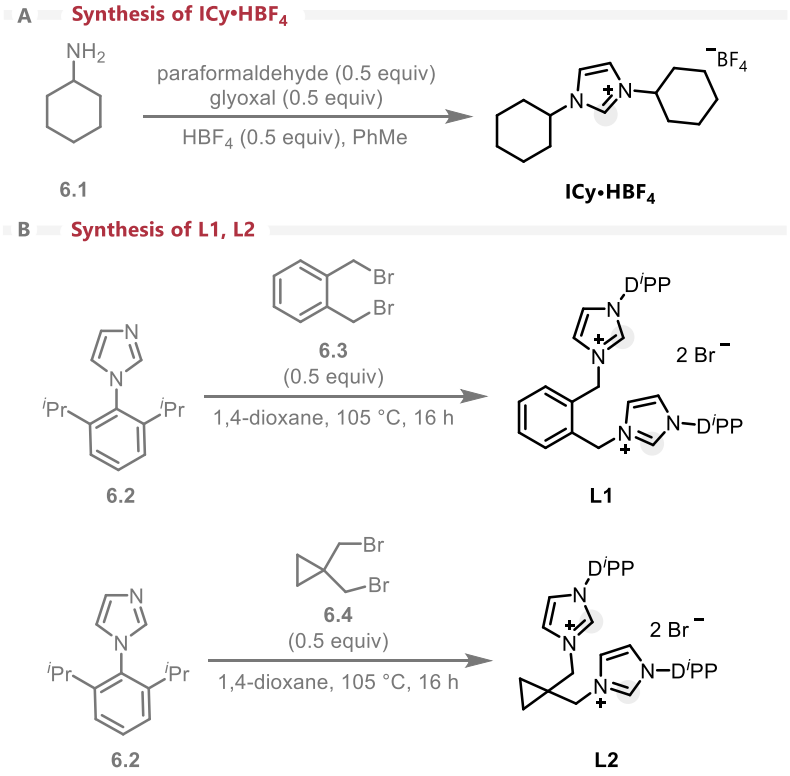




Chapter six references begin on page 435

All the transformations documented within this dissertation present practical alternatives to conventional methods to conduct the same transformation. For instance, the deoxygenative reductions developed in chapter two lack the requirement for hazardous reagents and difficult workups that are typically associated with deoxygenation chemistry.[11] In some cases, the reactions developed in chapter two are exceedingly difficult to carry out under alternative conditions. For instance, carbon-oxygen bonds in non-π-activated positions, as well as those in tertiary positions, are generally seen as difficult to activate in transition metal catalysis.[12,13] The methods developed in chapter two obviate these limitations in deoxygenative reduction reactions (e.g. reducing **6.5** to **6.6**), and the methods developed in chapters three through five do so in carbon-carbon or carbon-heteroatom bond forming transformations (e.g. the reaction of **6.7** to form **6.8**) (Scheme 6.2a). Notably, there are currently no other methods that react organoboron species with non-π-activated alcohols to achieve deoxygenative Suzuki-Miyaura coupling, and few methods that utilize π-activated alcohols.[12]

The findings of this dissertation are strengthened by the significant number of mechanistic investigations that were carried out. The mechanisms of nickel-catalyzed transformations are frequently cited as being difficult to study, largely in part due to nickels propensity to exist in a range of different oxidation states and its ability to participate in off-cycle reactions.[14] Within chapter two, extensive mechanistic information was gained through the use of carefully crafted substrate probes, often arising from questions such as "if the reduction of this substrate proceeds through a given reactive intermediate, then given product would be observed". For instance, various substrates were synthesized that would either isomerize, fragment, or cyclize if a radical intermediate was present; indeed, the observation of reactivity such as the 5-hexenyl cyclization of compound **6.9** to form **6.10** as the major product relative to **6.11** lent support to the existence of



Chapter six references begin on page 435

radical intermediates (Scheme 6.2b),[15] and the observation of 1,2-alkyl shifts, as in the reaction of **6.12** to yield **6.13**, in chapter three suggest carbocation intermediacy (Scheme 6.2b).[16] This dissertation is also littered with kinetic experiments. Modern kinetic techniques, including variable time normalization analysis, were employed in every chapter as a method to approximate the order of reactions in each component. Traditional kinetic techniques, including Hammett analyses, Eyring analysis and kinetic isotope effect studies were used to home in on specific aspects of each transformation, becoming especially valuable when looking for information to support or refute the existence of a carbocation-like intermediate in chapters three and four.

**Scheme 6.2.** Illustrating select strengths of this dissertation

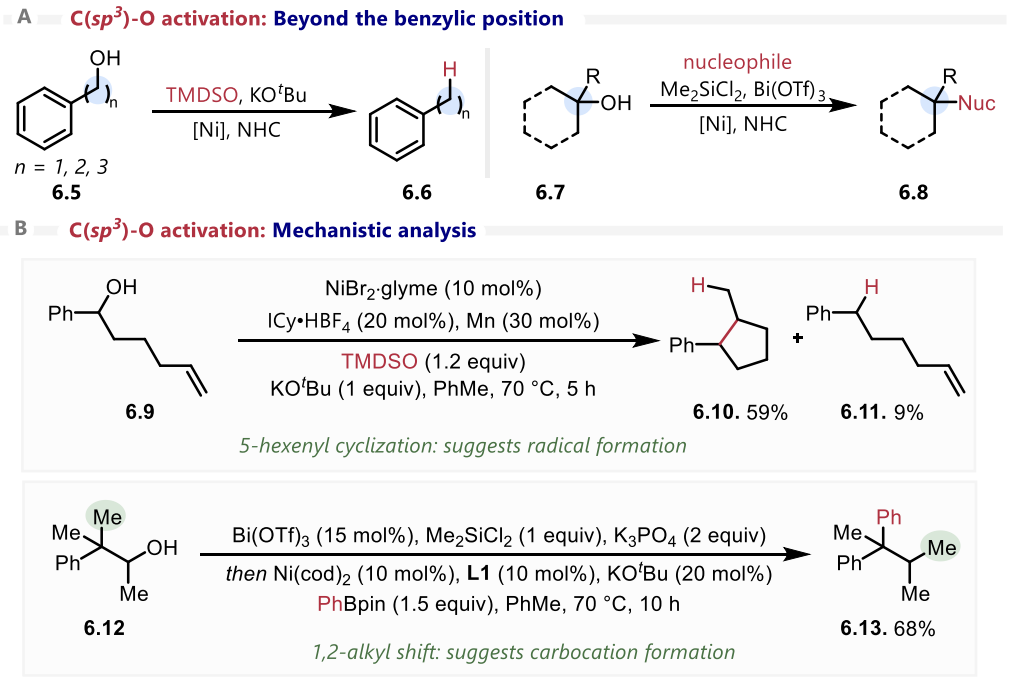




Chapter six references begin on page 435

### 6.2.2. Weaknesses

For all its strengths, this dissertation is not without weakness. While the catalysts and their associated ligands are indeed accessible, they must be employed at high loadings (5-10 mol%) relative to other transition metal catalyzed reactions (for instance, palladium-catalyzed reactions can sometimes employ ≤1 mol% of the metal).[17] This problem is exacerbated by the requirement for ligands that are either prohibitively expensive, in the case of ICy·$HBF_4$ (which was synthesized in house but can also be purchased from chemical vendors), or require in house synthesis, as in the case of **L1** and **L2**.

Each of the transformations developed within this dissertation also bear a range of synthetic limitations. As with most synthetic methodologies, certain functional groups could not be tolerated. While exceptions existed, it was frequently observed that reaction partners bearing unprotected N–H bonds (e.g. amines, amides), as well as those bearing carbon-halogen bonds or carbon-sulfur bonds did not yield successful reactivity. More pressing, however, is the "scaffold" limitations of each developed transformation. For instance, the deoxygenative reduction transformation discussed in chapter two failed when placing the target C–O bond greater than three carbons away from an aryl ring, as in the reaction of **6.14** to form **6.15**, as well as in the attempted reductions of compounds **6.16-6.18** (Scheme 6.3a). A related observation was made in chapter three, wherein only cyclic tertiary alcohols could be arylated, as in the reaction of **6.19** to form **6.20** (Scheme 6.3b). Subjecting other alcohols, such as **6.21-6.23**, to the general reaction conditions failed to afford arylated product. While this restriction could be exploited through the demonstration of chemoselective arylation, it greatly limits the general applicability of the deoxygenative Suzuki-Miyaura coupling. This restriction was alleviated by exploiting the $\beta$-silicon



Chapter six references begin on page 435

effect in chapter four, yet still reactivity was restricted to compounds that could stabilize a carbocation intermediate.

**Scheme 6.3.** Illustrating selected weaknesses within this dissertation

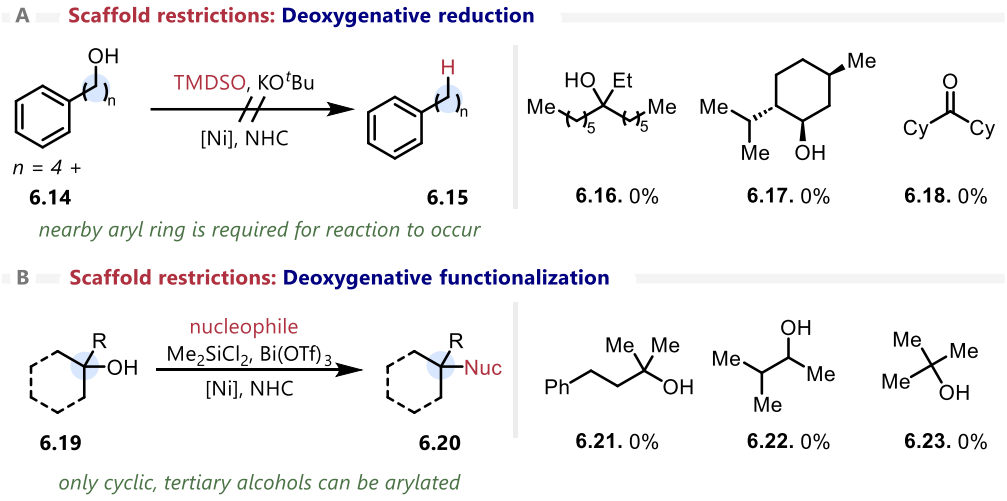


A significant weakness present throughout this dissertation is a lack of *in silico* data. Broadly, the weight of this thesis is carried by the development of two distinct catalytic systems, one system which permits deoxygenative reduction and one which permits deoxygenative functionalization. While a significant amount of data is gathered to support and/or refute the existence of various reactive intermediates (e.g. a radical intermediate in chapter two and a carbocation intermediate in chapters three/four), little data is gathered regarding the species which exist on the catalytic cycle. Computational analyses could help to better understand why the developed transformations work. It could reveal key factors that lead towards the observed scaffold limitations of each of the transformations and could shed light into the roles and existence of catalytic intermediates.



Chapter six references begin on page 435

### **6.2.3.** Overall contributions of this dissertation to the field of study: Summary

To the author of this dissertation, various aspects of this work stand out amongst the details as being significant advances to the field of synthetic chemistry. Chapter two began with the development of a selective, controllable single-step reduction of carboxylates into their corresponding tolyl-derivatives, a notable advance as the single-step reduction of carboxylates to the methyl oxidation state had previously been identified in a list of "long-standing problems" in organic chemistry in a popular textbook.[18] One notable application of this chemistry is in the conversion of esters into $–CD_3$ groups in a single catalytic step (Scheme 6.4). Esters are a prevalent functional group in pharmaceuticals, and the ability to convert them into methyl groups opens an avenue for exploiting the magic methyl effect, an effect which describes a range of beneficial pharmacological properties that are imparted when methylating a bioactive agent.[22] In one disclosure, boosts in potency up to 507 fold have been reported as a result of methylation.[23] Moreover, recent disclosures suggest that installing deuterium onto a bioactive scaffold can have advantageous properties.[24] As such, the ability to install $–CD_3$ groups – deuterated analogs of methyl groups – allows for the compounded exploitation of the magic methyl effect alongside the deuteration effect, potentially lending value to methods that can install $–CD_3$ groups in a single catalytic step. Select trideuteromethylated pharmaceuticals exist (**6.24-6.26**), and it is likely that more will be brought to market by the development of methods to install $–CD_3$ groups.



Chapter six references begin on page 435

**Scheme 6.4.** Installing –$CD_3$ groups

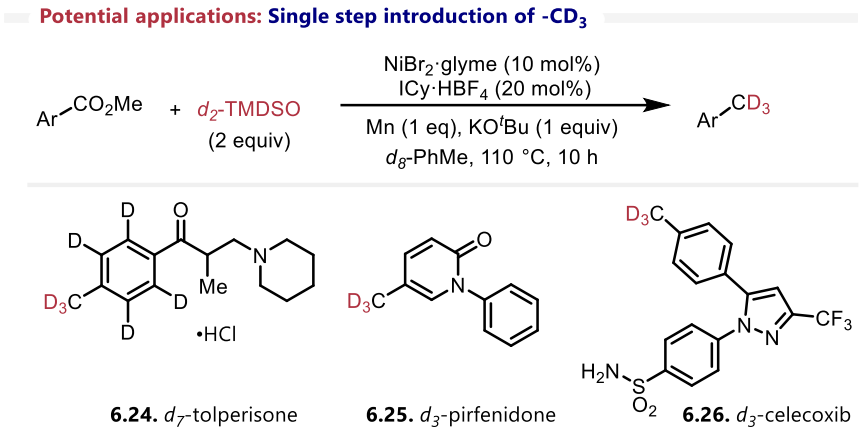


**6.24.** $d_7$-tolperisone **6.25.** $d_3$-pirfenidone **6.26.** $d_3$-celecoxib

The expansion of this transformation towards ketones, aldehydes, epoxides, ethers, and alcohols is notable as well, as this method presently exists as one of few methods that can deoxygenate such a broad range of functional groups under relatively practical, benign reaction conditions.

The subsequent development of a Suzuki-Miyaura arylation that permitted non-π-activated alcohols to act as electrophilic coupling partners is a notable advance in Suzuki-Miyaura chemistry as it expands the breadth of compounds amenable to this valuable transformation. A recent study suggests that aliphatic alcohols represent the most abundant and versatile alkyl source.[6] In the "escape from flatland",[25] chemists are likely to seek alkyl sources other than the more conventionally used alkyl halides, which often are synthesized through from alcohols as alkyl halides are not naturally occurring.[26] Lastly, the gathered evidence for an $S_N1$-type transition metal-catalyzed transformation is of note as it may contribute to how chemists consider oxidative additions and reaction mechanisms in cross-coupling chemistry.[19] Potentially, this work will exist



Chapter six references begin on page 435

as valuable precedent for future research projects that aim to exploit carbocation-like intermediates in cross-coupling reactions.

## 6.3. The future of C($sp^3$)–O bond activation, nickel catalysis: Enabling technologies in a modern era

The early days of cross-coupling saw the development of a myriad of methods that, generally, employed palladium catalysts alongside aryl halides.[27] As time went on, chemists – as they do – pushed the boundaries of what could be done in cross-coupling. Methods have been established for the incorporation of a wide range of nucleophilic coupling partners. from olefins in Mizoroki-Heck coupling, through various organometallic nucleophiles (organozincs, organostannanes, Grignard reagents, and so on), to organoboron species in Suzuki-Miyaura coupling. Similarly, the scope of amenable electrophilic coupling partners has been explored, from $sp^2$-hybridized species to $sp^3$-hybridized and from organo(pseudo)halides to more abundant, native functional groups such as esters.

Nickel catalysts have consistently proven formidable in the activation of carbon-oxygen bonds.[1] In particular, methods for the activation of C($sp^3$)–O bonds have utilized nickel catalysts. The author of this dissertation believes that the future of C($sp^3$)–O activation will continue to be tied to nickel catalysis. Significant advances may lie in the development of accessible ligands developed for the purpose of C($sp^3$)–O activation, as well as in the development of methods that permit stereochemical control over the functionalization of these bonds. Many of the discoveries made within this dissertation relied on the use of high-throughput experimentation. It is likely that this technology, along with other emerging technologies in synthetic chemistry (e.g. computational



Chapter six references begin on page 435

chemistry, machine learning, automation) will contribute towards advances in the future. Further, recent research has suggested that nickel catalysts are particularly privileged for merging with photo- and electrocatalysis.[28] The author of this dissertation believes that merging nickel catalysis with techniques including photocatalysis, electrocatalysis and even enzymatic catalysis will illuminate pathways towards C($sp^3$)–O activation that remain shadowed in the present day. The future of C($sp^3$)–O activation is likely to be led by a push towards simpler, native functional groups, such as alcohols. Finally, as methods continue to be developed for the activation of C($sp^3$)–O bonds, it is likely that an increased emphasis will be placed on applications towards biomass (i.e. lignin, tannin, cellulose) valorization.

## 6.4. Epilogue: Diet for a new Chem-merica

With the previous six chapters having been finally put on paper, its appropriate at this point to bring this dissertation to a close. We return to the question proposed at the beginning of this document – *what do we have, and what can we do with it?*

As a scientific answer to this question, we have explored within this dissertation the development of multiple chemical methods to use naturally abundant functional groups, including esters, ketones, and alcohols, as feedstock chemicals towards the synthesis of more (or less) complex molecules. Using the deoxygenative Suzuki-Miyaura arylation developed in chapter three as an example, it was observed that aliphatic alcohols – among the most abundant and versatile alkyl sources – could be functionalized to contain chemical moieties including variously-substituted arenes and heterocycles, thereby permitting the rapid build up of molecular complexity



Chapter six references begin on page 435

from accessible sources. Nickel is an earth-abundant catalyst; herein, we used this abundant catalyst to furnish molecules of rich complexities.

*What do we have and what can we do with it?*

Or, phrased differently – *what can we do with the things we have been given*? From wagons to automobiles, shacks to skyscrapers and fire to five-star Michelin meals this question has shaped modernity. As a chemist, I like to think that these developments have been spearheaded through a series of advances in chemistry. As we push towards the Sustainocene – a world where humanity seeks to live in harmony with the natural world – it is pivotal that this question remains at the forefront of thought. To it, however, the author of this dissertation suggests a change. Rather than simply asking what we can do with that which we are given, we should instead ask: ***what is the best thing that we can do with what we are given?*** Thomas Edison writes that "our greatest weakness lies in giving up. The most certain way to succeed is always to try just one more time." In chemistry, in science, and in life, we should continuously reflect upon the question: ***how can we make the best of what we are given using the skills that we learn.***

*"Th-th-that's all, folks."*

- *Porky Pig*



Chapter six references begin on page 435

## 6.5. References

(1) (a) Tobisu, M.; Chatani, N. Cross-Couplings Using Aryl Ethers via C–O Bond Activation Enabled by Nickel Catalysts. *Acc. Chem. Res.* **2015**, *48*, 1717–1726. (b) Rosen, B. M.; Quasdorf, K. W.; Wilson, D. A.; Zhang, N.; Resmerita, A.-M.; Garg, N. K.; Percec, V. Nickel-Catalyzed Cross-Couplings Involving Carbon−Oxygen Bonds. *Chem. Rev.* **2011**, *111*, 1346–1416.

(2) (a) Lee, B. C.; Liu, C.-F.; Lin, L. Q. H.; Yap, K. Z.; Song, N.; Ko, C. H. M.; Chan, P. H.; Koh, M. J. N-Heterocyclic Carbenes as Privileged Ligands for Nickel-Catalysed Alkene Functionalisation. *Chem. Soc. Rev.* **2023**, *52*, 2946–2991. (b) Matsubara, K. Well-defined NHC−Ni Complexes as Catalysts: Preparation, Structures and Mechanistic Studies in Cross-coupling Reactions. *Chem. Rec.* **2021**, *21*, 3925–3942.

(3) Labinger, J. A. Tutorial on Oxidative Addition. *Organometallics* **2015**, *34*, 4784–4795.

(4) (a) Krishnamurthy, S.; Brown, H. C. Forty Years of Hydride Reductions. *Tetrahedron*. **1979**, *35*, 567–607. (b) Conover, L.H.; Tarbell, D.S. Hydrogenolysis of Certain Substituted Aromatic Acids and Carbonyl Compounds by Lithium Aluminum Hydride. *J. Am. Chem. Soc.* **1950**, *72*, 3586-3588.

(5) Lackner, G. L.; Quasdorf, K. W.; Overman, L. E. Direct construction of quaternary carbons from tertiary alcohols via photoredox-catalyzed fragmentation of *tert*-alkyl *N*-phthalimidoyl oxalates. *J. Am. Chem. Soc.* **2013**, *135*, 15342−15345.

(6) Dong, Z.; MacMillan, D. W. C. Metallaphotoredox-enabled deoxygenative arylation of alcohols. *Nature* **2021**, *598*, 451-456.



Chapter six references begin on page 435

(7) Mills, R. J.; Monteith, J. J.; dos Passos Gomes, G.; Aspuru-Guzik, A.; Rousseaux, S. A. L. The cyclopropane ring as a reporter of radical leaving-group reactivity for Ni-catalyzed C($sp^3$)−O arylation. *J. Am. Chem. Soc*. **2020**, *142*, 13246-13254.

(8) Bullock, M. Catalysis without Precious Metals. Wiley September 8, 2010, p. 51.

(9) Hans, M.; Lorkowski, J.; Demonceau, A.; Delaude, L. Efficient Synthetic Protocols for the Preparation of Common *N*-Heterocyclic Carbene Precursors. *Beilstein J. Org. Chem.* **2015**, *11*, 2318–2325.

(10) Tulloch, A. A. D.; Danopoulos, A. A.; Winston, S.; Kleinhenz, S.; Eastham, G. N-Functionalized Heterocyclic Carbene Complexes of Silver. *J. Chem. Soc., Dalton Trans*. **2000**, *24*, 4499–4506.

(11) Surya Prakash, G. K.; Do, C.; Mathew, T.; Olah, G. A. Reduction of Carbonyl to Methylene: Organosilane-Ga(OTf)$_3$ as an Efficient Reductant System. *Catal. Letters* **2011**, 141, 507–511.

(12) Cook, A.; Newman, S. G. Alcohols as Substrates in Transition Metal-Catalyzed Arylation, Alkylation and Related Reactions. *ChemRxiv* **2023**. doi: 10.26434/chemrxiv-2023-7k37p.

(13) Lin, Q.; Tong, W.; Shu, X.-Z.; Chen, Y. Ti-Catalyzed Dehydroxylation of Tertiary Alcohols. *Org. Lett.* **2022**, *24*, 8459–8464.

(14) (a) Diccianni, J. B.; Diao, T. Mechanisms of Nickel-Catalyzed Cross-Coupling Reactions. *Trends Chem.* **2019**, *1*, 830–844. (b) Diccianni, J.; Lin, Q.; Diao, T. Mechanisms of Nickel-Catalyzed Coupling Reactions and Applications in Alkene Functionalization. *Acc. Chem. Res.* **2020**, *53* (4), 906–919.



Chapter six references begin on page 435

(15) Walling, C.; Cioffari, A. Cyclization of 5-hexenyl radicals. *J. Am. Chem. Soc*. **1972**, *94*, 6059-6064.

(16) Smith, M.B.; March, J. Carbocations. In *March's Advanced Organic Chemistry*; John Wiley and Sons, Inc.: Hoboken, NJ, USA, 2006; pp. 235-249.

(17) (a) Hazari, N.; Melvin, P. R.; Beromi, M. M. Well-Defined Nickel and Palladium Precatalysts for Cross-Coupling. *Nat. Rev. Chem.* **2017**, *1,* 3. (b) Chernyshev, V. M.; Ananikov, V. P. Nickel and Palladium Catalysis: Stronger Demand than Ever. *ACS Catal.* **2022**, *12*, 1180–1200.

(18) Hudlicky, T.; Reed, J. W. *The Way of Synthesis*; Wiley-VCH: Weinheim, Germany, 2007.

(19) Labinger, J. A. Tutorial on Oxidative Addition. *Organometallics* **2015**, *34*, 4784–4795.

(20) Ertl, P.; Altmann, E.; McKenna, J. M. The Most Common Functional Groups in Bioactive Molecules and How Their Popularity Has Evolved over Time. *J. Med. Chem.* **2020**, *63*, 8408–8418.

(21) Favi, G. Modern Strategies for Heterocycle Synthesis. *Molecules* **2020**, *25*, 2476.

(22) (a) Pinheiro, P. de S. M.; Franco, L. S.; Fraga, C. A. M. The Magic Methyl and Its Tricks in Drug Discovery and Development. *Pharmaceuticals (Basel)* **2023**, *16*, 1157. (b) Schönherr, H.; Cernak, T. Profound Methyl Effects in Drug Discovery and a Call for New C–H Methylation Reactions. *Angew. Chem. Int. Ed.* **2013**, *52*, 12256–12267.

(23) Steverlynck, J.; Sitdikov, R.; Rueping, M. The Deuterated "Magic Methyl" Group: A Guide to Site-selective Trideuteromethyl Incorporation and Labeling by Using $CD_3$ Reagents. *Chemistry* **2021**, *27*, 11751–11772.



Chapter six references begin on page 435

(24) Di Martino, R. M. C.; Maxwell, B. D.; Pirali, T. Deuterium in Drug Discovery: Progress, Opportunities and Challenges. *Nat. Rev. Drug Discov.* **2023**, *22*, 562–584.

(25)(a) Lovering, F.; Bikker, J.; Humblet, C. Escape from Flatland: Increasing Saturation as an Approach to Improving Clinical Success. *J. Med. Chem.* **2009**, *52*, 6752–6756. (b) Lovering, F. Escape from Flatland 2: Complexity and Promiscuity. *Medchemcomm* **2013**, *4*, 515.

(26) (a) Roughley, S. D.; Jordan, A. M. The Medicinal Chemist's Toolbox: An Analysis of Reactions Used in the Pursuit of Drug Candidates. *J. Med. Chem.* **2011**, *54*, 3451–3479.

(27) Johansson Seechurn, C. C. C.; Kitching, M. O.; Colacot, T. J.; Snieckus, V. Palladium-catalyzed Cross-coupling: A Historical Contextual Perspective to the 2010 Nobel Prize. *Angew. Chem. Int. Ed.* **2012**, *51*, 5062–5085.

(28) (a) Zhu, C.; Yue, H.; Chu, L.; Rueping, M. Recent Advances in Photoredox and Nickel Dual-Catalyzed Cascade Reactions: Pushing the Boundaries of Complexity. *Chem. Sci.* **2020**, *11*, 4051–4064. (b) Villo, P.; Shatskiy, A.; Kärkäs, M. D.; Lundberg, H. Electrosynthetic C−O Bond Activation in Alcohols and Alcohol Derivatives. *Angew. Chem. Int. Ed.* **2023**, *62*, e202211952.



Chapter six references begin on page 435

# Appendix

Chapters one and six do not have any associated characterization data as they are the introduction/conclusion of this dissertation. Spectra and other characterization data associated with chapter two are available free of charge at https://pubs.acs.org/doi/10.1021/jacs.0c02405 for experiments discussed in Section 2.3 and https://pubs.acs.org/doi/abs/10.1021/acscatal.1c03980 for experiments discussed in Section 2.4. Spectra and other characterization data associated with chapter three are available and free of charge at https://doi.org/10.1038/s44160-023-00275-w. Spectra and other characterization data associated with chapters four and five are present within this appendix.

4-Phenyl-1-(trimethylsilyl)butan-2-ol **4.87** ($CDCl_3$, 400 MHz for $^1H$ NMR, 100 MHz for $^{13}C$ NMR)

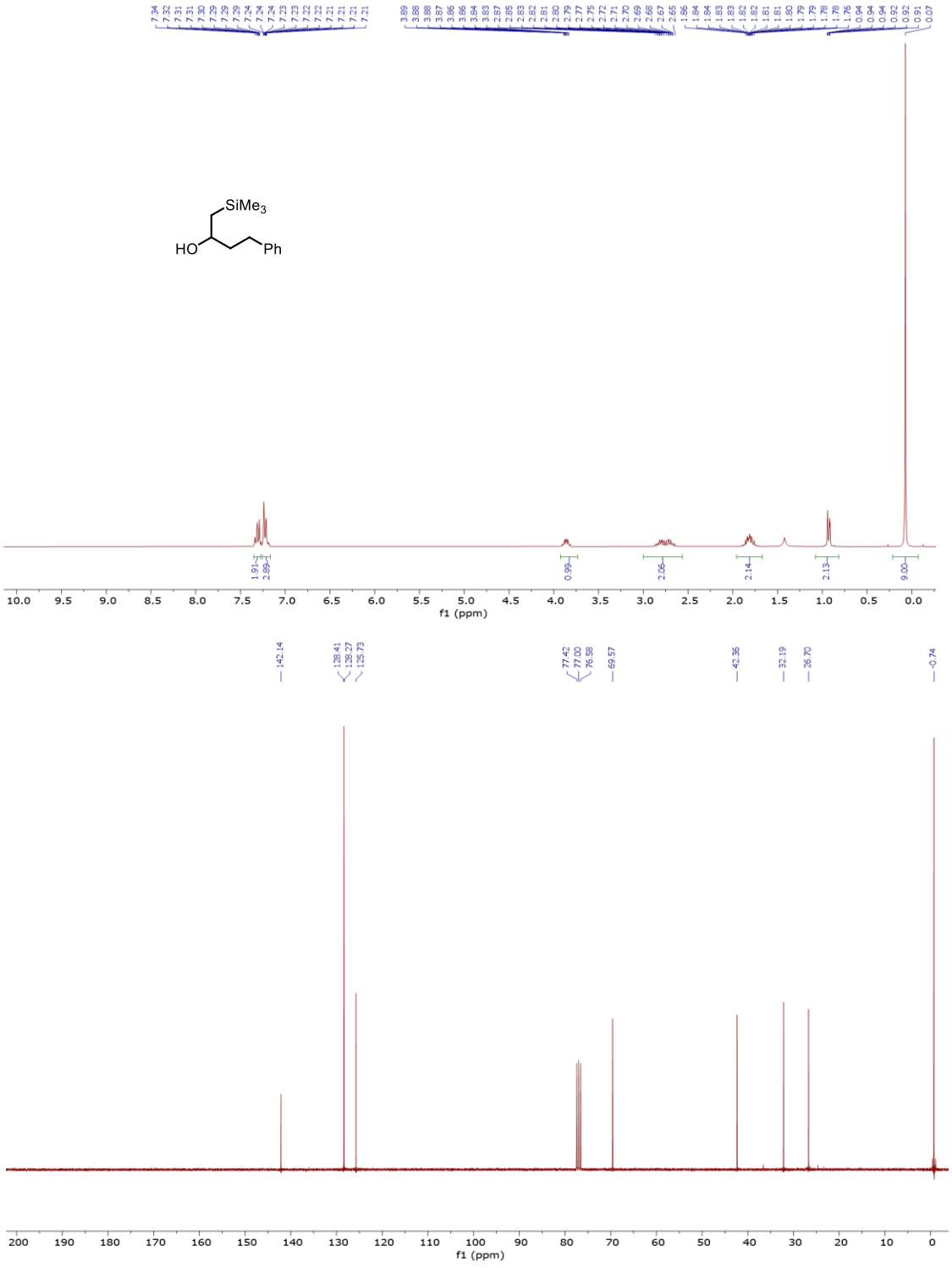

2-Methyl-4-(trimethylsilyl)butan-3-ol **4.88** ($CDCl_3$, 400 MHz for $^{1}H$ NMR, 100 MHz for $^{13}C$ NMR)

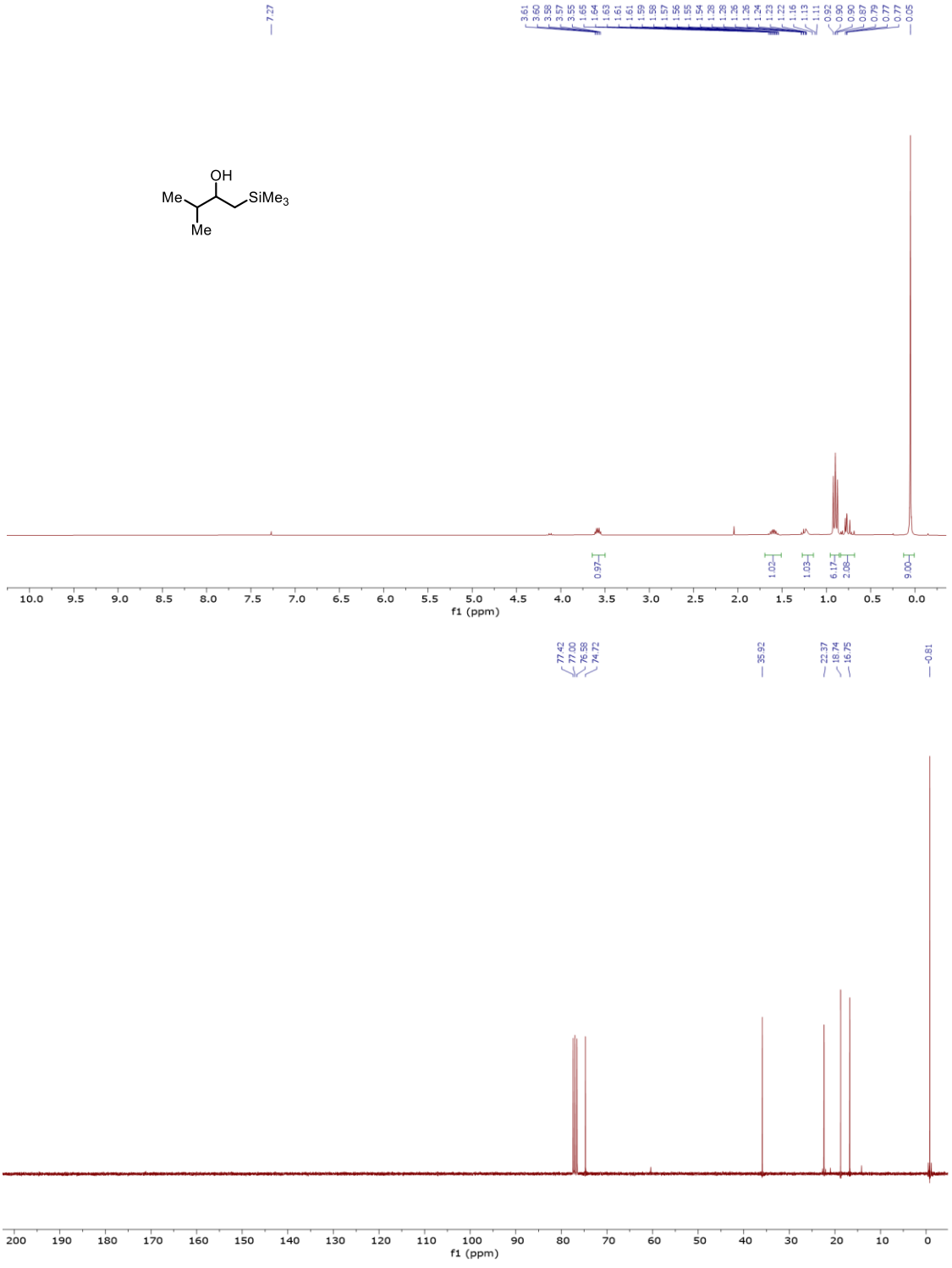

1-Cyclohexyl-2-(trimethylsilyl)ethan-1-ol **4.89** ($CDCl_3$, 400 MHz for $^1H$ NMR, 100 MHz for $^{13}C$ NMR)

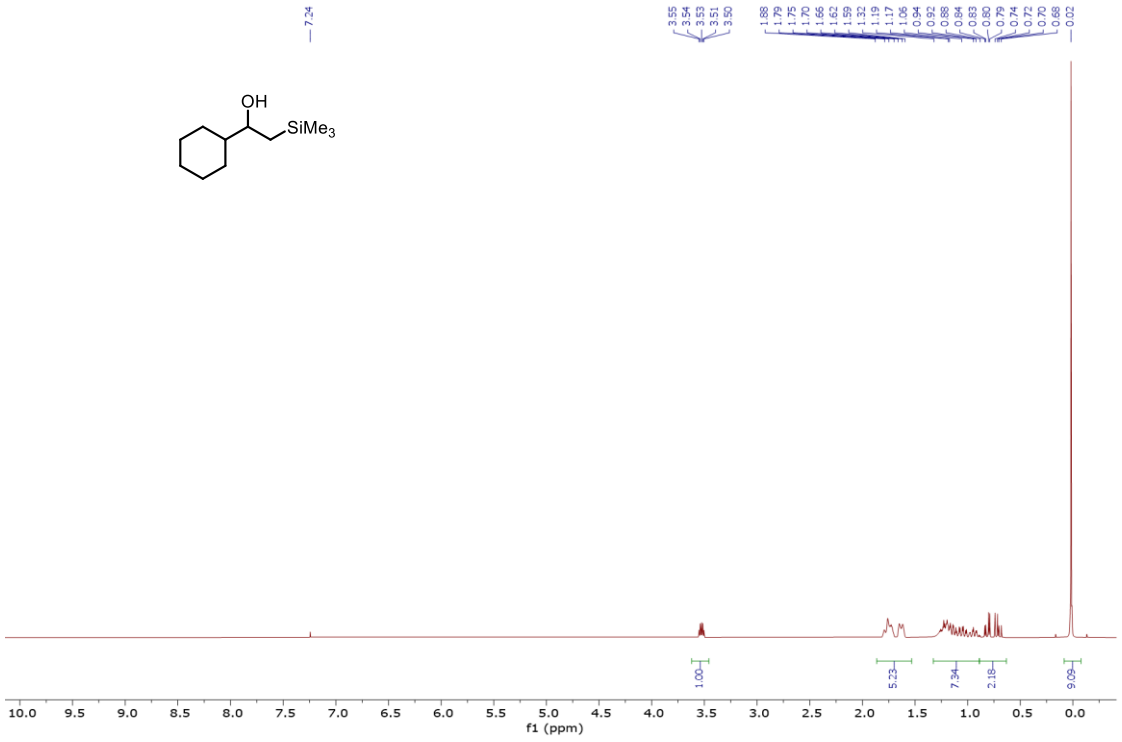


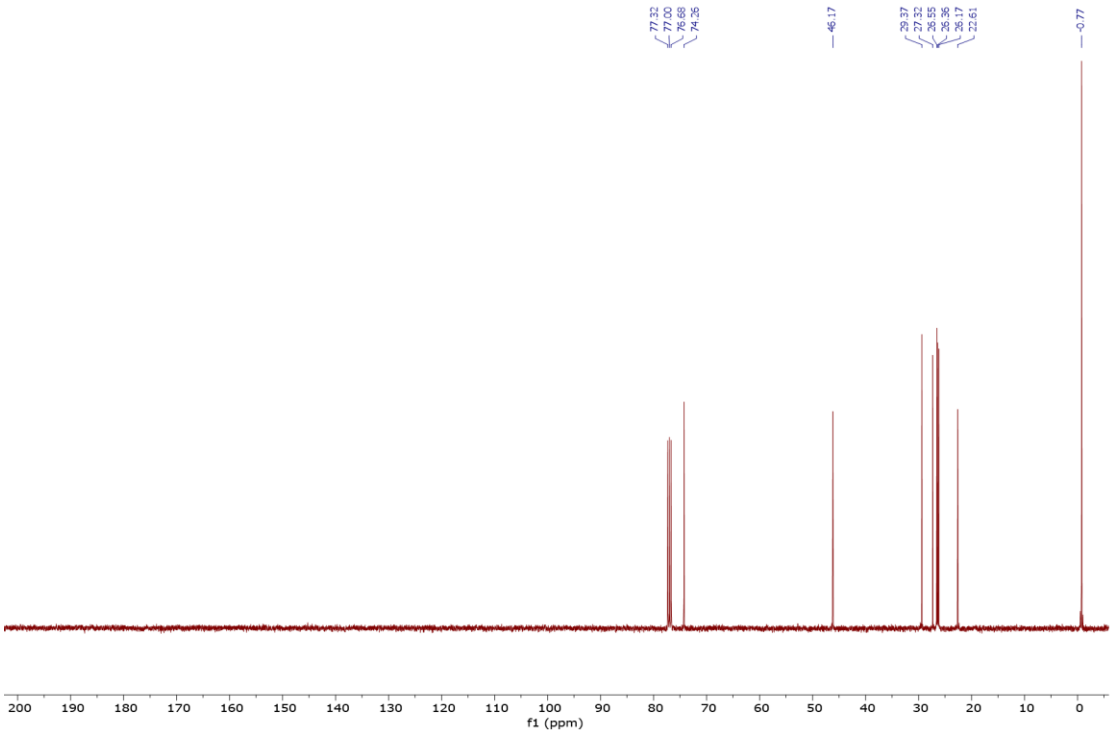

1-Phenyl-2-(trimethylsilyl)ethan-1-ol **4.90** ($CDCl_3$, 400 MHz for $^1H$ NMR, 100 MHz for $^{13}C$ NMR)

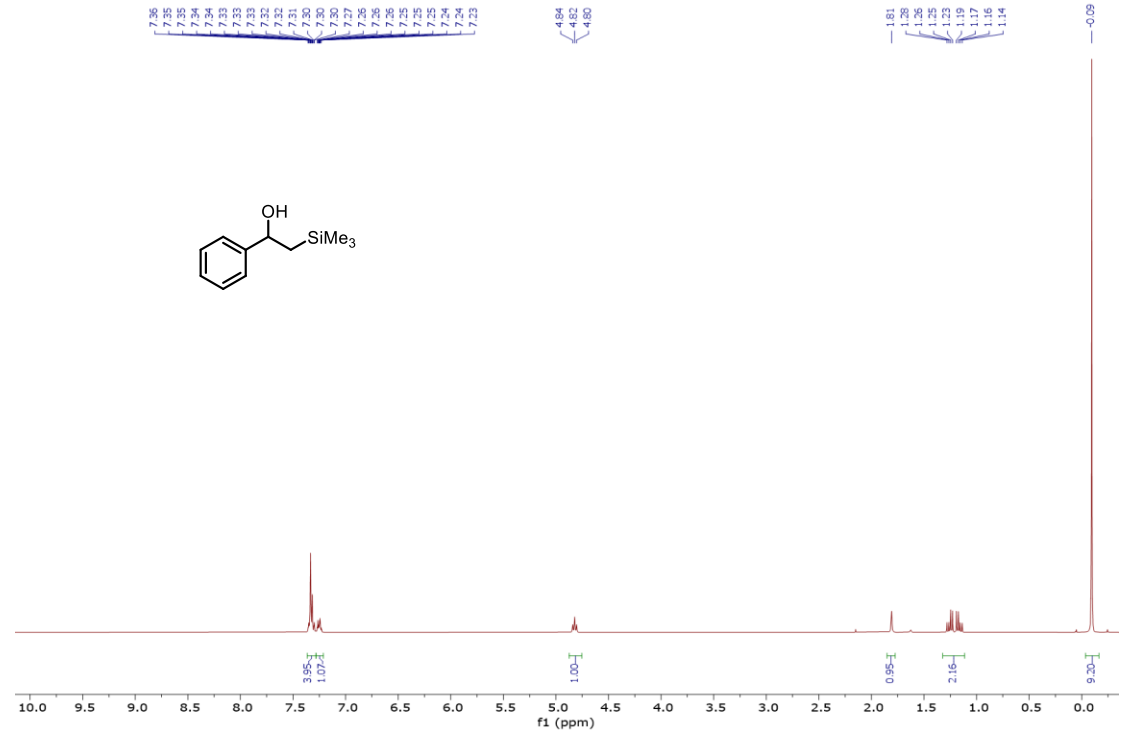


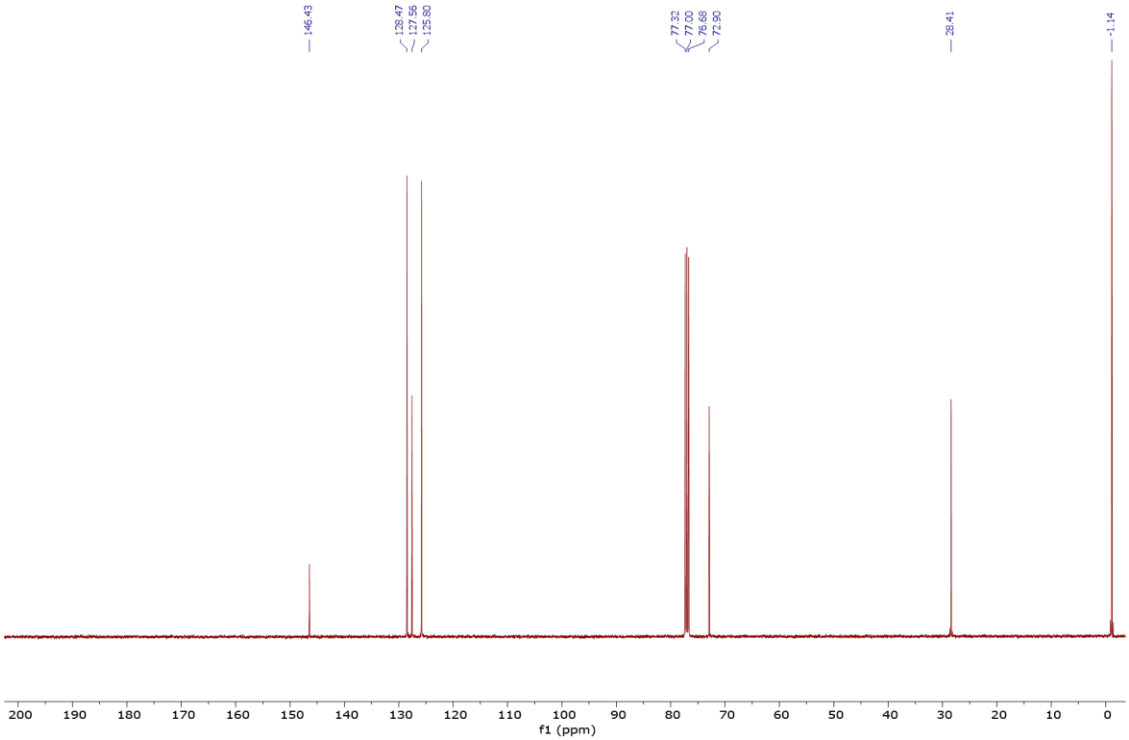

1-[Trimethylsilyl)methyl]cyclohexanol **4.91** ($CDCl_3$, 400 MHz for $^{1}H$ NMR, 100 MHz for $^{13}C$ NMR)

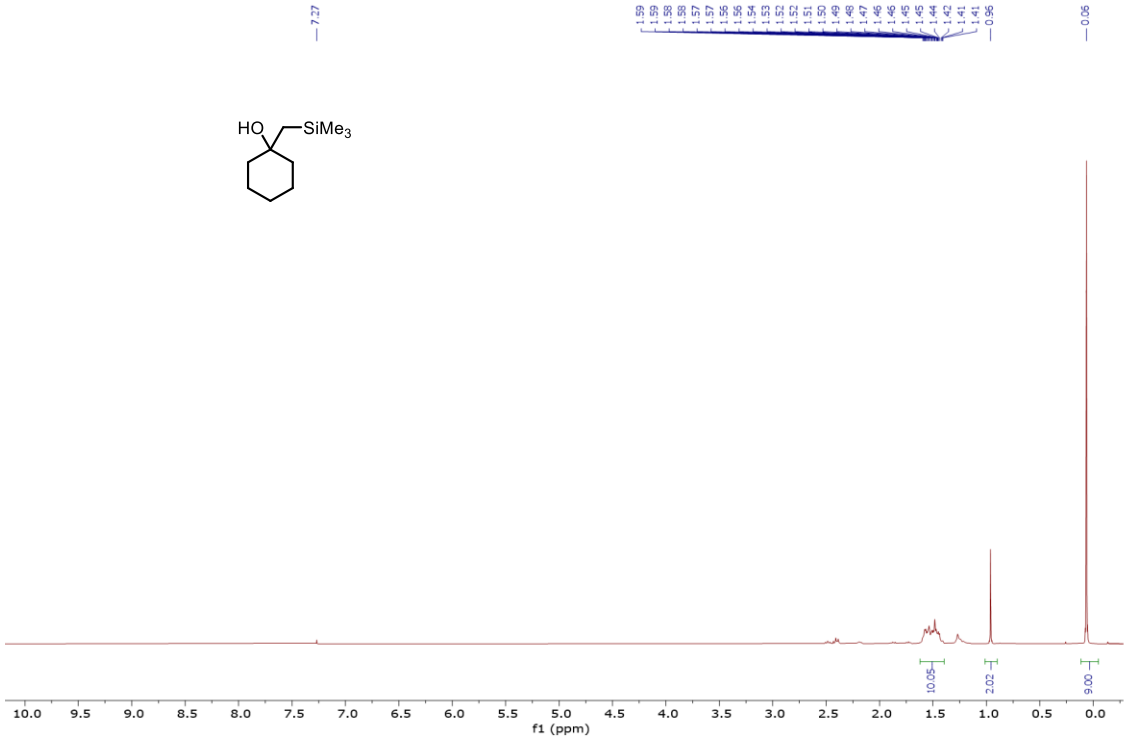


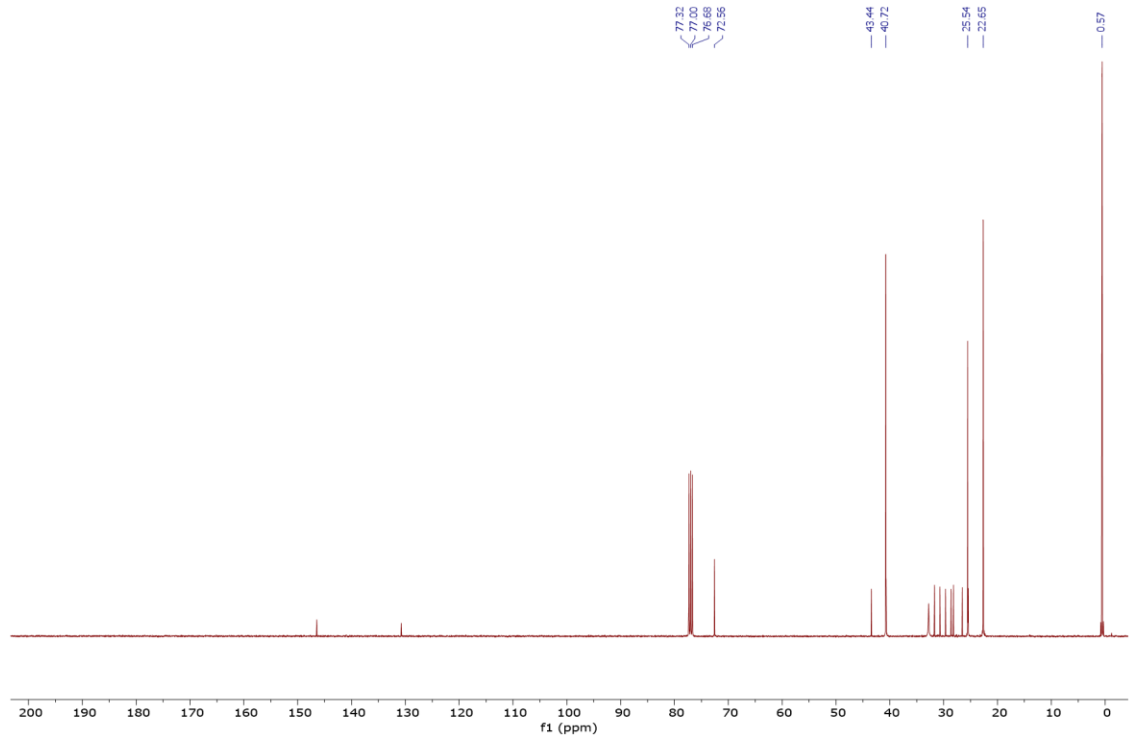

1-[4-(1*H*-pyrazol-1-yl)phenyl]-2-(trimethylsilyl)ethan-1-ol **4.92** ($CDCl_3$, 400 MHz for $^1H$ NMR, 100 MHz for $^{13}C$ NMR)

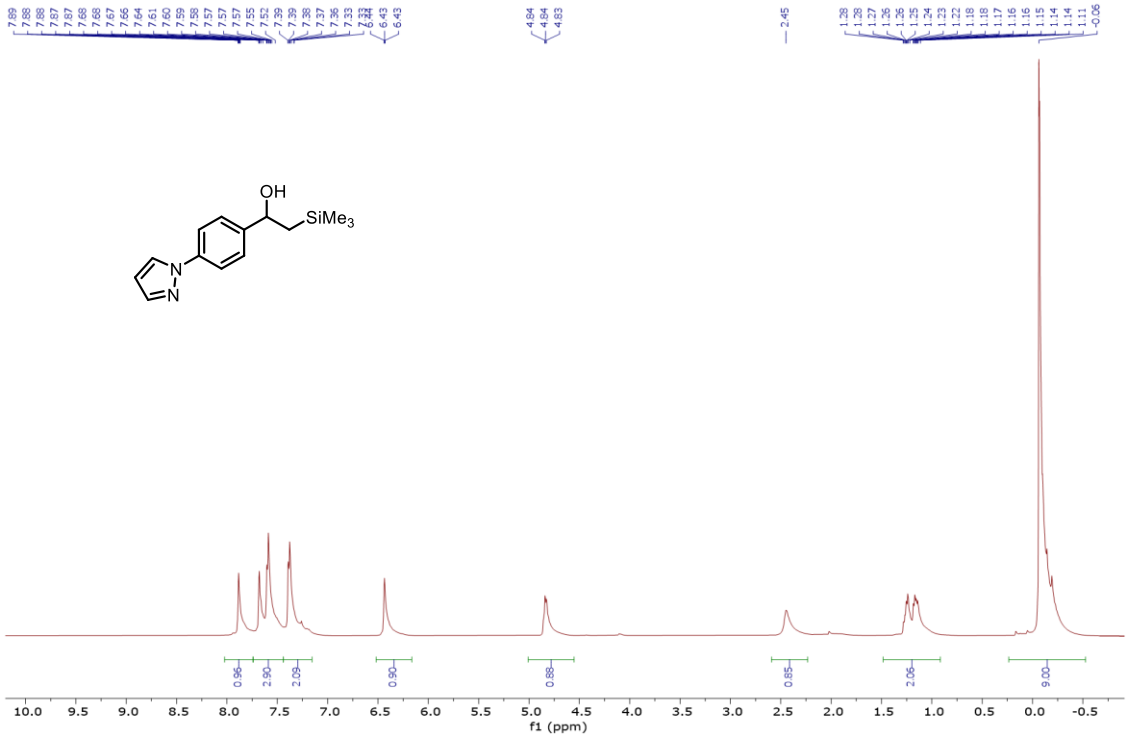


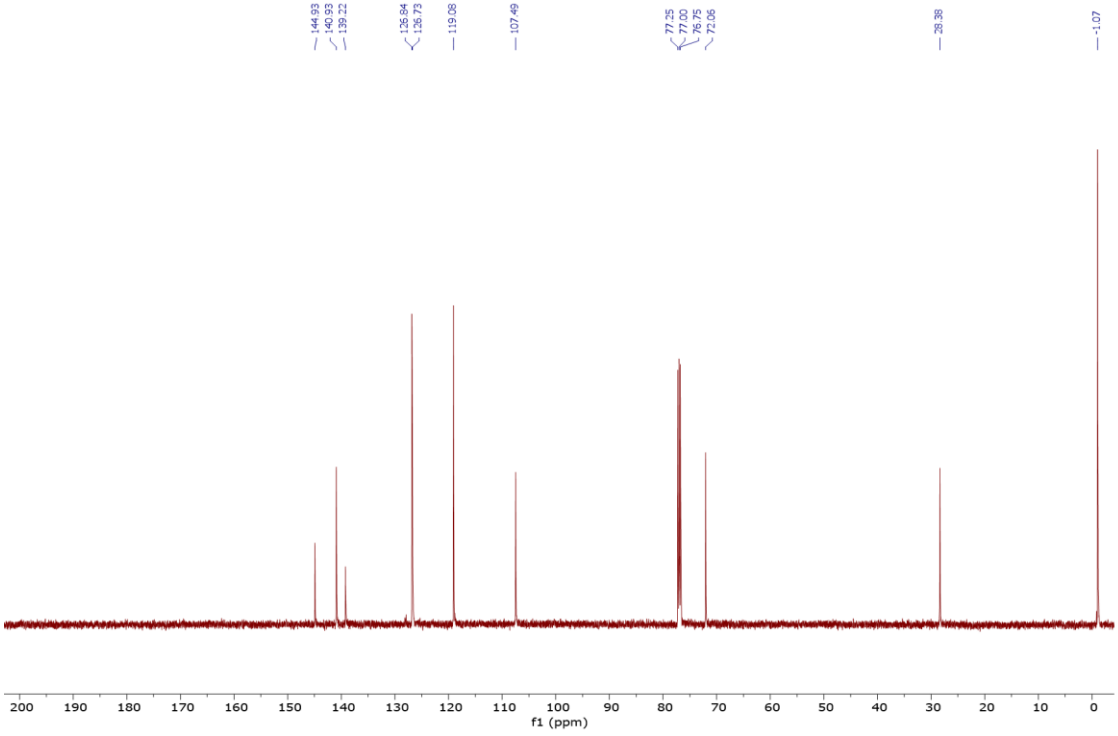

α-[(Trimethylsilyl)methyl]-3-thiophenemethanol **4.93** ($CDCl_3$, 400 MHz for $^1H$ NMR, 100 MHz for $^{13}C$ NMR)

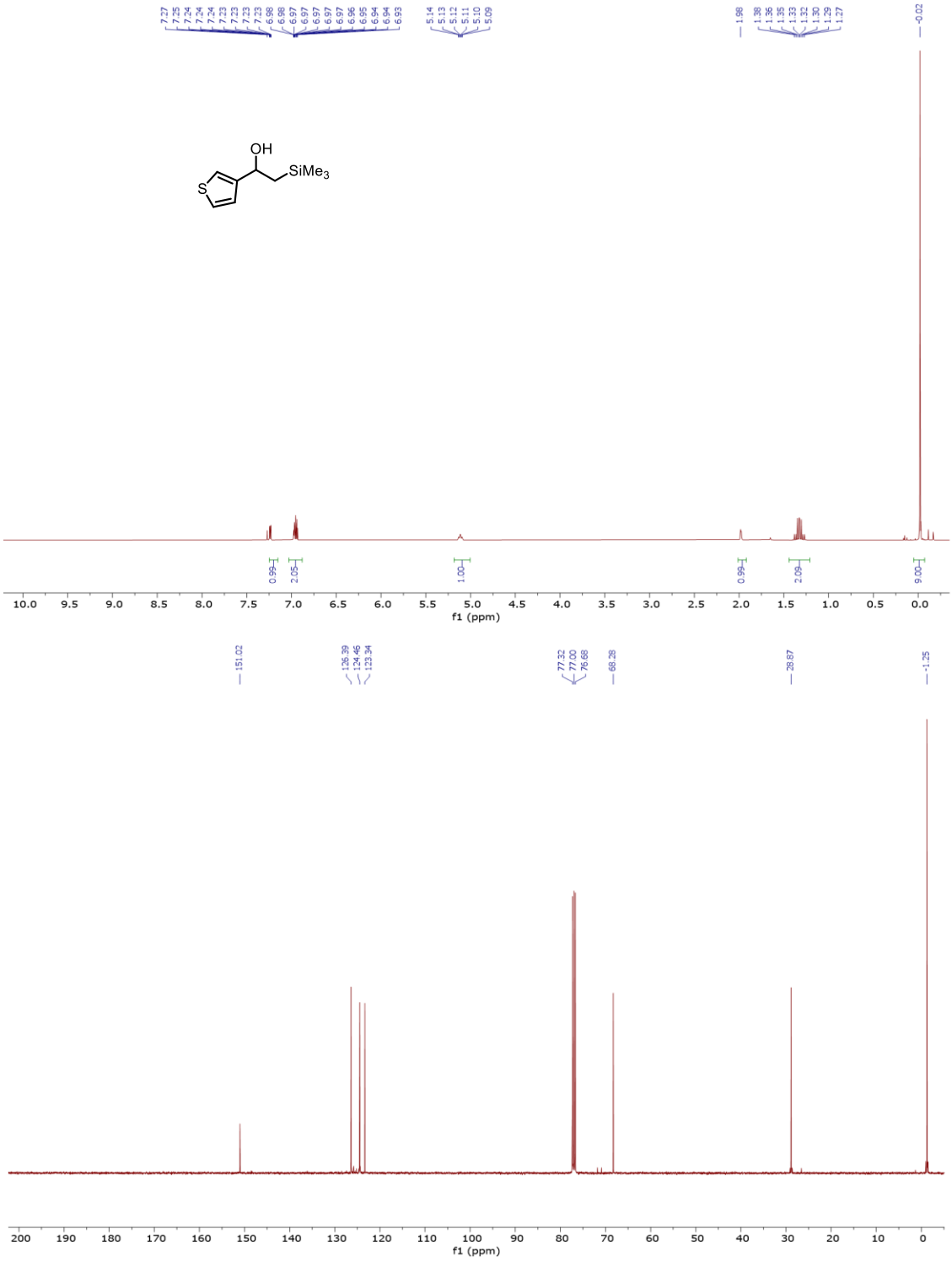

α-[(Trimethylsilyl)methyl]-5-quinolinemethanol **4.94** ($CDCl_3$, 400 MHz for $^1H$ NMR, 100 MHz for $^{13}C$ NMR)

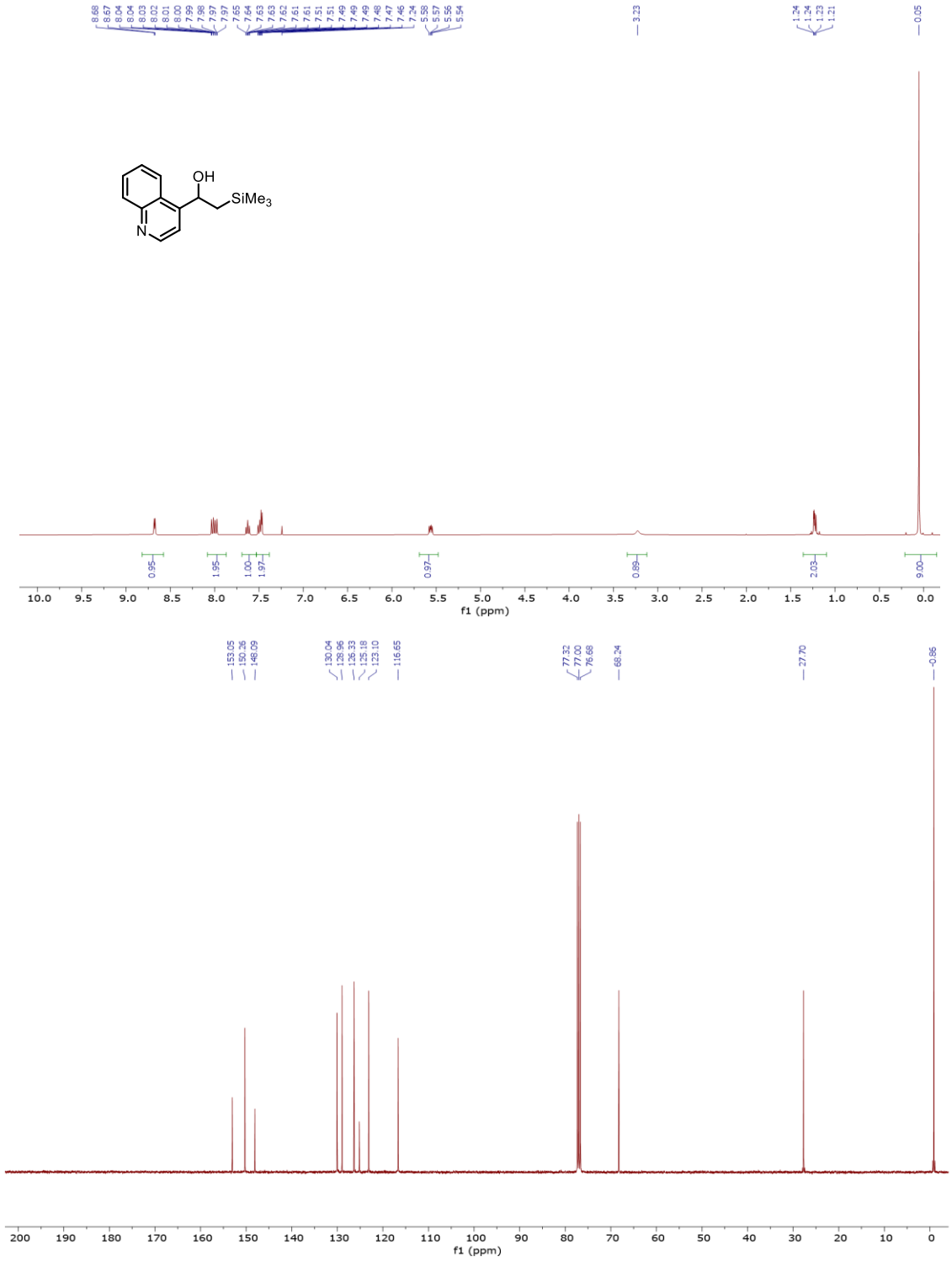

[2-[[(1,1-Dimethylethyl)dimethylsilyl]oxy]ethyl]trimethylsilane **4.35** ($CDCl_3$, 400 MHz for $^1H$ NMR, 100 MHz for $^{13}C$ NMR)

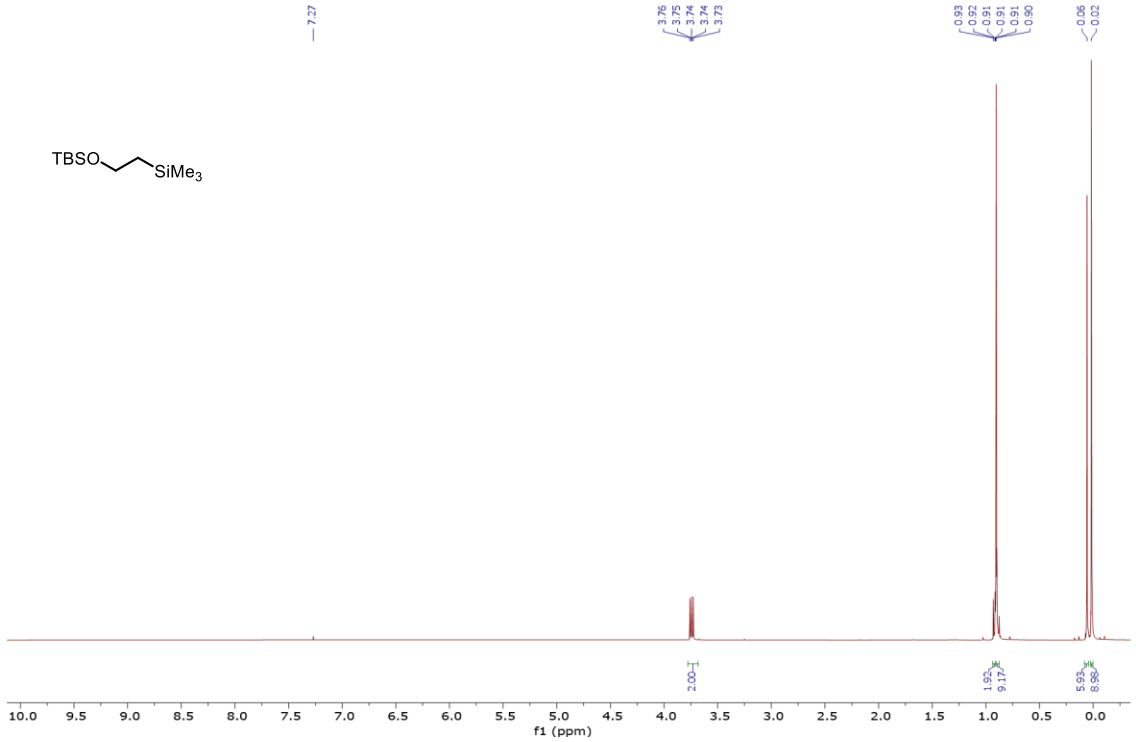


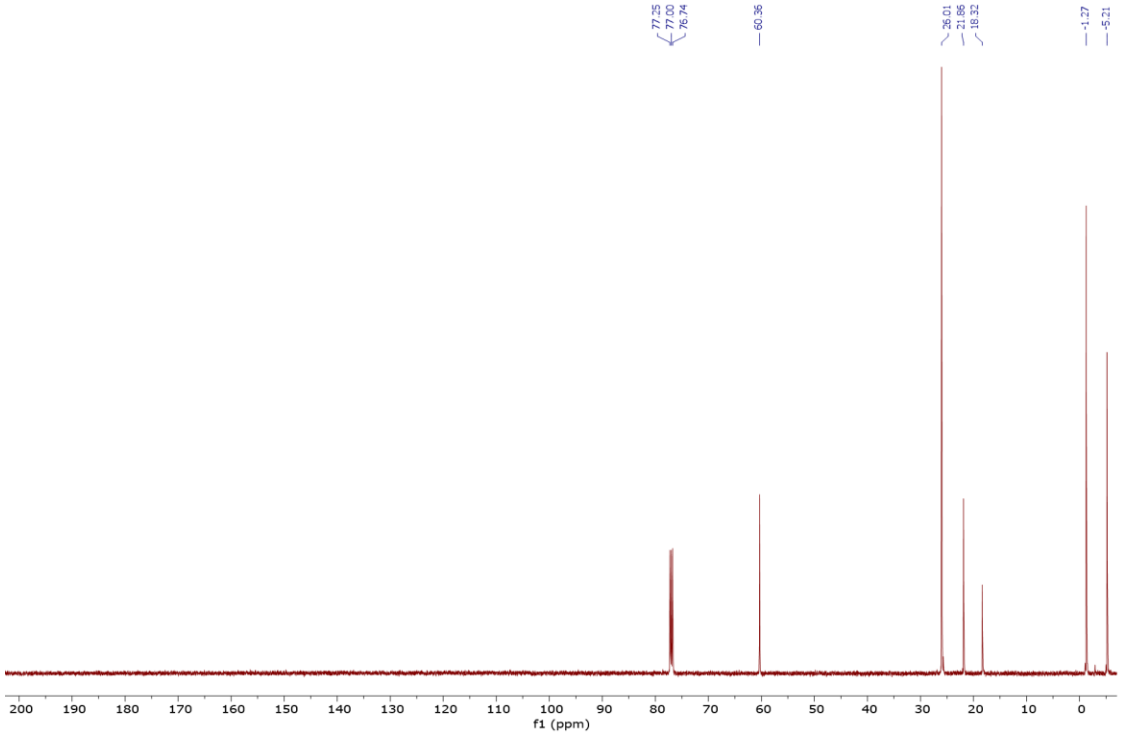

Trimethyl[2-(trimethylsilyl)ethoxy]silane **4.36** ($CDCl_3$, 400 MHz for $^1H$ NMR, 100 MHz for $^{13}C$ NMR)

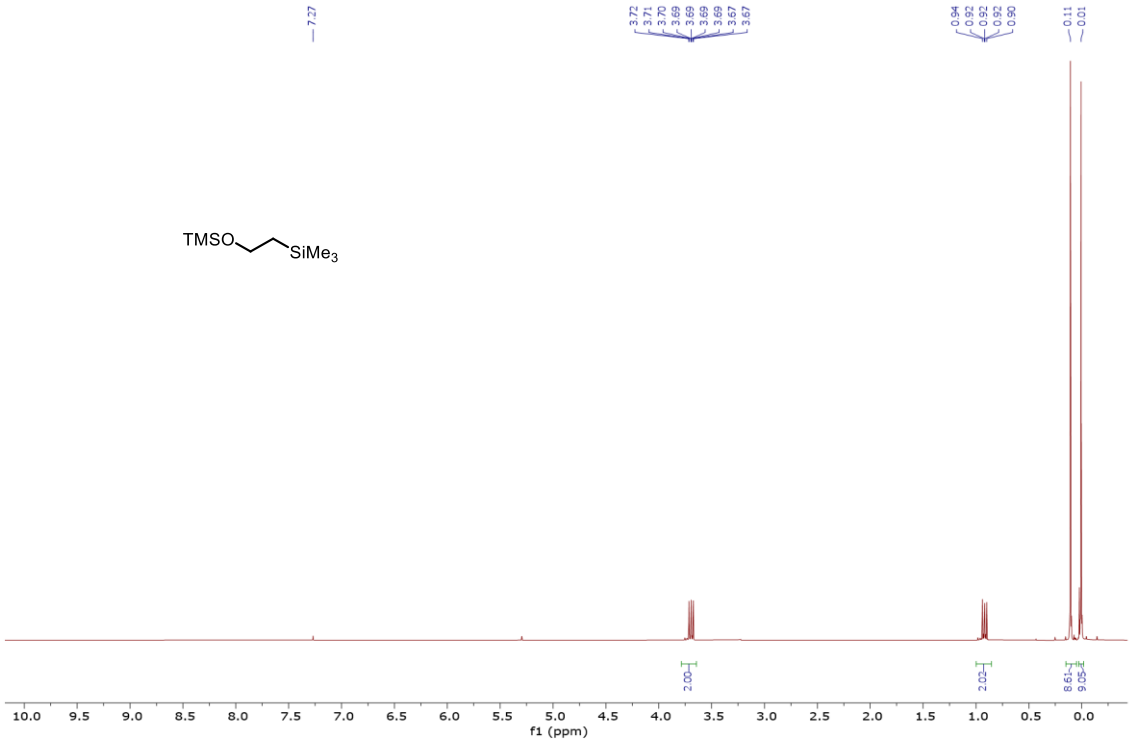


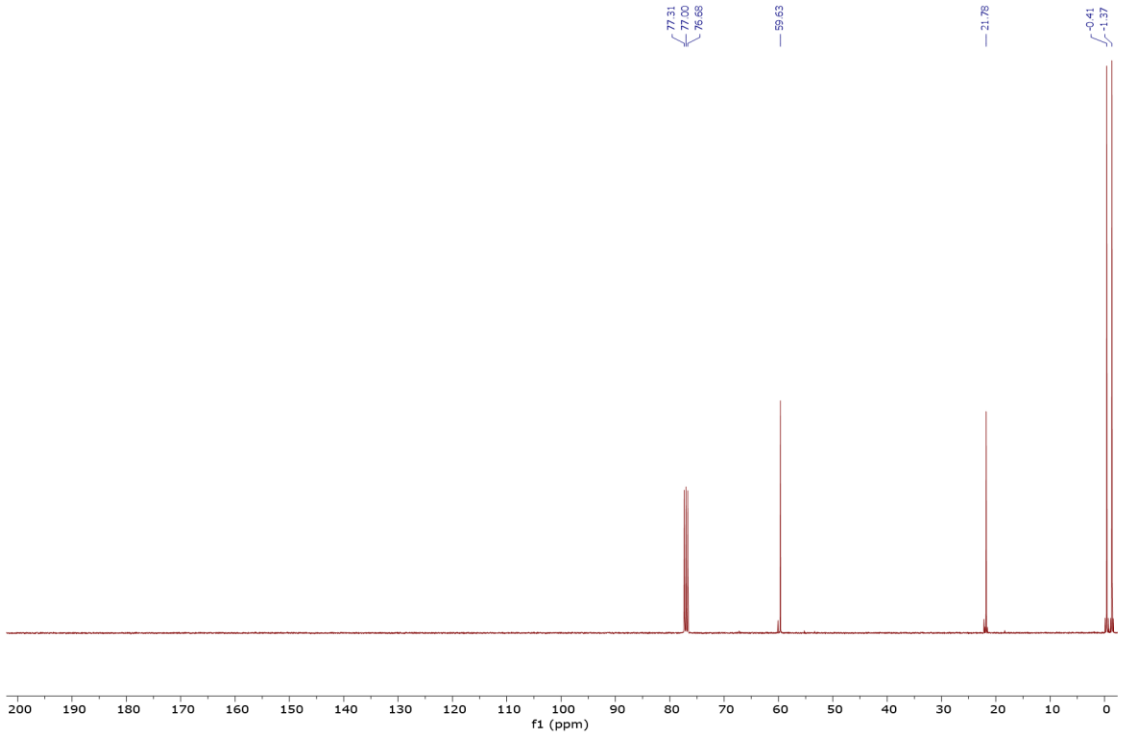

Benzyl-2-(trimethylsilyl)ethyl ether **4.37** ($CDCl_3$, 400 MHz for $^1H$ NMR, 100 MHz for $^{13}C$ NMR)

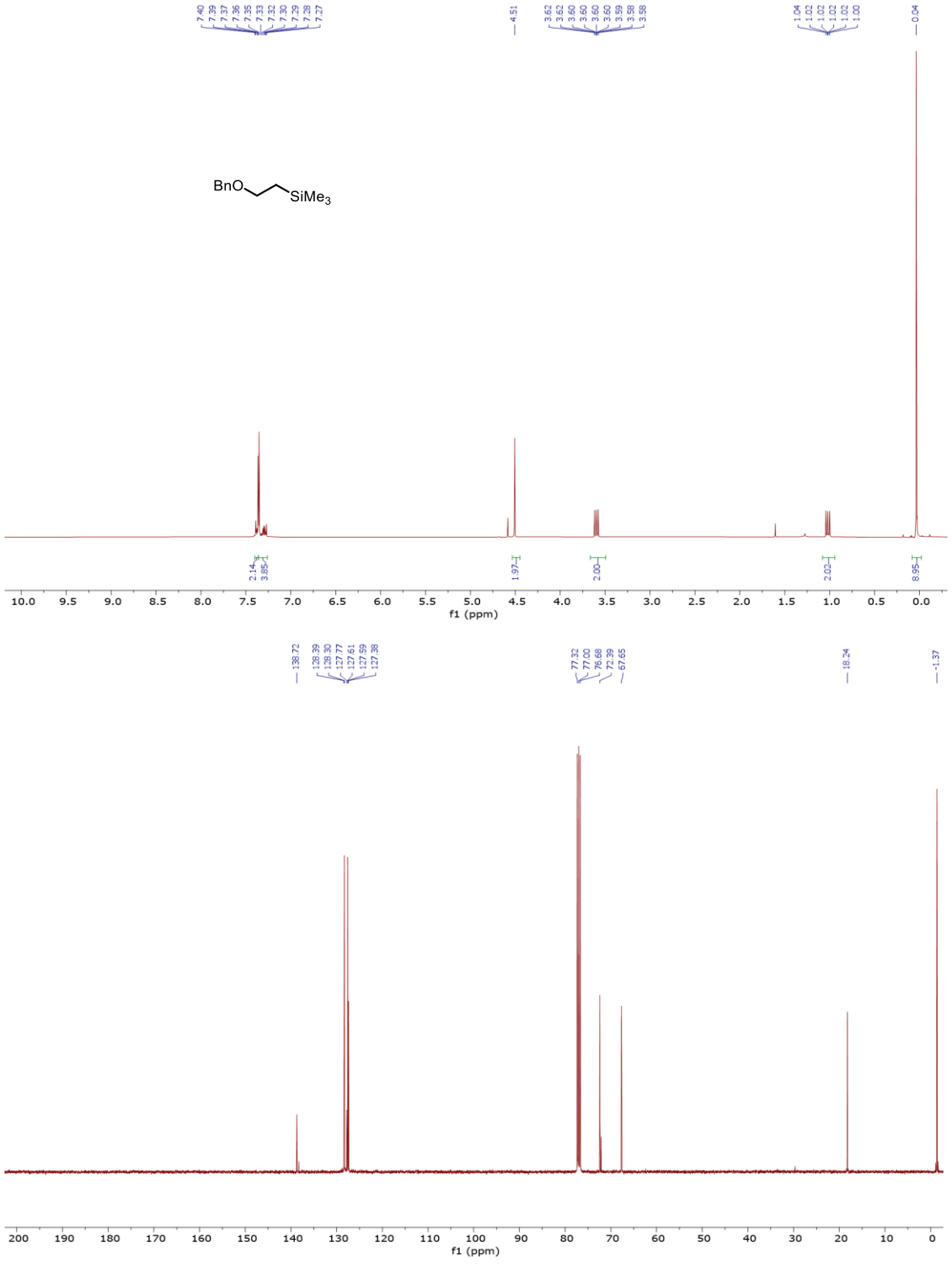

1-Cyclopropyl-2-(trimethylsilyl)ethan-1-ol **4.68** ($CDCl_3$, 400 MHz for $^1H$ NMR, 100 MHz for $^{13}C$ NMR)

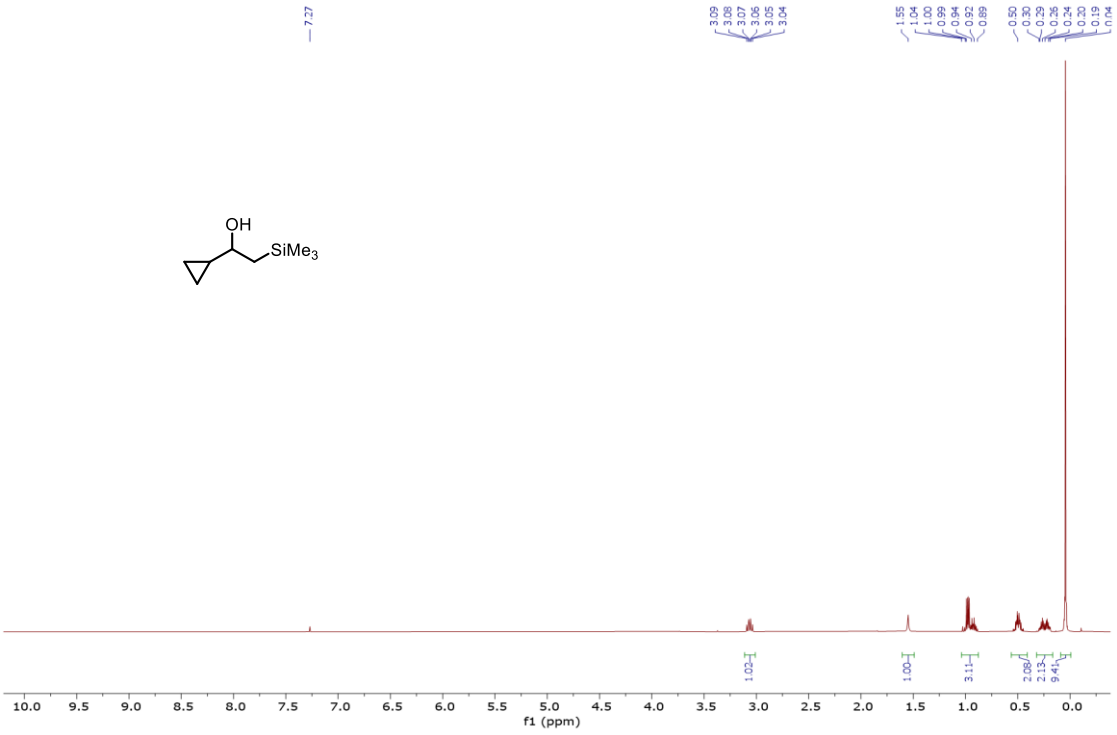


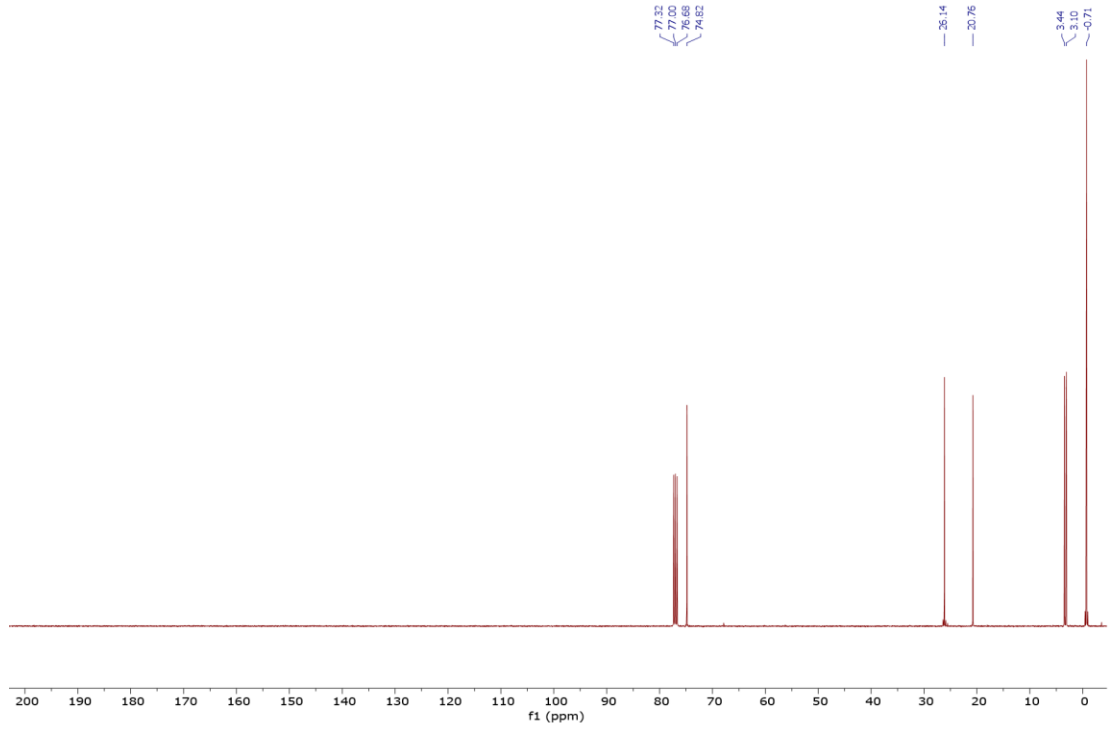

1-(Trimethylsilyl)hept-6-en-2-ol **4.71** ($CDCl_3$, 400 MHz for $^1H$ NMR, 100 MHz for $^{13}C$ NMR)

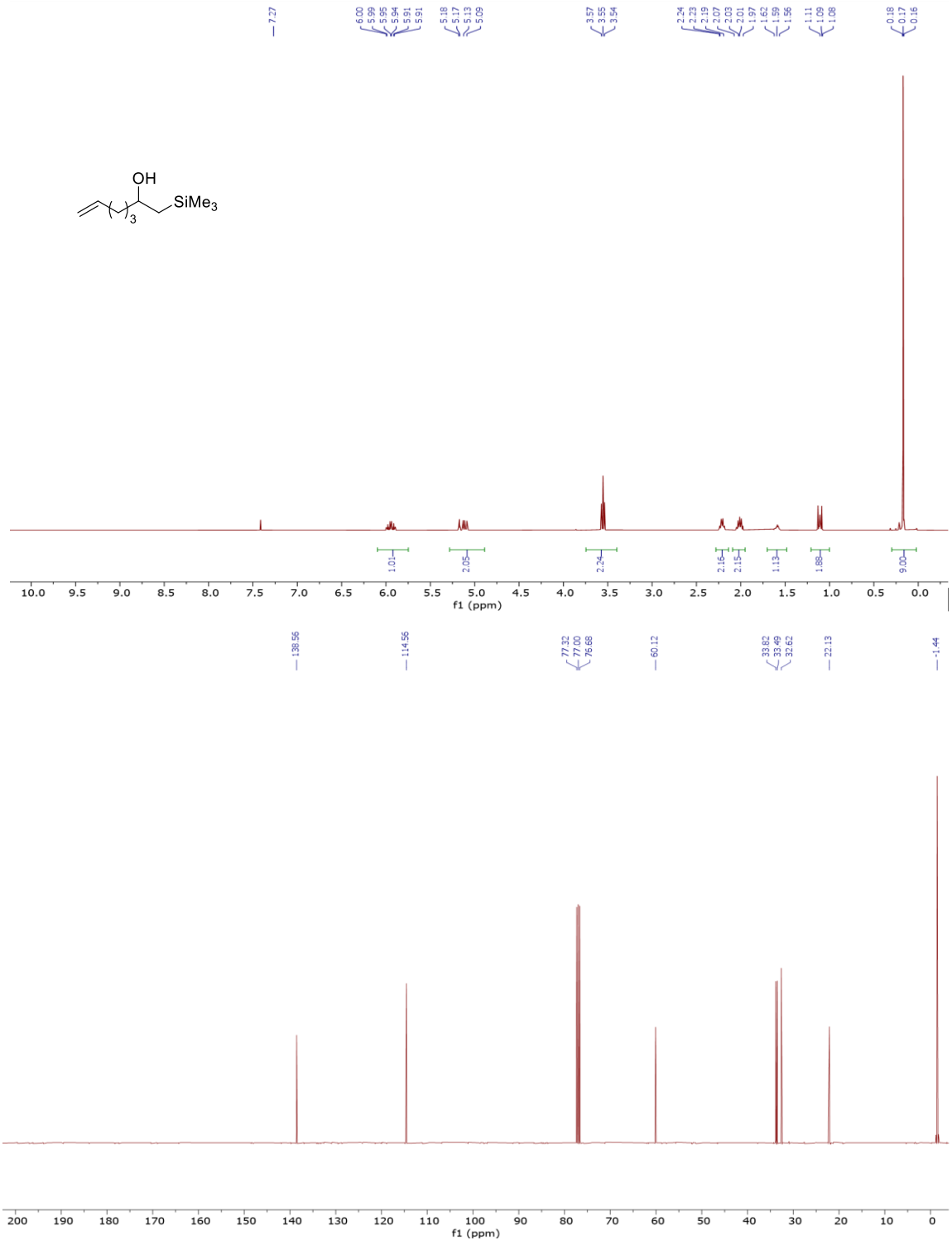

1,1’-Di(2,6-diisopropylphenyl)-3,3’-(2-cyclopropyl)propylenediimidazolium dibromide **L2** (*d*$_6$-DMSO, 400 MHz for $^{1}$H NMR, 100 MHz for $^{13}$C NMR)

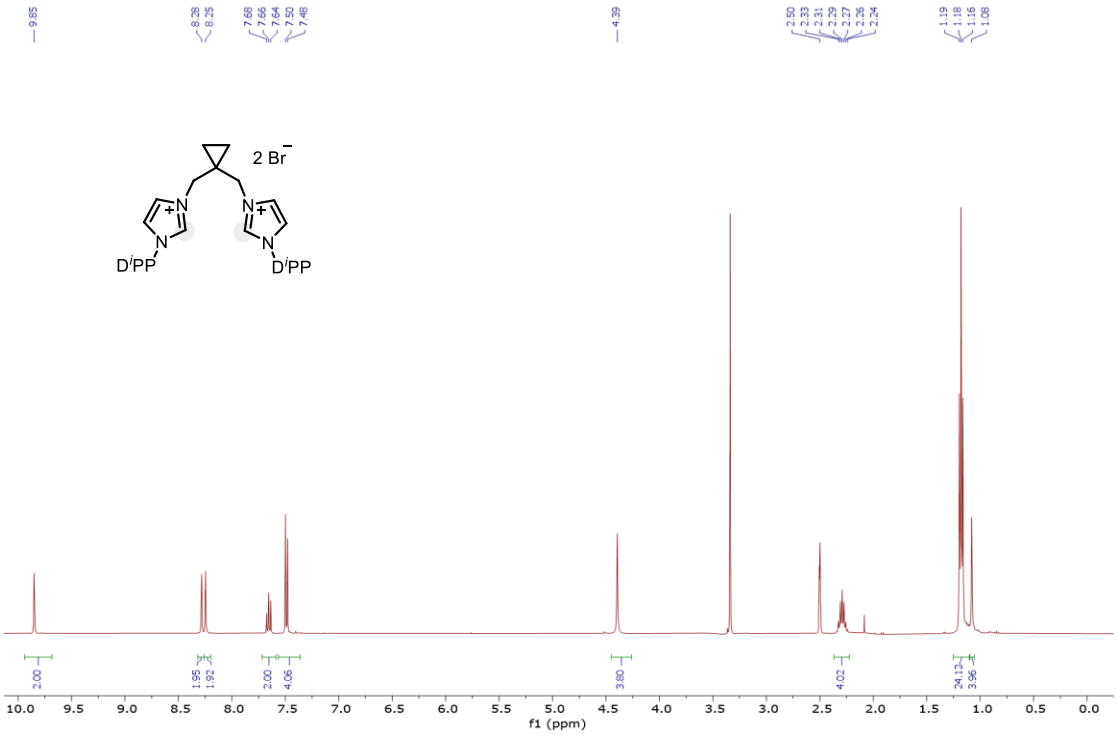


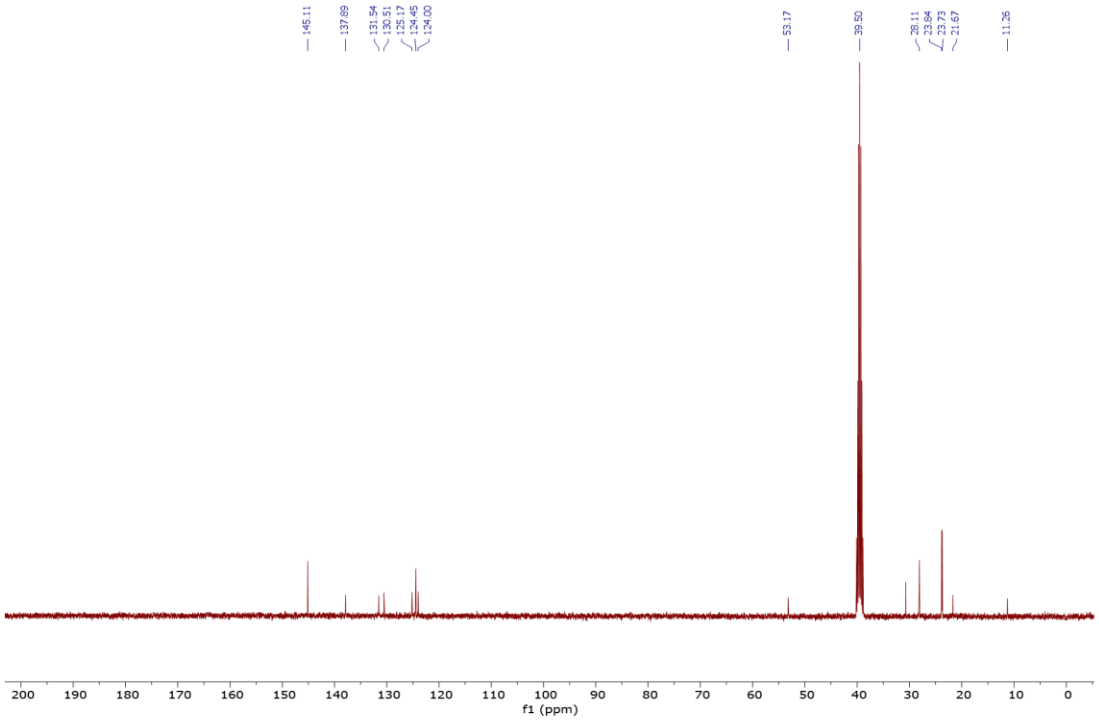

1,1’-Di(2,6-diisopropylphenyl)-3,3’-*o*-phenylenedimethylenediimidazolium dibromide **L1** ($CDCl_3$, 400 MHz for $^1H$ NMR, 100 MHz for $^{13}C$ NMR)

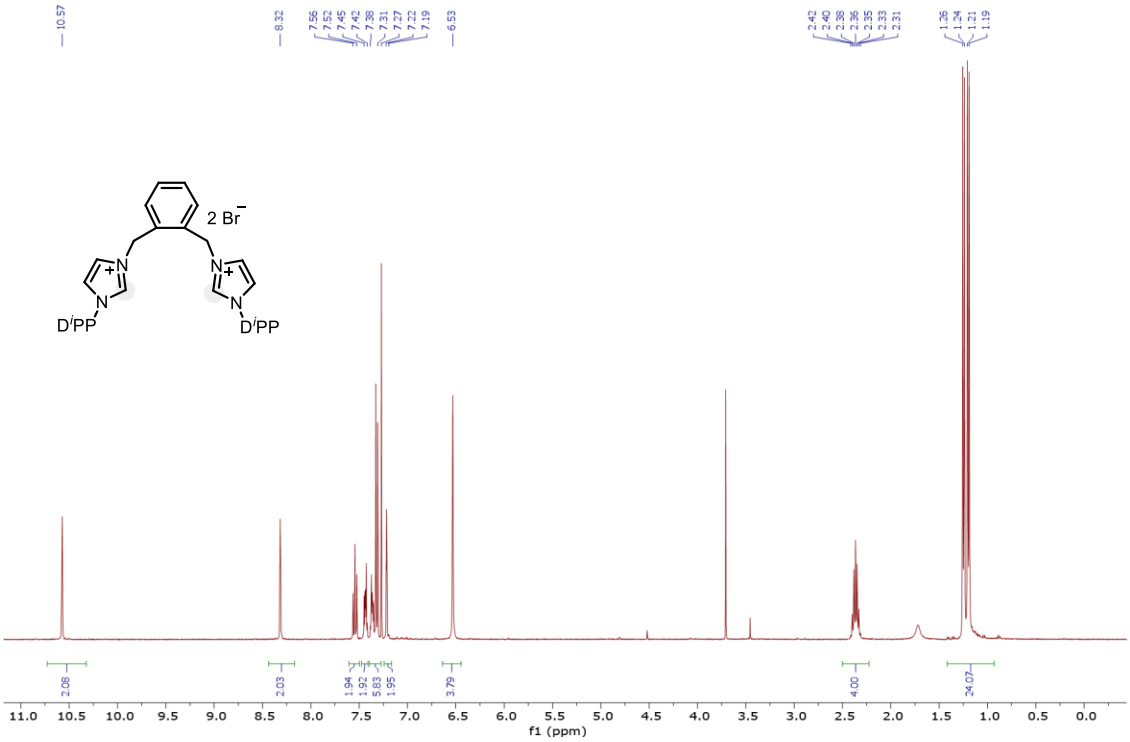


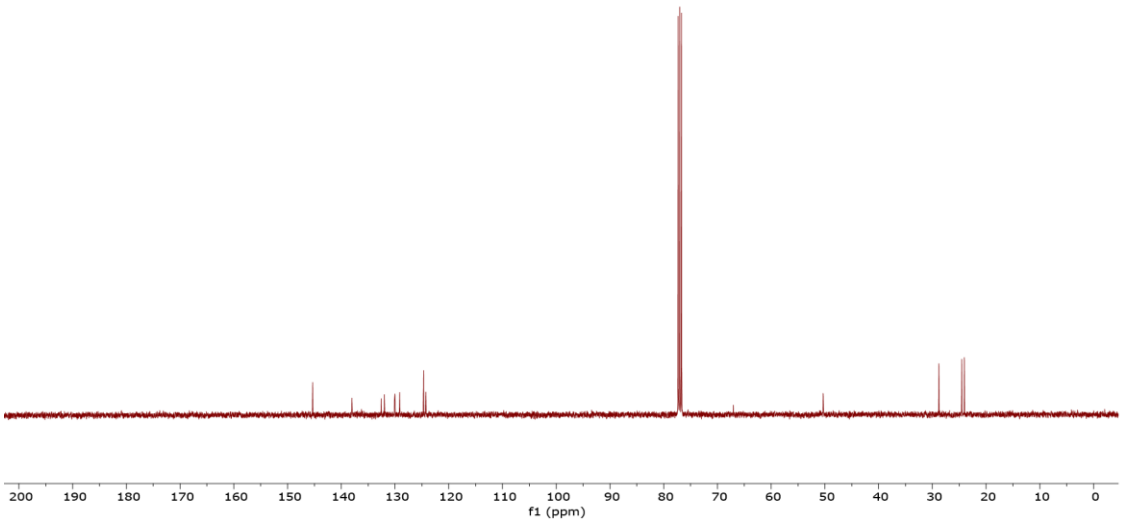

1,1’-Di(2,6-diisopropylphenyl)-3,3’-(2-methyl)propylenediimidazolium dibromide **L8** ($CDCl_3$, 400 MHz for $^1H$ NMR, 100 MHz for $^{13}C$ NMR)

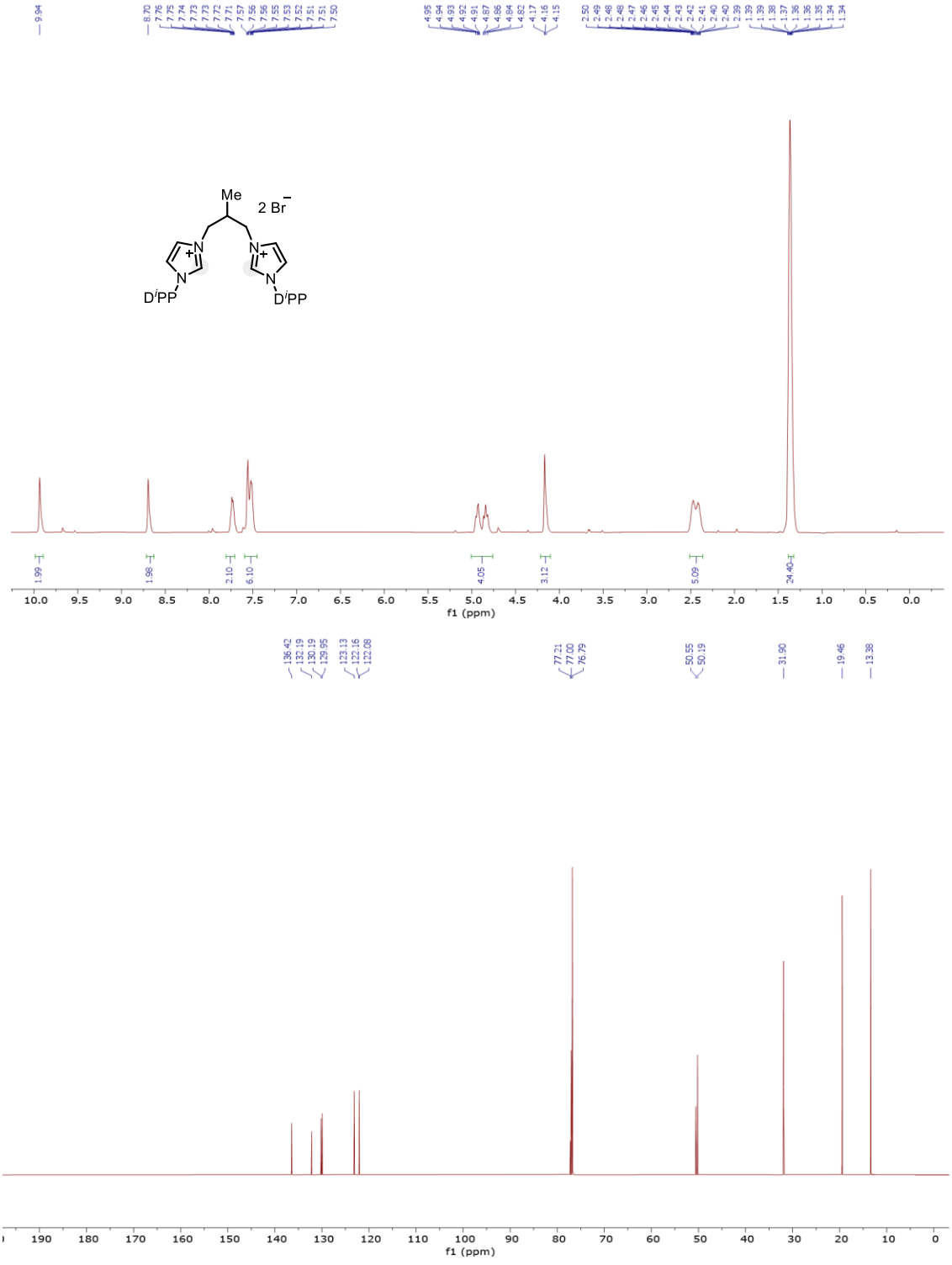

[2-(Trimethylsilyl)ethyl]benzene **4.9** ($CDCl_3$, 400 MHz for $^1H$ NMR, 100 MHz for $^{13}C$ NMR)

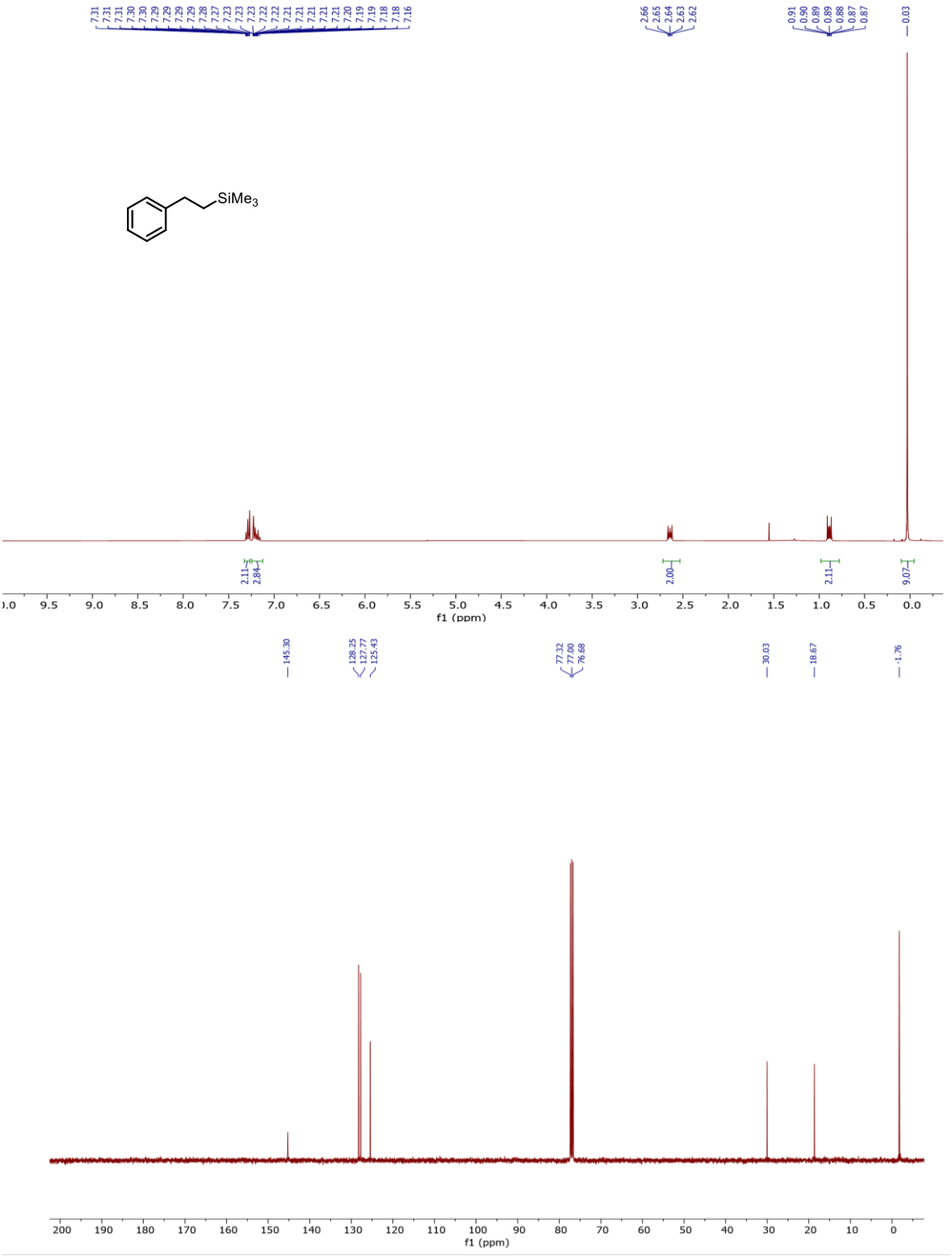

1-Methyl-4-[2-(trimethylsilyl)ethyl]-benzene **4.15** ($CDCl_3$, 400 MHz for $^1H$ NMR, 100 MHz for $^{13}C$ NMR)

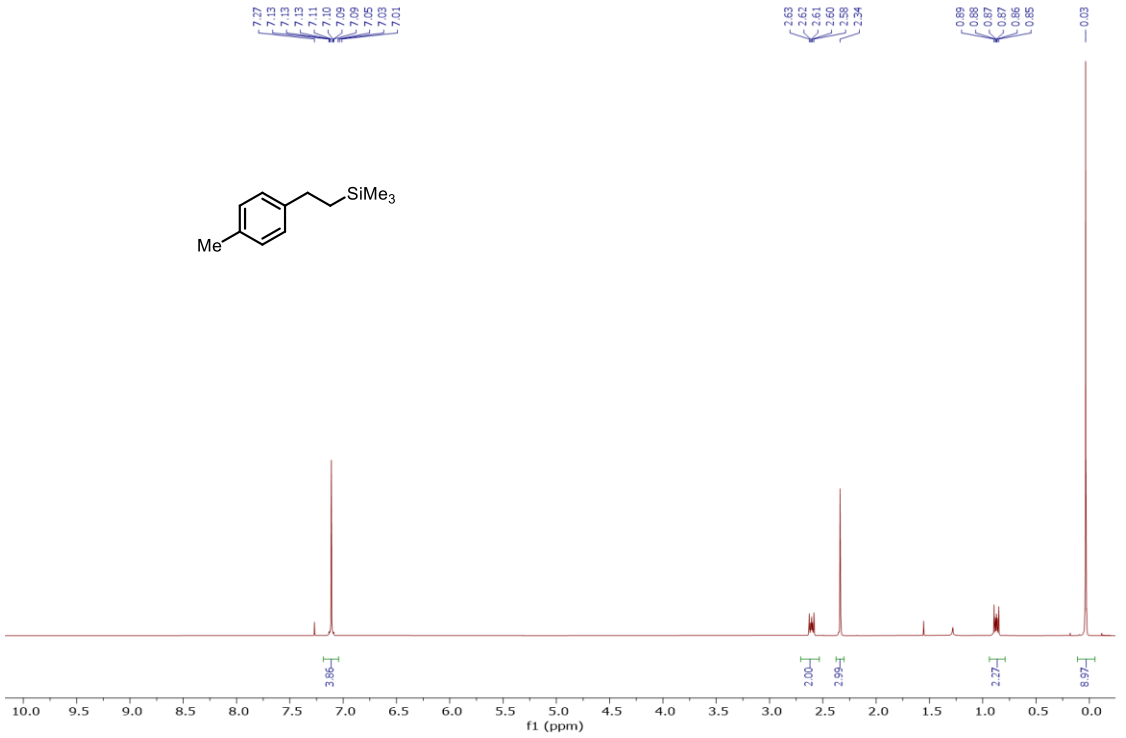


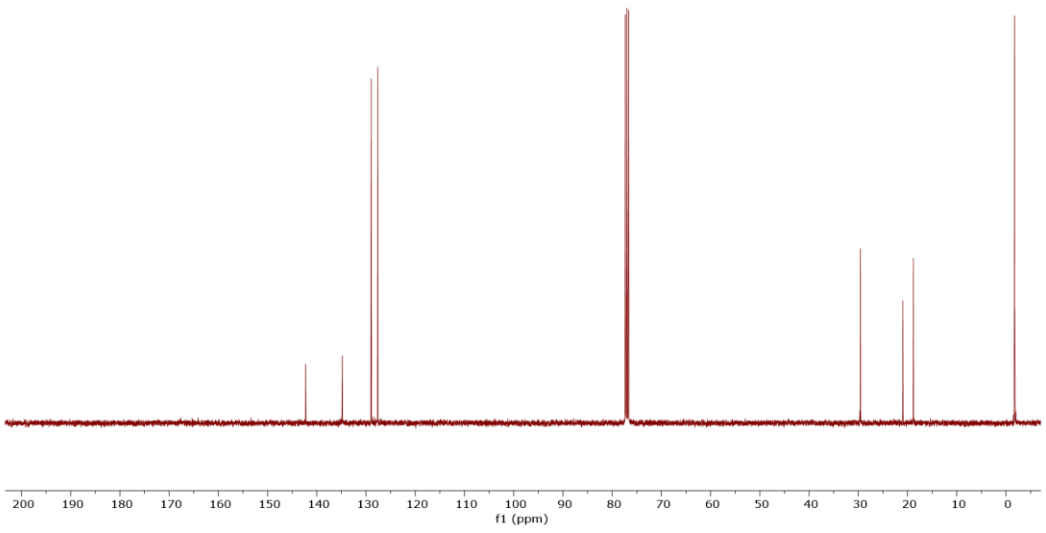

1-Methyl-2-[2-(trimethylsilyl)ethyl]benzene **4.16** ($CDCl_3$, 400 MHz for $^1H$ NMR, 100 MHz for $^{13}C$ NMR)

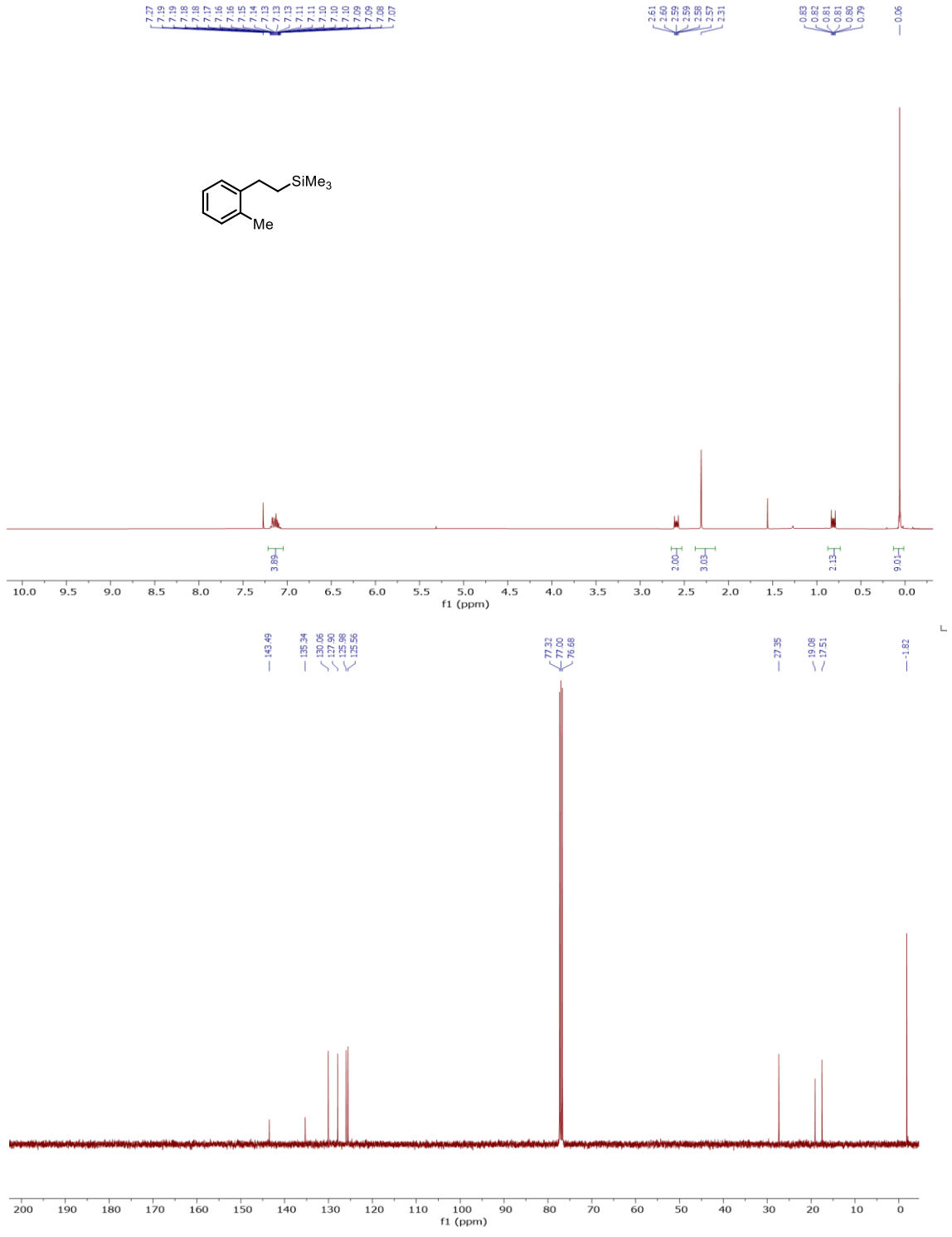

1-(1,1-Dimethylethyl)-4-[2-(trimethylsilyl)ethyl]benzene **4.17** ($CDCl_3$, 400 MHz for $^1H$ NMR, 100 MHz for $^{13}C$ NMR)

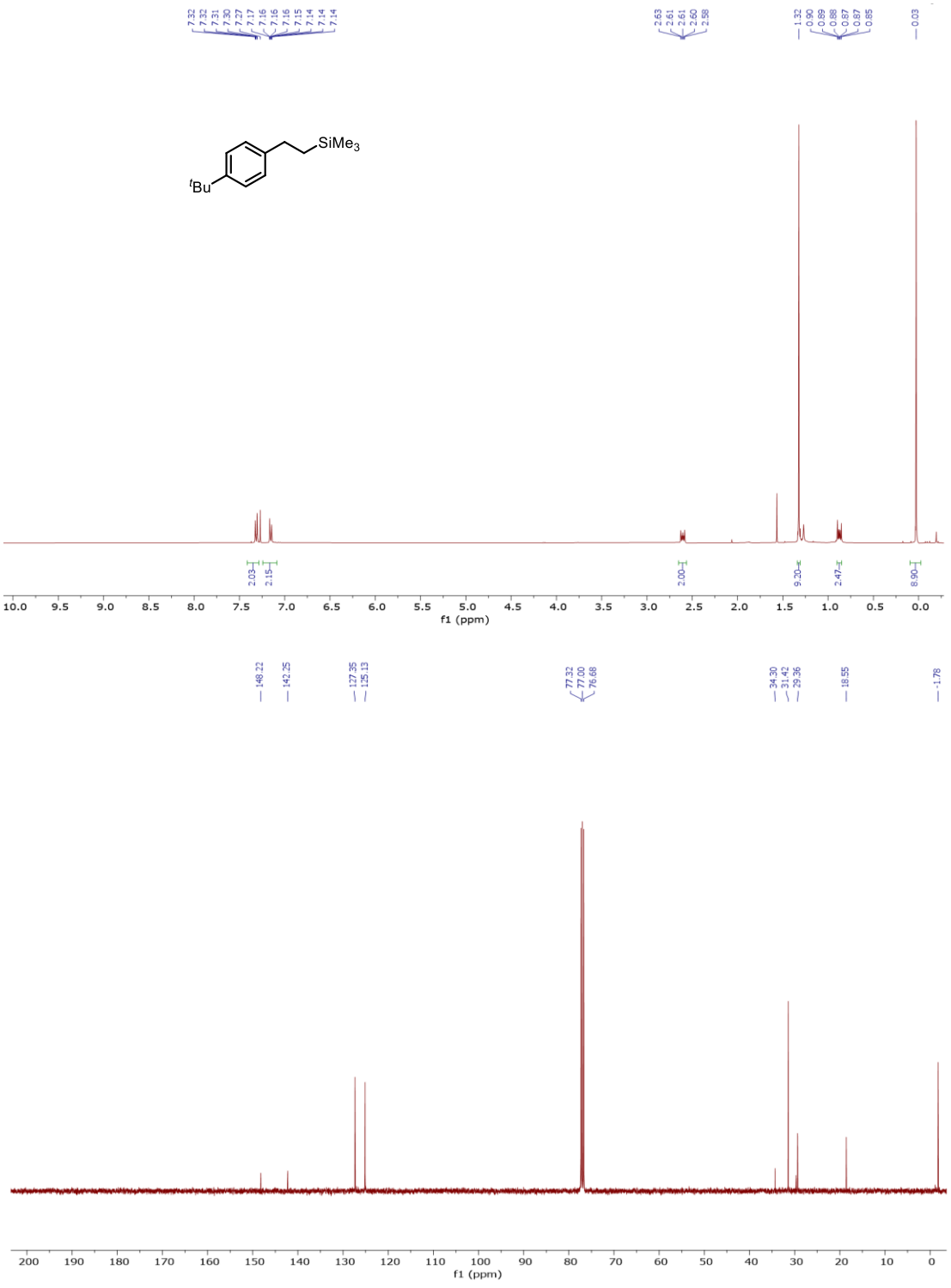

1-Fluoro-4-[2-(trimethylsilyl)ethyl]benzene **4.18** ($CDCl_3$, 400 MHz for $^1H$ NMR, 100 MHz for $^{13}C$ NMR)

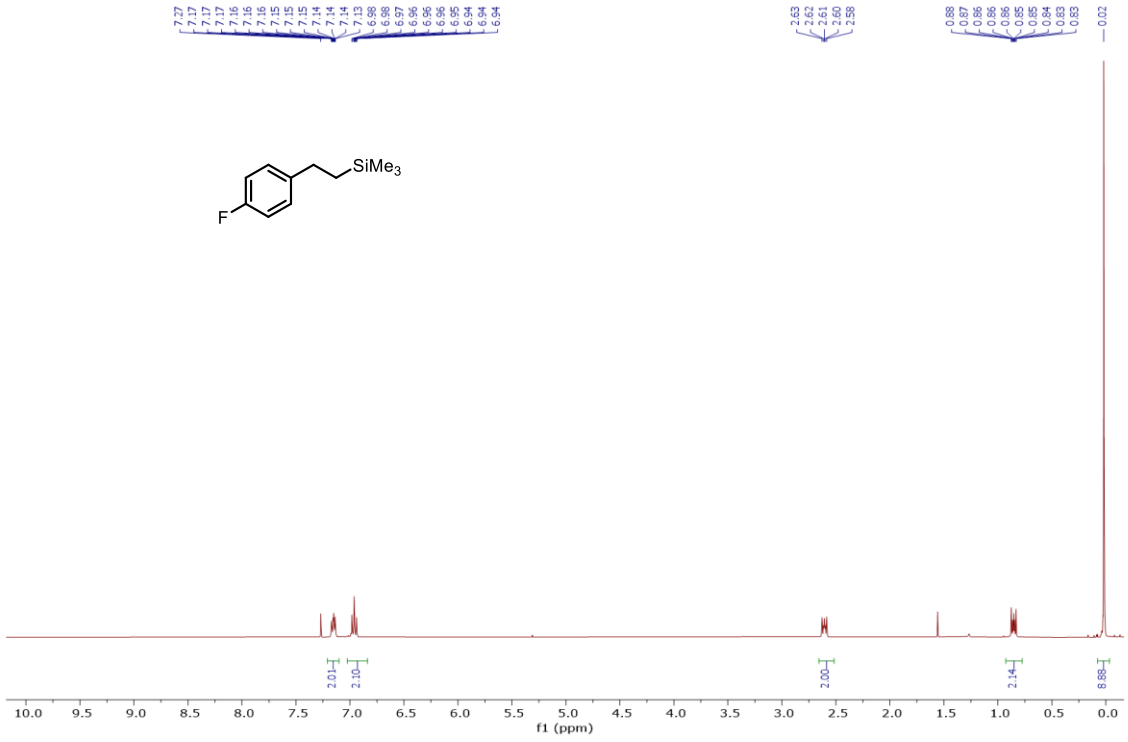


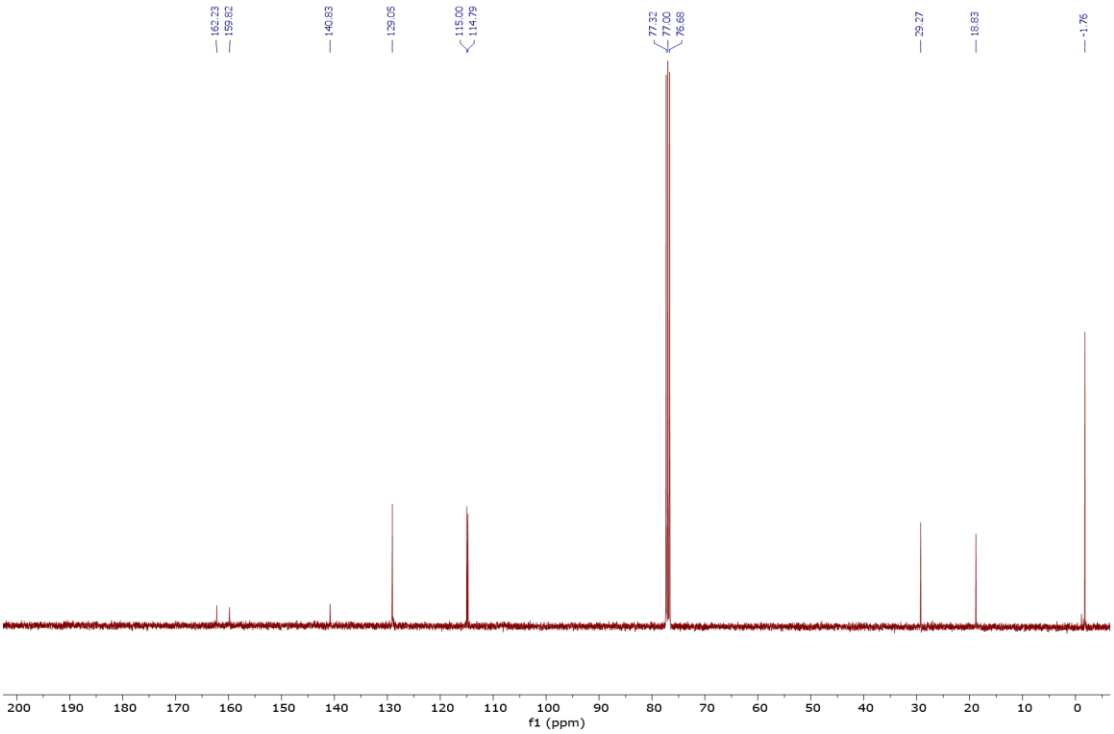

1-(Trifluoromethyl)-4-[2-(trimethylsilyl)ethyl]benzene **4.19** ($CDCl_3$, 400 MHz for $^1H$ NMR, 100 MHz for $^{13}C$ NMR)

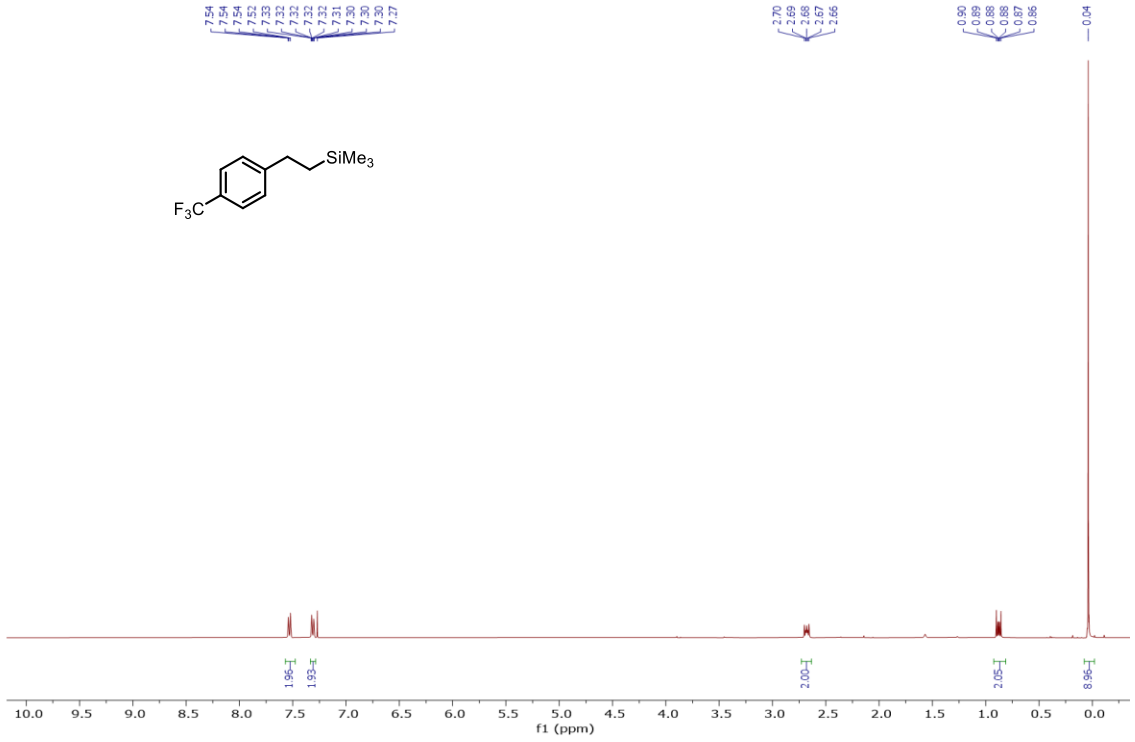


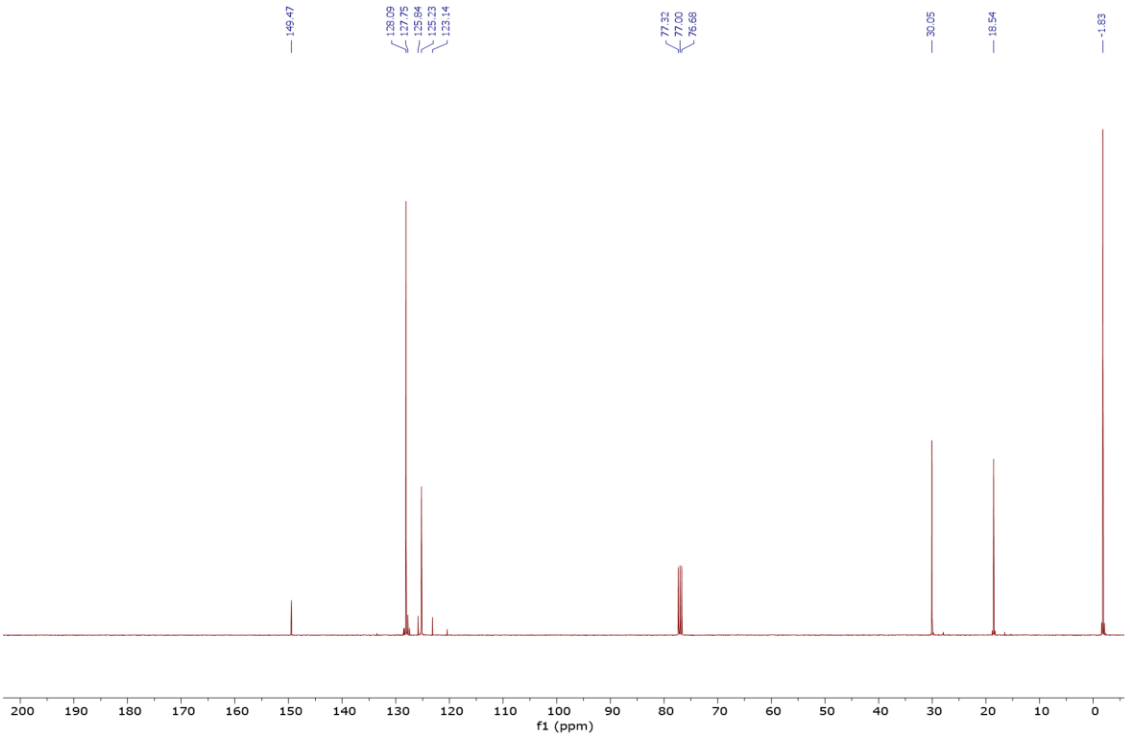

1-Chloro-4-[2-(trimethylsilyl)ethyl]benzene **4.20** ($CDCl_3$, 400 MHz for $^1H$ NMR, 100 MHz for $^{13}C$ NMR)

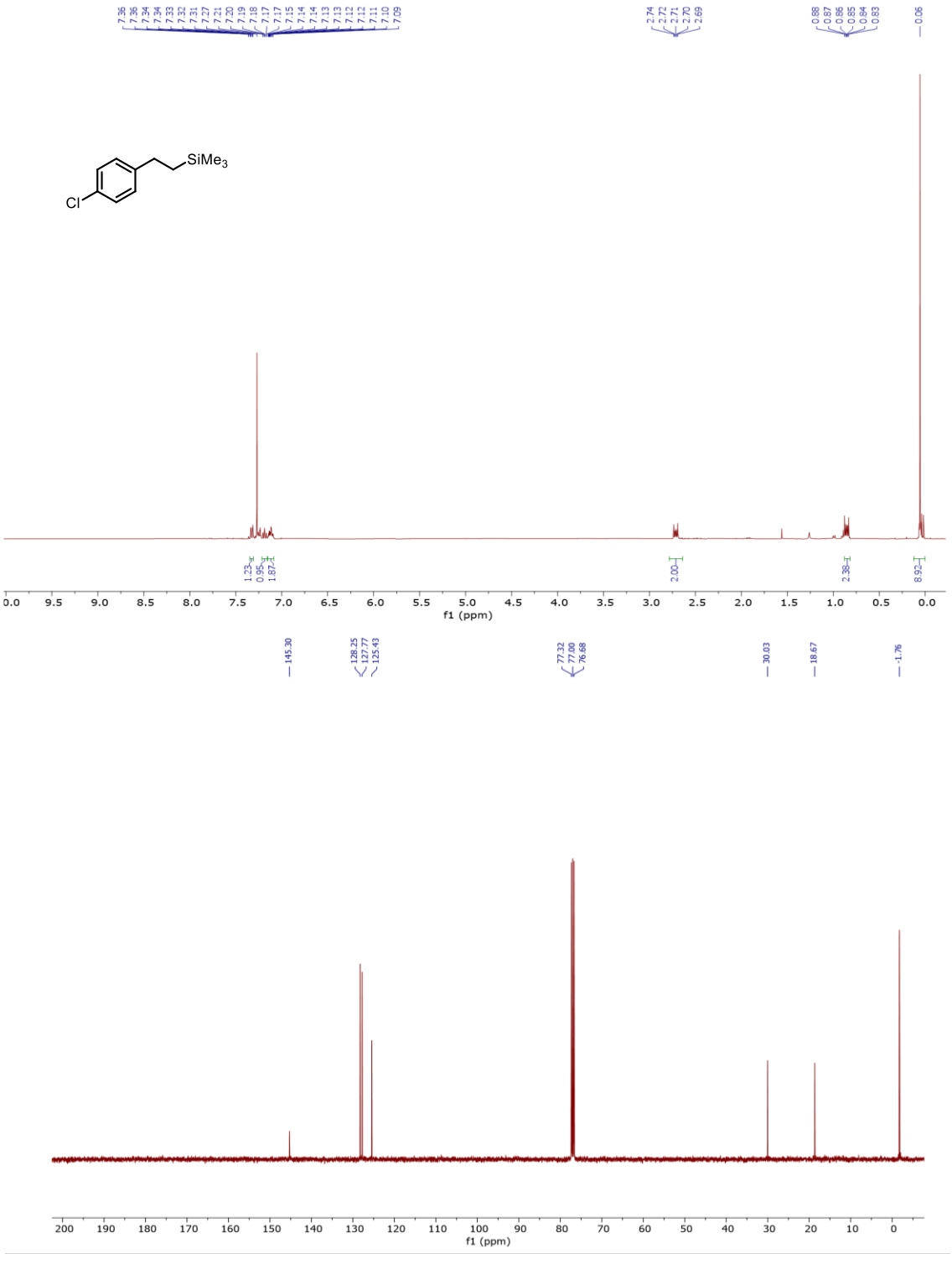

1-Methoxy-4-[2-(trimethylsilyl)ethyl]benzene **4.21** ($CDCl_3$, 400 MHz for $^1H$ NMR, 100 MHz for $^{13}C$ NMR)

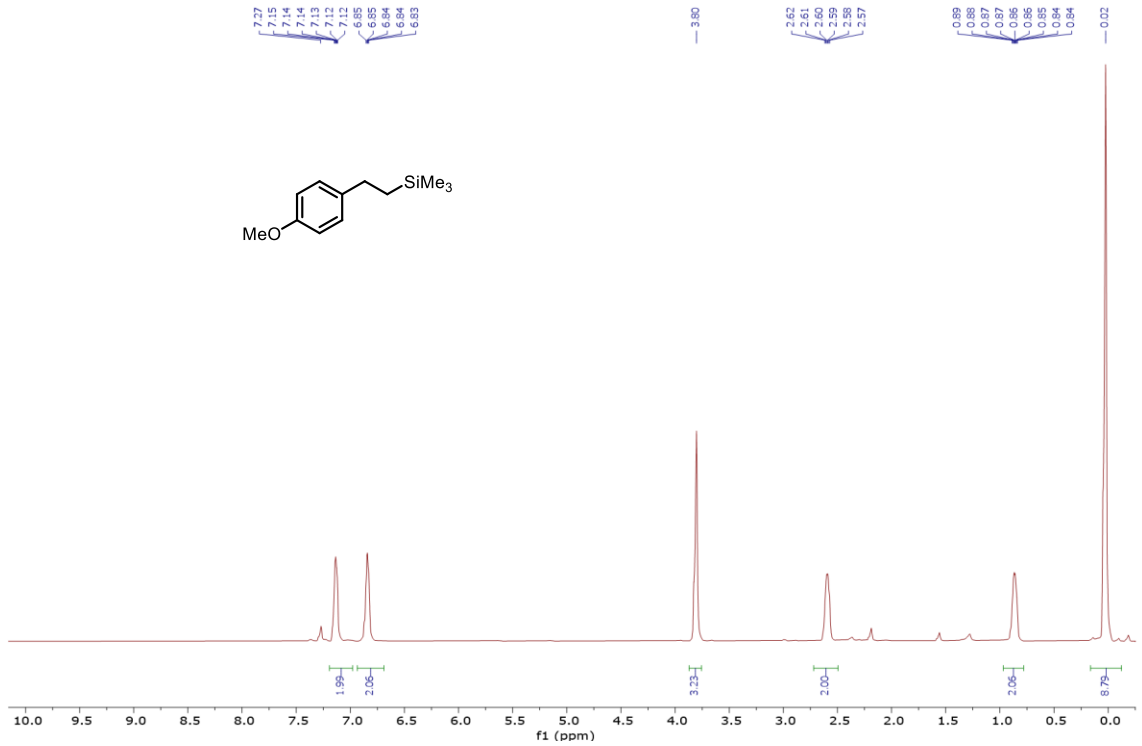


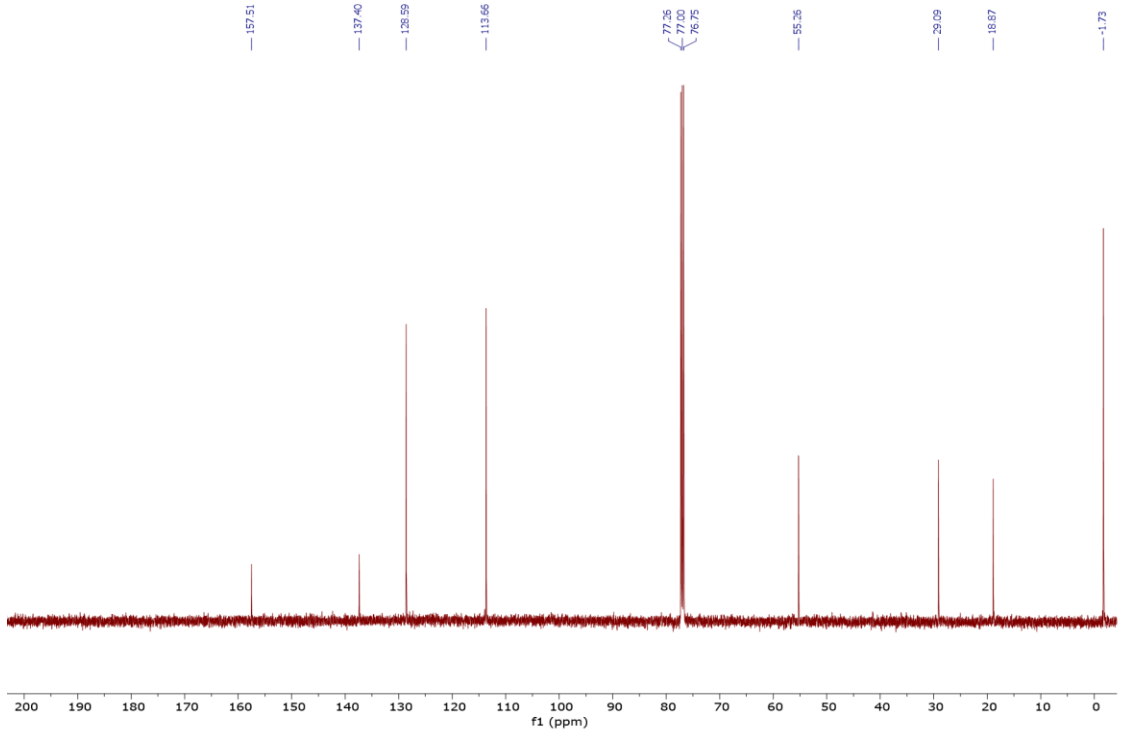

1-[2-(Trimethylsilyl)propyl]naphthalene **4.22** ($CDCl_3$, 400 MHz for $^1H$ NMR, 100 MHz for $^{13}C$ NMR)

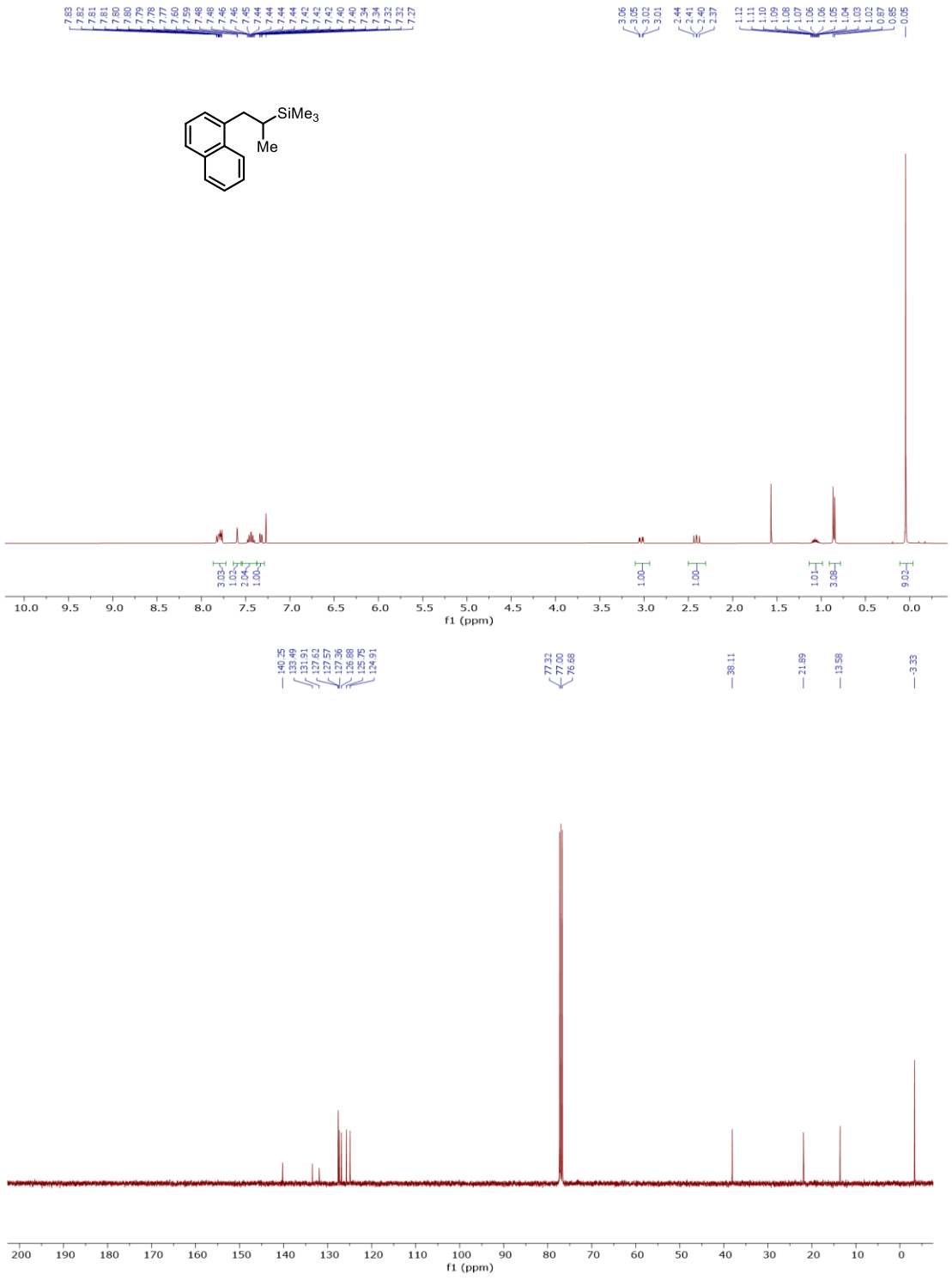

1-(2-Methylphenyl)-2-methyl-2-trimethylsilylethane **4.23** ($CDCl_3$, 500 MHz for $^1H$ NMR, 126 MHz for $^{13}C$ NMR)

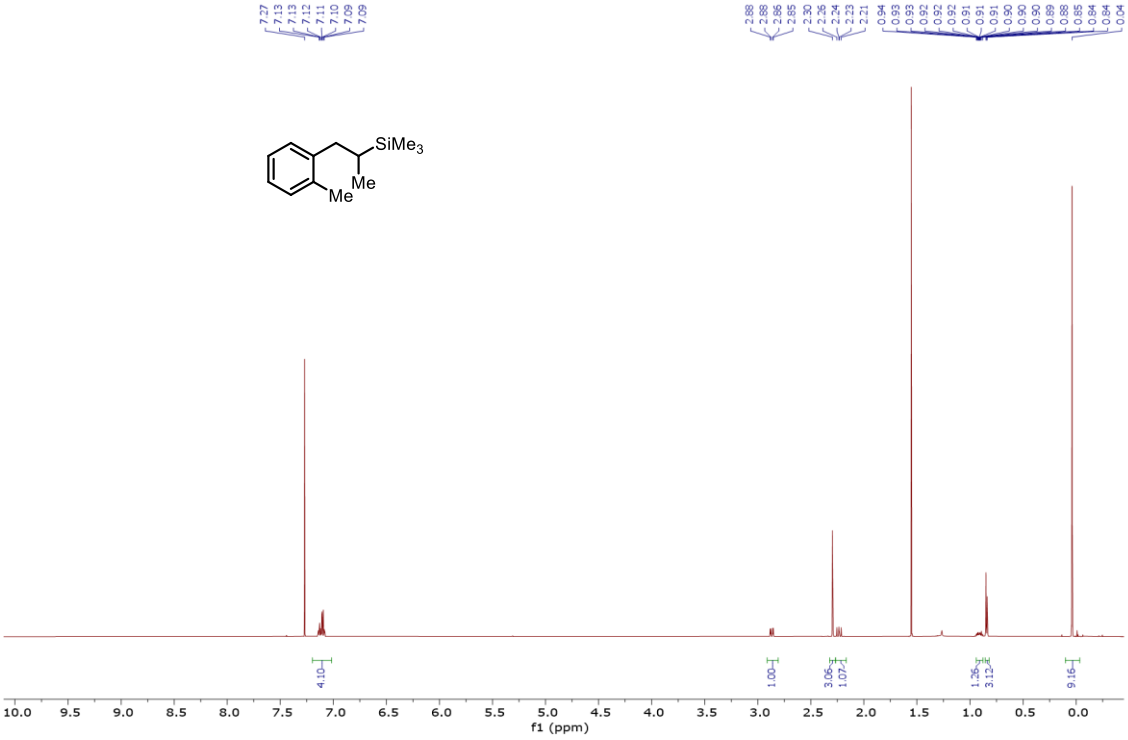


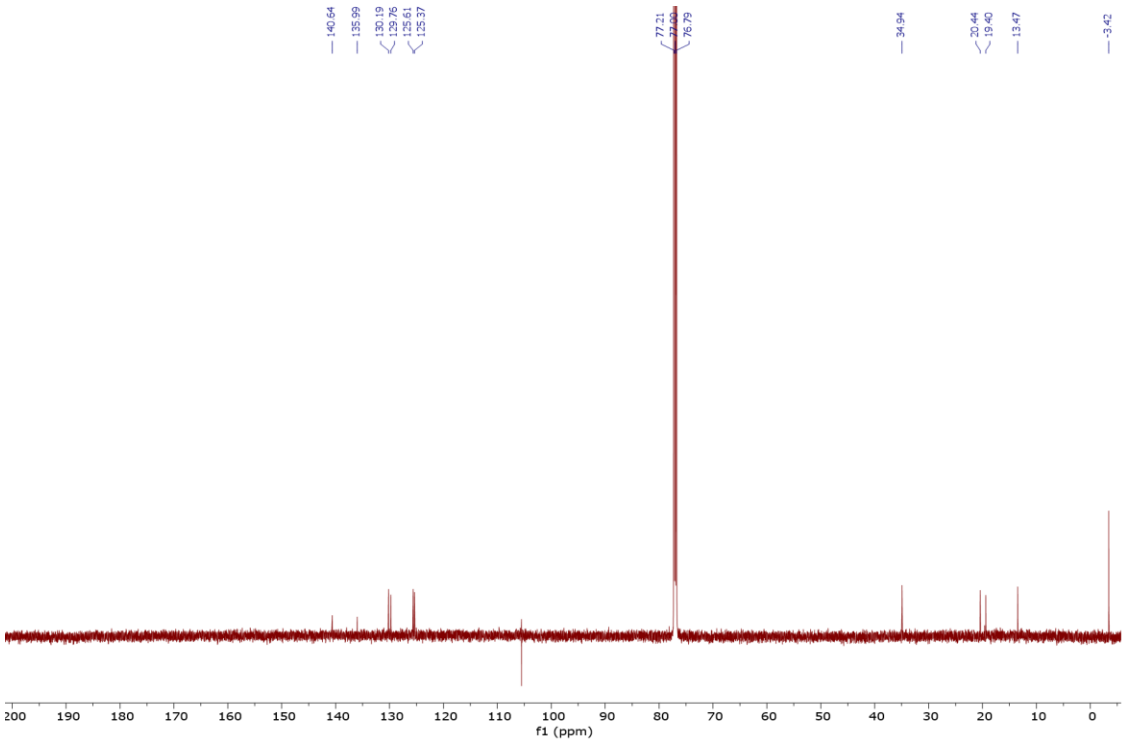

1-Methoxy-4-[2-(trimethylsilyl)ethyl]benzene **4.24** ($CDCl_3$, 400 MHz for $^1H$ NMR, 100 MHz for $^{13}C$ NMR)


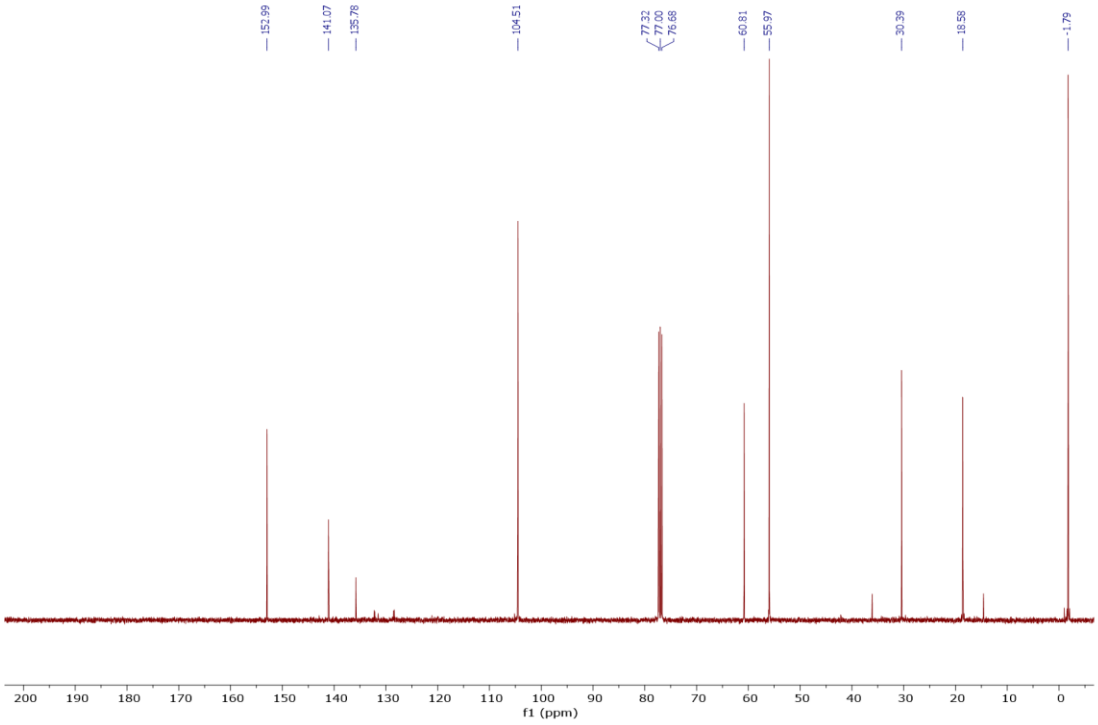

5-[2-(Trimethylsilyl)ethyl]benzo[*b*]thiophene **4.25** ($CDCl_3$, 400 MHz for $^1H$ NMR, 100 MHz for $^{13}C$ NMR)

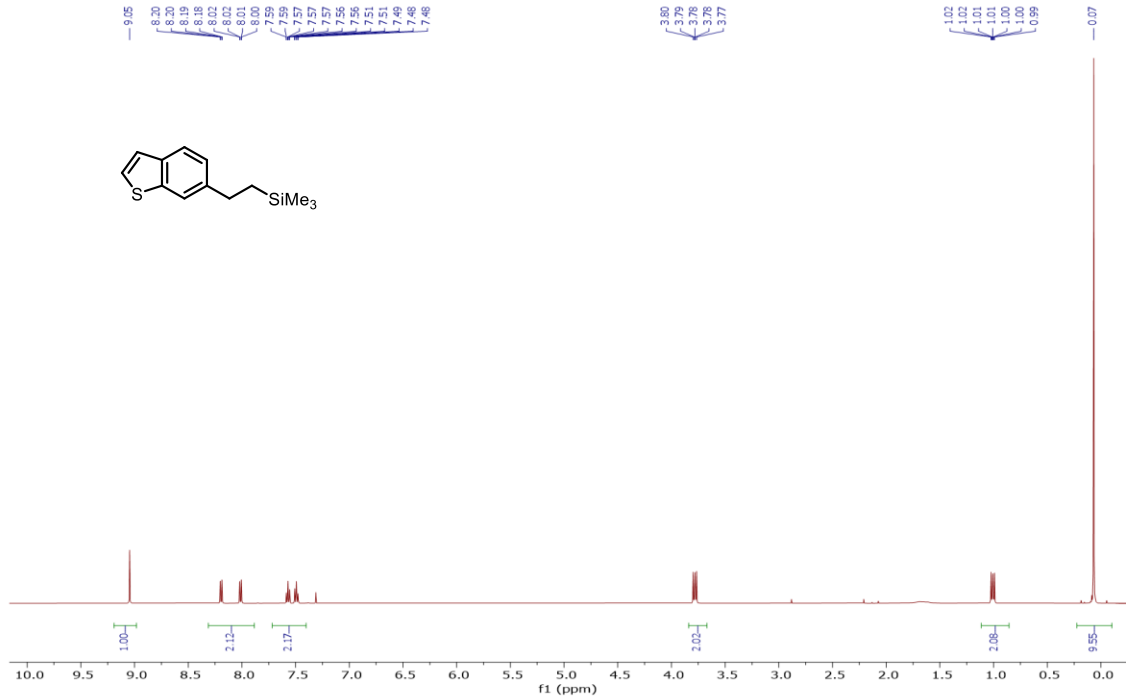


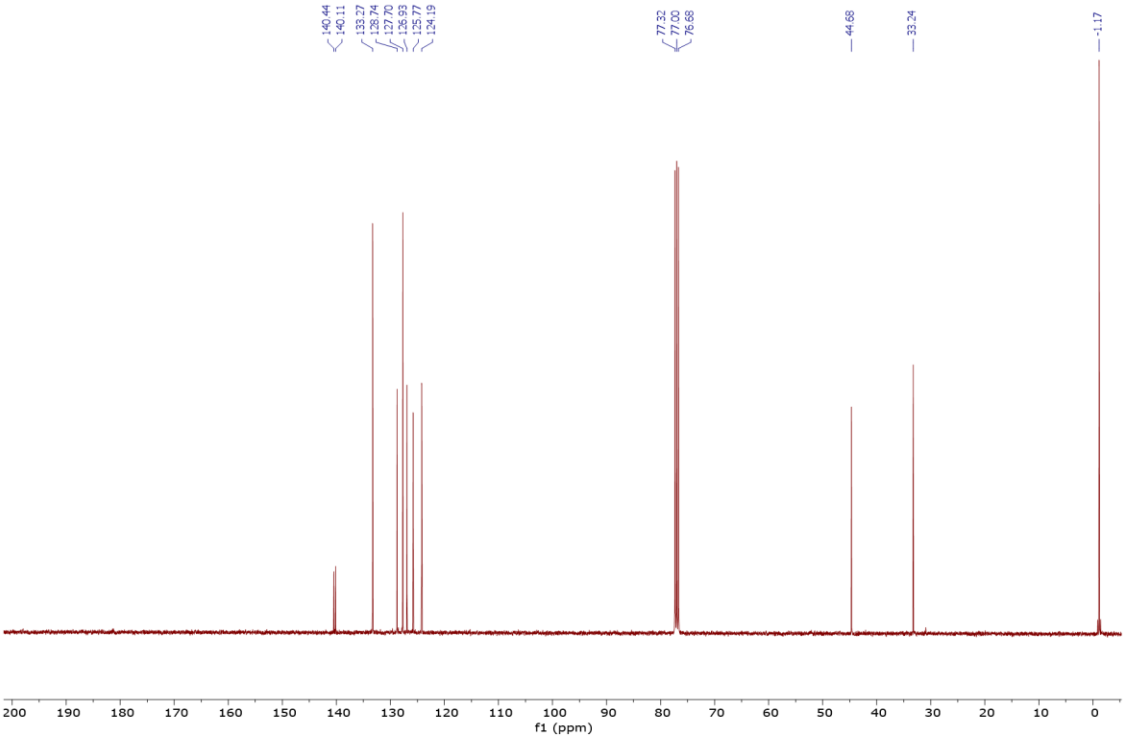

2-[2-(Trimethylsilyl)ethyl]benzofuran **4.26** ($CDCl_3$, 400 MHz for $^1H$ NMR, 100 MHz for $^{13}C$ NMR)

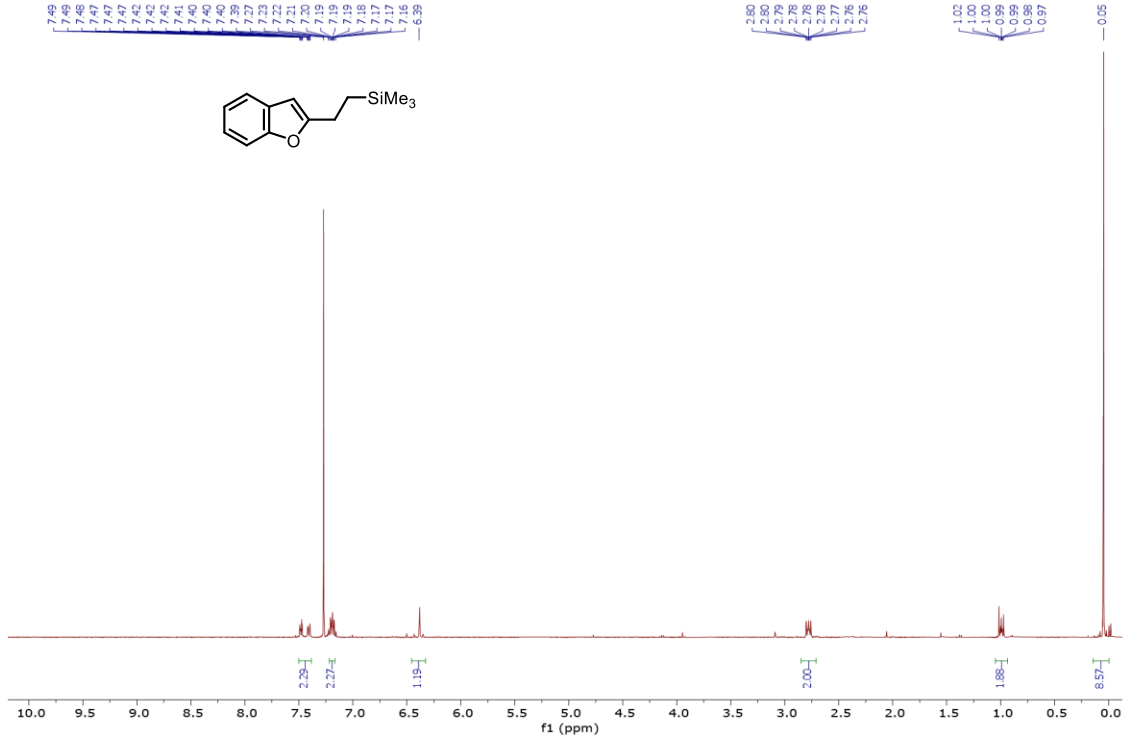


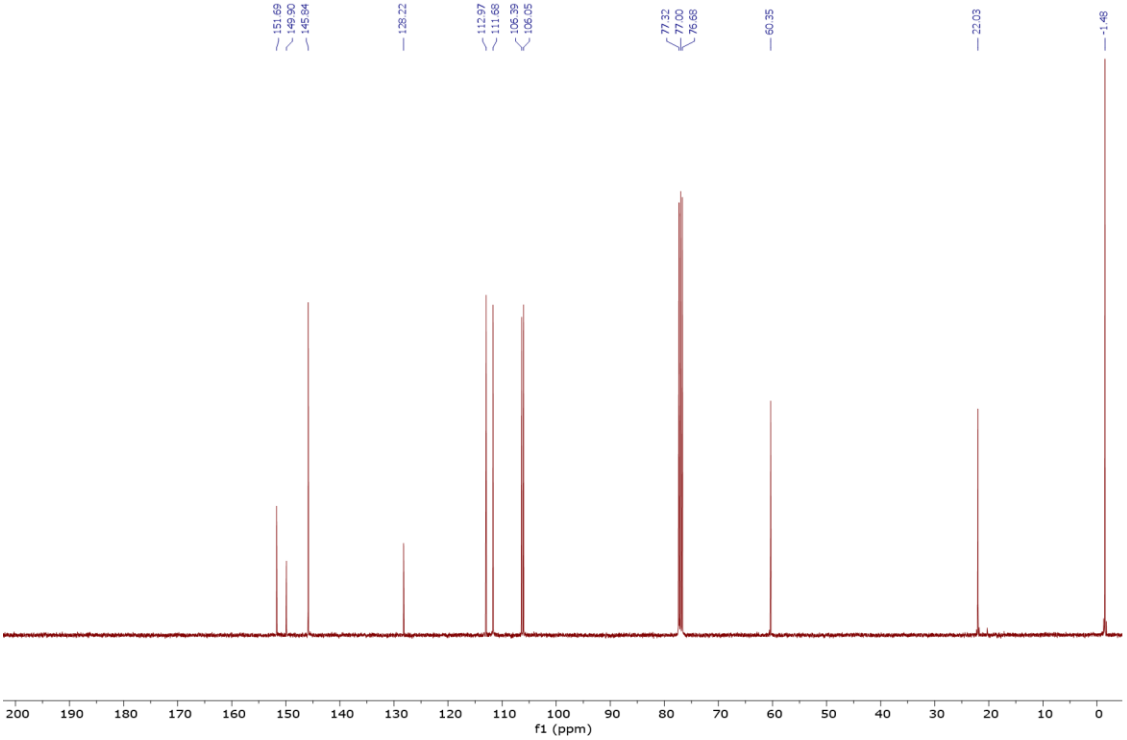

5-[1-(Trimethylsilyl)ethyl]-1,3-benzodioxole **4.27** ($CDCl_3$, 400 MHz for $^1H$ NMR, 100 MHz for $^{13}C$ NMR)

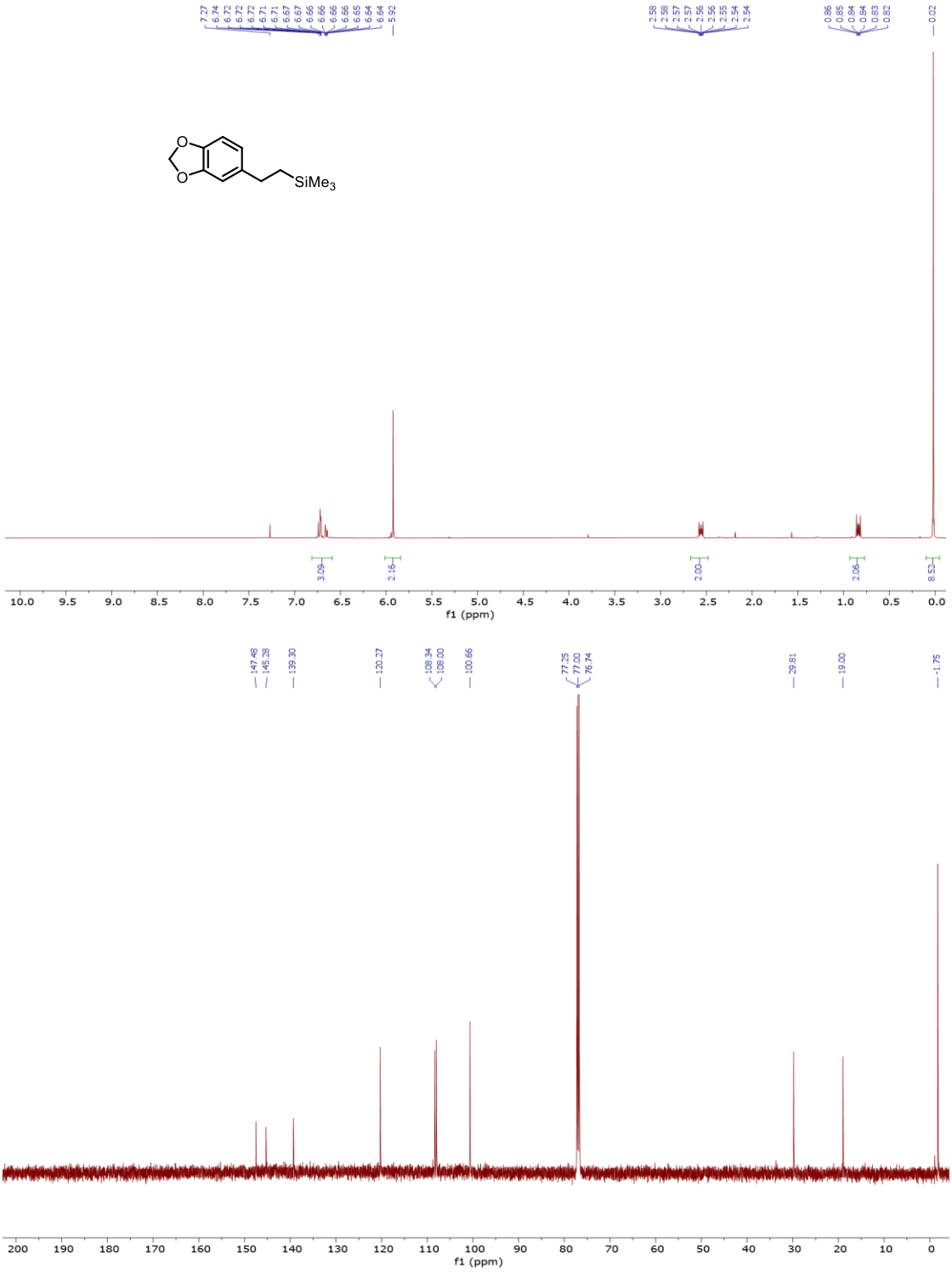

3-[2-(Trimethylsilyl)ethyl]pyridine **4.28** ($CDCl_3$, 400 MHz for $^1H$ NMR, 100 MHz for $^{13}C$ NMR)

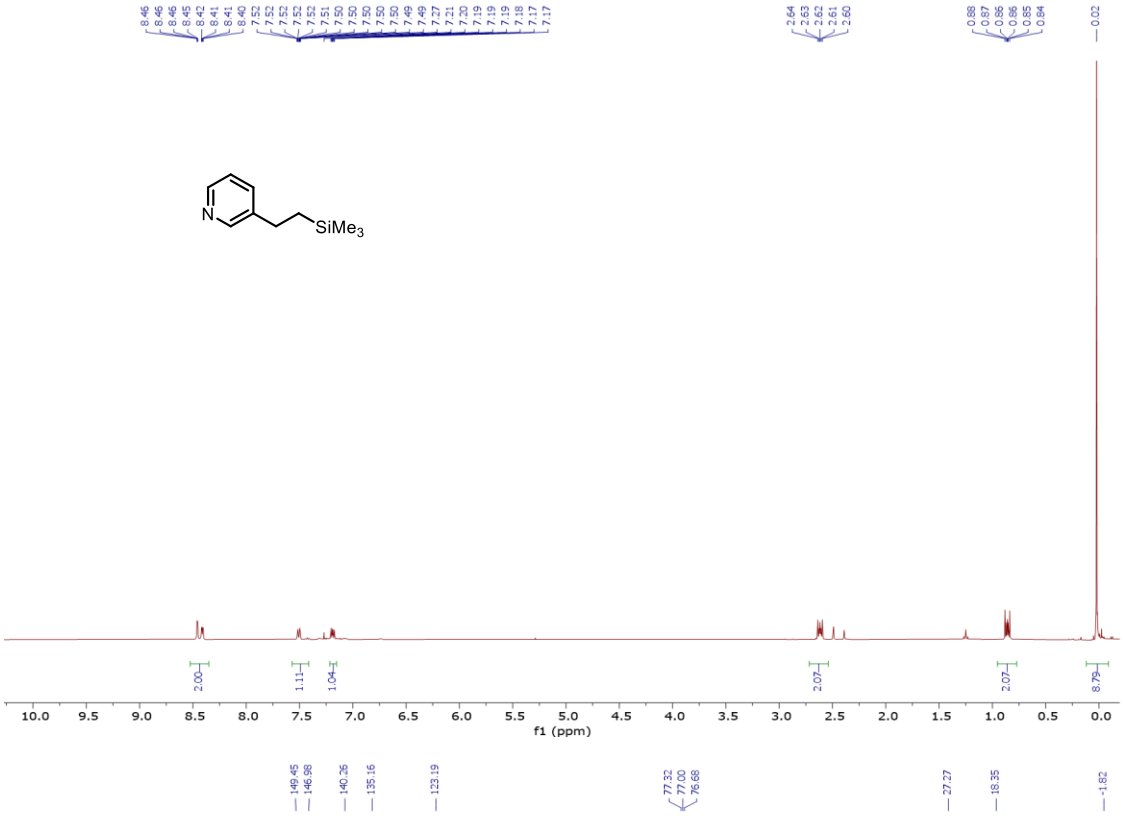


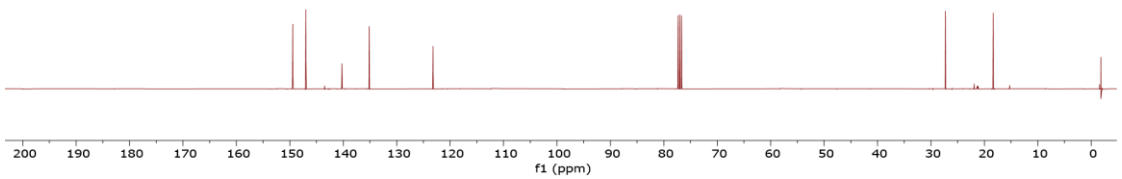

4-[4-[2-(Trimethylsilyl)ethyl]phenyl]morpholine **4.29** ($CDCl_3$, 400 MHz for $^1H$ NMR, 100 MHz for $^{13}C$ NMR)

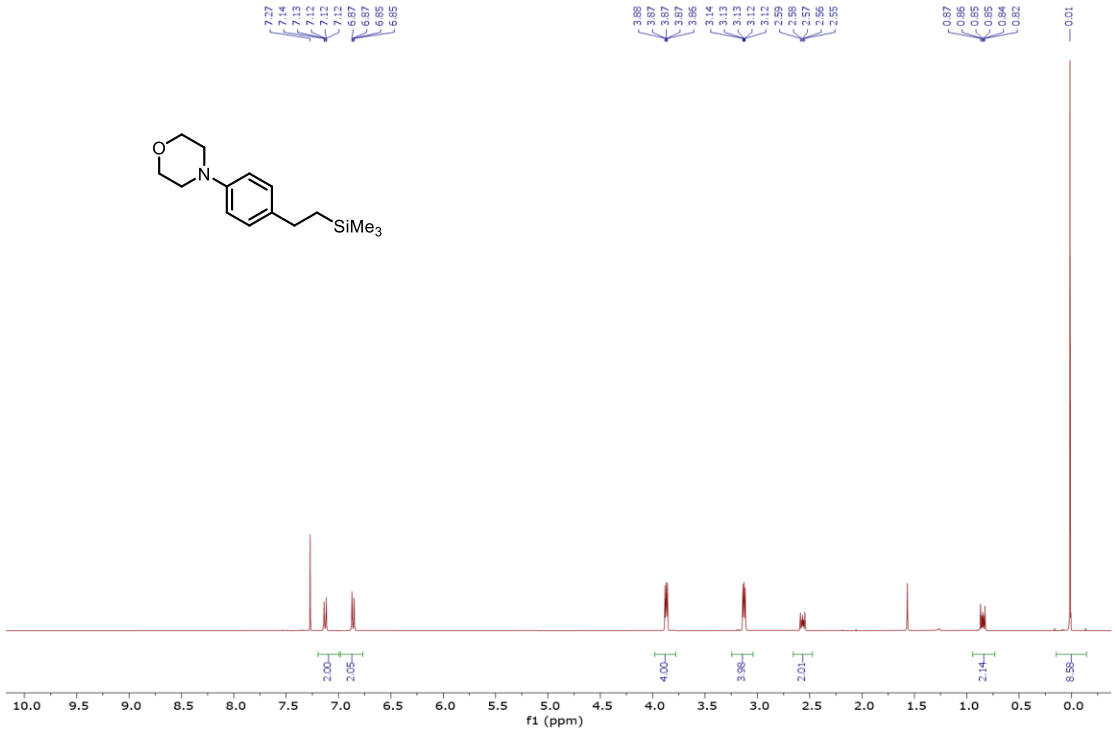


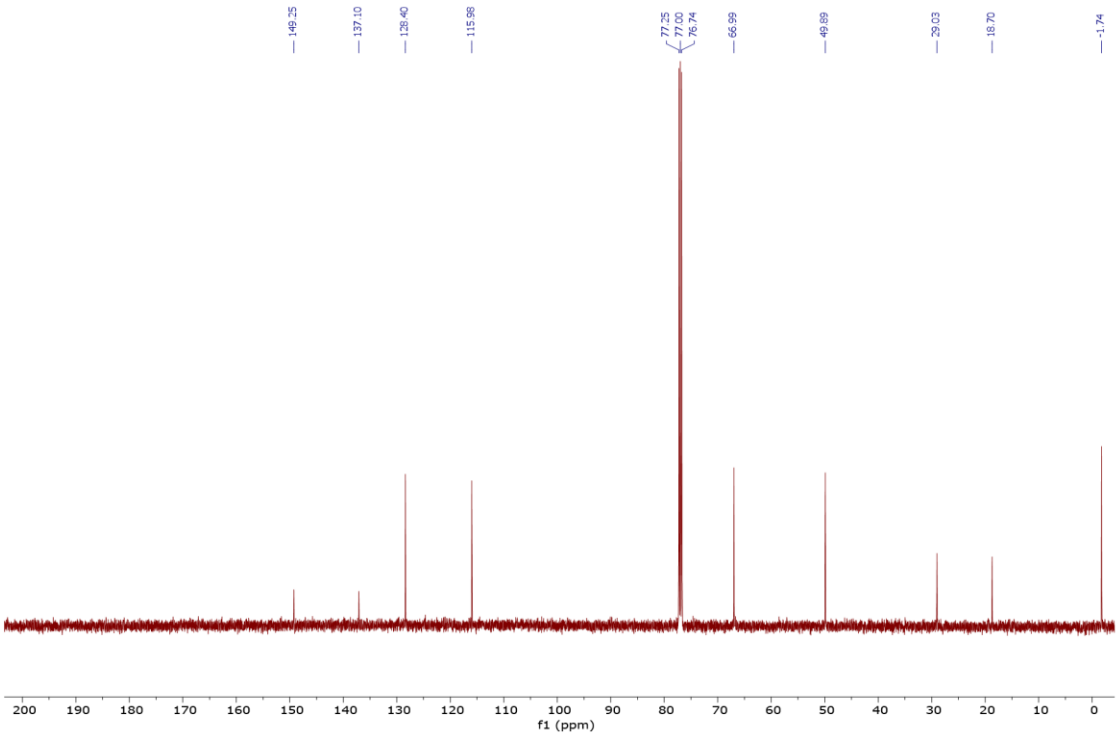

9-[4-[2-(Trimethylsilyl)ethyl]phenyl]-9*H*-carbazole **4.30** ($CDCl_3$, 400 MHz for $^1H$ NMR, 100 MHz for $^{13}C$ NMR)

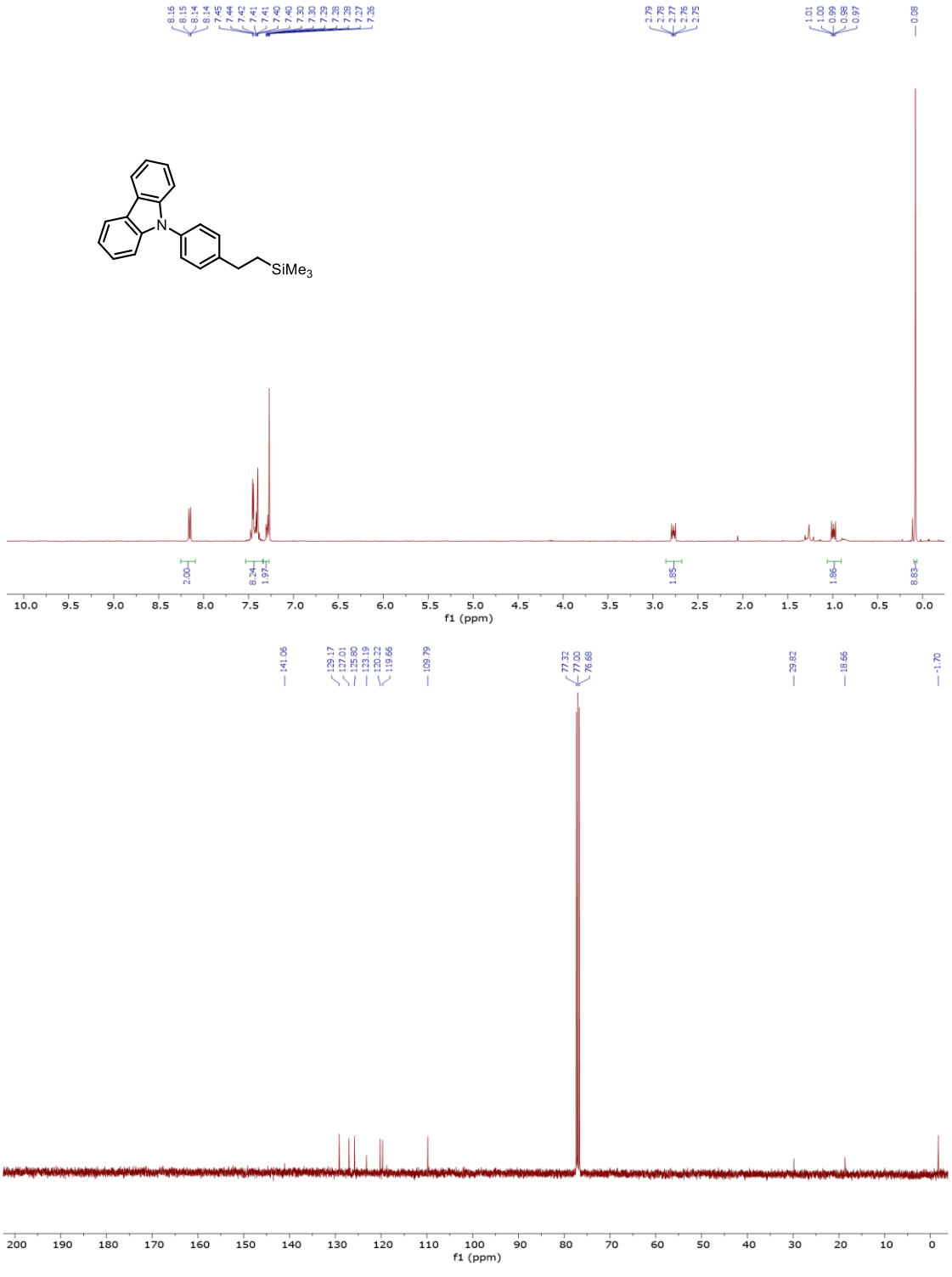

[3-(Trimethylsilyl)propyl]benzene **4.31** ($CDCl_3$, 400 MHz for $^1H$ NMR, 100 MHz for $^{13}C$ NMR)

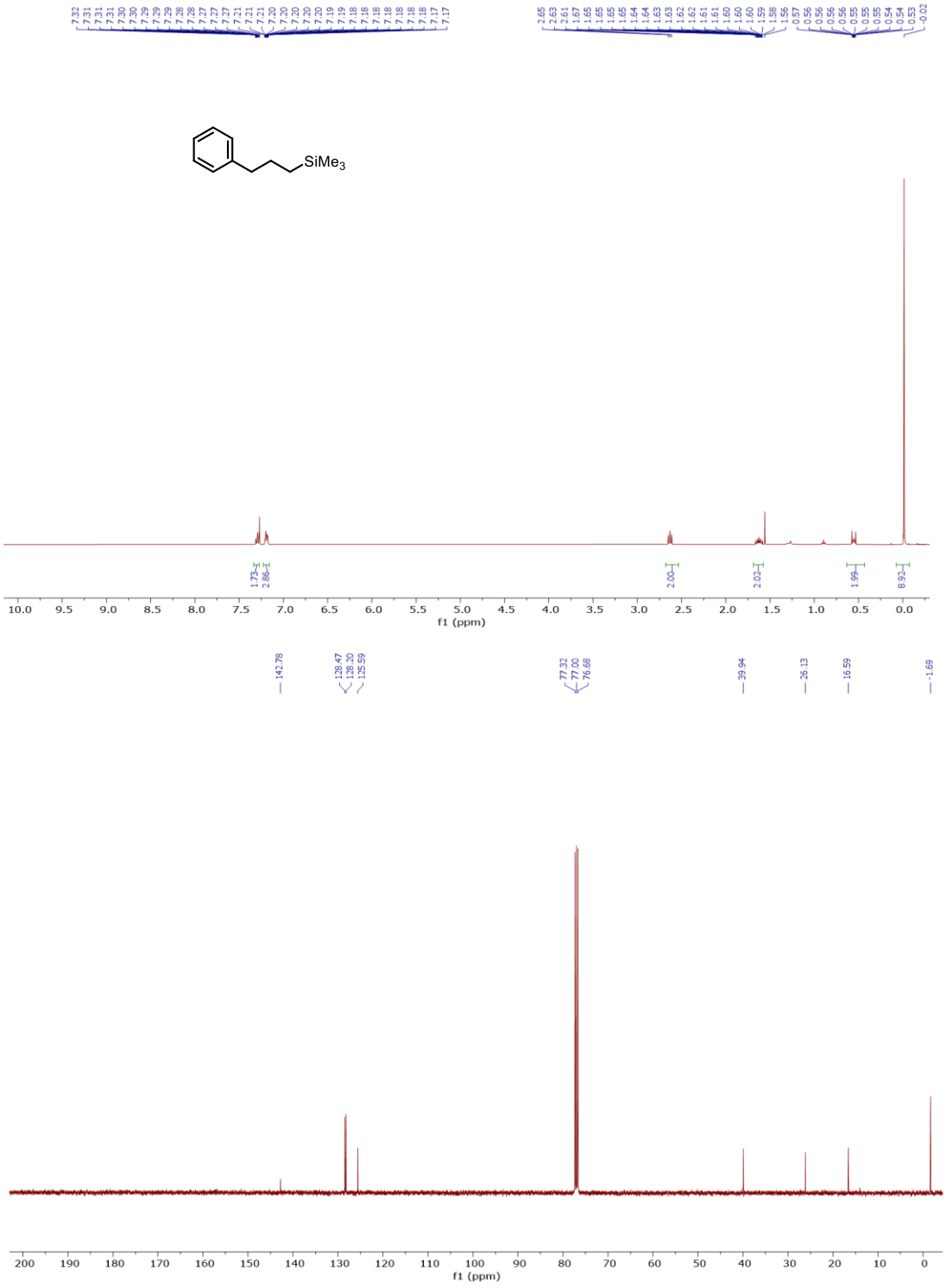

1-Phenyl-2-triethylsilylethane **4.32** ($CDCl_3$, 400 MHz for $^1H$ NMR, 100 MHz for $^{13}C$ NMR)

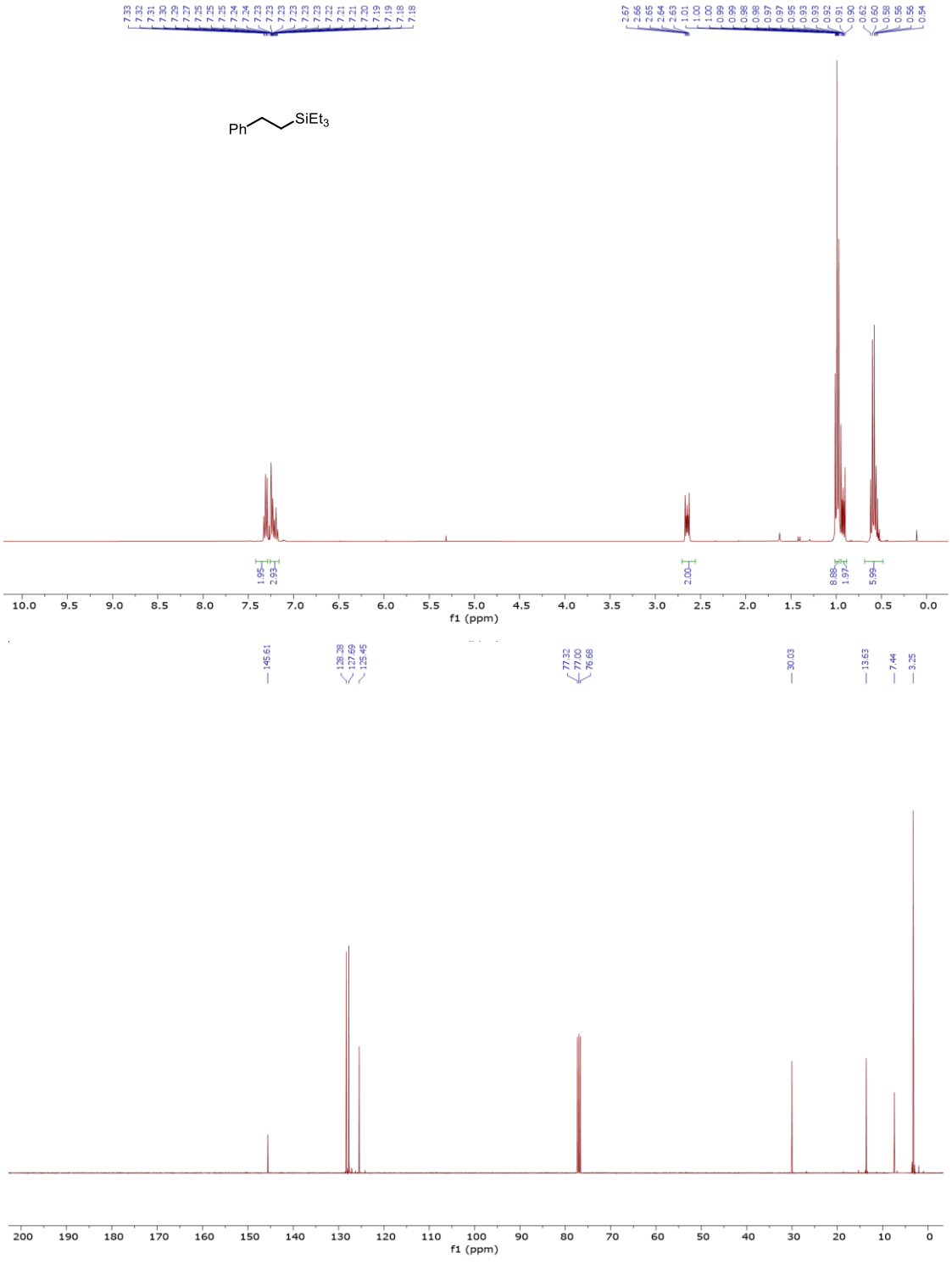

[Dimethyl(2-phenylethyl)silyl]benzene **4.33** ($CDCl_3$, 400 MHz for $^1H$ NMR, 100 MHz for $^{13}C$ NMR)

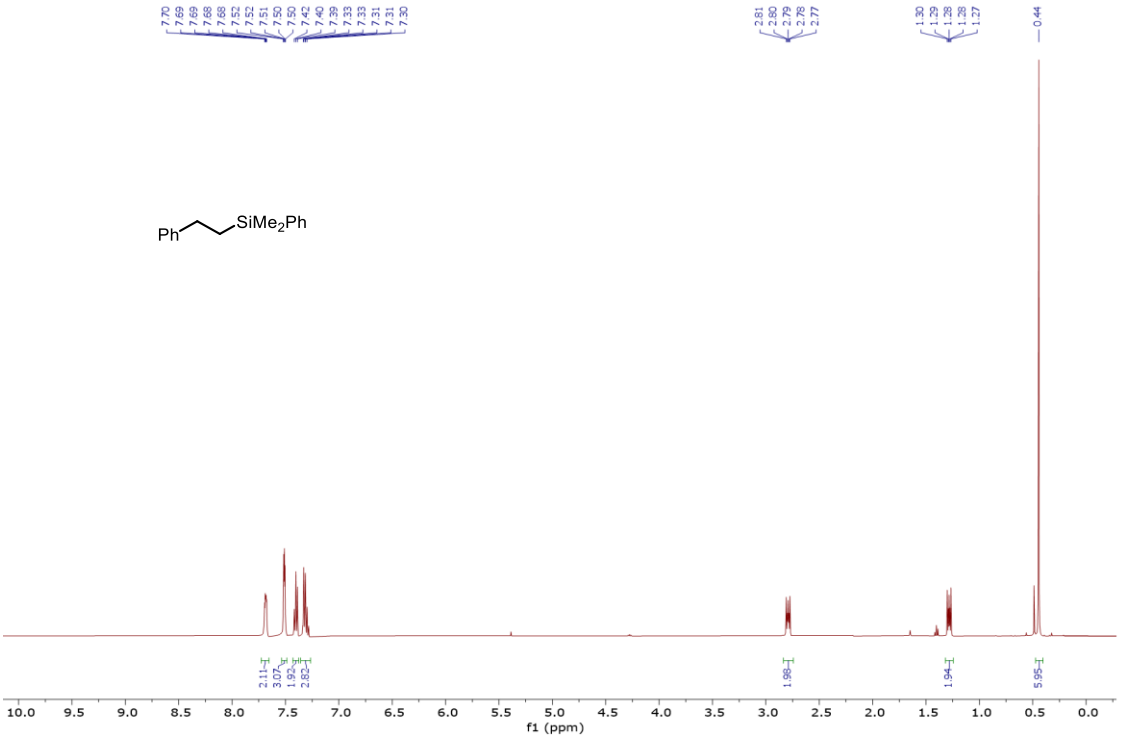


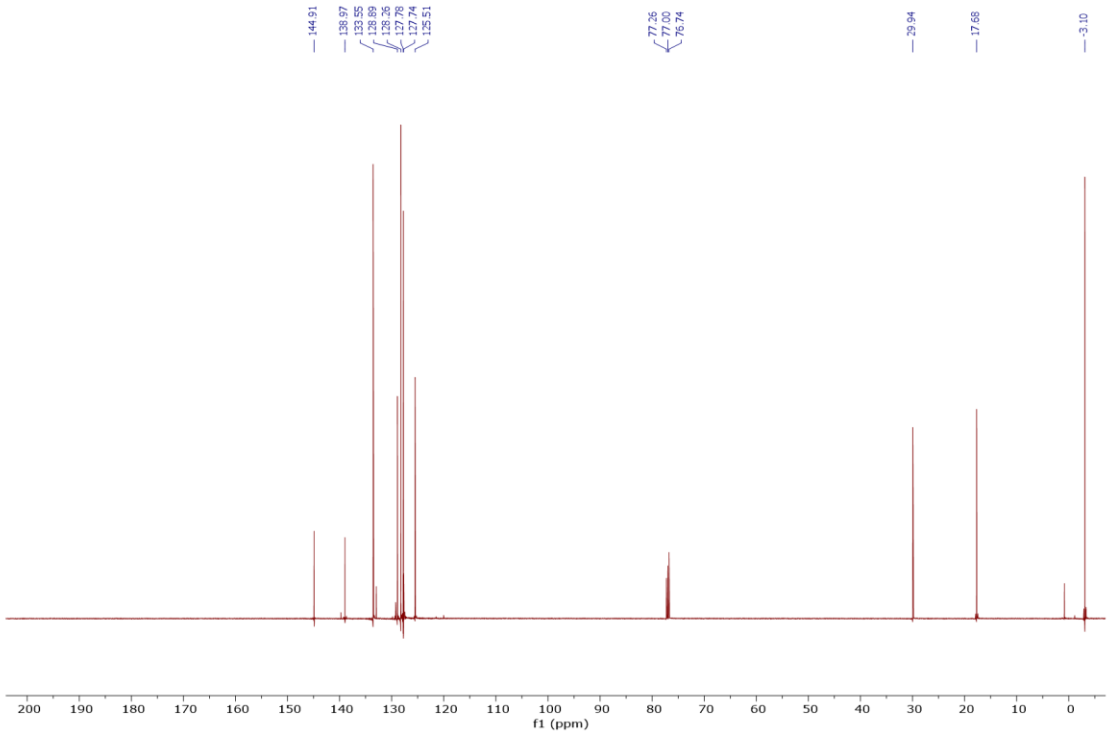

[3-[(1,1-Dimethylethyl)dimethylsilyl]propyl]benzene **4.34** ($CDCl_3$, 400 MHz for $^1H$ NMR, 100 MHz for $^{13}C$ NMR)

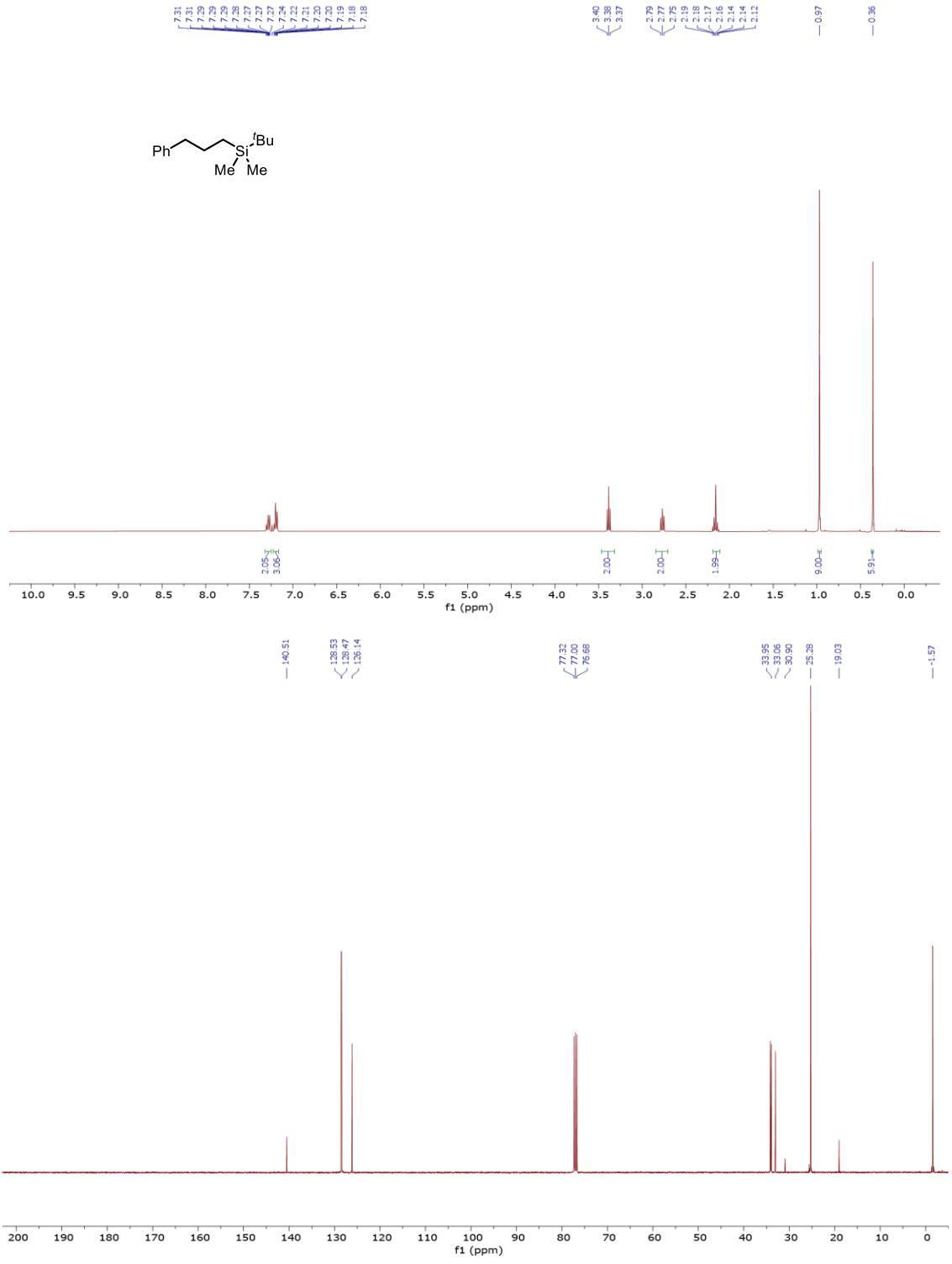

1-Methoxy-2-phenyl-3-(trimethylsilyl)propane **4.2** ($CDCl_3$, 400 MHz for $^1H$ NMR, 100 MHz for $^{13}C$ NMR)

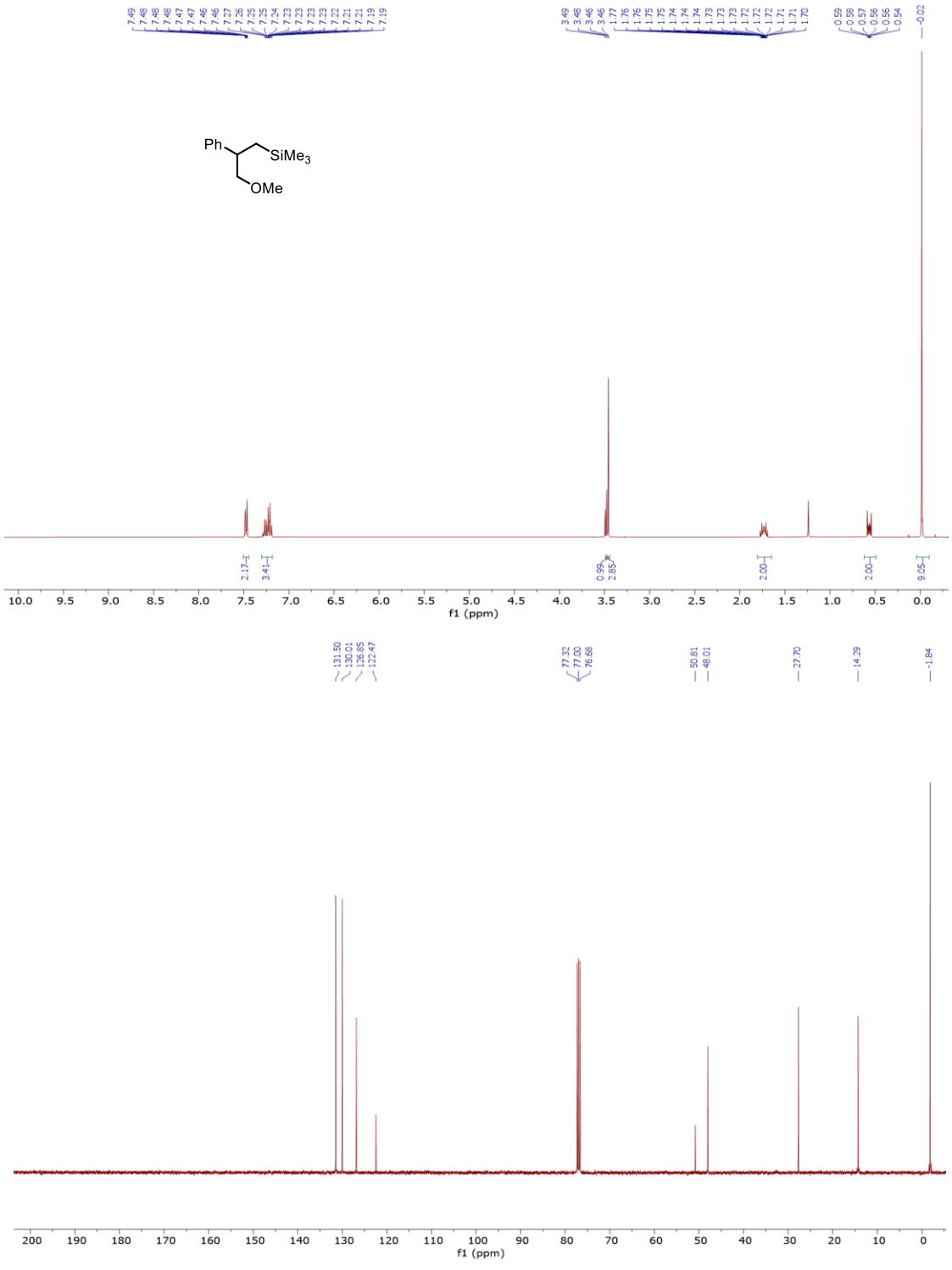

1,3-Diphenyl-4-trimethylsilylbutane **4.3** ($CDCl_3$, 500 MHz for $^1H$ NMR, 126 MHz for $^{13}C$ NMR)

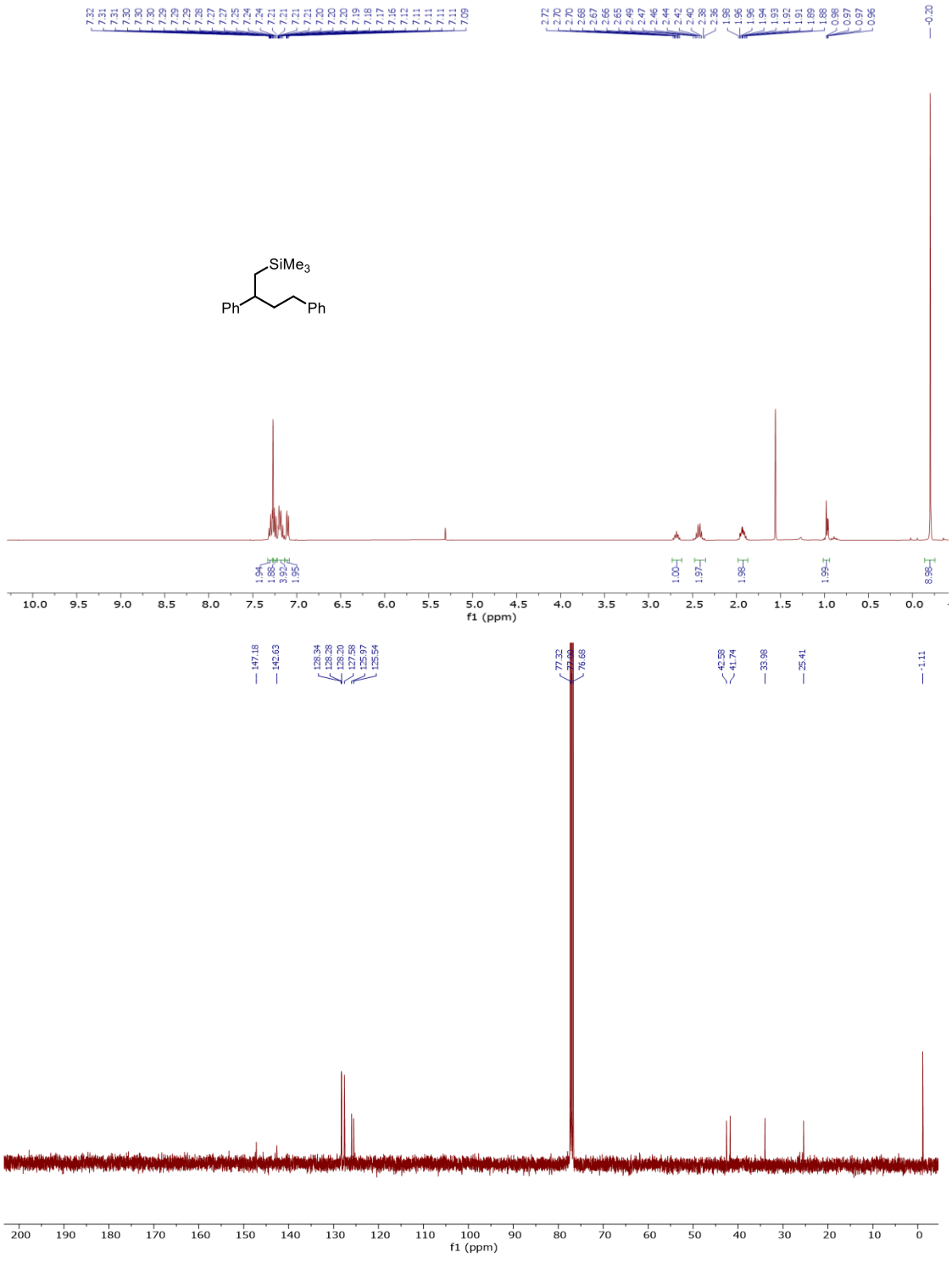

[1-Methyl-2-(trimethylsilyl)ethyl]benzene **4.4** ($CDCl_3$, 400 MHz for $^{1}H$ NMR, 100 MHz for $^{13}C$ NMR)

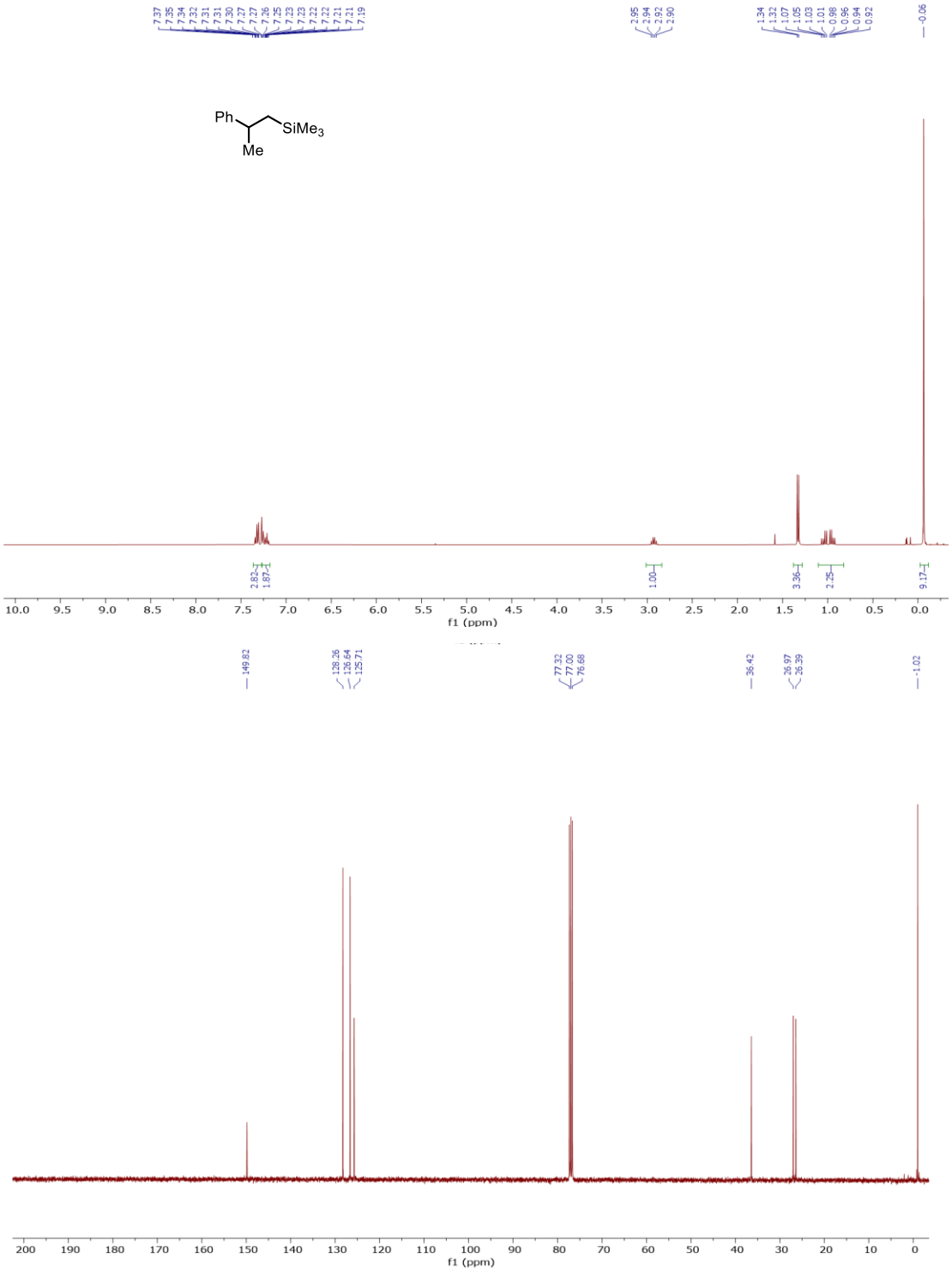

[2-Methyl-3-phenyl-4-(trimethylsilyl)]butane **4.5** ($CDCl_3$, 500 MHz for $^1H$ NMR, 126 MHz for $^{13}C$ NMR)

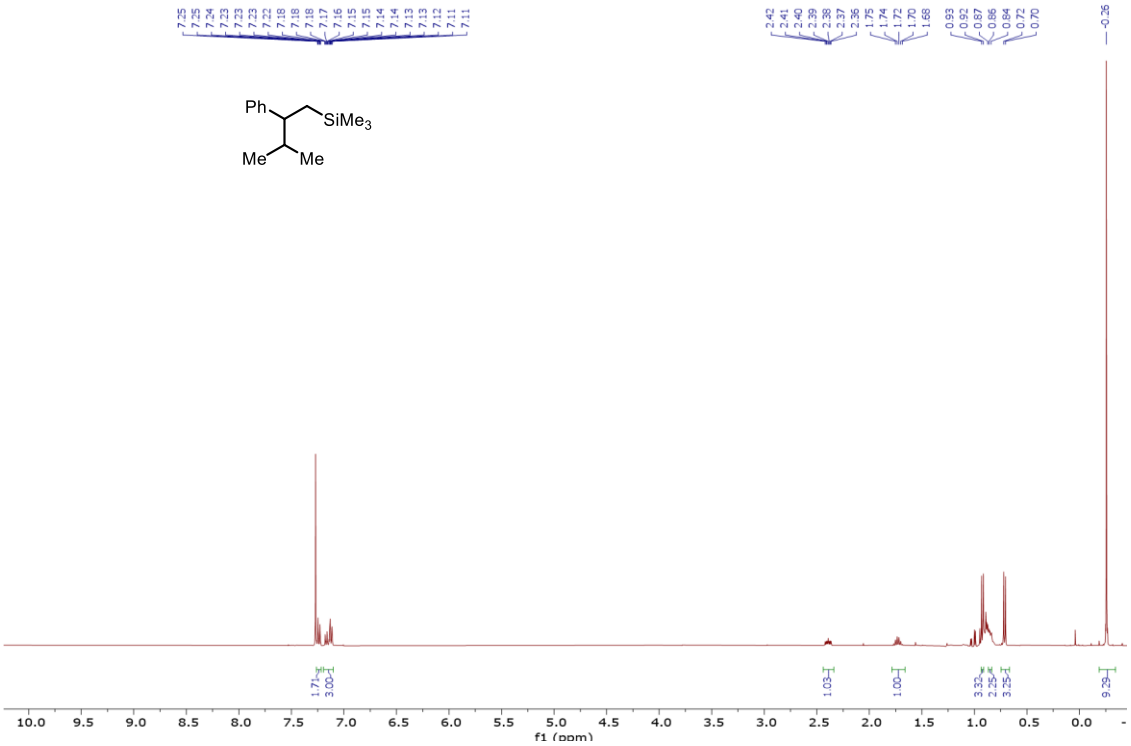


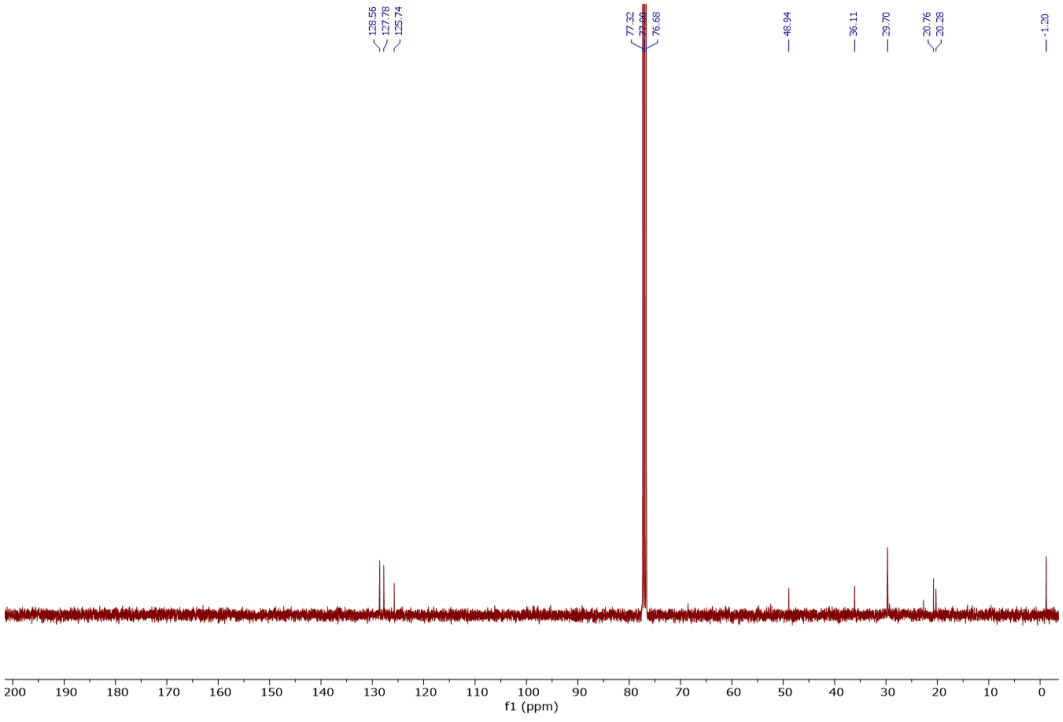

(2-Cyclohexyl-2-phenylethyl)trimethylsilane **4.6** ($CDCl_3$, 500 MHz for $^1H$ NMR, 126 MHz for $^{13}C$ NMR)

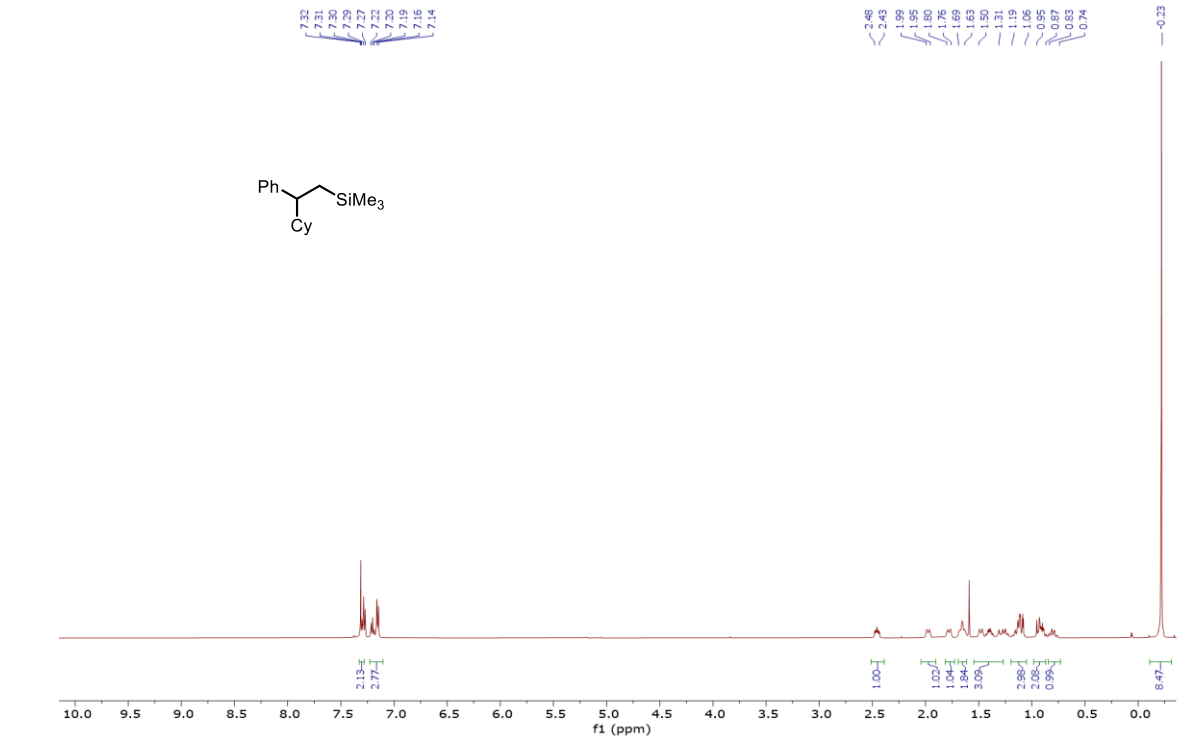


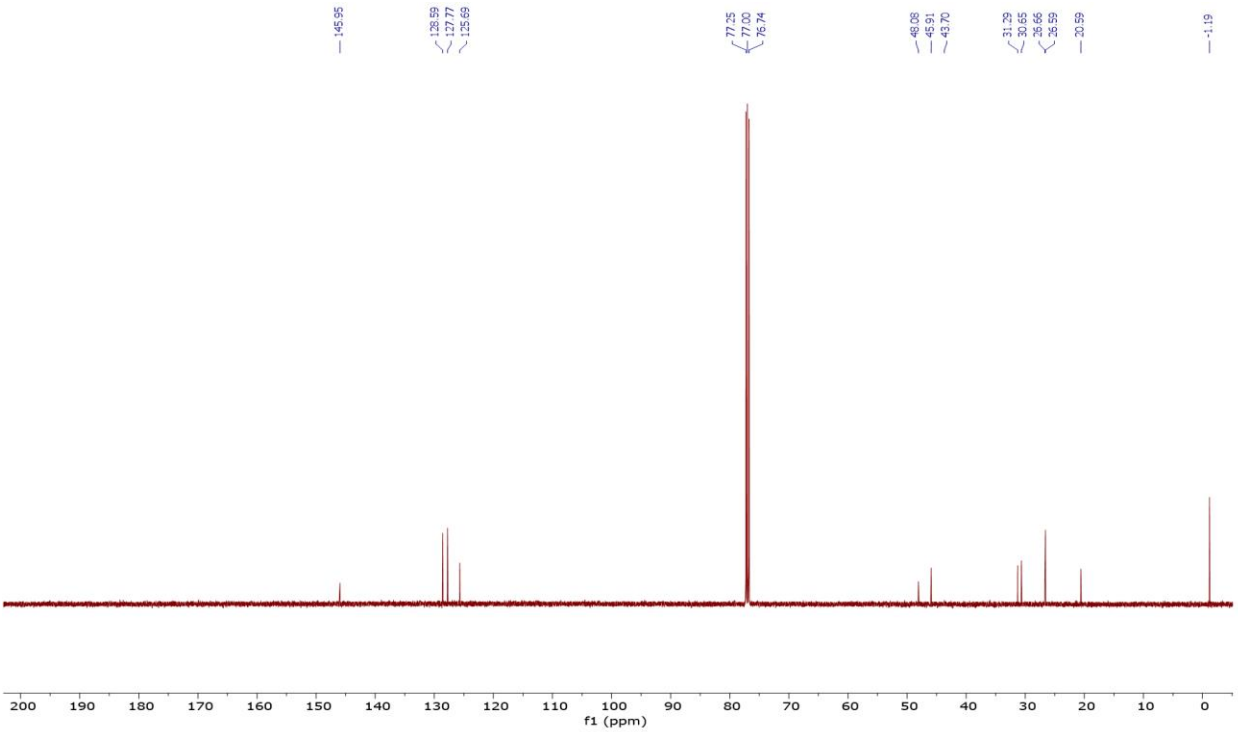

(2,2-Diphenylethyl)trimethylsilane **4.7** ($CDCl_3$, 400 MHz for $^1H$ NMR, 100 MHz for $^{13}C$ NMR)

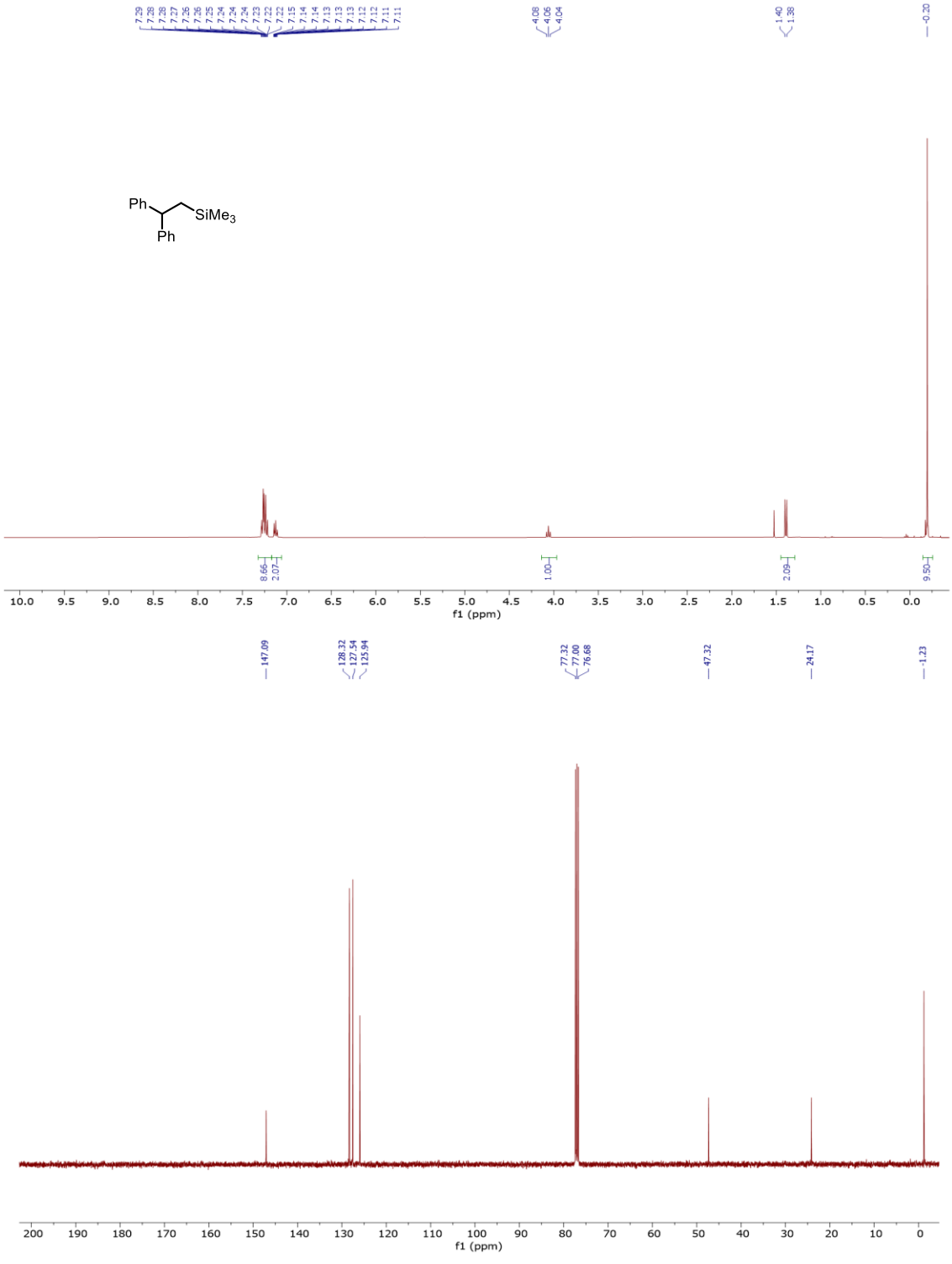

1,3-Diphenyl-4-trimethylsilylbutane **4.8** ($CDCl_3$, 400 MHz for $^1H$ NMR, 100 MHz for $^{13}C$ NMR)

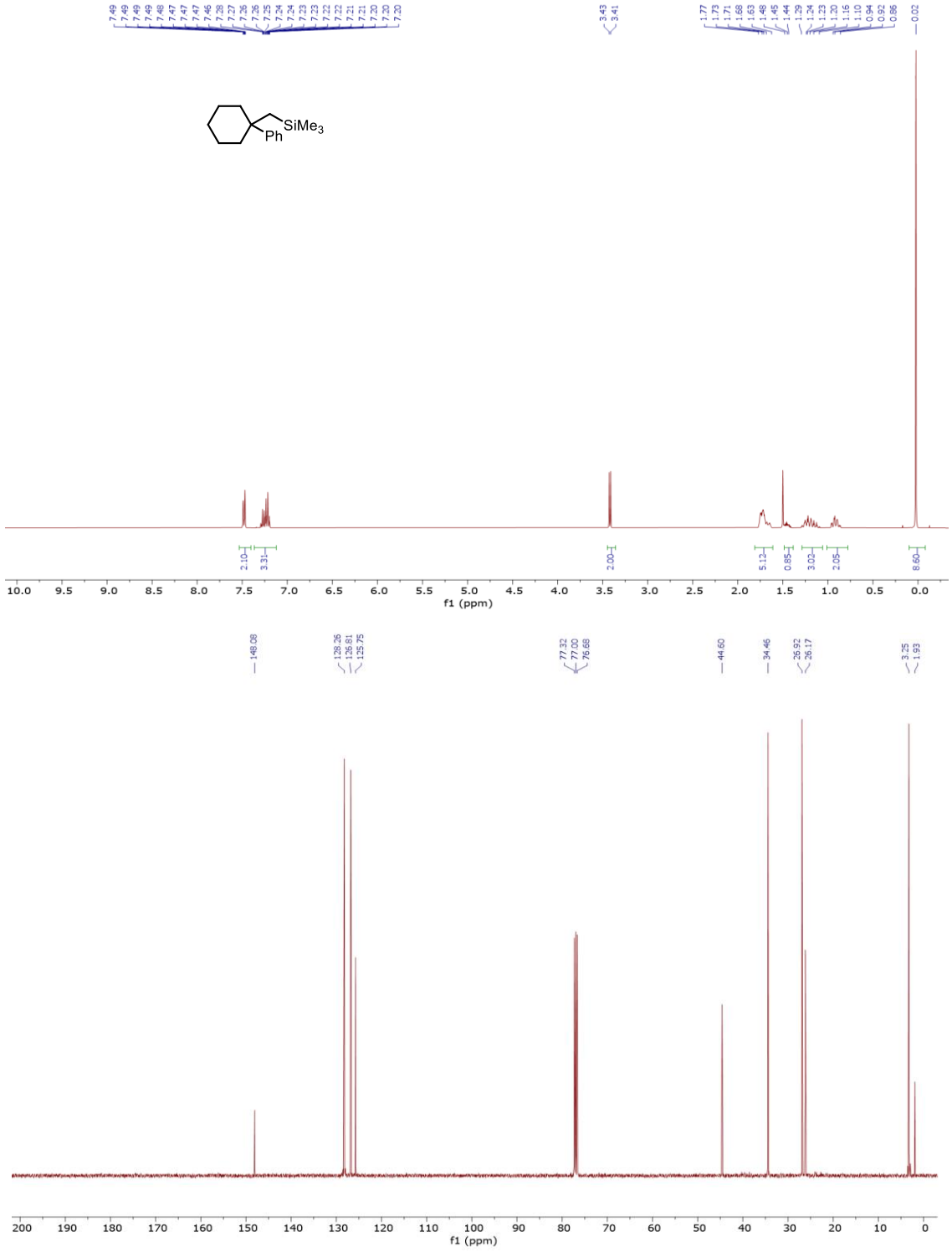

1-(Phenyl)-2-methyl-2-trimethylsilylethane **4.10** ($CDCl_3$, 500 MHz for $^1H$ NMR, 126 MHz for $^{13}C$ NMR)

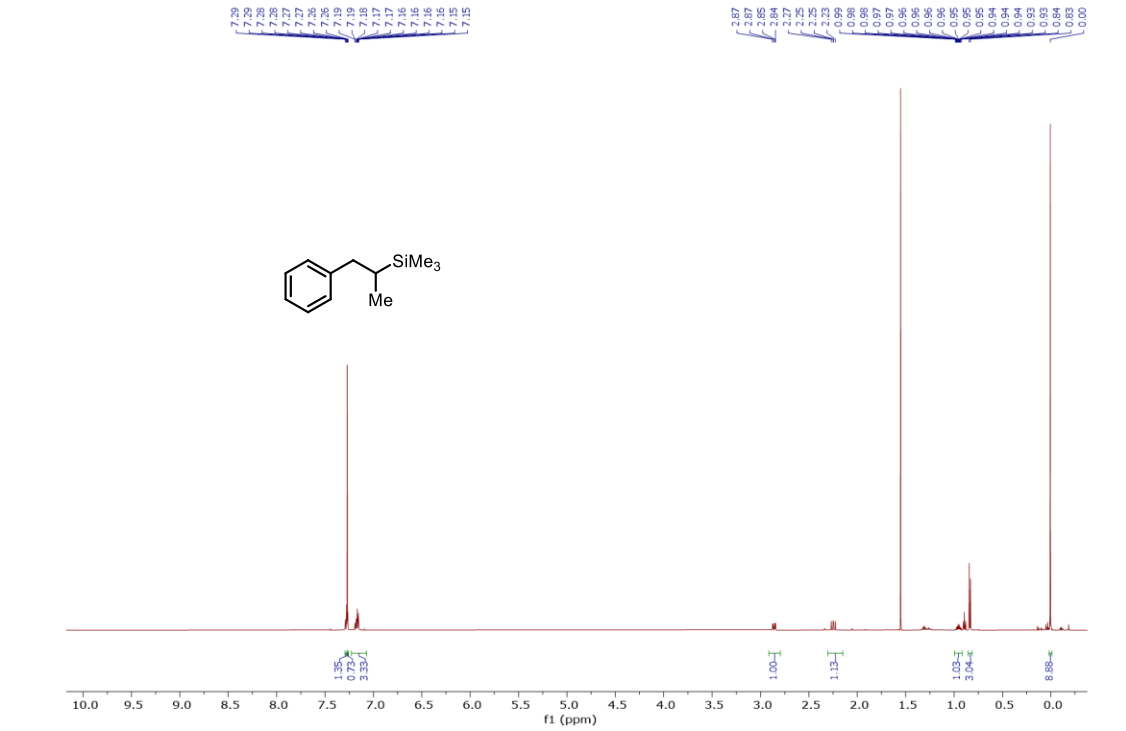


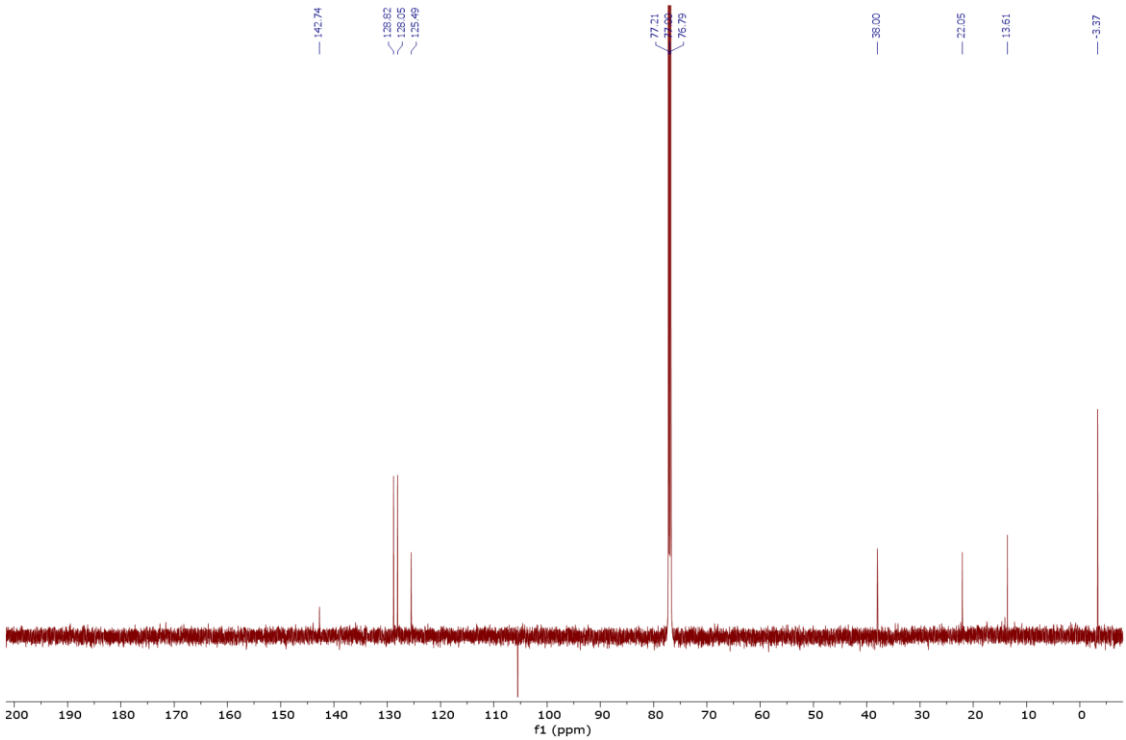

3-[2-Trimethylsilyl)-1-phenethyl]-thiazole **4.12** ($CDCl_3$, 400 MHz for $^1H$ NMR, 100 MHz for $^{13}C$ NMR)

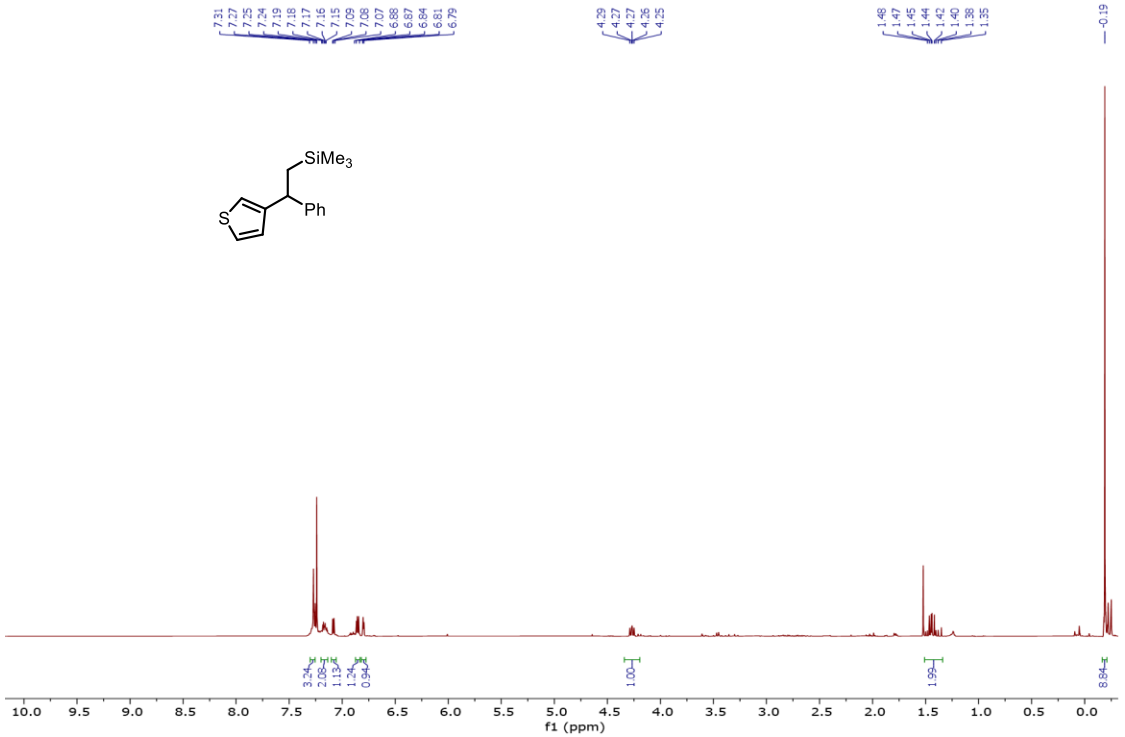


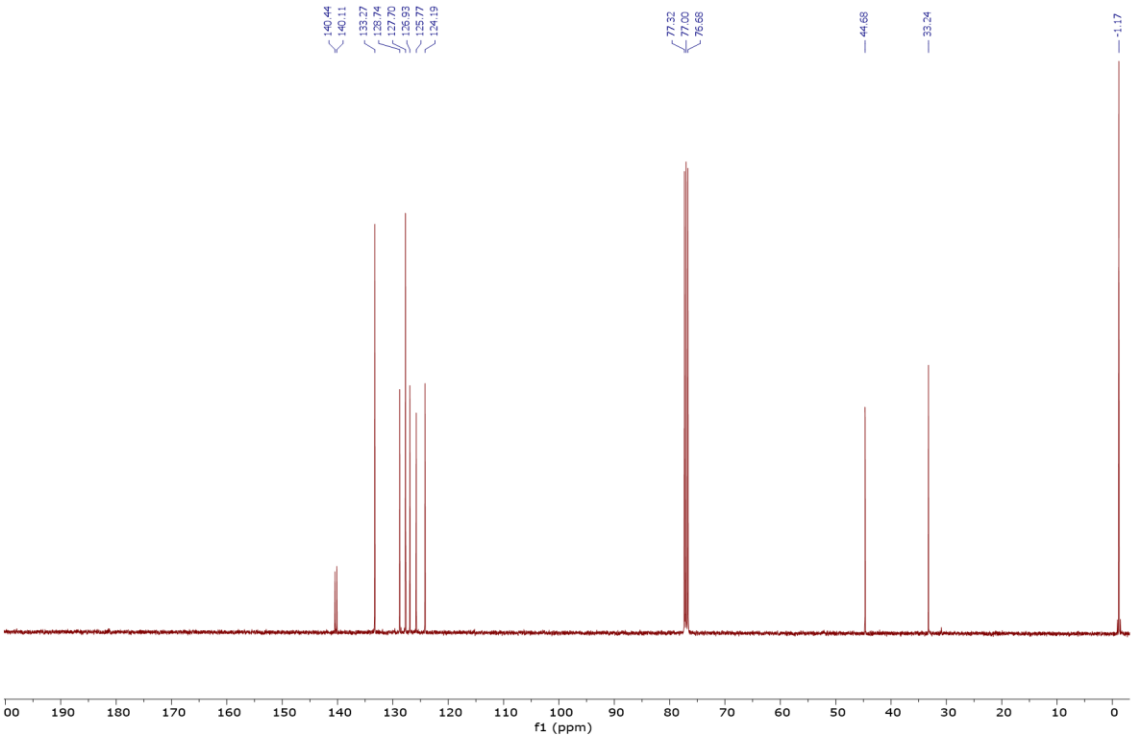

1-Cyclopropyl-1-phenyl-2-trimethylsilylethane **4.69** ($CDCl_3$, 400 MHz for $^1H$ NMR, 100 MHz for $^{13}C$ NMR)

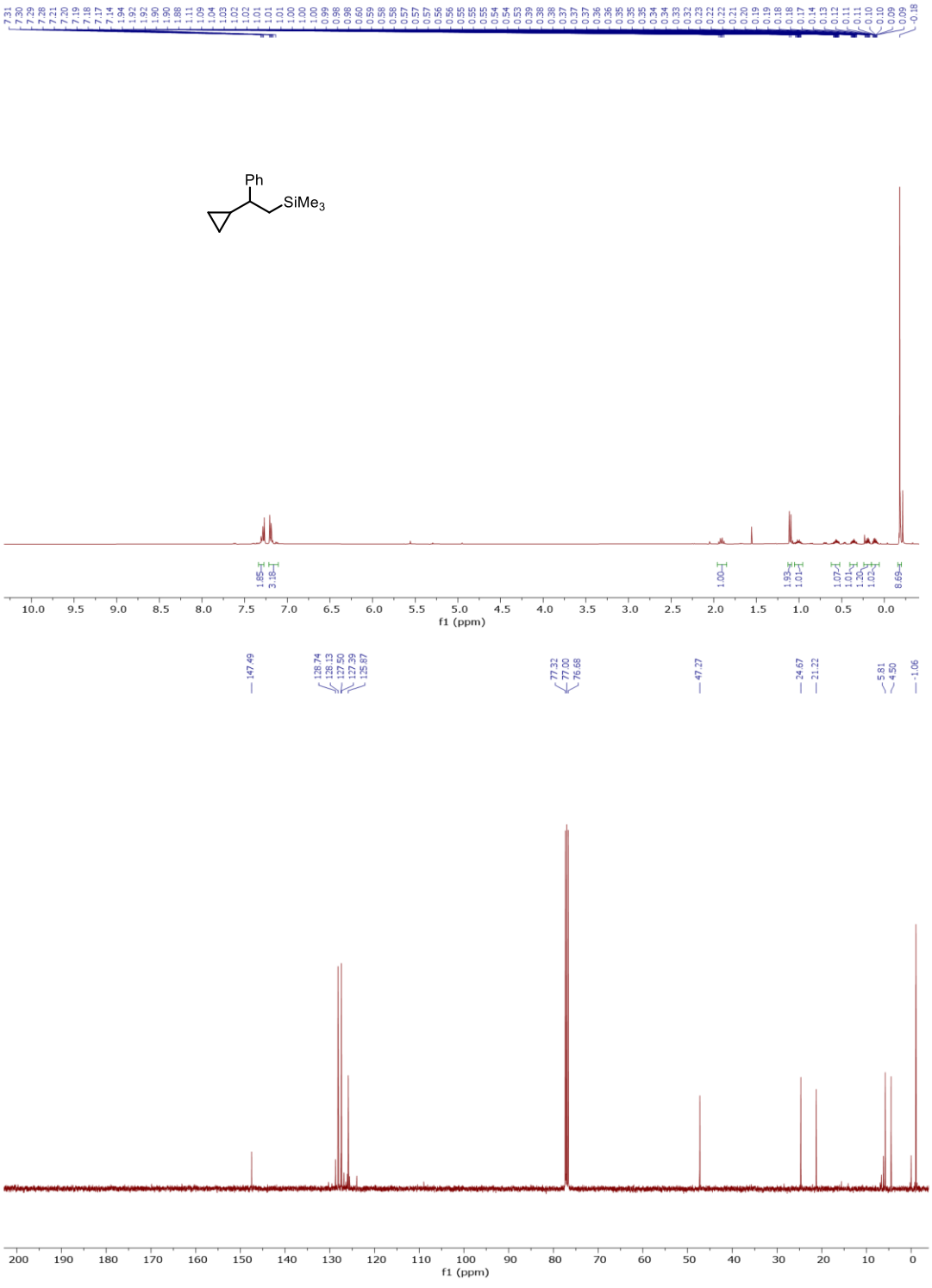

1-[(Trimethylsilyl)-6-heptenyl]benzene **4.72** ($CDCl_3$, 400 MHz for $^1H$ NMR, 100 MHz for $^{13}C$ NMR)

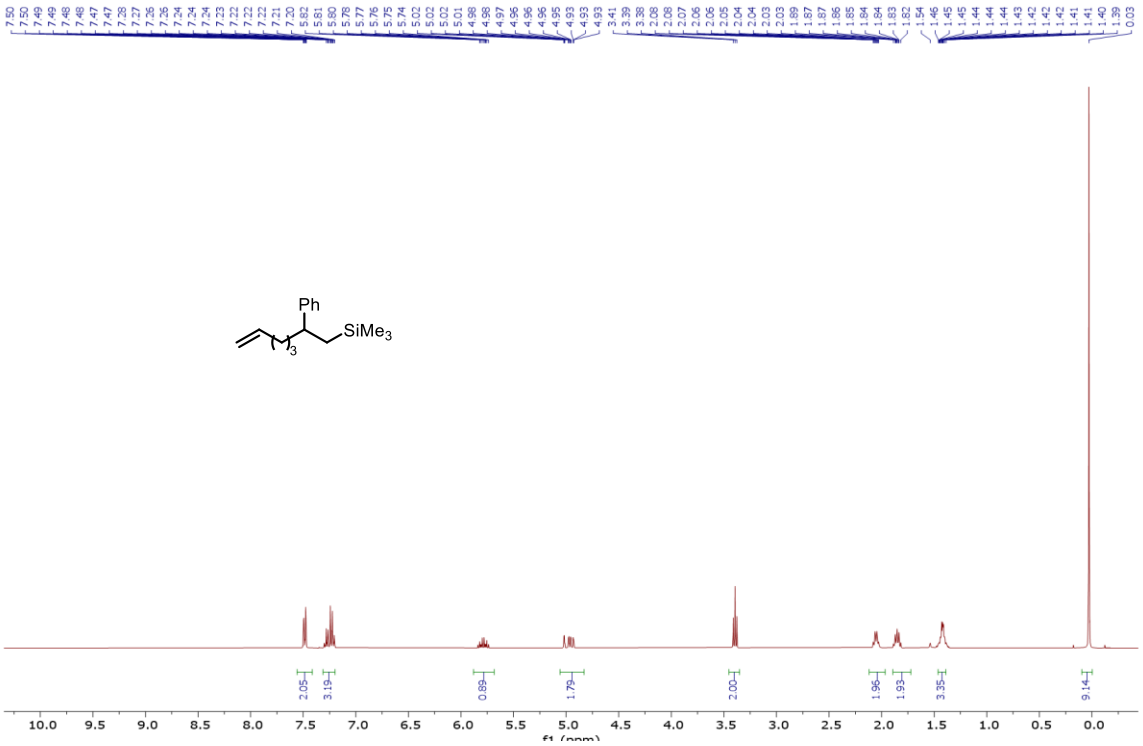


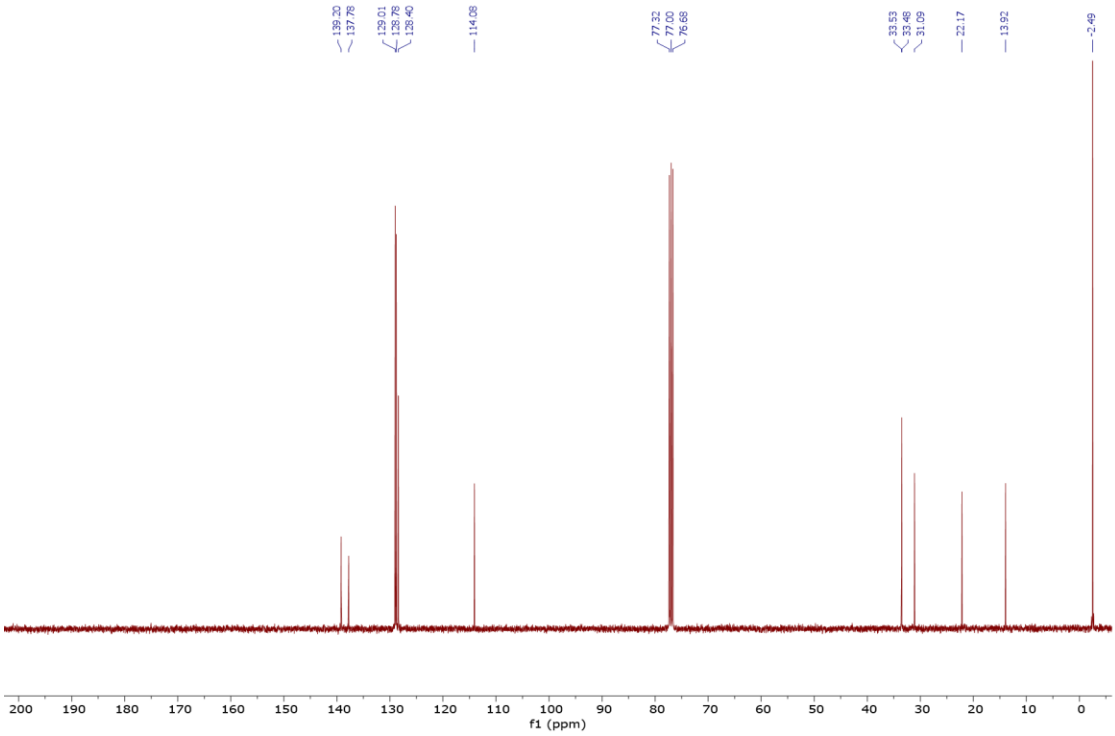

3-Methoxy-2-phenylpropan-1-ol **4.38** ($CDCl_3$, 400 MHz for $^{1}H$ NMR, 100 MHz for $^{13}C$ NMR)

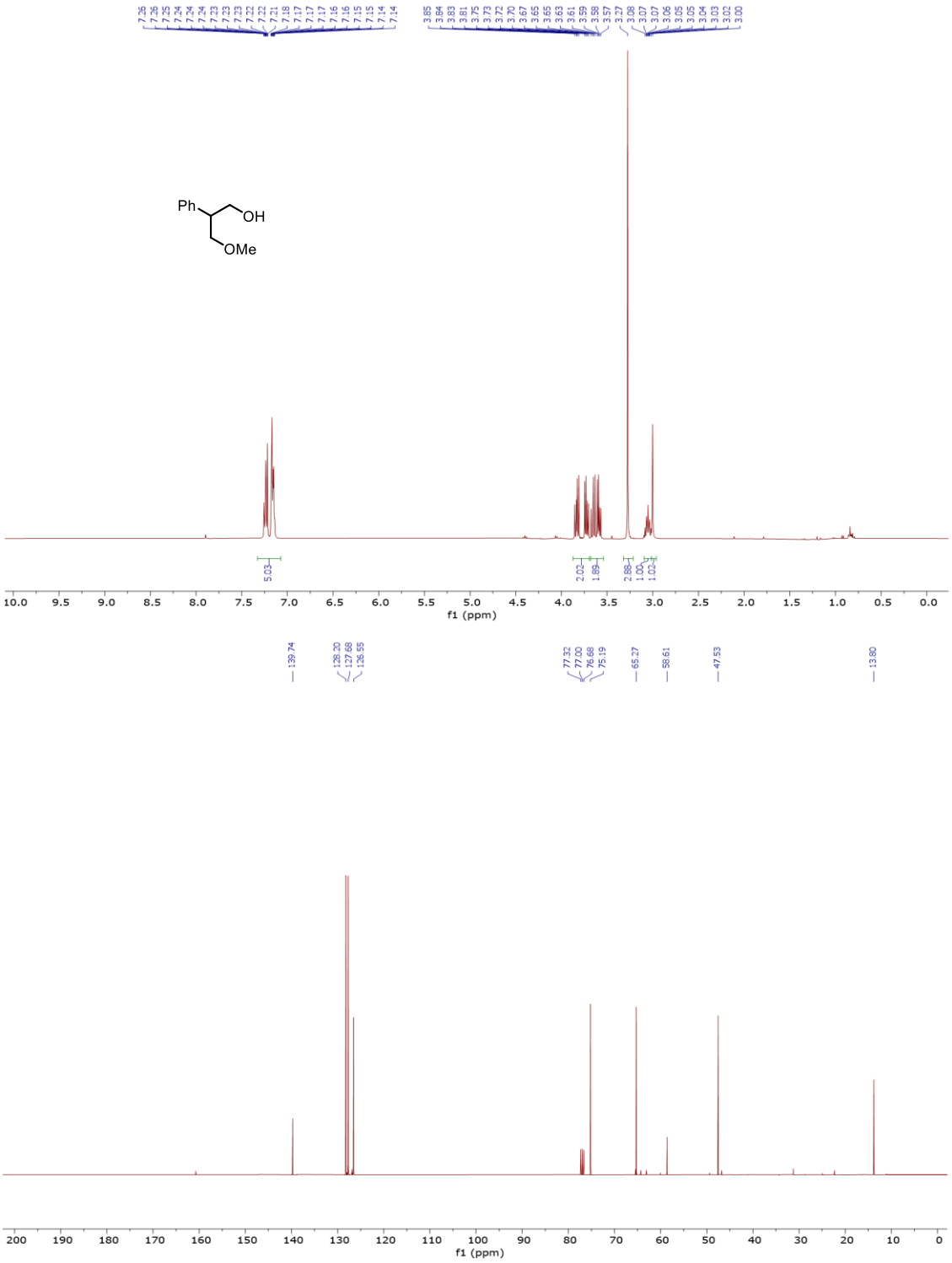

Phenylethanol **4.39** ($CDCl_3$, 400 MHz for $^1H$ NMR, 100 MHz for $^{13}C$ NMR)

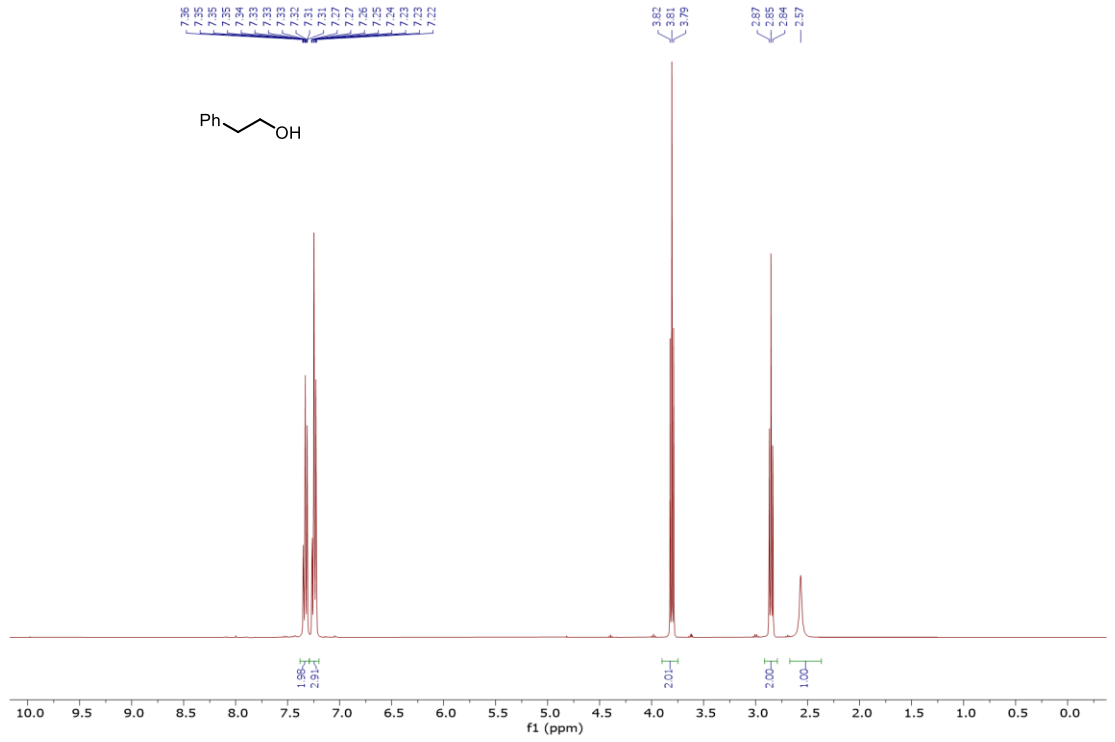


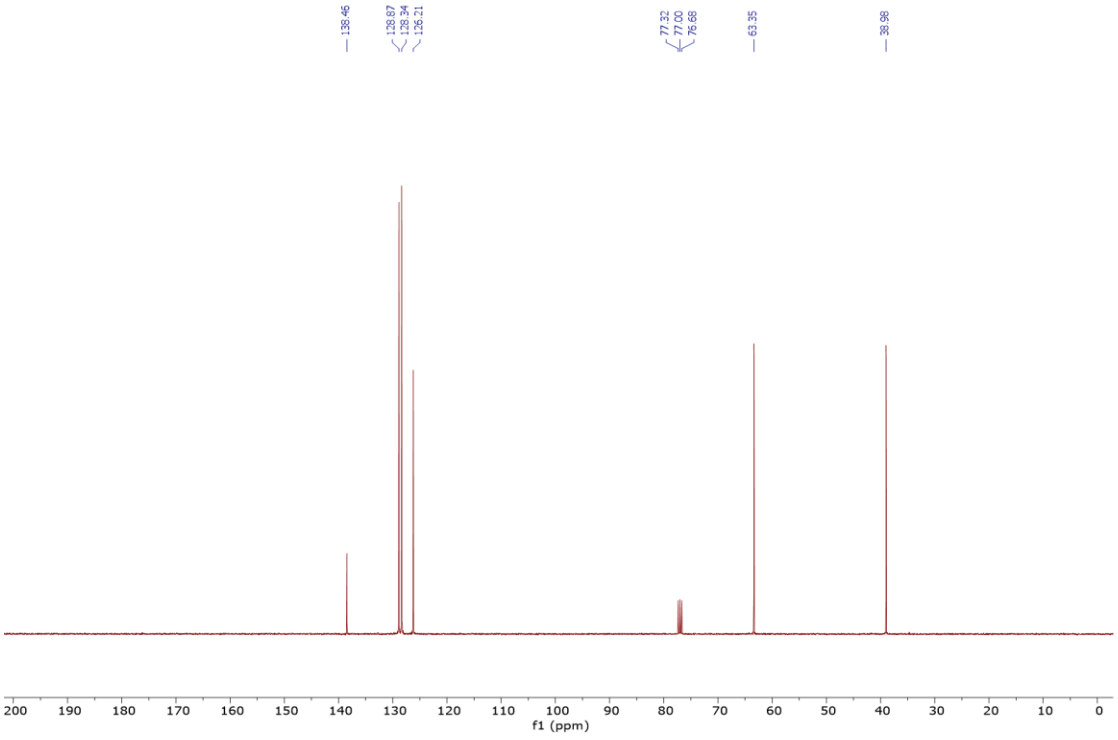

(2-Methoxy-1-methylethyl)benzene **4.40** ($CDCl_3$, 400 MHz for $^1H$ NMR, 100 MHz for $^{13}C$ NMR)

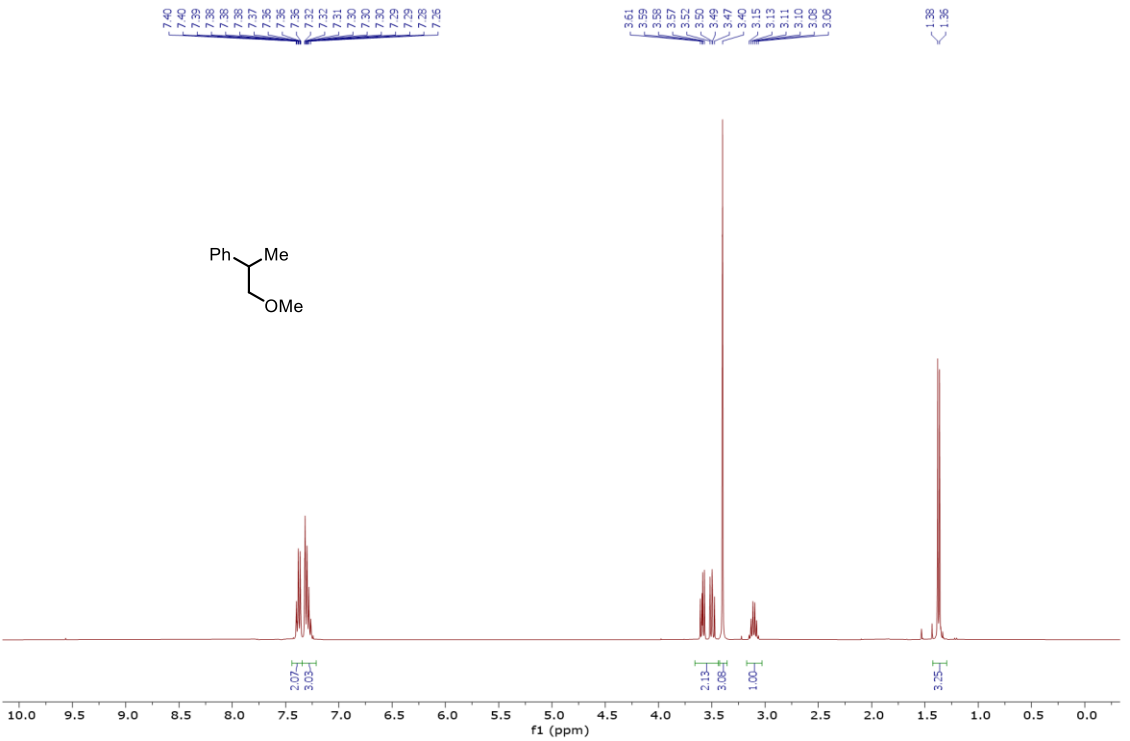


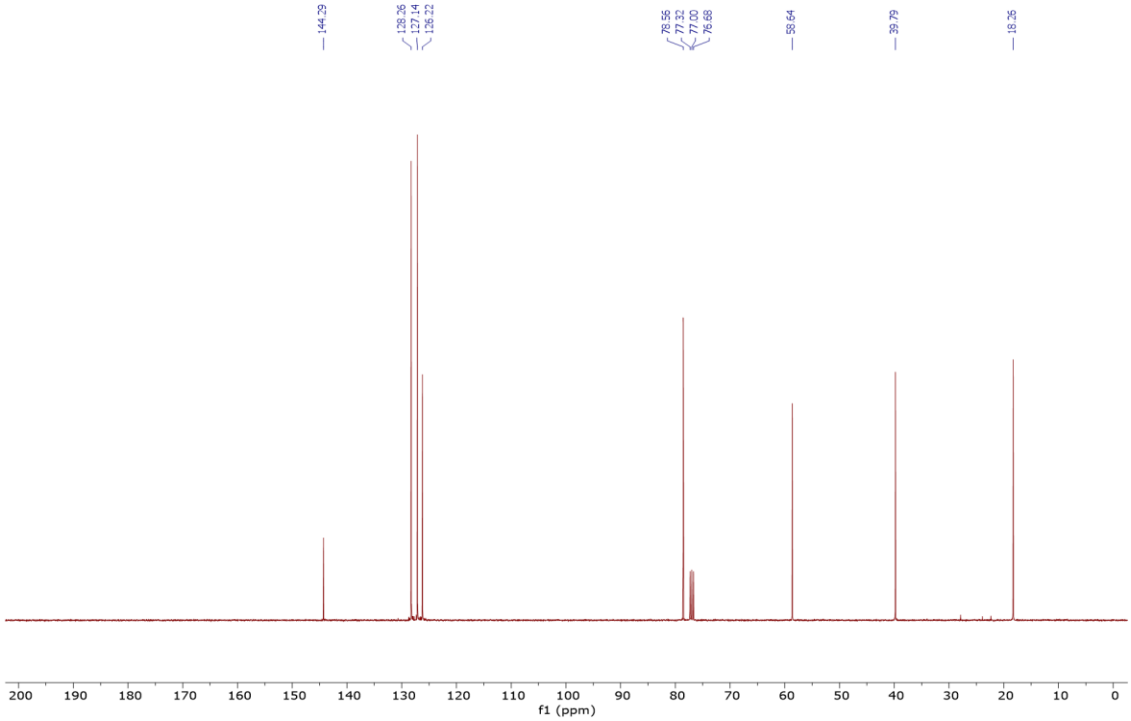

1-Cyclohexyl-1-phenylethane **4.41** ($CDCl_3$, 400 MHz for $^1H$ NMR, 100 MHz for $^{13}C$ NMR)

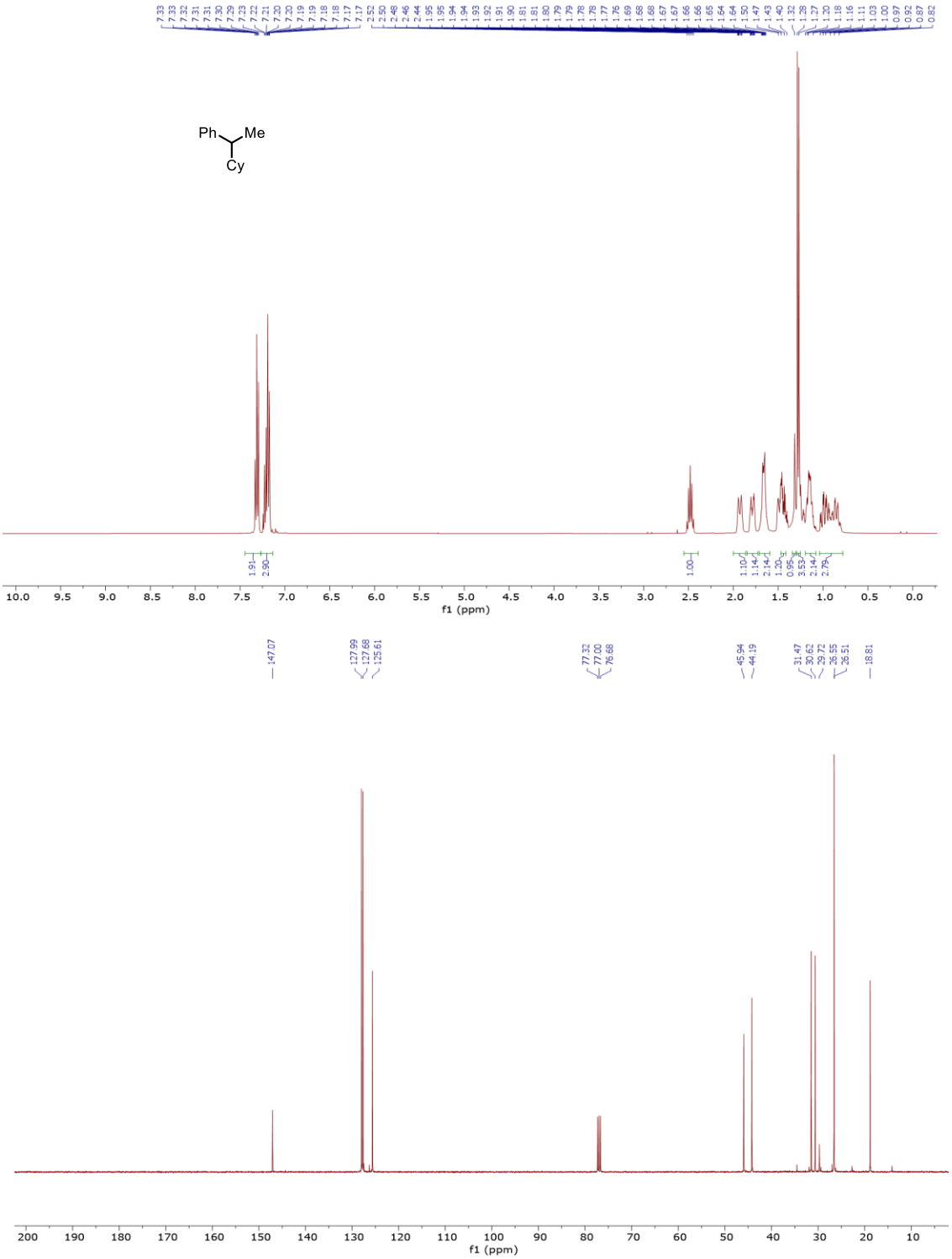

1-Methoxy-2-phenyl-3-(trimethylsilyl)propane **4.42** ($CDCl_3$, 400 MHz for $^1H$ NMR, 100 MHz for $^{13}C$ NMR)

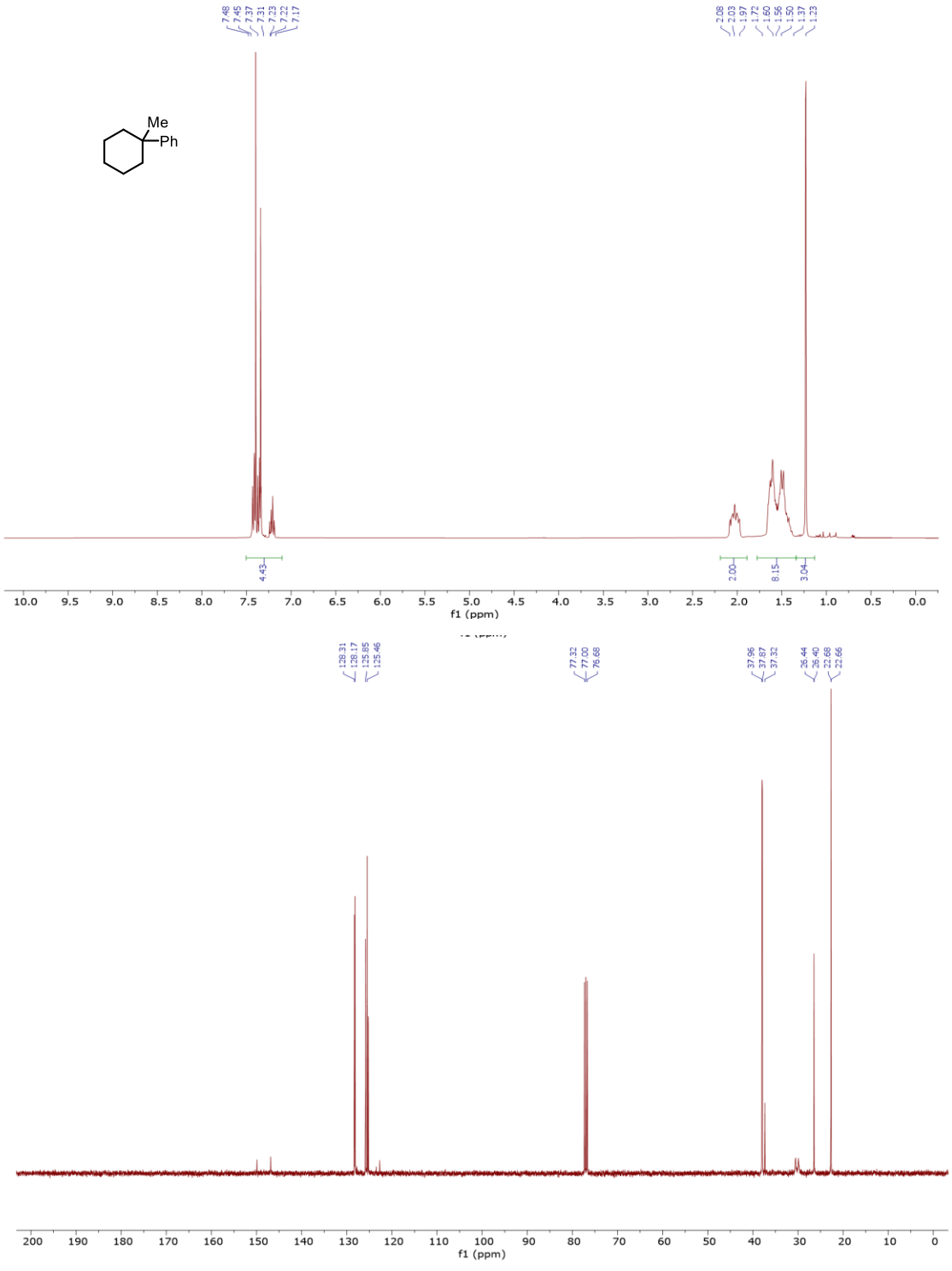

Nickel$^{(0)}$-**L1**-stilbene complex **4.61** ($CDCl_3$, 400 MHz for $^1H$ NMR, 100 MHz for $^{13}C$ NMR)

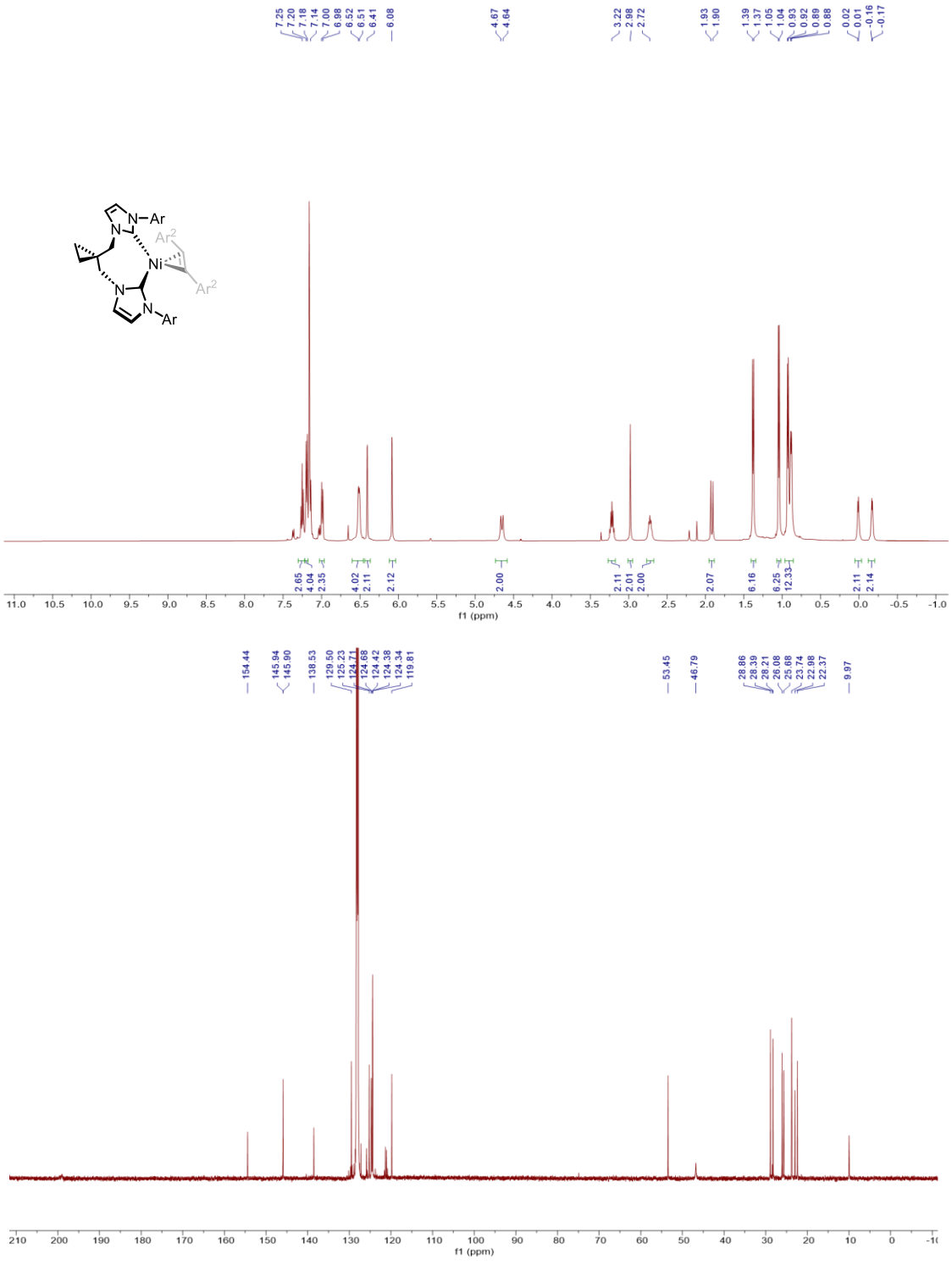

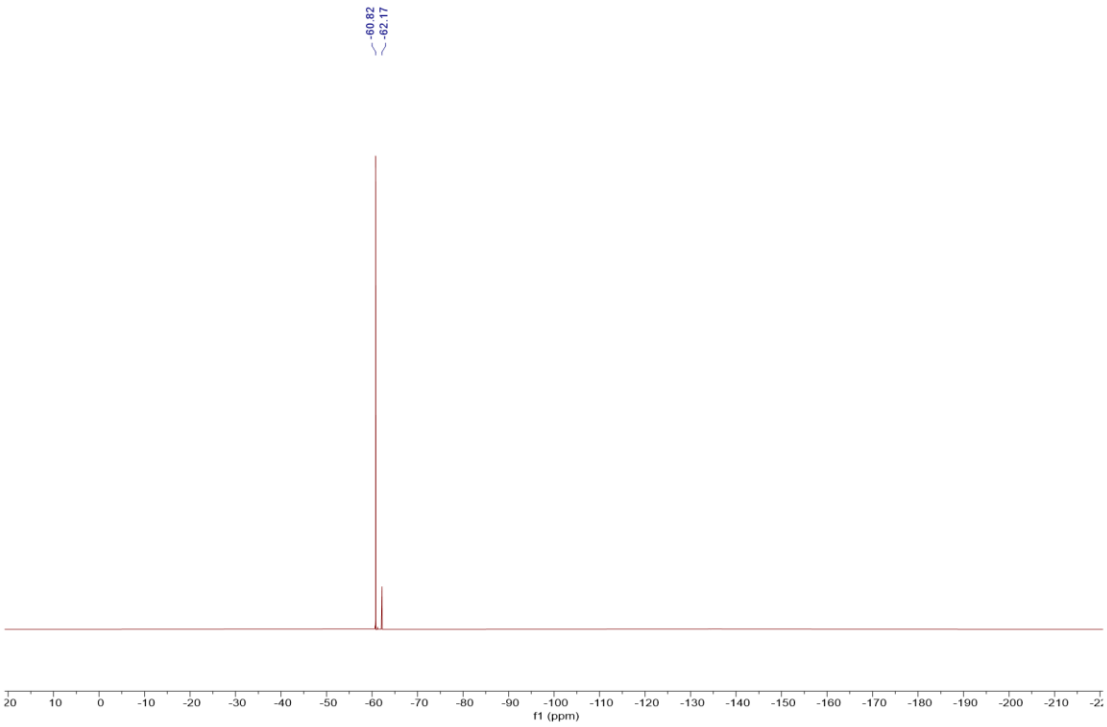
-60.82
-62.17
20 10 0 -10 -20 -30 -40 -50 -60 -70 -80 -90 -100 -110 -120 -130 -140 -150 -160 -170 -180 -190 -200 -210
f1 (ppm)

Nickel$^{(II)}$-**L1**-peroxo complex **4.59** ($CDCl_3$, 400 MHz for $^1H$ NMR, 100 MHz for $^{13}C$ NMR)

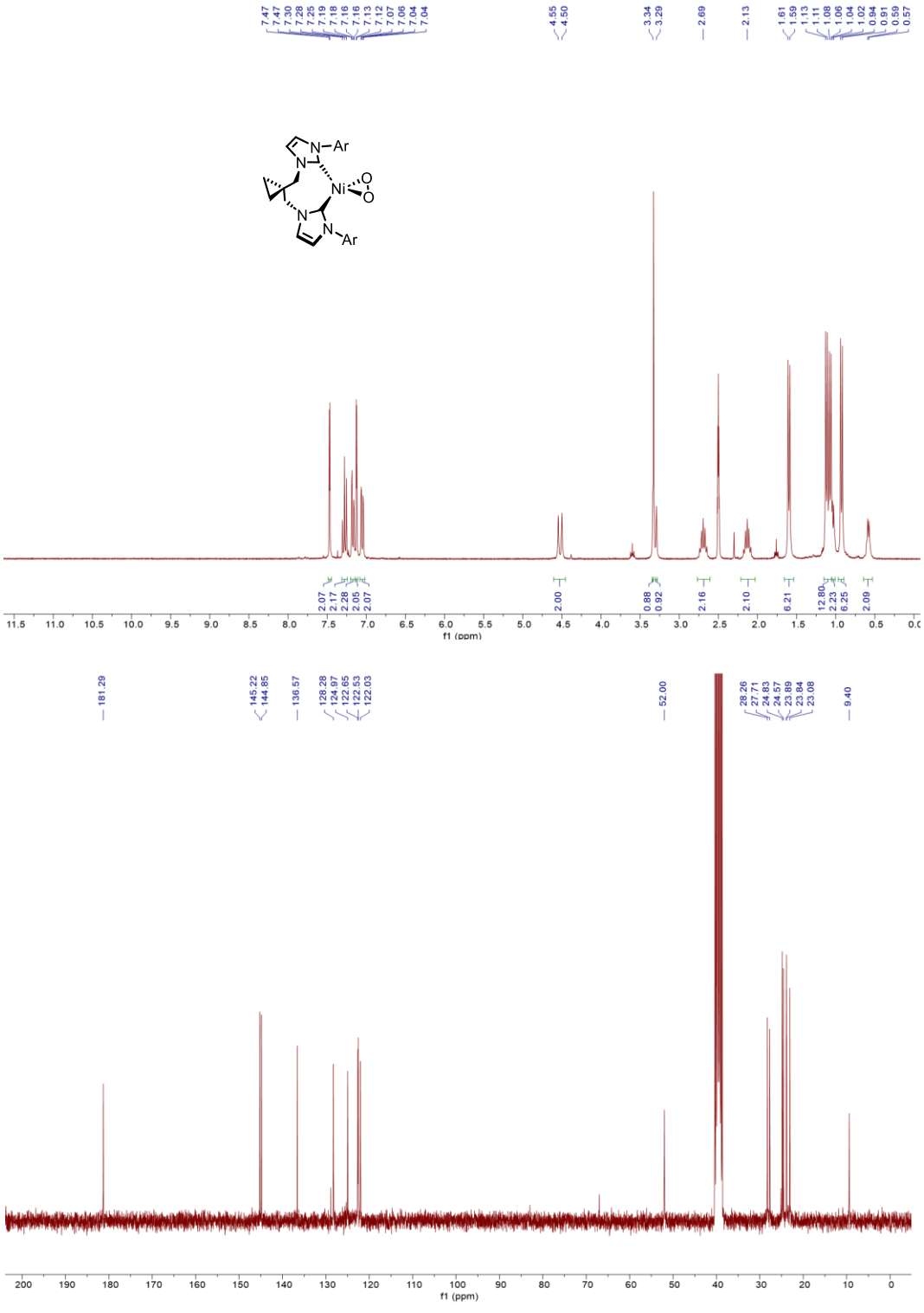

## *Spectra associated with chapter five*

4-(1,1-Dimethylethyl)tetrahydro-2*H*-pyran-4-ol **5.20** ($CDCl_3$, 400 MHz for $^{1}H$ NMR, 100 MHz for $^{13}C$ NMR)

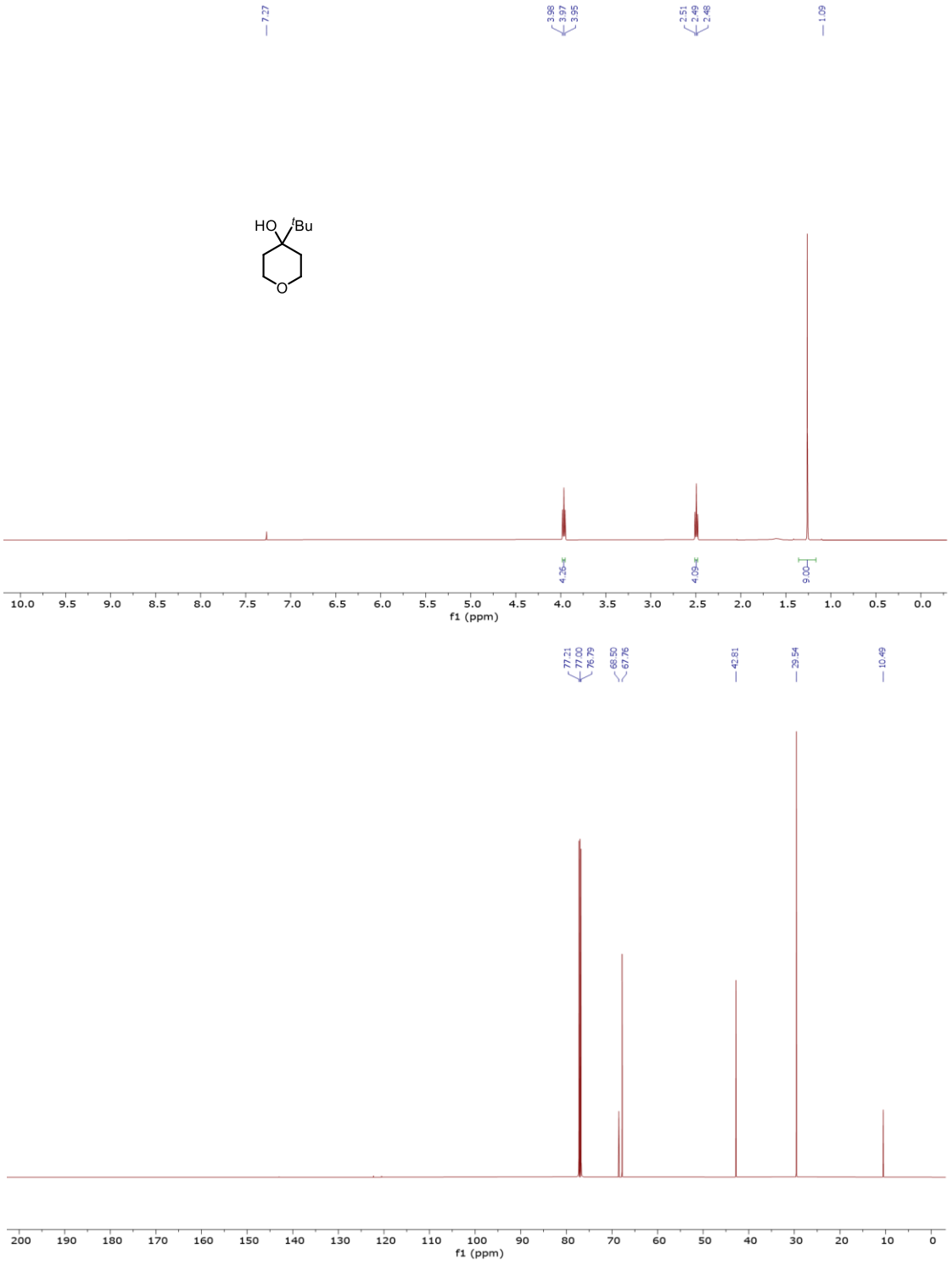

4-Alkynyl-4-(1,1-dimethylethyl)tetrahydro-2*H*-pyran **5.23** ($CDCl_3$, 400 MHz for $^1H$ NMR, 100 MHz for $^{13}C$ NMR)

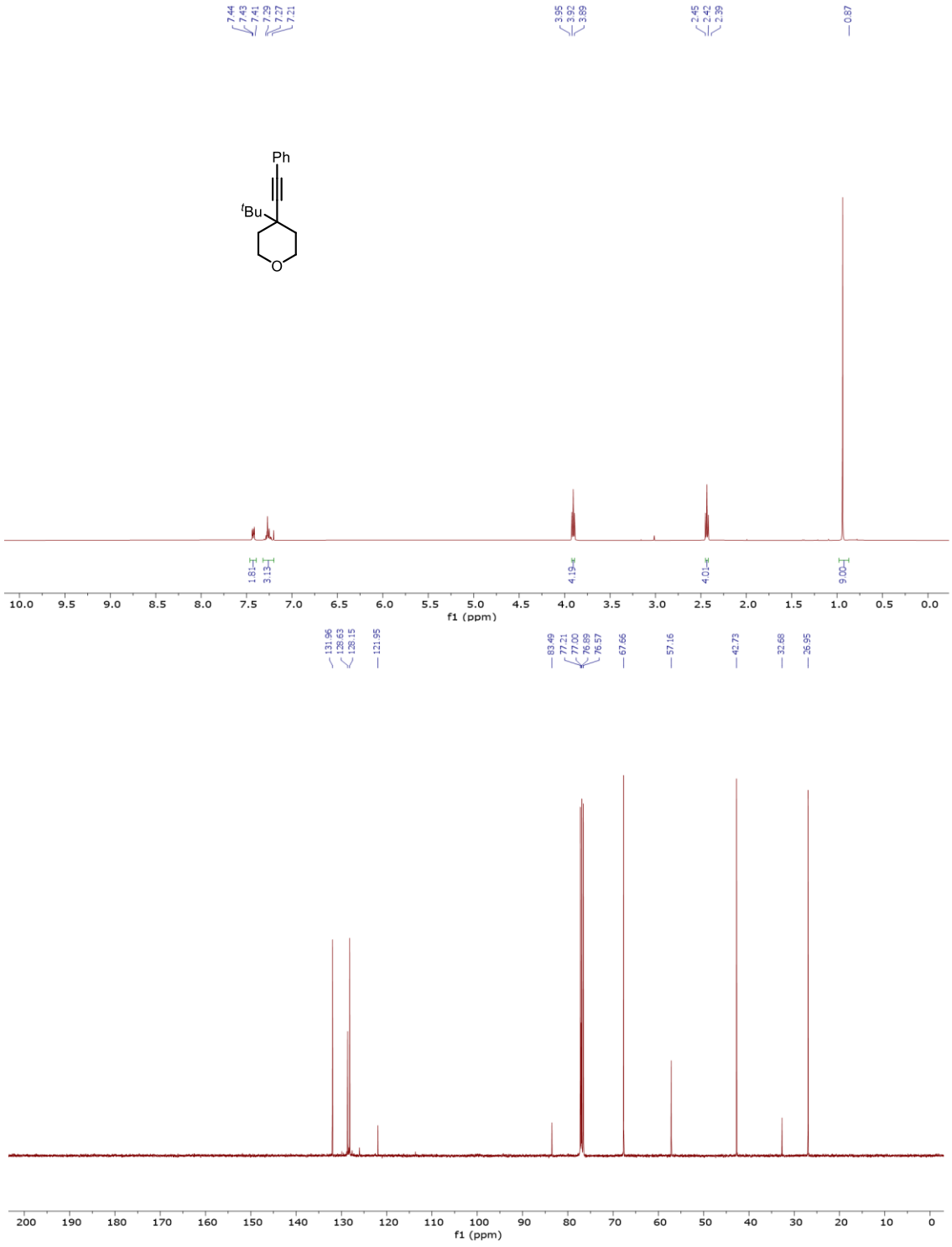

2-Methyl-1-tricyclo[3.3.1.1$^{3,7}$]dec-1-yl-1*H*-indole **5.18** ($CDCl_3$, 400 MHz for $^1H$ NMR, 100 MHz for $^{13}C$ NMR)

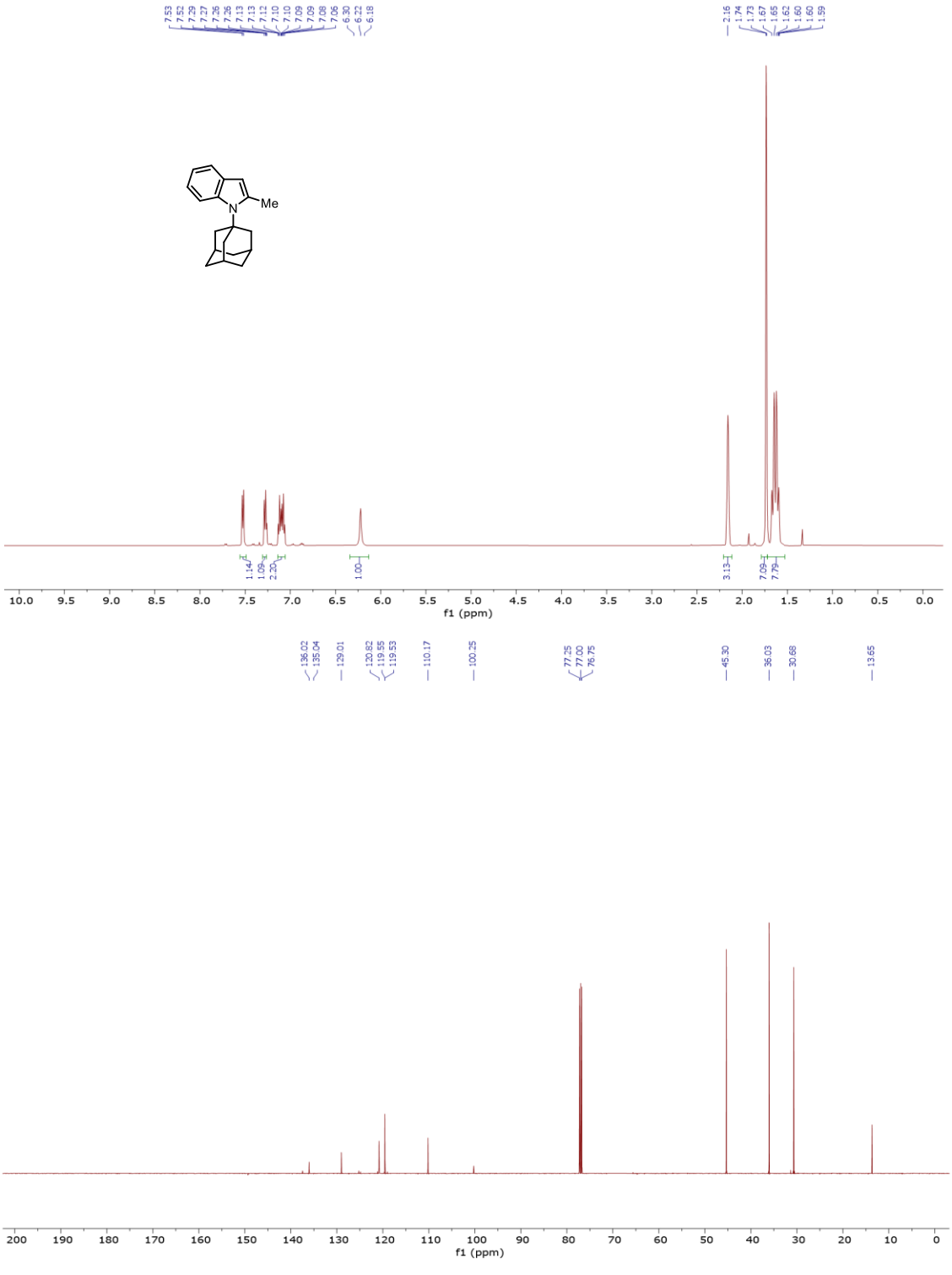

9-Tricyclo[3.3.1.1$^{3,7}$]dec-1-yl-9*H*-carbazole **5.19** ($CDCl_3$, 400 MHz for $^1$H NMR, 100 MHz for $^{13}$C NMR)

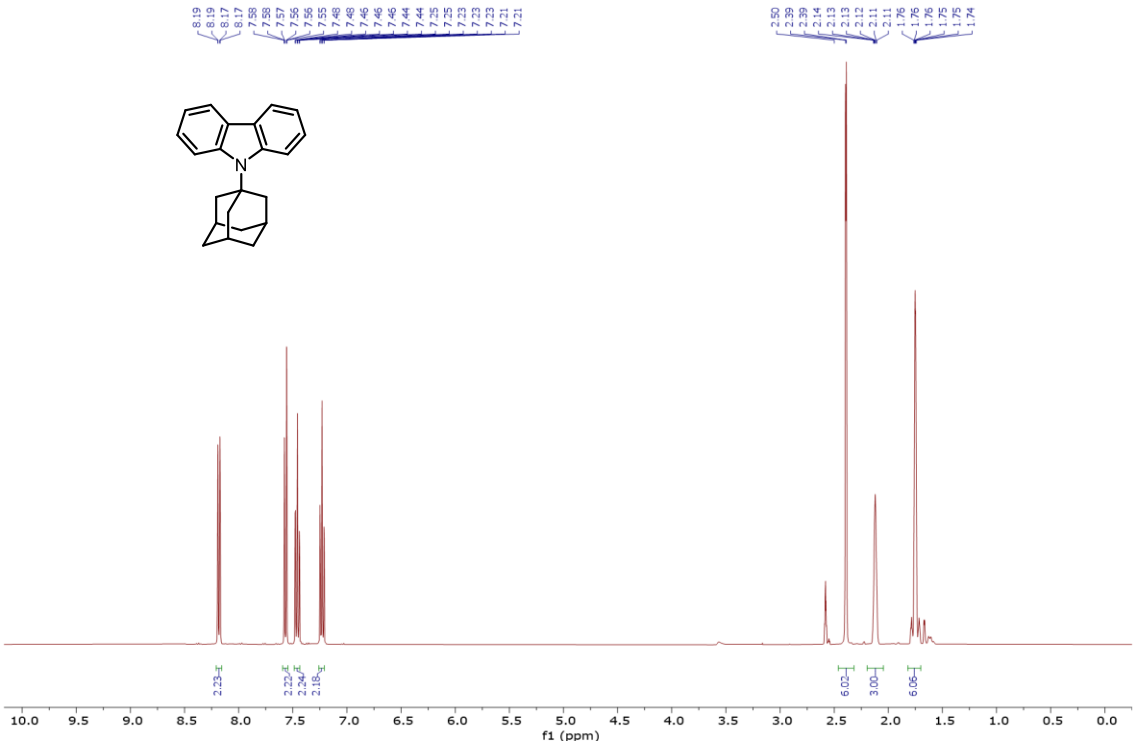

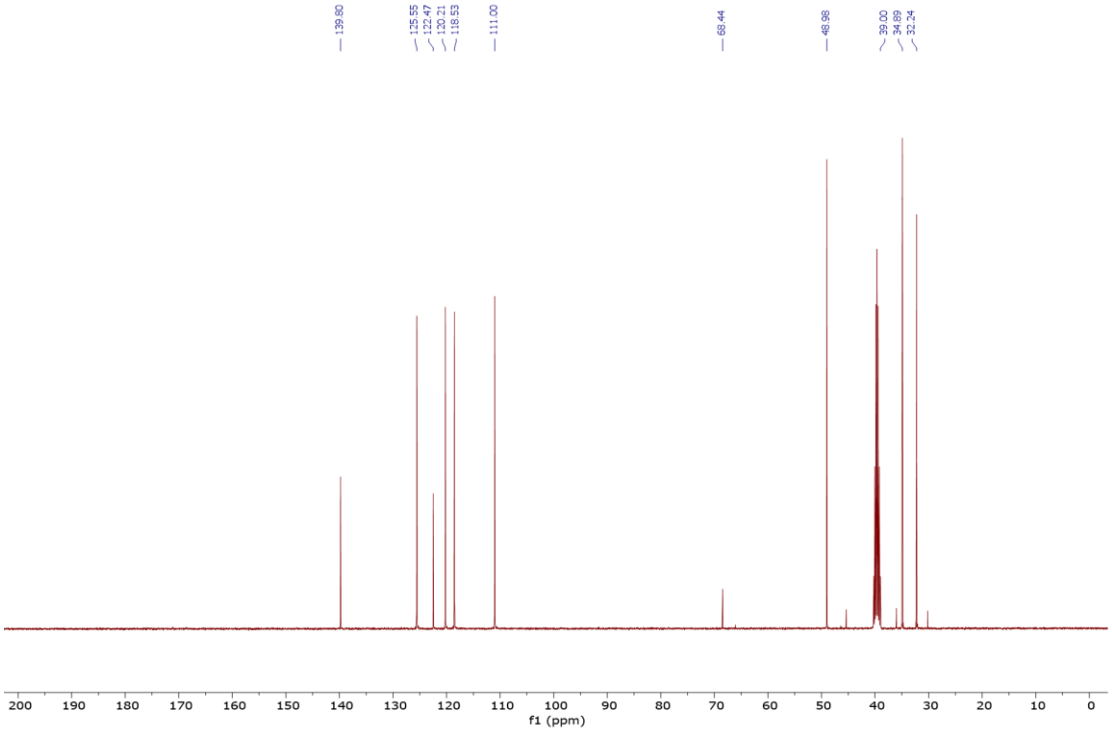

4-(*9H*-Carbazolyl)-4-(1,1-dimethylethyl)tetrahydro-2*H*-pyran **5.25** ($CDCl_3$, 400 MHz for $^1H$ NMR, 100 MHz for $^{13}C$ NMR)

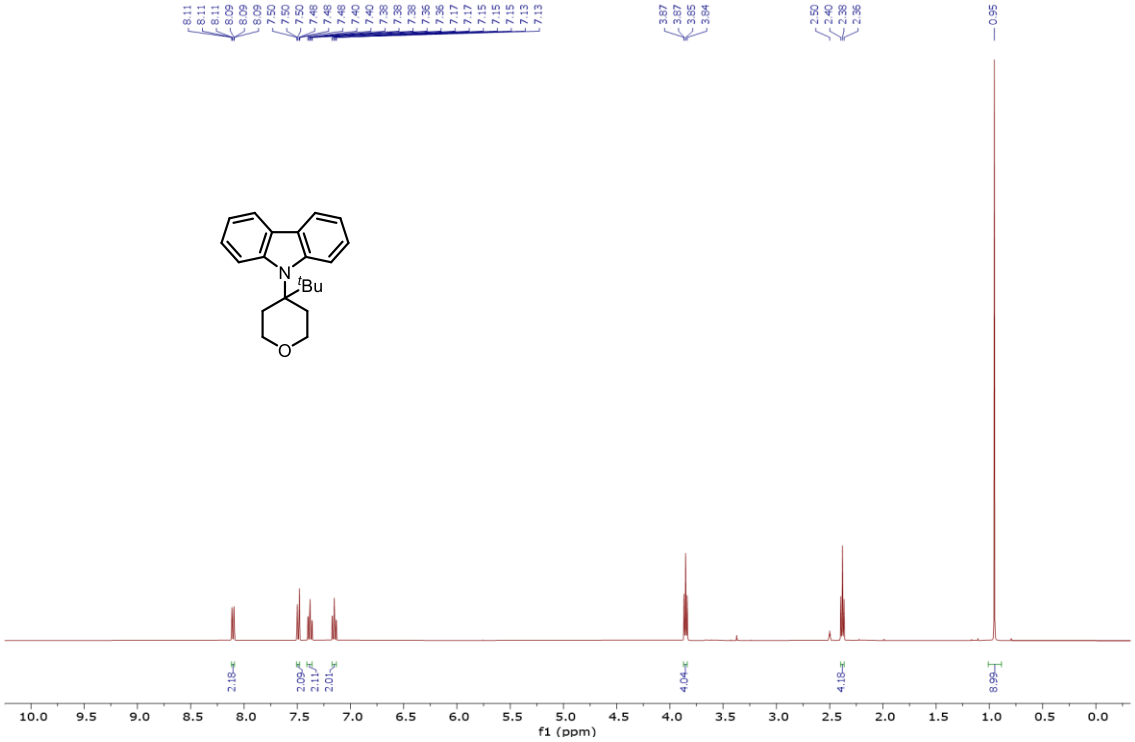


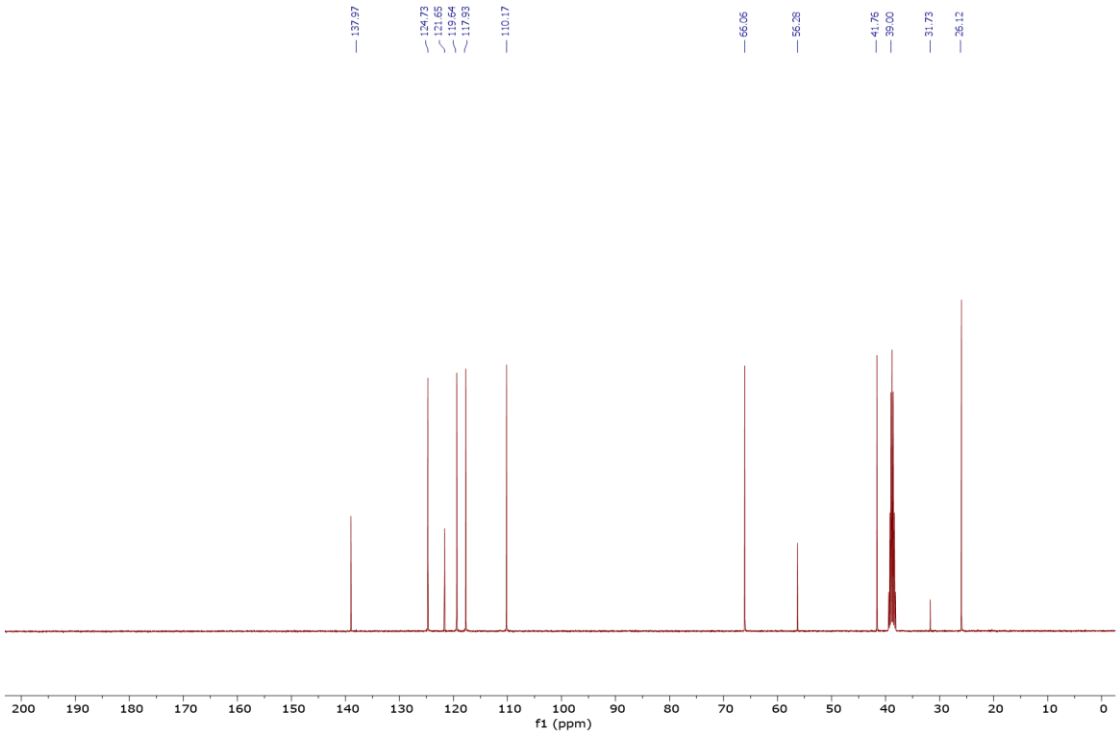

Methyl 1-(4-cyclohexyl-tetrahydro-2*H*-pyran-4-yl)-1*H*-indole-4-carboxylate **5.51** ($CDCl_3$, 400 MHz for $^1H$ NMR, 100 MHz for $^{13}C$ NMR)

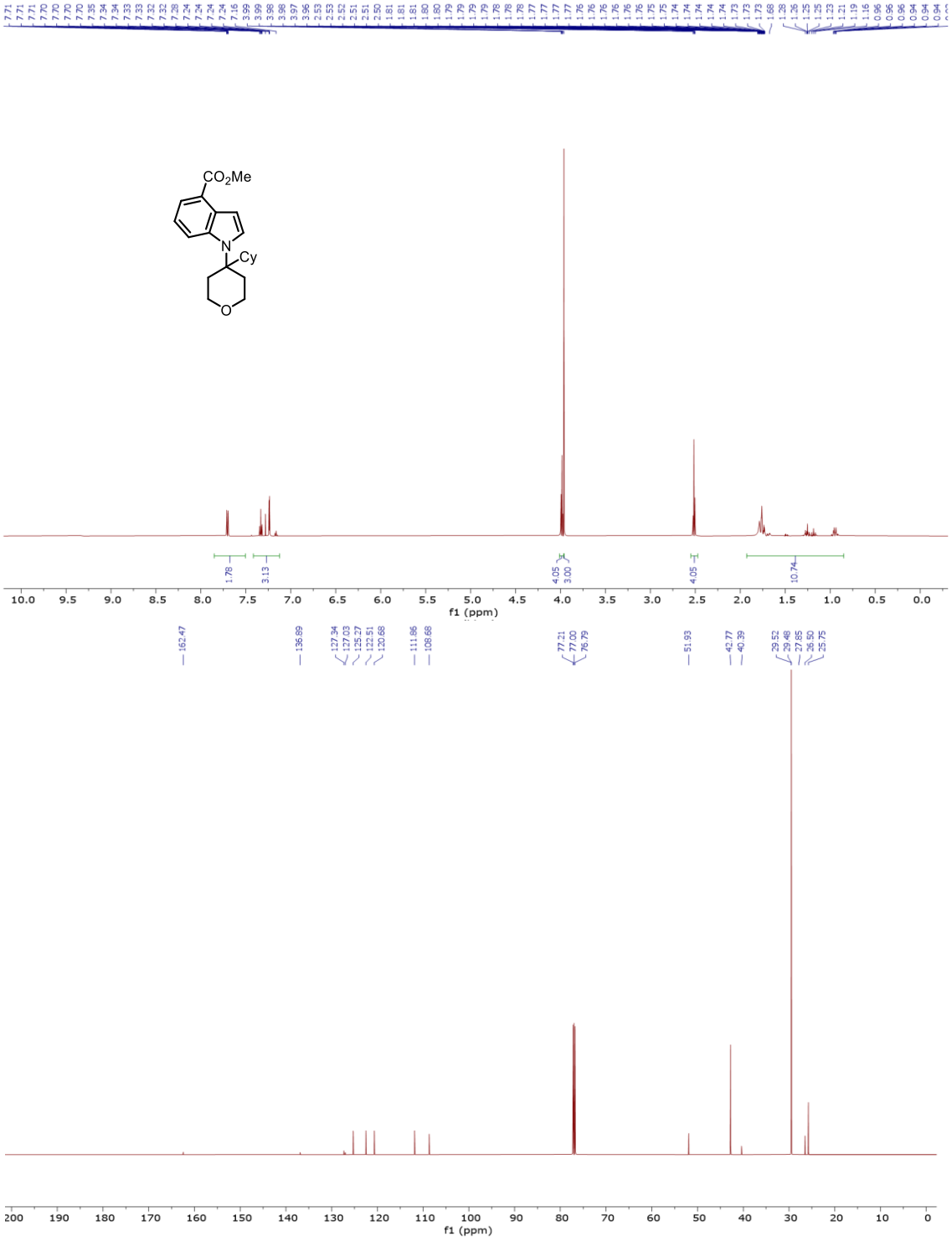

5-Bromo-1-(4-cyclohexyl-tetrahydro-2*H*-pyran-4-yl)-1*H*-indole **5.52** ($CDCl_3$, 400 MHz for $^{1}H$ NMR, 100 MHz for $^{13}C$ NMR)

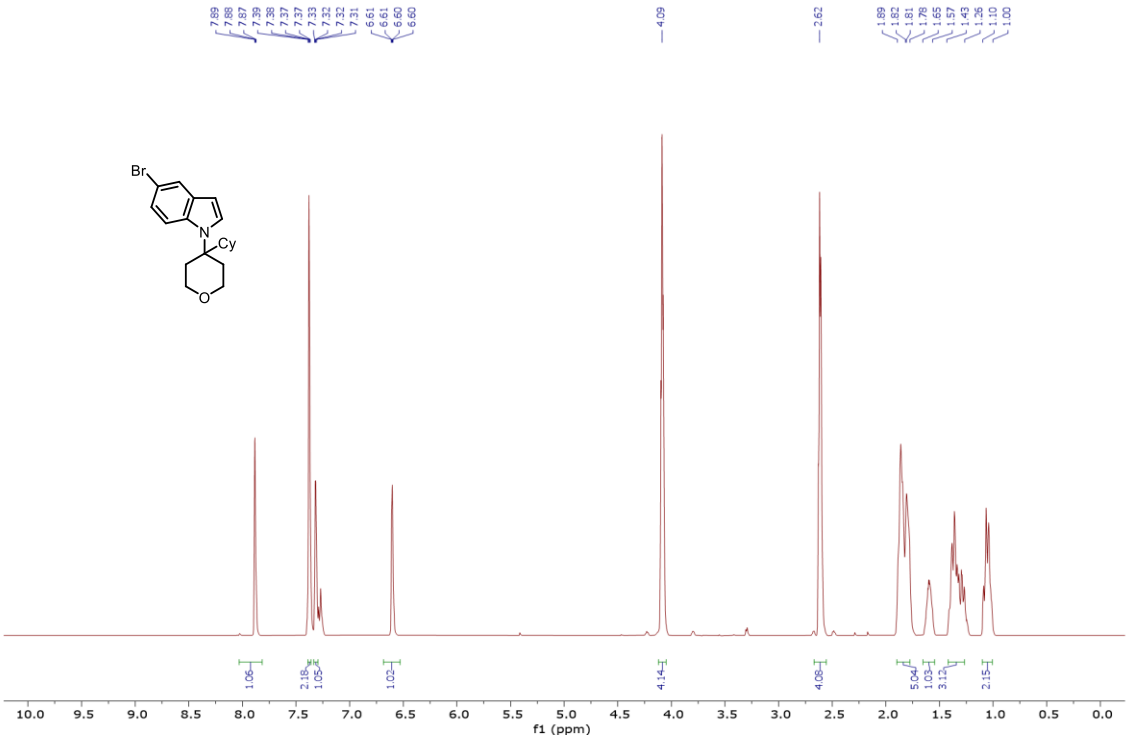


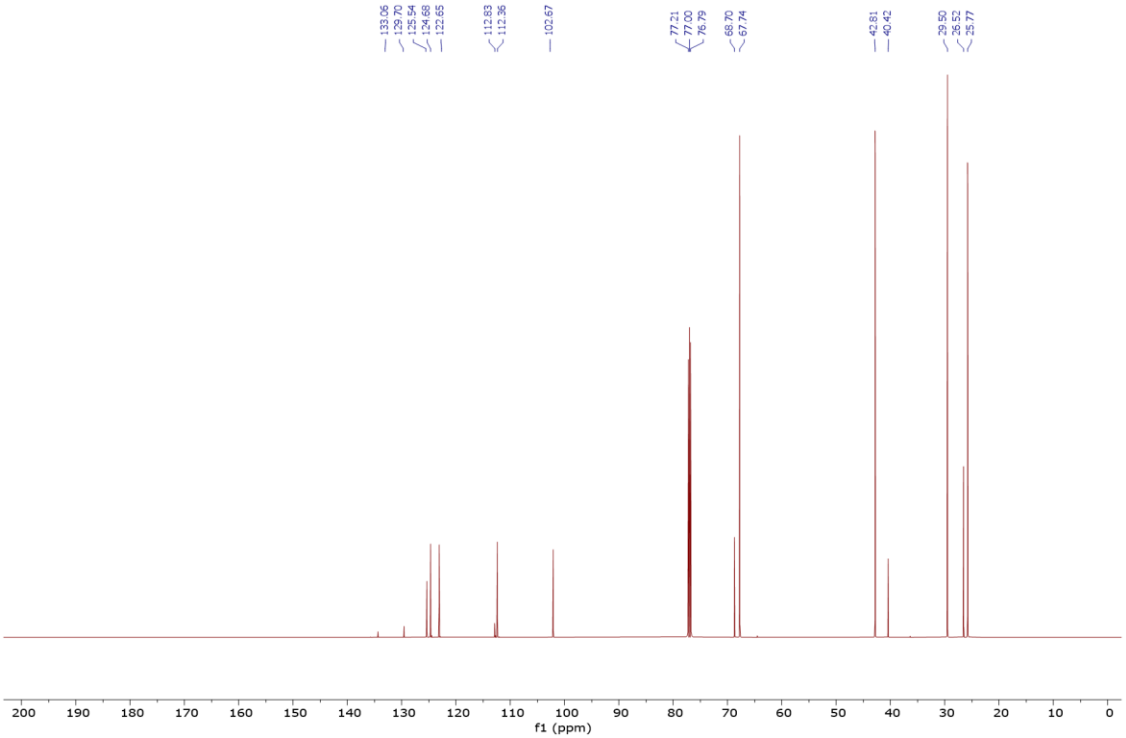

1-(4-Cyclohexyl-tetrahydro-2*H*-pyran-4-yl)-1*H*-indolyl-2-ethanol **5.53** ($CDCl_3$, 400 MHz for $^1H$ NMR, 100 MHz for $^{13}C$ NMR)

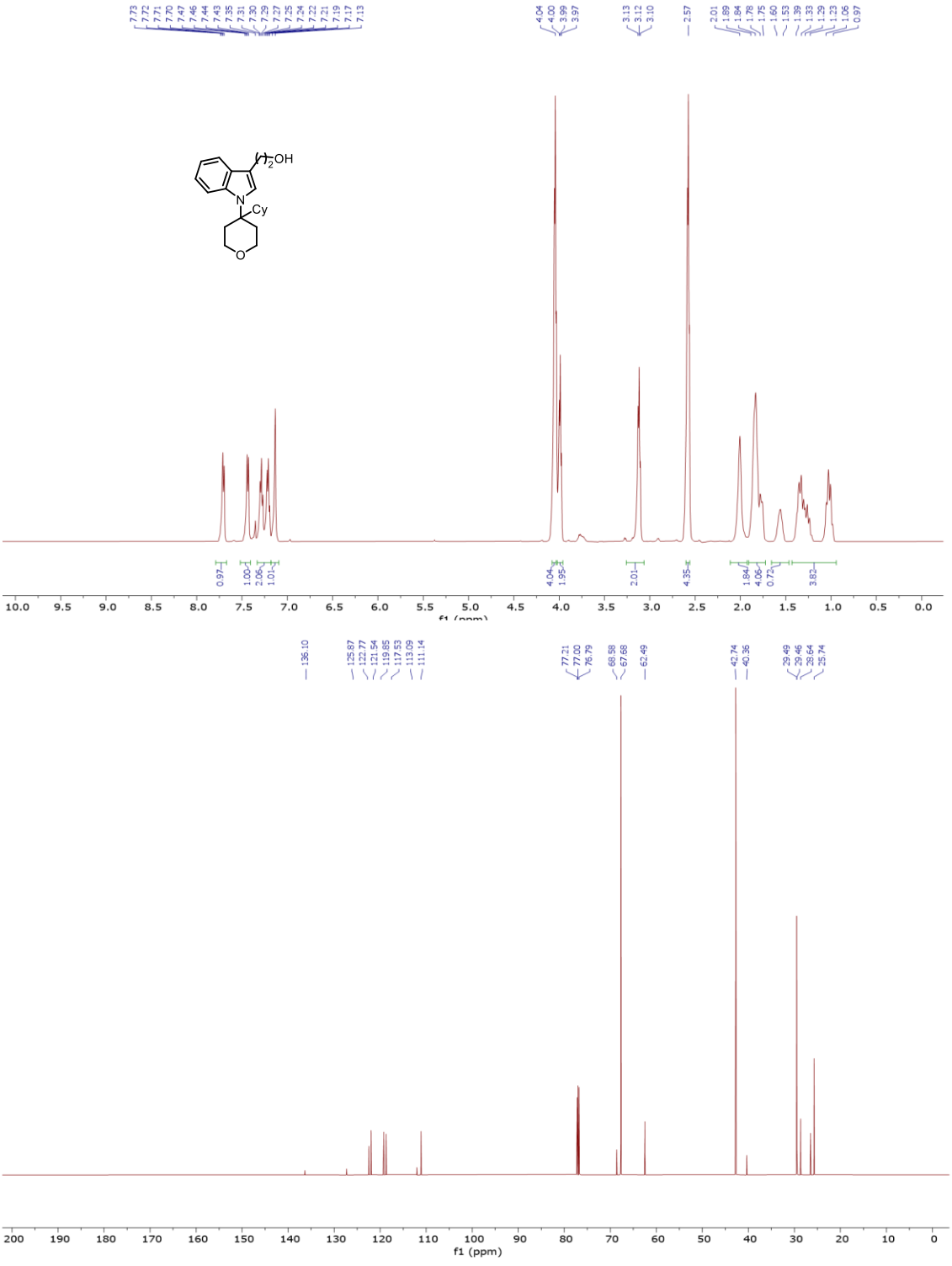

2-Methyl-(4-tertbutyl-1-methyl-piperidinyl)-1*H*-indole **5.54** ($CDCl_3$, 400 MHz for $^1H$ NMR, 100 MHz for $^{13}C$ NMR)

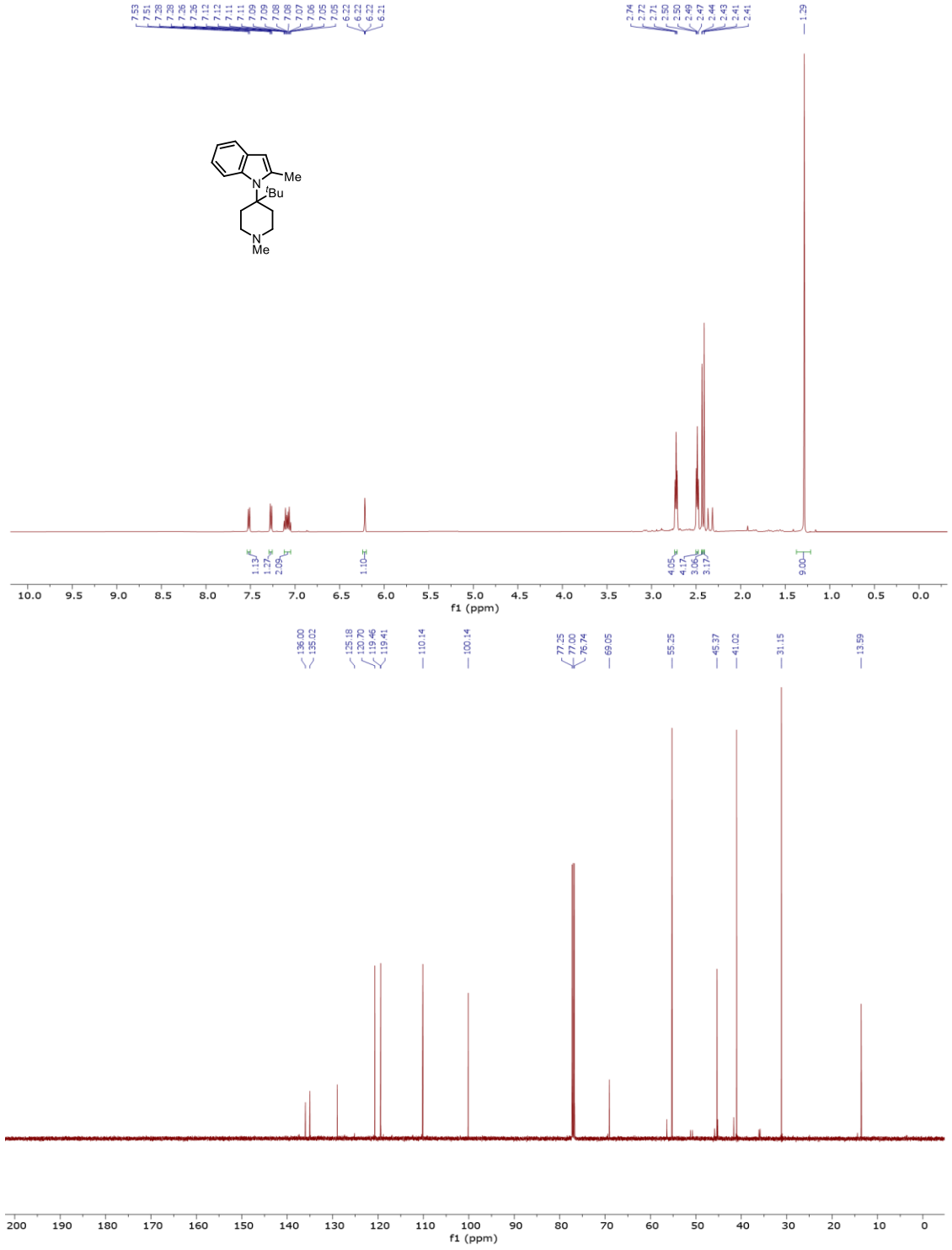

4-(*1H*-Chlorzoxazonyl)-4-(1,1-dimethylethyl)tetrahydro-2*H*-pyran **5.55** ($CDCl_3$, 400 MHz for $^1H$ NMR, 100 MHz for $^{13}C$ NMR)

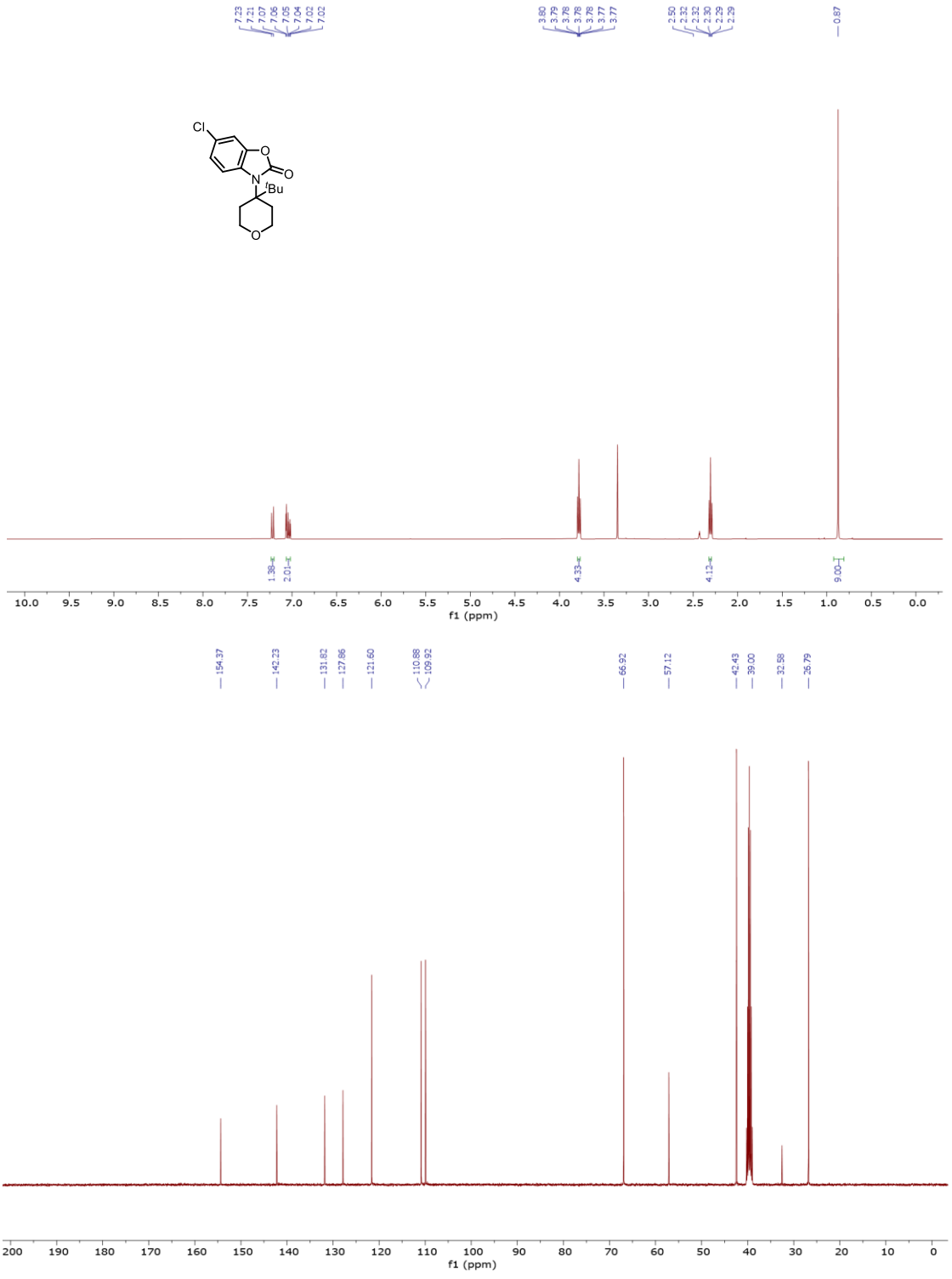

1-(Tetrahydro-4-cyclohexyl-2*H*-pyran-4-yl)-1*H*-pyrazole **5.56** ($CDCl_3$, 400 MHz for $^1H$ NMR, 100 MHz for $^{13}C$ NMR)

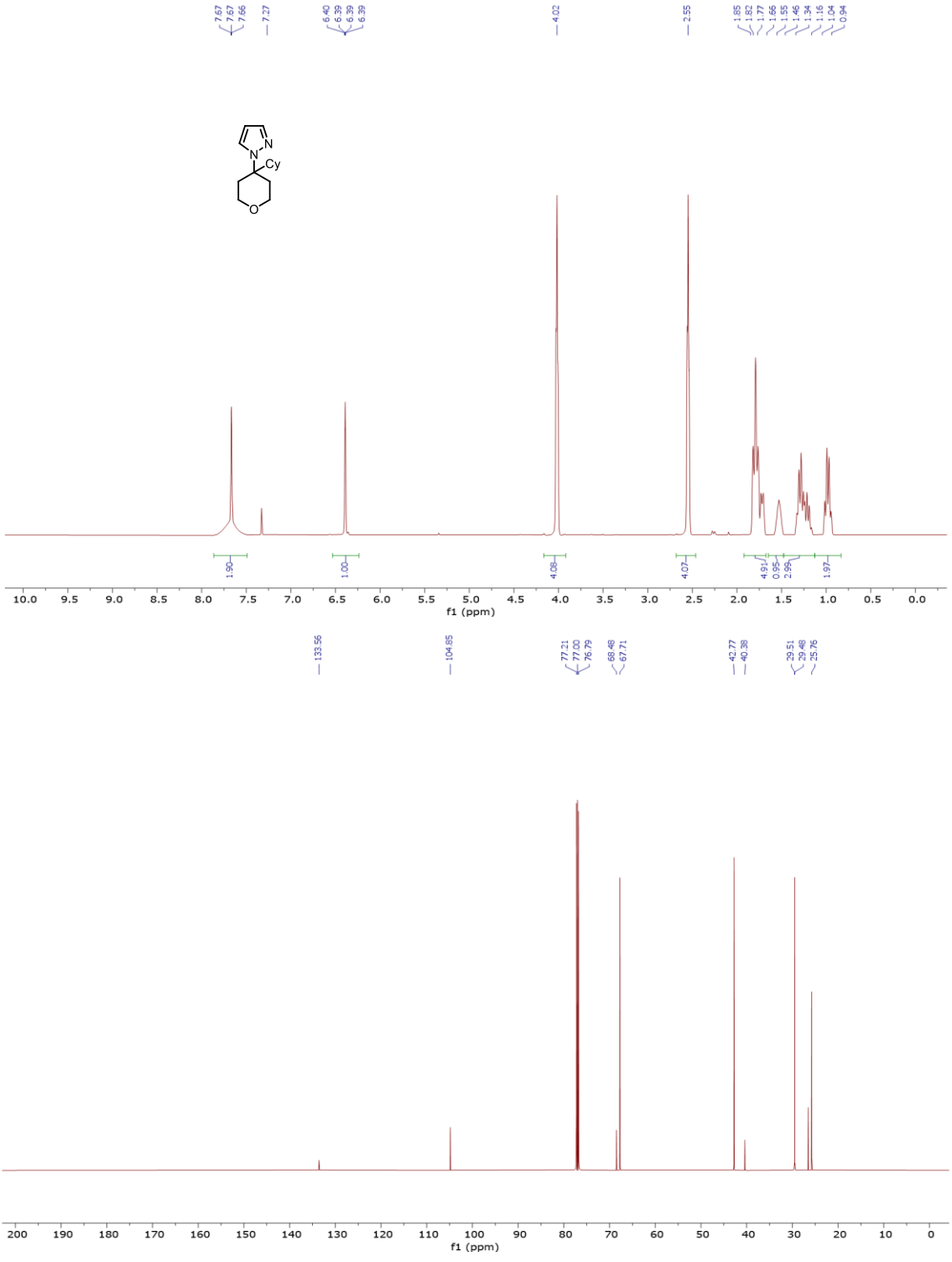

1-Tricyclo[3.3.1.1$^{3,7}$]dec-1-yl-1*H*-pyrazole **5.57** ($CDCl_3$, 400 MHz for $^1$H NMR, 100 MHz for $^{13}$C NMR)

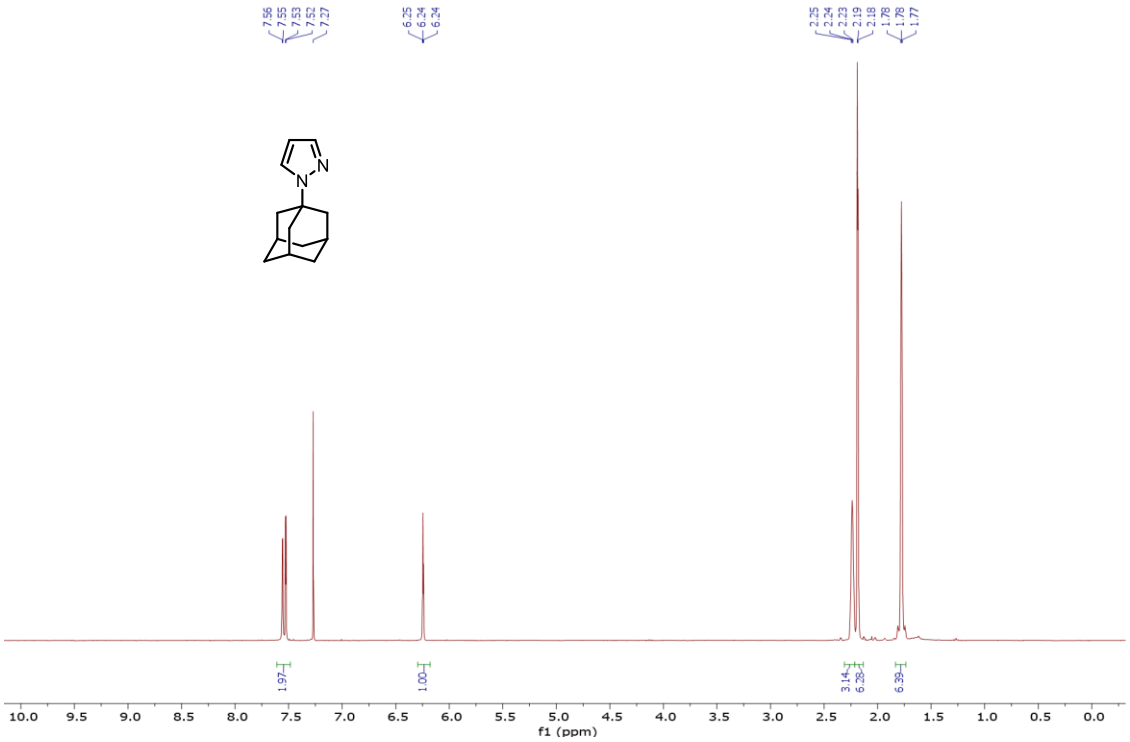


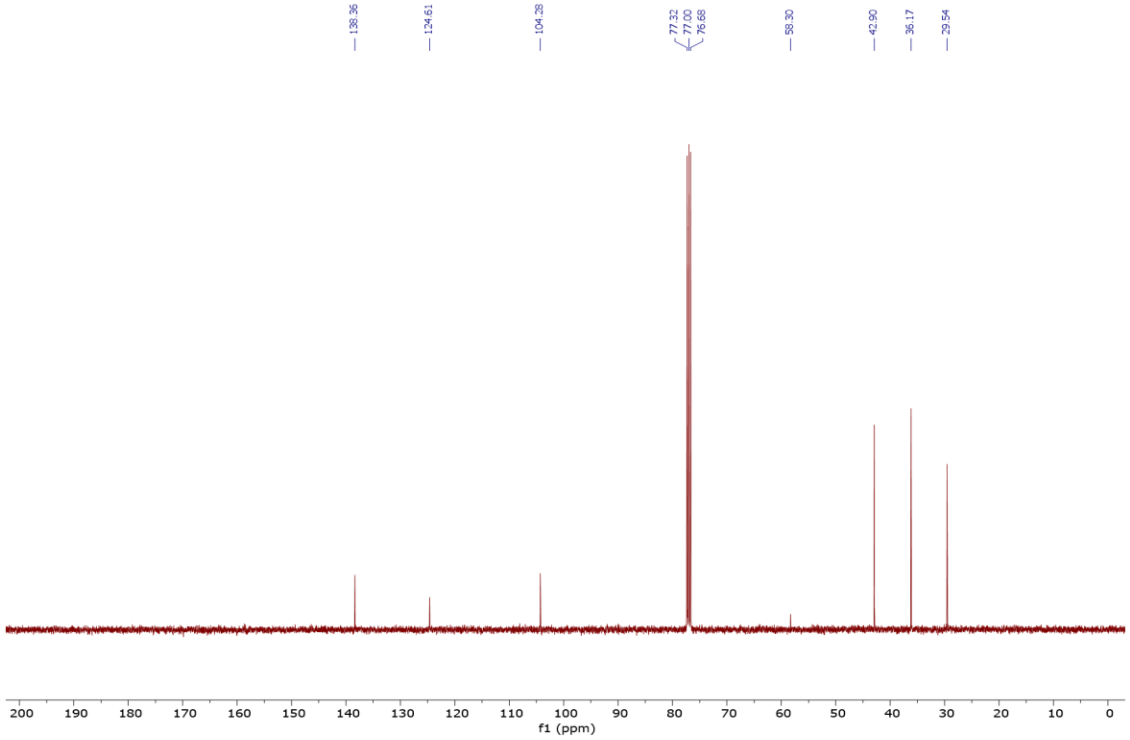

*N*-benzylindole **5.58** ($CDCl_3$, 400 MHz for $^1H$ NMR, 100 MHz for $^{13}C$ NMR)

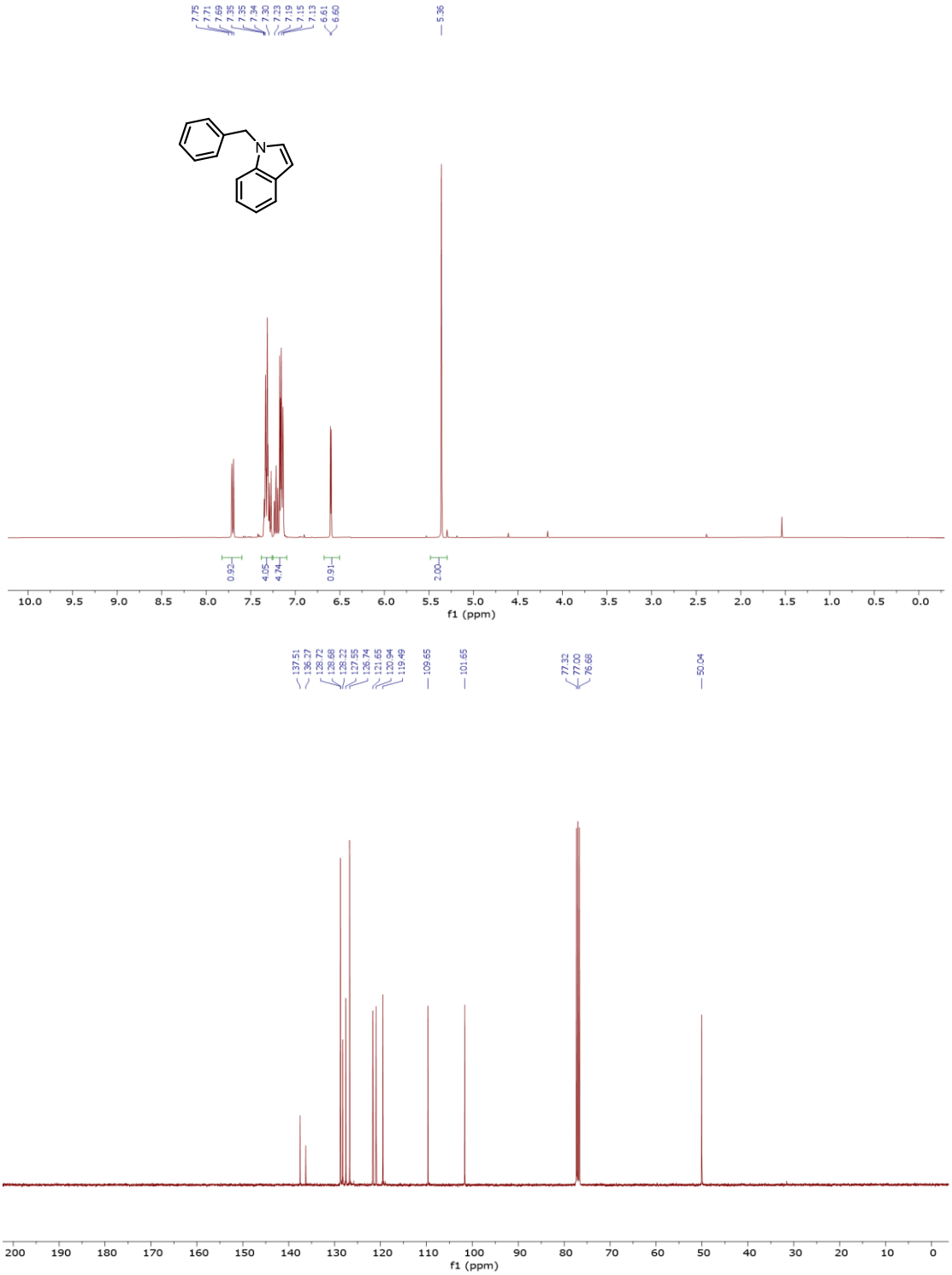

2-Methyl-(4-cyclopropyl-1-methyl-piperidinyl)-1*H*-indole **5.63** ($CDCl_3$, 400 MHz for $^1H$ NMR, 100 MHz for $^{13}C$ NMR)